

UNCLASSIFIED

| | |
|---|---|
| AD NUMBER | |
| AD385911 | |
| CLASSIFICATION CHANGES | |
| TO: | unclassified |
| FROM: | confidential |
| LIMITATION CHANGES | |
| TO: | Approved for public release, distribution unlimited |
| FROM: | Distribution authorized to U.S. Gov't. agencies and their contractors; Critical Technology; DEC 1967. Other requests shall be referred to Air Force Rocket Propulsion Laboratory, Attn: RPPR-STINFO, Edwards AFB, CA 93523. |
| AUTHORITY | |
| AFRPL LTR 15 MAR 1971; AFRPL LTR 5 FEB 1986 | |

THIS PAGE IS UNCLASSIFIED

AD 385 911

AUTHORITY:

PERP
to 5 Feb 86



THIS REPORT HAS BEEN DELIMITED
AND CLEARED FOR PUBLIC RELEASE
UNDER DOD DIRECTIVE 5200.20 AND
NO RESTRICTIONS ARE IMPOSED UPON
ITS USE AND DISCLOSURE.

DISTRIBUTION STATEMENT A

APPROVED FOR PUBLIC RELEASE;
DISTRIBUTION UNLIMITED.

SECURITY

MARKING

The classified or limited status of this report applies to each page, unless otherwise marked.

Separate page printouts **MUST** be marked accordingly.

THIS DOCUMENT CONTAINS INFORMATION AFFECTING THE NATIONAL DEFENSE OF THE UNITED STATES WITHIN THE MEANING OF THE ESPIONAGE LAWS, TITLE 18, U.S.C., SECTIONS 793 AND 794. THE TRANSMISSION OR THE REVELATION OF ITS CONTENTS IN ANY MANNER TO AN UNAUTHORIZED PERSON IS PROHIBITED BY LAW.

NOTICE: When government or other drawings, specifications or other data are used for any purpose other than in connection with a definitely related government procurement operation, the U. S. Government thereby incurs no responsibility, nor any obligation whatsoever; and the fact that the Government may have formulated, furnished, or in any way supplied the said drawings, specifications, or other data is not to be regarded by implication or otherwise as in any manner licensing the holder or any other person or corporation, or conveying any rights or permission to manufacture, use or sell any patented invention that may in any way be related thereto.

**Best
Available
Copy**

PATENT SECURITY NOTICE

Material in this publication relating to
DUAL ORIFICE INJECTION, LAMINATED
CHAMBER COOLING MEANS, and A VARIABLE
AREA INJECTOR CONCEPT

reveals subject matter contained in U.S. Patent Application Serial Nos. 426,711, 319,047, and 390,521 entitled "Rocket Injector," "High Pressure Rocket and Cooling Means" and "Controllable Injector for Rockets," respectively, which have been placed under Secrecy Orders issued by the Commissioner of Patents. These Secrecy Orders have been modified by SECURITY REQUIREMENTS PERMITS and a PERMIT "A", respectively.

A Secrecy Order prohibits publication or disclosure of the invention, or any material information with respect thereto. It is separate and distinct, and has nothing to do with the classification of Government contracts.

By statute, violation of a Secrecy Order is punishable by a fine not to exceed \$10,000 and/or imprisonment for not more than two years.

A SECURITY REQUIREMENTS PERMIT authorizes disclosure of the invention or any material information with respect thereto, to the extent set forth by the security requirements of the Government contract which imposes the highest security classification on the subject matter of the application, except that export is prohibited.

A PERMIT "A" authorizes disclosure of the subject matter of the patent application to any person of the classes hereinafter specified if such person is known to be concerned directly in an official capacity with the subject matter, provided that all reasonable safeguards are taken to otherwise protect the invention from unauthorized disclosure. The specified classes are:

- (a) Any officer or employee of any department, independent agency, or bureau of the Government of the United States.
- (b) Any person designated specifically by the head of any department, independent agency or bureau of the Government of the United States, or by his duly authorized subordinate, as a proper individual to receive the disclosure of the above indicated application.

A PERMIT "A" also authorizes disclosure to the minimum necessary number of person of known loyalty and discretion, employed by or working with United Aircraft Corporation or its licensees and whose duties involve cooperation in the development, manufacture or use of the subject matter by or for the Government of the United States, provided such persons are advised of the issuance of the Secrecy Order.

Disclosure of these inventions or any material information with respect thereto is prohibited except by written consent of the Commissioner of Patents or as authorized by the respective permits.

The foregoing does not in any way lessen responsibility for the security of the subject matter as imposed by any Government contract or the provisions of the existing laws relating to espionage and national security.

CONFIDENTIAL

AFRPL-TR-67-298-VOL II

(UNCLASSIFIED TITLE)

**ADVANCED
CRYOGENIC ROCKET ENGINE PROGRAM
STAGED-COMBUSTION CONCEPT
FINAL REPORT**

R. R. ATHERTON

**PRATT & WHITNEY AIRCRAFT
DIVISION OF UNITED AIRCRAFT CORPORATION
FLORIDA RESEARCH AND DEVELOPMENT CENTER**

**TECHNICAL REPORT AFRPL-TR-67-298-VOL II
DECEMBER 1967**

DECLASSIFIED AFTER 18 YEARS, DOD DIR. 5200.10

PATENT SECURITY NOTICE

PORTIONS OF THIS DOCUMENT CONTAIN SUBJECT MATTER COVERED BY A U.S. PATENT OFFICE SECURITY ORDER WITH MODIFYING SECURITY REQUIREMENTS PERMIT AND MODIFYING PERMIT "A". HANDLING SHALL BE IN ACCORDANCE WITH THE PERMIT AS DESCRIBED ON PAGE A AND INDICATED HEREIN. VIOLATORS MAY BE SUBJECT TO THE PENALTIES PRESCRIBED BY TITLE 36, U. S. C. (1962), SECTIONS 183 AND 185.

THIS DOCUMENT CONTAINS INFORMATION AFFECTING THE NATIONAL DEFENSE OF THE UNITED STATES WITHIN THE MEANING OF THE ESPIONAGE LAWS, TITLE 18, U. S. C., SECTIONS 793 AND 794, ITS TRANSMISSION OR THE REVELATION OF ITS CONTENTS IN ANY MANNER TO AN UNAUTHORIZED PERSON IS PROHIBITED BY LAW.

STATEMENT #2 CLASSIFIED

Best Available Copy

requires...
Special...
approval of

AFRPL-TR-67-298-VOL II
Edwards, Calif 935-23

CONFIDENTIAL

SECTION VIII MODULE CONTROL SYSTEM

| | |
|---------------------------------------|-----|
| A. Introduction and Summary | 247 |
| B. Mixture Ratio Valve and Seal Rig | 248 |
| 1. Hardware Description | 248 |
| 2. Test Program and Test Results | 284 |
| 3. Test Facilities and Procedures | 347 |
| 4. Conclusions | 352 |
| C. Flow Divider Valve and Seal Rig | 354 |
| 1. Hardware Description | 354 |
| 2. Test Program and Test Results | 392 |
| 3. Test Facilities and Procedures | 435 |
| 4. Conclusions | 440 |
| D. Thrust Control | 441 |
| 1. Hardware Description | 441 |
| E. Chamber Coolant Valve and Seal Rig | 469 |
| 1. Hardware Description | 469 |
| 2. Design of Selected Configuration | 471 |
| 3. Test Program and Test Results | 474 |
| 4. Summary and Conclusions | 486 |
| F. Electrical Ignition System | 486 |
| 1. Hardware Description | 486 |

~~CONFIDENTIAL~~

SECTION VIII
MODULE CONTROL SYSTEM

A. INTRODUCTION AND SUMMARY

(U) The objectives of the control tasks in the Phase I ADP program were (1) to build and test the valves needed for high pressure combustion rig tests and (2) to develop, through demonstration testing, the components of these valves considered critical to a high pressure cryogenic engine. In addition, the control system for the engine assembly was to be defined concurrently with the engine cycle analysis.

(U) To accomplish these objectives, a mode of control based on propellant flow metering was selected after preliminary analysis was conducted under the Module Design subtask (Section IV). In addition, points were located in the flowpath where regulation would be necessary.

(U) Of these regulation points, five were considered necessary to operate the high pressure combustion rigs. These points and the applicable valves were as follows:

1. Total oxidizer supply to the preburner regulated by a thrust control valve
2. Division of oxidizer flow between the primary and the secondary elements of the preburner injector regulated by a flow divider valve
3. Total oxidizer flow to the main chamber regulated by a mixture ratio valve
4. Fuel supply to the transpiration cooling passages regulated by a chamber coolant valve
5. Total fuel supply to the preburner regulated by a variable injector area.

(U) Four of these valves are discussed in this Section; the fifth, a variable-area fuel injector ultimately associated with the preburner, is discussed in Section IX.

(U) The electrical ignition systems were also defined as a part of the control task and these systems are described in this Section. The ignition system performance is reported in the preburner and main burner test Sections.

(U) Regulation and function requirements were defined for each of the valves, and the valve types were selected to satisfy these requirements in a configuration suitable for later development as an integral part of a demonstrator engine. An economical approach consistent with the intent of this program dictated the use of commercial actuation systems for these valves. This approach also allowed the test program to concentrate on the valve elements necessary to demonstrate high pressure cryogenic fluid regulation and control.

~~CONFIDENTIAL~~

(This page is Unclassified)

CONFIDENTIAL

(U) Definition of the control system was completed. The objective of this task was to define the engine and its control requirements in sufficient detail to permit analytical design of the control elements by competent control system manufacturers. To this end, complete simulations of the engine (both analog and digital) in a language and format common to the industry have been formulated for delivery to vendors. These simulations are described in Appendix II.

(U) Part of the control task was postponed by program redirection to use test stand equipment instead of the thrust control valve and the chamber coolant valve. As a result, the thrust control valve program was suspended when the detail parts were received and these parts were placed in storage. The chamber coolant valve program was suspended while the detail parts were on order and the orders were cancelled.

(U) Dynamic seals for the high pressure cryogenic valves were considered sufficiently unique to require supporting test programs. The objective of these programs was to demonstrate seal configurations that would contain liquid nitrogen at simulated operating pressures and limit overboard leakage to less than 10 standard cubic centimeters of nitrogen gas per second. This objective was accomplished.

(U) It was also an objective to seal propellants at tank pressures from the engine combustion chambers and demonstrate this by limiting liquid nitrogen leakage through the valves to 10 standard cubic centimeters of nitrogen gas per second. This objective was accomplished with the flow divider valve but was not accomplished with the mixture ratio valve. The mixture ratio valve seal performance was adequate for staged-combustion rig testing.

(U) Regulation characteristics of the flow divider valve and the mixture ratio valve were established by measuring water flow through the valves from a gas pressurized supply. These data were reduced to define the valve effective flow area, and the test results were in agreement with the requirements and design predictions to the extent that no modifications in valve regulation were required.

B. MIXTURE RATIO VALVE AND SEAL RIG

1. Hardware Description

a. Valve Type Selection

(U) The mixture ratio valve is required to regulate the oxidizer flow to the main injector. The flowmeter input control concept for the engine allowed definition of this unit as a simple regulating and shutoff valve.

(C) The mixture ratio valve design requirement was to pass 120% of its design flow at the valve operating point corresponding to the 100% thrust level and mixture ratio of 7. It was also required to provide shutoff for the main chamber oxidizer flow. Valve effective area, operating flow, and pressure drop requirements are shown in figure 304. Several design concepts were sketched and reviewed for selection.

CONFIDENTIAL

CONFIDENTIAL

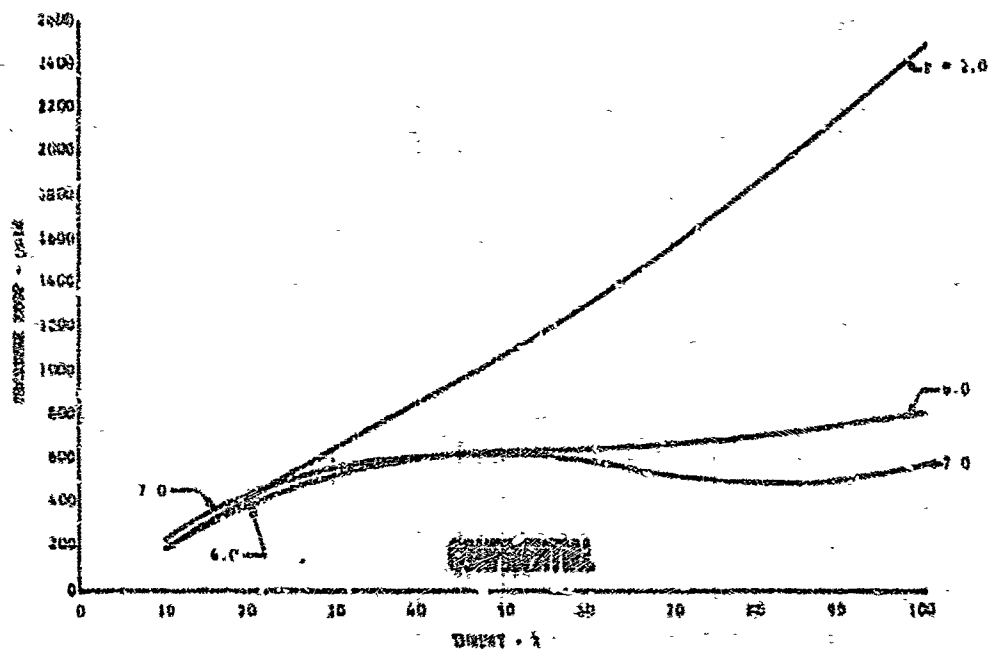
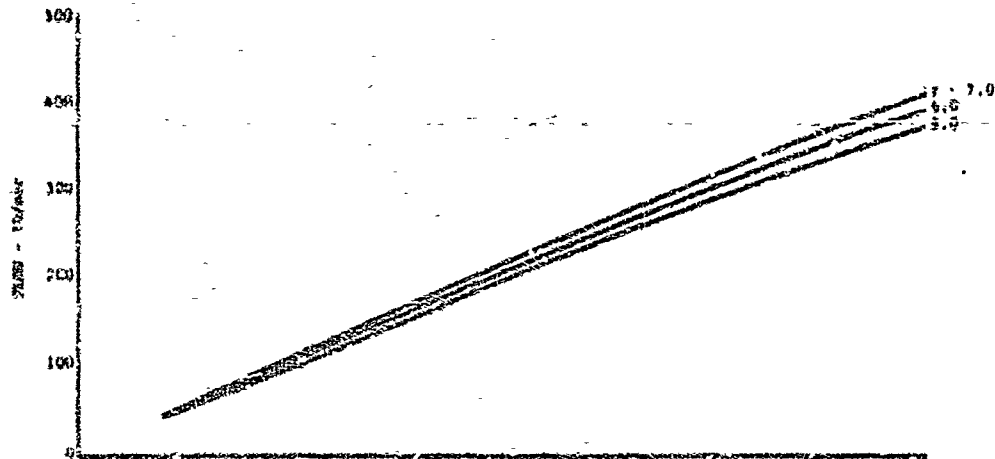
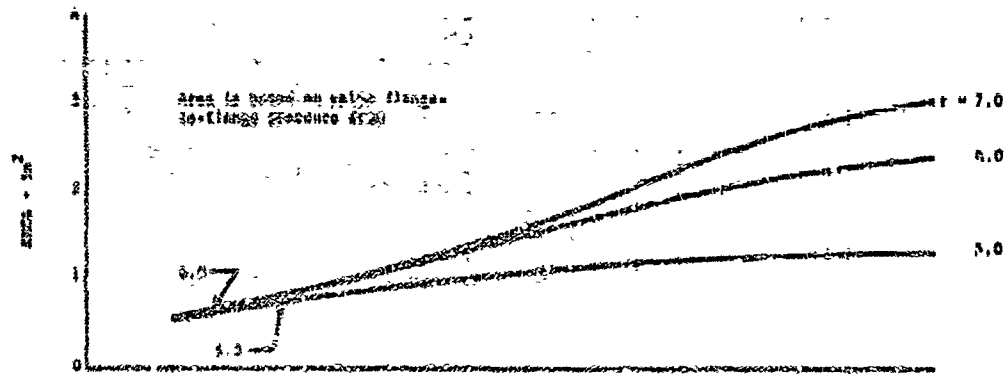


Figure 204. Mixture Ratio Valve Operating Requirements

DF 52377

CONFIDENTIAL

CONFIDENTIAL

(U) The object of the selection study was to evaluate the various valve types for use in the required engine application. The evaluation included the actuation requirements (load capacity and horsepower), accuracy, and general performance criteria (size, port contouring, mechanical feasibility, etc.). Detailed analysis of these candidates is discussed in the following paragraphs.

(U) As the result of the selection study a butterfly valve was selected for the mixture ratio valve.

b. Valve Type Selection

(1) Translating Sleeve Valve Candidate (See Figure 205)

(U) The translating sleeve valve scheme has a flowpath typical of most sleeve valves. Shutoff seals are located in the housing/sleeve area to avoid the alternative of having piston-mounted seals continually passing across the edges of contoured ports. As shown in figure 205, the piston makes contact with these seals only near the shutoff end of the stroke. This minimizes valve actuation force requirements throughout the engine operating range.

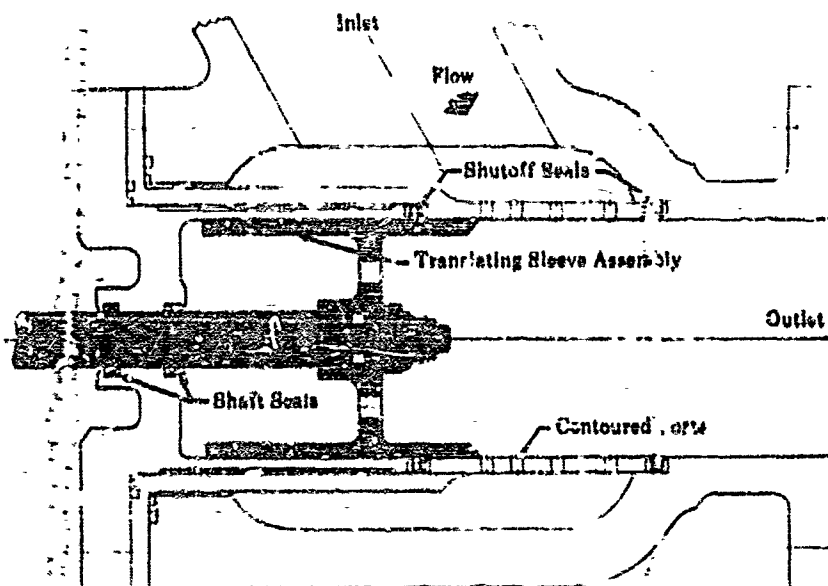


Figure 205. Mixture Ratio Valve, Sleeve Type

FD 160748

CONFIDENTIAL

(This page is Unclassified)

CONFIDENTIAL

(U) The required geometric flow area was established as a function of the rig operating point. Figure 206 is a plot of the required valve port geometric flow area as a function of thrust level and mixture ratio.

(U) When the valve turndown ratio was determined, the maximum port width depended only on the valve stroke. Figure 207 is a plot of this relationship. A valve-sizing family of curves is provided in figure 208, in which valve diameter is plotted as a function of stroke for various ratios of maximum port width to valve circumference.

(U) Figure 209 is a plot of geometric port areas as a function of stroke for 2-inch, 2.5-inch, and 3-inch total stroke valves. Figures 210, 211, and 212 are plots of the respective port contours for these valve strokes. The percent error in flow area vs percent positional error is plotted in figure 213 as a function of valve turndown ratio.

(C) The axial flow forces acting on the valve are shown in figure 214 as a function of thrust level as a mixture ratio of 5. A corresponding horsepower curve is shown in figure 215.

(U) The inverted pintle type valve yields considerably higher loads than the contoured port sleeve valve (thus higher power requirements) because the fluid induced static pressure gradient is exposed to a larger area.

(C) The mechanical design features established for comparing candidate sleeve valves in the mixture ratio control function were as follows:

1. Inlet and outlet size to be 4.00-in. diameter for a maximum fluid velocity of 60 ft/sec at 100% thrust nominal flow rate.
2. Sleeve flow area of 5.30-in.² is based on maximum flow and minimum ΔP condition at 90% thrust and 7 to 1 mixture ratio. Applying the 120% capacity requirement to the physical maximum port total area resulted in an area of 6.50-in.².
3. Sleeve stroke was established at 3.00-in. with 4.00-in. diameter sleeve and minimum sleeve area of 0.655-in.².
4. Housing losses were set at 4.5 times velocity head at rated flow of 379 lb/sec, or 142 psid.
5. Required shutoff seal loading was estimated to be 450 lb, and piston rod seal loading under maximum pressure conditions was 350 lb.
6. Wall thickness was sized for 32,000-psi yield strength aluminum alloy.

(2) Pintle Orifice Valve Candidate (See figure 216)

(U) The configuration of the pintle orifice type mixture ratio valve is basically the same as for the other components. The inlet port is 90 degrees from the axis of the valve. Shutoff sealing is accomplished through a plastic O-ring seal mounted in the pintle.

CONFIDENTIAL

CONFIDENTIAL

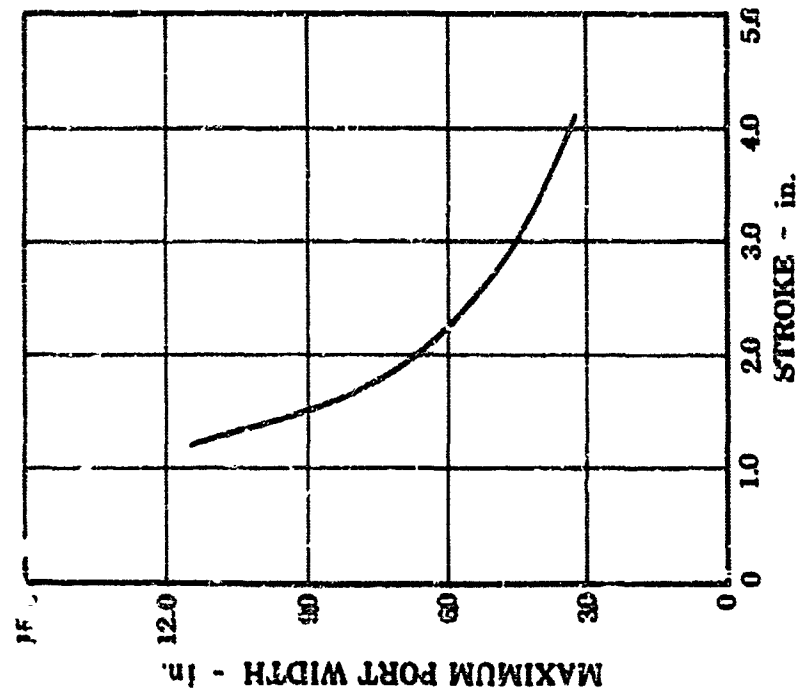


Figure 207. Maximum Width of Constant Area Error Contoured Port vs Stroke of Sleeve Valve (Mixture Ratio Valve) FD 18261

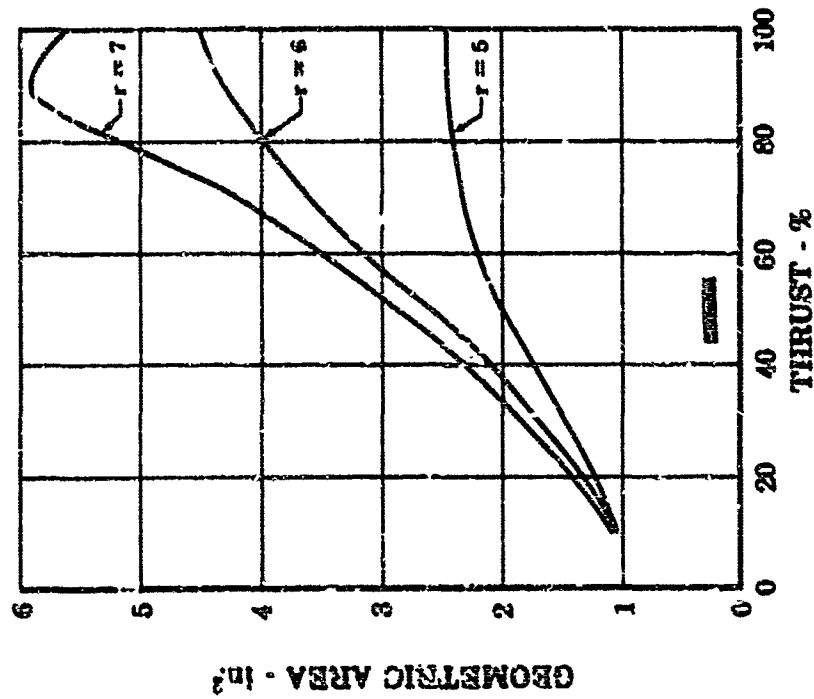


Figure 206. Sleeve Valve Geometric Area vs Percent Thrust (Mixture Ratio Valve) FD 18189

CONFIDENTIAL

UNCLASSIFIED

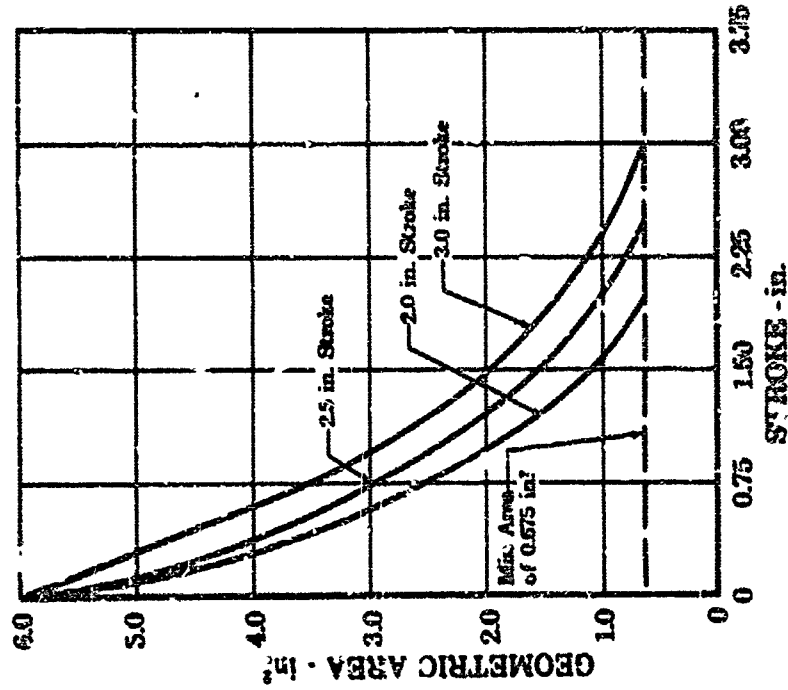


Figure 209. Port Area vs Stroke for Constant Percentage Port Contour on Sleeve Valve (Mixture Ratio Valve)

FD 18282

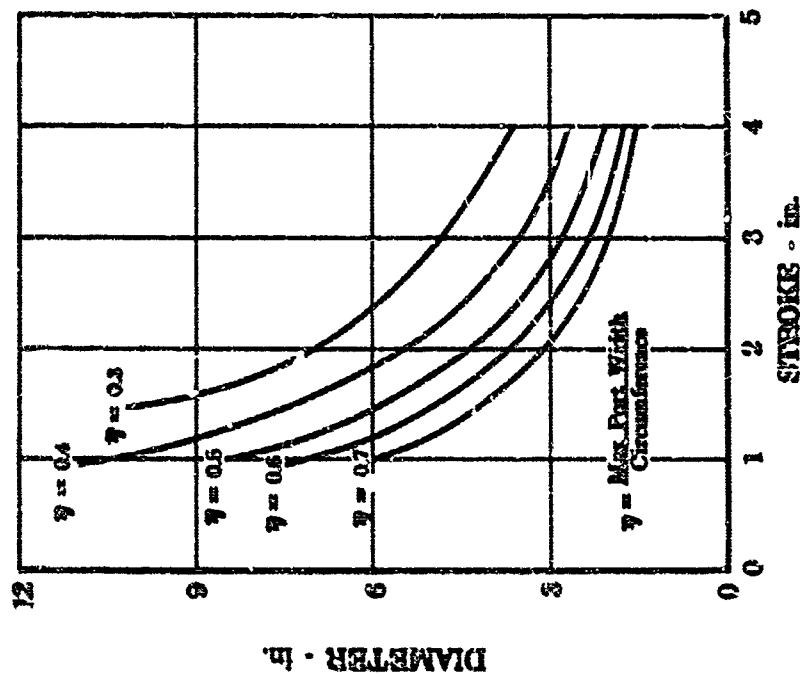


Figure 208. Sleeve Valve Diameter vs Stroke (Mixture Ratio Valve)

FD 18238

UNCLASSIFIED

UNCLASSIFIED

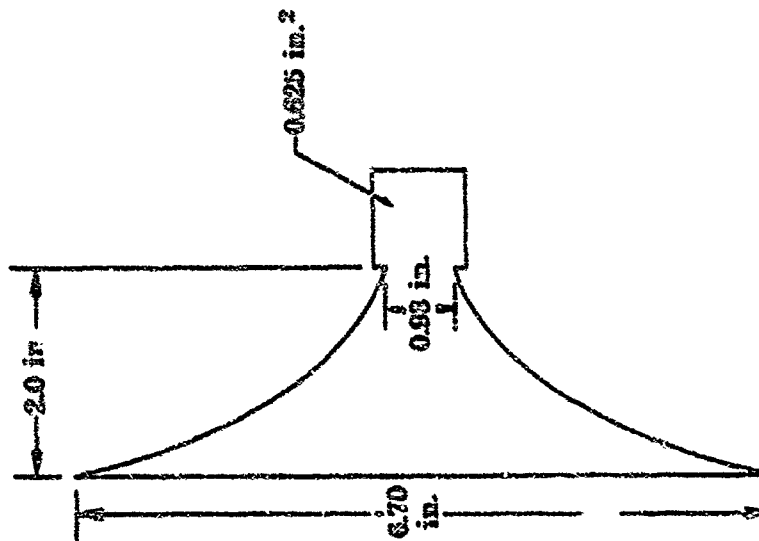


Figure 210. Sleeve Port Contour for 2.0-inch Stroke (Mixture Ratio Valve)

PD 18210 Figure 211.

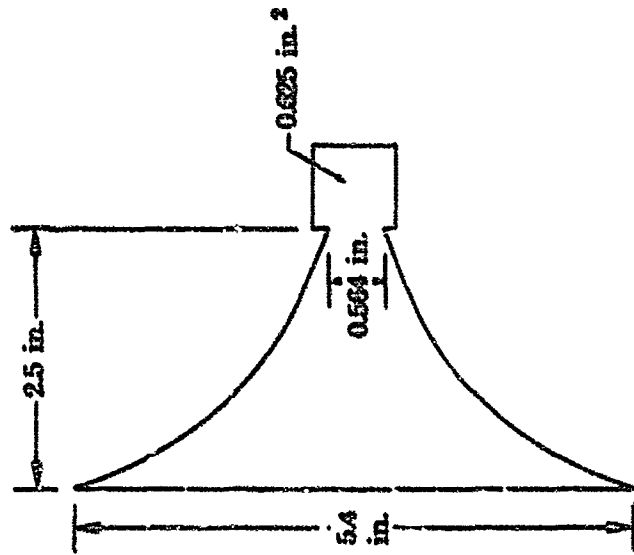


Figure 211. Sleeve Port Contour for 2.5-inch Stroke (Mixture Ratio Valve)

PD 18.

UNCLASSIFIED

CONFIDENTIAL

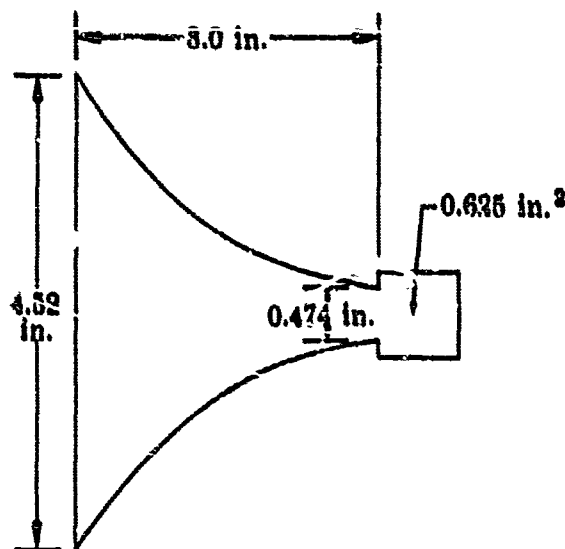


Figure 212. Sleeve Port Contour for 3.0-inch Stroke (Mixture Ratio Valve)

FD 18212

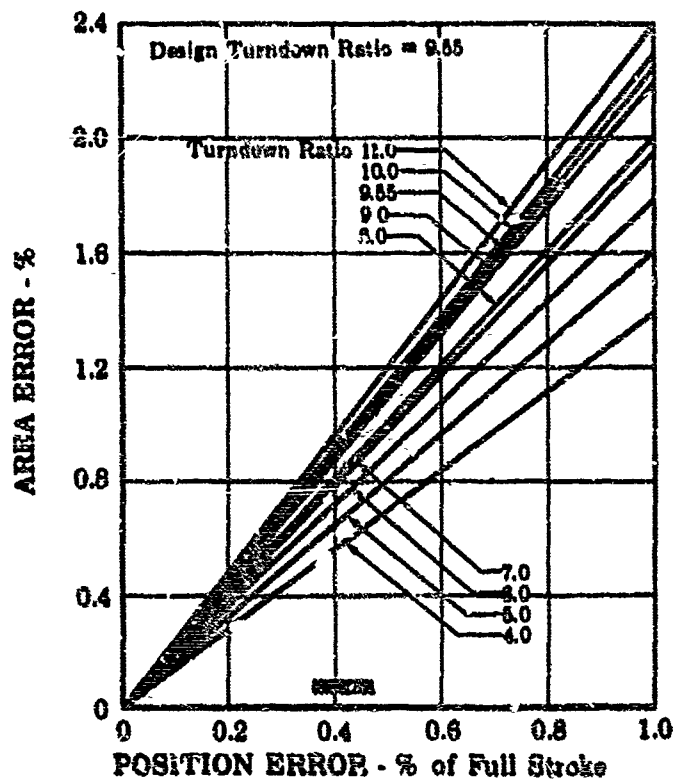
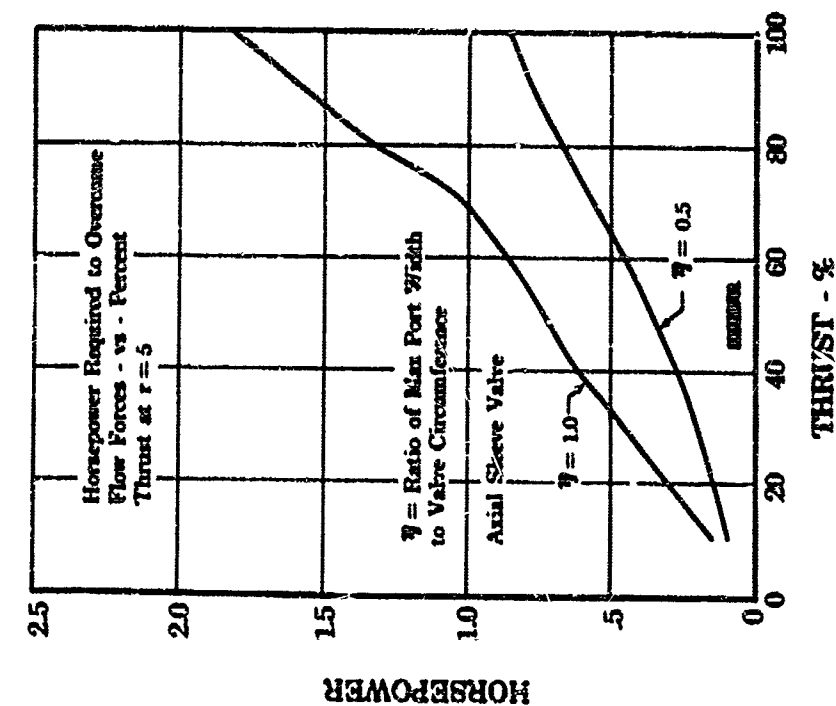


Figure 213. Percent Area Error vs Percent Stroke Error for Various Valve Turndown Ratios (Mixture Ratio Valve)

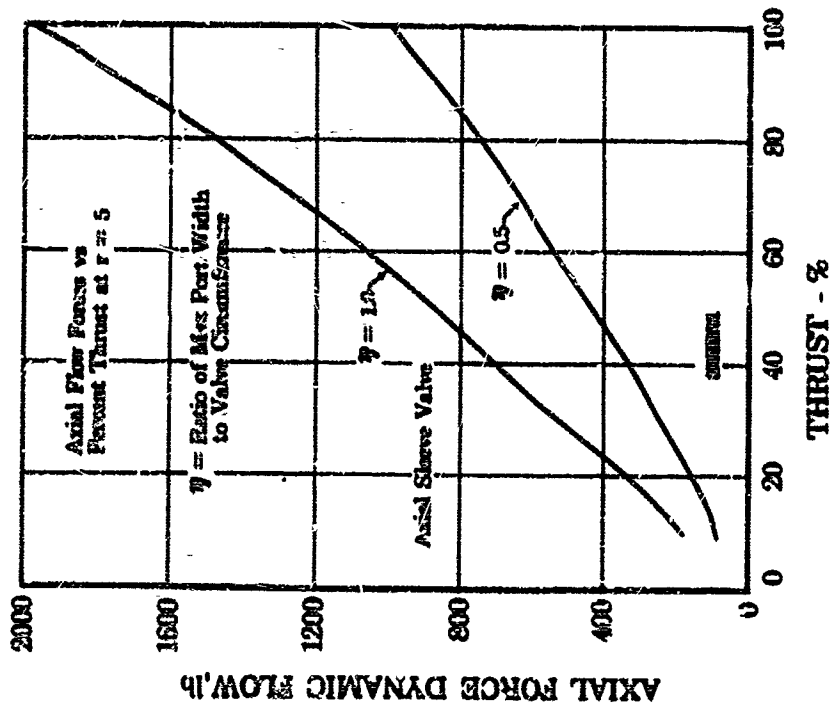
FD 18259

CONFIDENTIAL



FD 18176

Figure 215. Horsepower Required to Overcome Flow Forces vs Percent Thrust at $r = 5$ (Mixture Ratio Valve)



FD 18233

Figure 214. Axial Flow Forces vs Percent Thrust at $r = 5$ (Mixture Ratio Valve)

CONFIDENTIAL

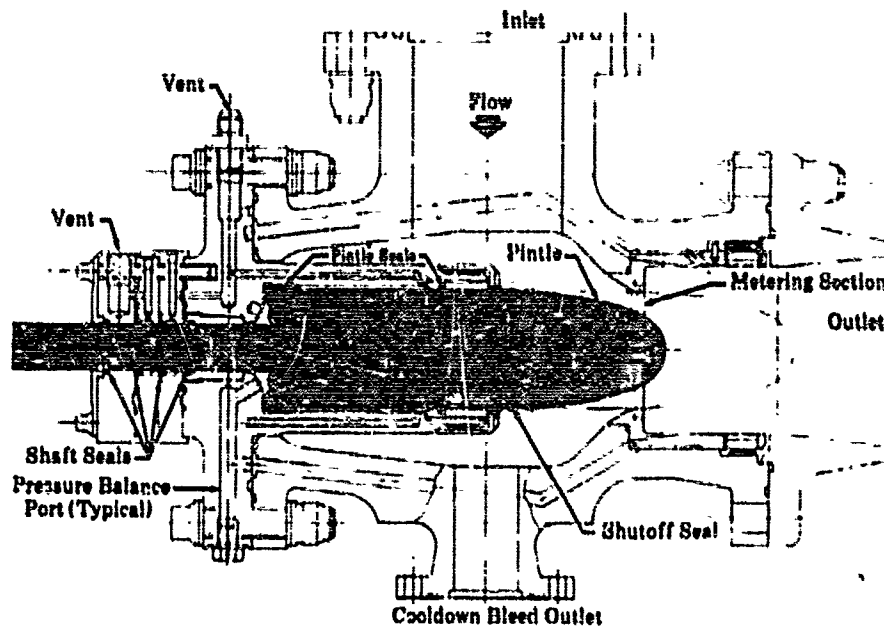


Figure 2i6. Mixture Ratio Valve, Pintle Orifice Type

FD 16073A

(U) In sizing the pintle orifice valve, a limiting condition occurs when the system request for valve flow area results in sufficient pintle withdrawal to cause a drop-off in discharge coefficient. This results in operation that deviates from a constant percentage contour. This drop-off effect is illustrated in figure 217, where the flow coefficient is plotted as a function of wall diameter for various valve strokes.

(U) Figure 218 is a plot of required geometric flow vs percent thrust and mixture ratio. The effect of pressure recovery is influential in this analysis. The percent recovery factor is shown in figure 219 as a function of thrust and mixture ratio.

(C) Figure 220 is a plot of axial valve opening force as a function of percent thrust and mixture ratio. Figure 221 is a plot of the net axial force acting on the pintle, which is compensated for by shaft sizing, as a function of thrust and mixture ratio. Coupling the simulated rig transient data with the forces generated in figure 221 yields a power requirement of 0.98 horsepower (1.96 horsepower if no force reversal is allowed).

(U) Operational and mechanical problems in pintle valve schemes with respect to concentricities, sealing, and dirt sensitivity also apply to the mixture ratio valve.

(C) The housing parts and pintle body illustrated in figure 216 are aluminum alloy. The pintle bullet is AMS 5735 (stainless steel) to match the thermal characteristics of its retaining bolt and the valve orifice. The bearings used to guide the pintle are of lead- or Teflon-filled bronze.

CONFIDENTIAL

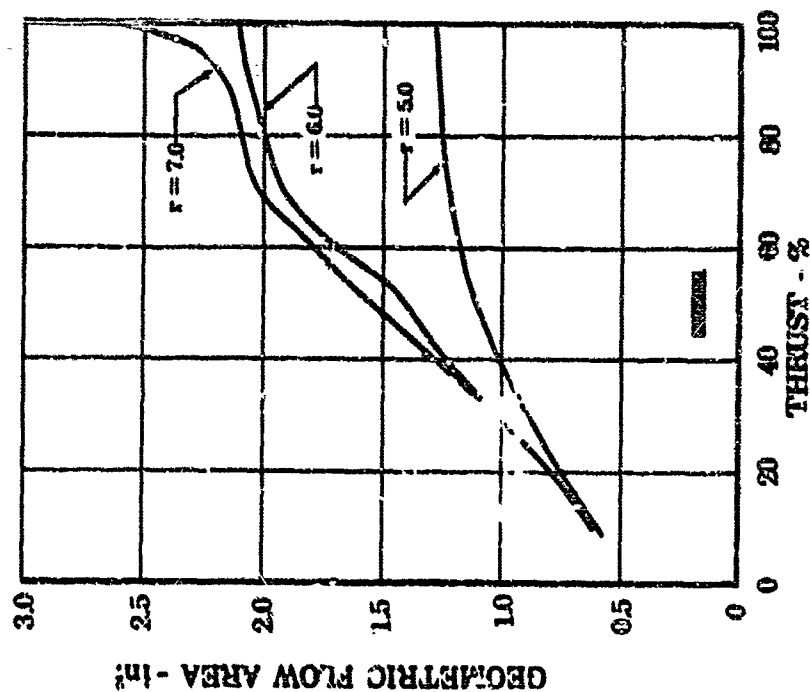
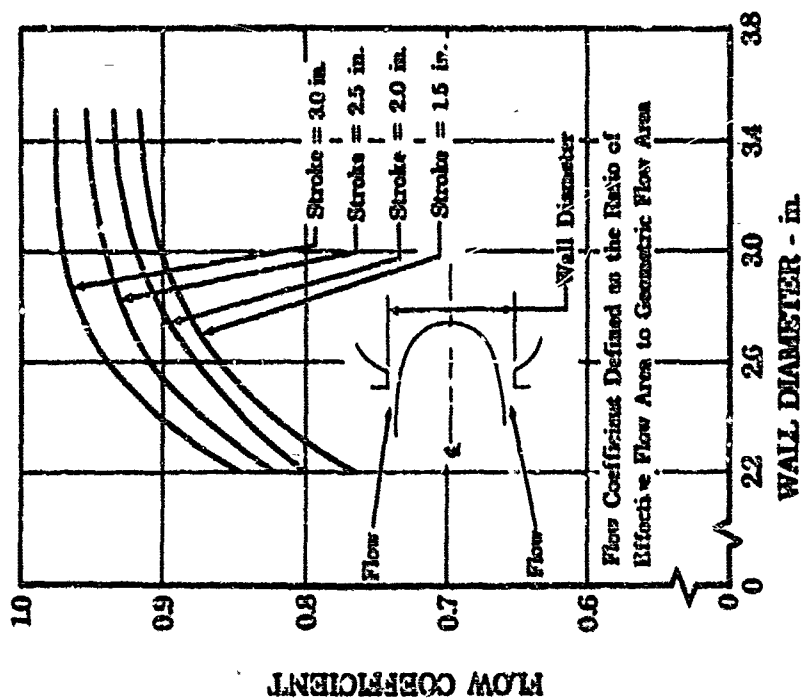


Figure 218. Required Geometric Flow Area vs Percent Thrust (Mixture Ratio Valve)

Figure 217. Pintle Valve Sizing Criteria (Mixture Ratio Valve)



CONFIDENTIAL

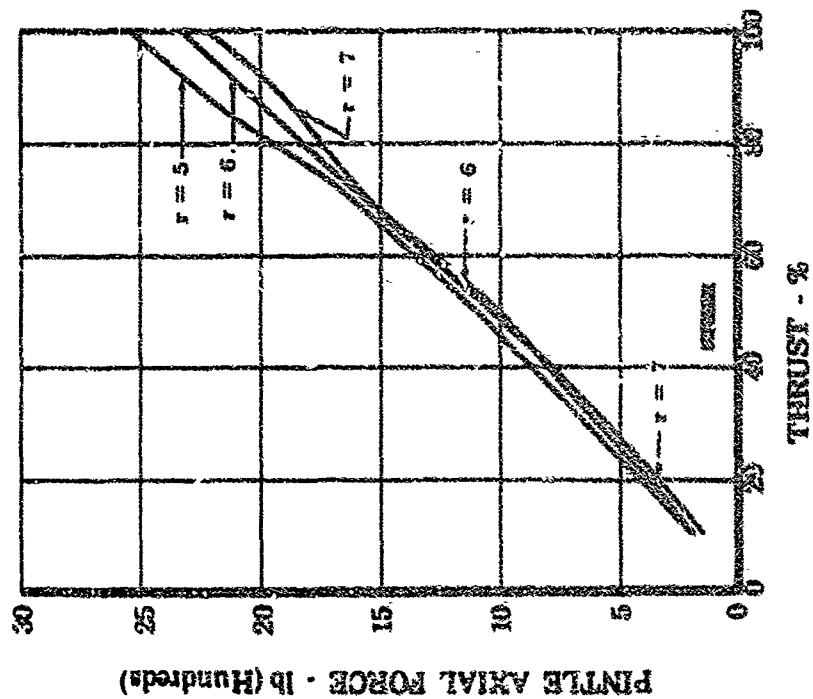


Figure 220. Axial Force vs Percent Thrust (Mixture Ratio Valve)

FD 18195

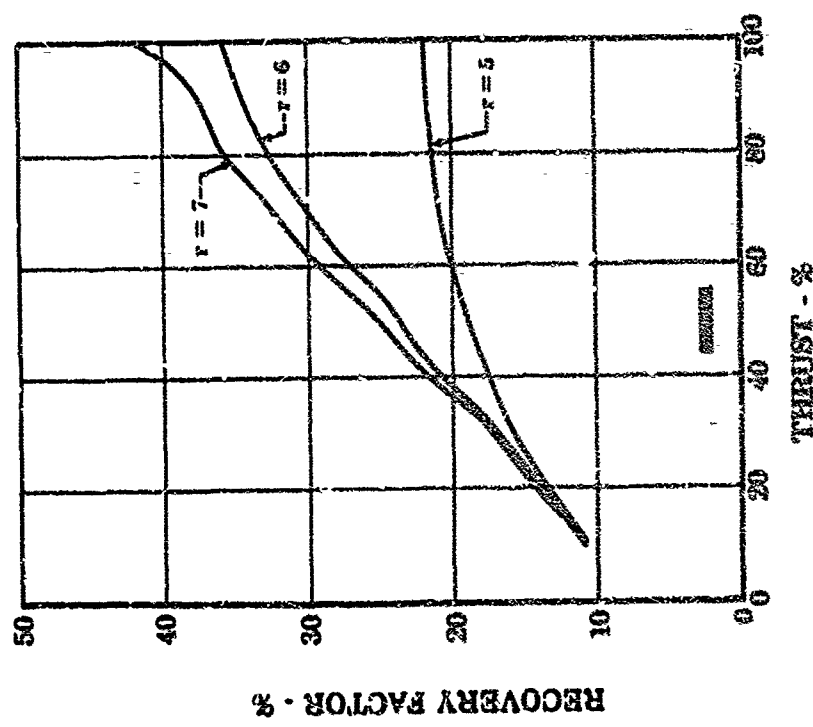


Figure 219. Percent Pressure Recovery vs Percent Thrust (Mixture Ratio Valve)

FD 18190

CONFIDENTIAL

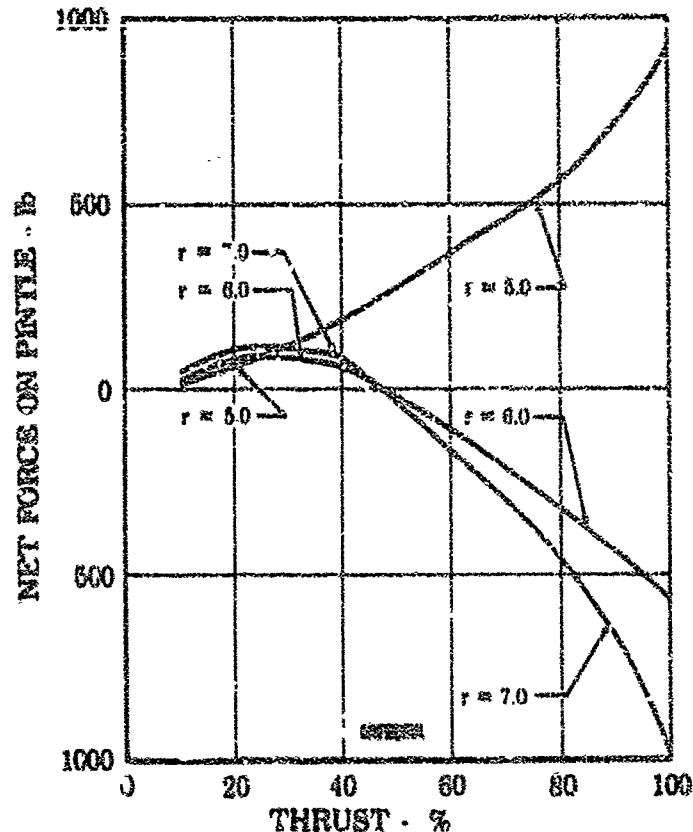


Figure 221. Net Axial Force vs Percent Thrust as a Function of Mixture Ratio (Mixture Ratio Valve)

FD 18260

(C) The mechanical design features established for evaluation of a pintle-orifice valve in the mixture ratio valve were as follows:

1. A 2.60-in. diameter orifice and a 3-in. stroke were selected to satisfy the flow and ΔP requirements.
2. Thrust balance of the pintle valve was difficult to achieve because of uncertainty of the analysis, the effects of leakage, eccentricities, and the static pressure distribution along the pintle. The wide range of flows and pressure drops means unbalance will always exist, probably in the order of 1000 lb maximum in each direction.
3. Confidence in the thrust balance of the pintle valve was low because of the wide range of flow and pressure drop. Variable effects of leakage, eccentricity, and static pressure distribution may add ± 1000 lb to the predicted unbalance, particularly in a transient.

CONFIDENTIAL

CONFIDENTIAL

(3) Pintle Venturi Valve Candidate

(a) Noncavitating Venturi

(C) It was required for this type valve that the venturi throat pressure (static) always be maintained above the saturation pressure of the fluid. Figure 222 shows that below 60% thrust and at a mixture ratio of 7, cavitation will occur. No further consideration of this type valve was given.

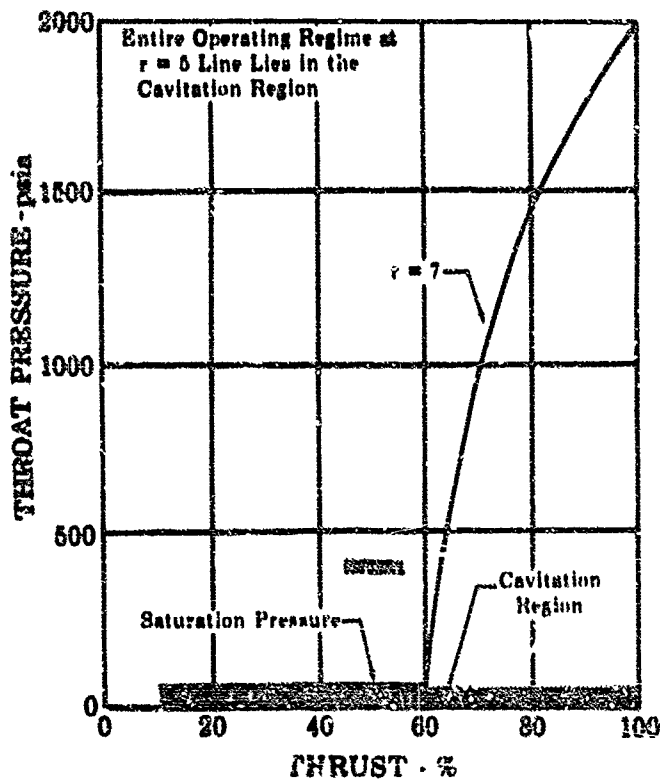


Figure 222. Throat Pressure vs Percent Thrust for Noncavitating Venturi Pintle Scheme (Mixture Ratio Valve)

PD 18279A

(b) Cavitating Venturi (See figure 223)

(C) To maintain cavitation and meet stability requirements, the venturi throat pressure (static) must not exceed the saturation pressure of the fluid. Figure 224 illustrates that the fluid will not be in cavitation between 87 and 93% thrust at a mixture ratio of 7; this rules out use of this type of valve.

CONFIDENTIAL

CONFIDENTIAL

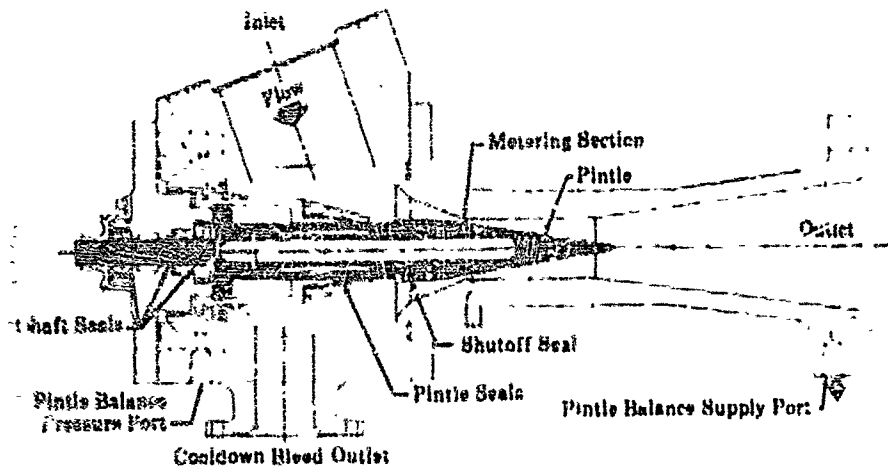


Figure 223. Mixture Ratio Valve, Cavitating Venturi Type

FD 16076B

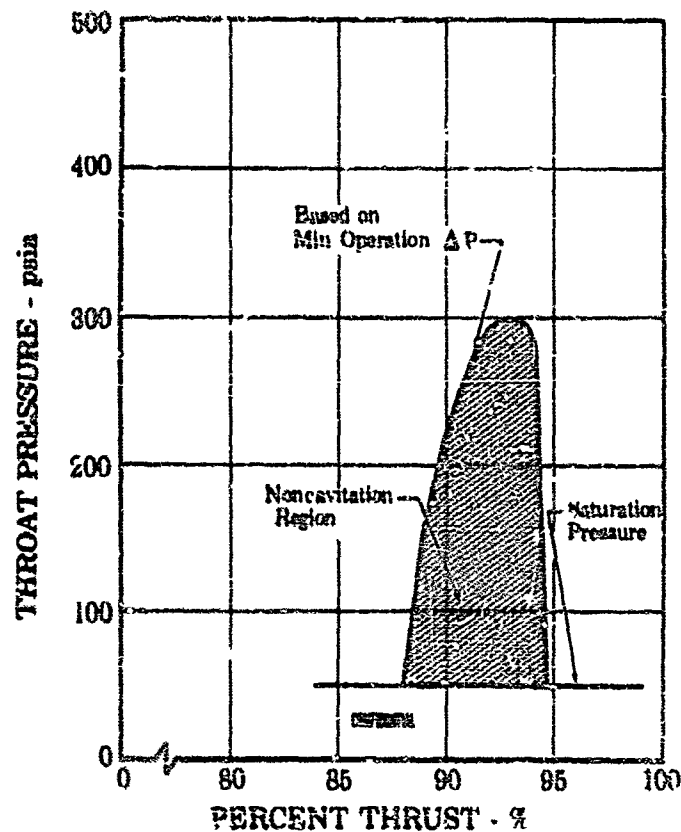


Figure 224. Venturi Throat Pressure vs Percent Thrust for Cavitating Venturi Scheme (Mixture Ratio Valve)

FD 18175

CONFIDENTIAL

CONFIDENTIAL

(C) The mechanical design features established for evaluation of a cavitating venturi valve in the mixture ratio valve selection were as follows:

1. The valve housings were 32,000-psi yield strength aluminum, except for a throat insert to avoid cavitation damage. The stainless steel pintle assembly was split to enable assembly of the shutoff seal.
2. The cavitating venturi valve envelope was 9 by 12 by 30 in., and the estimated weight was 70 lb.

(4) Ball Valve Candidate (See figure 225.)

(U) A ball valve has much the same performance characteristics and actuation requirements as a butterfly valve and it offers relatively low actuation forces and a small package size. Determination of these characteristics is described in the following paragraphs.

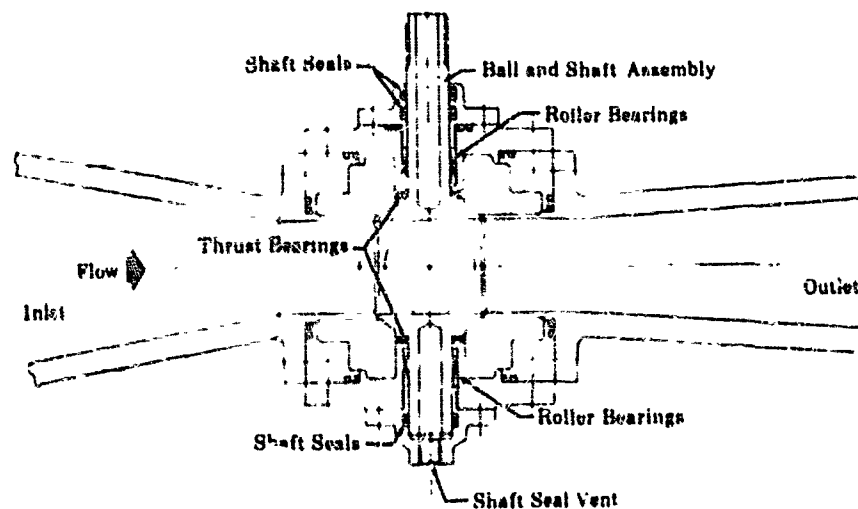


Figure 225. Mixture Ratio Valve, Ball Type

FD 16075A

(U) The "K" factor used in determining the pressure loss across a ball valve as a function of throat pressure or angular opening is given in figure 226. This K factor may be used to establish a valve flow-pressure drop relationship as follows:

$$\left[\frac{1}{2g} v^2 \right] K = (P_{in} - P_d)$$

when

$P_{in} - P_d$ = the pressure loss

P_{in} = Inlet pressure (total)

P_d = Discharge pressure (total)

CONFIDENTIAL

CONFIDENTIAL

ρ = Fluid density

V = Velocity of fluid at throat

K = Loss factor

(U) Since

$$\dot{W} = AV = \text{Weight Flow}$$

Then

$$\frac{1}{2g} \left(\frac{\dot{W}^2}{\rho A^2} \right) K = P_{in} - P_d$$

Solving for flow rate:

$$\dot{W} = \sqrt{2g \rho (P_{in} - P_d)} \sqrt{A} \frac{1}{K}$$

Since

K = Function of angular opening

A = Function of angular opening

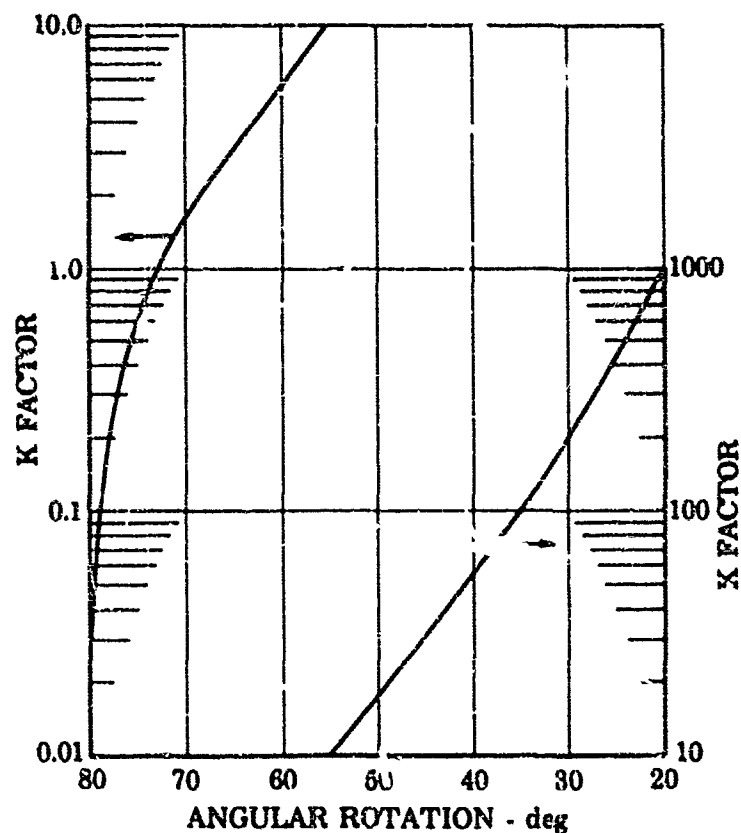


Figure 226. K Factor for Ball Valve vs Angular Rotation

FD 17946

264

CONFIDENTIAL

(This page is Unclassified)

CONFIDENTIAL

(U) For a fixed pressure drop and fluid density the flow through the ball valve is a unique function of valve opening.

(C) To size the ball passage diameter, valve flange-to-flange pressure loss was plotted as a function of passage diameter with the valve full open. Figure 227 indicates that at a required pressure loss of 585 psi the required passage diameter is 2-in.

(U) With the 2-in. diameter passage, the required angular opening was determined as a function of thrust level and mixture ratio. (See figure 228.)

(U) The effective area of the valve as a function of angular position was established by lumping the K factor with the geometric area. Figure 229 shows this parameter to be similar to that of the butterfly valve.

(U) To establish the area sensitivity to positional error, figure 230 was determined by taking the slope of the effective area curve at a point and dividing the slope by the effective area at the point. By taking a number of points, figure 230 was generated, yielding the percent area error per positional error as a function of angular position. Within the required range of operation, the sensitivity characteristics were similar to the butterfly valve.

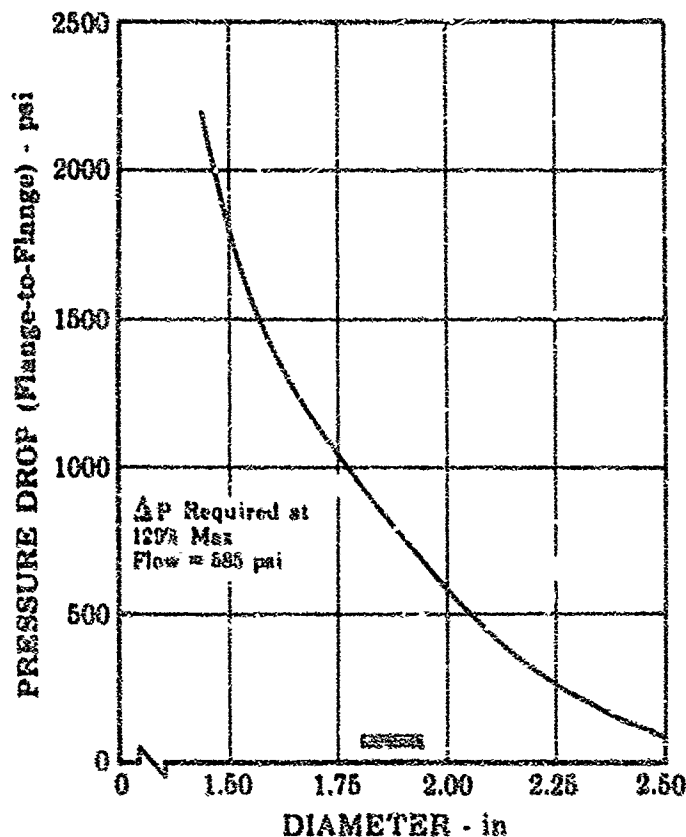


Figure 227. Pressure Drop vs Diameter of Ball Passage (Mixture Ratio Valve)

FD 18220

CONFIDENTIAL

CONFIDENTIAL

266

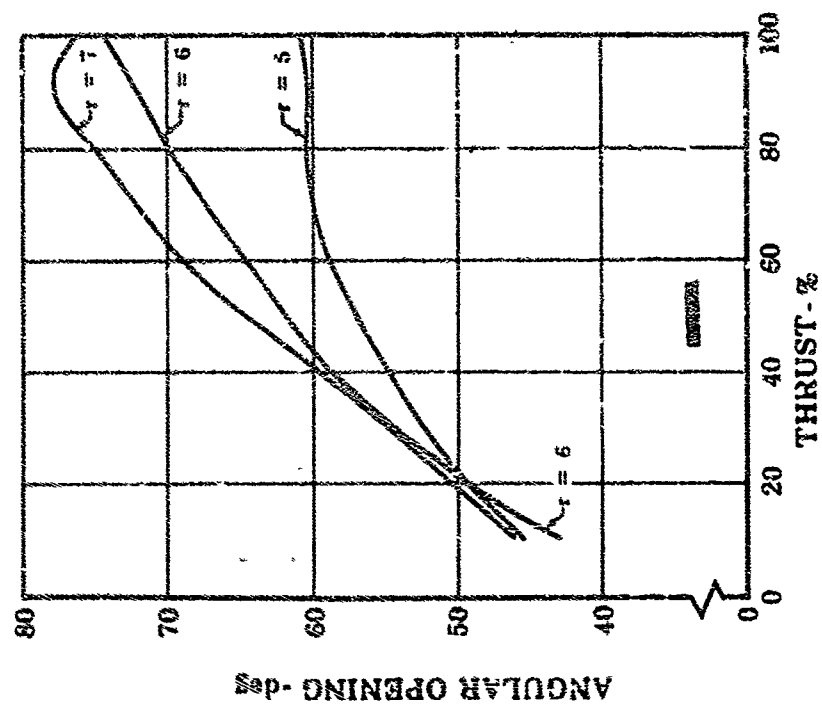
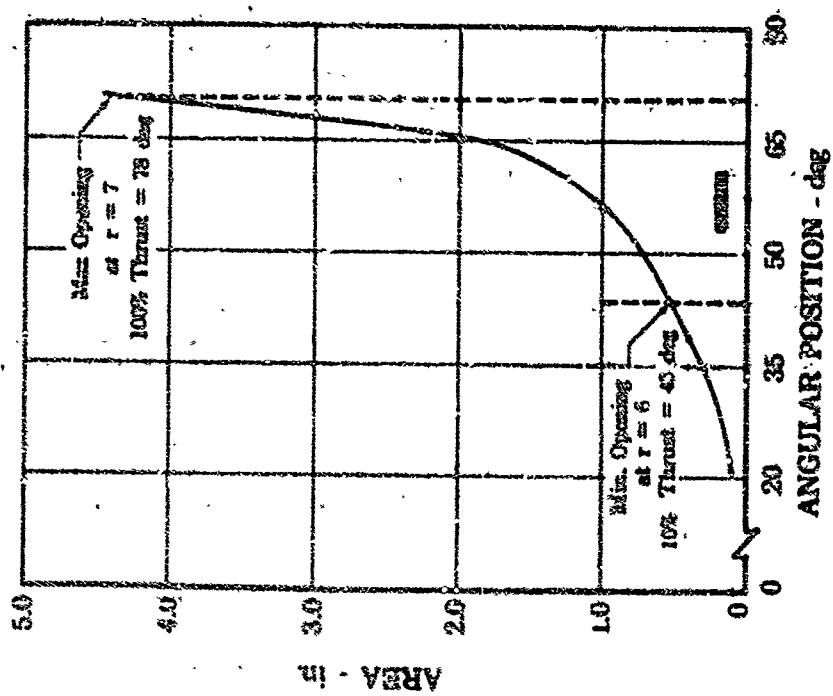


Figure 228. Angular Opening of Ball vs Percent Thrust (Mixture Ratio Valve)

FD 18243



FD 18256

Figure 229. Effective Area of Ball Valve vs Angular Position (Mixture Ratio Valve)

CONFIDENTIAL

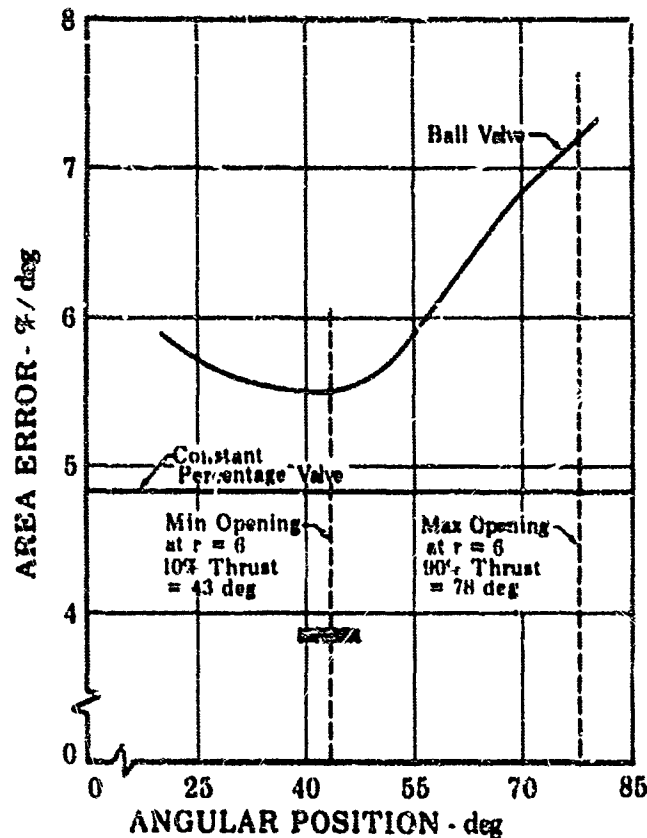


Figure 230. Area Error for Ball Valve and Constant Percentage Valve (Mixture Ratio Valve)

FD 18255

(U) After integrating the pressure profiles in the ball passage and establishing the centroids of these profiles, the net flow torque was evaluated. Figure 231 is a plot of the dynamic torque acting on the ball valve as a function of thrust level and mixture ratio.

(C) An area rate of change was determined from the simulated rig transient. When this area rate of change was converted to angular velocity and combined with dynamic torque, the result was a power requirement of 0.42 horsepower.

(C) The mechanical design features established for evaluation of a ball valve in the mixture ratio valve selection were as follows:

1. A 2.00-in. diameter hole through a 3.125-in. diameter ball was selected to pass 120% of the maximum required flow at the pressure drop required for 100% flow with the ball fully open.
2. Influence of 1000-psi allowable bearing stress on the Teflon shutoff seal produced 33 in.-lb of torque. The influence seal loading on shaft torque was determined to be 53 in.-lb.

CONFIDENTIAL

CONFIDENTIAL

3. The required needle roller bearings have a 4390-lb dynamic load capacity and will support the 4000-lb hydraulic load reaction at the 2480-psi pressure drop condition.
4. Total shaft torque required to operate the ball valve, excluding the hydraulic unbalance forces acting on the ball, was 75 in.-lb.
5. The ball valve design used a 32,000-psi yield strength aluminum alloy housing. The ball and shaft were Inconel 718.

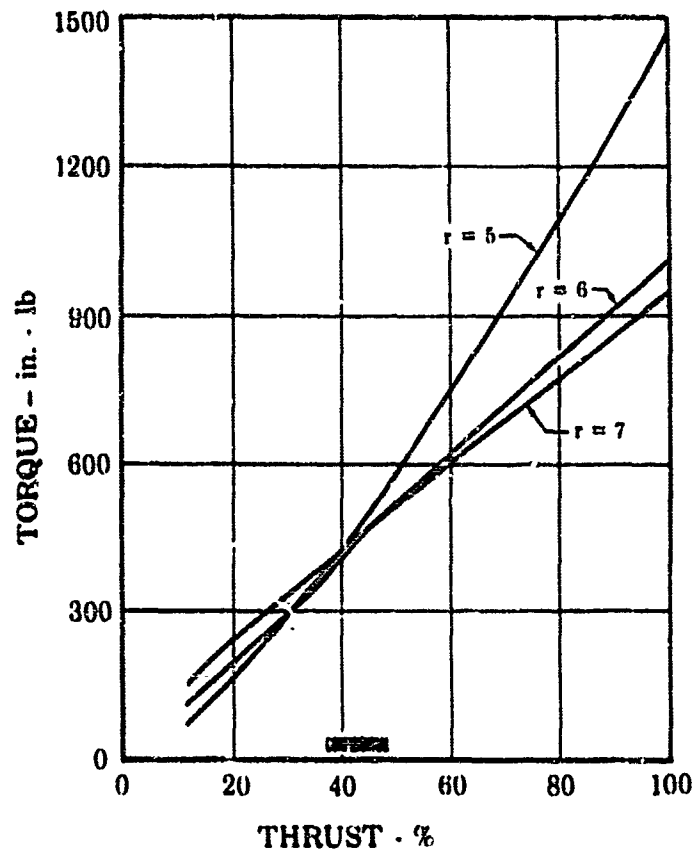


Figure 231. Dynamic Torque vs Percent Thrust (Ball Valve)

FD 18242

(5) Butterfly Valve Candidate (See figure 232)

(U) Shaft deflection considerations suggested an integral disk and shaft. This, in turn, required a split main housing for assembly. Low actuation forces and high durability were provided through the use of roller bearings on each end of the shaft. To accommodate the shutoff feature, a canted shaft with uninterrupted disk sealing surface was provided.

CONFIDENTIAL

CONFIDENTIAL

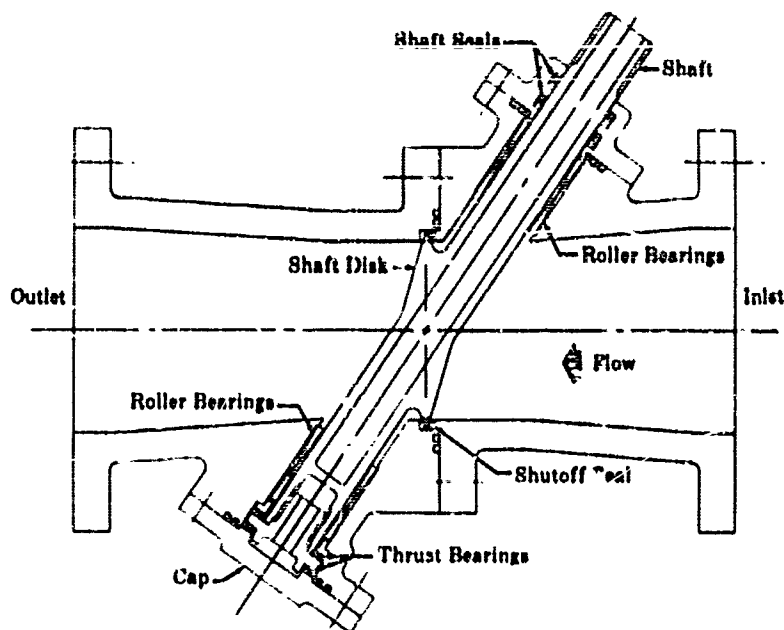


Figure 232. Mixture Ratio Valve, Butterfly Type Candidate

FD 16079A

(C) The canted shaft angle and sealing mechanism result in a high shaft-to-throat diameter ratio. This physical characteristic affected the basic flow-pressure drop relationship for the valve. The resulting effect was comparatively low valve gain between 60- and 90-degree valve opening. Because of this relative insensitivity, a 60-degree valve opening at maximum flow conditions was selected for conservative sizing. Figure 233 is a plot of required valve disk position as a function of valve throat diameter for 100% and 10% thrust level conditions. The 60-degree valve opening at the 120% flow point is shown to occur at a throat diameter of 3 inches. Figure 234 is a plot of valve angular opening as a function of thrust level and mixture ratio. The valve effective area is shown as a function of angular opening in figure 235. The effective area sensitivity with respect to positional error is shown in figure 236.

(C) Figure 237 is a plot of dynamic torque as a function of thrust level and mixture ratio. From a simulated engine transient, an area rate of change requirement was established for the mixture ratio control valve. Coupling the dynamic torque with the angular shaft velocity yielded a maximum power requirement of 0.49 horsepower. A cross-plot of dynamic torque versus angular opening for various mixture ratios is shown in figure 238.

CONFIDENTIAL

CONFIDENTIAL

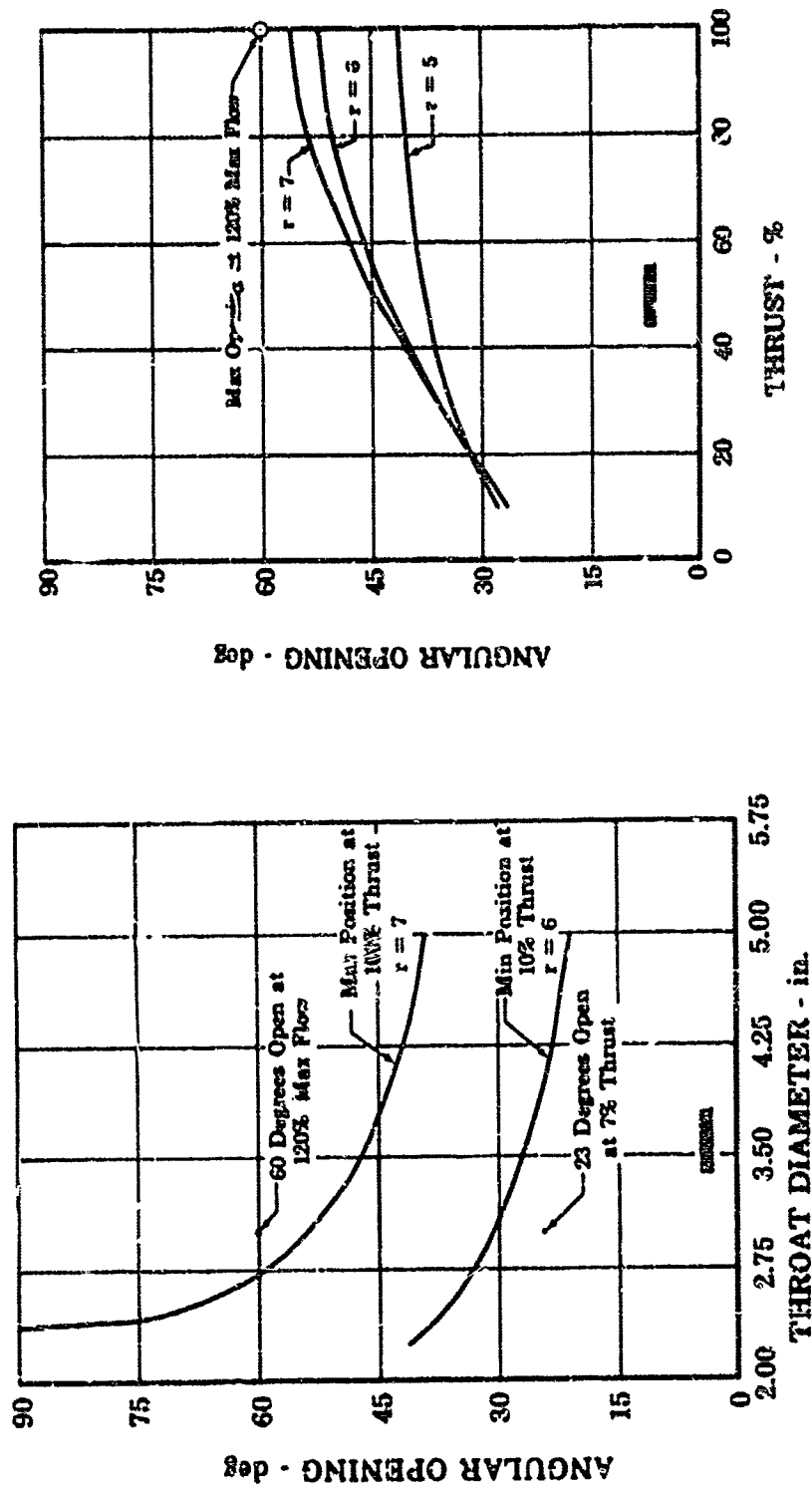
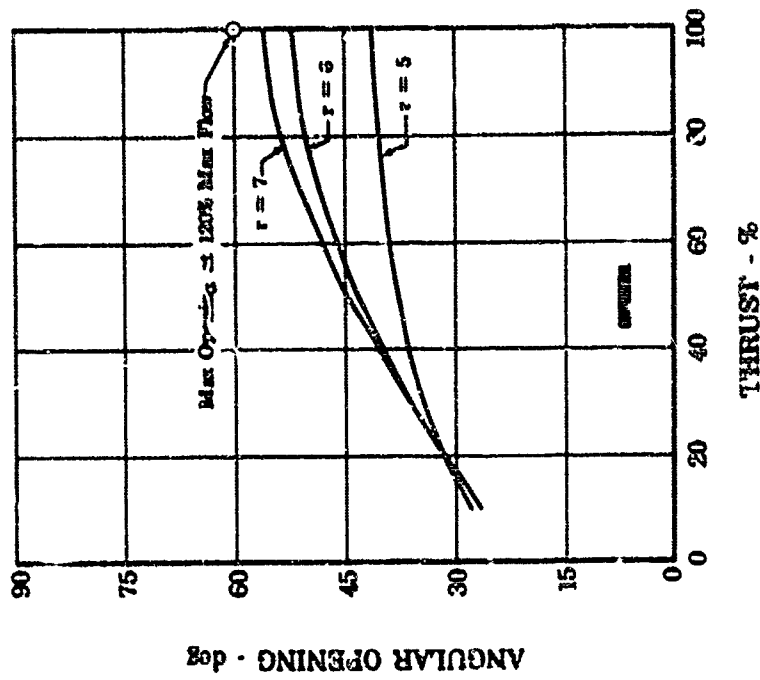


Figure 233. Butterfly Position vs Throat Diameter (Mixture Ratio Valve)

FD 18214 Figure 234. Butterfly Angular Opening vs Percent Thrust for 3.0-inch Inlet Diameter (Mixture Ratio Valve)



CONFIDENTIAL

CONFIDENTIAL

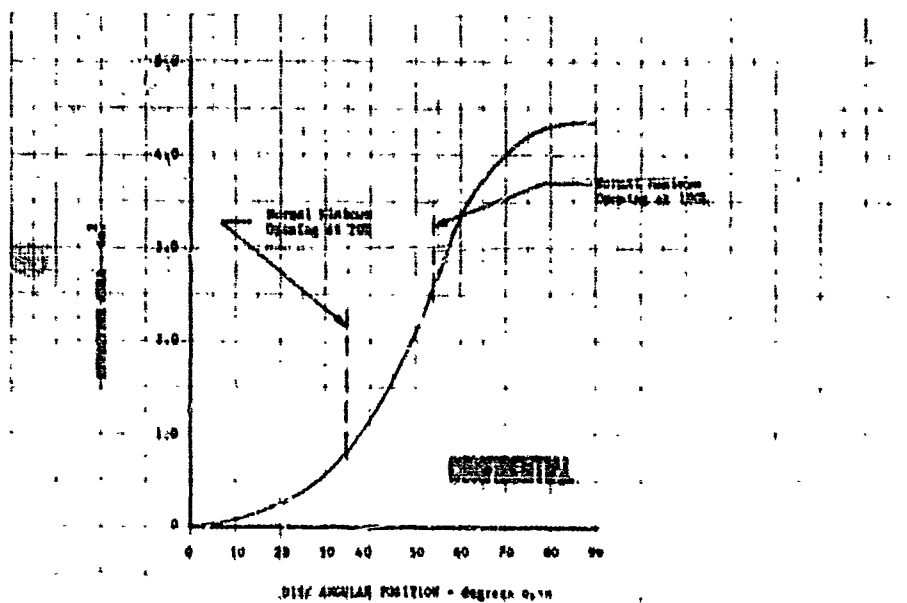


Figure 235. Butterfly Angular Opening vs Effective Area for 3.0-inch Inlet Diameter (Mixture Ratio Valve)

DF 58761

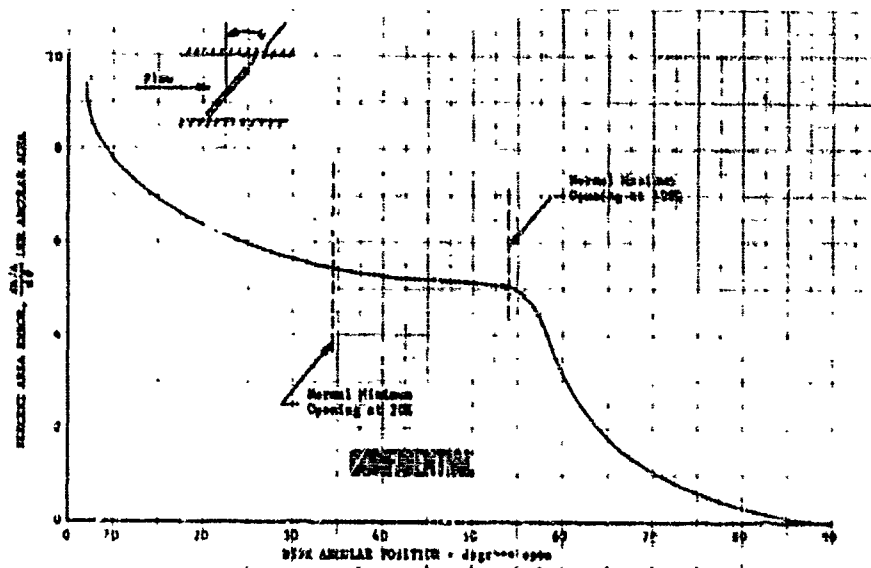


Figure 236. Area Error Per Degree in Percent vs Disk Angle

DF 58899

CONFIDENTIAL

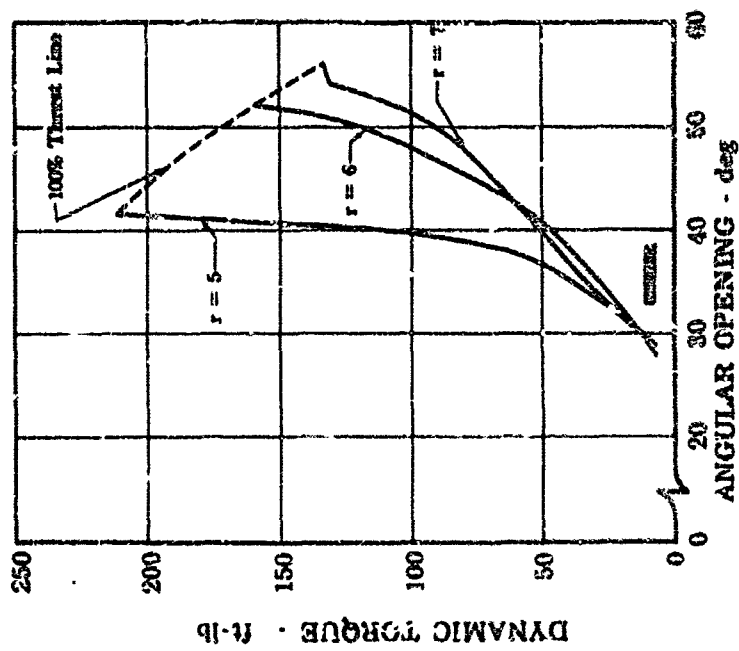


Figure 232. Butterfly Dynamic Torque vs Angular Opening for 3.0-inch Inlet Diameter (Mixture Ratio Valve) FD 18177

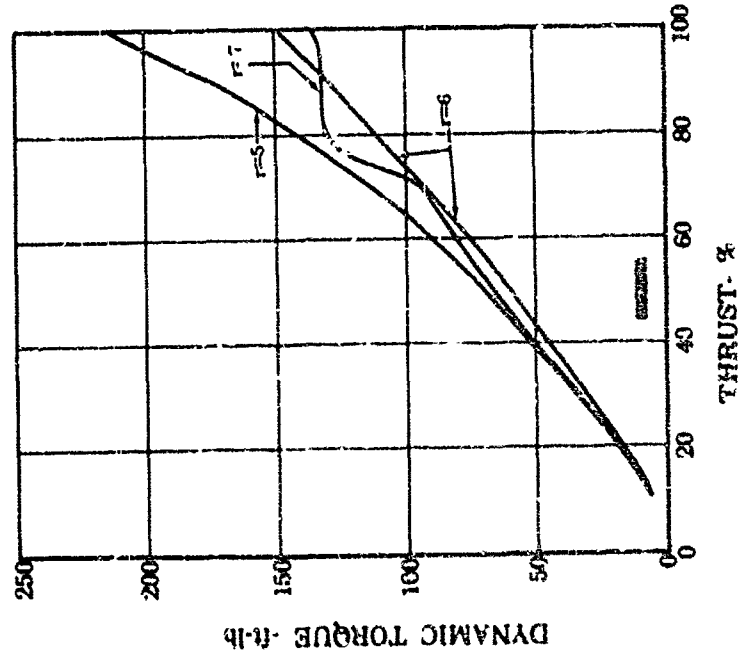


Figure 237. Butterfly Dynamic Torque vs Percent Thrust for 3.0-inch Inlet Diameter (Mixture Ratio Valve) FD 18227

CONFIDENTIAL

(C) The mechanical design features established for evaluation of a butterfly valve in the mixture ratio valve selection were as follows:

1. The flow area was sized to allow 120% flow at 60-degree disk opening and 440 psi pressure drop. This gave a 3.00-in. disk diameter and a 1.00-in. shaft diameter.
2. Shaft loading was determined by multiplying 100% of the disk area by the maximum pressure drop of 2200 psi. The resultant force was 15,800 lb. This load was divided equally between the shaft bearings, allowing for component forces associated with the 30-degree shaft tilt.
3. The radial load acting on the shaft roller bearing was 6850 lb. A suitable roller bearing was determined to be adequate to handle this load (neglecting the effects of shaft deflection that was not yet calculated).
4. The axial force tending to act on the roller thrust bearing, which is located at the end of the shaft opposite the drive spline, is 7900 lb. This is the 30-degree component of the 15,800 lb load on the butterfly disk. The actual thrust loading acting on the bearing is probably closer to 1000 lb for two reasons: (1) because the disk is partly open (45 degrees) under maximum loading, about 1/2 of the thrust component is taken out in the radial direction because of the offset shaft geometry. (2) The compensating force generated by the internal pressure acting on the shaft at the exposed drive end was 3000 pounds.

(6) Comparison Summary

(U) Table XXX is a quantitative summary of the significant features used in the selection study of the different valve candidates. Table XXXI is an estimated qualitative summary of the different valve candidates.

c. Design of Selected Configuration

(1) General

(U) The mixture ratio valve, which is located upstream of the main injector, is a butterfly type that incorporates a shutoff seal for the oxidizer flow to the main burner. To accommodate this shutoff feature, a canted shaft with integral disk was selected to provide an uninterrupted disk sealing surface. This resulted in a higher ratio of shaft diameter to throat diameter than would occur in a 90-degree design. Incorporation of the disk seal in the mixture ratio valve eliminated the need for a separate shutoff valve between the mixture ratio valve and the injector.

(U) The canted shaft and disk arrangement required a split main housing for assembling the valve. It was also necessary to incorporate widely spaced double roller bearings to support the loads produced by the maximum valve pressure drop. Shaft thrust bearings were incorporated to restrain the shaft against the flow-pressure thrust loads resulting from the canted shaft. These flow loads were minimized by pressure balancing the shaft to oppose them.

CONFIDENTIAL

CONFIDENTIAL

(C) Table XXX. Quantitative Valve Summary Comparison

| Valve Function | Valve Candidate | Required Horsepower (1) | Valve Torque or Axial Force (2) | Acc. μ V, (3) |
|-----------------------|-------------------------------------|--------------------------------|---------------------------------|-------------------|
| Mixture Ratio Control | Butterfly Valve | 0.49 | 264 ft-lb | 1.85 - 2.59 |
| | Translating sleeve - port contoured | 1.34 | 1200 lb | 2.24 |
| | Pintle orifice valve | 1.96 | 2160 lb | 2.2 |
| | Pintle venturi valve | Refer to applicable paragraph. | | |
| | Rotating ball valve | 0.42 | 121 ft-lb | 2.82 |

(1) Horsepower required to actuate the valve to follow engine transient under worst operating conditions.

(2) Maximum (total) valve torque or axial force due to flow forces.

(3) Percent area error per percent positional error.

(4) All configurations meet cycle balance requirements except as noted.

CONFIDENTIAL

CONFIDENTIAL

(C) Table XXI. Qualitative Valve Summary Comparison

| Valve Candidate | Remarks |
|---|--|
| Butterfly Valve | Appeared the smallest and most compact of all the valve candidates for the mixture ratio control. Simple mechanism with low actuating power requirements. Flow characteristics have built-in constant percentage regulating traits. Mixture ratio control valve required a sealing butterfly flapper. |
| Translating Sleeve Valve | |
| (Inverted Pintle) | Required higher actuation power than butterfly valve. Constant percentage contour on housing more difficult to machine than on a ported sleeve. Frictional effects more pronounced than rotational friction effects of butterfly. Small area metering (when sleeve plugs to housing bore) may give undesirable flow characteristics. |
| (Contoured Port) | better characteristics than inverted pintle. Flow forces act on smaller areas. Possibility of temperature (transient) sensitivity as well as dirt sensitivity. |
| Pintle Orifice | Appeared large compared to other valve candidates. Shaft and pintle area load compensation was necessary to obtain reasonable actuation power requirements. |
| Pintle Venturi (Cavitating and Noncavitating) | The venturi could not be operated wholly cavitated or wholly noncavitated over the entire engine operating envelope for mixture ratio control application. |
| Ball Valve | Constant percentage regulating trait inferior to that of the butterfly valve. Offers medium package size and low actuation power requirement. Seal erosion and wear could be a problem. |

CONFIDENTIAL

(This page is Unclassified)

CONFIDENTIAL

(2) Mechanical Description

(C) The mixture ratio valve housings and the integral disk-shaft are made of Inconel 718. The 4-inch diameter inlet and discharge were sized for a maximum oxidizer velocity of 60 ft/sec at 100% thrust and a mixture ratio of 6. The valve metering area was sized to produce a pressure drop of 570 psi at 100% thrust and a mixture ratio of 7. This condition fixed the disk diameter at 3.0 inches with a shaft diameter of 1.125 inches. The inlet converges at a 10-degree angle and the discharge diverges at a 30-degree angle. Dowel pins are used to maintain the alignment between the two valve housings. The housing flange seals are Teflon (AMS 2515) coated metal (AMS 7325) stainless steel O-rings with interseal vents.

(U) Continuing effort to improve the operational characteristics of the mixture ratio valve produced hardware design changes in three significant areas: (1) shutoff seal configuration, (2) dynamic shaft seals, and (3) actuator mount assembly. Figure 239 illustrates the initial design configuration. Figure 240 illustrates the final design configuration.

(U) The final shutoff seal configuration is shown in figure 241. This seal, made of laminated Kapton and FEP Teflon, replaced the original metallic piston ring seal.

(U) Dynamic lip-type shaft seals are used on the splined end of the shaft. These are formed lip seals of laminated Kapton F and FEP Teflon (1.750-in. OD x 0.875-in. ID (unformed) x 0.035-in. thick). Spring-loaded Teflon cup seals 1.125-in. nominal OD x 1.000-in. nominal ID x 0.090-in. cup depth are used on each side of the nitrogen purge cavity. The other end of the shaft does not incorporate dynamic seals. The high pressure on this end of the shaft is contained by the Inconel 718 cap.

(U) The valve actuation system consists of a rotary hydraulic servo-actuator utilizing commercial parts.

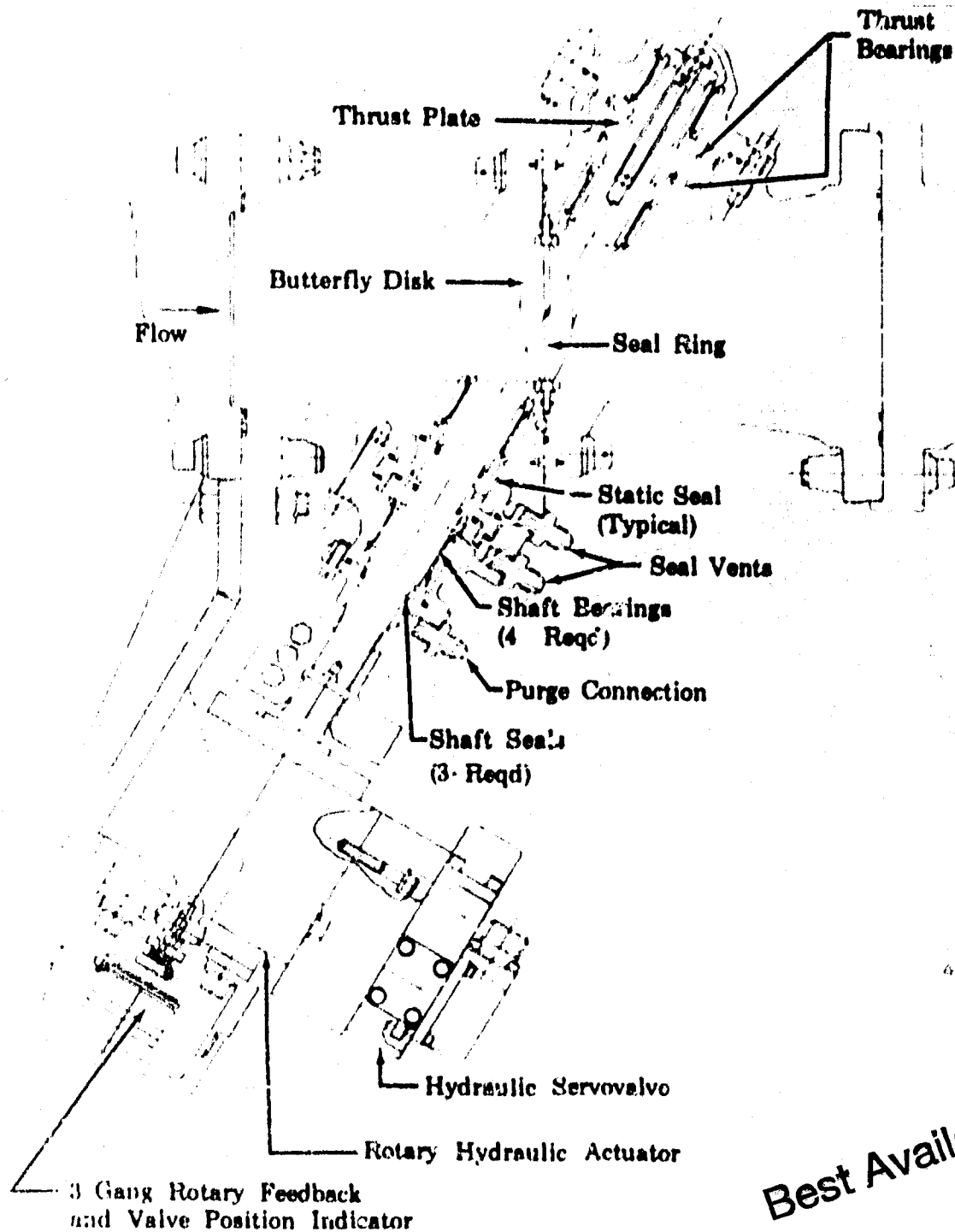
(U) Test stand flowmeter measurements of total flow are input to a control system computer, sending an electrical command to the actuator servovalve. The servovalve supplies hydraulic pressure to the actuator, which sets the mixture ratio valve flow area. The oxidizer flow is constantly measured by the oxidizer line flowmeter and compared with the programmed computer requirements. An error signal commands the servovalve and mixture ratio valve position and corrections are made until the actual flow equals the required flow.

(U) The original actuator mount assembly was redesigned because of excessive flexure during operation.

(U) The actuator torque required to turn the shaft as a function of thrust and mixture ratio is shown in figure 242. The major portion of the torque is developed from flow sources. The remaining torque is required to overcome the resistance of the dynamic seals, bearings, and the shutoff seal. The actuator torque was minimized by incorporating roller bearings on the shaft.

CONFIDENTIAL

UNCLASSIFIED



Best Available Copy

Figure 239. Mixture Ratio Valve Initial Design

FD 18114

UNCLASSIFIED

UNCLASSIFIED

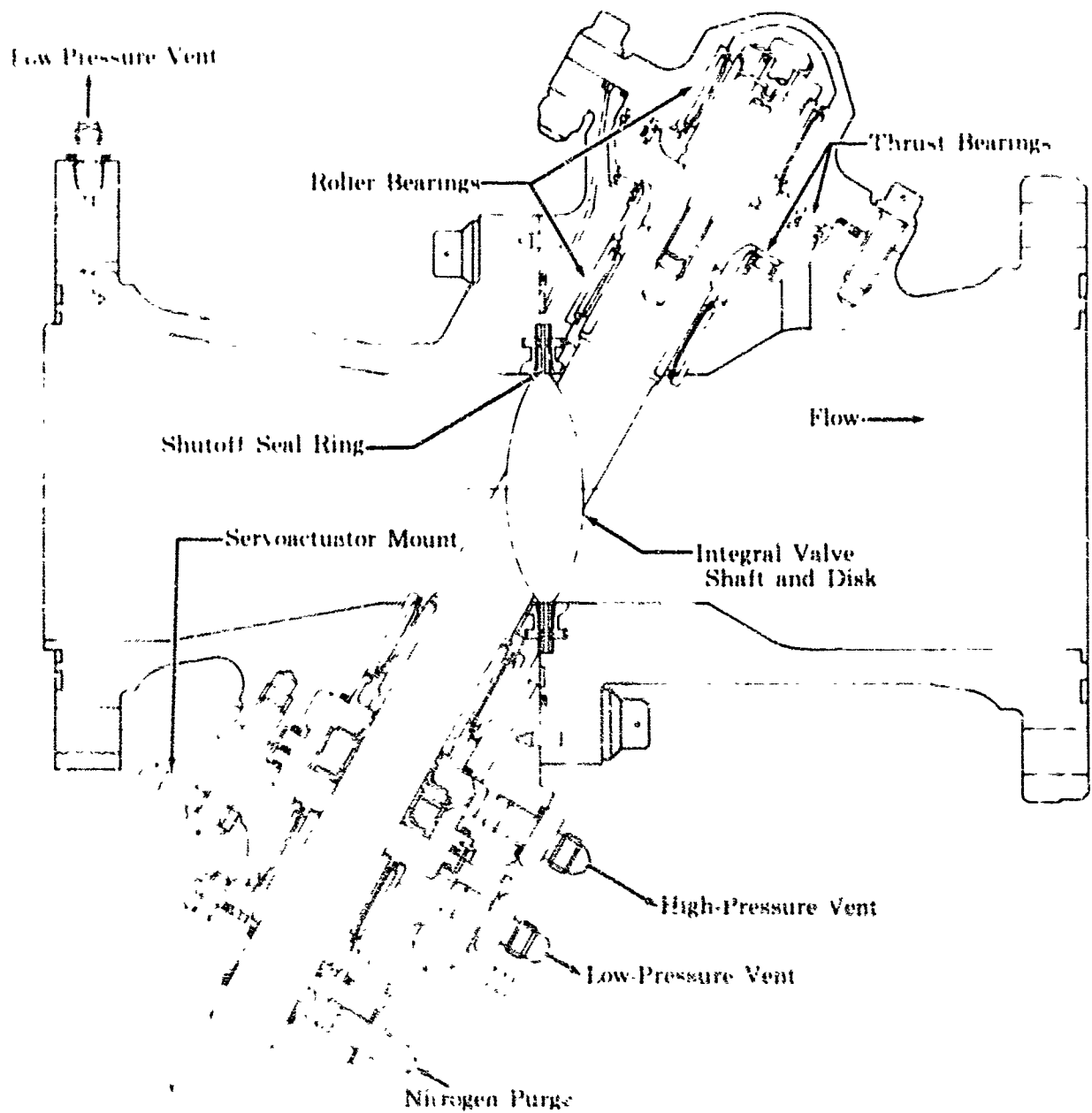


Figure 240. Mixture Ratio Valve Final Design

FD 18938A

UNCLASSIFIED

CONFIDENTIAL

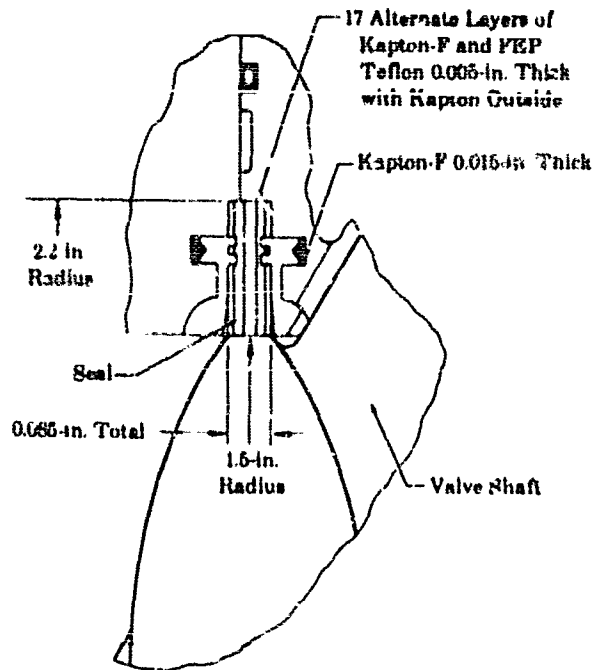


Figure 241. Mixture Ratio Valve Shutoff Seal FD 19002A

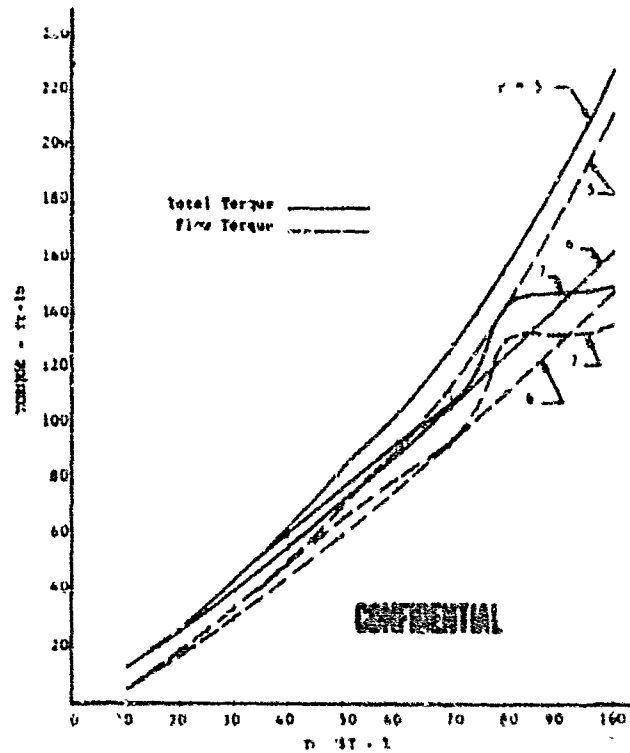


Figure 242. Mixture Ratio Valve Torque vs Percent Thrust DF 52376

CONFIDENTIAL

CONFIDENTIAL

(C) The four roller bearings were spaced to provide a maximum radial capacity while preventing excessive angular misalignment on the inner bearings. The load deflection diagram for the shaft at its maximum load condition (100% thrust, $r = 5$) is shown in table XXXii. Stress levels for other major parts of the valve are also presented along with the angular opening relationship of the shaft to the butterfly disk. The axial thrust on the shaft is taken by two roller thrust bearings. The maximum load shown on each bearing occurs at different operating conditions and is a result of the shifting of the shaft thrust load during the valve excursion. All of the bearing races and rollers are made of AMS 5630. The materials used in separators for the thrust and roller bearings are AMS 5613 and AMS 5640, respectively.

(J) Operating Characteristics

(C) The mixture ratio valve was designed to pass 120% of the design flow at 100% thrust and a mixture ratio of 7. Figure 204 shows the operating requirements for the valve.

(U) The valve effective area versus disk angle is shown in figure 235. Included in this curve is the pressure recovery downstream of the valve, as well as the valve discharge coefficient. Related to this curve is the disk angle versus percent thrust curve shown in figure 234. The area error per degree versus disk angle is shown in figure 236. This curve shows that the valve operating range occurs in the section of the curve where the area error is essentially constant and provides an accurate area schedule.

(U) A 1-inch diameter rotary shaft seal test rig was designed and parts were procured to test spring-loaded Teflon cup seals and lip-type seals; seal materials were varied throughout the test program. The rig was designed to test two types of seals simultaneously. Duplicate seal rig materials and dimensional details were selected to simulate corresponding mixture ratio valve parts. Figure 243 shows the rotary shaft seal test rig parts in exploded detail. The test rig assembly is shown in figure 244.

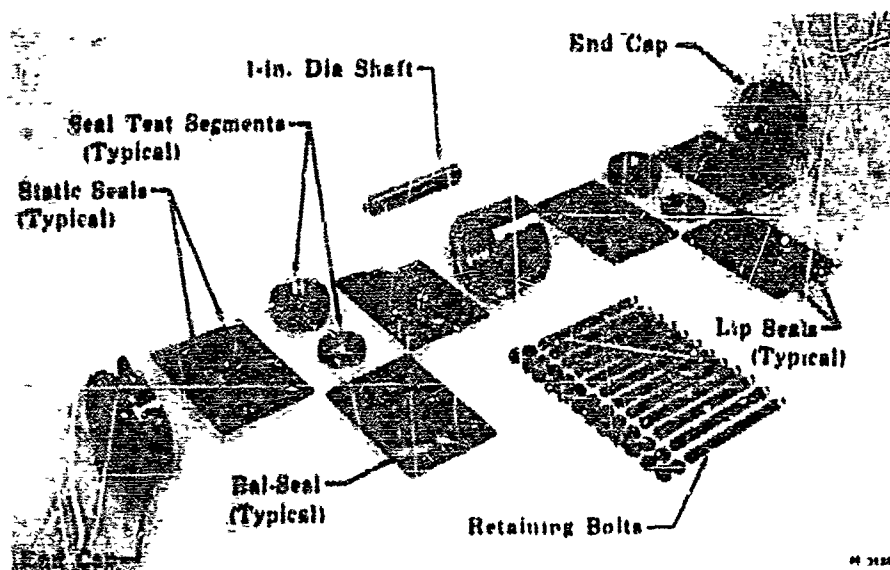


Figure 243. Rotary Shaft Seal Test Rig Parts

FD 23419

CONFIDENTIAL

(C) Table XXVII. Allowable Mixture Ratio Control Valve Loads and Stresses

| Load Condition | Torque, in.-lb | Angular Displacement, deg | | Stress, psi | | Load, lb |
|------------------------------------|-------------------|---------------------------------|-------|---------------------|--------------------------|-------------|
| | | Disk | Shaft | Room Temperature | Operating Temperature | |
| Shaft Operating Torque | | | | | | |
| 100% Thrust | 2360 | | | | | |
| 120% Thrust | 3060 | | | | | |
| Maximum Actuator Torque | 6840 | | | | | |
| Shaft Rotation Limits | | | | | | |
| Shutoff | | 0 | 0 | | | |
| Minimum Area (7% Flow) | | 23.8 | 29.0 | | | |
| Minimum Flow (10% and $r = 5$) | | 28.3 | 34.5 | | | |
| Maximum Flow (93% and $r = 7$) | | 57.5 | 70.0 | | | |
| Maximum Area (120% Flow) | | 60.0 | 73.0 | | | |
| Full Actuator Stroke | | 82.0 | 90.0 | | | |
| Full Open (Theoretical) | | 90.0 | 109.5 | | | |
| Shaft Stress ¹ | | | | | | |
| Bending | 2220 | | | 134,000 | | 168,000 |
| Shear | 2220 | | | 11,800 | | 95,000 |
| Combined | 2220 | | | 135,000 | | |
| Combined | 2920 | | | 136,000 | | |
| Spline Tooth Bearing Stress | | | | | | |
| 100% Thrust $r = 5$ | 2360 | | | 5,400 | | |
| 120% Thrust | 3060 | | | 7,000 | | |
| Maximum Actuator Torque | 6840 | | | 15,600 | | |
| Flange Bending Stress ² | | | | | | |
| Inlet Flange | | | | 76,000 | | |
| Outlet Flange | | | | 70,000 | | |
| Split Flange | | | | 45,000 | | |
| Bearing Cap Flange | | | | 98,000 | | |

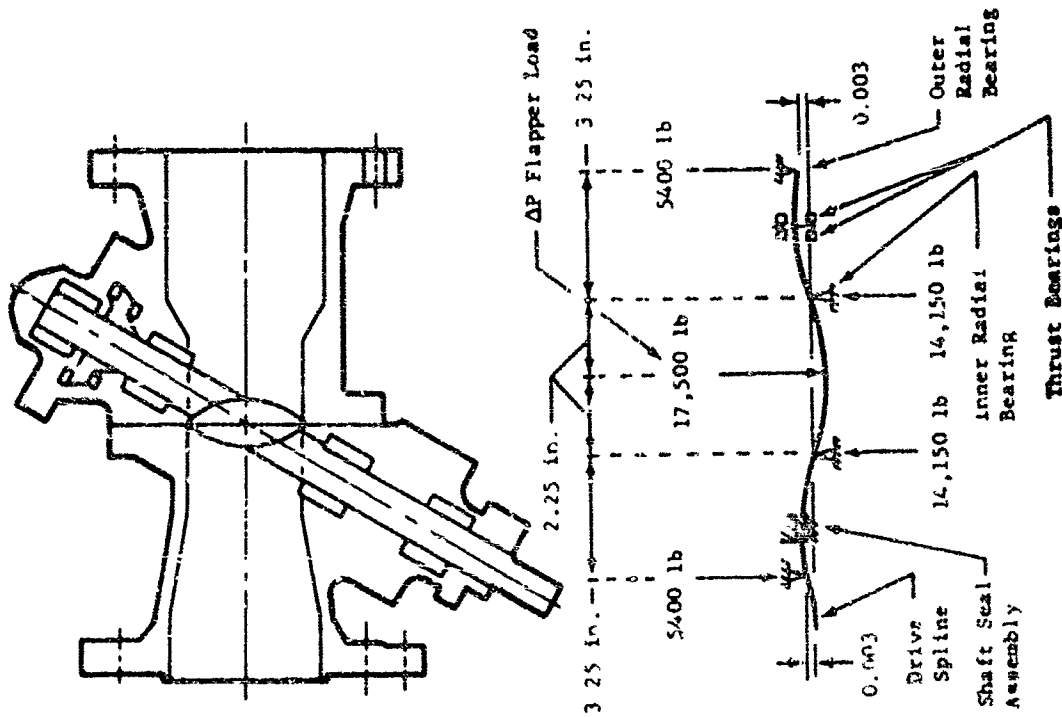
(C) Table XXXII. Allowable Mixture Ratio Control
Valve Loads and Stresses (Continued)

| Load Condition | Torque, in -lb | Angular Displacement, deg | Stress, psi Room Temperature | Operating Temperature | 0.2% Yield Strength | Load, lb |
|---|-------------------|---------------------------------|---------------------------------|--------------------------|---------------------------|-------------|
| Bolt Combined Tensile Stresses | | | | | | |
| Inlet Flange | | | 107,000 | 107,000 | | 14,150 |
| Outlet Flange | | | 90,000 | 95,000 | | 5,400 |
| Split Flange Long Bolt | | | 107,000 | 107,000 | | 1,650 |
| Split Flange Short Bolt | | | 90,000 | 101,000 | | 2,480 |
| Bearing Cap | | | 86,000 | 97,000 | | |
| Drive Cap | | | 77,500 | 90,300 | | |
| End Cap | | | 80,000 | 85,000 | | |
| Bearing Load | | | | | | |
| Radial, Inner | | | | | | |
| Radial, Outer | | | | | | |
| Thrust, Inner | | | | | | |
| Thrust, Outer | | | | | | |
| Maximum Internal Pressure Differential | | | | | | |
| Inlet | | | 7,600 | 9,000 | | |
| Discharge | | | 6,000 | 7,200 | | |
| Maximum Valve Pressure Drop | | | 2,400 | 2,700 | | |

CONFIDENTIAL

CONFIDENTIAL

(C) Table XXXII. Allowable Mixture Ratio Control Valve Loads and Stresses (Continued)



Shaft Load-Deflection Diagram

- 1 Operation at 100%, thrust $r = 5$ 2480 psi pressure drop, and -270°F.
- 2 Stresses are based on flange deflection, of 0.0003 in. at the location of the inner O-ring seals, under maximum operating pressures.
- 3 Stresses are based on maximum scheduled operating pressures, and include an inlet pipe installation moment of 72,000 in. lb, the maximum specified wrench torques and a 0.10 coefficient of friction.
- 4 Load is based on a 2480 psi pressure drop and a 0.003 in. shaft deflection. (See shaft load-deflection diagram.)
- 5 Load is based on a 2480 psi pressure drop.
- 6 Load is based on a 400 psi pressure drop and 410 psi inlet pressure.
- 7 With the specified inlet and discharge pressures, the valve housing bolts made of AMS 5731 material are stressed to the 0.2% yield point.
- 8 Pressure drop limits shown are based on a 200°F temperature shaft yield strength of 150,000 psi and an operating temperature yield strength of 168,000 psi.

CONFIDENTIAL

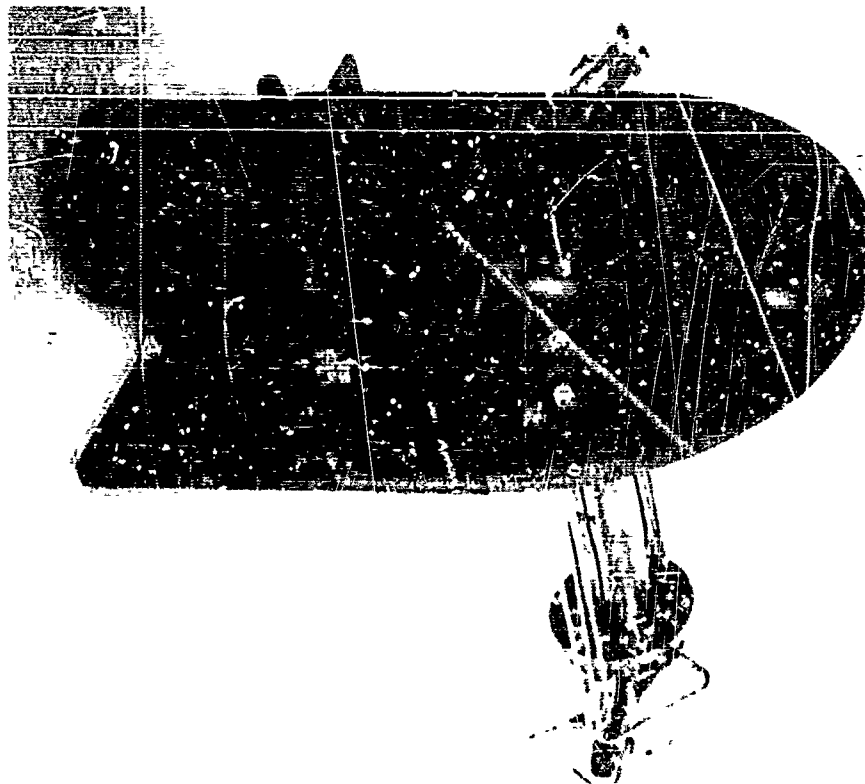


Figure 244. Rotary Shaft Seal Test Rig

FE 66018

2. Test Program and Test Results

(U) The first mixture ratio valve (F-33466) completed eight build, test, and inspection cycles. The second valve (F-35106) completed five similar cycles. Five water flow calibrations, three environmental endurance tests, and five environmental leakage tests were performed on the valves.

(C) An 11,292 cycle environmental endurance test proved the structural integrity of the valve. Water calibration and environmental leakage tests indicated that major changes in actuator support hardware, butterfly disk seal configuration, and shaft seal configuration were required for optimum performance.

a. Mixture Ratio Valve F-33466 (Refer to table XXIII for Test Summary)

(1) Build No. 1

(U) The initial build of rig F-33466, which is shown in figure 245, incorporated the following features:

1. Tufam-coated aluminum bushings and thrust bearings
2. Graphite-filled TFE Teflon Bal Seal shaft seals
3. Seal carrier inside diameters and tie bolt tabwasher silver plated to prevent galling
4. Inlet and outlet flange static pressure taps
5. The original design hydraulic servomotor and mount bracket.

CONFIDENTIAL

(C) Table XXXIII. Test Summary, Mixture Ratio Valve F-33466

| Build No. | Features | Configuration | Seal Description | Program | Test and Testdown Remarks |
|-----------|--|--|--|--|--|
| 4 | <ol style="list-style-type: none"> Tufcon coated aluminum bushings and thrust washers. Seal retaining segments ID silver pinned. Pressure taps in inlet and outlet bushings. Titan O-Rings substituted for Teflon coated metallic O-Rings. Protractor attached to valve shaft to indicate valve position. | <p>Primary Secondary Vent</p> <p>Disk</p> | <p>Graphite-filled Tufcon Bal-Seal.</p> <p>Copper Beryllium split piston ring</p> | <ol style="list-style-type: none"> Water calibration Flow torque calibration | <ol style="list-style-type: none"> Experienced excessive leakage at inlet flange and primary seal vent. Excessive actuator bracket deflection when shaft hit stops. Flow torque calculated from load cell data. Load cell was attached by a distance from shaft along torque arm. Piston ring was broken and two pieces were missing. |
| - | <ol style="list-style-type: none"> As k-to-back Bal-Seals in cap Lip-Seal, dynamic seal, package Revised actuator support. Internal actuator stops. Protractor removed. Valve position determined from potentiometer calibration and post-test resistance data. | <p>Primary, Secondary</p> <p>Vent - 1 Vent - 2</p> <p>Disk</p> | <p>Laminated 500F-131 Kaptan and PTF Teflon (Teflon sealing surface)</p> <p>Graphite-filled Teflon Bal-Seal</p> <p>Laminated 500F-131 Kaptan and PTF Teflon ring X sealing surface.</p> | <ol style="list-style-type: none"> Environmental endurance test | <ol style="list-style-type: none"> Rig pulled because of excessive leakage at primary seal vent. Inlet pressure varied from 50 to 2500 psig CH_4 for dynamic leakage measurements. Inlet pressure varied from 40 to 60 psig CH_4 for disk seal leakage measurement. Moderate to severe rolling on rig shaft and Tufcon bearing assemblies. Primary and secondary seals were improperly installed utilizing Kaptan as sealing surface. |
| 3 | <ol style="list-style-type: none"> Roller Bearings Seal groove in shaft was filled with nichrome / metal spray for utilization of ID sealing disk seal | <p>Primary</p> <p>Secondary Vent - 1 Vent - 2 Disk</p> | <p>Laminated 500F-131 Kaptan and PTF Teflon Lip-Seal (Kaptan sealing surface).</p> <p>Same as Build 2</p> <p>Seal Bal-Seals from Build 2</p> <p>Laminated 500F-131 Kaptan and PTF Teflon 0.195-in. thick</p> | <ol style="list-style-type: none"> Water Calibration | <ol style="list-style-type: none"> Nichrome V filler in shaft cracked and was chipped in several places. |

CONFIDENTIAL

(C) Table XXIII. Test Summary, Mixture Ratio Valve F-33/66 (Continued)

| Build No. | Features | Configuration | Seal Description | Program | Test and Remarks |
|-----------|--|--|---|--|---|
| 4 | 1. OD of disk on shaft nickel plated. 2. Viton O-Rings were substituted for Teflon-coated metallic O-Rings. | Primary Secondary Vent - 1 Vent - 2 Disk | Used seals from Build 3 | 1. Water circulation test. | 1. Section of nickel plate on shaft disk missing after test. |
| 5 | 1. Disk seal rings housing 0.415-in. thick laminated Teflon-Kapton disk seal. 2. OD of disk on shaft was machined and filled with Nichrome 3 metal spray. 3. Inconel rings with Krypton on each side were substituted for O-Rings. 4. All secondary O-Rings vented on ID. | Primary Secondary Vent - 1 Vent - 2 Disk | Laminated 500F-131 Kapton and PEP Teflon 0.175-in. thick (Kapton sealing surface) Graphite-filled Teflon PEP Seal Teflon Seal Laminated 500F-131 Kapton and PEP Teflon 0.045-in. thick | 1. Environmental endurance test. | 1. Total of 11,892 shaft cycles completed at inlet pressures up to 4200 psi. 2. No excessive and immediate test test completed. 3. Frequency response complete and satisfactory. 4. Excessive primary seal leakage. 5. Lower thrust bearing failing. 6. Secondary O-Ring between Inconel rings had been omitted during assembly. 7. Sealing surface on disk was satisfactory. |
| 6 | 1. Loose leaf disk seal Kapton "T". 2. Inconel rings substituted for O-Rings. Rings compressed Krypton as seal master oil. 3. All secondary O-Rings vented on ID. | Primary Secondary Vent - 1 Vent - 2 Disk | Same as Build 5 Laminated 500F-131 Kapton and 500R Kapton looseleaf 0.08-in. thick | 1. Environmental test prior to staged combustion installation. | 1. Excessive primary seal leakage. 2. Test included 1500 shaft cycles at inlet pressures to 6000 psi. 3. Portion of metal spray on shaft disk was broken during test. 4. Lower thrust bearing failed - 2 grn. |
| 7 | 1. OD of disk on rip shaft was nickel plated with silver-chromium (Rellarc welded). 2. Inconel ring substituted for primary O-Ring. 3. Thrust plate ID silver plated. 4. Teflon coated thrust washer used as lower thrust bearing. Upper and lower washers silver plated. 5. All secondary O-Rings vented on ID. | Primary Secondary Vent - 1 Vent - 2 Disk | Same as Build 5 Laminated PEP Teflon with 1 piece of 500F-131 Kapton. 0.045-in. thick. | 1. Same as Build 6 | 1. Excessive primary and disk seal leakage. 2. ID of disk seal was extruded and flayed. |

CONFIDENTIAL

(C) Table XXVII, Test Summary, Mixture Ratio Valve 1-33466 (Continued)

[illegible]

CONFIDENTIAL

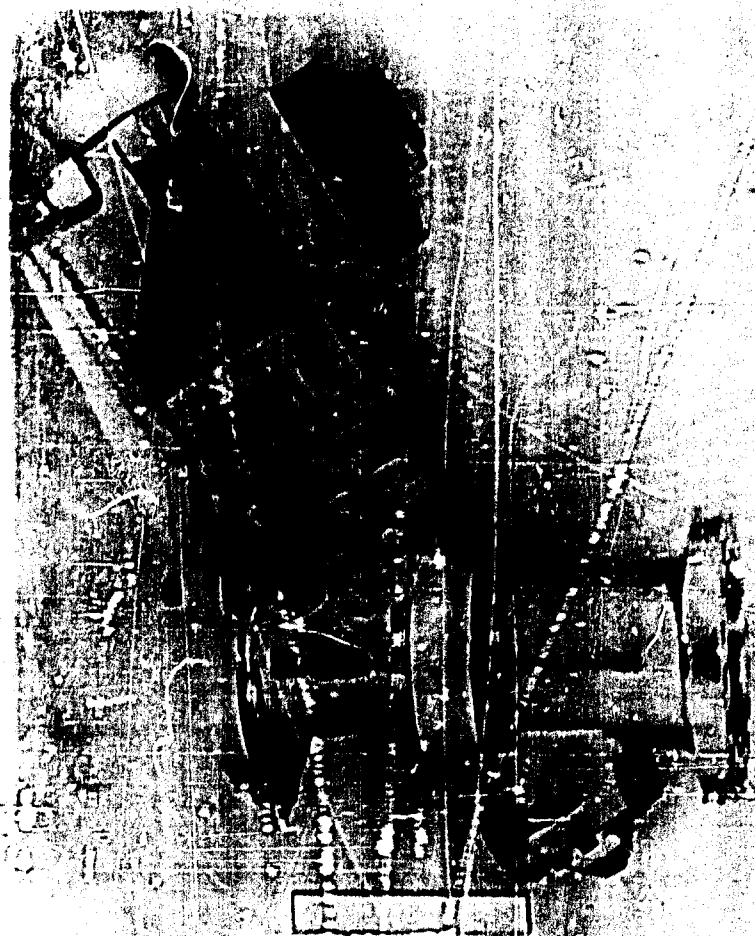


Figure 245. Mixture Ratio Valve Assembly
F-33466-1

FE 67914

(C). Prior to assembly, the outer housings were assembled and hydrostatically proof-pressure tested at 6900 psig internal pressure for 15 minutes.

(D). The valve was mounted in the B-21 water flow test stand, as shown in Figure 246, and was instrumented.

(E). The water flow calibration was performed on B-21 by positioning the valve shaft and setting specified valve differential pressures. During flow calibration, the following were noted:

1. Excessive actuator mount bracket deflection at high torque levels, and when the shaft was rotated to the full travel stops.
2. The inlet flange primary static seal and valve internal primary seats leaked excessively.

Figure 247 shows the water flow calibration results.

CONFIDENTIAL

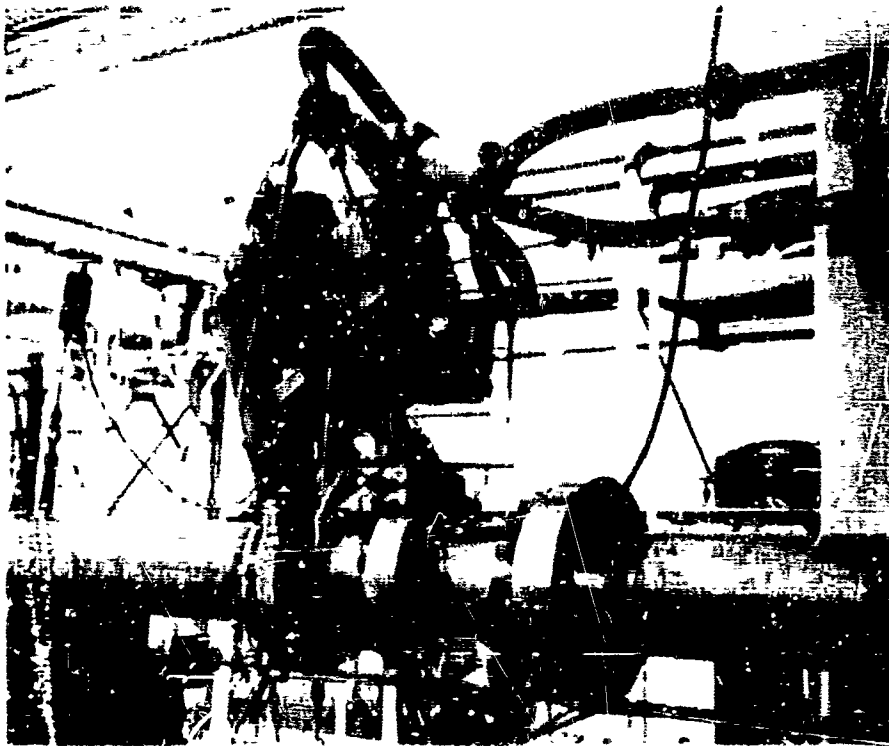


Figure 249. Mixers Ratio Valve Assembly
Mounted in 1" Filter Flow
Test Stand

FI 68510

Figure 250. Mixers Ratio Valve Assembly
Mounted in 1" Filter Flow
Test Stand

FI 68511

CONFIDENTIAL

(This page is Unclassified)

CONFIDENTIAL

(U) For the flow torque tests, the valve actuator was removed and a torque arm was attached to the shaft coupling. A load cell was used to measure applied torque at various shaft positions and differential pressure settings. Internal shaft and seal friction caused considerable data scatter. Externally applied mechanical vibration improved the data, but did not eliminate the problem. The torque data are shown in figure 248.

(U) After the flow torque tests, the valve was vacuum baked at 150°F for 2 hours to determine if the vacuum bake would completely dehydrate the internal valve and seal vent passages.

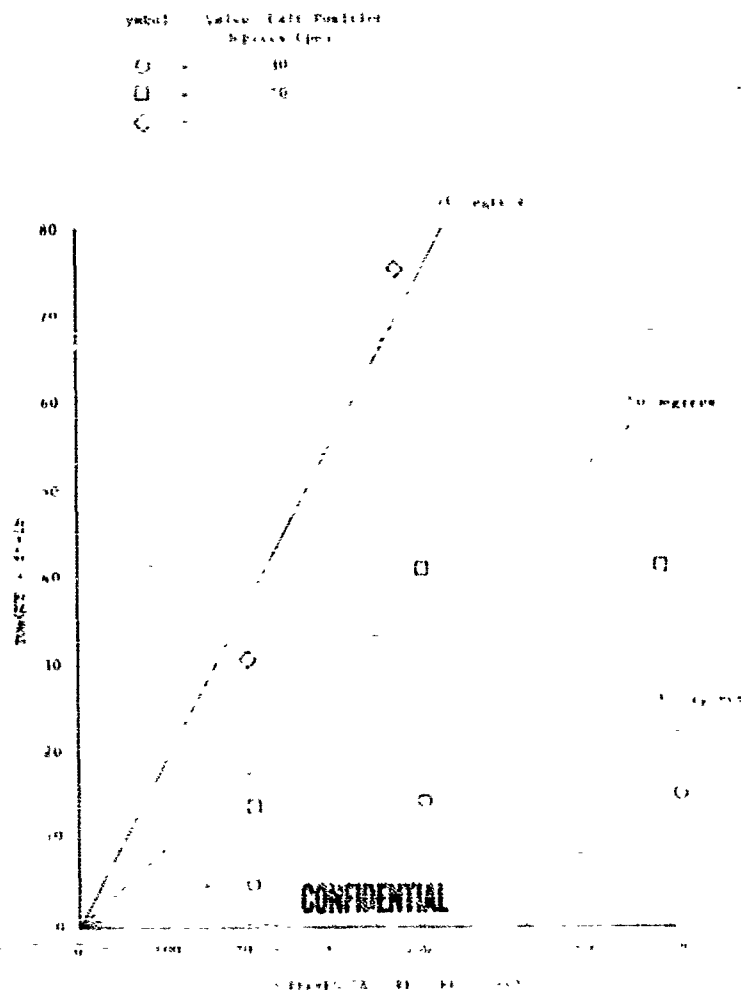


Figure 248. Mixture Ratio Valve Torque vs Differential Pressure, Rig F-31466-1

DF 58765

CONFIDENTIAL

CONFIDENTIAL

(U) No moisture was found in the valve assembly during disassembly. Two parts of the beryllium-copper piston ring were missing and some iron oxide deposits were found in the valve bearing areas. Other parts were generally in excellent condition with no other evidence of damage. No reason for the inlet flange and valve internal primary seal leakage was found and all seals and glands were in good condition.

(U) A metallurgical analysis of the remaining piston ring pieces indicated tensile failure. One part was sheared during valve closure, as shown in figures 249, 250 and 251.

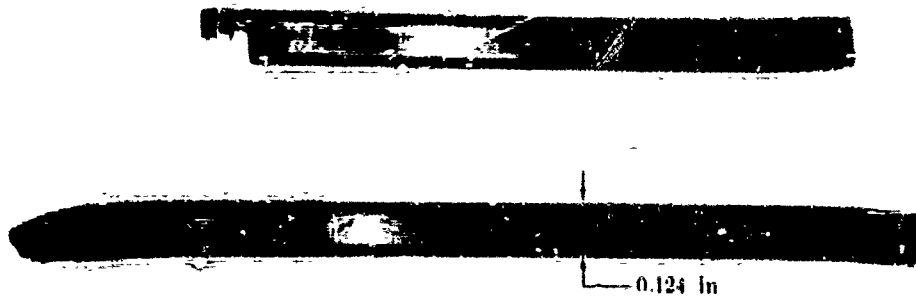


Figure 249. Disk Seal Piston Ring After
Test on Rig F-33466-1

FD 23-36



Figure 250. Tensile Failed Areas of Disk Seal
Piston Ring After Test on
Rig F-33466-1

FD 23-36

CONFIDENTIAL

(This page is Unclassified)

CONFIDENTIAL

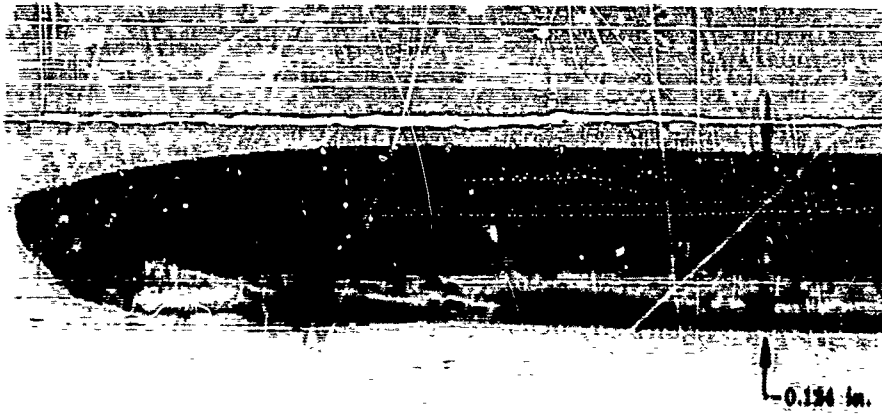


Figure 251. Sheared Area of Disk Seal Piston
Ring After Test on Rig F-33466-1

FD 23434

(2) Build No. 2

(U) The second build of mixture ratio valve F-33466 incorporated the same parts as build No. 1 except for the following:

1. The vent seal cap was reoperated for incorporation of an additional shaft Bal-Seal (reversed) to prevent moisture intrusion.
2. Laminated 500-F-131 Kapton (Kapton F) - Hf Teflon primary and secondary lip seals
3. A laminated Kapton-F-FEP Teflon disk seal
4. A revised actuator support.

(U) The revised actuator support fully enclosed the coupling, as shown in figure 252. Internal stops were incorporated.

(U) The torque required to rotate the shaft at ambient temperature was 20 to 25 in-lb.

(C) The mixture ratio valve was mounted in the B-22 stand for a planned 10,000 actuation cycle cryogenic endurance test. A total of 3375 shaft actuation cycles, including 500 shutoff cycles, was accumulated during the endurance test. The initial 2375 cycles were performed at 500 psig inlet pressure. An inlet pressure of 2500 psig was maintained from 2500 to 3000 cycles. All shutoff cycles were run at 50 psig inlet pressure.

CONFIDENTIAL

CONFIDENTIAL

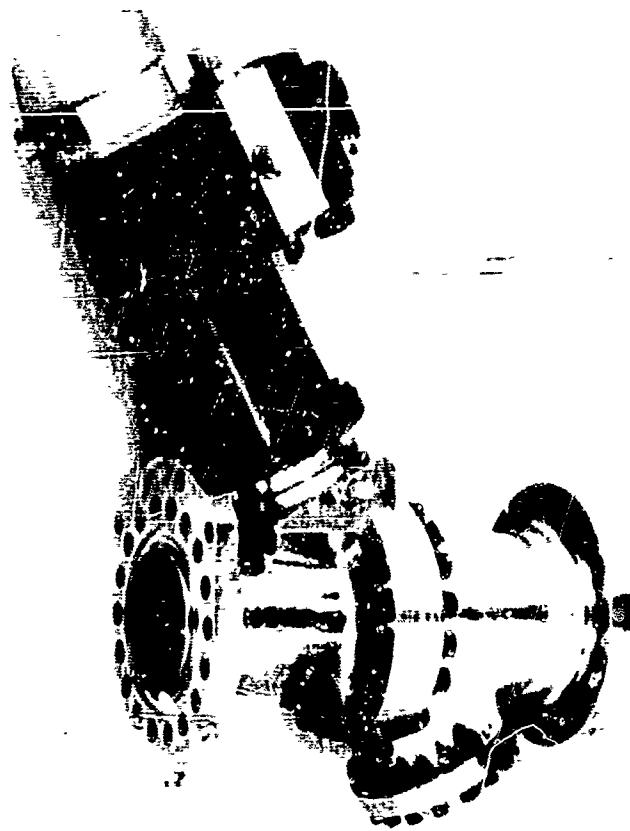


Figure 2-2. Revised Actuator Mount

11 69878

(f) During the test, both the inlet and outlet flange primary static O-ring leakages exceeded the flowmeter range (>7.0 scs). Disk seal and primary seal leakage are shown in figure 2-3. Disk seal leakage varied inversely with rig temperature (162 to 260°R) during the final 37 shut-off cycles. The maximum secondary seal leakage was less than 1.0 scs throughout the run. The hydraulic pressure required to move the actuator varied from 100 to 220 psid.

(g) Valve disassembly after the test revealed evidence of severe galling between the butterfly shaft, butterfly sleeves, and fully coated shaft bushings. (See figures 2-4, 2-5, and 2-6.) Severe galling between the fully coated thrust bearings, thrust washer, spacer, and butterfly sleeves also observed. The laminated Teflon and RFP Teflon shaft seals and disk seal were in excellent condition.

(h) Leakage inspection did not reveal the reason for excessive inlet and outlet static O-ring and internal primary and secondary seal leakage.

CONFIDENTIAL

(This page is Unclassified)

CONFIDENTIAL

MIXTURE RATIO VALVE LEAKAGE VS ACTUATION CYCLES - RIG F-33466-2

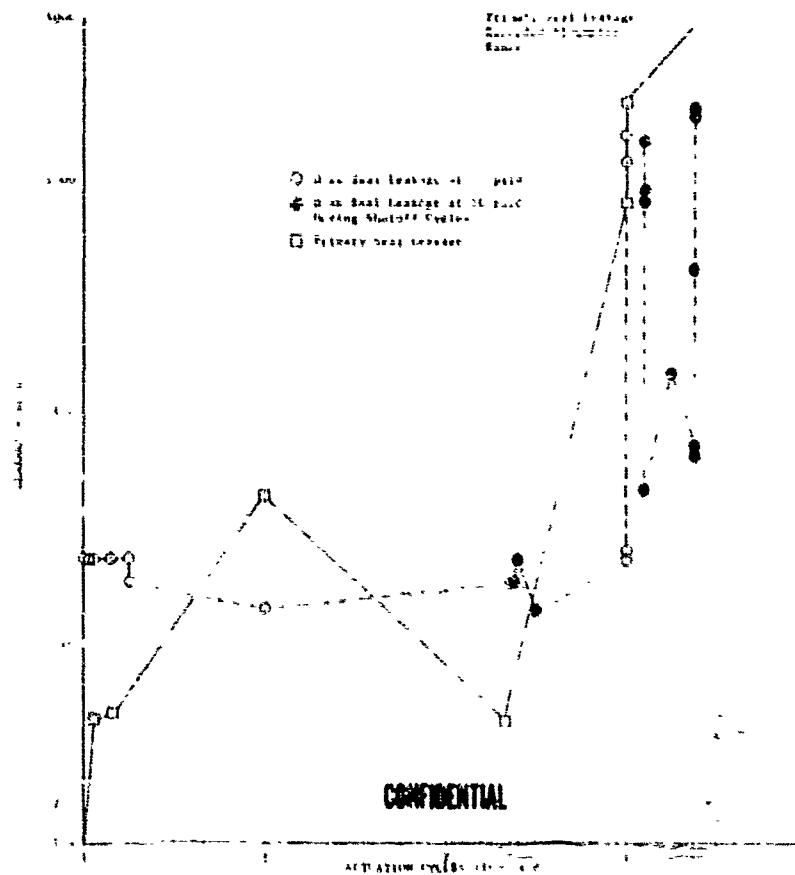
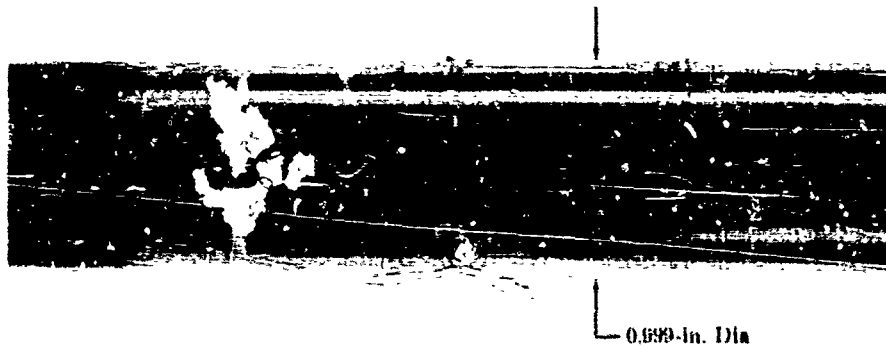


Figure 253. Mixture Ratio Valve Leakage vs Actuation Cycles, Rig F-33466-2

DE 58880



DE 58880

Figure 254. Butterfly Shaft After Test, Rig F-33466-2

DE 58880

CONFIDENTIAL

UNCLASSIFIED

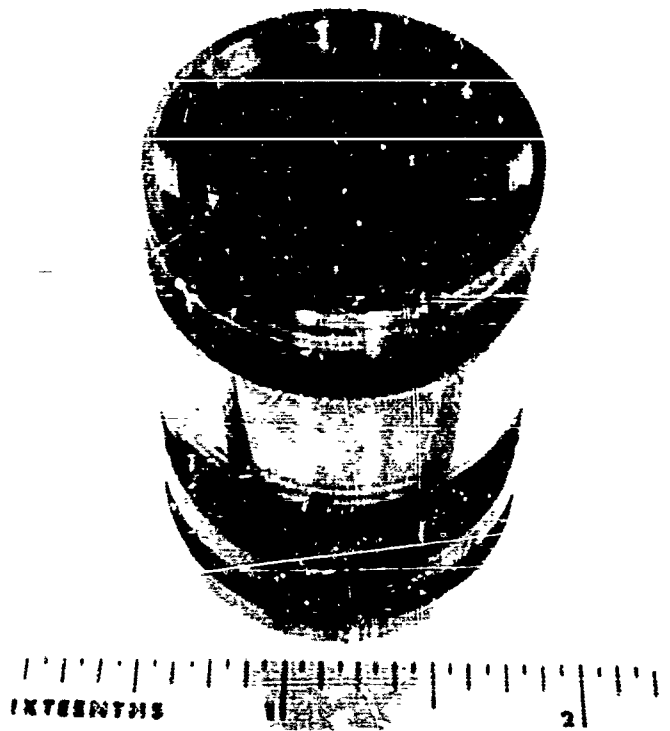


Figure 255. Bearing Sleeve After Test of
Rig F-33466-2

FE 69035

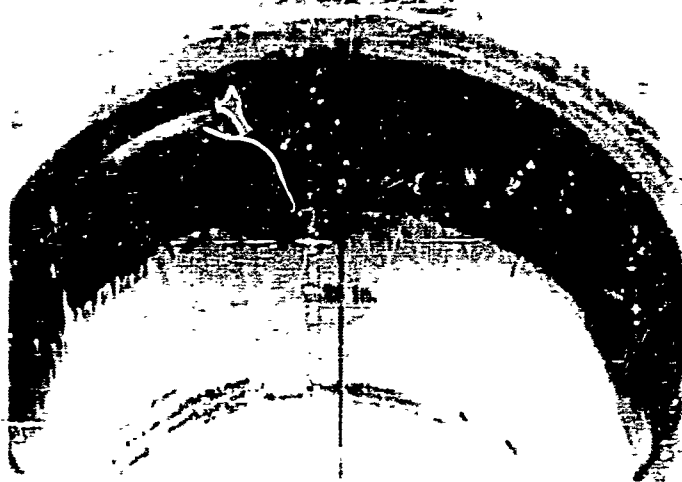


Figure 256. Outward Faces Coated by Slush
After Test of Rig F-33466-2

FE 69035

UNCLASSIFIED

UNCLASSIFIED

(3) as 11 50. 3

(4) The third build of mixture ratio valve F-33466 was the same as build no. 2 except for the following features:

1. Roller shaft bearings and thrust bearings
2. shaft seal groove filled with Nichrome V metal spray
3. Viton O-rings substituted for all Teflon covered metal O-rings except for the two primary O-rings.

(5) The torque required to rotate the valve at ambient temperature was 100 to 110 in-lb. The torque required to rotate the shaft into a position of the disk seal was 130 in-lb.

(6) The water flow calibration was performed on the B-21 test stand and the results are shown in Figure 257.

(7) Disassembly and inspection revealed the following:

1. Iron oxide deposits were observed on the bearings
2. The metal spray on the shaft disk and several small cracks across the groove and the edges were slightly chipped. (See Figures 258, 259, and 260.)
3. The inside diameter of the disk seal was slightly traced as shown in Figure 261.
4. The primary lip seal had a slight radial crack in the Teflon at the lip edge.

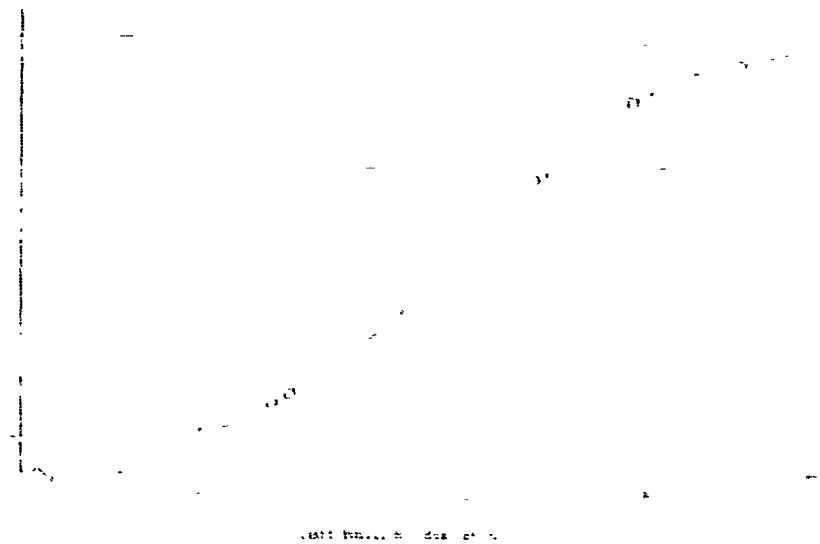


Figure 257. Mixture Ratio Valve Effective Area vs. Shaft Position, Rig F-33466-3

at 58864

UNCLASSIFIED

UNCLASSIFIED

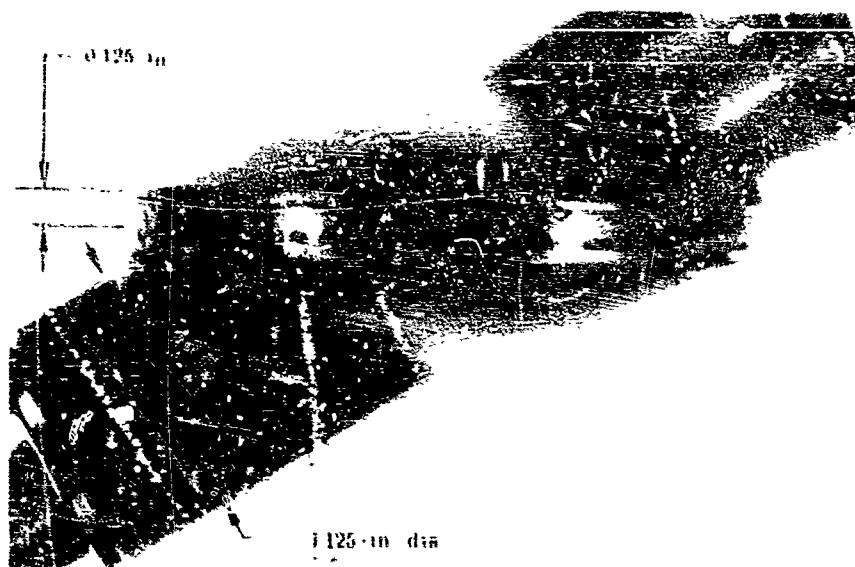


Figure 10. Shaft End After Test of Top 1-Station

1.125 in dia

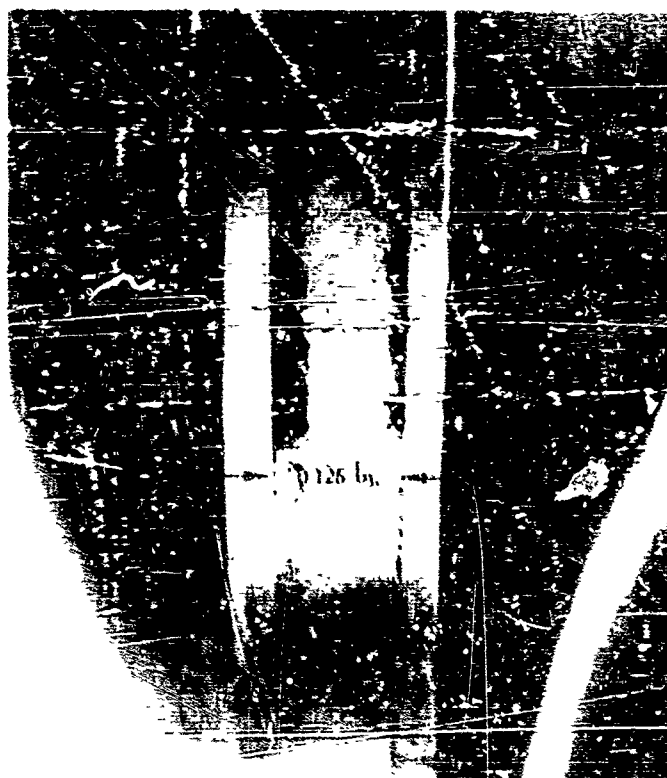


Figure 11. Shaft End After Test of Top 1-Station

UNCLASSIFIED

UNCLASSIFIED

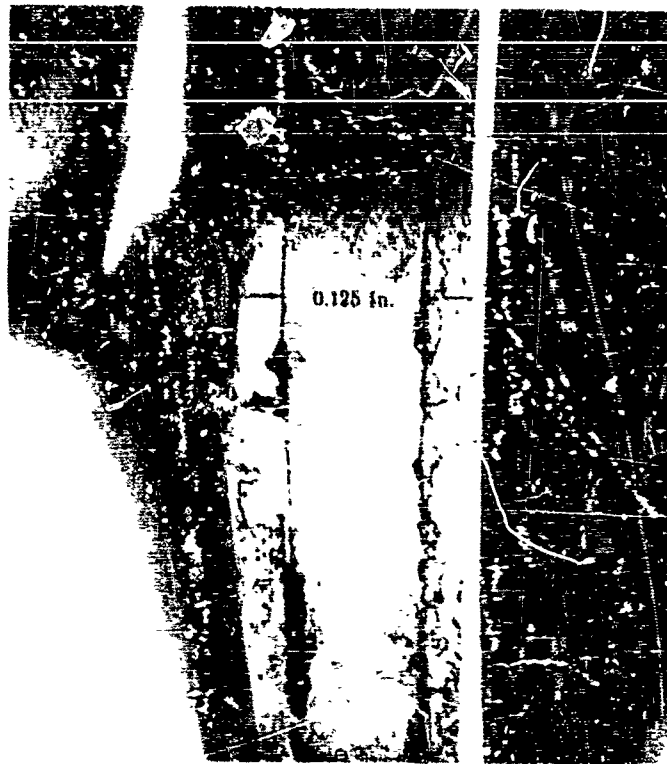


Figure 260. Shaft Pipe After Test of
Rik 1-33460-1 Showing chips
in "Metal" spray

FD 23442

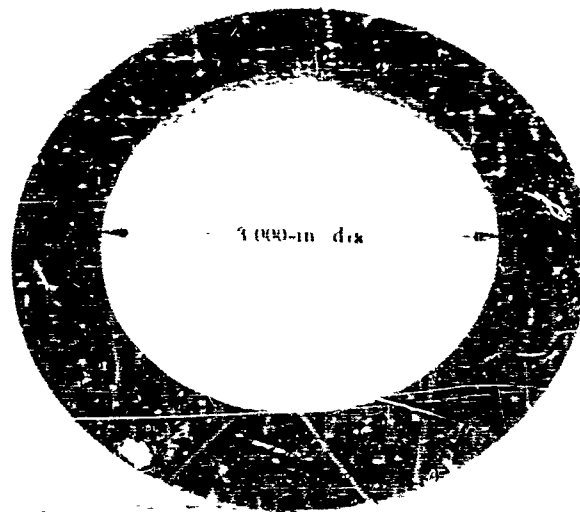


Figure 261. Disk 101 After Test of
Rik 1-33460-1

FD 23442

2/5

UNCLASSIFIED

CONFIDENTIAL

(4) Build No. 4

(U) The fourth build of mixture ratio valve F-33466 incorporated the following changes to the third build configuration:

1. The shaft disk outside diameter was machined and nickel plated
2. A laminated Kapton-F and FEP Teflon disk seal (0.175-inch thick) was used.

(U) The torque required to rotate the valve at ambient temperature was as follows:

| | |
|---|--------------|
| Rotation out of disk seal | 350 in-lb |
| Clockwise and counterclockwise rotation | 65-110 in-lb |
| Rotation into disk seal | 700 in-lb. |

(U) The water flow calibration was performed on the B-21 test stand and the results are shown in figure 262.

(U) Valve disassembly after the test revealed that the inside diameter of the disk seal was frayed and a large portion of the nickel plate on the shaft disk was missing. All other parts appeared in good condition.

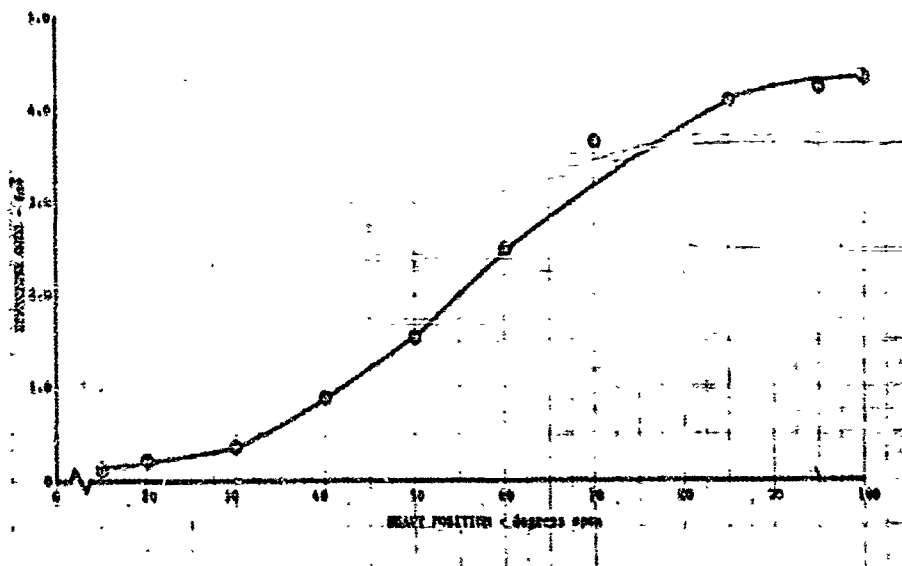


Figure 262. Mixture Ratio Valve Effective Area vs Shaft Position.
Rig F-33466-4

DF 58879

CONFIDENTIAL

(This page is Unclassified)

CONFIDENTIAL

(5) Build No. 5

(U) The fifth build of mixture ratio valve F-33466 was the same as build No. 4 except for the following:

1. The inside diameter of the laminated Kapton-F and FEP Teflon primary and secondary lip seals was increased.
2. The shaft disk seal groove was machined and filled with Nichrome V metal spray.
3. A laminated Kapton-F and FEP Teflon disk seal (0.085-inch thick) was used.
4. Disk seal rings that trapped two layers of Kapton-F in the primary static seal grooves were used.
5. Seal rings with two layers of laminated Kapton-F on each side were substituted for the primary O-rings.
6. All secondary O-rings were vented on the inside diameter.
7. Four layers of Kapton-F replaced the primary O-ring at the inlet flange. The mating pressure plate compressed the Kapton approximately 50%.

(U) The torque required to rotate the valve at ambient temperature was 35 to 50 in-lb. The ambient temperature disk seal leakage at 50 psid GN₂ was 16.7 sccs. No other seal leakage was detected.

(C) The mixture ratio valve was mounted in the B-22 test stand for a cryogenic endurance test. A total of 11,892 cycles was completed at internal pressures up to 4200 psig. This included 500 partial-stroke shutoff cycles, 9500 partial-stroke control cycles, 892 partial-stroke response test cycles, and 1000 full-stroke shutoff cycles.

(U) Disk seal leakage at 50 psid and primary seal leakage are illustrated in figure 263. During the test, the maximum leakages from the inlet static seal and outlet O-ring seal were 2640 sccs and 154 sccs GN₂, respectively. The maximum secondary seal leakage of 363 sccs occurred with the primary seal vent capped; however, additional leakage was evident from the valve housing center flange. Vent seal leakage remained less than 1.4 sccs throughout the test. The hydraulic pressure required to turn the valve shaft varied from 100 to 180 psid.

(U) Hysteresis, linearity, and frequency response tests were conducted with the valve controlled by an open loop circuit as illustrated in figure 264. Hysteresis and linearity tests were conducted with valve movement in incremental steps of approximately 20% of the total valve travel (0 to 20%, 20% to 40%, etc.). The results of these tests are presented in figures 265 and 266. A linearity test was conducted with valve movement in increasing step increments (0 to 20%, 0 to 40%, etc.) and the results are presented in figure 267. Valve frequency response and phase lag to a sine wave input with increasing frequency are shown in figures 268 and 269.

300

CONFIDENTIAL

REPORT

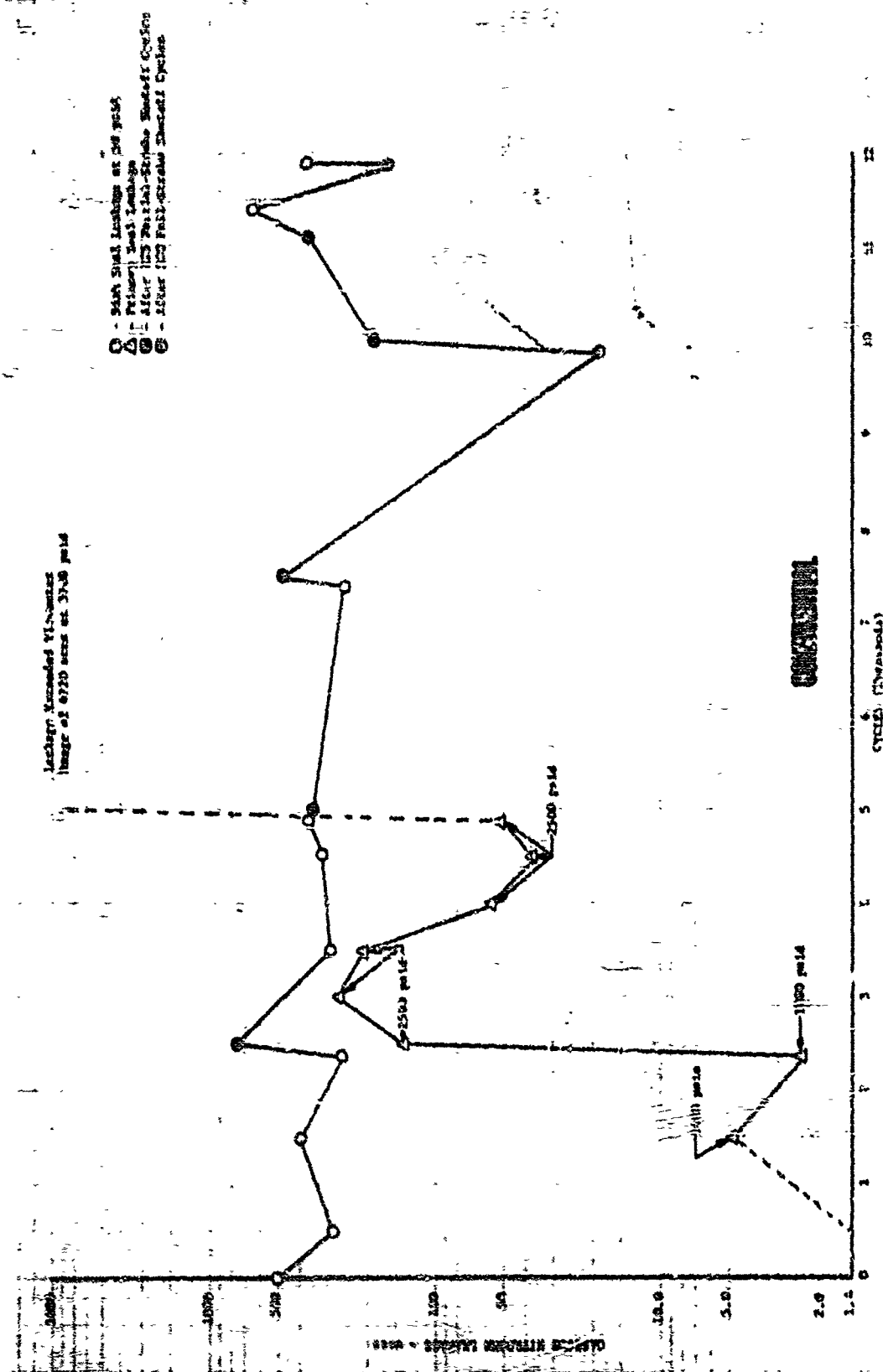


Figure 263. Leakage vs Cycles, Mixture Ratio Valve Rig F-33466-5

DF 58769

CONFIDENTIAL

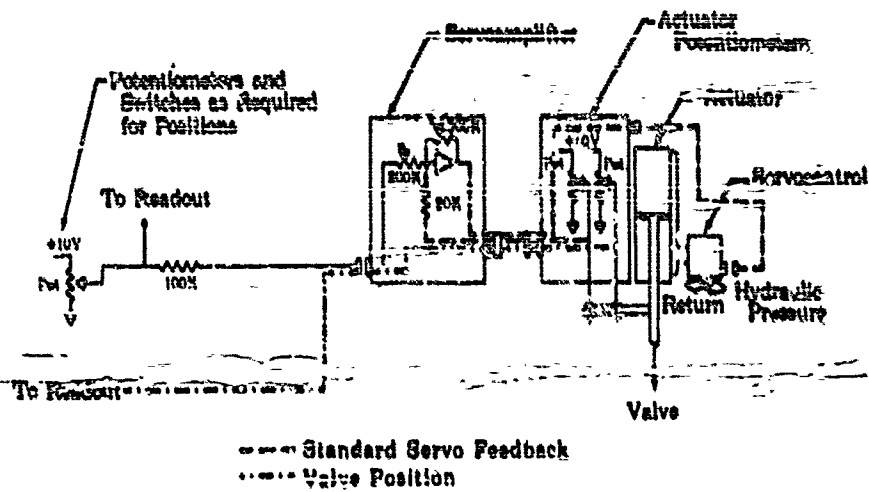


Figure 264. Control System Schematic, Mixture Ratio Valve Rig F-33466-5

FD 22797

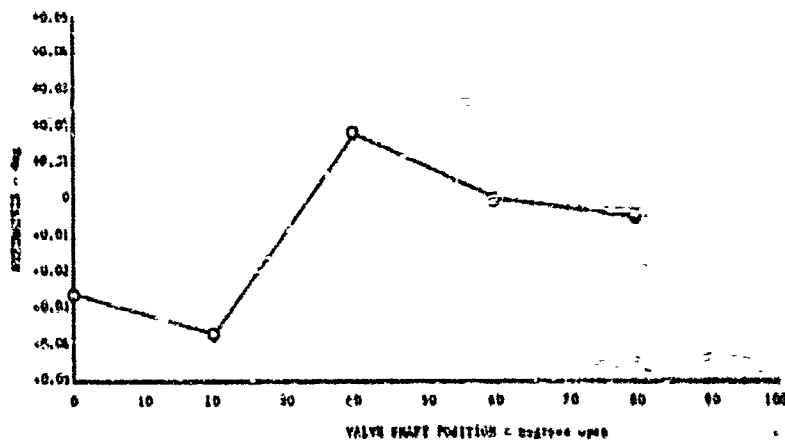


Figure 265. Hysteresis vs Shaft Position (Fixed Step Increments)

DF 58772

302
CONFIDENTIAL
(This page is Unclassified)

UNCLASSIFIED

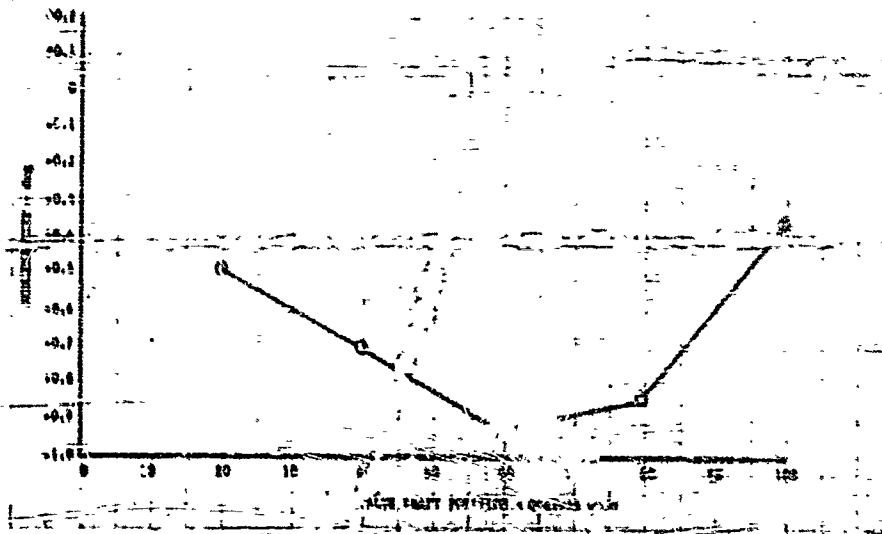


Figure 266. Nonlinearity vs Valve Shaft Position (Fixed Step Increments)

DF 58773

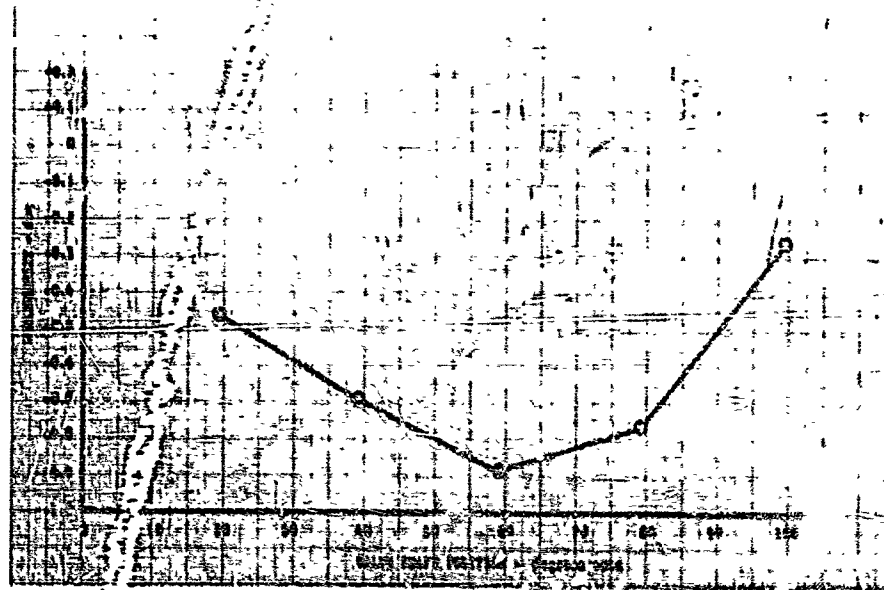


Figure 267. Nonlinearity vs Shaft Position (Increasing Step Increments)

DF 58774

UNCLASSIFIED

UNCLASSIFIED

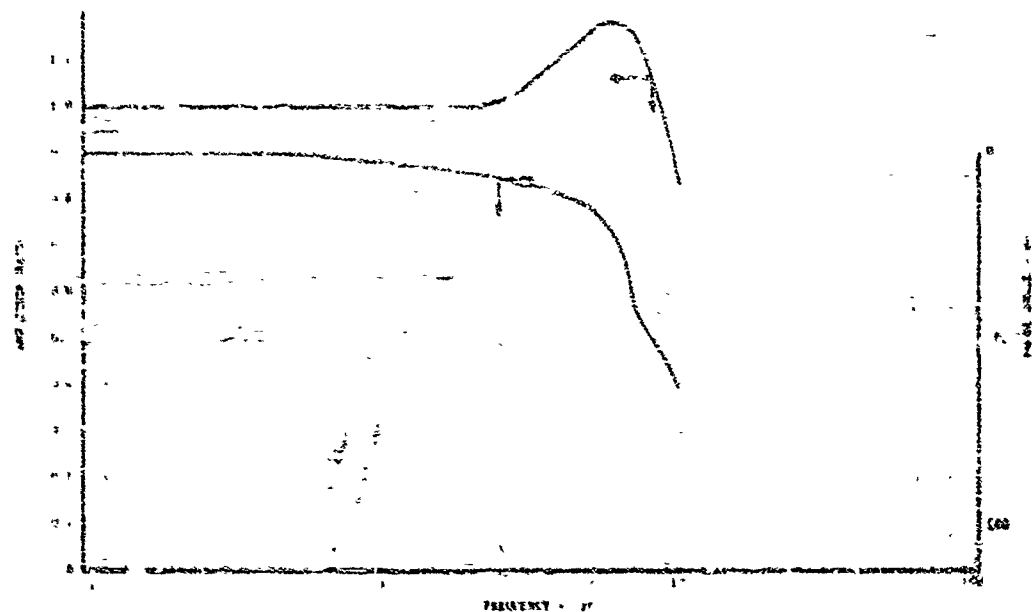


Figure 268. Amplitude Ratio vs Frequency
(Inlet Pressure = 0 psig)

DF 58770

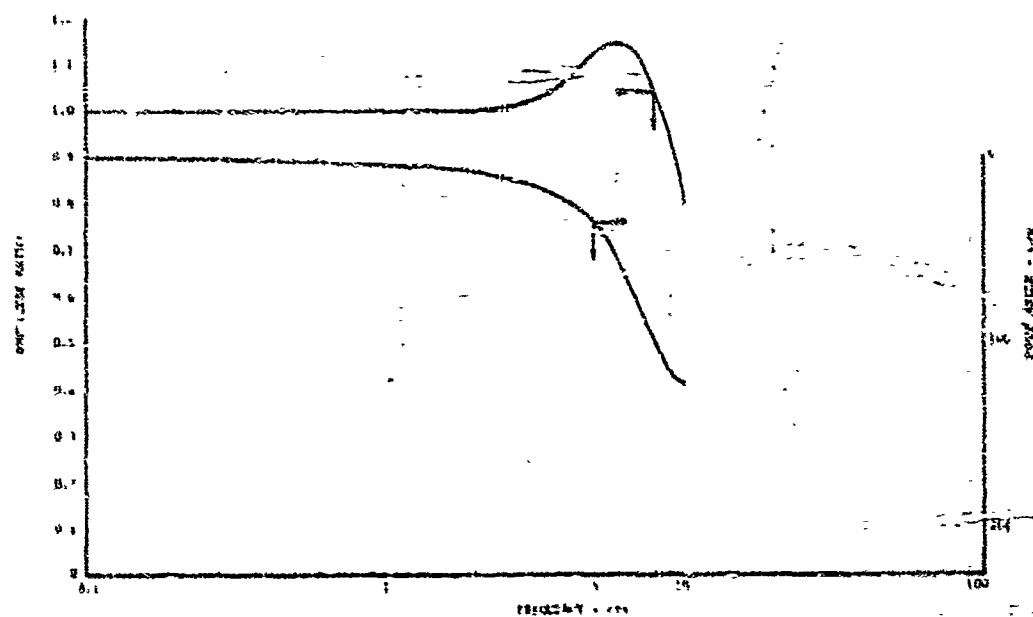


Figure 269. Amplitude Ratio vs Frequency
(Inlet Pressure = 3000 psig)

DF 58771

UNCLASSIFIED

UNCLASSIFIED

(C) Valve disassembly after the test revealed that all parts were in good condition and capable of continued testing. The lower thrust bearing, figure 270, had galled with the thrust washers and spacer. The shaft and shaft disk were in good condition as shown in figure 271. However, the inside diameter of the disk seal was slightly frayed as shown in figure 272. The primary lip seal was in excellent condition as shown in figure 273.

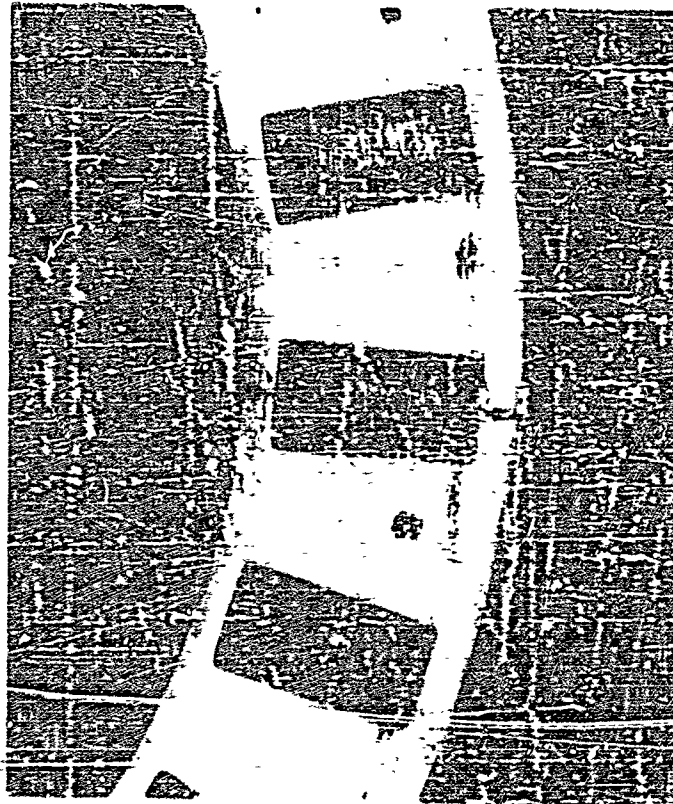


Figure 270. Lower Thrust Bearing After Test
of Rig F-33466-5

SD 23443

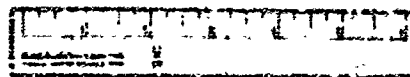
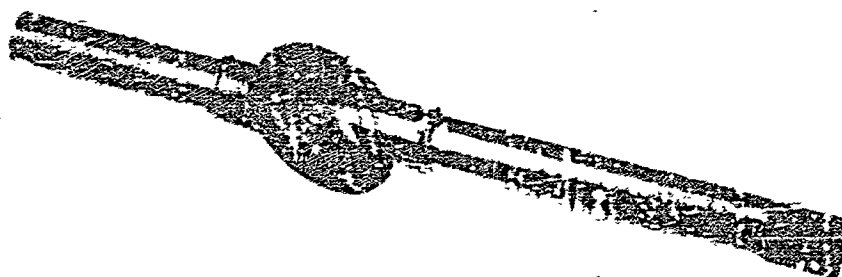


Figure 271. Shaft and Shaft Disk After Test of
Rig F-33466-5

FE 71429

305

UNCLASSIFIED

UNCLASSIFIED

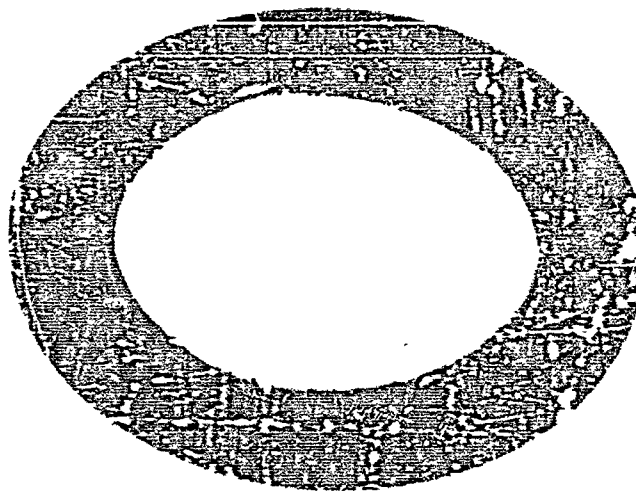


Figure 274. Disk Seal After Test of
Rig F-33466-5

FE 71436

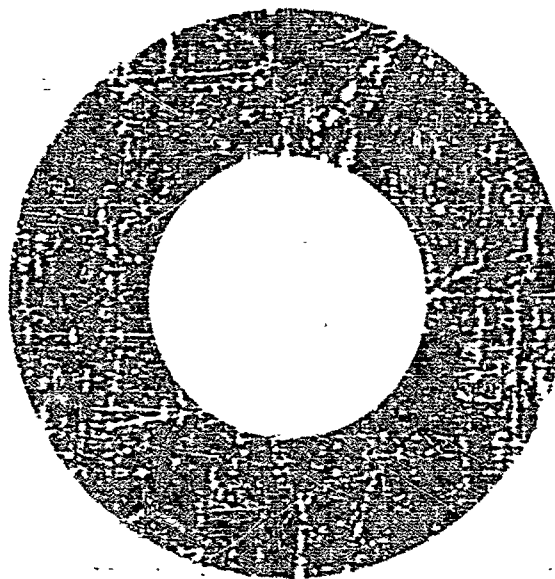


Figure 275. Primary Lip Seal After Test of
Rig F-33466-5

FE 71432

UNCLASSIFIED

(U) The two loose layers of Kapton-F trapped in the inlet primary O-ring groove by the disk seal ring were extruded by pressure and sheared, causing the high primary seal leakage. The secondary O-ring was not installed during assembly.

(6) Build No. 6

(U) The sixth build of mixture ratio valve F-33466 was the same as build No. 5 except for the following:

1. Disk seal rings that compressed three layers of laminated Kapton-F in the primary static seal grooves approximately 66% were used.
2. A laminated Kapton F-Kapton H disk seal (0.085 in. thick) was used.
3. Primary static seal rings were reworked to compress two layers of laminated Kapton-F on each side approximately 50%.
4. The upper bearing spacer outside diameter was silver plated to prevent galling with the thrust bearing.
5. The shaft vent seal housing inside diameters were silver plated to prevent galling with the shaft.

(U) The torque required to rotate the valve at ambient temperature was as follows:

| | |
|--|------------|
| Rotation out of disk seal | 210 in.-lb |
| Clockwise and counter-clockwise rotation | 25 in.-lb |
| Rotation into disk seal | 325 in.-lb |

The ambient temperature disk seal leakage at 50 psid GN₂ was 15 sccs. No other seal leakage was detected.

(C) The mixture ratio valve was mounted in the B-22 test stand for a cryogenic endurance test. A total of 1500 cycles was complete at internal pressures up to 6000 psig. This included 5 partial-stroke shutoff cycles, 20 partial-stroke control cycles, and 1475 full-stroke shutoff cycles.

(U) Disk seal leakage at 50 psid is shown in figure 2/4. The primary seal vent was capped when the leakage exceeded the flowmeter range (4729 sccs) at 20 cycles. The outlet static seal leakage exceeded flowmeter range at 1000 psig inlet pressure (10 cycles) and was capped. The maximum inlet flange static seal leakage was 18.9 sccs. The secondary and vent seal leakage remained less than 1.4 sccs throughout the test.

CONFIDENTIAL

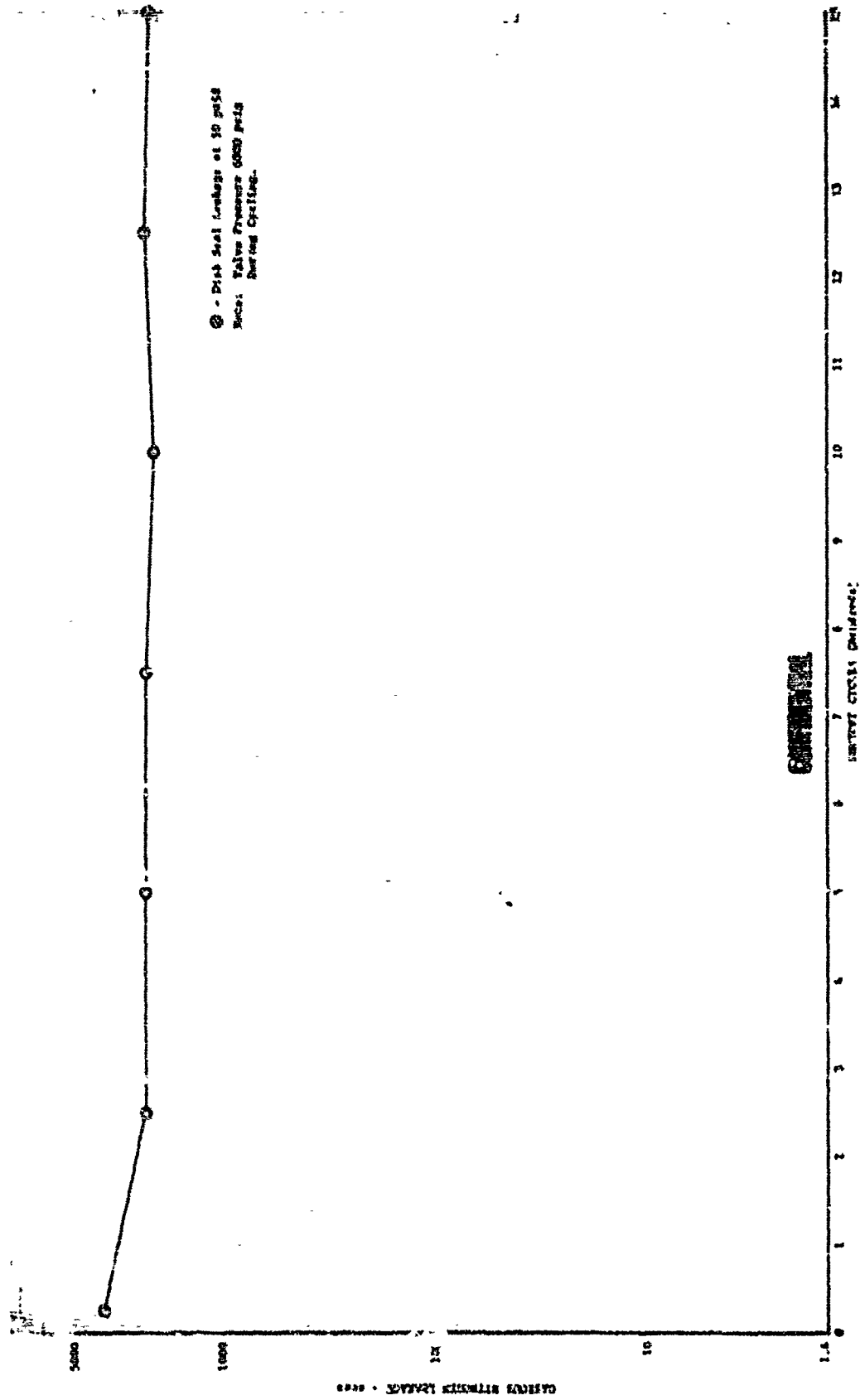


Figure 274. Disk Seal Leakage vs Shaft Cycles, Mixture Ratio Valve, Fig F-33466-6

DF 59122

CONFIDENTIAL

UNCLASSIFIED

(U) Valve disassembly after test revealed the following:

1. A portion of the metal spray area on the shaft disk OD was broken off causing the high disk seal leakage. (See figure 275.) The disk seal appeared in good condition.
2. The lower thrust bearing had galled slightly with the thrust washer as shown in figure 276.
3. The lip seals were in good condition and capable of full test cycling as shown in figure 277.
4. There was evidence of bearing cap flange separation from the laminated Kapton ring primary static seal.
5. The laminated Kapton V-ring was not centered in the outlet static seal groove.

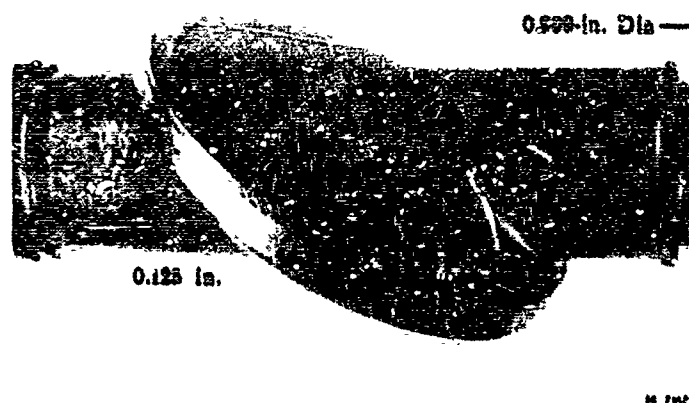


Figure 275. Shaft Disk After Test of
Rig F-33466-6

FD 23444



Figure 276. Lower Thrust Bearing After Test
of Rig F-33466-6

FE 71747

UNCLASSIFIED

UNCLASSIFIED

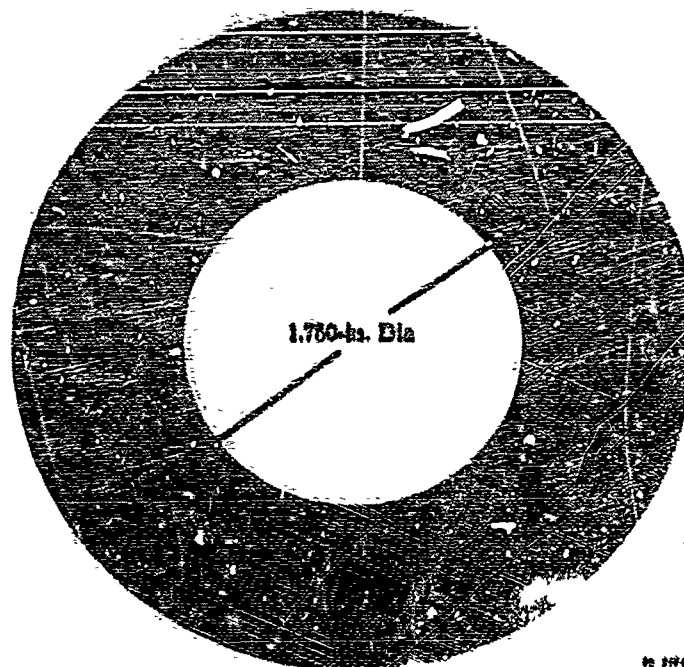


Figure 277. Lip Seal After Test of
Rig F-33466-6

FD 23443

(7) Build No. 7

(U) The seventh build of mixture ratio valve F-33466 was the same as build No. 6 except for the following:

1. The shaft disk seal groove was machined and filled with silver-lithium (puddle welded).
2. A laminated Kapton F (one piece) - FEP Teflon disk seal (0.085-in. thick) was used.
3. Standard Teflon-covered metal O-rings were used for the primary static seal in the bearing cover and outlet housing.
4. The bearing cover flange was undercut to increase effective seal load.
5. The thrust plate ID was silver plated to prevent galling with the shaft.
6. A Tuftram-coated thrust bushing was substituted for the inner thrust bearing, and the mating thrust washers were silver plated to prevent galling.
7. Lockwire holes were incorporated in the shaft bolt and plug.

(U) The torque required to rotate the valve at ambient temperature was as follows:

| | |
|---------------------------|--------------|
| Rotation out of disk seal | 400 in.-lb |
| CW and CCW rotation | 50-52 in.-lb |
| Rotation into disk seal | 700 in.-lb |

UNCLASSIFIED

CONFIDENTIAL

No disk seal leakage was detected at 50 psia GN₂ pressure (ambient temperature).

(C) The mixture ratio valve was mounted in the B-22 test stand for a cryogenic leakage test. A total of 37 cycles was completed. Included in the total were 5 partial-stroke shutoff cycles, 30 partial-stroke cycles, and 2 response test partial-stroke shutoff cycles. Valve internal pressures varied from 50 to 6000 psig.

(C) Disk seal leakage at 50 psia and primary seal leakage are illustrated in figure 278. The primary seal vent was capped when the leakage exceeded the flowmeter range, as indicated. The outlet primary O-ring leakage exceeded the flowmeter range at 1000 psig and was capped. The maximum inlet static seal leakage was 193 sccs. The secondary and vent seal leakage remained less than 1.4 sccs throughout the run. Average valve response to a step input was 1.04 milliseconds/degree.

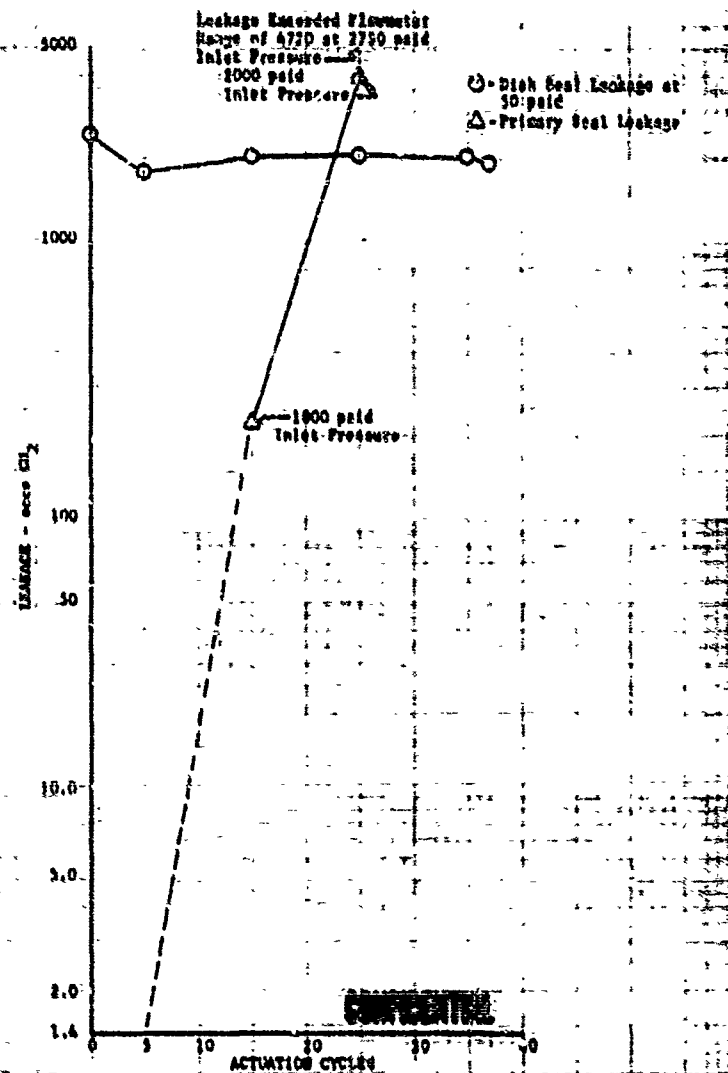


Figure 278. Leakage vs Actuation Cycles, Rig F-33466-7

DF 59531

CONFIDENTIAL

~~CONFIDENTIAL~~

(U) Valve disassembly after test revealed all parts were in good condition. The disk seal ID was slightly frayed, but otherwise satisfactory.

(8) Build No. 8

(U) The eighth build of the mixture ratio valve was the same as build No. 7 with the following exceptions:

1. A looseleaf (OD bonded) Kapton F-FEP Teflon disk seal was used (0.003-in. thick sheets in alternate layers).
2. The interconnecting primary static seal vent passages in the inlet and outlet housings were plugged to isolate the leakages from the bearing cover primary static seal, housing center flange primary static seal, and primary shaft lip and static seals. Separate vent outlets were added.
3. An Inconel-supported O-ring of laminated Kapton F (two layers) were used as primary static seal in the bearing cover.
4. Used O-rings were employed at the outlet flange cover.
5. Both main housings were reoperated and two 0.375-24 bolts were added in the center flange bolt circle to increase flange bolt load.

(U) The torque required to rotate the valve at ambient temperature was as follows:

| | |
|--|--------------|
| Rotation out of disk seal | 120 in.-lb |
| Clockwise and counter-clockwise rotation | 25-60 in.-lb |
| Rotation into disk seal | 100 in.-lb |

(C) The valve was mounted in the B-22 test stand for an environmental leakage test; 35 cycles were completed including 5 shutoff cycles and 30 partial-stroke actuation cycles. Leakages from the disk seal, primary shaft and static seal, housing center flange primary static seal, and bearing cover static seal are shown in figure 279. The housing center flange seal vent was capped when leakage exceeded the flowmeter range at 4000 psid (35 cycles) internal pressure. External leakage was visible from the valve center flange after this vent was capped. The secondary and vent shaft seal leakages remained less than 1.4 acs throughout the run. The outlet primary O-ring static seal vent was capped at 15 cycles (1000 psid) due to excessive leakage. External flange leakage was visible at internal pressures above 2000 psig.

~~CONFIDENTIAL~~

CONFIDENTIAL

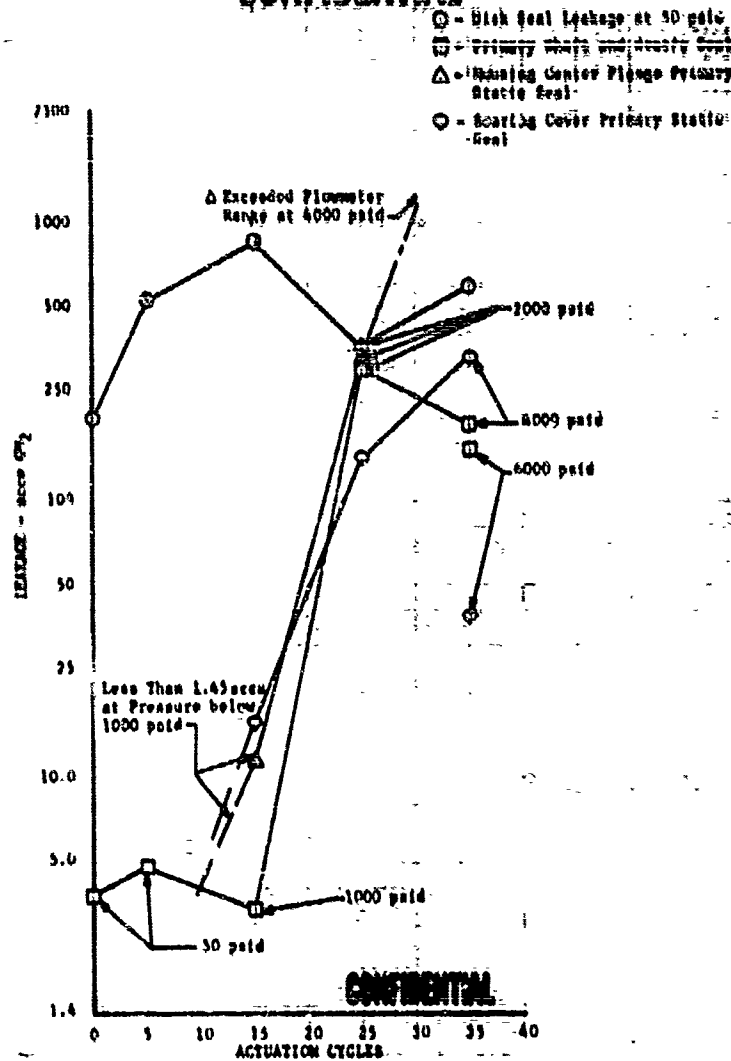


Figure 279. Leakage vs Actuation Cycles, Rig F-33466-8

DF 59532

(C) The valve was pulled from the B-22 test stand and the valve center flange torques were found to be below specification. These bolts were retorqued and the valve was returned to test. The valve was pressurized to 6000 psig internal pressure, and external leakage from the valve center flange was still evident. After test, the torque required to rotate the valve at ambient temperature was as follows:

| | |
|--|--------------|
| Rotation out of disk seal | 20 in.-lb |
| Clockwise and counter-clockwise rotation | 20-25 in.-lb |
| Rotation into the disk seal | 22 in.-lb |

CONFIDENTIAL

CONFIDENTIAL

(U) Disassembly of the valve revealed the following:

1. The disk seal was in good condition, although the outer layers were sheared by the static seal rings.
2. The laminated Kapton F-FEP Teflon lip seals were in excellent condition.
3. Portions of the Kapton F on the bearing cover static seal were extruded between the flanges, indicating flange separation.
4. The reason for external leakage at the valve housing center flange was not evident.

(C) The valve housings and bearing cover were assembled using Viton O-rings. The housing assembly was stresscoated and hydrostatically pressure tested to 6000 psig to indicate areas of high stress concentration. Stresscoat patterns appeared on the bearing cover at 2500 psig and on the inlet and outlet housings at 4500 psig internal pressure. The stresscoat threshold strain indicated tensile stress of approximately 34,000 psi in the inlet and outlet housings and 61,000 psi in the bearing cover at maximum internal proof pressure of 6000 psig. Figures 280, 281, and 282 show the stress concentrations that occurred during the test.

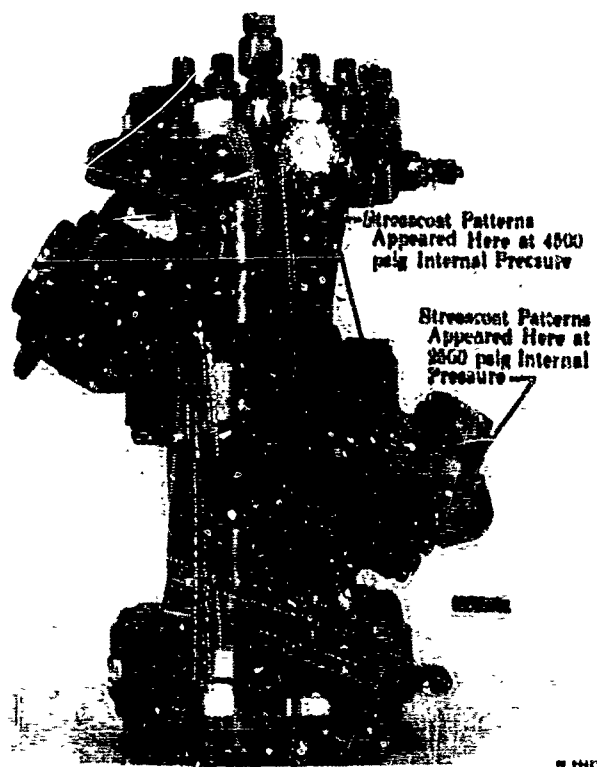
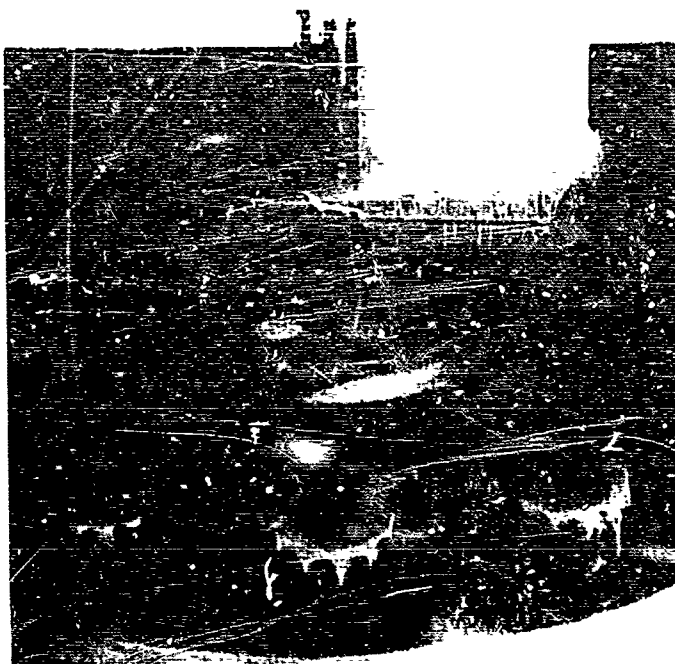


Figure 280. 150K Mixture Ratio Valve Housing Assembly Showing Stresscoat Patterns Due to 6000 psig Internal Proof Pressure

FD 23062

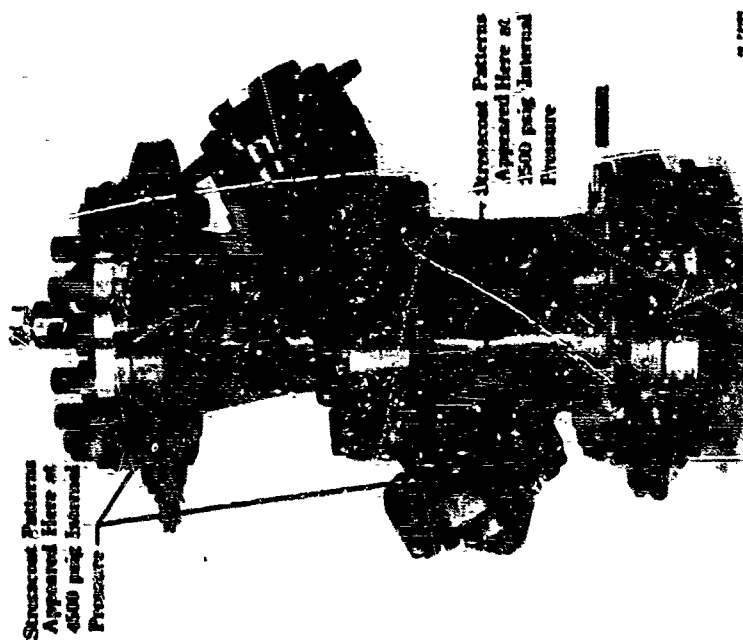
CONFIDENTIAL



250K Mixture Ratio Valve
Housing Assembly Showing
Stresscoat Patterns on
Bearing Cap Due to 6000 psig
Internal Proof Pressure

FD 23064

Figure 282.



250K Mixture Ratio Valve
Housing Assembly Showing
Stresscoat Patterns Due to
6000 psig Internal Proof
Pressure

FD 23063

Figure 281.

CONFIDENTIAL

(C) After removing the stresscoat the housing assembly was again hydrostatically pressure tested to 6000-psig internal pressure. Measurements indicated approximately 0.001-in. separation at the housing center flange and 0.006-in. separation at the bearing cover flange. Further testing will be required to accurately determine flange separation and incorporate design corrections.

b. Mixture Ratio Valve F-35106 (Refer to table XXXIV for test summary.)

(U) Four build, test, and disassembly inspection cycles were completed on this valve. The fifth build was subjected to an environmental leakage check and installed on the staged combustion rig. It performed satisfactorily for all tests on that rig, except for excessive static seal leakage during the maximum thrust run.

(1) Build No. 1

(C) Prior to assembly, the outer housings were assembled and hydrostatically proof pressure tested at 6000-psig water internal pressure.

(U) The initial build of rig F-35106 incorporated the following features:

1. Roller bearings throughout
2. A solid TFE Teflon disk seal
3. Kapton F-FEP Teflon primary and secondary lip-type shaft seals
4. Revised actuator support.

(U) The revised actuator support incorporated internal stops in the actuator and fully enclosed the coupling as shown in figure 252.

(U) The water flow calibration was performed by positioning the valve shaft and setting specified valve differential pressures. Figure 283 shows the water flow calibration results.

(U) Flow torque tests were performed by positioning the valve shaft, setting the valve differential pressure, and recording the output from the load cell. The torque data are shown in figure 284.

(U) Post-test inspection revealed a failed Teflon disk seal. (See figure 285.)

CONFIDENTIAL

(C) Table XXIV. Test Summary, Mixture Ratio Valve F-35106

| Build No. | Examination | Configuration | Seal Description | Program | Remarks |
|-----------|---|--|--|--|---|
| 1 | 1. Boiler bearings. 2. Seal between DB oiler placed 3. DB disk seal. 4. Viton O-rings. 5. Sealed window mount. 6. Lip-balls as primary and secondary dynamic shaft seals. 7. Back-to-back vent Ball-balls. 8. Key-C Journal steps in actuator. | Primary Secondary Vent - 1 Vent - 2 Disk | Laminated 502F-131 Krypton FEP Teflon (Teflon sealing surface) Vaporite filled Teflon Ball- balls VTE Teflon Disk Seal (DB sealing surface) Vented seals from Build 1 | 1. Flow meter calibration 2. Meter calibration | 1. Disk seal leaking after test - Retrieved from Run Tank. |
| 2 | Same as Build 1 | Primary Secondary Vent - 1 Vent - 2 Disk | Laminated 502F-131 Krypton FEP Teflon, DB sealing sur- face | 1. Meter calibration | 1. Disk seal leaking after test - except for small piece. |
| 3 | 1. Sizer in disk on rig shaft filled with Xichrome 7 metal spray to sealize ID Disk Seal. 2. Retainic Teflon coated O-Rings. | Primary Secondary Vent - 1 Vent - 2 Disk | Laminated 502F-131 Krypton FEP Teflon (Krypton sealing surface) Same as Build 1 Laminated 502F-131 Krypton and FEP Teflon 2d sealing surface 0.175-in. thick. | 1. Environmental test prior to staged combustion rig installation. 2. Transfer to 0.25:1 combustion rig for calibration. | 1. Excessive primary and Disk seal leakage. 2. Average valve response 1.2 ± 10-3 sec/deg. |
| 4 | Same as Build 3 | Primary Secondary Vent - 1 Vent - 2 Disk | Same as Build 3 | 1. Same as Build 3 | 1. Excessive primary seal leakage. 2. Small cracks in ID of Lip-Balls. |
| 5 | 1. O-Ring sealant of the primary Lip-Seal was substituted with lacquer. Two pieces of 502F-131 Krypton were bonded to each side of this over as retain- material. 2. O-Ring was substituted with seal tape as (1) above 3. All secondary O-Rings were vented on ID. 4. Torque on 0.375-in. dia. bolts increased to 150 in.-lb. 5. Torque on 0.543-in. dia. bolts increased to 1200 in.-lb. | Primary Secondary Vent - 1 Vent - 2 Disk | Loose stacking of 502F-131 Krypton and FEP Teflon 0.175-in. thick Laminated 502F-131 Krypton FEP Teflon (Krypton sealing surface) Same as Build 1 Laminated 502F-131 Krypton and FEP Teflon, Loose lead ID sealing surface 0.175-in. thick | 1. Environmental test prior to staged combustion rig installation. 2. Transfer to 0.25:1 combustion rig for calibration. 3. Staged combustion test- ing; compiled 502F-131 records of total test time. | 1. During environmental testing, high leakage experienced at the primary vent; however, leak was acceptable for staged combustion testing. 2. Average valve response was 1.2 ± 10-3 sec/deg. 3. During staged combustion test- ing external leakage was apparent. 4. A "breastplate" bond was fabricated and installed around the valve body. Indio bond collected the leakage which was vented away from the staged rig. 5. The valve was visually inspected during staged combustion test- ing. In rear, near the disk seal, built and other leakable areas of the valve were in excellent condition. |

CONFIDENTIAL

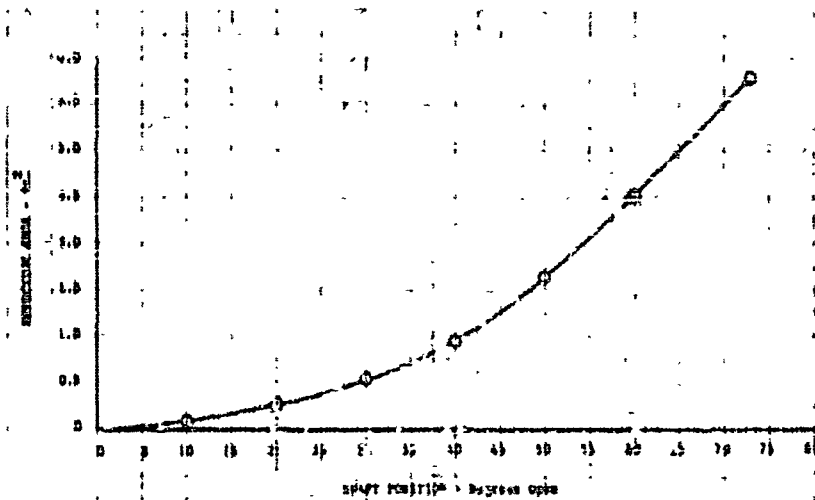


Figure 283. Mixture Ratio Valve Effective Area vs Shaft Position, Rig F-35106-1 DF 59010

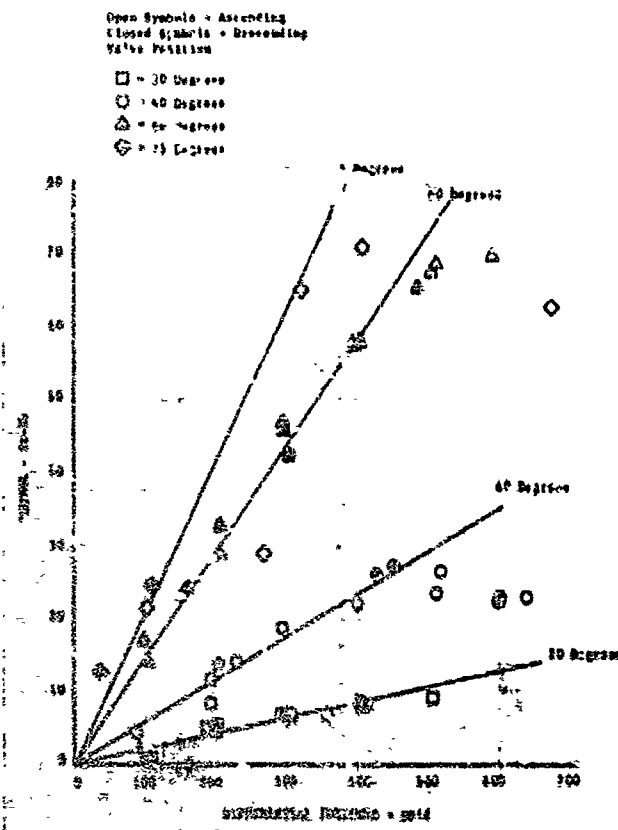


Figure 284. Torque vs Differential Pressure for Mixture Ratio Valve Rig F-35106-1 DF 59011

318

CONFIDENTIAL

(This page is Unclassified)

UNCLASSIFIED

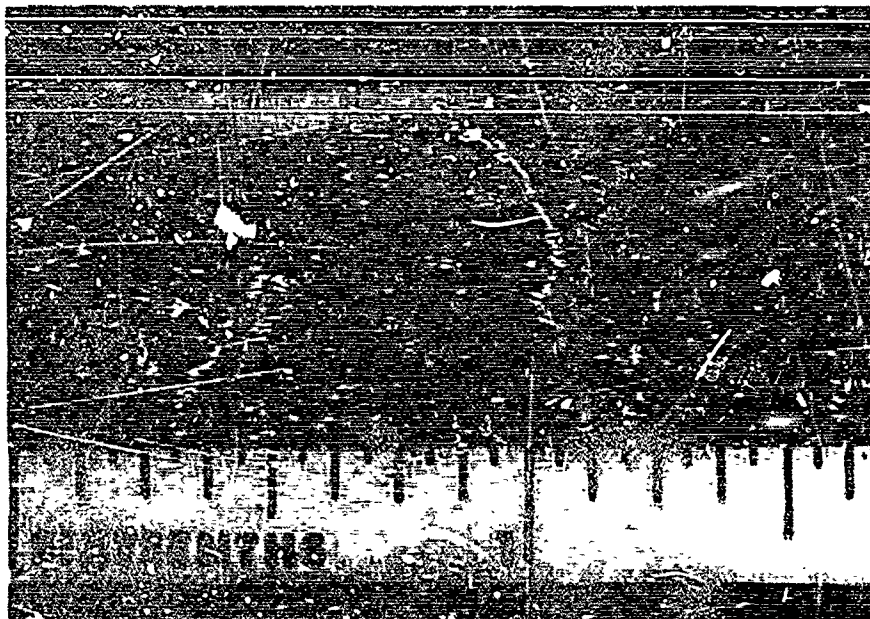


Figure 285. Teflon Disk Seal After Test of
Rig F-35106-1

FE 70305

(2) Build No. 2

(U) This build of mixture ratio valve F-35106 incorporated a laminated Kapton F-FEP Teflon material disk seal. All other seals and O-rings were reused from build No. 1. The torque required to rotate the valve at ambient temperature was 800 in.-lb to rotate out of the disk seal, and 35-40 in.-lb for rotation.

(U) The valve was mounted in the B-21 water flow test stand and the calibration was performed by positioning the valve shaft and setting specified valve differential pressures. Static seal leakage was not evident during calibration; figure 286 illustrates the flow calibration results.

The torque required to rotate the shaft was 12 in.-lb in all positions. Valve disassembly after test revealed the following:

1. The disk seal was missing except for a piece approximately 1 inch long remaining in the seal gland. (See figure 287.)
2. Moisture was present in the cap and on the thrust bearings.
3. Slight iron oxide deposits were on the shaft roller bearings.

UNCLASSIFIED

UNCLASSIFIED

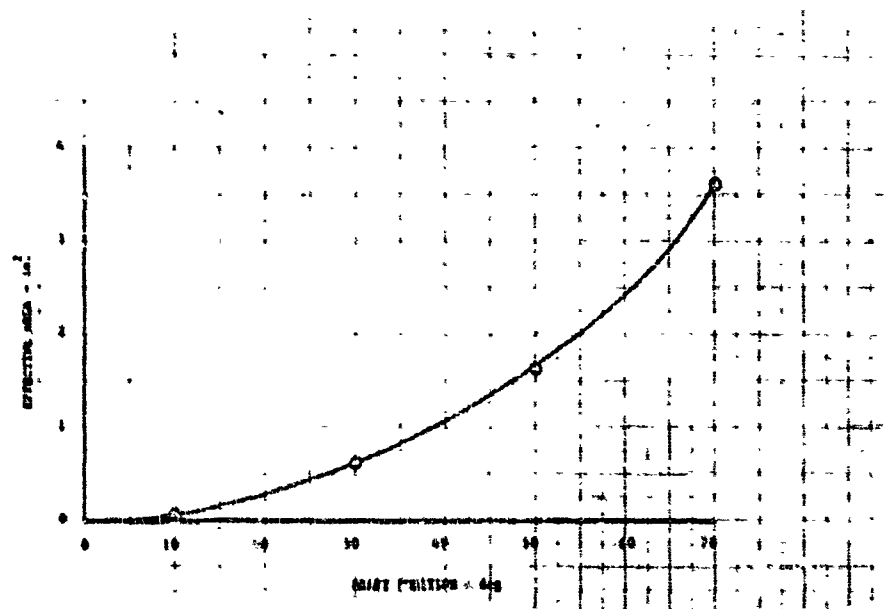


Figure 286. Mixture Ratio Valve Effective Area vs Shaft Position, Rig F-35106-2 DF 38766

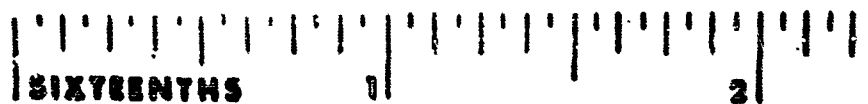


Figure 287. Laminated Kapton-FEP Teflon Disk Seal After Test of Rig F-35106-2 FE 70306

(3) Build No. 3

(U) The third build of mixture ratio valve F-35106 incorporated the same parts as the second build except the following:

1. Graphite-filled Teflon Bal-Seals as back-to-back vent shaft seals
2. Seal carrier inside diameters and tie bolt tabwasher were silver plated to prevent galling

320

UNCLASSIFIED

CONFIDENTIAL

3. Shaft seal groove was filled with Nichrome V metal spray
4. A laminated Kapton F and FEP Teflon disk seal were incorporated
5. The inlet flange primary O-ring was replaced with a 0.015-inch thick laminate of Kapton F. The mating flange was reoperated to compress this laminate by 30%, and trap it in the gland.
6. Teflon-coated metal O-rings were incorporated in all other static seal glands.

(U) The mixture ratio valve was mounted in the B-22 test stand for a cryogenic leakage test. No operational malfunctions or irregularities were noted during the test. A total of 45 cycles was accumulated.

(C) Disk seal leakage at 50 psid varied from 684 sccs to 1550 sccs. Primary seal leakage (includes primary static seals and primary shaft seal) exceeded the flowmeter range (4720 ccm) at inlet pressures in range of 500 to 5000 psig. The seal leakages are illustrated in figure 288. Maximum static seal leakage at the inlet flange was 14 sccs. Static seal leakage at the outlet flange varied from 27 sccs to 850 sccs. Average valve response to a step input was determined to be 1.2×10^{-3} sec/deg.

(U) Valve disassembly after test revealed the disk seal was frayed on the inside diameter and small Kapton F particles were found in the valve housings.

(4) Build No. 4

(U) The fourth build of mixture ratio valve F-35106 had the same features as build No. 3, with the following exceptions:

1. A looseleaf stackup of Kapton F and FEP Teflon disk seal was used.
2. The inlet flange primary O-ring was replaced with a 0.020-inch thick laminate of 0.005-inch Kapton F. The mating flange compressed this laminate 50%, trapping it in the gland.

(U) The mixture ratio valve was mounted in the B-22 test stand for cryogenic operation. No malfunctions or irregularities were noted during the test program, during which a total of 30 cycles was accumulated.

(U) Disk seal leakage at 50 psid varied from 198 to 300 sccs. Primary seal leakage (includes primary static seals and primary shaft seal) exceeded the flowmeter range at inlet pressures greater than 500 psig. Maximum static seal leakage at the inlet flange was 47 sccs. Static seal leakage at the outlet flange varied from 1.4 sccs to 2000 sccs. Seal leakage summary is presented in figure 289.

(U) Valve disassembly after test revealed small cracks on the inside diameter in the Kapton F material of the primary and secondary lip seals.

CONFIDENTIAL

CONFIDENTIAL

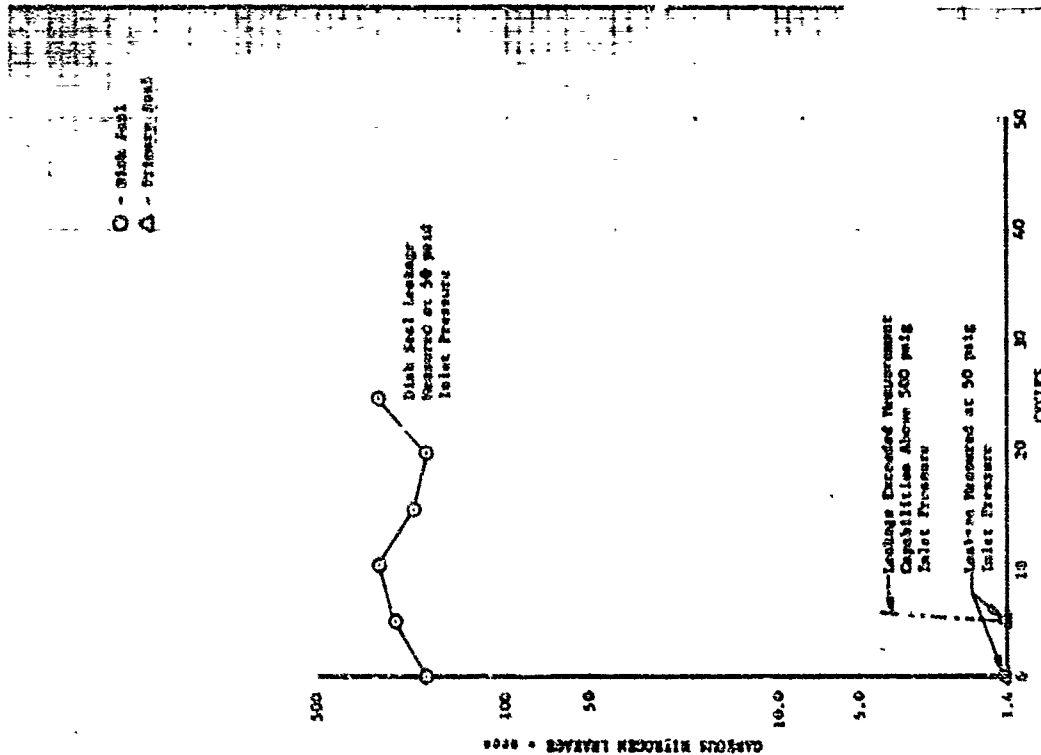


Figure 289. Leakage vs Cycles, Mixture Ratio Valve Rig F-35106-4 DF 58768

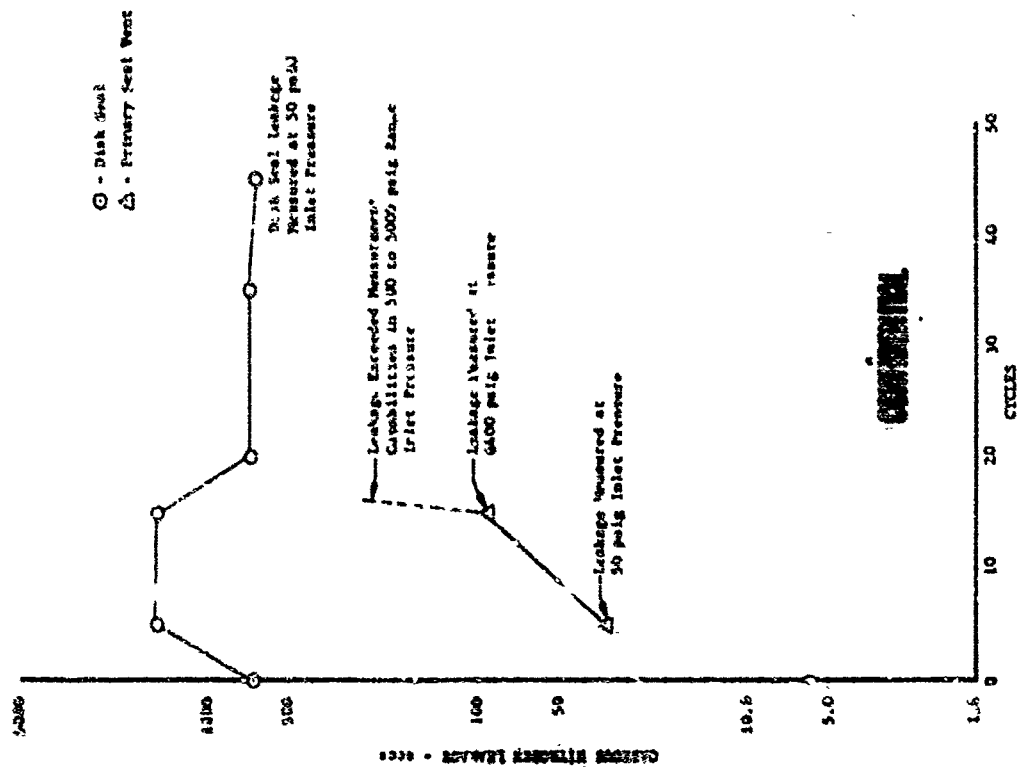


Figure 288. Leakage vs Cycles, Mixture Ratio Valve Rig F-35106-3 DF 58767

322
CONFIDENTIAL

CONFIDENTIAL

(5) Build No. 5

(U) The fifth build of mixture ratio valve F-35106 and actuator assembly was the same as build No. 4 with the following exceptions:

1. Solid metal rings with rectangular cross section and two layers of Kapton F on each side were substituted for the primary O-rings at the bearing cover interface and at the primary shaft seal interface.
2. All secondary O-rings were vented on the ID.
3. The inside diameter of the laminated Kapton F and FEP Teflon Primary and Secondary Lip Seals was 0.875-in. (before forming).
4. A laminated 0.175-in. thick Kapton F and FEP Teflon (loose-leaf ID) disk seal was used.
5. Flange bolt torques were increased.

(U) The torque required to rotate the valve at ambient temperature was as follows:

| | |
|--|--------------|
| Rotation out of disk seal | 275 in.-lb |
| Clockwise and counter-clockwise rotation | 40-50 in.-lb |
| Rotation into disk seal | 250 in.-lb |

(U) The valve was mounted in the B-22 test stand for an environmental leakage test. A total of 25 cycles was completed, including 5 shutoff cycles and 20 partial-stroke actuation cycles. Leakage at the primary seal vent and the disk seal are shown in figure 290. The secondary and vent seal leakage remained less than 1.4 sccs throughout the test.

(U) The valve was returned from environmental testing and given a thorough visual examination and all visible areas were in excellent condition. The valve was then mounted on the staged-combustion rig.

(U) During staged combustion testing, external leakage was visible at the valve center flange interface. When the staged-combustion rig was returned from test for parts modification, the mixture ratio valve was removed from the rig and visually examined. All parts were in excellent condition. A sheetmetal cover was fabricated for the valve center flange and bearing cap. This cover enabled the leakage to be collected and routed away from the rig. The valve was reinstalled on the rig for continued testing, after which the mixture ratio valve remained on the test stand with the staged-combustion rig.

(U) Mixture ratio valve 35106-5 was operative during a total of 34 firings for 573.1 seconds of hot time during staged-combustion testing. No malfunctions were noted other than the external leakage.

CONFIDENTIAL

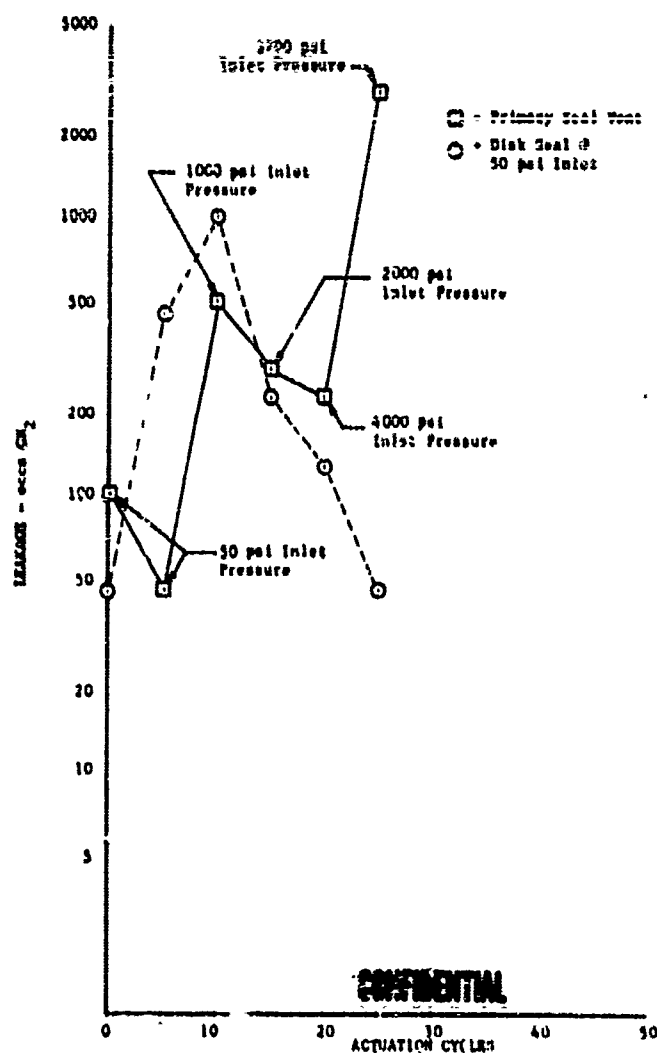


Figure 290. Leakage vs Cycles, Mixture Ratio
Valve Rig F-35106-5

DF 59533

c. Rotary Shaft Seal Test Rig (Refer to table XXXV for test summary.)

(C) The rotary shaft seal test rig was designed to test the mixture ratio valve shaft seal packages. Lip-type seals and spring-loaded cup-type gland seals were tested in liquid nitrogen with seal differential pressures up to 6000 + psig. An exploded view of the initial test assembly was previously shown in figure 243. Ten build, test, and inspection cycles were completed on this rig. The final lip seal design of laminated Kapton F and FEP Teflon passed the 10,000 actuation cycle and 500 pressure cycle (0 to 5000 + psig) test with overboard primary shaft seal leakage less than 1.4 cc/cycle throughout the test. The 10 environmental endurance tests completed on this rig are summarized in the following paragraphs. All tests were conducted with the rig submerged in liquid nitrogen (-140°R). Actuation cycles were performed with 5000 to 6400 psig rig inlet pressure. Pressure cycles were to 5000 + psig.

CONFIDENTIAL

CONFIDENTIAL

(C) Table XXXV. Test Summary, Rotary Shaft Seal Test Rig F-33443

| Build No. | Configuration | | Cryogenic Test Results | | | Remarks |
|-----------|---|---|---|---|---|---------|
| | Features | Seal Description | Leakage Range, sec/c | Cycles | | |
| 1 | 1. Rig designed to test Bal Seals and Lip-Seals simultaneously. 2. Teflon coated O-Rings as static seals. 3. Pneumatic Hydraulic actuator used to turn rig shaft. | Test: Graphite-filled Teflon Bal Seal Primary Secondary Vent Test: Nylon - TFE Teflon Lip-Seals Primary Secondary Vent | Less than 1.4 1.6 22 Less than 1.4 | 10 | 1. Rig pulled because of shaft binding. | |
| 2 | 1. Bearing bushing fitted to actuator mount to ensure shaft alignment. 2. ID's of rig segments silver plated to preclude galling on shaft. | Test: Secondary - All new seals - Same as Build 1 Primary - Secondary - Vent | Less than 1.4-2.8 Less than 1.4 Less than 1.4-2.6 Less than 1.4-28.4 Less than 1.4-2.6 Less than 1.4-4.7 | 10,115 Shaft Cycles 250 Presure Cycles | 1. Leakage at primary Bal-Seal increased substantially after 40 pressure cycles. 2. Primary Bal-Seal split during test. 3. Primary Lip-Seal split during test. 4. Vent seal leakage due to environmental Li_2 boil-off. | |
| 3 | 1. Bal-Seals installed in end test-seals to isolate vent and test-seals from environmental Li_2 . 2. PEP Teflon O-Ring in shaft used in Lip-Seal. | Test: TFE Teflon Bal-Seal Secondary - Primary Secondary - Vent Test: Nylon - PEP Teflon Lip-Seal Primary Secondary - Vent | Less than 1.4 Less than 1.4 120-200 Less than 1.4 Less than 1.4 Less than 1.4 | 500 Presure Cycles | 1. The primary Bal-Seal was split. | |
| 4 | 1. Lip-Seals utilized for dual function-Static and dynamic seals. (Thin O-Rings utilized at Lip-Seal interfaces). 2. Fixture rails valve parts list static seals (Teflon coated metallic O-rings used in Bal-Seal Portion of rig). | Test: Secondary - Primary - Secondary - Vent Test: All new seals - Same as Build 3 | 2.3 - 19 1. - 122 240-850 Less than 1.4-50 Less than 1.4 2.2-3.2 | 10,000 Shaft Cycles 500 Presure Cycles | 1. Primary Bal-Seal was split. 2. Superficial cracks in primary Lip-Seal. 3. Test Seal leakage due to environmental Li_2 boil-off (Vent isolation Bal-Seals damaged during assembly). 4. Torque investigation: Temp Inlet Press Torque Pressure Data In.-lb Ambient 0 psi 42-44 Li_2 287 psi 43-45 600 psi 83-86 Post-run Data Li_2 0 48-50 200 54-55 600 48-53 | |

CONFIDENTIAL

(C) Table XXV. Test Summary, Rotary Shaft Seal Test Rig F-33443 (Continued)

| Build No. | Configuration | | Dynamic Test Results | | | Remarks |
|-----------|---|--|-----------------------|---------------------|--|--|
| | Features | Seal Description | Leakage-Rate, p. sec. | Cycles | | |
| 5 | 1. Rig p. is pumped with 0.0005-in. diam glass beads | Test - Graphite-filled Teflon | Less than 1.4 | 10,000 | 1. Superficial fatigue cracks in Primary Lip-Seal. | 2. Distorted secondary Lip-Seal. 3. White residue in rig. 4. Overall photo of dynamic seals. 5. Torque investigation: |
| | | Primary - Lip-Seal | Less than 1.4 | Shaft | | |
| | | Primary - Laminated 500F-131 Kapton-FEP Teflon Lip-Seal (Teflon sealing surface) | Less than 1.4-37.5 | 500 Pressure Cycles | | |
| | | Secondary - Stacked 500F-131 Kapton FEP Teflon Lip-Seal (Teflon Sealing Surface) | Less than 1.4 | | | |
| 6 | Same as previous builds | Test - Mylar-FEP Teflon Lip-Seal | Less than 1.4 | 10,000 | 1. Superficial cracks in Primary Lip Seal. | 2. Leakage interaction noted between Primary Lip-Seal and Static Seals on Bal-Seal portion of rig. 3. Bal-Seal leakage was generally higher prior to cycling and after pressure cycles. 4. O-Ring compression appeared satisfactory. |
| | | Primary - Same seals | Less than 1.4 | Shaft | | |
| | | Primary - Recured from Build 5 | Less than 1.4 | 500 Pressure Cycles | | |
| | | Secondary - Same as Build 5 | Less than 1.4-3.3 | | | |
| 7 | OD vent holes in dynamic leakage isolation O-Ring (Bal-Seal portion of rig). This O-Ring was also sandwiched between two pieces of 500F-131 Kapton (0.105 in. thick). | Test - Graphite-filled Teflon Bal-Seal | Less than 1.4 | 14,000 | 1. Leakage interaction noted between Primary Bal-Seal and Static seals on Bal-Seal portion of rig. | 2. Leakage isolation O-Ring was scalloped, indicating OD pressurization. 3. Appearance of all Dynamic Seals was good. |
| | | Primary - Laminated 500F-131 Kapton-FEP Teflon Lip-Seal (Kapton Sealing Surface) | Less than 1.4-2.8 | 700 Pressure Cycles | | |
| | | Secondary - Same as Build 6 | Less than 1.4 | | | |
| | | Test - All seals same as Build 7 | Less than 1.4 | 2,400 Shaft Cycles | 1. Polled rig because of excessive leakage at primary Lip-Seal. | |
| 8 | All secondary O-Rings vented on ID. 2. Bolt torque increased from 300 to 500 in.-lb. | Test - All seals same as Build 7 | Less than 1.4-42 | 55 Pressure Cycles | 2. Primary Lip-Seal split. | 3. Leakage interaction noted between Primary Bal-Seal and Static Seals on Bal-Seal portion of rig. 4. Compression of O-Rings was normal. |
| | | Primary - Same as Build 7 | Less than 1.4 | | | |
| | | Secondary - Same as Build 7 | Less than 1.4 | | | |
| | | Test - Same as Build 7 | Less than 1.4 | | | |

(C) Table XXXV. Test Summary, Rotary Shaft Seal Test Rig F-33443 (Continued)

| Build No. | Configuration | | Crucial Test Results | | Remarks |
|-----------|--|---|------------------------|---------------------|---|
| | Features | Seal Description | Leakage Rate, in./min. | Cycles | |
| 9 | 1. Leakage isolation O-ring and the Primary O-ring at Primary Bal-Seal interface were sand-wiched between two pieces of 500F-131 Kapton. | Vent Secondary | Less than 1.0 | 10,000 Shaft Cycles | 1. Superficial cracks in Primary Lip-Seal 2. Leakage interaction did not occur during test. |
| | 2. The inboard secondary O-ring (Bal-Seal end of rig) was shimmed with 0.010-in. thick TFE Teflon. | Primary - Graphite-filled Teflon Bal-Seal | Less than 1.0-1.2 | 500 Pressure Cycles | |
| | 3. All secondary O-rings were on ID. | Primary Secondary - Same as Build 9 | Less than 1.0 | | |
| | 4. Bolt torque was 500 in.-lb. | | | | |
| 10 | 1. All O-ring substituted with one 0.005-in. thick layer of 50. Kapton was positioned between adjacent segment surfaces. | Vent Secondary | Less than 1.2 | 10,000 Shaft Cycles | 1. Leakage interaction did not occur during test. 2. Static seal leakage was less than 1.5 in./min throughout test. 3. Photos were taken of rig with seal in place. |
| | 2. Bolt torque 500 in.-lb. | Primary - TFE Teflon Bal-Seal Primary - Laminated 500F-131 Kapton TFE Teflon Lip-Seal (Kapton sealing surface) | 6-2500 Less than 1.0 | 500 Pressure Cycles | |
| | | Secondary - Laminated 500F-131 Kapton TFE Teflon Lip-Seal (Teflon sealing surface) | Less than 1.2 | | |
| | | Vent - Nylon-722 Teflon Lip-Seal | Less than 1.2 | | |

CONFIDENTIAL

(1) Build No. 1

(a) Objective

(U) This build of the rotary shaft seal test rig was to investigate the leakage and endurance of graphite-filled Teflon Bal-Seals and Mylar/Teflon (TFE) lip seals.

(b) Configuration

(C) The test rig, which was previously shown in figure 244, incorporates a pneumatic translating actuator (5-inch diameter piston) that rotates the rig shaft through a linkage assembly. The rig shaft was chrome-plated AMS 5735 stainless steel with a 6 microinch average surface roughness. Prior to cryogenic test, the rig was hydrostatically proof pressure tested at 6000 psig water and then vacuum baked.

(c) Test Summary

(U) During initial cycling of F-33443-1 the shaft alignment bushing id slipped from the actuator adapter bracket and had allowed the unsupported adapter shaft to bend. No meaningful seal leakage data were taken.

(U) The rig was disassembled and water was found in all segments of the rig. This was attributed to the rig vent lines that were not tightly capped prior to removing the rig from LN₂ environment.

(U) The shaft and adapter shaft were galled at the pinned connection. The shaft was also bent approximately 0.050-inch.

(C) The secondary Bal-Seal had a small chip in the inside diameter sealing lip. All the primary static Teflon coated metal O-ring seals not rigidly contained at the inside diameter had a scalloped appearance; this was attributed to pressurization of the static seal vents during the 6000-psig hydrostatic water test.

(2) Build No. 2

(a) Objective

(U) This build of the rotary shaft seal test rig was to investigate the leakage and endurance of graphite-filled Teflon Bal-Seals and Mylar/Teflon (TFE) lip seals.

(b) Configuration

(U) The second build of the Rotary Seal Test Rig, shown in figure 291, was the same as build No. 1. Actuation and pressure cycle rates for these tests were each approximately 10 cycles per minute.

CONFIDENTIAL

CONFIDENTIAL

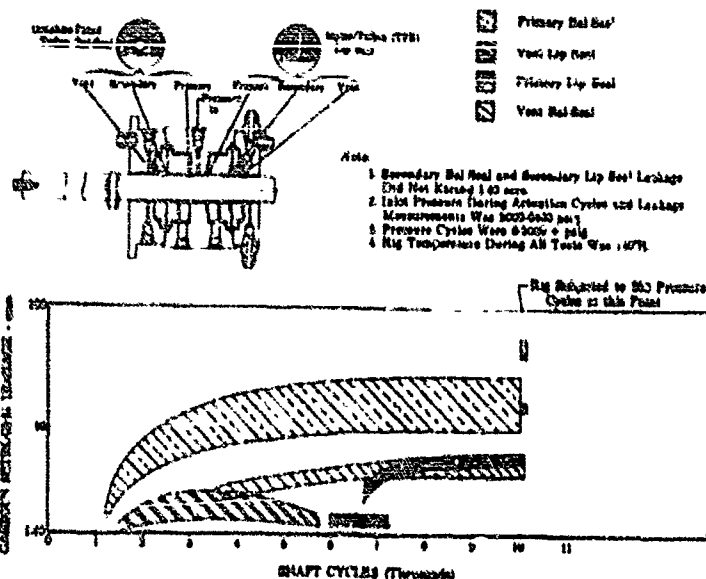


Figure 291. Rotary Shaft Seal Test Rig Leakage vs Cycles for Rig F-33443-2 FD 20151A

(c) Test Summary

(C) Leakage measurements with the shaft stationary were taken prior to shaft cycling, prior to the pressure cycle period, and during the pressure cycle period. All other leakage measurements were taken during actuation cycling. Inlet pressure to the rig varied from 5000 to 6400 psig during actuation cycling. The leakage rates for the various seals tested are shown in the curves in figure 291.

(C) After 10,000 actuation cycles, the actuator was stopped and the rig was subjected to 250 inlet pressure cycles (0-5000 + psig). Final seal leakage measurements were taken during an additional 115 actuation cycles conducted after the pressure cycles.

(U) After completion of these tests, the teardown inspection revealed the following:

1. No moisture was evident in the rig.
2. Slight contamination was found on all shaft seals and in glands.
3. The primary Bal-Seal was split at the base of the seal as shown in figure 292.
4. The primary lip seal Teflon was split at two locations on the formed radius as shown in figure 293.

(U) Leakage past the primary Bal-Seal increased by a factor of 6 between 40 and 100 pressure cycles. The seal apparently failed during this period. It was not possible to determine when the primary lip seal failed because of fluctuating leakage; it is presumed to have failed during the pressure cycle period.

CONFIDENTIAL

CONFIDENTIAL

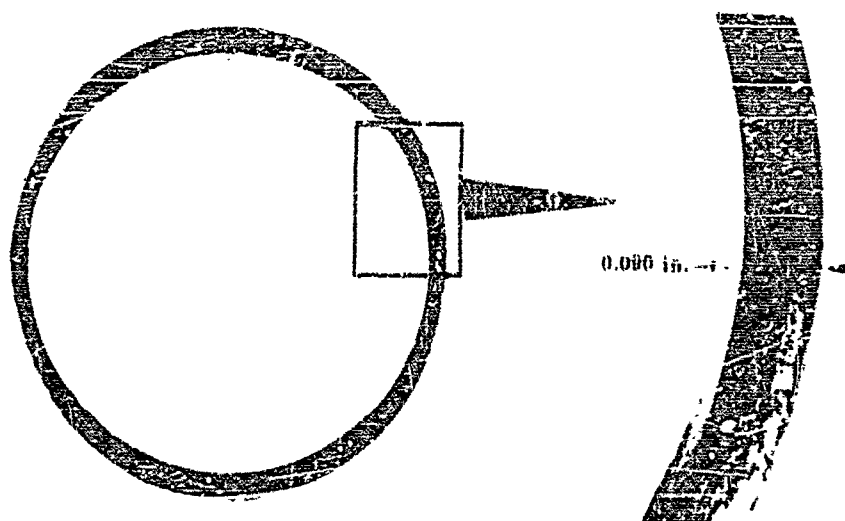


Figure 292. Primary Bal-Seal After Test

FD 20062A

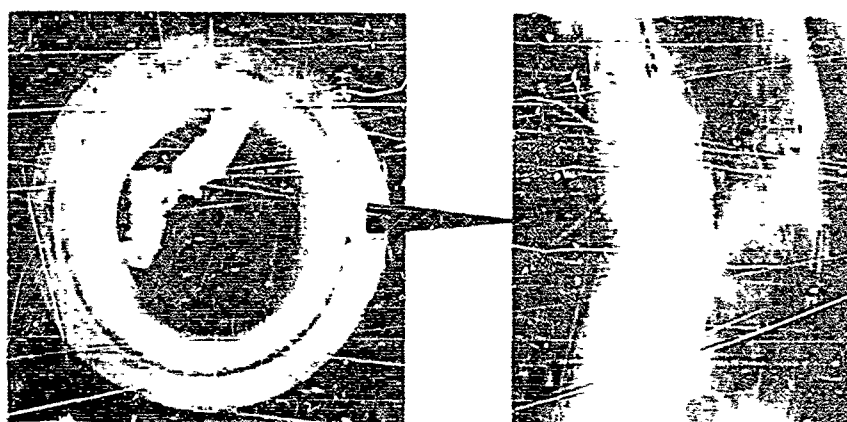


Figure 293. Primary Lip Seal After Test

FD 20061A

(3) Build No. 3

(a) Objective

(U) This build of the rotary shaft seal test rig was to investigate the leakage and endurance of FEP Teflon Bal-Seals and Mylar/FEP Teflon lip seals.

(b) Configuration

(U) The third build of the test rig is shown in figure 294. Further modifications of the seal rig were as follows:

1. Lip seal retainers were modified to accept the thinner (0.020-inch thick) FEP Teflon lip seals.

330

CONFIDENTIAL

(This page is Unclassified)

CONFIDENTIAL

2. The end plates were reoperated to accept graphite-filled Teflon Bal-Seals that were used to isolate the vent cavities from the LN₂ bath.
3. A shaft fabricated of AMS 5735 (stainless steel) was used with a measured surface finish of 3 to 5 microinch surface roughness.

(c) Test Summary

(C) A total of 500 pressure cycles was completed. Pressure cycling was done with the rig shaft stationary.

(U) The primary Bal-Seal leakage was 120 sccs prior to cycling. During the test, the primary Bal-Seal leakage varied from 120 to 376 sccs. The leakage rates for the seals tested are shown in figure 294.

(U) The rig was disassembled and a split was found at the base of the primary Bal-Seal as shown in figure 295. A small amount of contamination was found on all shaft seals and in the glands.

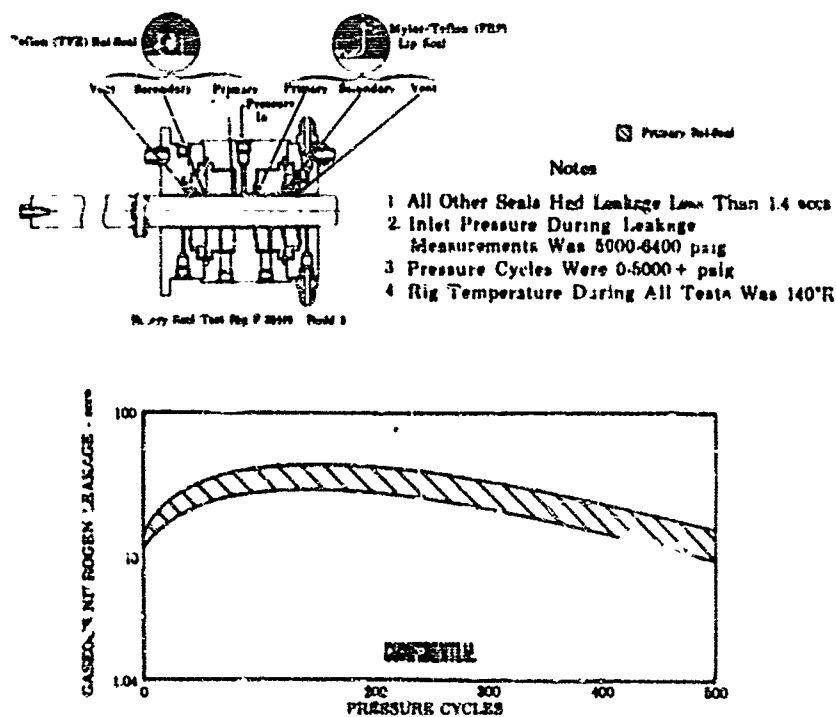


Figure 294. Rotary Shaft Seal Test Rig Leakage vs Cycles for Rig F-33443-3

FL 20074A

CONFIDENTIAL

CONFIDENTIAL

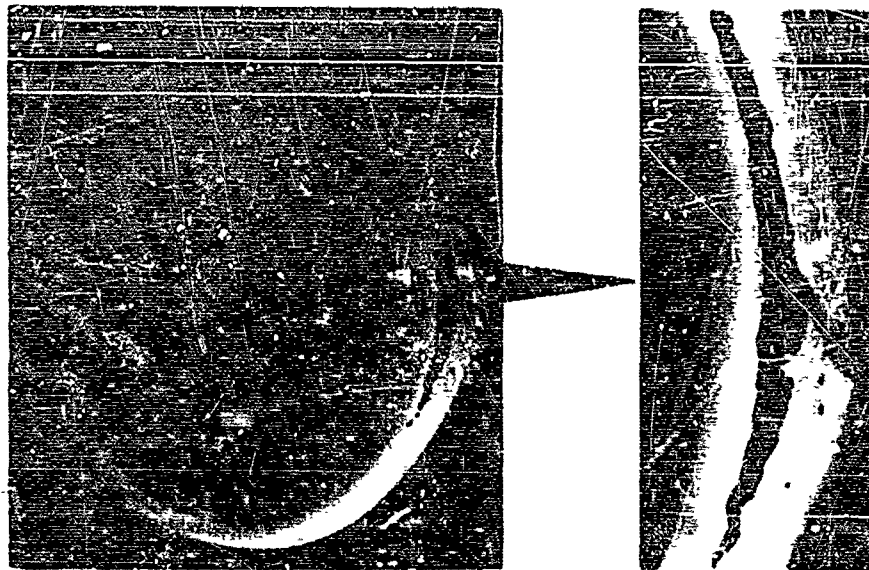


Figure 295. Primary Bal-Seal After Test

FD 20068A

(4) Build No. 4

(a) Objective

(U) This build of the rotary shaft seal test rig was to investigate the leakage and endurance of TFE Teflon Bal-Seals and Mylar/FEP Teflon lip seals

(b) Configuration

(U) The fourth build of the test rig is shown in figure 296. Further modifications of the seal rig were as follows:

1. The primary Teflon-coated metal O-rings at the primary and secondary lip seal were omitted.
2. Teflon coated metal O-rings were used on the Bal-Seal end of the rig.

(c) Test Summary

(C) A total of 10,000 shaft cycle and 500 pressure cycles was completed. Pressure cycles were accomplished at four intervals of approximately 2000 actuation cycles. At each interval the rig was subjected to 125 pressure cycles. During the pressure cycle period, shaft actuation cycling continued.

(C) Leakage at the vent Bal-Seal exceeded the established limit of 10 sccm at approximately 5500 shaft cycles. The leakage rates for the seals tested are shown in figure 296.

CONFIDENTIAL

CONFIDENTIAL

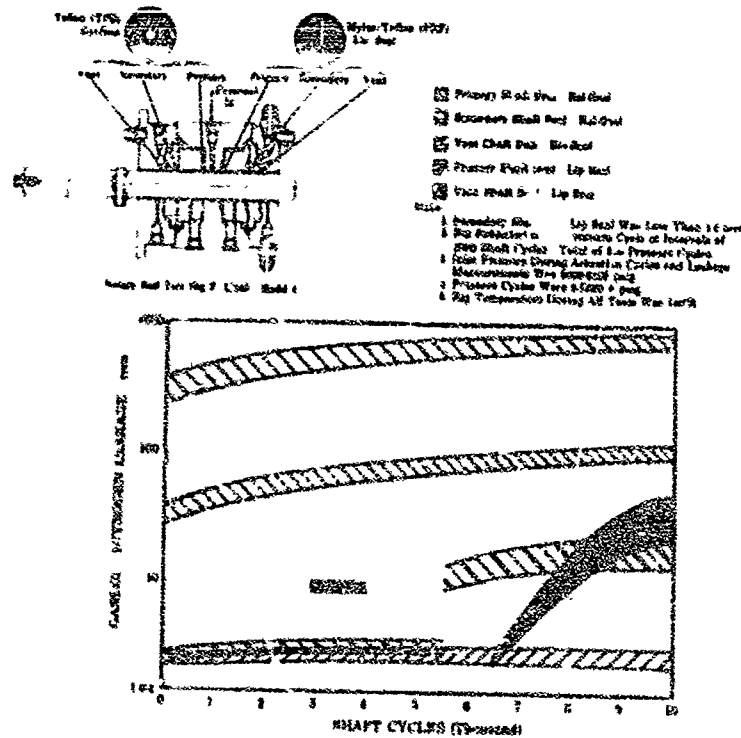


Figure 296. Rotary Shaft Seal Test Rig Leakage vs Cycles for Rig F-33443-4 FD 20075B

(U) After completion of these tests, the teardown inspection revealed the following:

1. The primary Bal-Seal was split at the corner of the base surface and the inside diameter, as shown in figure 297.
2. The primary lip seal had superficial fatigue cracks, as shown in figure 298, but could not be made to leak during post disassembly testing.
3. A small amount of contamination was found on the secondary and vent Bal-Seals. A powdery Teflon wear residue was found in the lip seal end of the rig.
4. Figure 299 shows all of the dynamic seals tested on rig F-33443-4.

CONFIDENTIAL

CONFIDENTIAL

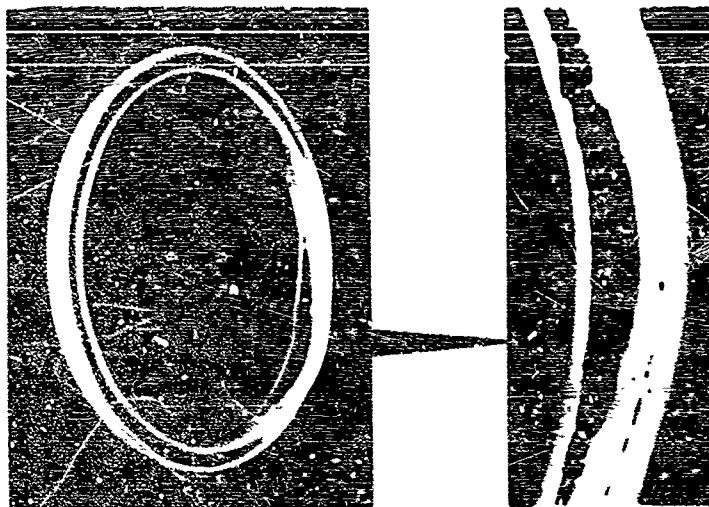


Figure 297. Primary Bal-Seal After Test

FD 20067A

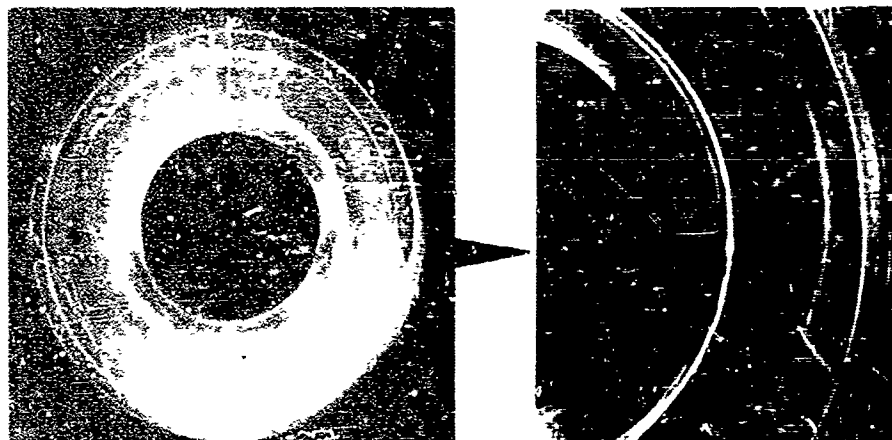


Figure 298. Primary Lip Seal After Test

FD 20071A

CONFIDENTIAL

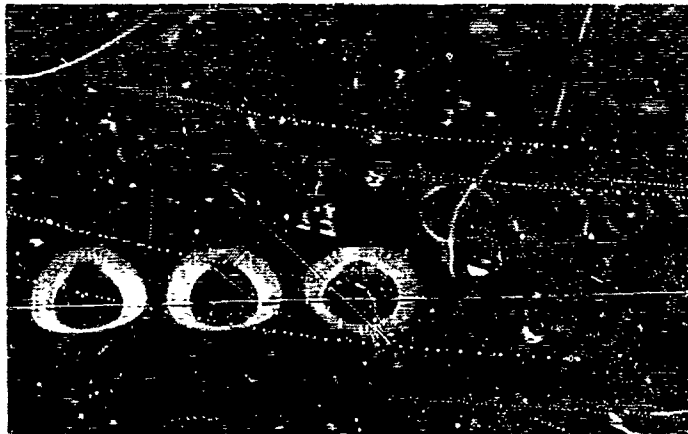


Figure 299. All Dynamic Seals Tested on
Rig F-33443-4

FD 23446

(5) Build No. 5

(a) Objective

(U) This build of the rotary shaft seal test rig was to investigate the leakage and endurance of graphite-filled Teflon Bal-Seals and laminated and stacked 500 F-131 Kapton (Kapton F) and FEP Teflon lip seals.

(b) Configuration

(U) The fifth build of the test rig is shown in figure 300. Further modifications of the seal rig were as follows:

1. The laminated Kapton F and FEP Teflon lip seal was made by fusing three pieces of 500 F-131 Kapton (0.005-in.) and one piece of FEP Teflon (0.020-in.). The laminate was fused at 525°F for 15 minutes at approximately 10 psia load. This seal was used as the primary lip seal.
2. A stacked Kapton F and FEP Teflon lip seal was used as the secondary lip seal. It consisted of three pieces of 500 F-131 Kapton and one piece FEP Teflon.

(c) Test Summary

(C) A total of 10,000 shaft cycles and 500 pressure cycles was completed. Pressure cycles were accomplished at approximate intervals of 2000, 4000, 6000, and 8000 shaft cycles. The rig was subjected to 125 pressure cycles at each interval. Shaft cycling continued during the pressure cycle period.

CONFIDENTIAL

CONFIDENTIAL

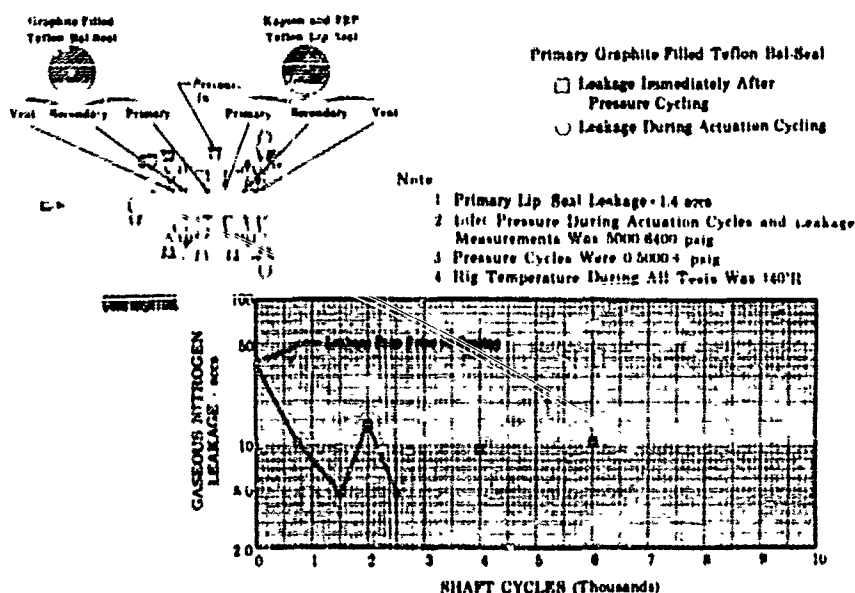


Figure 300. Rotary Shaft Seal Test Rig Leakage vs Cycles for Rig F-33443-5 FD 22247A

(C) Leakage rates experienced during the test were highest prior to cycling; the primary Bal-Seal leaked at a rate of 37.5 sccs. This leakage decreased to less than 1.4 sccs after 3000 shaft cycles. However; immediately after the second and third pressure cycle series, detectable leakage recurred (9.8 sccs and 10.8 sccs, respectively). All other seal leakage rates during the test were less than 1.4 sccs. The leakage rates for the seals tested are shown in figure 300.

(C) Cycling was stopped after completion of 10,000 shaft cycles and 500 pressure cycles. Minor installation alterations were made so that the secondary lip seal could be pressurized to 5000-6400 psig. However, when pressurizing this seal, secondary O-ring seal leakage under outside diameter pressurization prevented isolation and pressurization of the secondary seal. The test rig was removed for disassembly.

(U) The teardown inspection revealed the following:

1. All Bal-Seals had slight inside diameter wear. No splitting was detected and seal appearance was good.
2. The primary lip seal (bonded Kapton F and FEP Teflon) had superficial fatigue cracks. (See figure 301.) Microscopic observation indicated that these cracks occurred in the intermediate layers of the Kapton film.

CONFIDENTIAL

UNCLASSIFIED

3. The Kapton P film on the secondary lip seal (stacked Kapton P and FEP Teflon) had a scalloped edge on the inside diameter. (See figure 302.) No cracking was detected.
4. A white residue was found on the primary and secondary lip seals and on the retainers. X-ray inspection of this residue revealed Teflon particles. A more complete analysis could not be made because of insufficient material sample.
5. No evidence of moisture was found in the rig.
6. Figure 303 shows all of the dynamic seals tested on rig F-33443-5.

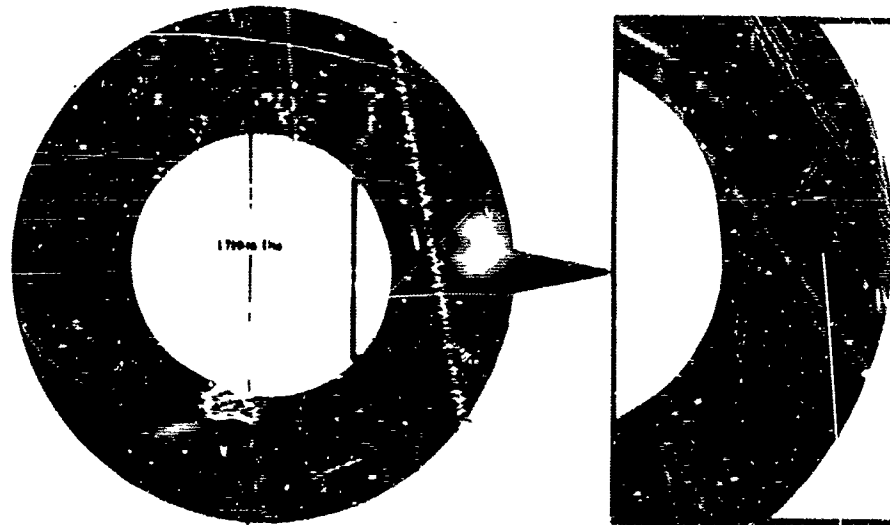


Figure 301. Primary Lip Seal After Test on
Rig F-33443-5

PD 22283A

UNCLASSIFIED

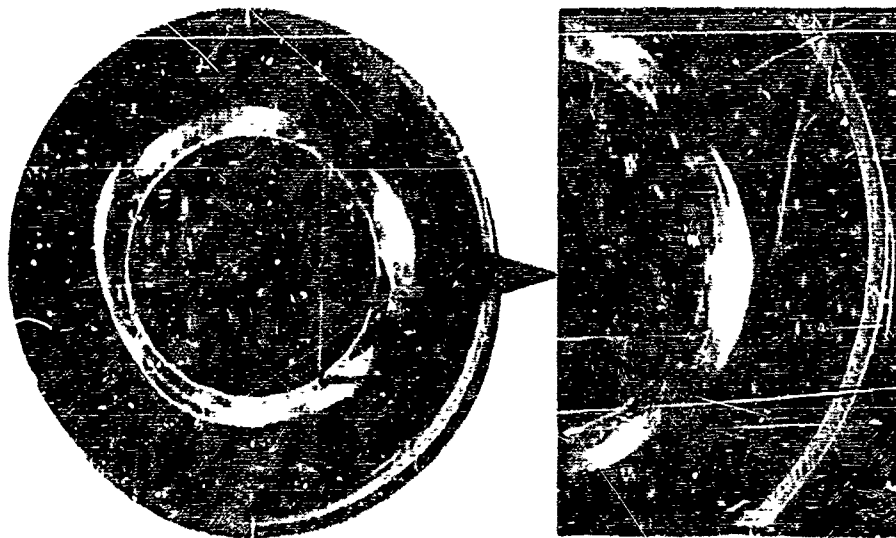


Figure 302. Secondary Lip Seal After Test
on Rig F-33443-5

FD 22253A

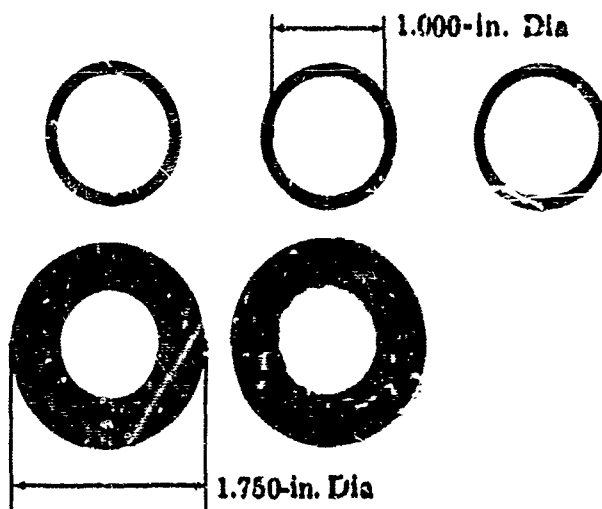


Figure 303. All Dynamic Seals Tested on
Rig F-33443-5

FD 23447

UNCLASSIFIED

CONFIDENTIAL

(6) Build No. 6

(a) Objective

(U) This build of the rotary shaft seal test rig was to investigate the leakage and endurance of graphite-filled Teflon Bal-Seals and laminated Kapton F and FEP Teflon lip seals.

(b) Configuration

(C) The sixth build of the test rig is shown in figure 304. Further modifications of the seal rig were as follows:

1. The secondary and vent lip seals were Mylar-FEP Teflon materials.
2. All Bal-Seals used in this build had been previously subjected to 10,000 actuation cycles and 500 pressure cycles during test of Rig F-33443-5.

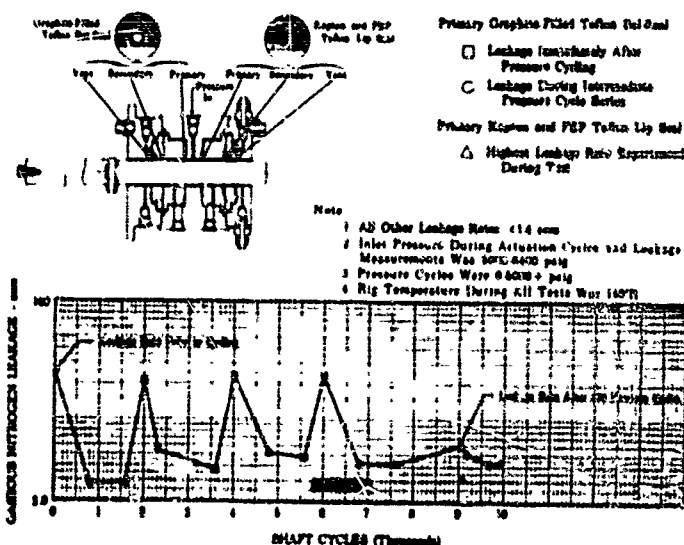


Figure 304. Rotary Shaft Seal Test Rig Leakage vs Cycles for Rig F-33443-6 FD 20151D

(c) Test Summary

(C) A total of 10,000 shaft cycles and 500 pressure cycles was completed. Pressure cycles were accomplished at approximate intervals of 2000, 4000, 6000, and 8000 shaft cycles. The rig was subjected to 125 pressure cycles at each interval. Shaft cycling was continuous throughout the test.

CONFIDENTIAL

(C) The primary Bal-Seal leakage rates during the test were highest prior to cycling and immediately after the 125, 250, and 375 pressure cycle series. The Kapton-Teflon lip seal leakage exceeded 1.4 acs only one time (at 9100 shaft cycles, 500 pressure cycles). All other seal leakage rates were less than 1.4 acs. The seal leakage rates experienced during the test are shown in figure 304.

(G) The test indicated that the static O-ring leakage rate for the Bal-Seal portion of the rig was affected by the primary Bal-Seal leakage rate. Post-test data with the rig at LN₂ temperature verified this condition.

(U) After completion of these tests, the teardown inspection revealed the following:

1. All Bal-Seals had inside diameter wear; however, no splitting was detected and seal appearance was good.
2. The primary lip seal (bonded Kapton F and FEP Teflon) was cracked through the Teflon Layer. The Kapton material had superficial fatigue cracks that looked like partial separation in the intermediate layers. (See figure 305.)
3. Graphite deposits were found on the rig shaft and in the seal glands on the Bal-Seal portion of the rig.
4. No evidence of moisture was found in the rig.
5. O-ring compression and sealing surfaces on the Bal-Seal portion of the rig appeared satisfactory.
6. The post-teardown inspection did not reveal any reason for the primary-to-static seal leakage interaction.

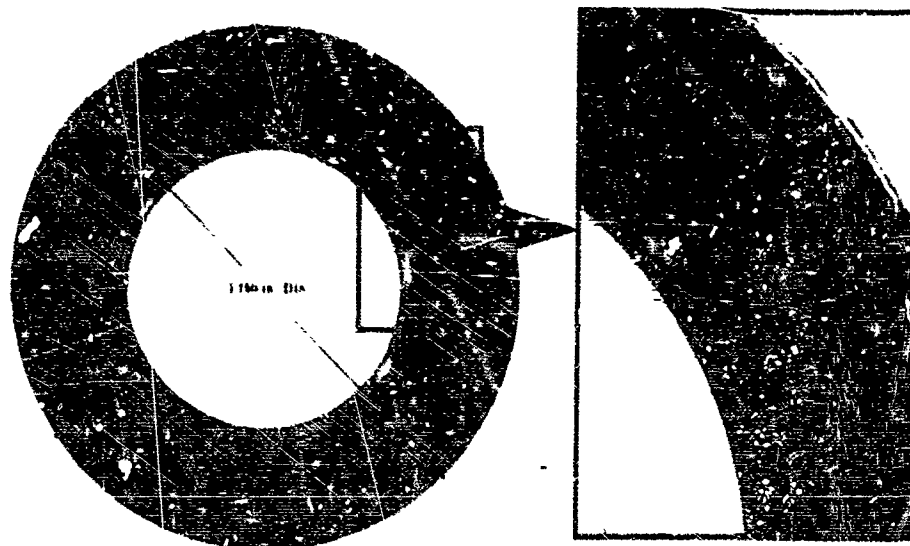


Figure 305. Primary Lip Seal After Test on
Fig F-33443-6

FD 22254A

CONFIDENTIAL

(7) Build No. 7

(a) Objective

(U) This build of the rotary shaft seal test rig was to investigate the leakage and endurance of graphite-filled Teflon Bal-Seals and laminated Kapton F and FEP Teflon lip seals.

(b) Configuration

(C) The seventh build of the test rig is shown in figure 306. Further modifications of the seal rig were as follows:

1. The secondary and vent lip seals were Mylar-FEP Teflon materials
2. All Bal-Seals used in this build had been subjected to more than 10,000 actuation cycles and 500 pressure cycles during testing of previous builds of this rig.
3. Outside diameter vent holes were made in the leakage isolation O-ring (Bal-Seal portion of rig only) and the seal was sandwiched between two pieces of 0.005-in thick Kapton F.

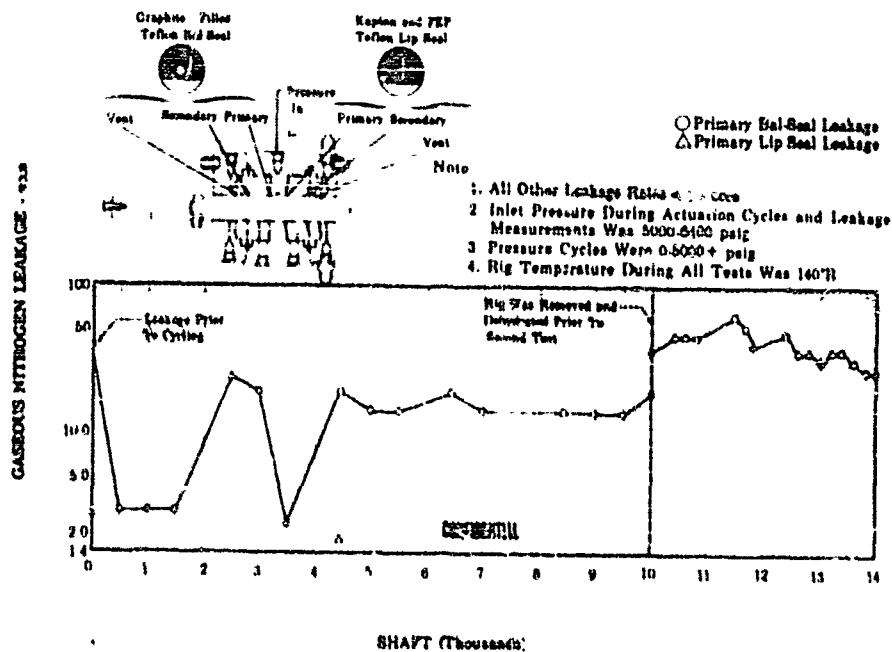


Figure 306. Rotary Shaft Seal Test Rig Leakage vs Cycles for Rig F-33443-7 FD 22234A

(c) Test Summary

(C) A total of 14,000 shaft cycles and 700 pressure cycles was completed. An initial 10,000 shaft cycles and 500 pressure cycles were performed (125 pressure cycles at approximate intervals of 2000, 4000, 6000, and 8000 shaft cycles). The test rig was vacuum baked at 160°F for 2 hours

CONFIDENTIAL

and then subjected to an additional 4000 shaft cycles and 200 pressure cycles. One hundred pressure cycles were conducted at approximate intervals of 1000 and 2000 shaft cycles. Data recorded during the additional 4000 shaft cycles and 200 pressure cycles indicated less interaction between the primary Bal-Seal and the static seals.

(C) The primary Bal-Seal had the highest measured seal leakage during the test. The Kapton F and FEP Teflon lip seal leakage exceeded 1.4 sccs only two times: prior to cycling and at 4463 shaft cycles and 250 pressure cycles. All other dynamic seal leakages were less than 1.4 sccs. The leakage rates for the seals tested are shown in figure 306.

(U) The teardown inspection revealed the following:

1. All Bal-Seals had inside diameter wear; however, no splitting was detected and seal appearance was good.
2. A yellow residue was found on the primary lip seal. No splitting or separation was observed and seal appearance was good. (See figure 307.)
3. Graphitic deposits were found on the rig shaft and in the seal glands on the Bal-Seal portion of the rig.
4. Slight moisture was detected in the secondary lip seal vent line and in the inlet line.
5. The leakage isolation O-ring was bent inward, indicating outside diameter pressurization.

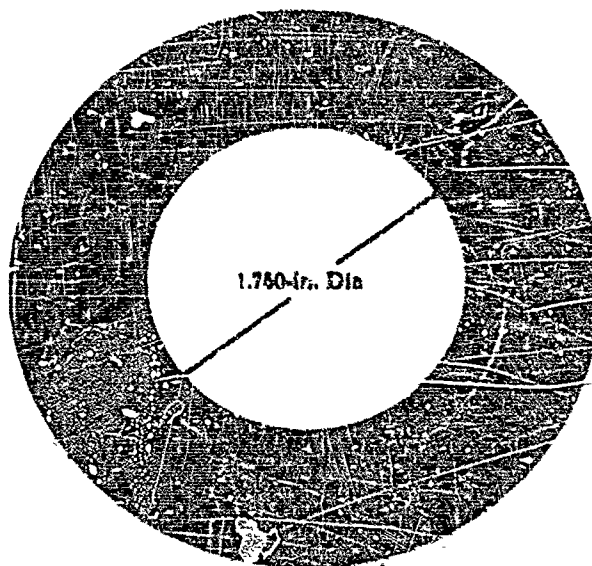


Figure 307. Primary Lip Seal After Test
on Rig F-33443-7

FD 23448

CONFIDENTIAL

(8) Build No. 8

(a) Objective

(U) This build of the rotary shaft seal test rig was to investigate the leakage and endurance of graphite-filled teflon Bal-Seals and a laminated Kapton F and FEP Teflon lip seal.

(b) Configuration

(U) The eighth build of the test rig is shown in figure 308. Further modifications of the seal rig were as follows:

1. The secondary and vent lip seals were Mylar-FEP Teflon materials.
2. Secondary and vent Bal-Seals used in this build had been subjected to actuation and pressure cycles during previous builds of this rig.
3. Bolt torque was increased to 500 in.-lb.

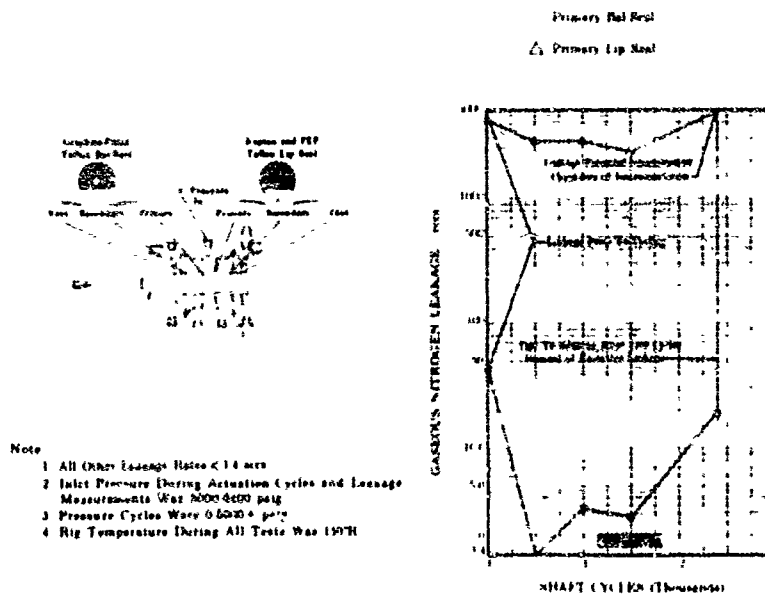


Figure 308. Rotary Shaft Seal test Rig Leakage vs Cycles for Rig F-33 43-8 FD 22578A

(c) Test Summary

(U) A total of 2400 shaft cycles and 15 pressure cycles was completed before excessive primary lip seal leakage was observed. Seal leakage interaction was also apparent between the primary Bal-Seal and the static seals on this portion of the rig.

CONFIDENTIAL

CONFIDENTIAL

(C) Primary Bal-Seal leakage was in the range of 42 to less than 1.4 secs. The primary lip seal leakage exceeded measurement capabilities at 2400 cycles. All other dynamic seal leakages were less than 1.4 secs. Leakage rates for the seals tested are shown in figure 308.

(E) The teardown inspection revealed the following:

1. All Bal-Seals had inside diameter wear; however, no splitting was detected and seal appearance was good.
2. The primary lip seal was split. (See figure 309.)
3. Kapton and graphite deposits were found on the rig shaft and graphite was found in the Bal-Seal glands.
4. No moisture or galling was detected in the rig.
5. All O-rings indicated normal compression.

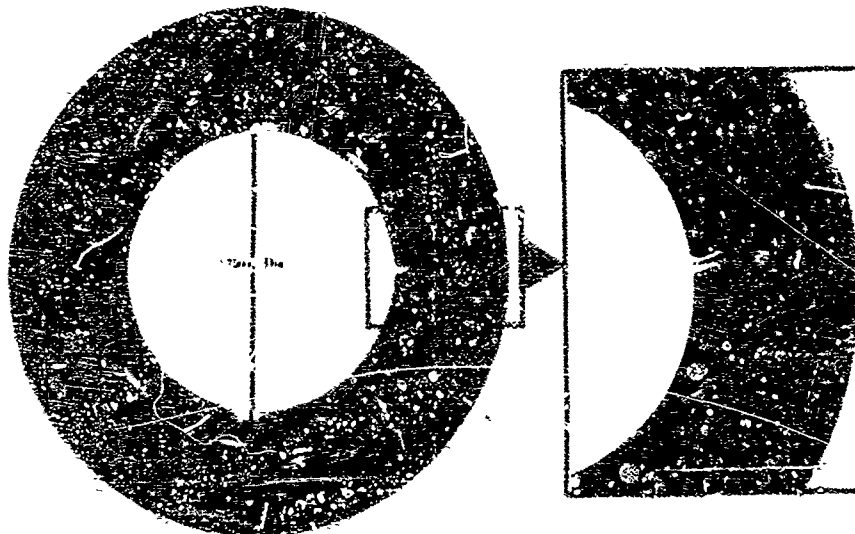


Figure 309. Primary Lip Seal After Test
on Rig F-33443-8

FD 2-784A

(7) build No. 9

(a) Objective

(1) This build of the rotary shaft seal test rig was to investigate the leakage and endurance of graphite-filled teflon Bal-Seals and a laminated Kapton I and FFI teflon lip seal.

(b) Configuration

(C) The ninth build of the test rig is shown in figure 310. Further modifications of the seal rig were as follows:

1. The secondary and vent lip seals were Nylar-FEP teflon materials.

CONFIDENTIAL

2. Secondary and vent Bal-Seals used in this build had been subjected to actuation and pressure cycles during previous builds of this rig.
3. The leakage isolation O-ring and the primary O-ring, located at the primary Bal-Seal interface, were placed between two pieces of 0.005-inch thick Kapton F.

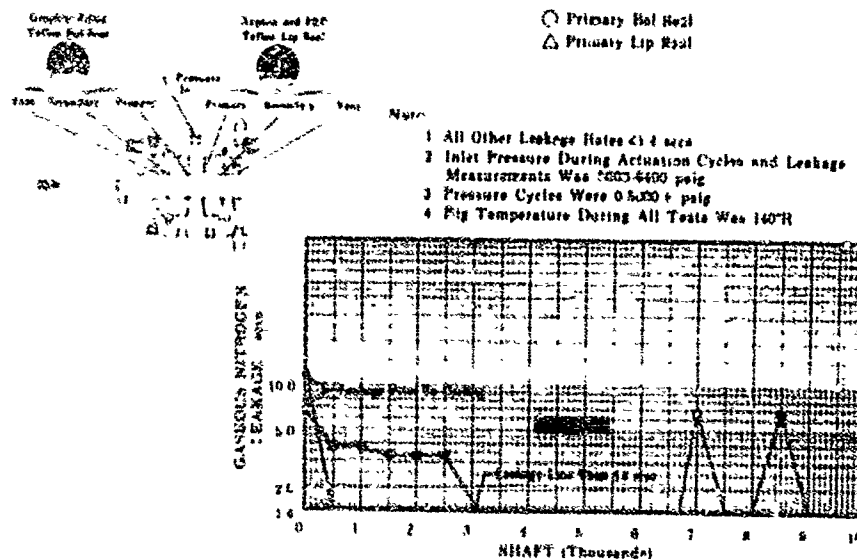


Figure 310. Rotary Shaft Seal Test Rig Leakage vs Cycles for Rig F-33443-9 FD 22579A

(c) Test Summary

(C) A total of 10,000 shaft cycles and 500 pressure cycles was completed. Pressure cycles were accomplished at approximate intervals of 2000, 4000, 6000, and 8000 shaft cycles. The rig was subjected to 125 pressure cycles at each interval and shaft cycling was continuous throughout the test.

(U) The primary Bal-Seal leakage rates during the test were highest prior to cycling and immediately after the first 125 pressure cycles. All other seal leakage rates were less than 1.4 ccs. The seal leakage rates experienced during the test are shown in figure 310.

(U) The test indicated that the static O-ring leakage rate for the Bal-Seal portion of the rig was not affected by the primary Bal-Seal leakage rate.

(U) After completion of these tests, the teardown inspection revealed the following:

1. All Bal-Seals had inside diameter wear; however, no splitting was detected and seal appearance was good.
2. The primary lip seal (bonded Kapton-Teflon) had superficial fatigue cracks that appeared to be partial separation in the intermediate layers.

CONFIDENTIAL

CONFIDENTIAL

3. Graphite deposits were found on the rig shaft and in the seal glands on the Bal-Seal portion of the rig.
4. Yellow Kapton powder was found on the rig shaft and in the primary lip seal gland.
5. Slight moisture was found in the primary lip seal vent line.
6. O-ring compression and sealing surfaces on the Bal-Seal portion of the rig appeared satisfactory.

(10) Build No. 10

(a) Objective

(U) This build of the rotary shaft seal test rig was to investigate the leakage and endurance of a laminated Kapton F and FEP Teflon lip seal with increased unformed inside diameter (9.875 in.).

(b) Configuration

(U) The tenth build of the test rig is shown in figure 311.

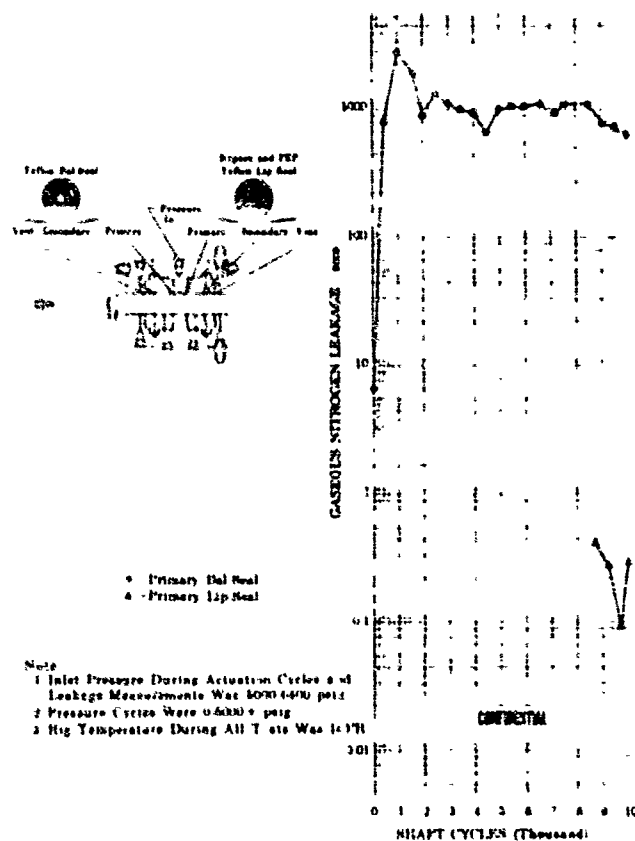


Figure 311. Rotary Shaft Seal Test Rig Leakage vs Cycles for Rig F-33443-10 FD 22749A

CONFIDENTIAL

CONFIDENTIAL

(U) Build No. 10 incorporated the following features:

1. The secondary lip seal was Kapton F and FEP Teflon and the vent lip seal was Mylar-FEP Teflon.
2. The secondary and vent Bal-Seals had been used in build No. 9.
3. All O-rings were replaced with one layer of 0.005-inch thick Kapton F positioned between adjacent interfaces.
4. Bolt torque was increased to 500 in.-lb.

(c) Test Summary

(C) A total of 10,000 shaft cycles and 500 pressure cycles was completed. Pressure cycles were accomplished at approximate intervals of 2000, 4000, 6000, and 8000 shaft cycles. The rig was subjected to 125 pressure cycles at each interval and shaft cycling was continuous throughout the test.

(C) The primary Bal-Seal leakage rate was highest at 100 cycles and decreased during the remainder of the test. Slight leakage was detected at the vent lip seal cavity. All other leakages were less than 1.4 scs. The seal leakage rates experienced during the test are shown in figure 311.

(U) The test indicated that the static seal leakage rate for the Bal-Seal portion of the rig was not affected by the primary Bal-Seal leakage rate.

(U) After completion of these tests, valve disassembly revealed the following:

1. All Bal-Seals had inside diameter wear and the primary Bal-Seal was split.
2. The primary lip seal had inside diameter wear as shown in figure 312.
3. Kapton powder was in the primary lip seal cavity.
4. Graphite deposits were found on the rig shaft and in the secondary seal glands on the Bal-Seal portion of the rig.

3. Test Facilities and Procedures

a. B-21 and B-22 Test Stands

(U) Test stands B-21 and B-22 (See figures 313 and 314.) were used for control component tests. Control calibrations and cycle tests are conducted on the closed loop water blowdown facility, B-21 stand, and on the high pressure GN2 flow bench with cryogenic cooldown capabilities. The water flow loop consists of a 2100-gallon run tank, which when filled is pressurized to the required level from a 5000-psia nitrogen source. The tank is capable of supplying 1500-psia water to the inlet of the test item at flow rates up to 450 lb/sec. The water passes through electro-

CONFIDENTIAL

hydraulic control valves that will set the preprogramed flow versus pressure ramp to the test item. A 20-channel analog computer is used for this purpose. The water flows through the test section and into a catch tank, which recovers the working fluid. The recovered water is then pumped back to the run tank for reuse. Turbine flowmeters are used for flow measurement, and data are recorded on strip charts and on an 18-channel oscillograph. A minimum test duration of 30 seconds is attainable with this system when operating at the maximum flow rate.

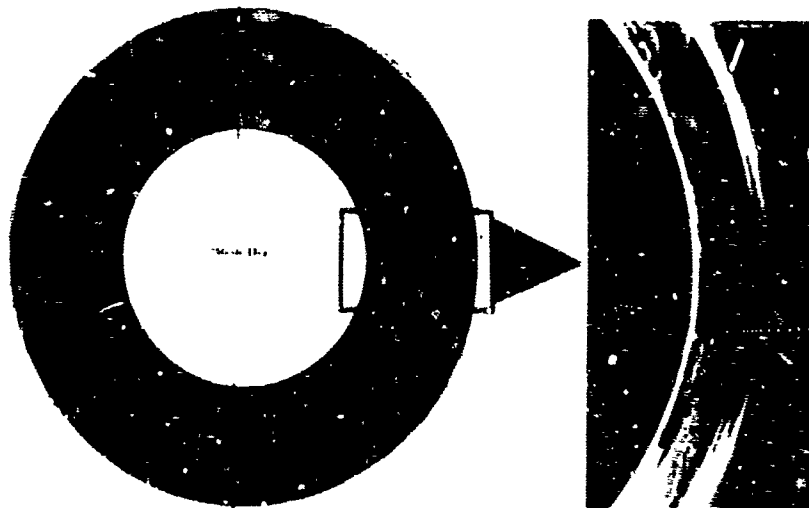


Figure 312. Primary Lip Seal After Test
on Rig F-3443-10

FD 22726A

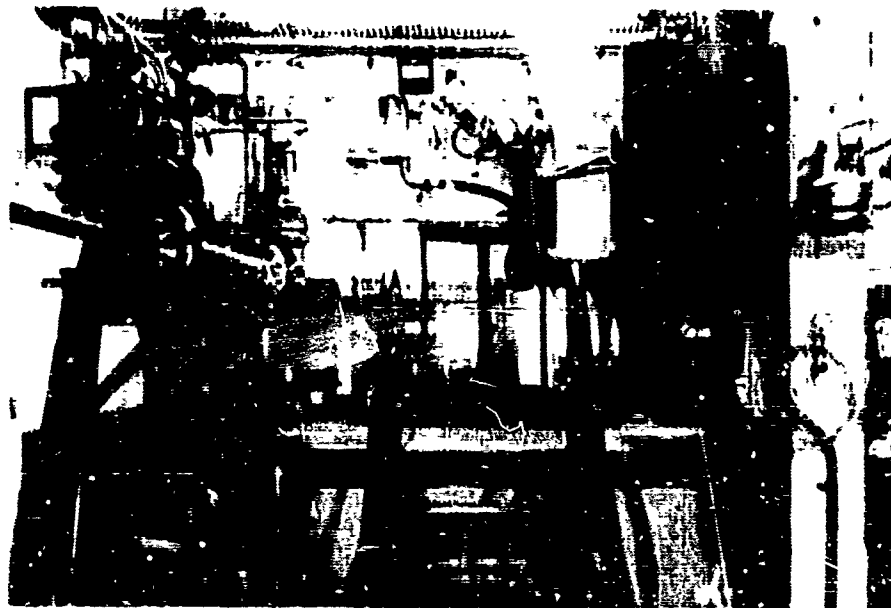


Figure 313. B-21 Control Calibration Facility

FC 13775

CONFIDENTIAL

(This page is Unclassified)

CONFIDENTIAL

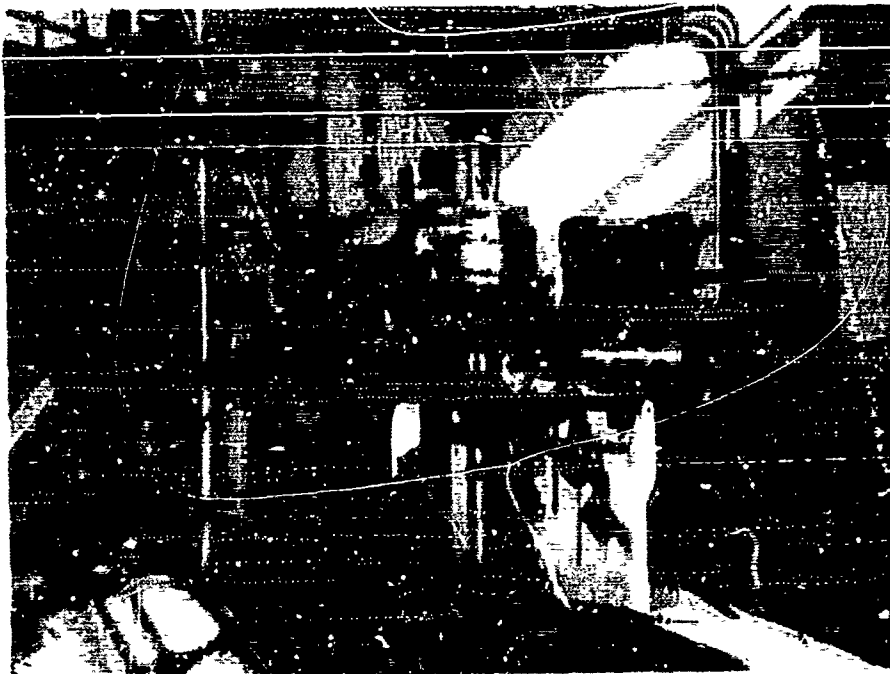


Figure 314. B-22 Cryogenic Static Cycle Stand FC 13799

(U) The high pressure GN_2 flow loop on B-22 stand consists of a 10,000 psig GN_2 supply, electropneumatic control valves, and turbine flowmeters. A large dewar cooldown tank is available for cryogenic temperature tests. This stand uses the same analog computer, strip charts, and other control and recording facilities as B-21 stand.

b. Test Procedures

(U) For water flow calibration, the valves were mounted in the B-21 water flow test stand as shown in figure 315 and were instrumented as shown schematically in figure 316.

(U) The water flow calibration was performed by positioning the shaft and setting specified valve differential pressures. Data were recorded on strip charts and O-graphs.

(U) For the flow torque test, the valve actuators were removed and a torque arm attached to the shaft coupling. A load cell was used to measure the applied load, as shown in figure 317.

(U) The tests were performed by positioning the valve shaft, setting the valve differential pressure, and recording the output from the load cell. The data were recorded on strip charts and O-graphs.

(C) For environmental tests, the valves were mounted in the B-22 test stand as shown in figure 318 and instrumented as shown schematically in figure 319. Environmental tests were performed by pressurizing the valve with LN_2 at internal pressures from 50 to 6000 psig. The valves were cycled at these conditions and valve seal leakages were measured periodically.

CONFIDENTIAL

CONFIDENTIAL

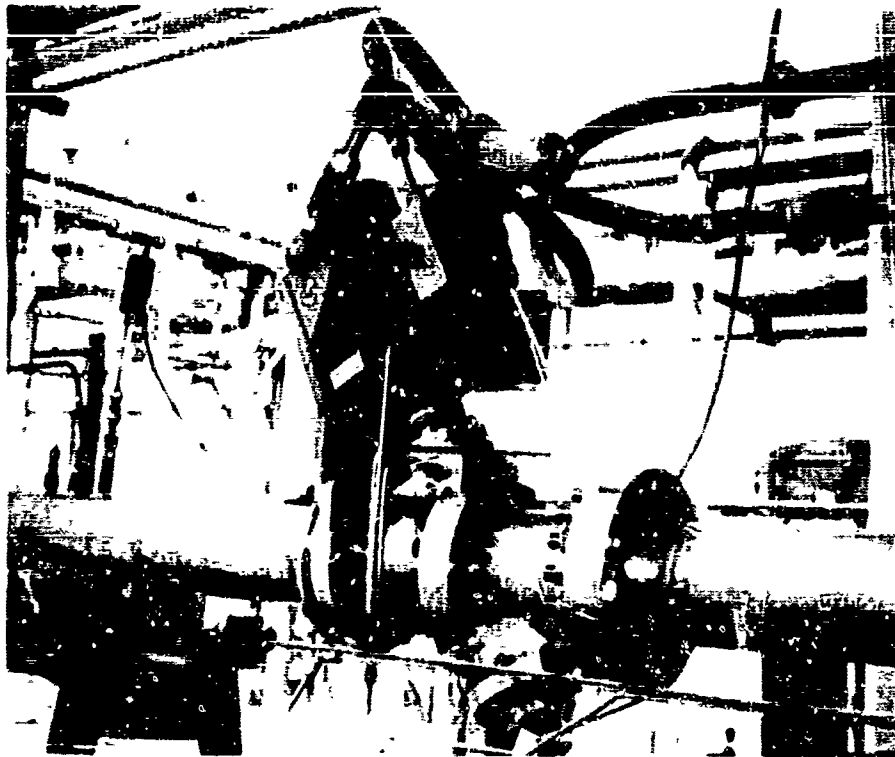
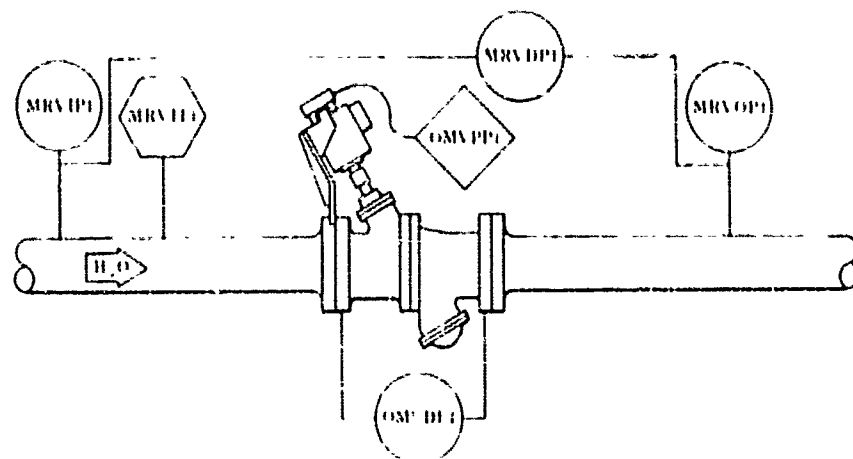


Figure 315. Mixture Ratio Valve Assembly
Mounted in B-21 Waterflow Test
Stand

FE 68515



| Header | Description | Header | Description |
|---------|-----------------------|---------|---------------------------|
| MRV DPI | MRV Inlet Pressure | OMV DPI | MRV Differential Pressure |
| MRV TI | MRV Inlet Temperature | OMV OPI | MRV Orifice Pressure |
| MRV OPI | MRV Orifice Pressure | | |

Figure 316. Mixture Ratio Valve Instrumenta-
tion Schematic (B-21 Stand)

FD 22750A

CONFIDENTIAL

(This page is Unclassified)

CONFIDENTIAL

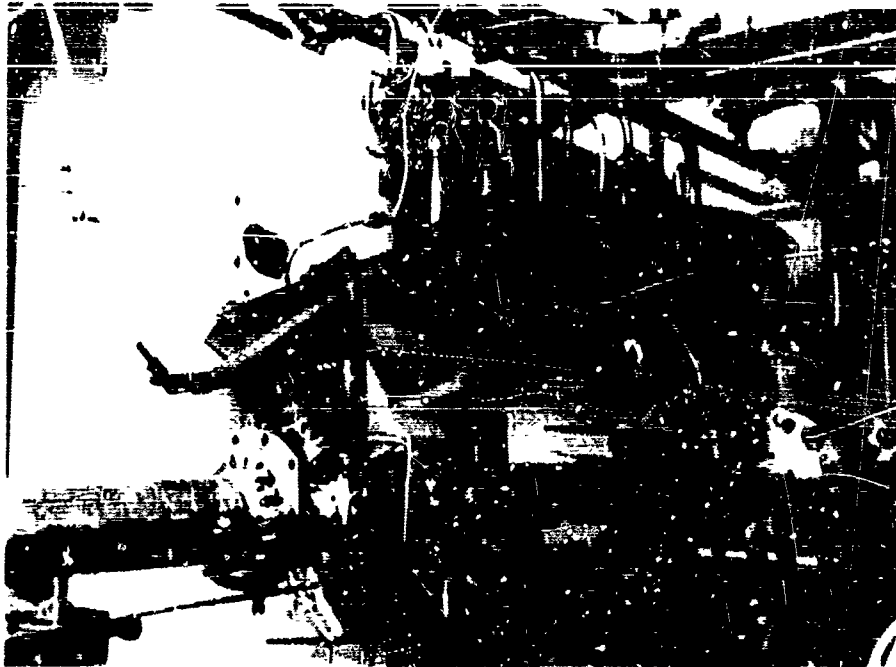


Figure 317. Flow Torque Test Installation

FE 67780

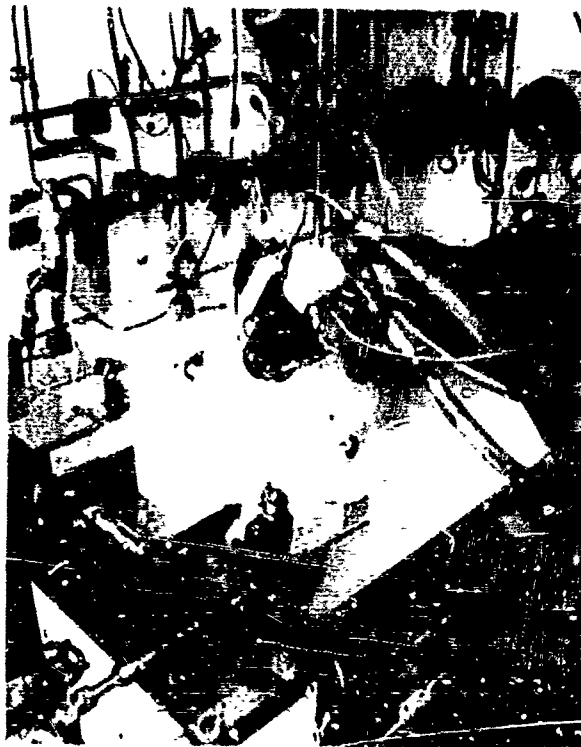


Figure 218. Mixture Ratio Valve Rig F-33466-5
During Cryogenic Endurance Testing

FE 71279

3 of

CONFIDENTIAL

(This page is Unclassified)

CONFIDENTIAL

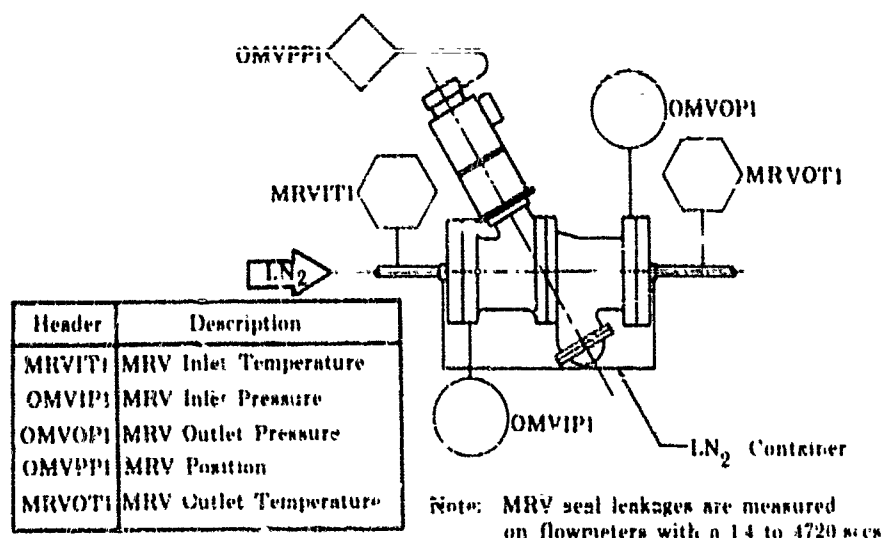


Figure 319. Mixture Ratio Valve Instrumentation Schematic (B-22 Stand)

FD 23066

(C) For environmental endurance tests, the rotary shaft seal test rig was mounted in B-22 test stand as shown in figure 320. Environmental tests were performed by conditioning the rig at LN₂ temperature and pressurizing with GN₂ up to 6700 psig. The rig shaft was cycled by a double-acting pneumatic actuator. Pressure cycles were performed by alternately increasing and decreasing rig inlet pressure. Seal leakages from the rig vents were measured periodically throughout the continuous cycle program. The standard program was a 10,000 shaft actuation cycle with 500 pressure cycles (0-5000 psig) performed in 125-cycle increments at intervals of 2000 shaft cycles.

4. Conclusions

(U) Control of the overall engine mixture ratio required a valve upstream of the main injector. Based on results of the valve-type selection study, a 3-inch diameter butterfly valve was selected for design, procurement, and test. A commercial rotary hydraulic servoactuator was adapted to the valve, and two valve assemblies were procured.

(U) Some changes to the valve were incorporated during Phase I to obtain the required position accuracy and seal durability. The actuator support was changed to a cylindrical shape to improve torsional stiffness. The original design piston ring seal, which was mounted in the butterfly disk, was replaced with a housing-mounted laminated plastic seal.

(U) A rotary shaft seal test rig was built and a shaft seal test program was conducted to define an acceptable seal.

(U) The mixture ratio valve met its primary objectives of substantiating the design calculations for flow modulation, and providing satisfactory

CONFIDENTIAL

CONFIDENTIAL

modulation, response, and shutoff capability for the staged-combustion rig tests. Static seal problems were encountered. The Teflon-coated metal O-rings used for static seals throughout the valve leaked during high pressure component tests and during staged-combustion rig tests. The leakage is attributed to flange deflection with internal pressure and the inability of small diameter metal O-rings to accommodate deflection and maintain a seal. Tests to determine the flange deflection were started near the end of the program; additional work is necessary to solve the problem.

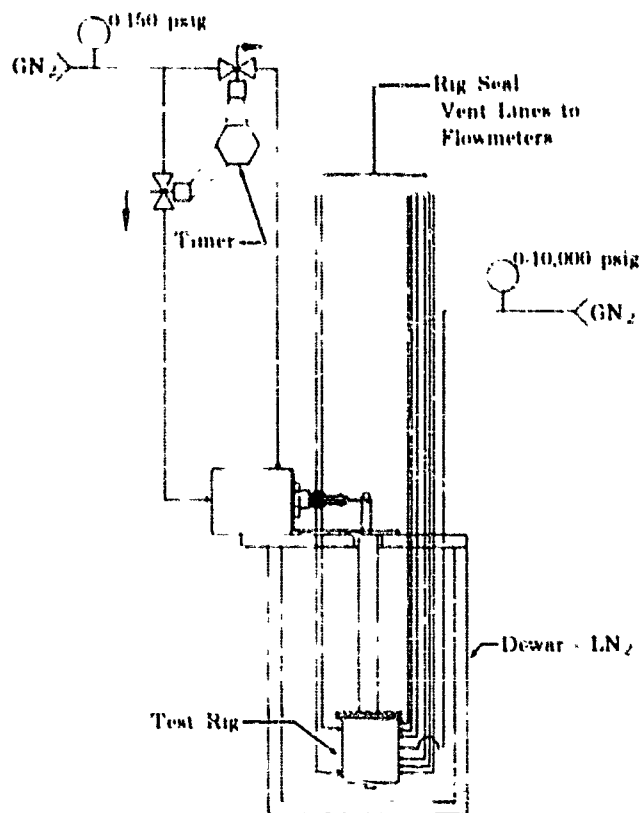


Figure 320. Rotary Shaft Seal Test Rig
Schematic for B-22 Stand

FD 23067

(U) The target disk seal leakage of 10 secs was not attained. After incorporation of the housing-mounted disk seal, which was required for seal durability, several seal modifications were tested, but none met the target.

(U) Valve operation was consistent and reliable throughout the staged-combustion rig test program, and the rig requirements for the valve were satisfied.

CONFIDENTIAL

(This page is Unclassified)

CONFIDENTIAL

(C) Ten build, test, and inspection cycles were completed on the rotary shaft seal rig and are summarized in table XXV. The first tests indicated that the formed lip-type seal was superior to spring-loaded cup seal designs. Lip seals combining Mylar and Teflon sheet did not possess satisfactory life during pressure cycling. Substitution of FEP Teflon for the TFE Teflon, and replacement of the Mylar with Kapton F, resulted in a seal configuration that passed the 10,000 actuation cycle and 500 pressure cycle (0-5000 psig \pm) test exposure with no failure and less than 1.4 secs GN₂ primary seal leakage throughout the test.

(U) The heat bonding procedures used for laminating the Kapton and FEP Teflon lip seals were later applied to static seal and disk seal parts fabricated from these materials.

(U) The rotary shaft seal test rig test goal of 10 secs maximum overboard leakage was attained. The rig was stored at the end of the program.

(U) Solution of the static seal problem will require additional tests and analysis, and the solution will be applicable to seal areas throughout the high pressure engine.

(U) Achieving disk seal leakage below 10 secs with an adequate seal life will require more development.

C. FLOW DIVIDER VALVE AND SEAL RIG

1. Hardware Description

a. General

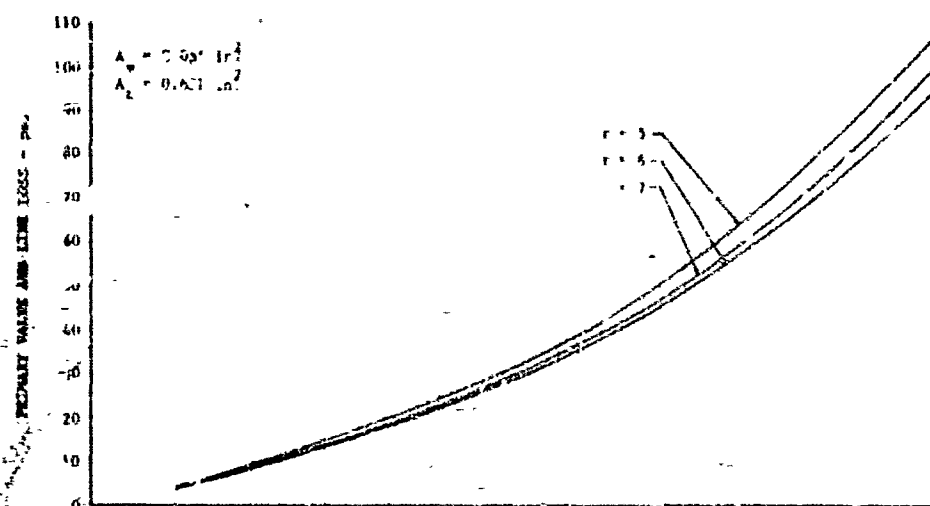
(U) Figures 321, 322, and 323 define the performance requirements for the flow divider valve as established by engine cycle analysis. In addition, the valve was required to shut off the preburner oxidizer flow and sequence the igniter oxidizer supply.

(U) The four most promising candidates for the flow divider valve were studied in sufficient detail to compare their overall performance. These were valves using the pintle-orifice, the pintle-venturi, the translating sleeve, and the ball and rotating sleeve concepts. In addition to these studies, five other concepts were investigated until a critical problem or disadvantage was determined that resulted in elimination from further consideration. If no critical problem developed, the scheme was compared with the original four concepts.

(U) Those concepts investigated to a point where a serious problem arose were: (1) rotating plate, (2) rotary sleeve with a cam-activated poppet shutoff, (3) ball, (4) butterfly, and (5) rotary sleeve.

CONFIDENTIAL

CONFIDENTIAL



CONFIDENTIAL

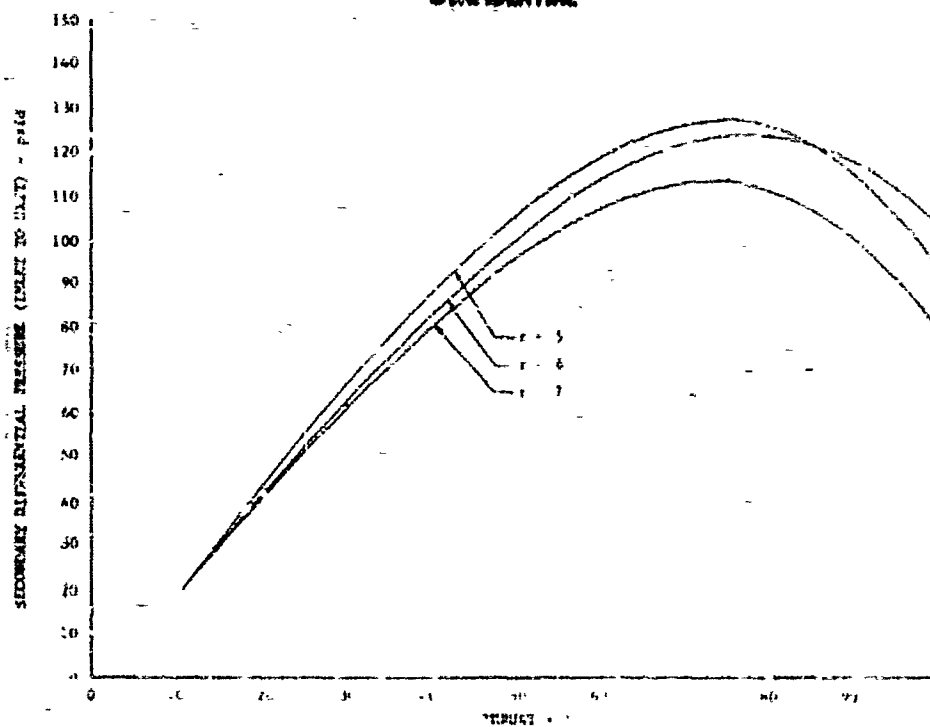


Figure 321, Flow Divider Valve R₁ Pressure Drop vs Percent Thrust DB 52262

CONFIDENTIAL

CONFIDENTIAL

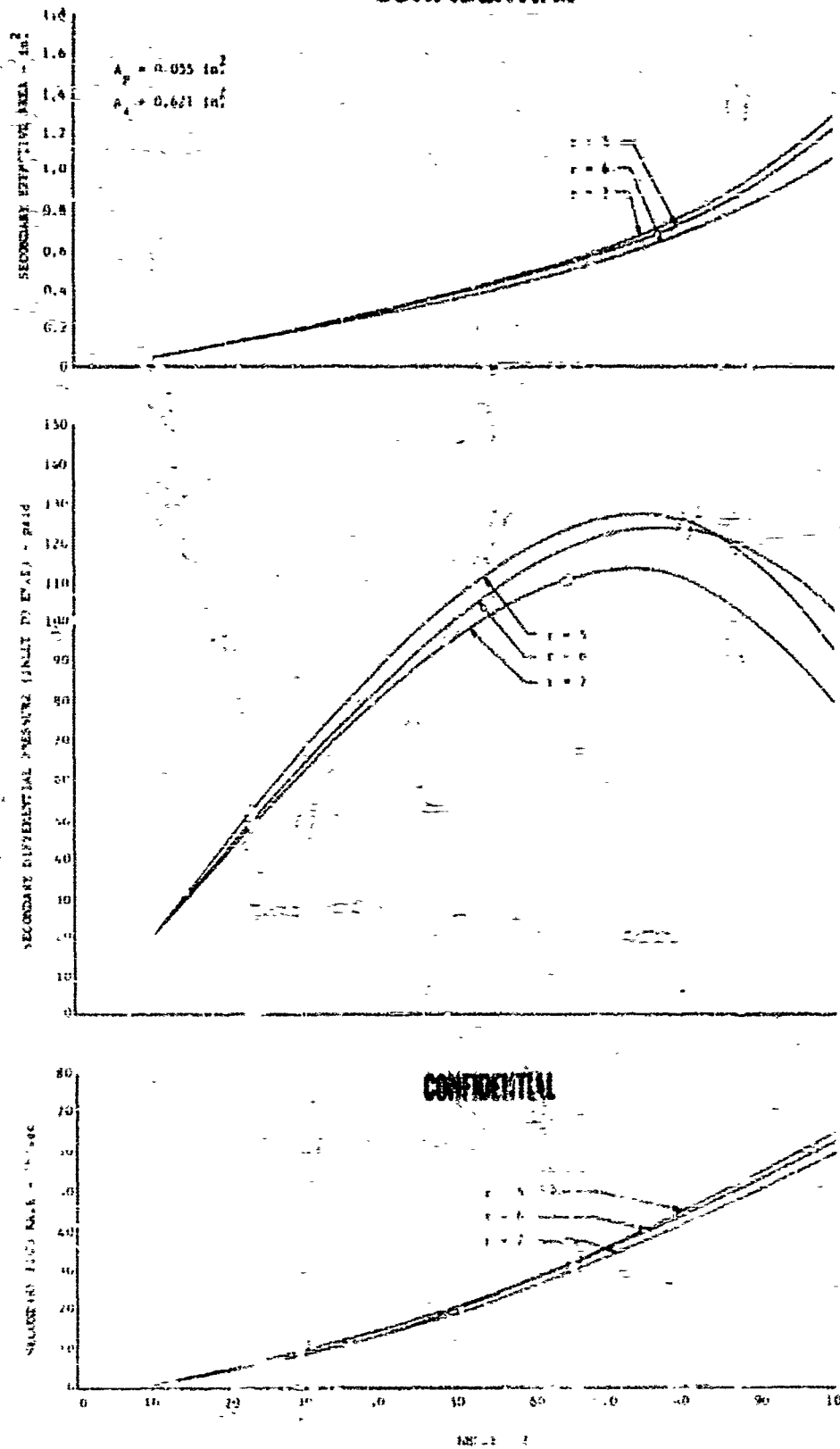


Figure 322. Flow Divider Valve Rig Design
 Requirements for Operation
 from 10 to 100% Thrust

D-32267

- 356 -

CONFIDENTIAL

CONFIDENTIAL

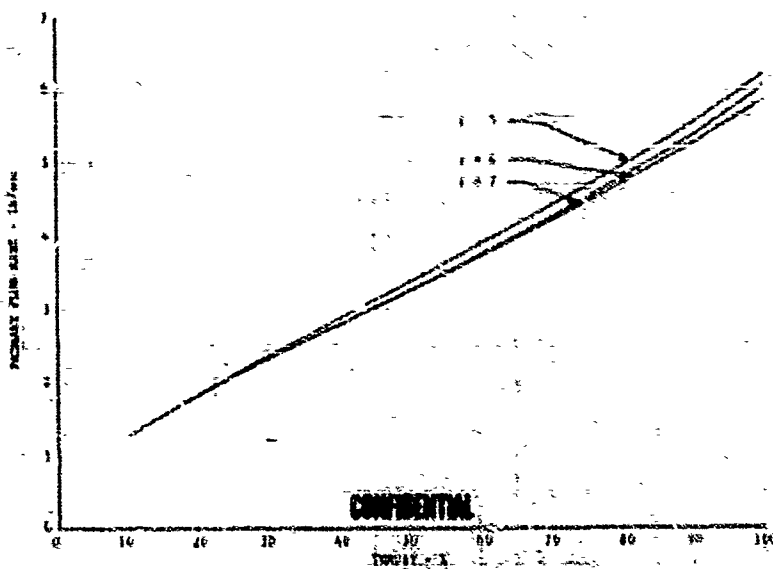


Figure 323. Flow Divider Valve Primary
Flow Rate vs Percent Thrust

DF 39534

(C) All concepts considered were to satisfy the following basic ground rules:

1. The valve should have a flow capacity equal to 120% of the maximum secondary flow with a secondary valve ΔP of 150 psi to allow for injector modification.
2. Primary flow must be scheduled from zero to 10% thrust to include the engine starting sequence.
3. Secondary flow must be shut off to approximately 10% and scheduled to the maximum area required.
4. The valve must fit inside the preburner injector dome and be removable from the dome as a unit for calibration.
5. The valve must be removable from the dome without removing the dome from the preburner.
6. The valve must be pressure balanced to minimize the required actuation force.
7. The valve must provide positive shutoff of preburner oxidizer flow.
8. The valve type must be suitable for use as a thrust control.

CONFIDENTIAL

b. Valve Type Selection

(1) Pintle-Orifice Candidate (See figure 324.)

(C) The pintle-orifice concept distributes the primary flow by exposing a series of slots in the valve housing, with more open area being exposed as the pintle moves toward opening the secondary area. Secondary flow remains shut off until the full 10% thrust primary flow area is exposed. Secondary flow is regulated by moving a contoured plug into the fixed orifice.

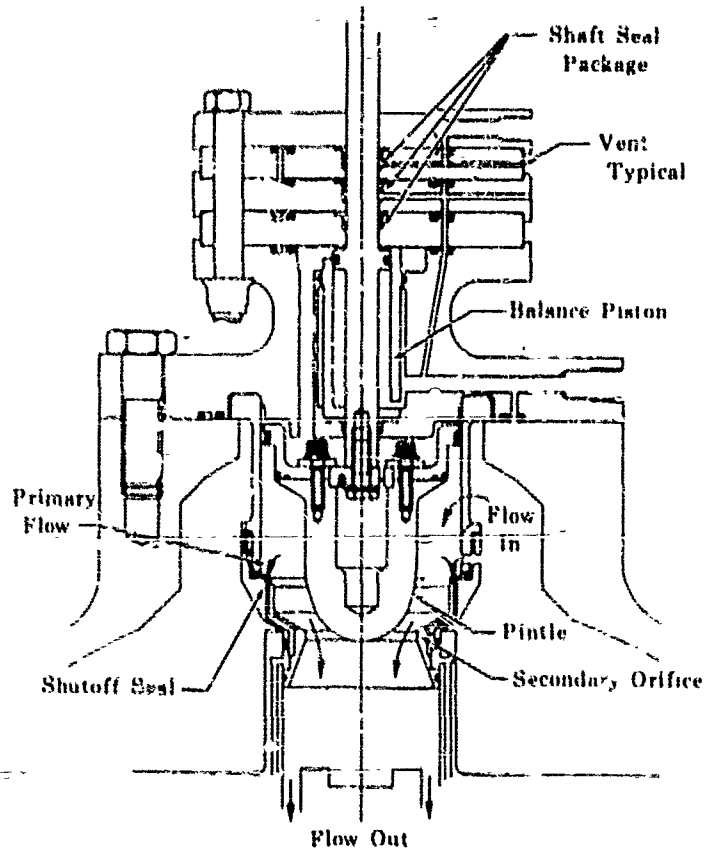


Figure 324. Flow Divider Valve, Pintle-Orifice Candidate

FD 18173A

(U) The required valve geometric flow area is determined from the secondary flow rate, valve pressure drop, and pressure recovery conditions. Figure 325 is a plot of geometric flow area as a function of thrust level and mixture ratio.

(U) Figure 326 is a contour plot of the pintle based on a constant percentage profile.

(U) The percent area error is plotted as a function of percent positional error in figure 327. The sensitivity of area error with respect to valve windup ratio is illustrated in this plot.

CONFIDENTIAL

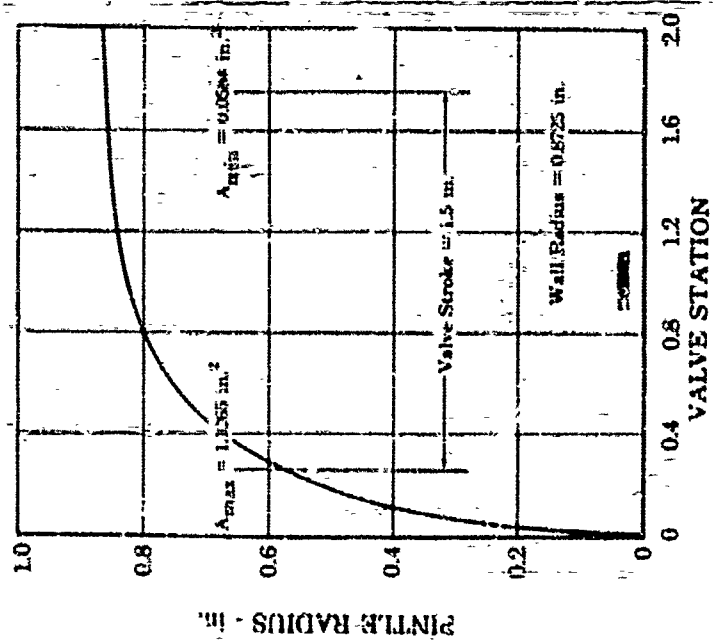
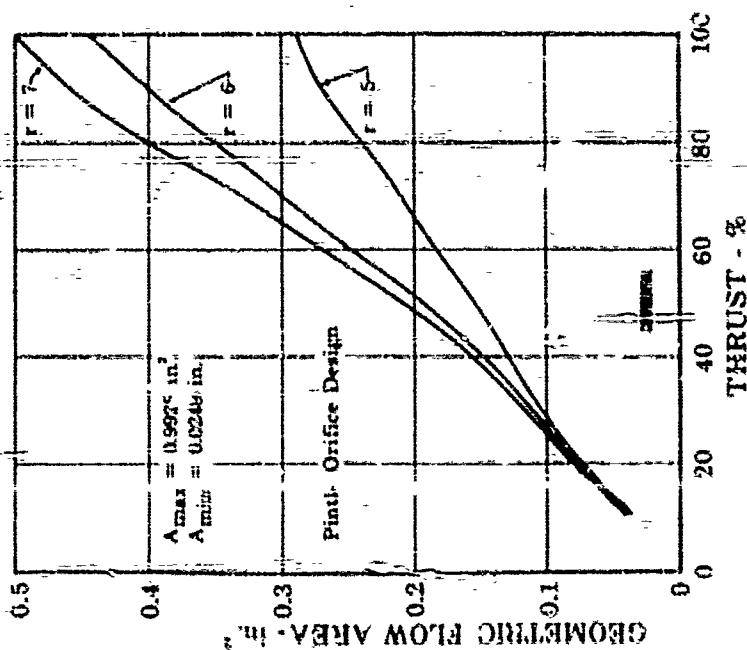


Figure 326. Flow Divider Valve Required Contour

Figure 325. Preliminary Flow Divider Valve Required Area



CONFIDENTIAL

CONFIDENTIAL

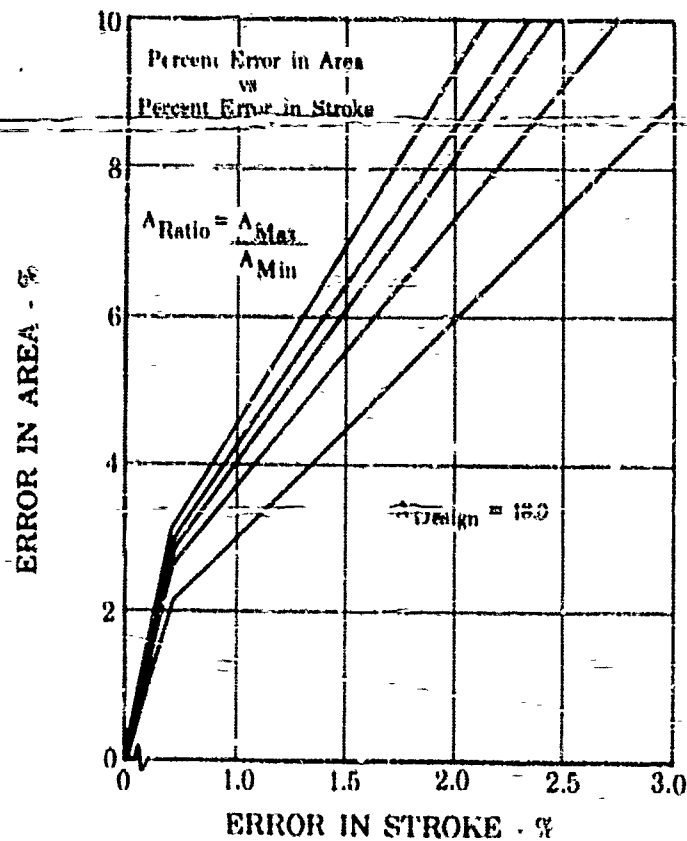


Figure 327. Percent Error in Area vs Percent Error in Stroke for Preburner Flow Divider Valve FD 18159

(U) Integrating the static pressure profile over the bullet face yields the valve opening force. This force is illustrated in figure 328 as a function of thrust level and mixture ratio.

(C) The maximum hydraulic force acting on the pintle was determined to be 2510 lb at maximum power and a mixture ratio of 5. A thrust balance piston area c. 0.442-in.² was incorporated to offset these forces. This piston area resulted in a predicted force unbalance of 60 lb over the engine operating range. Seal and bearing friction was not investigated for this scheme.

(U) Positive shutoff at zero thrust was provided by axial contact of the pintle with a plastic seat inset in the valve housing. The secondary flow area remain shut off during the start and idle transient. This is accomplished by a piston ring seal upstream of the primary ports and a radial seal in the approach to the orifice throat.

CONFIDENTIAL

CONFIDENTIAL

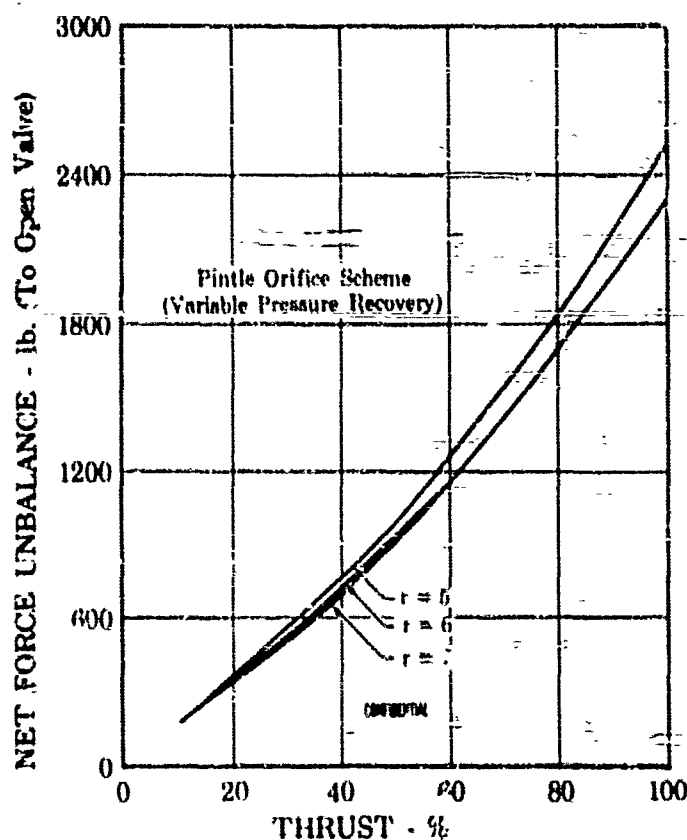


Figure J28. Noncompensated Force Balance
vs Percent Thrust (Preburner
Flow Divider Valve)

FD 18158

(U) Because the secondary flow area around the pintle is an extremely narrow annulus at the low flow condition, concentricity control is critical and has a great effect on discharge coefficient. At larger areas, concentricity becomes less important. This characteristic required that squareness and concentricity be held to very close tolerances, and that special assembly techniques be used in sizing the annulus.

(U) The orifice size was based on a predicted pressure drop and discharge coefficient. Therefore, results of initial bench testing must be used to modify the pintle contour and orifice size to provide desired performance. Possible development problems were predicted with the piston ring seal at high pressure differentials. Another problem was predicted with the radial secondary seal, because it was fully withdrawn from its sealing surface in most of the valve operating range, and it was susceptible to damage when re engaged.

CONFIDENTIAL

CONFIDENTIAL

(2) Pintle-Venturi Candidate (See figure 329.)

(5) The pintle-venturi candidate shown in figure 329 to the flow divider valve was investigated to take advantage of the pressure recovery made available by the venturi, allowing the use of a smaller pintle and throat diameter and resulting in a large weight flow per unit throat area for a given valve flange-to-flange pressure loss. Combining the pressure recovery factor with the required flow rate and valve loss yields a required geometric flow area. Figure 330 is a plot of the required geometric flow area as a function of thrust level and mixture ratio. The pressure recovery factor varies with the venturi throat area and the shape of the pintle at the throat. Figure 331 is a plot of valve pressure recovery as a function of thrust level and mixture ratio. Once the turndown ratio of the valve is determined, the pintle contour can be established. Figure 332 is a plot of the required pintle position as a function of thrust level and mixture ratio. This was determined by establishing a constant percentage contour based on a valve stroke and turndown ratio. Knowing the required flow area then established the pintle position with a constant percentage contour.

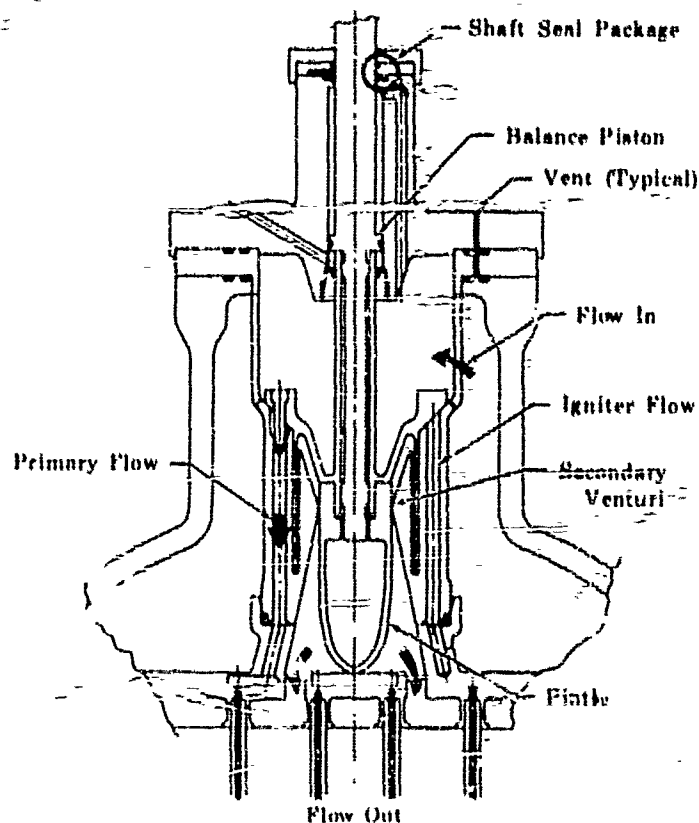


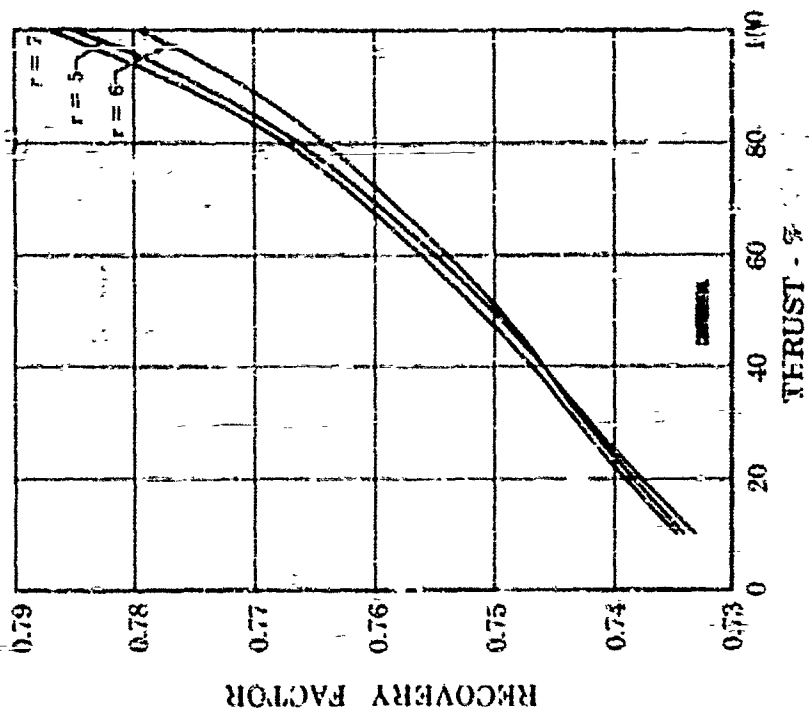
Figure 329 Flow Divider Valve, Pintle-Venturi Candidate

FD 18000A

CONFIDENTIAL

(This page is Unclassified)

CONFIDENTIAL



FD 17998

Pressure Recovery vs
Percent Thrust (Flow
Divider Valve)

Figure 331.

FD 17997

Pintle Venturi Flow Area
vs Percent Thrust
(Flow Divider Valve)

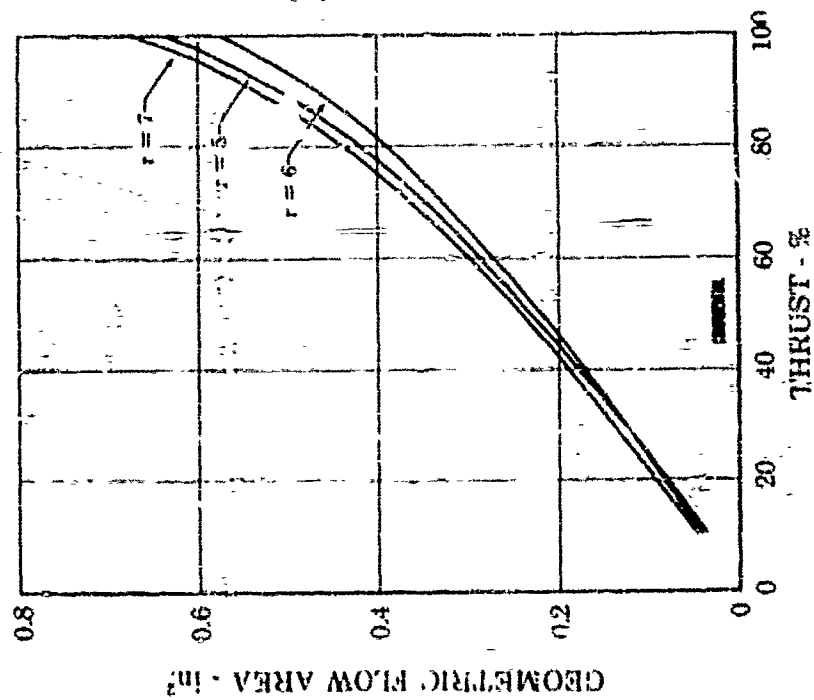


Figure 336.

CONFIDENTIAL

CONFIDENTIAL

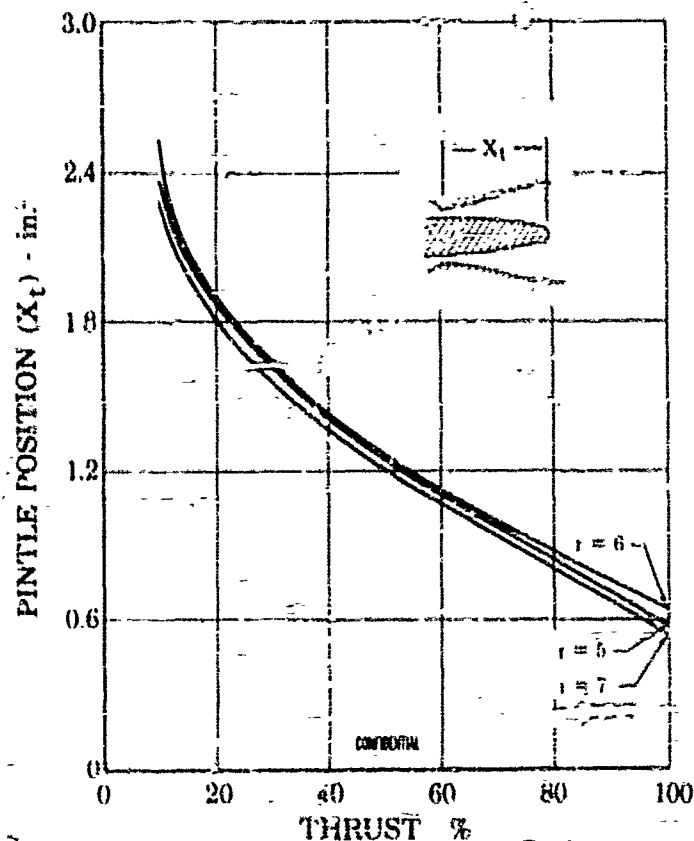


Figure 332 - Pintle Position vs Percent Thrust
(Flow Divider Valve)

FD 18217

(U) Integrating the static pressure profile along the face of the pintle yields the valve opening force. Figure 333 is a plot of this force as a function of thrust level and mixture ratio.

(U) Summing the various pressure area terms that tend to close the valve, and adding them vectorially with the opening force yields the net axial force. This force is plotted in figure 334 as a function of thrust and mixture ratio. If an attempt is made to "match" the closing force with the opening force (compensation), the resulting net force is shown in figure 335 as a function of thrust and mixture ratio.

(C) Selecting a 0.750-in. diameter shaft produced a net force unbalance of 2100 lb, which required incorporation of a thrust balancing area. This was established as 0.344-in.². Adding this to the shaft diameter produced a piston diameter of 1.000 inch. Bearing and seal friction was not considered in this investigation.

(U) Shutoff was accomplished with a poppet valve coupled to the main pintle. This feature presented a disadvantage in that the poppet must be lapped to the seat, which is a part of the valve housing, and must remain as a matched set.

CONFIDENTIAL

CONFIDENTIAL

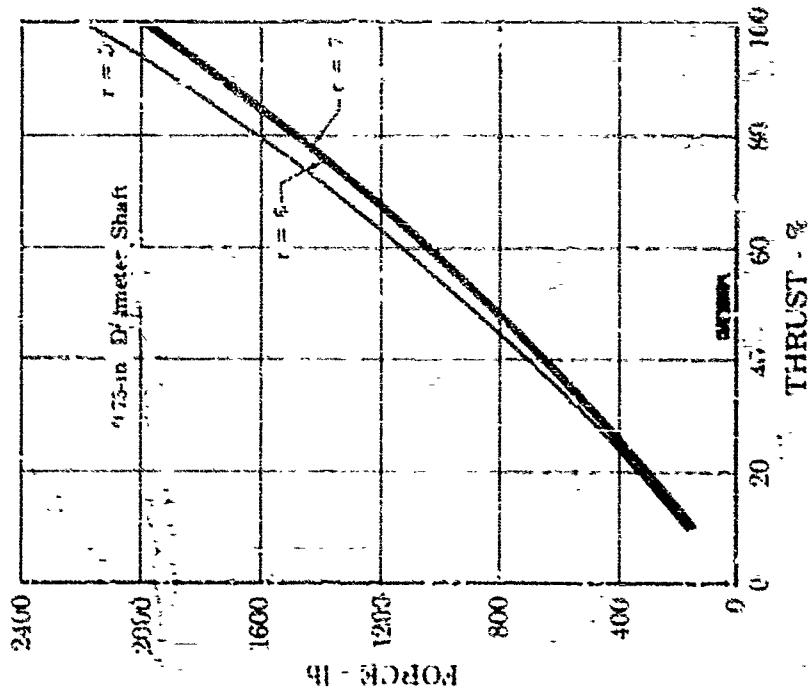


Figure 335. Flow Divider Valve Net
Pintle Force vs Percent
Thrust (Noncompensated)

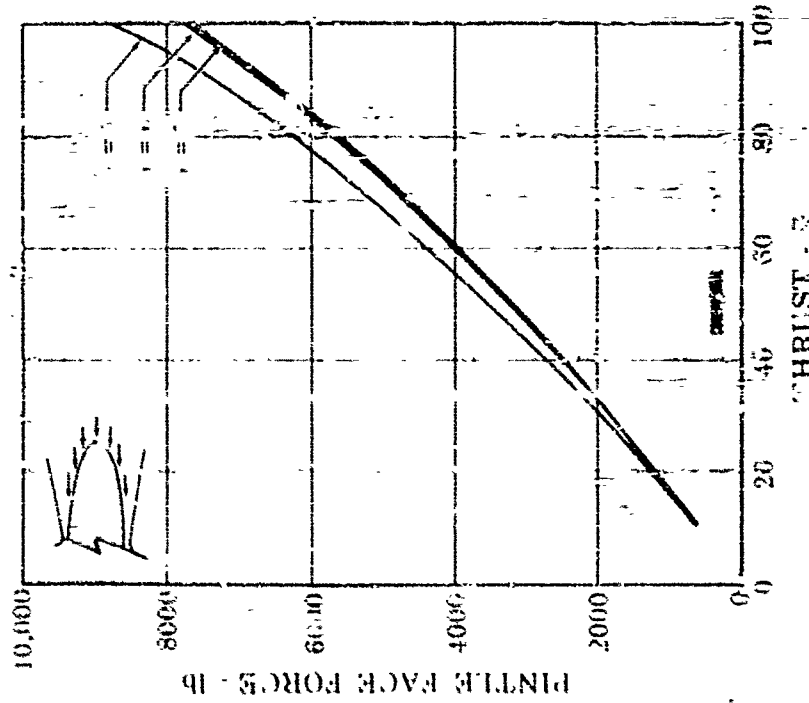


Figure 333. Pintle Face Force vs
Percent Thrust (Flow
Divider Valve)

CONFIDENTIAL

CONFIDENTIAL

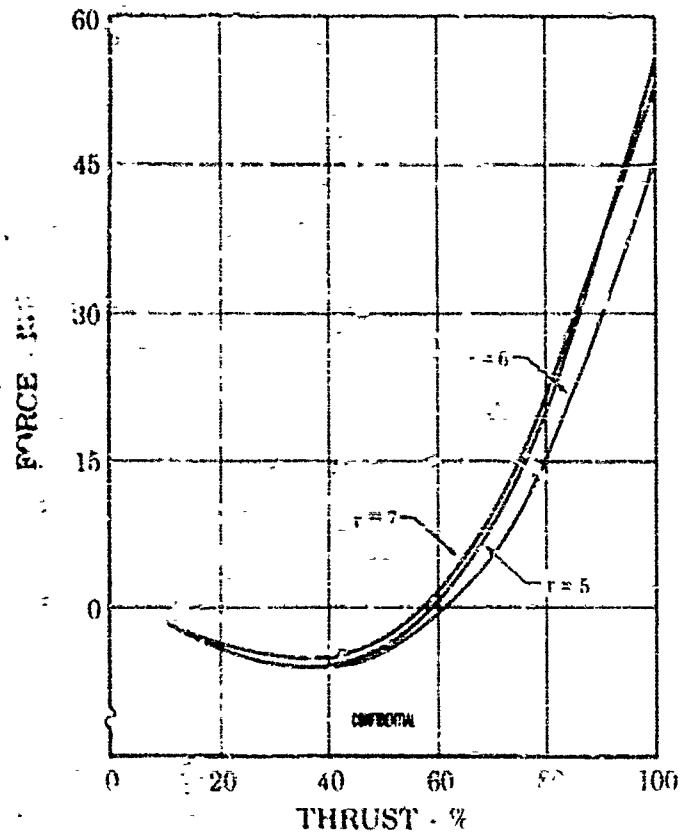


Figure 335. Flow Divider Valve Net Pintle
Force vs. Percent Thrust
(Compensated)

FD 18207

(C) The primary flow was modulated with centered rods, which are located in the poppet valve head, that protrude into the orifices in the poppet valve seat. These rods regulate primary flow through the starting transient and become completely disengaged above 10% thrust, allowing distribution to be accomplished by the injector nozzles. To assure accurate flow distribution, these rods must be located with extreme accuracy to minimize discharge coefficient variation through the orifices.

(U) Secondary flow proportioning was accomplished in the same manner as in the pintle-orifice scheme with the contour being determined similarly. As with the pintle-orifice scheme, valve performance could be optimized only through bench testing where throat diameter and venturi divergence angle can be varied.

(U) Little advantage was found in using the venturi concept because the diameter gains were offset by the added length of the venturi diffusion section.

(3) Ball and Rotating Sleeve Candidate (See figure 336.)

(C) A combination of a rotating ball (for shutoff sealing) and a rotating sleeve (for flow distribution) as shown in figure 336 was evaluated as a

CONFIDENTIAL

CONFIDENTIAL

candidate for the flow divider valve. This concept consists of a ball type valve for thrust and a sleeve valve for secondary modulation. Ball diameter and a passage diameter were selected so that 30 degrees of rotation was required before the ball portion of the valve exposed area to the flow. The distribution sleeve included three ports requiring 36 degrees of angular rotation for minimum to maximum required flow area. The angular distance between the maximum port width and the maximum port width of the next port was 24 degrees. The port contour and sleeve port arrangement are shown in figure 337. Figure 338 is a plot of geometric inlet area of the ball valve as a function of angular opening. Figure 339 is a plot of the effective inlet area of ball valve vs angular position.

(U) Pressure losses across the valve entrance (ball position) are established by determining an entrance "K" factor to relate pressure loss to ball valve angle and flow rate.

(U) To illustrate the use of this "K" factor the following parameters are defined:

A_{in} = Valve inlet area

ρ = Fluid density

P_L = Pressure loss

F_{in} = Fluid velocity (entrance)

\dot{w} = Flow rate

The pressure loss may be written as

$$P_L = (K) \frac{1}{2g} v_{in}^2$$

since $\dot{w} = (A_{in})(v_{in})$

$$\text{then } P_L = (K) \frac{1}{2g} \frac{(\dot{w})^2}{(A_{in})^2}$$

(U) Figure 340 is a plot of this "K" factor as a function of angular opening. Because the required valve flow rate is a function of thrust and mixture ratio, the valve entrance loss may be calculated as a function of the operating point. Figure 341 is a plot of the ball valve inlet pressure loss as a function of thrust level and mixture ratio. Figure 342 is a plot of the required geometric flow area for the sleeve section as a function of thrust and mixture ratio. Because the flow divider valve circuit is sized according to system flow rate and a 4.5% (of preburner pressure) pressure drop across the primary injector, the valve entrance loss must be made up by either (1) increased pressure rise from the oxidizer turbopump, or (2) reduced pressure drop across the thrust control valve.

CONFIDENTIAL

CONFIDENTIAL

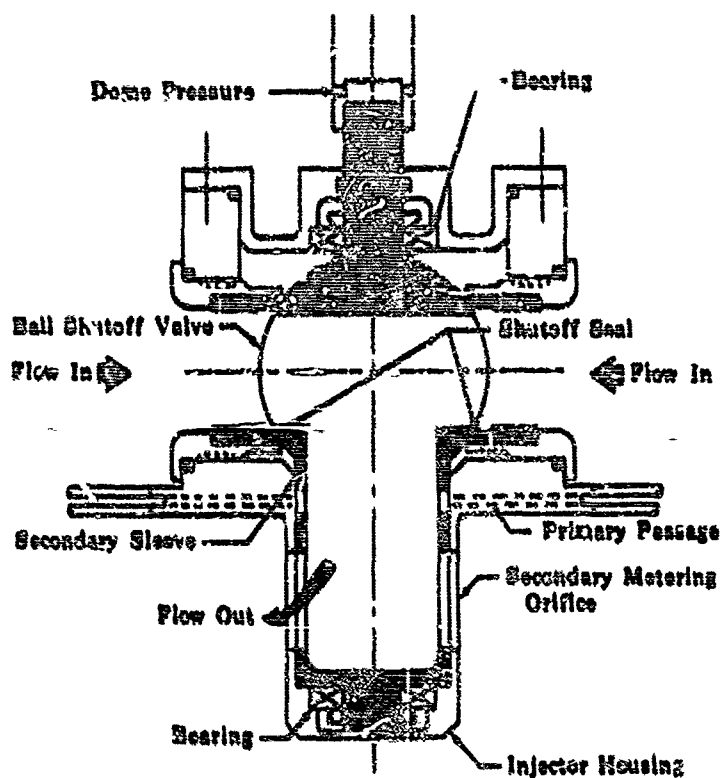


Figure 336. Flow Divider Valve, Ball and Rotating Sleeve Candidate

FD 18211A

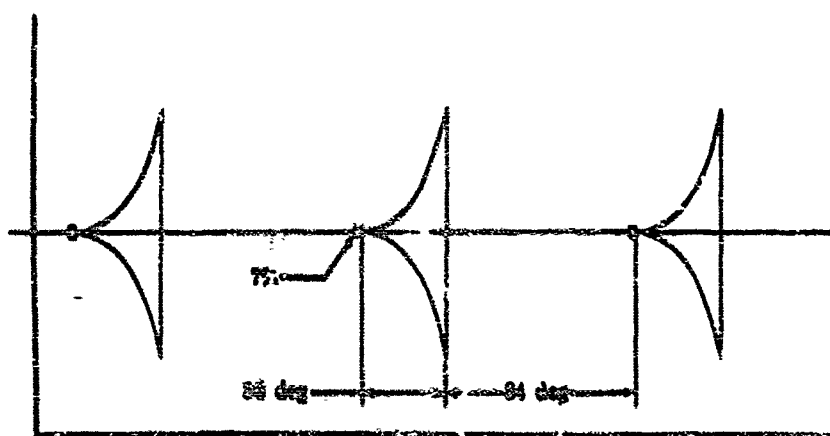


Figure 337. Development of Sleeve Valve with Three Constant Percentage Contour Ports

FD 17999

368

CONFIDENTIAL

(This page is Unclassified)

CONFIDENTIAL

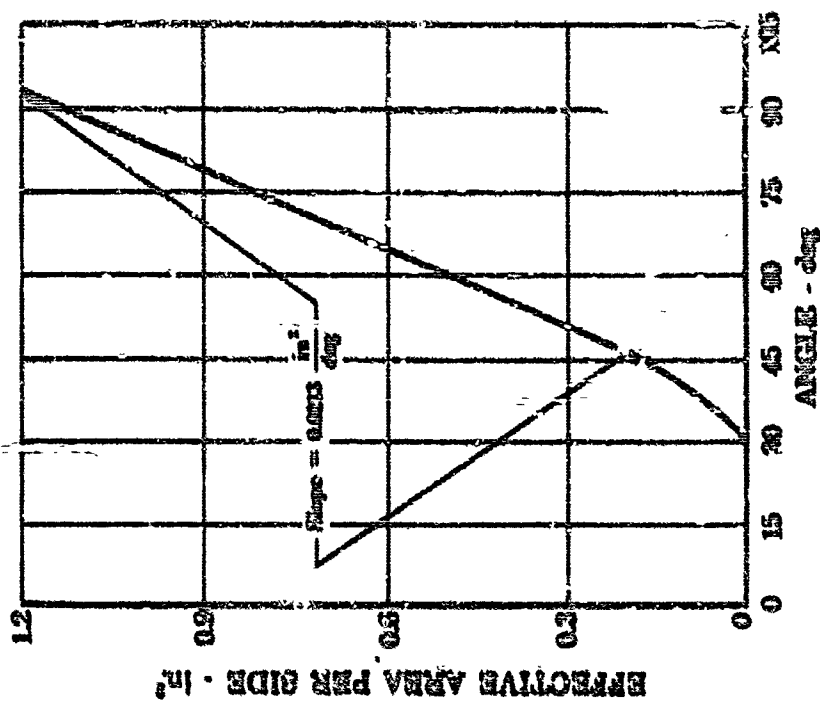


Figure 339. Effective Area of Inlet to Ball Valve vs Angular Position for 1.5-inch Diameter

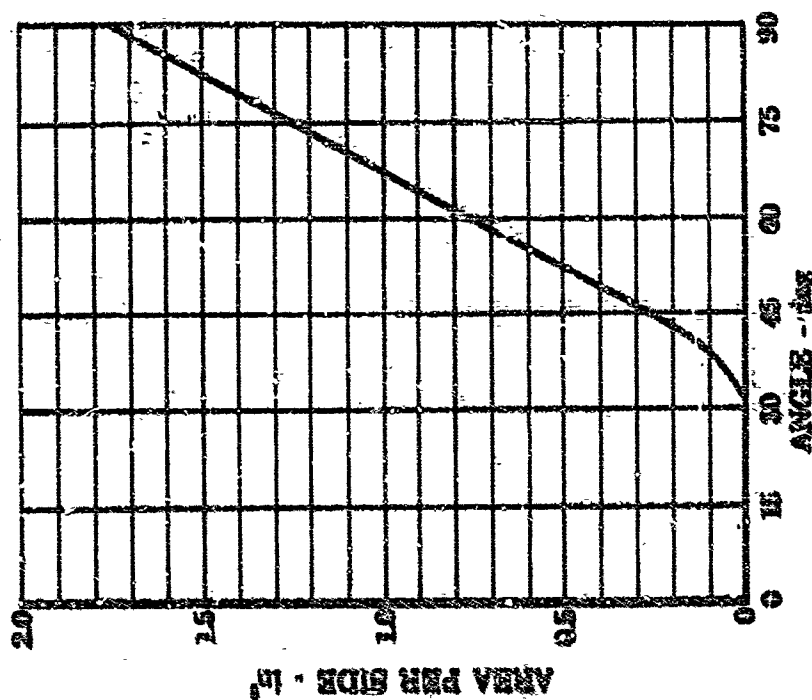


Figure 338. Geometric Inlet Area of Ball Valve vs Angle of Rotation for 1.5-inch Inlet Diameter

CONFIDENTIAL

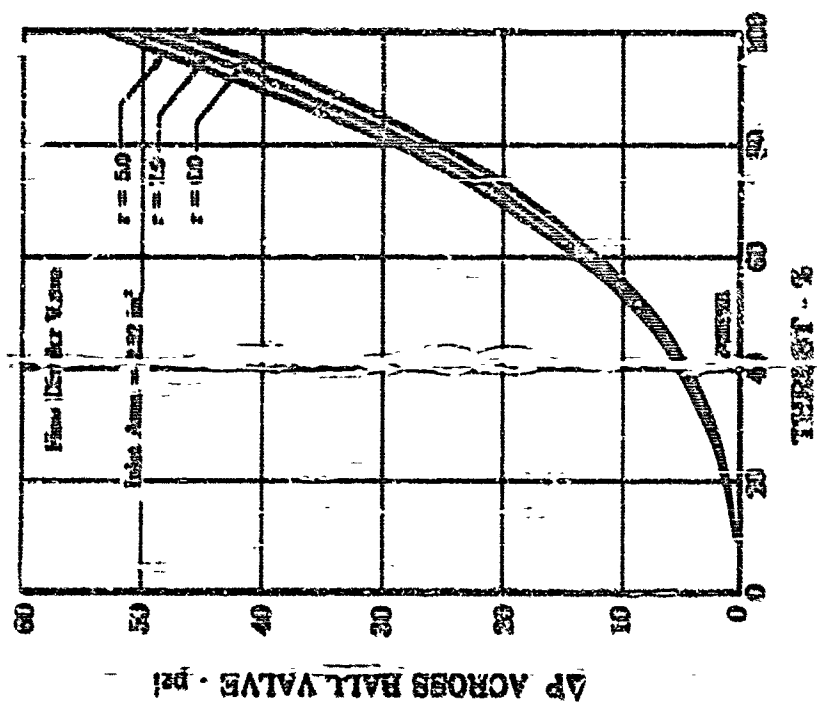
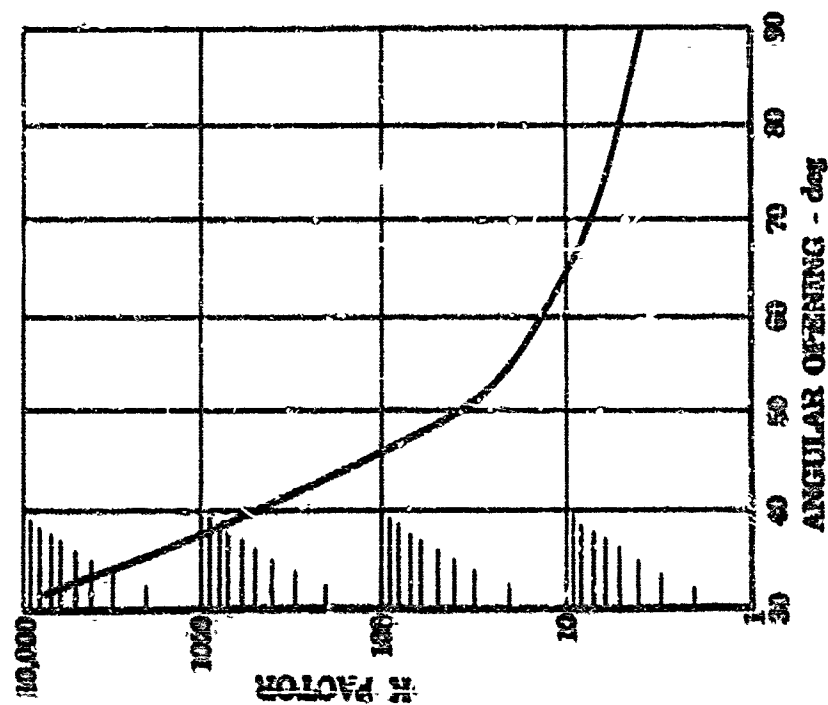


Figure 341. Pressure Drop Across Ball Valve vs Percent Throat

FD 18221

Figure 340. K-Factor for Ball Valve vs Angular Opening (Flow Divider Valve)



FD 18225

CONFIDENTIAL

CONFIDENTIAL

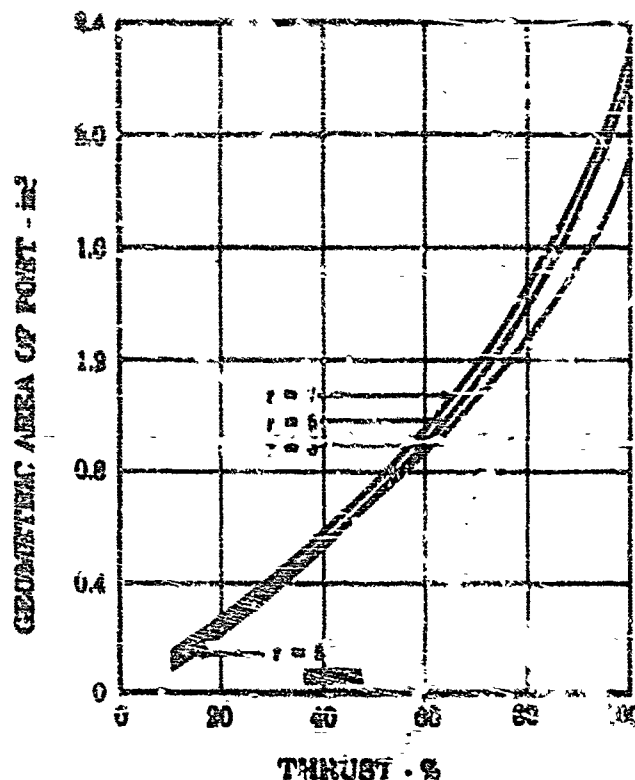


Figure 342. Geometric Area of Contoured Port vs Percent Thrust (Flow Divider Valve) FD 18257

(U) Figure 343 is a plot of the valve geometric flow area for the sleeve section as a function of angular position based on a constant percentage port contour.

(U) Knowing the valve effective area as a function of angular position and the required geometric pore area as a function of thrust and mixture ratio, the required valve angular position can be determined. This is plotted in Figure 344 as a function of thrust and mixture ratio.

(U) When the valve turndown ratio and the valve stroke have been set, (the valve stroke of a rotary sleeve can be evaluated in terms of valve diameter and angular rotation, the maximum port width can be determined. Figure 345 is a plot of maximum port width as a function of valve diameter for a three-port valve. This phenomenon is discussed in more detail in the corresponding thrust control section. The percent area error is shown plotted as a function of percent positional error in figure 346. The effect of turndown ratio on the area error is also illustrated.

CONFIDENTIAL

CONFIDENTIAL

372

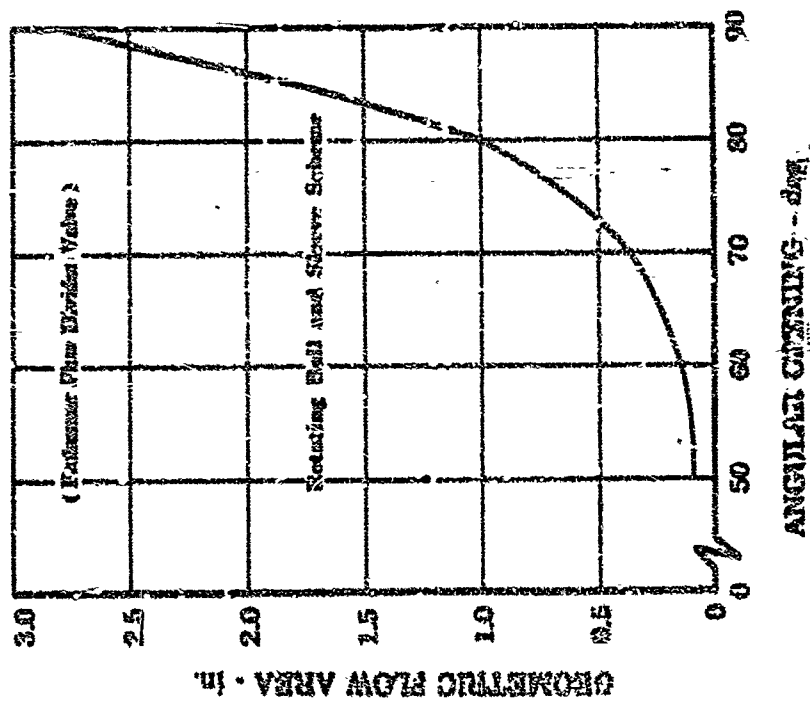


Figure 363. Flow Area of Contoured Port vs Angular Opening of Sleeve Port Valve

FD 18216

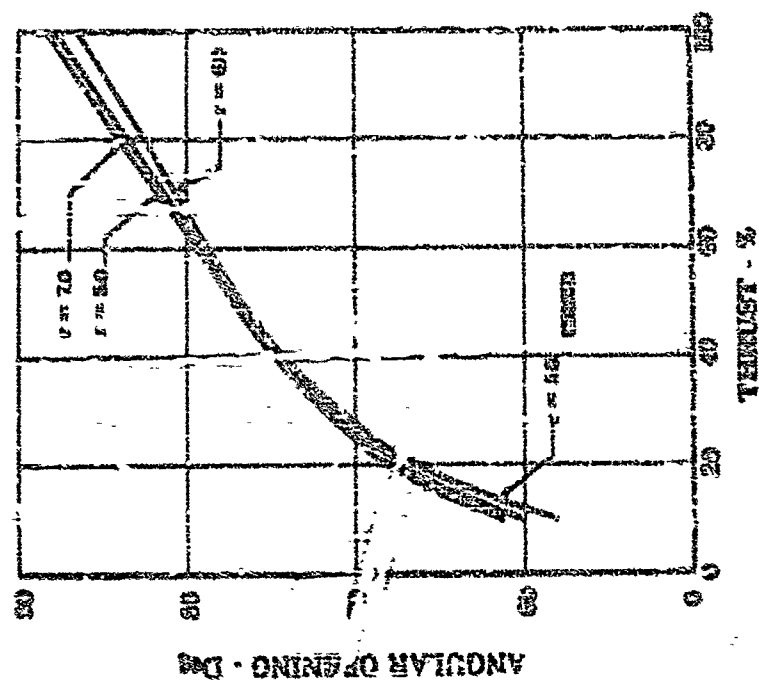


Figure 364. Angular Opening of Sleeve vs Percent Thrust (Flow Divider Valve)

FD 18201

CONFIDENTIAL

573

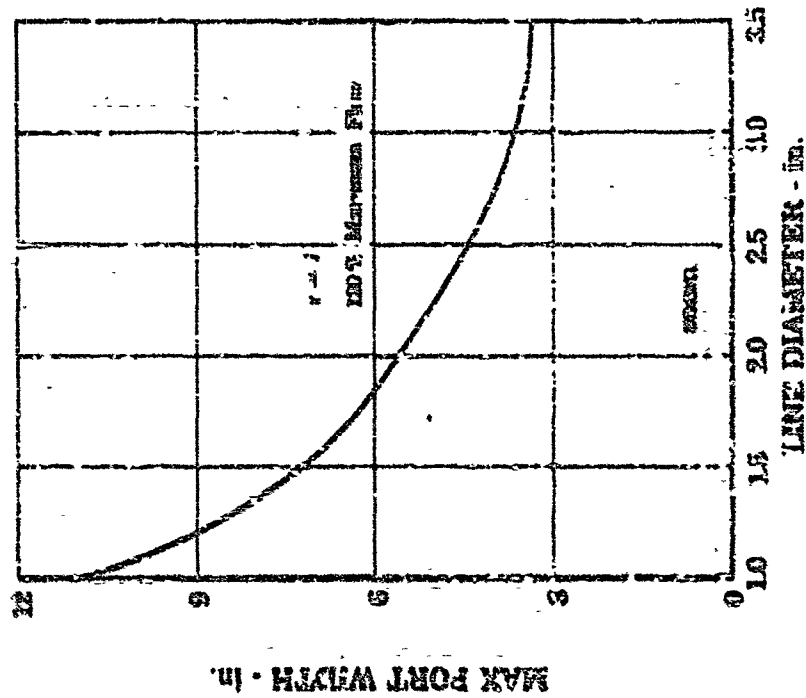


Figure 345. Maximum Port Width vs Line Diameter (Flow Divider Valve)

ED 18202

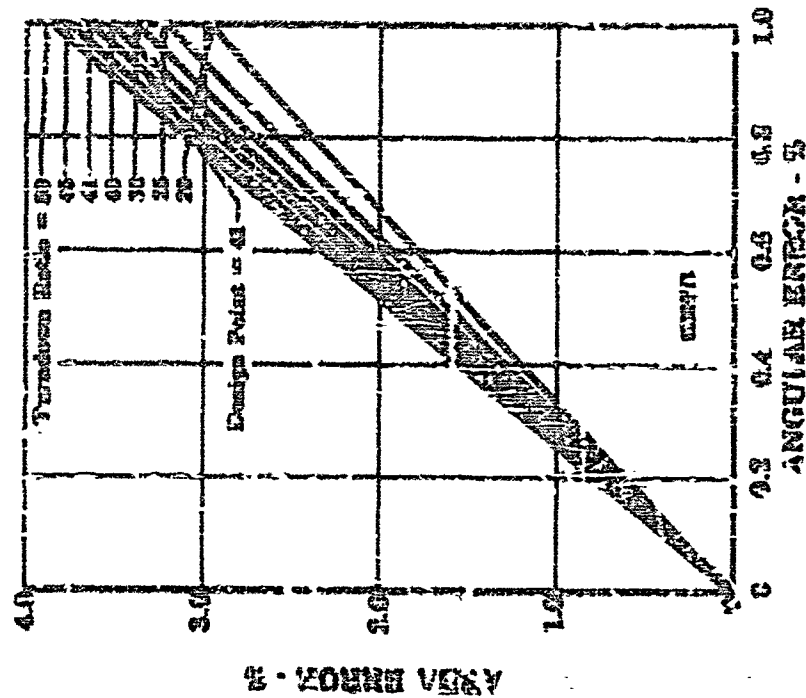


Figure 346. Percent Area Error vs. Percent Position Error (Flow Divider Valve)

ED 18166

CONFIDENTIAL

~~CONFIDENTIAL~~

(4) Rotary Plate Candidate

(b) This scheme is simply a better valve that opens and closes primary and secondary areas in a shuffling motion. It has the advantage of compact height, good leakage control, and positive shutoff. Once the valve is cracked open, leakage will exist between primary and secondary, but leakage is easily controlled by the proximity of the plate to the seating face. In reality, an amount of leakage to secondary is not only permissible, but even desired for injector element cooling.

(c) Seal durability in this design could be a problem because of continual scrubbing on the seat plate. However, the primary reason for rejecting the scheme was the requirement for complicated manifolding in the injector to accommodate the nonconcentric primary and secondary flowpaths.

(5) Rotary Sleeve Candidate (See figures 347.)

(b) Rotary sleeve valves are basically the same as sliding flat plate valves except that the ports are cut in concentric cylinders that are rotated relative to each other to vary area. This valve was eliminated from further consideration because of difficulty in sealing around the ports and failure to provide a positive shutoff. The performance of this scheme would be the same as the combination ball and sleeve except for the difference in entrance losses. (See figures 341 and 348.)

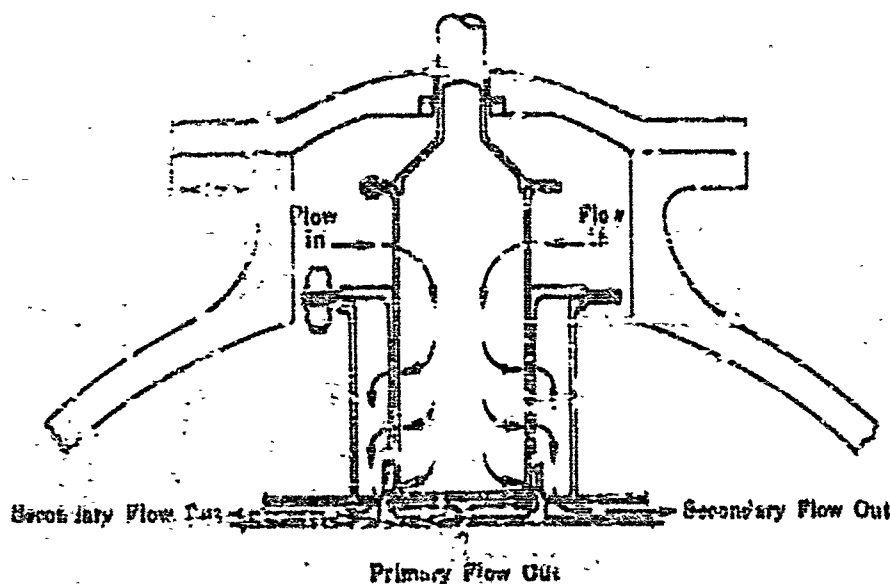


Figure 347. Flow Divider Valve, Rotary Sleeve Candidate

FD 10168

~~CONFIDENTIAL~~

(This page is Unclassified)

CONFIDENTIAL

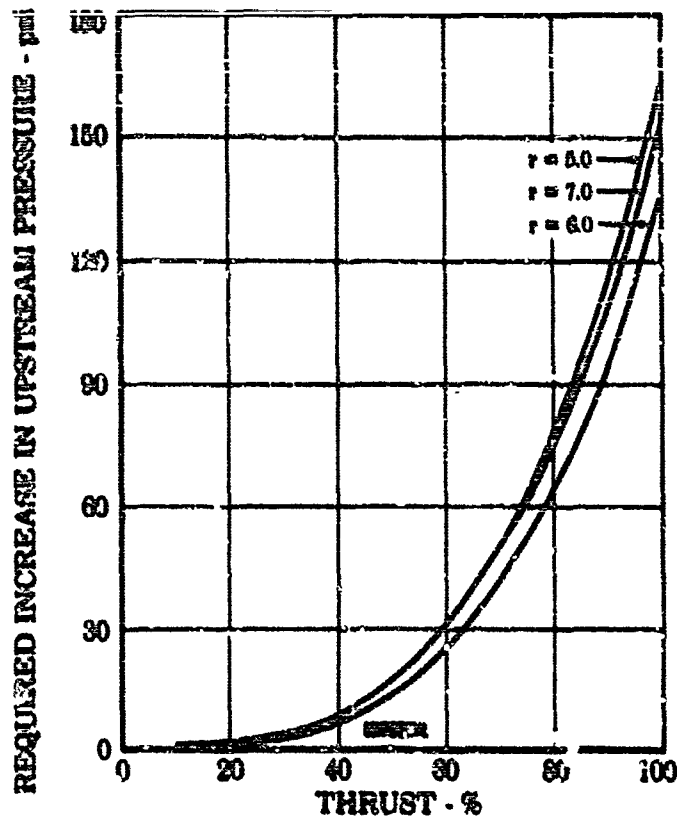


Figure 348. Required Increase in Pressure Upstream of Flow Divider Sleeve Valve vs Percent Thrust

FD 18155

(5) Rotating and Translating Sleeve Candidate

(U) This concept combines a pure rotary sleeve valve with a poppet that provides positive oxidizer flow shutoff. When the valve stem is rotated, cam followers attached to the inner cylinder ride on a contoured surface, opening or closing the poppet.

(U) Weak points in this concept are the problem of leakage control between the sleeves, high degree of positioning error, and complexity; also, at the time of investigation, it appeared that the unit could not control leakage flow.

(7) Ball Valve Candidate

(U) A pure ball valve cannot perform combined functions. Therefore, for the system under study, at least two ball valves would be required: one to regulate primary flow and another to regulate secondary flow. Ball valves were considered to be undesirable as distribution valves because of possible damage to the seals during throttling caused by their high-velocity flows. However, they do provide excellent shutoff features.

CONFIDENTIAL

CONFIDENTIAL

(8) Butterfly Valve Candidate

(U) The butterfly valve provides primary flow modulation by wiping a seal on the flapper across a port cut in the valve housing. This method of modulation would be extremely sensitive to positioning error. In addition, the seal would likely be subject to frequent replacement because of wear generated by the frequent passage over the primary port. The seal would be subjected to flow forces across it as in the ball valve.

(9) Translating Sleeve Candidate (See figure 349.)

(U) The translating sleeve valve shown in figure 349 of two stationary and two movable cylinders. The outer movable cylinder provides the shut-off function for the entire valve and provides the device for exposing the flow distribution ports to supply pressure. The contoured secondary flow distribution ports are in the stationary member, while the primary ports are on the inner movable cylinder that also provides the pressure balance function. The primary ports are located in the movable unit because this part is more readily changed or modified during the development program.

(U) Preburner oxidizer flow was shut off by driving the secondary valve sleeve against a trapped Teflon seal at the end of its stroke, which minimized its tendency to cold flow.

(U) Primary flow was initiated by moving the secondary sleeve axially. This motion exposed several passages by drawing a piston ring seal over them. These passages supply flow to the primary valve. The primary flow was controlled by two contoured ports machined in the primary shaft. With the primary area full open, primary flow distribution was accomplished at the injector nozzle. Further motion exposes five contoured ports in the stationary cylinder of the secondary valve. The number of ports was optimized at five so that the minimum port opening at the low thrust level would be 0.030-inch; it was considered that an opening less than this would be sensitive to contamination.

(U) Based on the secondary flow rate and the flow divider valve pressure drop, the required effective valve area was determined. Figure 350 shows the required effective valve area as a function of thrust level and mixture ratio.

(U) The valve turndown ratio and stroke established the maximum required port width. Figure 351 shows maximum port width as a function of valve stroke and the number of ports.

(U) Figure 352 is a valve-sizing family of curves. The required valve diameter is plotted as a function of total valve stroke for various ratios of maximum port width to valve circumference.

(U) Figures 353 and 354 are plots of the port contours for a 1.25-in. and a 2-inch valve stroke, respectively. Figure 355 is a plot of the valve flow forces (noncompensated) as a function of thrust level and mixture ratio.

CONFIDENTIAL

(This page is Unclassified)

CONFIDENTIAL

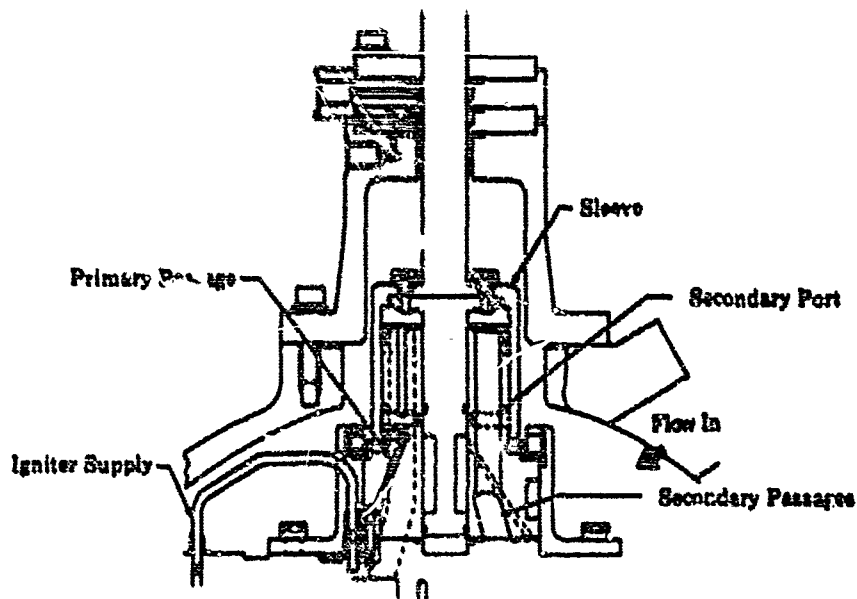


Figure 349. Flow Divider Valve, Translating Sleeve Candidate

FD 18174A

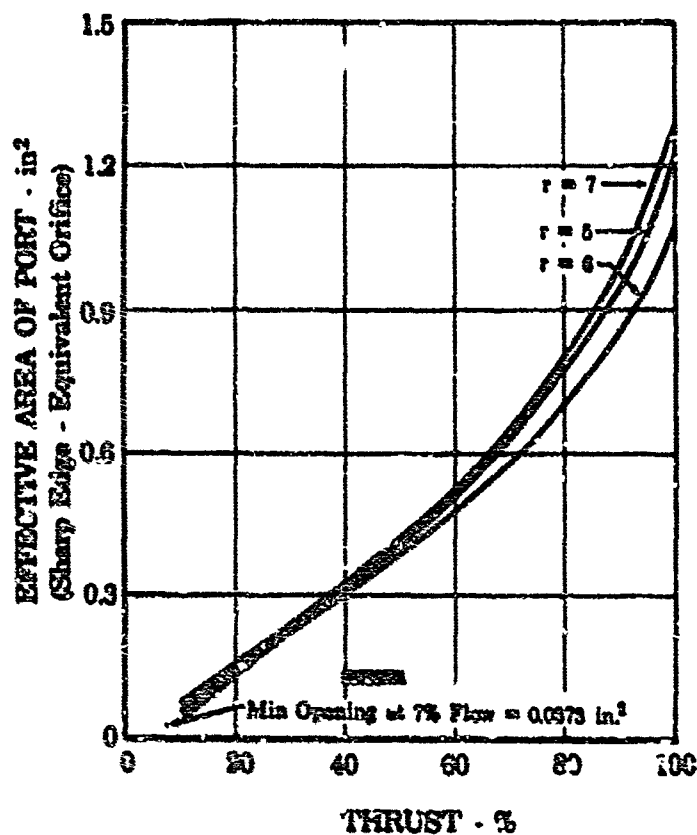


Figure 350. Effective Area of Secondary Valve vs Percent Thrust (Preburner Flow Divider Valve)

FD 18223

CONFIDENTIAL

CONFIDENTIAL

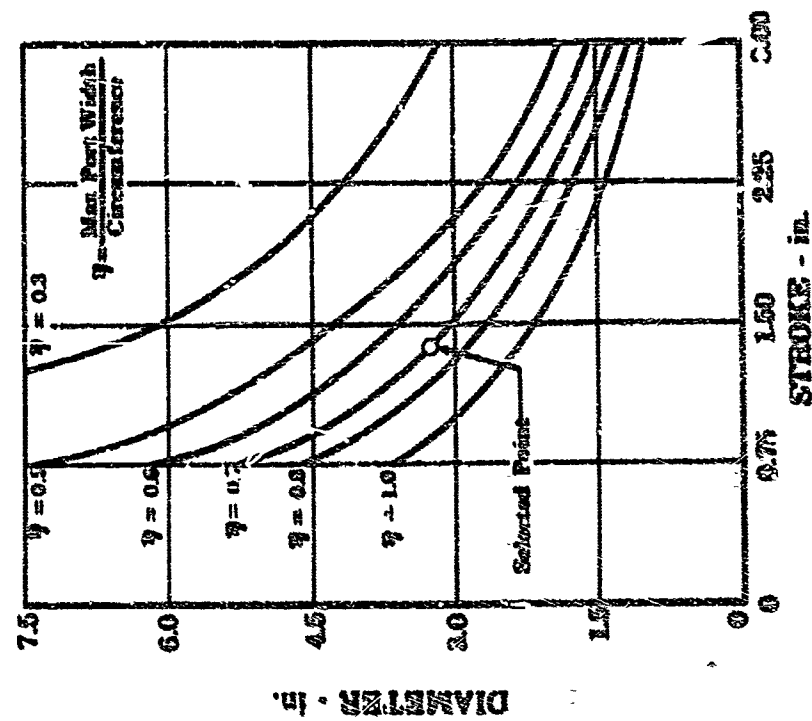


Figure 352. Stroke vs Diameter for Translating Sleeve Valve (Preburner Flow Divider Valve) FD 18253

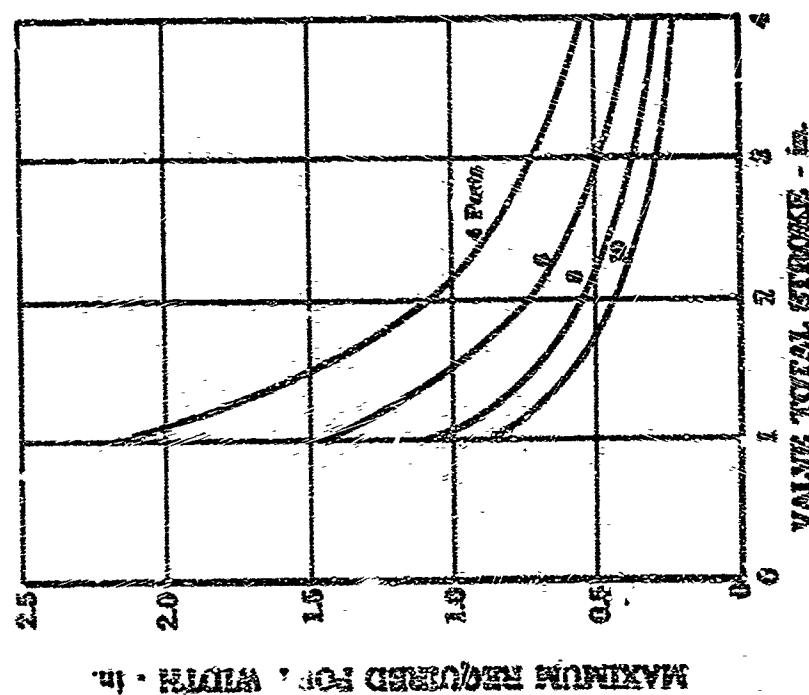


Figure 351. Maximum Required Port Width vs Valve Stroke FD 18265

CONFIDENTIAL

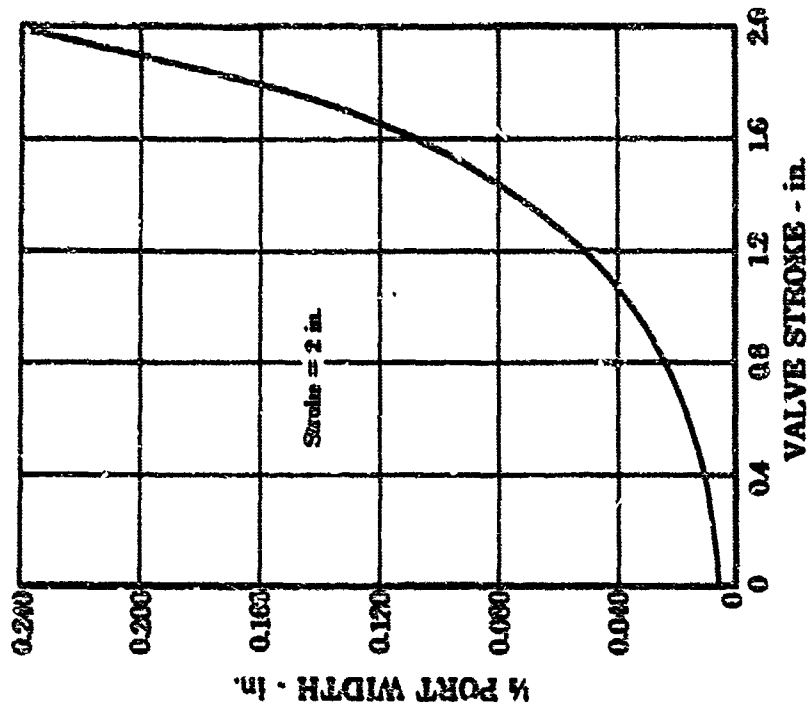


Figure 354. Flow Divider Valve Port Contour (10 Ports Required)

FD 18256

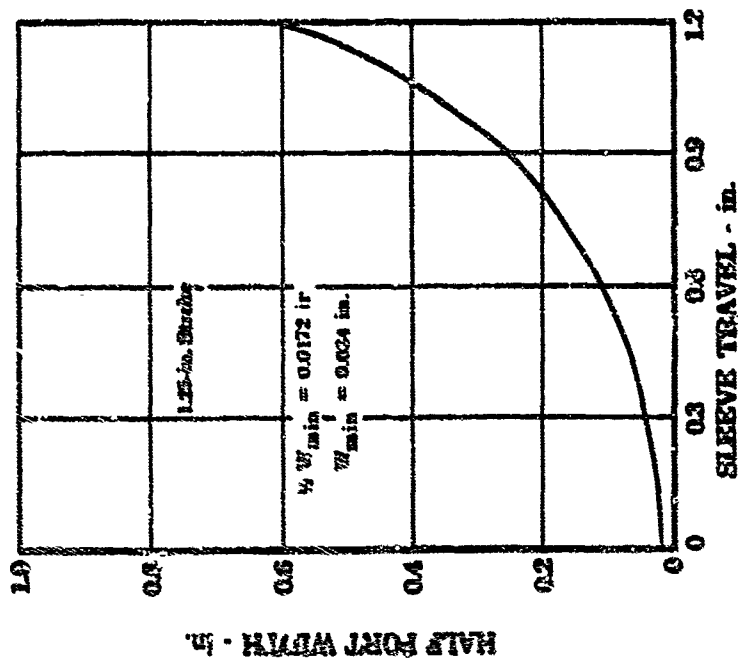


Figure 353. Port Contour of Constant Area Error Port Based on 5 Equal Ports

379

CONFIDENTIAL

(This page is Unclassified)

CONFIDENTIAL

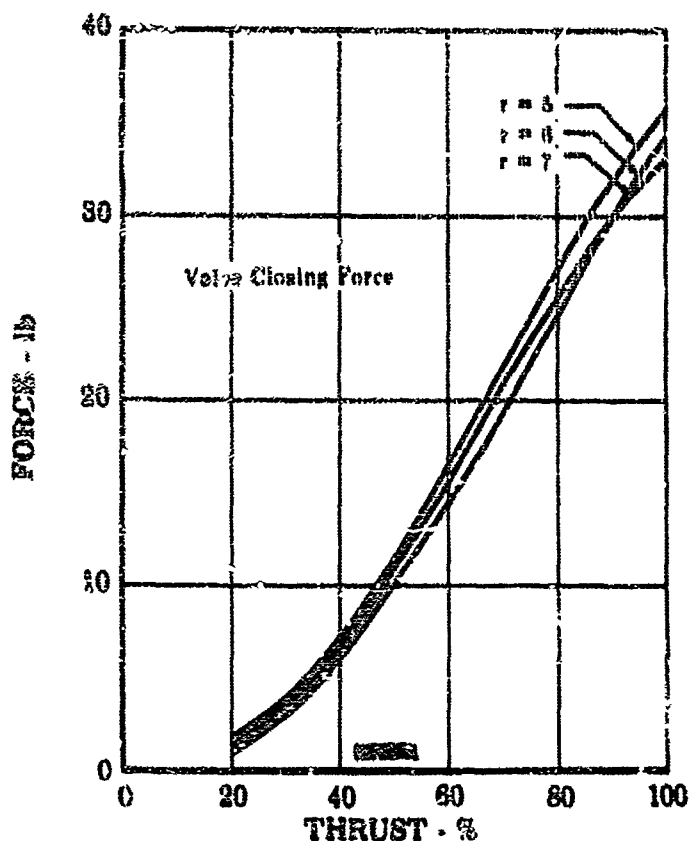


Figure 355. Valve Force (Noncompensated) vs Percent Thrust (Preburner Flow Divider Valve)

FD 19278

(U) Figure 356 is a plot of the valve flow forces just discussed, with the addition of a compensating force from a sleeve cutback. Net forces are plotted as a function of thrust level and mixture ratio. Pressure balance of the sleeve is such that during operation, unbalanced force is negligible, and at shutoff the force acts to keep the valve sealed.

(U) With the requirement for a high degree of flow control accuracy at low thrust levels, it was desirable to minimize leakage flow. This was accomplished through use of piston ring seals for distributing as well as pressure balancing.

(U) The translating sleeve valve has the ability to include the thrust control function through modification of the ports to provide a higher turndown ratio and a greater pressure drop across the secondary valve. Through use of a classified spacer under the main sleeve, the relationship of primary open area to secondary open area during start can be provided. These two features provide experimental valve flexibility.

CONFIDENTIAL

CONFIDENTIAL

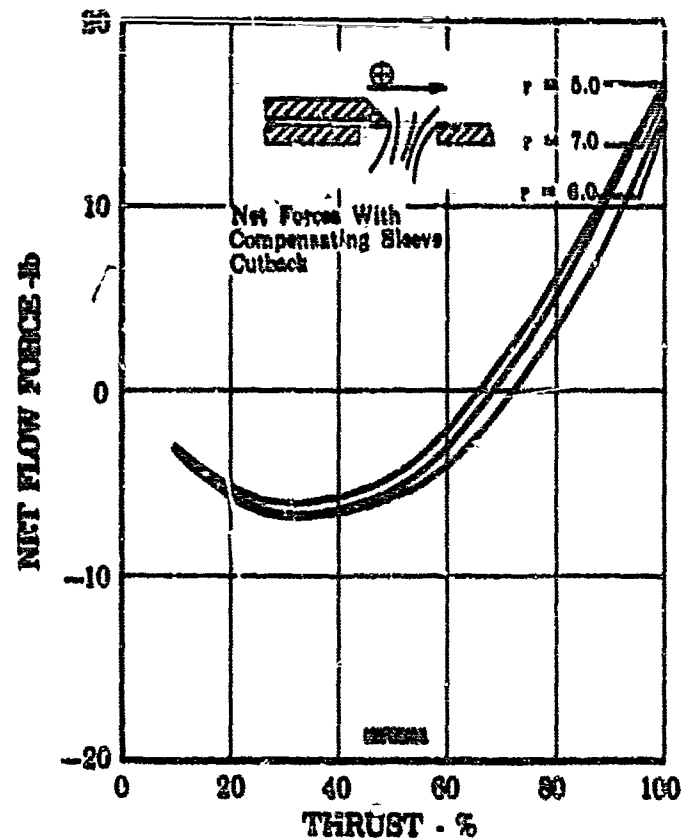


Figure 356. Flow Forces vs Percent Thrust
(Preburner Flow Divider Valve)

FD 18225

(10) Comparison Summary

(U) As a result of this study, the translating sleeve valve was selected from the candidates shown in table XXXVI, with the added requirement to provide starting flow modulation in addition to modulating the primary-to-secondary flow ratio over the operating range.

(U) Table XXXVI. Flow Divider Valve Candidates

| Valve Type | Comments |
|--------------------------|---|
| Translating Sleeve | Selected configuration on basis of positive shutoff, pressure and flow balance and desirable metering characteristics |
| Pintle Orifice | Undesirable metering characteristics and tolerance requirements |
| Pintle Venturi | Same comments as pintle orifice with added length of diffuser section |
| Ball and Rotating Sleeve | Rotary sleeve acquires close fit for metering with attendant contamination sensitivity |

CONFIDENTIAL

CONFIDENTIAL

c. Design of Selected Configuration

(U) The demonstrator engine flow divider valve, illustrated assembled on the preburner injector in figure 357 and in exploded layout figure 358, divides the oxidizer supply into two separate flows to the preburner dual-orifice oxidizer system. Figure 357 also summarizes the areas of design changes incorporated during development testing. This valve also provides an oxidizer supply for both the preburner and main chamber igniters, and incorporates a positive shutoff for the total preburner oxidizer supply. The flow divider valve is located in the preburner dome with the servoactuator mounted outside the dome. To permit more flexibility in the valve operating schedule, the demonstrator valve is longer than a flight design and does not include the thrust control function, which may be incorporated in the flight valve.

(C) The rig and demonstrator flow divider valve is shown in figure 359 without associated hardware. The valve has two metering systems; an inner spool valve to meter primary flow from ignition to 10% thrust, and an outer sleeve valve to meter secondary flow from 10% to 100% thrust. As the rig valve was initially opened, the oxidizer began to flow to the igniters, loading the fuel supply. After ignition, the valve was opened further to permit the oxidizer to purge the secondary injectors. This purge was maintained as the primary spool valve opened. The secondary valve was then opened to an effective area of 0.064-in.² corresponding to a thrust of 10%. The shim may be changed between the secondary and primary valves to permit an effective secondary area of 0.064-in.² to be opened anytime between start and the full-open position of the primary valve, if rig results indicate that an oxidizer effective area corresponding to 10% thrust can be opened at start.

(C) Thrust modulation between 10% and 100% required variation of the secondary port effective area. This area was changed in response to the control system output that scheduled the required secondary valve position to give the area required for a given mixture ratio and thrust level setting.

(U) The cross-sectional view of the demonstrator preburner oxidizer flow divider valve (figure 357) shows the valve mounted on the preburner, completely enclosed by the preburner dome (Inconel 718) and dome cap (AMS 5646 stainless steel). The dome serves as a plenum chamber in conjunction with the flow divider valve baffle to reduce the velocity of the entering oxidizer and distribute it to the six primary and five secondary supply ports with equal pressure drops across the ports. The valve could be removed from the dome for calibration by removing the dome cap, seal assembly, and servoactuator and mount.

(C) Figure 360 shows a cross section through the primary passages. The path the oxidizer takes from dome inlet through the baffle and into the secondary ports is shown in figure 361. The material used for the primary spool was AMS 4650 (copper alloy), for the secondary sleeve was AMS 5735 (iron-base alloy), and for the valve housing was AMS 5646 (stainless steel). These materials were selected to provide parts that were thermally compatible with seal sliding surfaces capable of being chrome plated and given an RMS 8 finish to provide wear resistance. They were designed to minimize the thermal drift problem associated with a valve having a secondary turndown ratio of 25.3:1.

CONFIDENTIAL

CONFIDENTIAL

FD 148911D

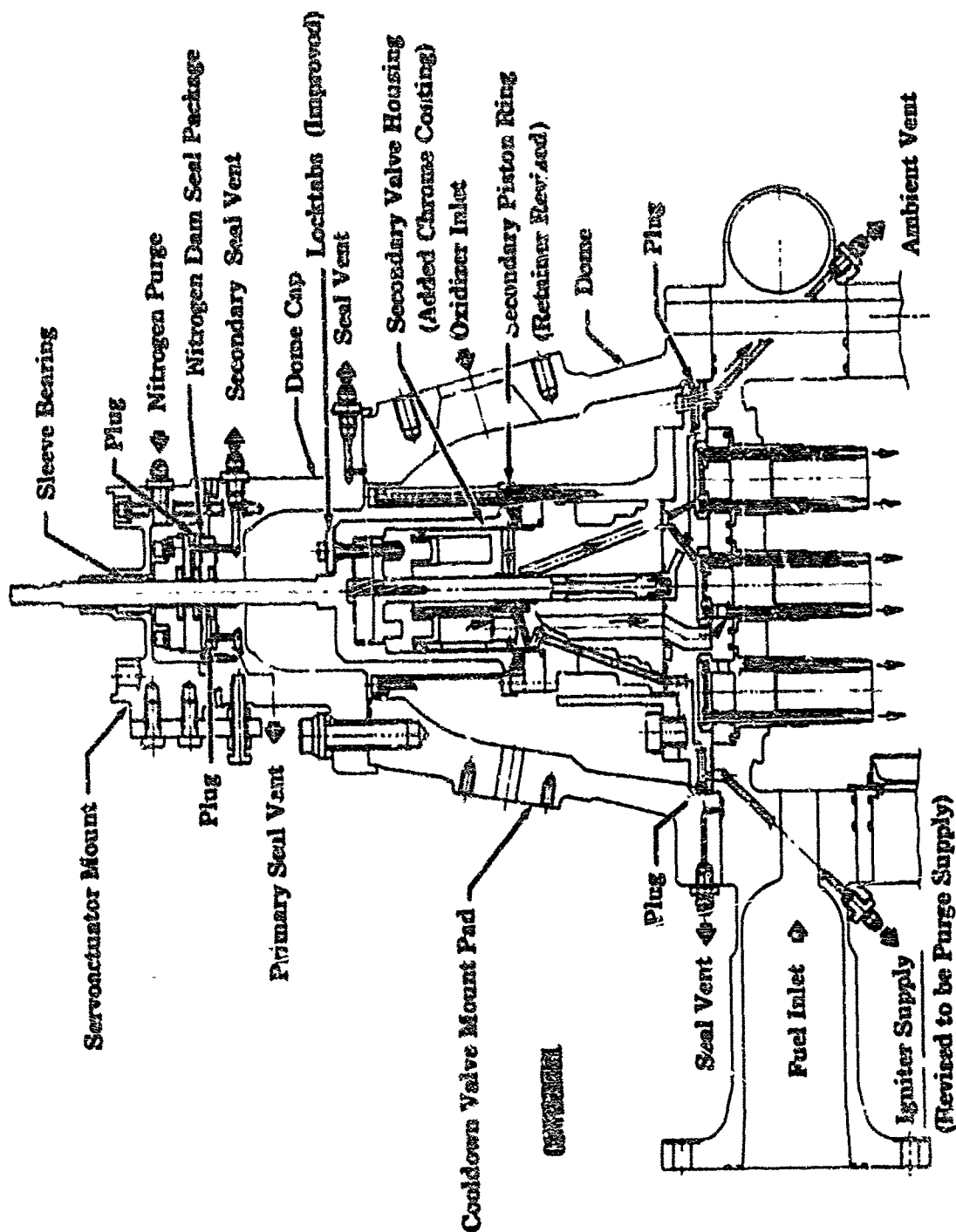


Figure 357. Flow Divider Valve with Oxidizer Side of Preburner Injector

CONFIDENTIAL

SECRET

CS-6130

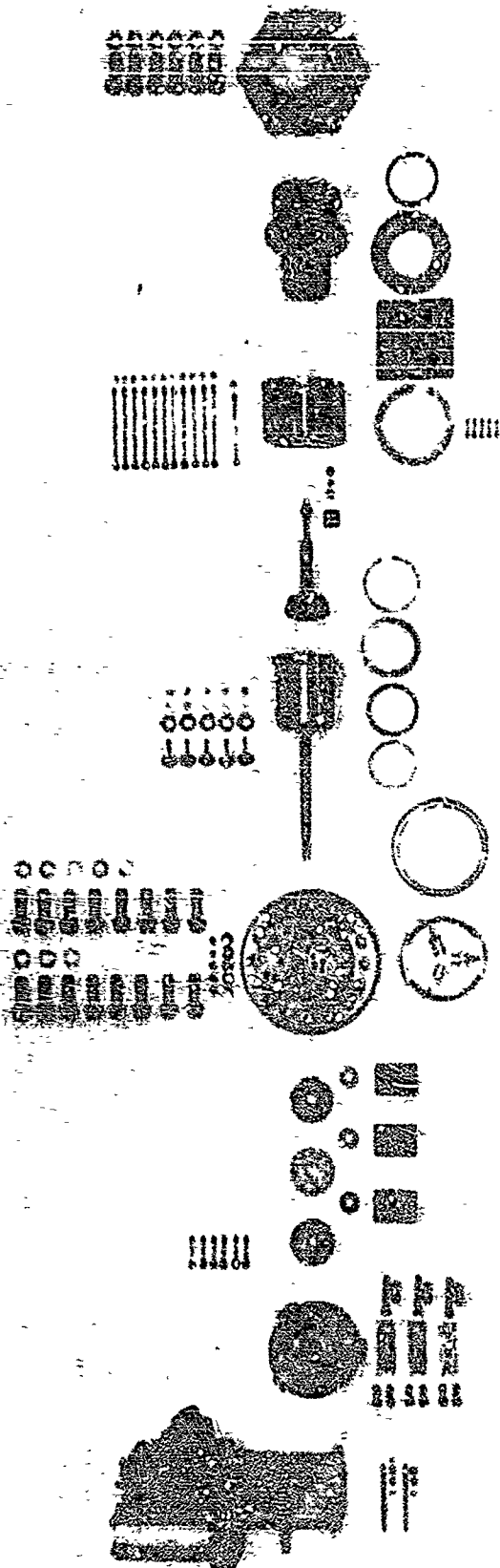


Figure 358. Flow Rider Valve Parts

384

CONFIDENTIAL

(This page is Unclassified)

CONFIDENTIAL

made of Teflon and was trapped to prevent cold flowing. Labyrinth grooves on the outside diameter of the seal retainer reduced leakage between the tight fitting seal and retainer when the valve was shut off. The seal has the capability of sealing a maximum pressure differential of 200 psid.

(U) The secondary metering piston ring seal shown in figure 362 was made of Berylco 25 (AMS 4650). The piston ring was pinned to the secondary sleeve valve to maintain the ring gap orientation with respect to the valve housing ports. This prevented a possible bind should the piston ring gap align with one of the tapered port edges. The upper piston ring seal, shown in figure 363, was also made of Berylco 25. Both seals were capable of sealing a maximum pressure differential of 125 psi. The upper seal ring dimensions are 3.375-in. ID x 3.719-in. OD x 0.200-in. maximum axial thickness. The lower seal ring dimensions are 3.144-in. ID x 3.440-in. OD x 0.140-in. maximum axial thickness.

(C) The high-pressure (5100 psia) primary spool valve seal configuration is illustrated in figure 364. This seal package consisted of two Berylco 25 piston rings in series with a spring energized Teflon lip seal (0.683-in. OD x 0.563-in. ID x 0.090-in. axial thickness) on the ambient pressure side. During normal valve operation, full pressure was developed across the lip seal. If the lip seal failed, the piston rings would permit the valve to continue functioning with only a small quantity of overboard leakage (approximately 0.031 lb/sec).

(C) The dome cap nitrogen dam seal package shown in figure 365 contains three floating seal plates capable of compensating a 0.034-in. radial deflection because of valve machining tolerances. Each seal plate contains a shaft seal (0.811-in. OD, 0.681-in. ID, and 0.065-in. axial thickness) and a static face seal (1.187-in. OD, 1.35-in. ID, and 0.075-in. axial thickness). Oxidizer leakage past the primary and secondary seals is vented overboard. Leakage past the vent seal is combined with a 50 psi dry nitrogen purge in the dome cap which vents to ambient around the sleeve valve shaft; this prevents ice from accumulating around the shaft. The design leakage valve for the seal package is 10 scs GN₂ past the vent shaft seal.

(U) The high-pressure static seals between the dome cap and dome, and between the preburner and dome consisted of two Teflon-coated metal O-rings in series. The inner O-rings were of the self-energized configuration and the volume between these seals was vented overboard.

(U) The servoactuator mount housed the leaded-bronze (Bearium B-10) sleeve bearing that supported the sleeve valve shaft. This bearing isolated the critical piston ring seal surfaces of the flow divider valve from misalignment loads and vibration loads from the servoactuator. The mount also included aligning shims (figure 366) to compensate for tolerance accumulation between the sleeve bearing and the valve housing. The actuator mount was secured in place by 3 alignment plates and 10 external bolts.

CONFIDENTIAL

CONFIDENTIAL

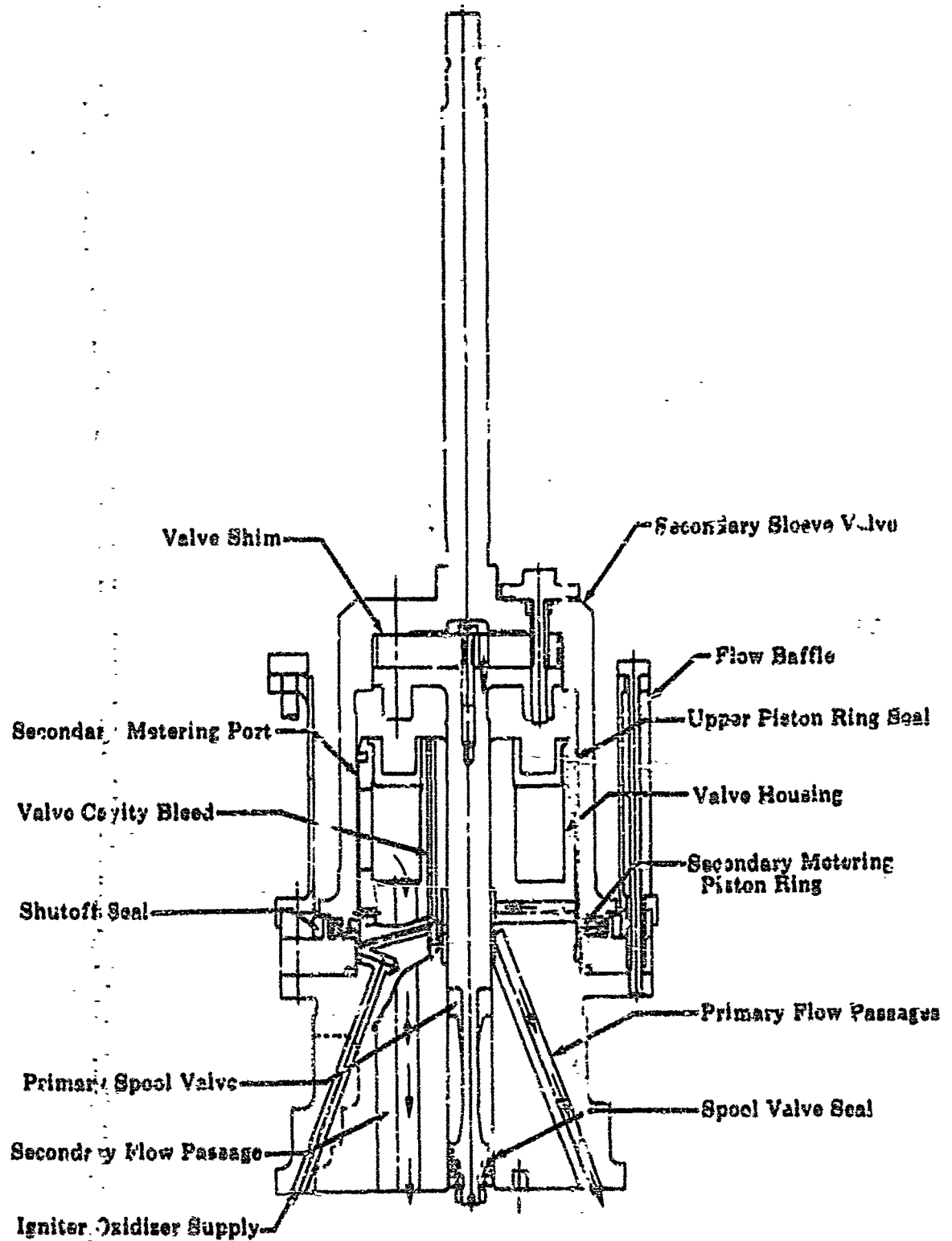


Figure 359. Rig and Demonstrator Flow Divider Valve

FD 1A909C

386

CONFIDENTIAL

(This page is Unclassified)

UNCLASSIFIED

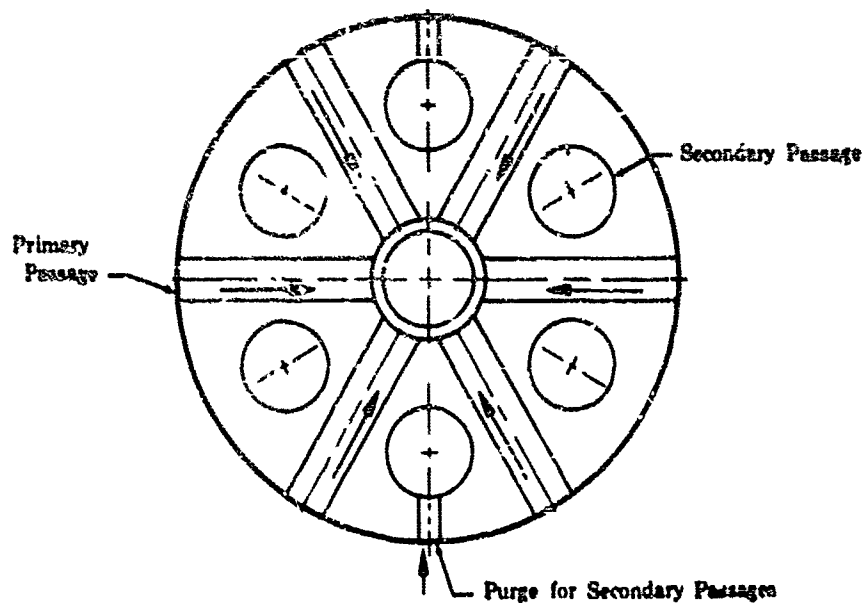


Figure 360. Cross Section of Primary Ports

FD 18891

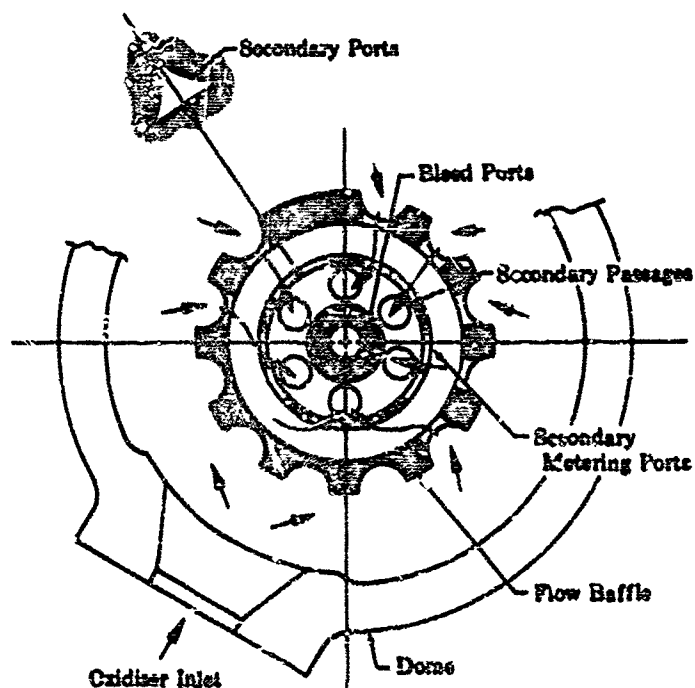


Figure 361. Cross Section of Secondary Ports

FD 18894

(U) Because the valve was pressure balanced the full length of travel, the required servoactuator forces were caused mainly by seal breakaway and friction forces. The maximum required servoactuator force of 21.2 lb occurred at start when the valve was opened against the 35 psi pressure differential across the shutoff seal. The shutoff seal (figure 362) was

UNCLASSIFIED

UNCLASSIFIED

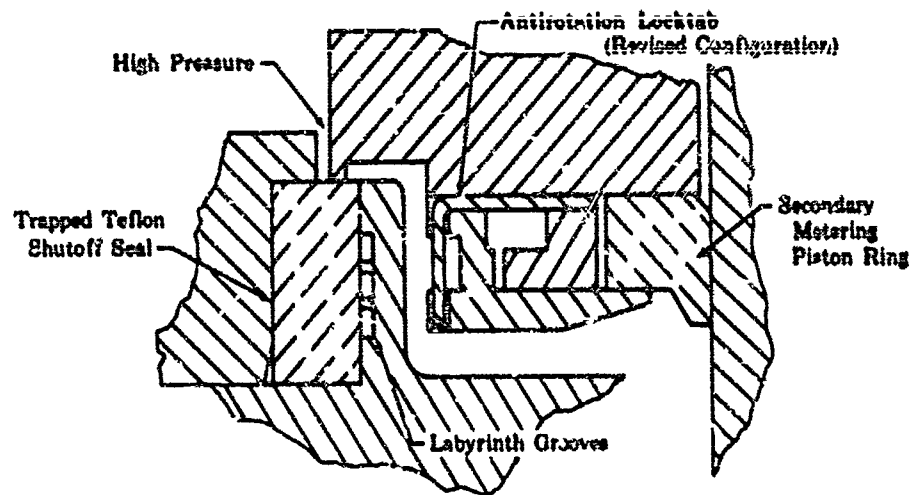


Figure 362. Secondary Metering Piston Ring and Shutoff Seal

FD 18887B

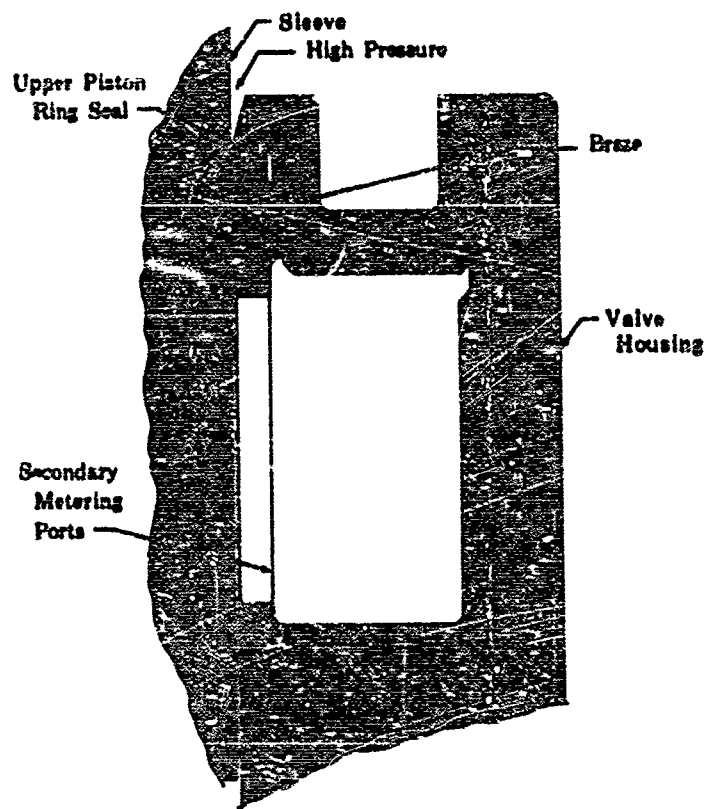


Figure 363. Upper Piston Ring Seal

FD 18888A

UNCLASSIFIED

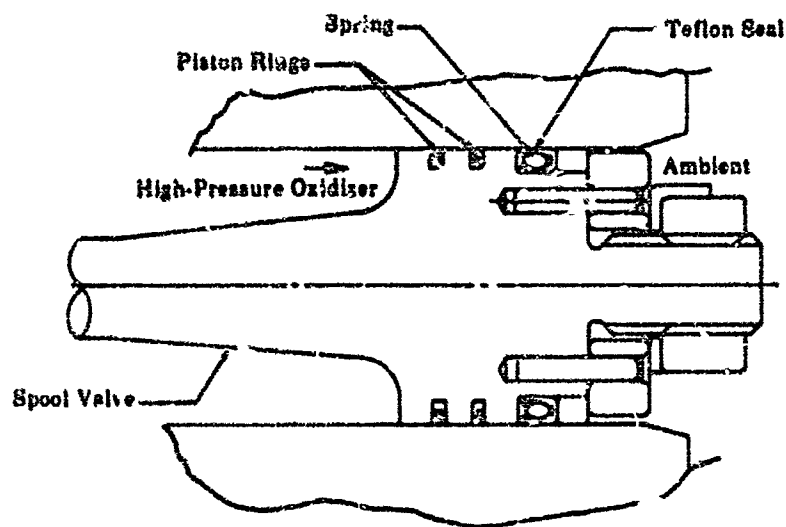


Figure 364. High-Pressure Spool Valve Seal Package

FD 18893

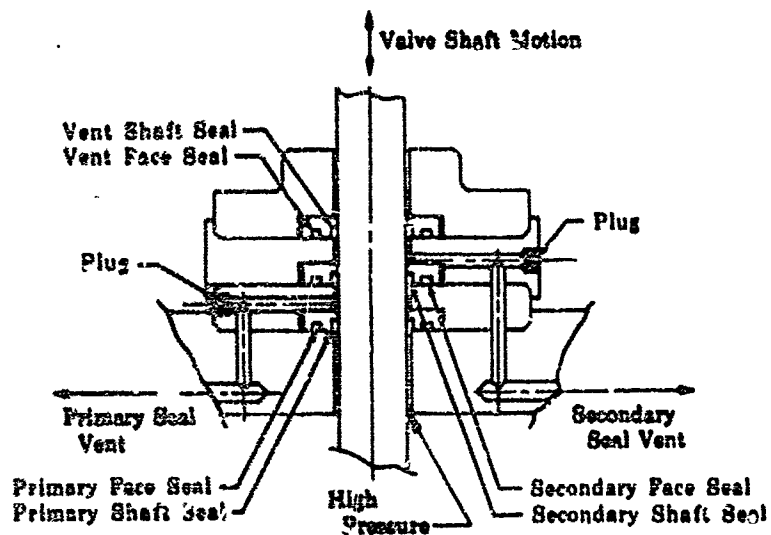


Figure 365. Nitrogen Dam Seal Package

FD 18896B

UNCLASSIFIED

UNCLASSIFIED

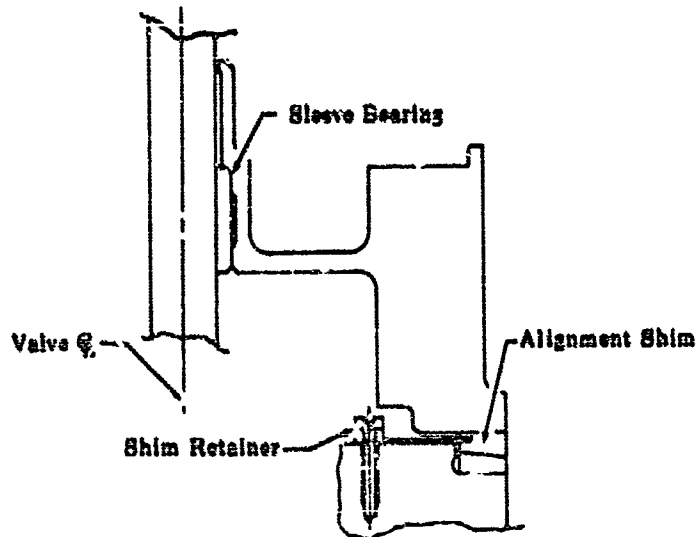


Figure 366. Servoactuator Mount

FD 18990

(U) The predicted flow divider valve operating characteristics, including valve line loss are shown in figure 367.

(U) Design changes incorporated in the flow divider valve and actuator as a result of testing are listed below:

1. During flow tests of the first valve assembly, the spring lock for the secondary sleeve piston ring retainer became disengaged and caused damage to the shutoff scaling edge and shutoff seal retainer. A revised piston ring retainer lock incorporating locktabs, as shown in figure 362, was designed, fabricated, and included on later builds, eliminating problems in this area.
2. Wear resulting from a 41,000-cycle endurance test at LN₂ temperatures indicated a need for chrome coating the valve housing on the port area surface that was in rubbing contact with the Be-Cu piston ring. The housing surface was chrome coated, and a subsequent test revealed a marked improvement in resistance to wear.
3. The locktabs for the valve retaining bolts were redesigned to simplify installation. The new tab design, which is shown in figure 368 accommodated two bolts and eliminated the requirement to externally hold the locktabs in the required position during the torquing procedure.
4. Linearity tests of the flow divider valve actuator indicated that an improved potentiometer mount was required. The original mount allowed a shift in potentiometer position during violent actuator movement. The mount was redesigned to provide better support, and tests revealed no shift in potentiometer position.

UNCLASSIFIED

CONFIDENTIAL

5. The igniter oxidizer supply passage was converted to provide a secondary oxidizer purge. The igniter supply passage was connected to two of the secondary flow channels, and the original entrance port was plugged.

(C) The piston seal test rig shown in exploded assembly in figure 369 was designed to simulate the flow divider valve piston and shaft seal packages. The rig was designed to test 0.681-in. ID shaft seals, 1.357-in. ID face seals, and a 0.683-in. OD piston seal. Design operating conditions were temperature of 140°R, 5000 to 6400 psig GN₂ inlet pressure, shaft stroke of 1.25-in., and shaft cycle rate of 1 cps. Seal vent passages were provided to measure leakage flows. The rig was translated by a pneumatic actuator. Materials and pertinent dimensions were the same as corresponding flow divider valve parts.

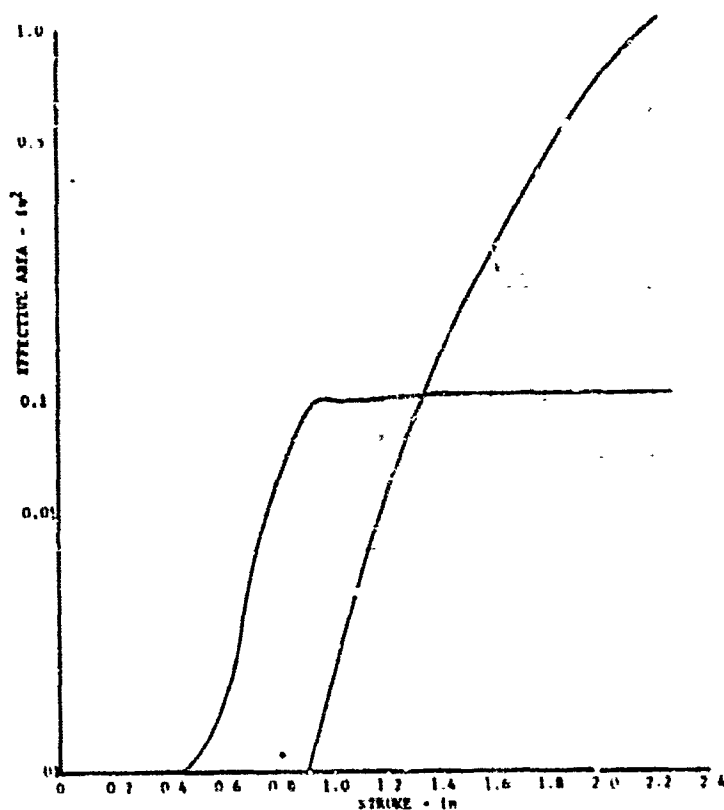


Figure 367. Preburner Oxidizer Flow Divider Valve (Predicted Effective Area vs Stroke)

DF 59535

CONFIDENTIAL

CONFIDENTIAL

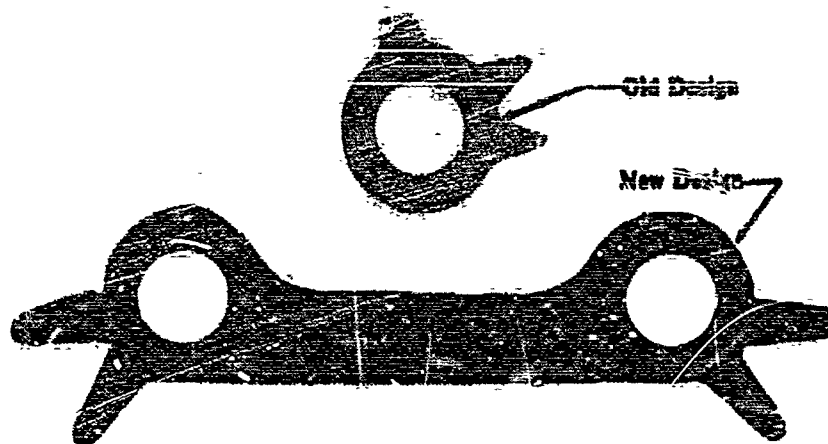


Figure 368. Revised Flow Divider Valve Locktab Design FD 22058

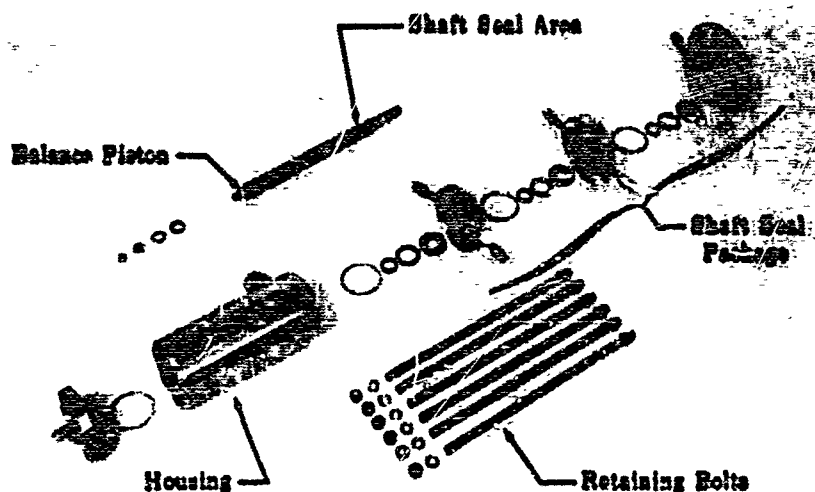


Figure 369. Exploded View of Piston Seal Test Rig FD 23420

2. Test Program and Test Results

a. Evaluation of Reynolds Number Effect

(U) This test series was conducted to assure that the Reynolds number range used in the water calibration was above the value that affects the flow coefficient. Exact Reynolds number simulation during calibration was not possible because of the pressure limitations of the water flow calibration stand. For the same volumetric flow rate, the Reynolds number in liquid oxygen was approximately 4.6 times the Reynolds number

CONFIDENTIAL

in water because of viscosity differences. However, data published on the relation of flow coefficient to Reynolds number for square edged orifices showed that above a critical value, Reynolds number had no further effect on flow coefficient.

(C) This effect was evaluated by calculating the valve effective area for a fixed valve position from data recorded at several flow rates. Figures 370 and 371 show the effect of the valve pressure drop on the effective area for the primary and secondary circuits. The equivalent pressure drop for liquid oxygen was included for reference. These data show that no Reynolds number effect was seen above 100 psi pressure drop for the primary and 150 psi pressure drop for the secondary. The valve calibrations were conducted above these critical values.

(U) Further verification of the calibration techniques is illustrated in figure 372, where the total valve effective area as determined by water flow calibration was compared to the effective area as derived from combustion rig testing with liquid oxygen.

b. Water Flow Calibrations

(U) Water flow calibrations of the flow divider valve were conducted to define the relation of valve stroke to effective area. These data were correlated with the design predictions as shown on figure 373. Deviation from the design predictions occurred in the full open position of the primary circuit where the passage losses were less than predicted.

(U) Definition of the valve stroke to effective area relationship was necessary to allow valve positioning during staged-combustion testing to provide the proper flow split between the preburner primary and secondary flow circuits. The relationship of valve effective area to other flow parameters is illustrated by the nomograph shown in figure 374.

c. Actuator/Servocontrol Response and Linearity

(U) Tests were conducted with the flow divider valve actuator to determine (1) the frequency response and linearity with the standard servovalve control loop, and (2) improvement in linearity with addition of a position feedback circuit to the standard servocontrol loop.

(U) A sine wave generator was used to cycle the valve position input signal, and a precision voltage source was used with a potentiometer to define the valve position. Frequency response and phase lag were defined by oscillograph traces of the actuator, and the desired actuator position as the input signal was cycled at various frequencies. The frequency response and phase lag data are shown in figure 375.

(U) Nonlinearity for the test series was defined as the measured deviation from a linear position vs voltage relationship between the minimum and maximum valve positions. Calibration of the valve position potentiometers indicated their linearity to be $\pm 0.05\%$ of full-scale.

(U) The standard servovalve open loop control was evaluated using the system illustrated in figure 376. The test conducted with an external closed loop on valve position is also shown in figure 376.

CONFIDENTIAL

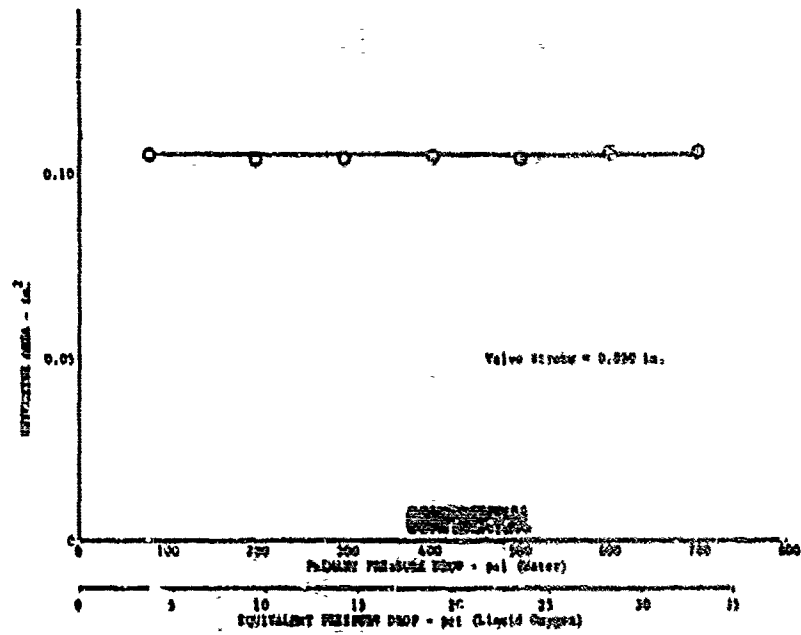


Figure 370. Effective Area vs Pressure Drop for Primary Circuit

DF 56038

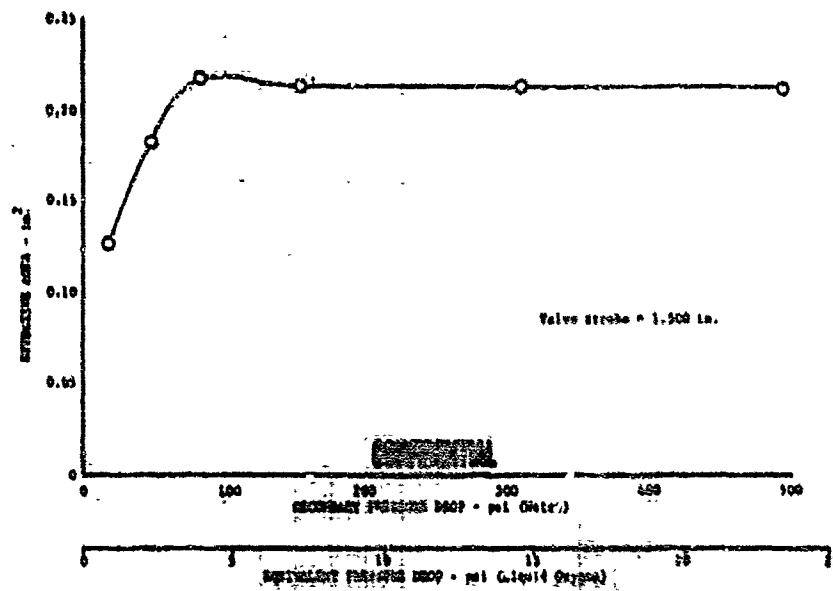


Figure 371. Effective Area vs Pressure Drop for Secondary Circuit

DF 56039

CONFIDENTIAL

UNCLASSIFIED

Water Calibration, 1-21
Test Stand
Oil Calibration, 1-6
Test Stand

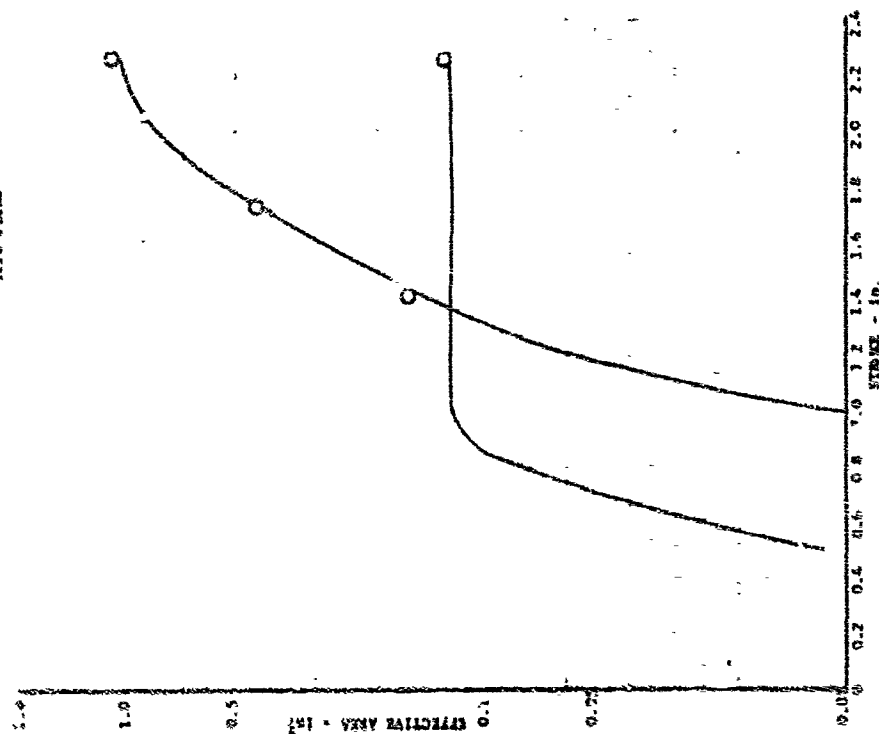


Figure 372. Flow Divider Valve
Effective Area vs Stroke -
Rig F-33469

DF 59536

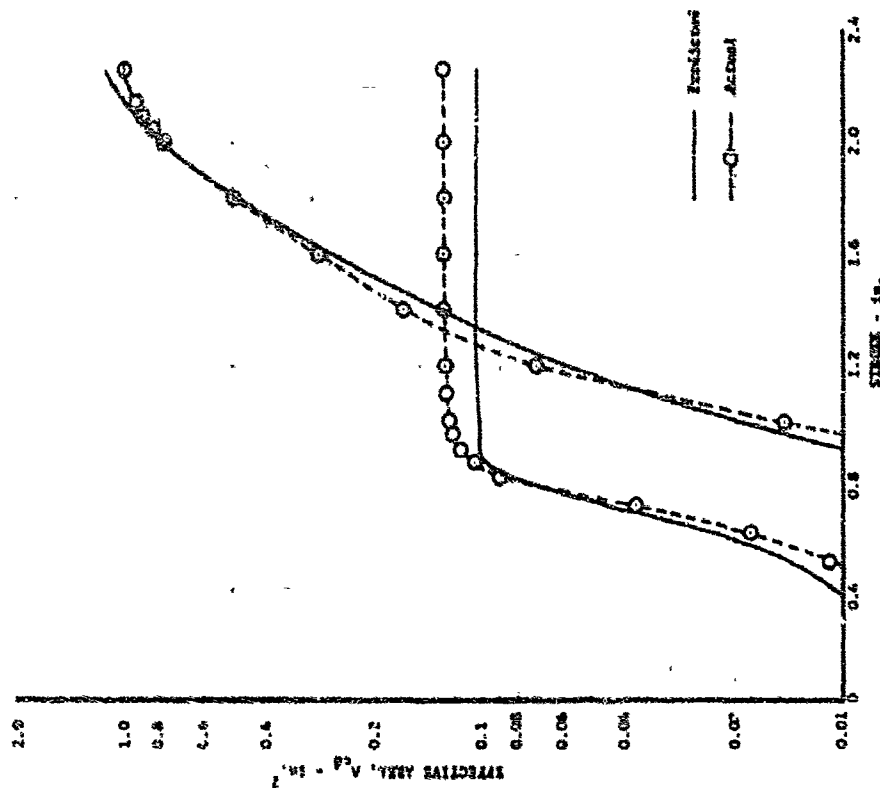


Figure 373. Preburner Oxidizer
Flow Divider Valve Effective
Area vs Stroke - Rig F-33458.2

DF 57179

UNCLASSIFIED

UNCLASSIFIED

Equation:

$$\dot{W} = AC \sqrt{\frac{2g\Delta P}{144}}$$

\dot{W} = Flow (lb/sec)

AC = Effective Area (in²)

g = Gravitational Constant (32.2 ft/sec²)

ΔP = Differential Pressure (lb/in²)

ρ = Density (lb/ft³)

Key:

$\rho \propto \Delta P \rightarrow R$

$R \propto AC \rightarrow W$

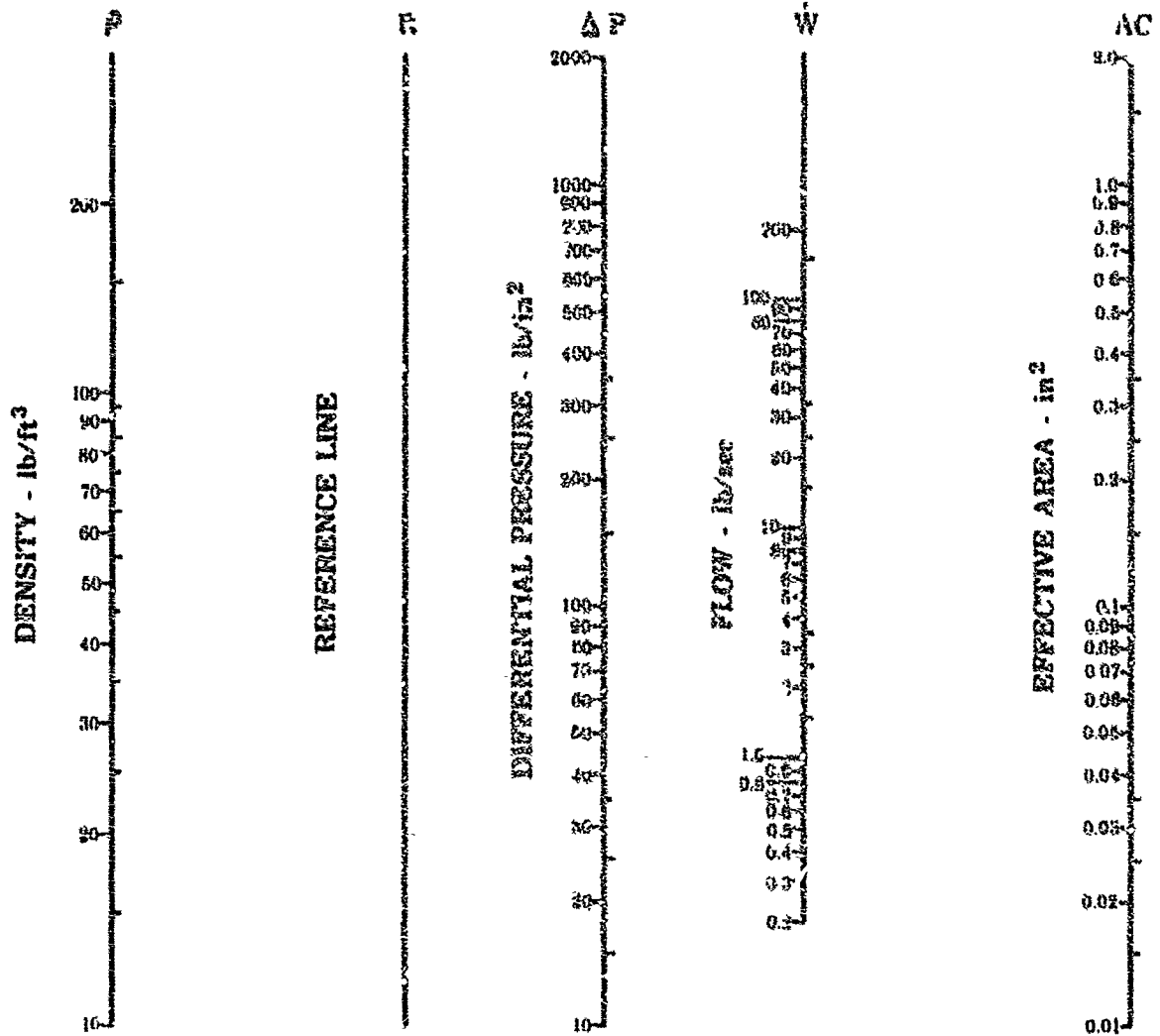
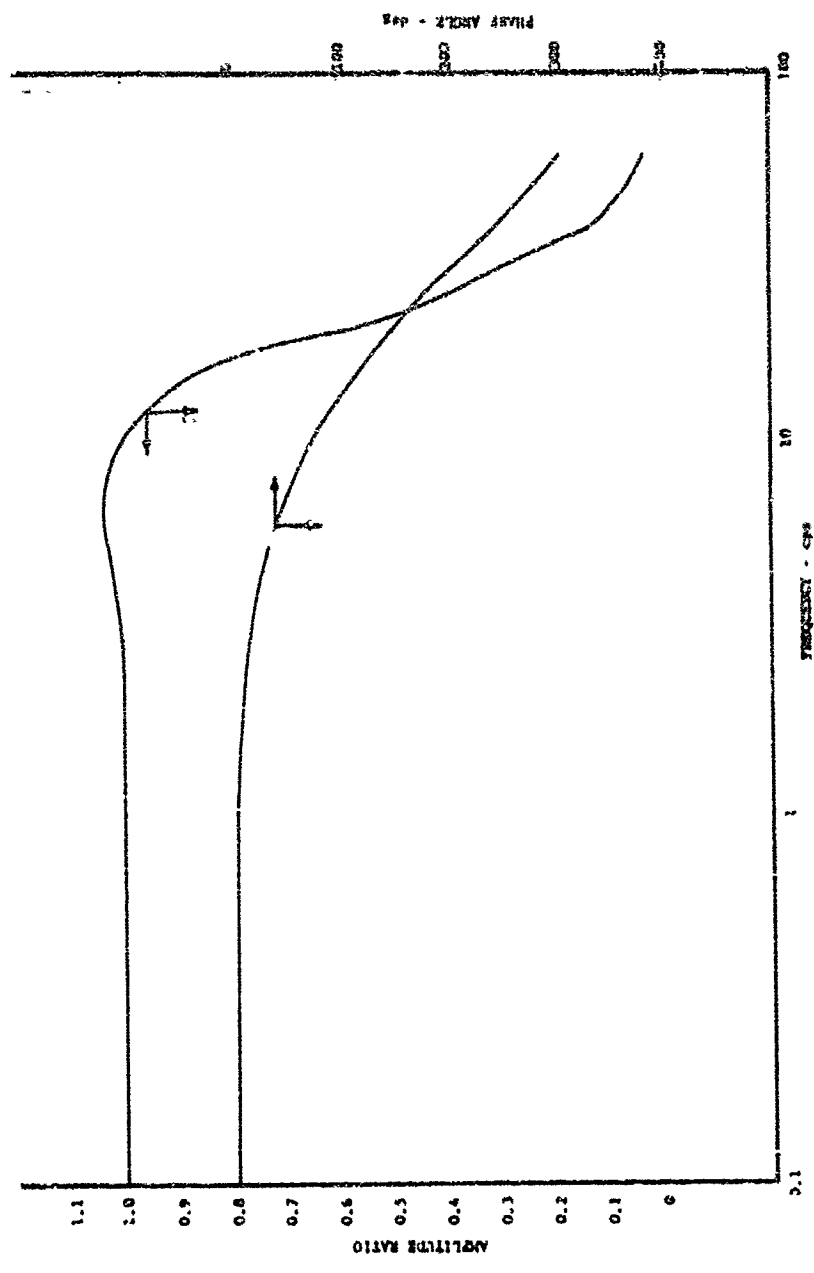


Figure 374. Flow Nomograph

FD 23068

UNCLASSIFIED

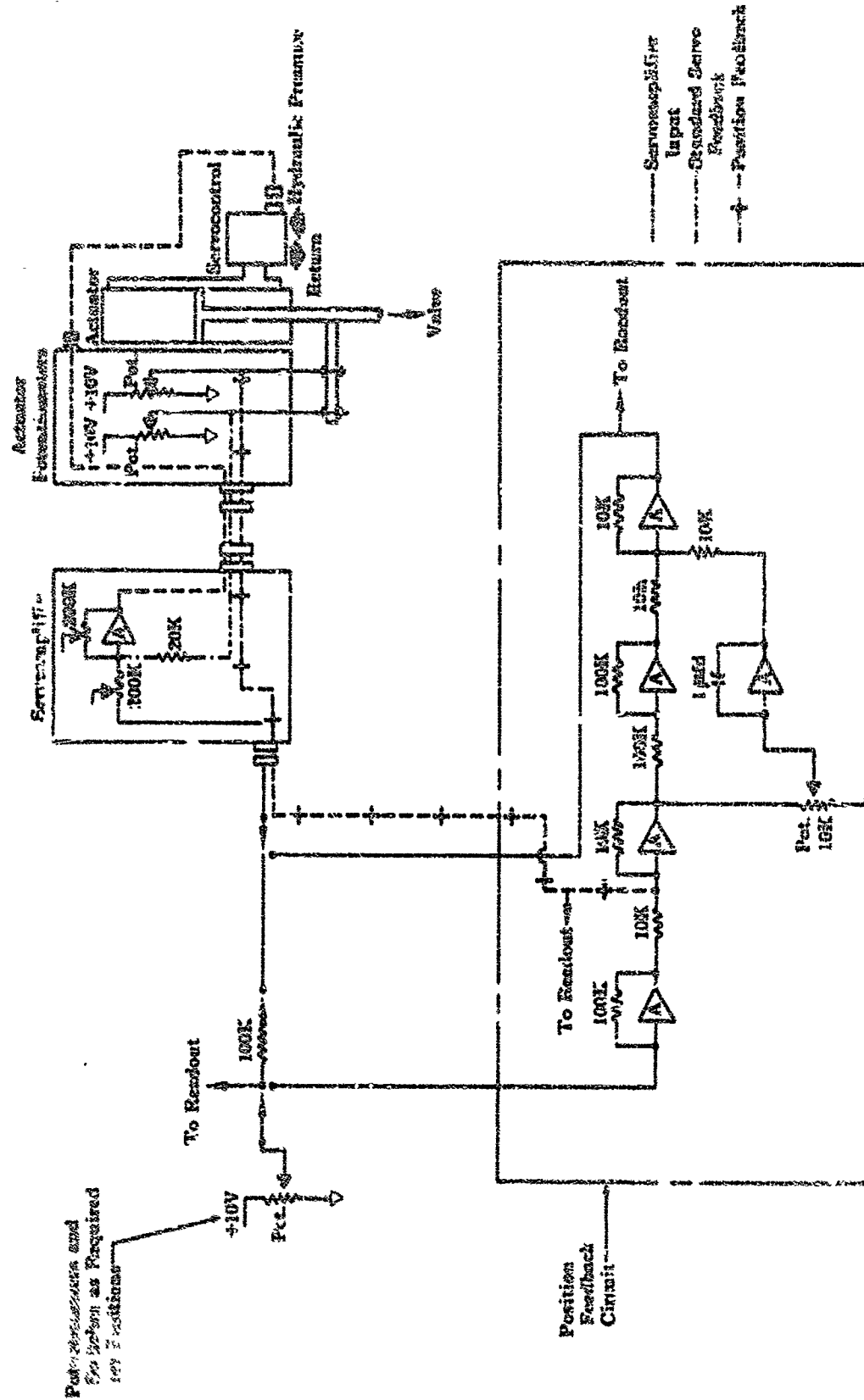
UNCLASSIFIED



REF 56861

Figure 375. Bode Plot for Flow Divider Valve Actuator Rig F-33465.

UNCLASSIFIED



CONFIDENTIAL

(U) Two types of step input tests were conducted for both open loop and closed loop control. The first test called for valve movement in incremental steps of approximately 10% of the total valve travel (0-10%, 10%-20%, 20%-30%, etc.). The second test series called for actuator movement in step increments (0-10%, 0-20%, 0-30%, etc.). Both test series were conducted with increasing and decreasing actuator strokes to evaluate hysteresis.

(U) The results of the open loop and closed loop tests with fixed step increments are shown in figure 377 and the hysteresis is shown in figure 378. The results of the open loop and closed loop test with increasing step increments are shown in figure 379 and the hysteresis is shown in figure 380.

(U) The majority of the open loop test points were within the goal of $\pm 0.5\%$ linearity. A maximum deviation of 1.06% occurred at the 70% position for the fixed step input series. Linearity for the closed loop test series with both fixed and increasing step increments was within $\pm 0.06\%$.

(U) This test series indicated that the observed linearity and hysteresis were suitable for demonstrator engine use, although the open loop servocontrol system did not meet the intended goal of $\pm 0.5\%$ linearity over the entire range. The closed loop system would provide a linearity well within the $\pm 0.5\%$ goal, but does not warrant the additional complexity for this application.

d. Power Requirements

(U) A test program was conducted to determine the maximum power requirements of the flow divider valve. Because of the balanced nature of the valve design, flow forces were minimal and were neglected for this evaluation. The maximum forces occurred during breakaway and were caused by seal and piston ring static friction. The piston ring and seal drag was measured at cryogenic conditions and ambient pressure during the valve cyclic endurance program. The results of this test are shown in figure 381.

(C) Endurance tests of the flow divider valve were conducted to evaluate the wear characteristics of parts in rubbing contact and the integrity of parts subject to pressure and impact loading. The first test was a 41,000 cycle endurance test conducted at LN₂ temperatures.

(C) The valve was subjected to 11,000 cycles to test the Teflon shutoff seal sealing endurance and mechanical integrity. Figure 382 shows the shutoff seal leakage at intervals during these cycles.

CONFIDENTIAL

DF 56857

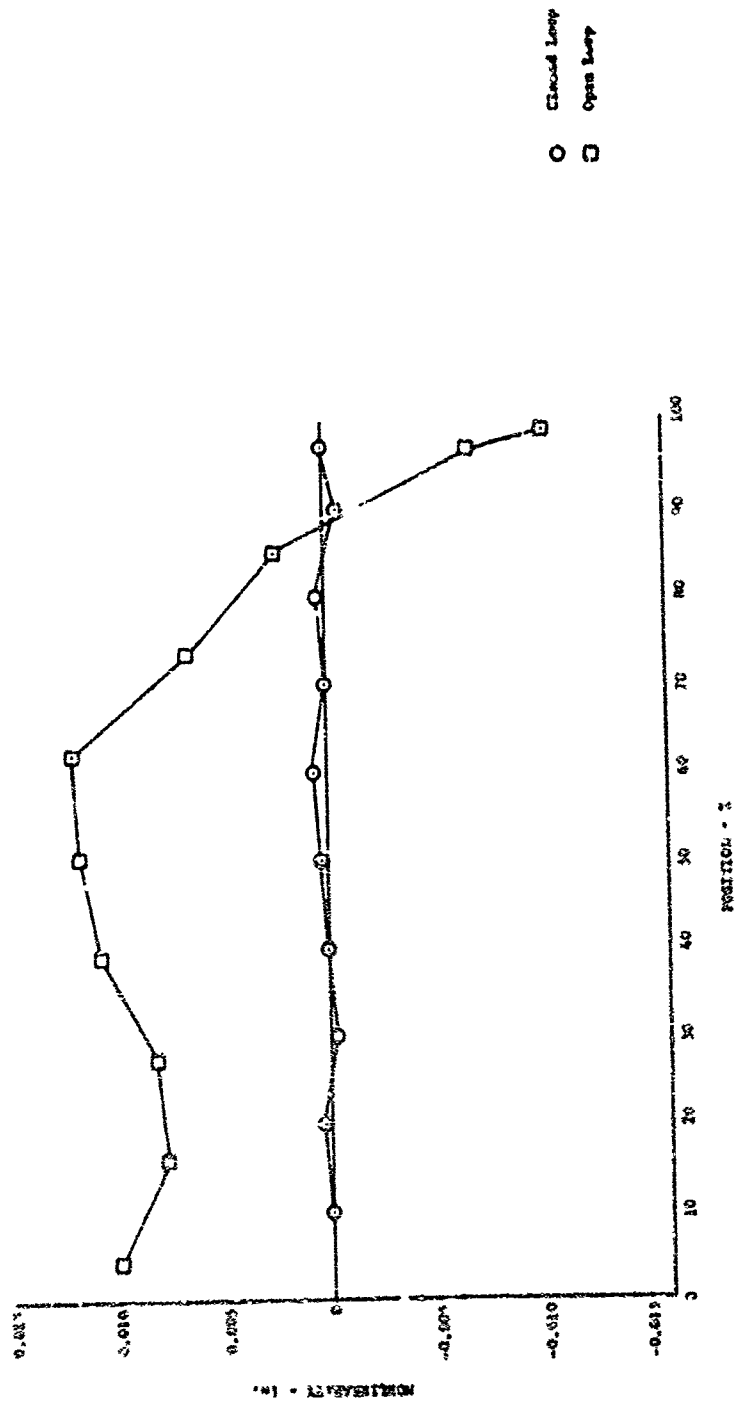


Figure 377. Nonlinearity vs Percent Valve Stroke for Flow Divider Valve Actuator
Rig F-33465-1 (Fixed Step Increments)

400

CONFIDENTIAL

(This page is Unclassified)

UNCLASSIFIED

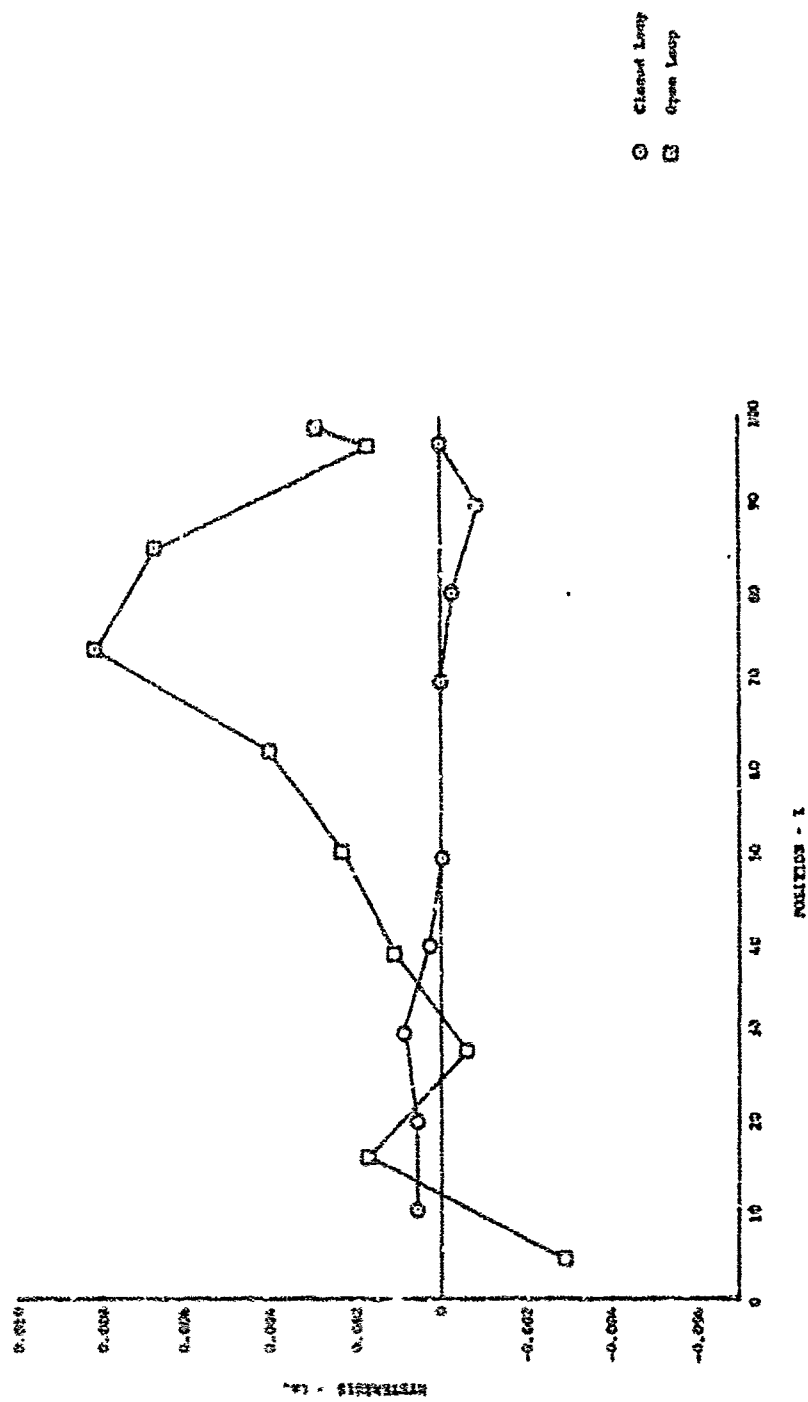


Figure 378. Hysteresis vs Percent Valve Stroke for Flow Divider Valve Actuator Rig F-33465-1
(Fixed Step Increments)

DF 56858

UNCLASSIFIED

UNCLASSIFIED

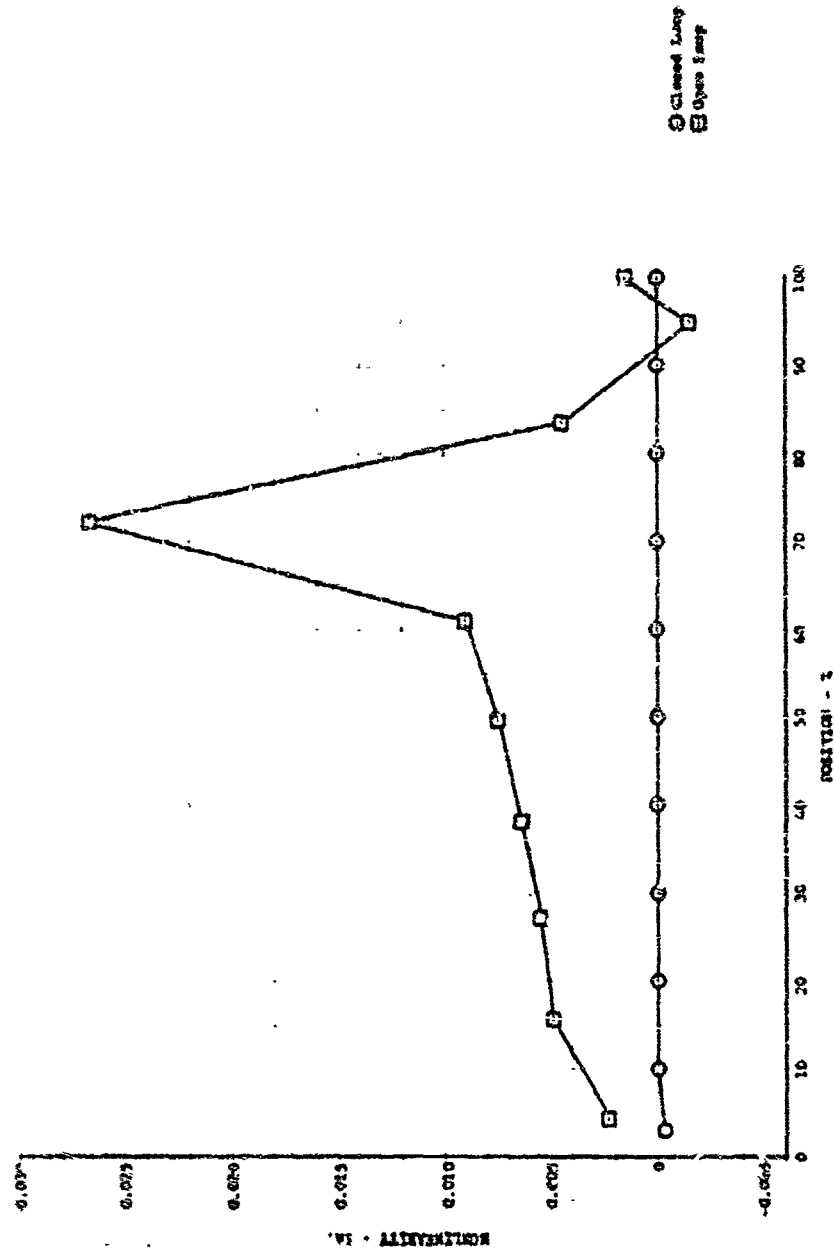


Figure 379. Nonlinearity vs Percent Valve Stroke for Flow Divider Valve Actuator Rig F-33465-1
(Increasing Step Increments)

DF 56859

UNCLASSIFIED

CONFIDENTIAL

DF 56860

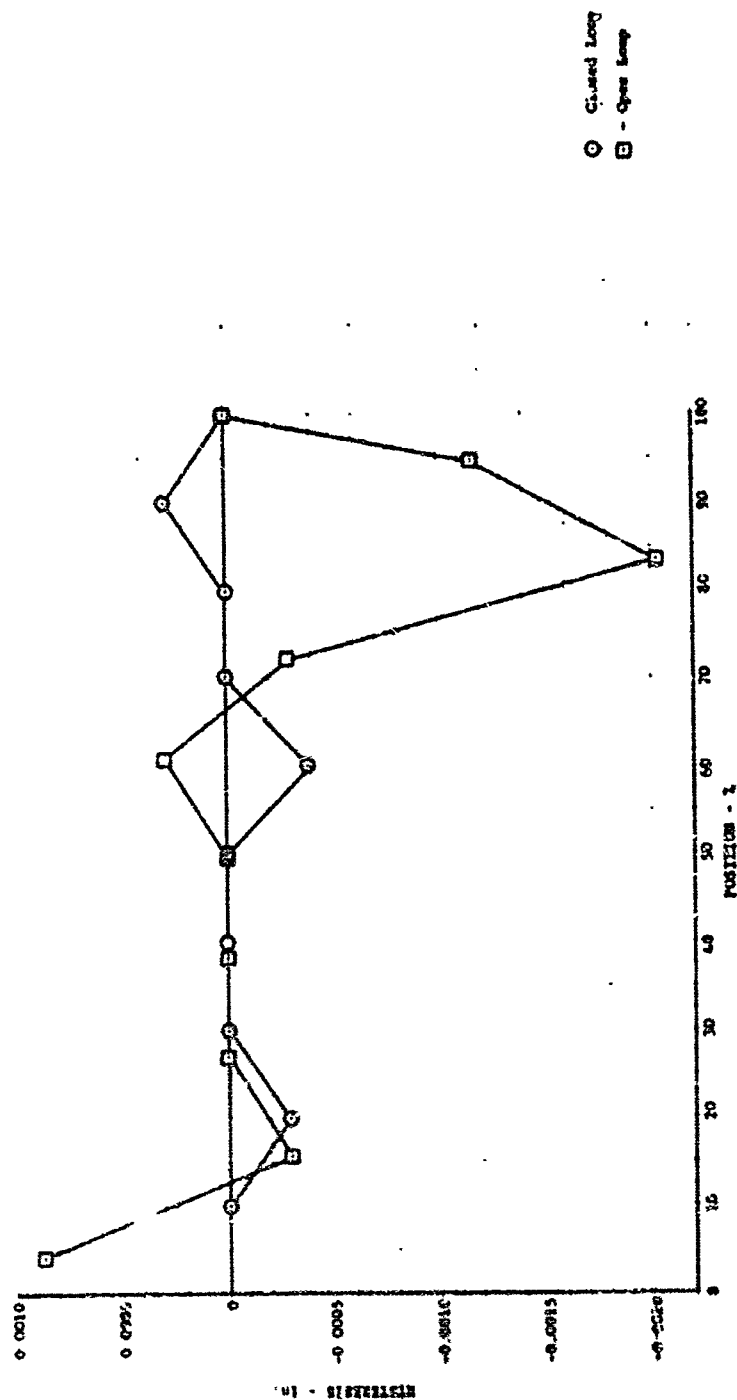


Figure 380. Hysteresis vs. Percent Valve Stroke for Flow Divider Valve / tuator Rig F-33465-1
(Increasing Step Increments)

CONFIDENTIAL

(This page is Unclassified)

CONFIDENTIAL

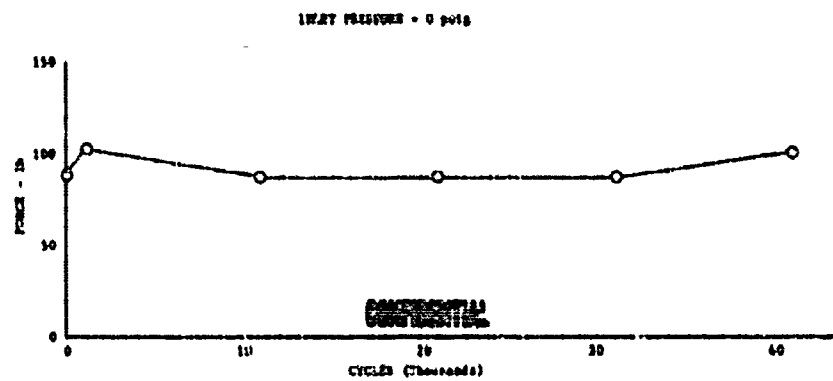


Figure 381. Actuator Breakaway Force vs Cycles DF 36862
for Flow Divider Valve Rig F-33458-4

CONFIDENTIAL

CONFIDENTIAL

DF 58010

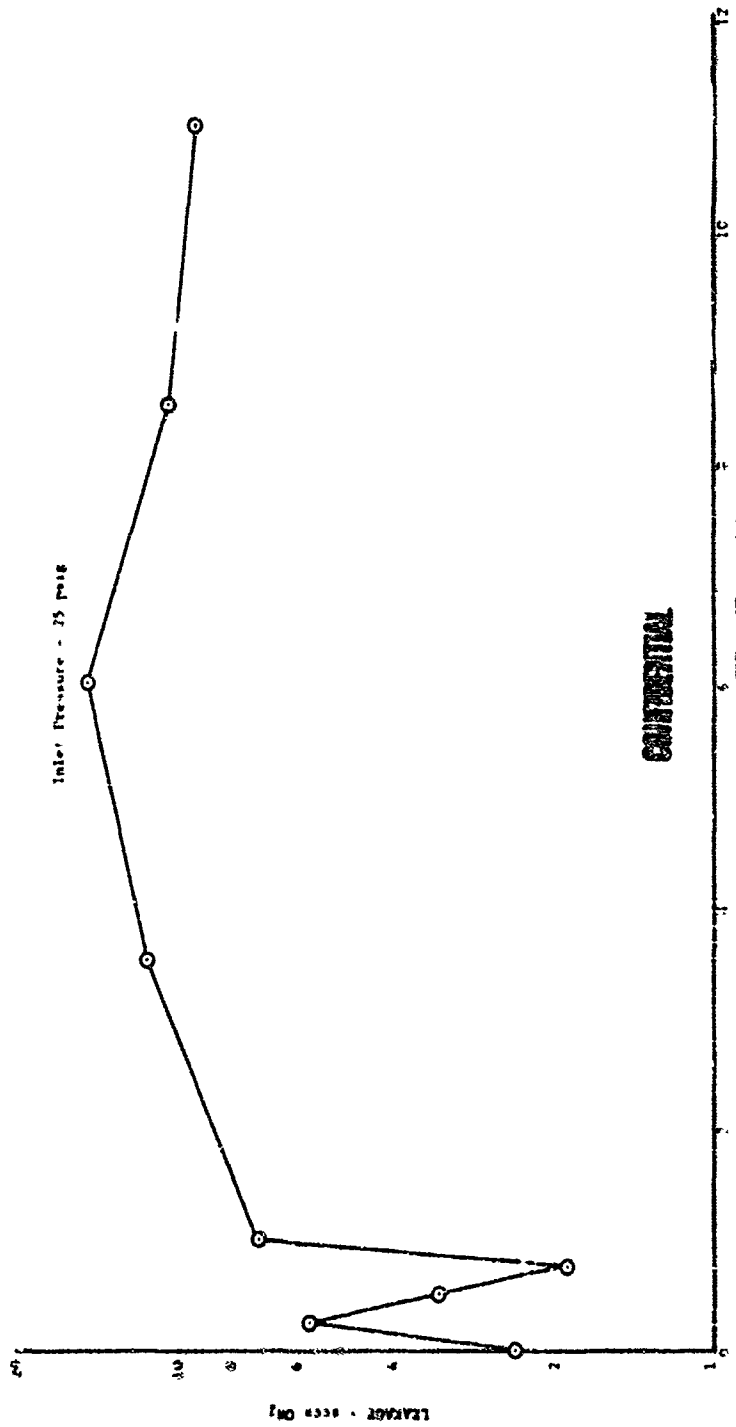


Figure 382. Teflon Shutoff Seal Leakage vs Cycles for Flow Divider Valve Rig F-33458-4

CONFIDENTIAL

CONFIDENTIAL

(U) No appreciable wear of the shutoff mechanical stop surface was observed. (See figure 383.)

(U) The secondary sleeve sealing edge and stop surface showed no appreciable wear as shown in figure 384.

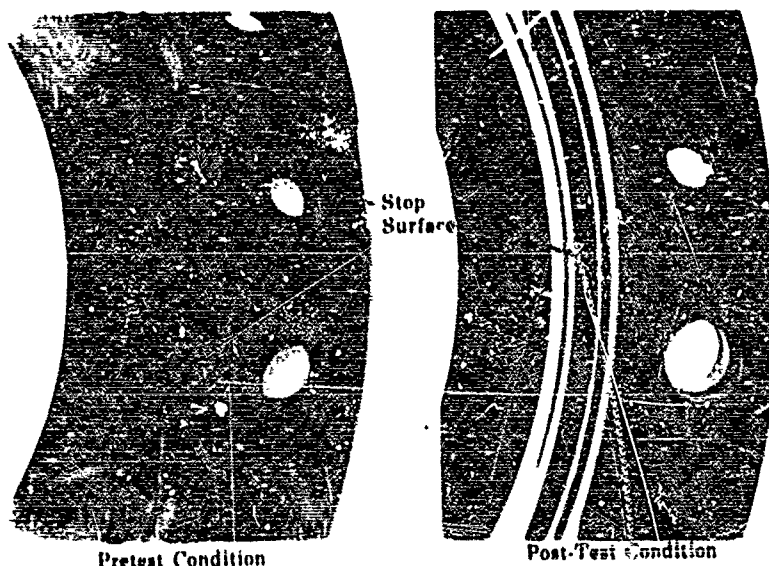


Figure 383. Pretest and Post-Test Condition of Shutoff Mechanical Stop Surface

FD 22189

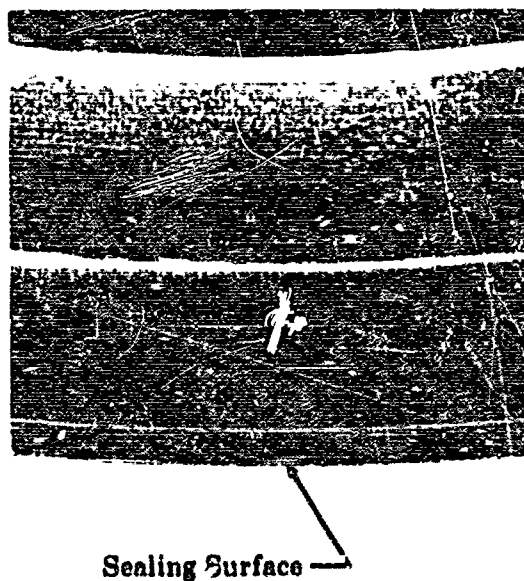


Figure 384. Post-Test Condition of Secondary Sleeve Sealing Edge

FD 22198

406

CONFIDENTIAL

(This page is Unclassified)

CONFIDENTIAL

(C) Leakage past the secondary piston rings was measured during 30,000 cycles of the test. Ten thousand cycles were performed in the primary range with 100-psi differential pressure across the rings. A second 10,000 cycles were performed at a different valve position in the primary range with no pressure drop across the rings. The amplitude for both sets of cycles was 0.10-inch. A third set of 10,000 cycles, with an amplitude of 1.40-inch and no pressure load on the rings, was conducted over the secondary port area. Leakage past the rings was measured at 100-psi differential pressure and is shown in figure 385.

(U) Figure 386 illustrates the effects of pressure loading versus no pressure loading on the rings by showing the difference in ring wear and Be-Cu deposits on the valve housing. Figure 387 shows the valve housing prior to testing.

(U) The upper secondary piston ring exhibited some outside diameter wear, and there were Be-Cu deposits around the secondary port area on the valve housing. Figure 388 illustrates pretest and post-test conditions of these parts.

(U) Be-Cu deposits were found on the inside diameter of the secondary sleeve as a result of upper secondary piston ring wear. The lower secondary piston ring exhibited some inside diameter wear as shown in figure 389.

(U) Slight contamination and wear were found on the primary, secondary, and vent Omniseal shaft seals. The primary spool piston, piston rings, the piston seal showed moderate wear, and the piston seal was slightly contaminated. These results are illustrated in figure 390. There was little evidence of wear in the housing bore area that engages the primary spool piston seal and rings. Figure 391 shows the condition before and after the test. Axial gall marks found on the shaft surface of the primary spool are shown in figure 392.

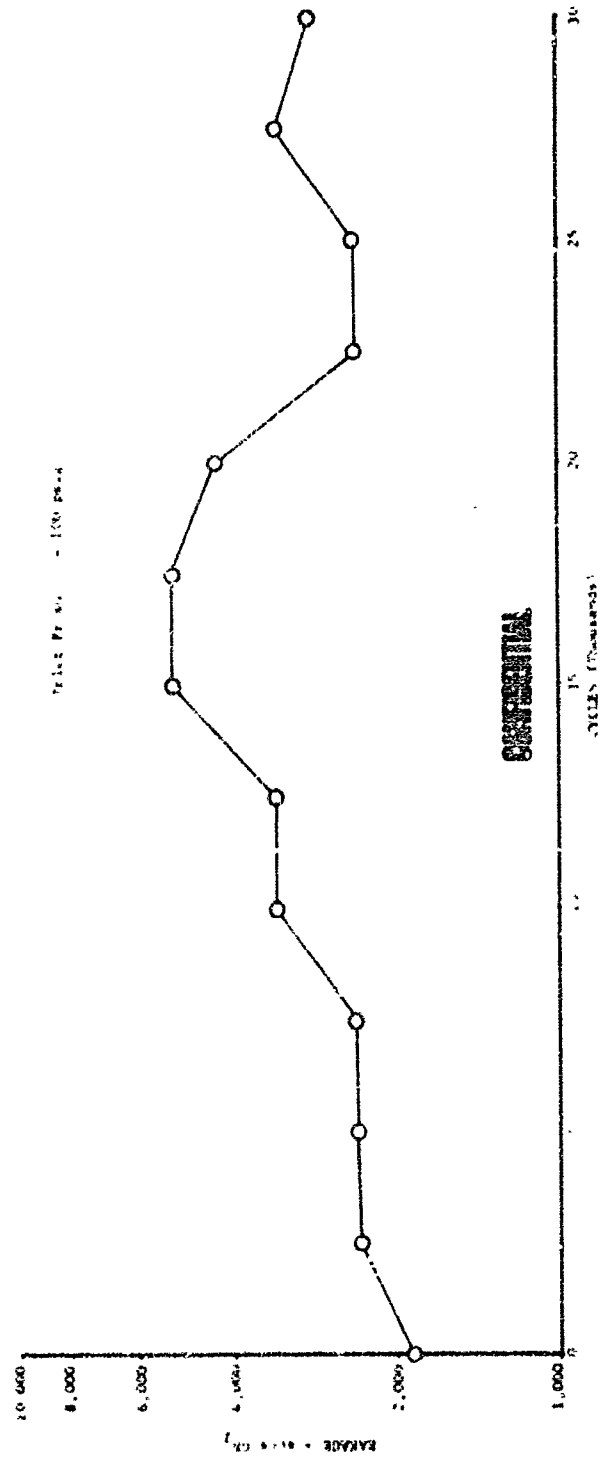
(U) The pre- and post-endurance water calibration data are shown in figure 393.

(U) The chrome-plated secondary sleeve inside diameter exhibited superior wear characteristics as compared to the AMS 5646 (stainless steel) valve housing. Chrome coating of the valve housing was indicated for future applications.

(C) A second cryogenic endurance test was conducted to evaluate chrome coating the valve housing as a means of improving the wear characteristics. In addition, it was desired to determine the effect of valve pressure drop on piston ring and housing wear. The housing was chrome coated per PWA 48 (0.0001 - 0.0002 thick) and subjected to a 35,000-cycle test at LN₂ temperature under various differential pressure loads. The valve mount and installation were similar to the first test.

CONFIDENTIAL

CONFIDENTIAL



DF 58031

Figure 385. Secondary Seal Ring Leakage vs Cycles for Flow Divider Valve Rig F-33458-4

CONFIDENTIAL

UNCLASSIFIED

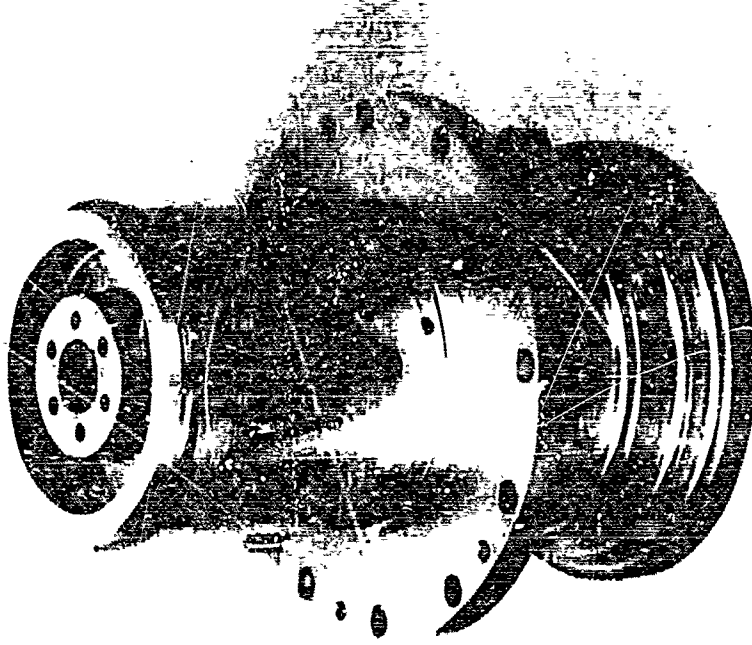
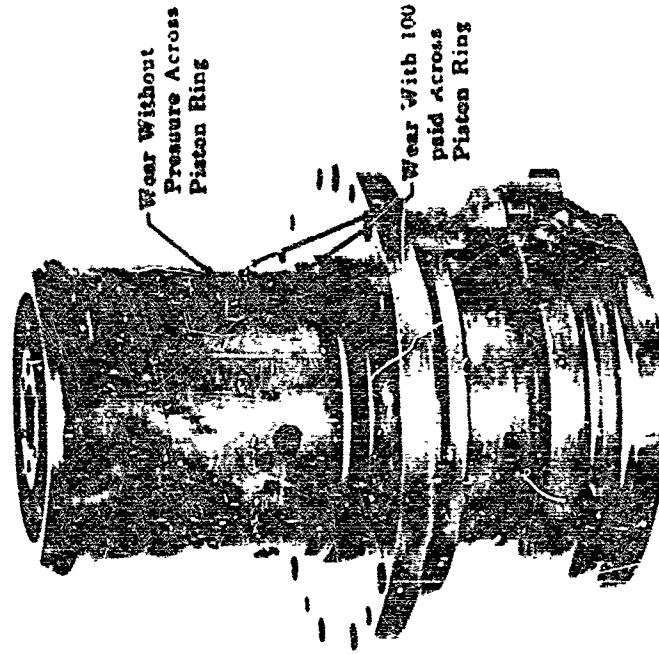


Figure 387. Flow Divider Valve Housing
Prior to Testing

FD 22207

Figure 386. Effects of Pressure
Loading



UNCLASSIFIED

UNCLASSIFIED

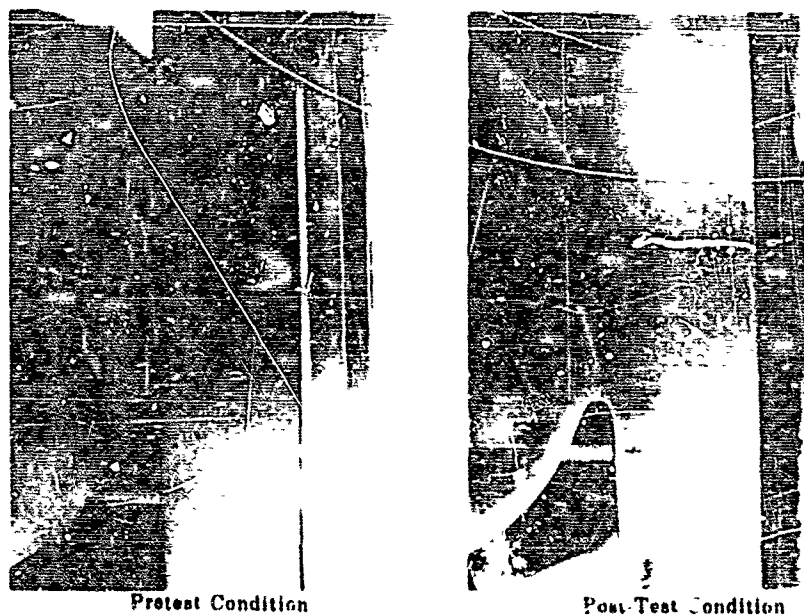


Figure 388. Pretest and Post-Test Condition of Upper Secondary Piston Ring and Secondary Post Area in the Valve Housing FD 22208

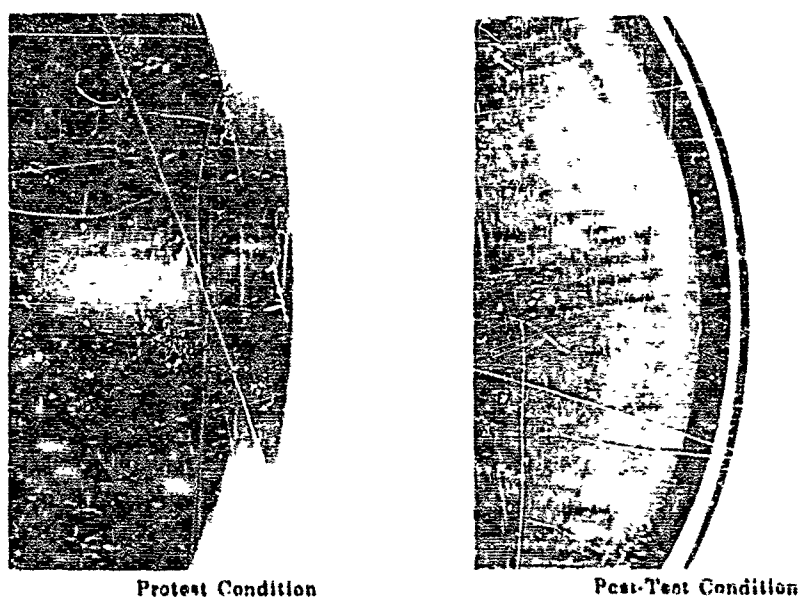
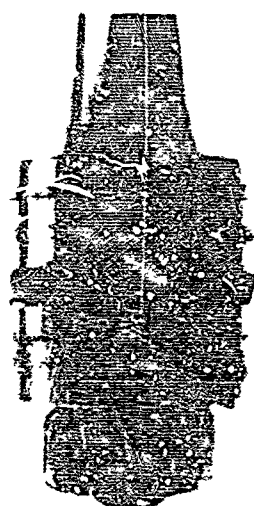


Figure 389. Pretest and Post-Test Condition of Lower Secondary Piston Ring FD 22209

UNCLASSIFIED

UNCLASSIFIED



Pretest Condition



Post Test Condition

Figure 390. Pretest and Post-Test Condition
of Primary Spool

FD 22210



Pretest Condition



Post Test Condition

Figure 391. Pretest and Post-Test Condition
of Spool Bore Area

FD 2 212

UNCLASSIFIED

UNCLASSIFIED

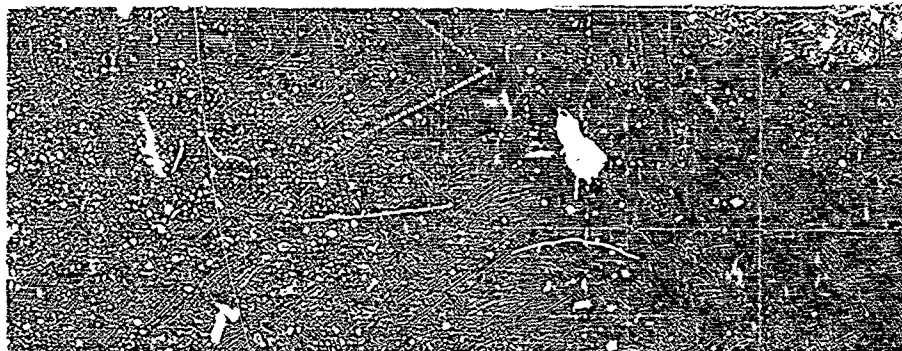


Figure 392. Post-test Condition of Primary Spool Shaft Surface

FE 64044

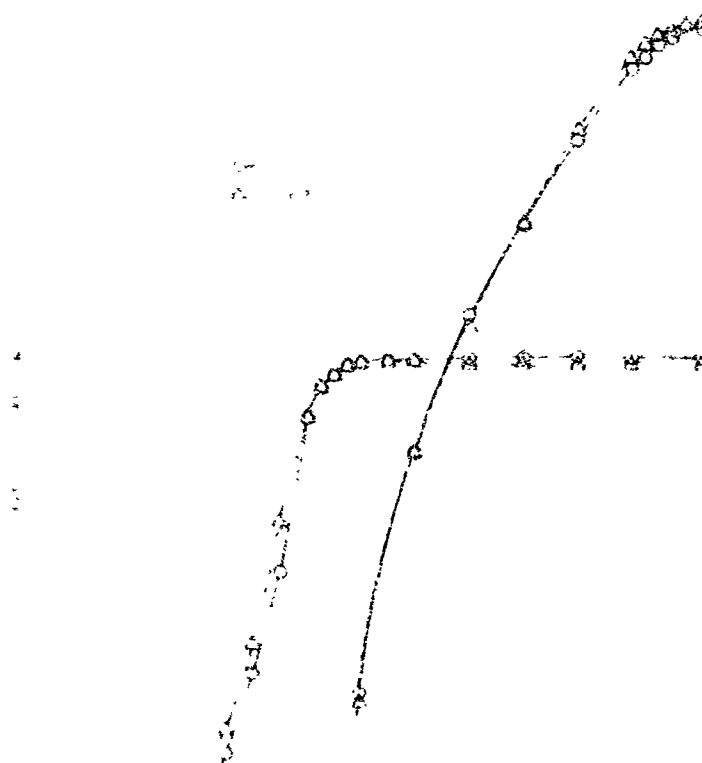


Figure 393. Flow Under Valve Effective Area vs Stroke - Rip F-33458

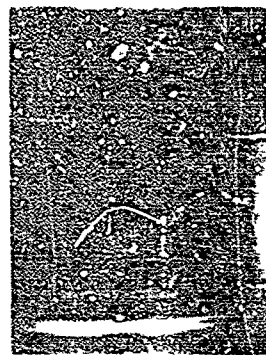
DF 58677

UNCLASSIFIED

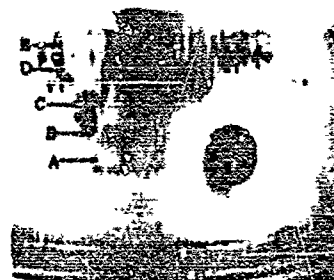
CONFIDENTIAL

(C) the surface areas, A through F in figures 394 and 395 were subjected to cycles at 5 cps at the differential pressures given below:

| Area | Cycles | Pressure Drop (psid) |
|------|--------|-------------------------|
| A | 5,000 | 200 |
| B | 5,000 | 400 |
| C | 5,000 | 600 |
| D | 5,000 | 800 |
| E | 5,000 | 1,000 |
| F | 10,000 | 0 |



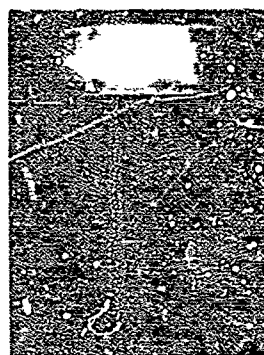
Pretest Condition



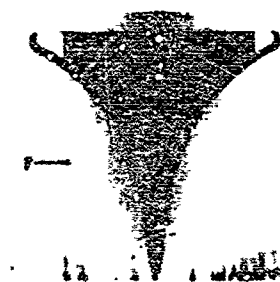
Post Test Condition

Figure 394. Pretest and Post-Test Condition of the Secondary Valve Housing Showing the Effects of Piston Ring Differential Pressure

FD 23019



Pretest Condition



Post Test Condition

Figure 395. Pretest and Post-Test Condition of Secondary Port Area on the Valve Housing

FD 23018

CONFIDENTIAL

(U) Figure 396 shows the leakage past these seals following each cycle set. Figure 397 illustrates the pre- and post-test condition of the upper piston seal ring that was in contact with the secondary sleeve chrome coated inside diameter. Figure 398 shows the pre- and post-test condition of the lower piston seal ring that was in contact with the valve housing. Figure 398 shows the secondary sleeve inside diameter that was in contact with the upper piston seal ring.

(C) The high leakage rate indicated by point (1) on figure 396 is explained by figure 399, where two distinct leakage areas are indicated by the data points. The upper line, showing data taken after 5,000 cycles in area B, as shown on figure 399, indicates a larger leakage than the remaining data points, which are shown in the lower line. This was probably because of a local buildup of Be-Cu at this valve position. The effect of wear as a result of valve cycles is also reflected in the lower line.

(U) In conclusion, the wear characteristics of the Be-Cu piston rings on a chrome coated housing were acceptable for the design differential pressure range. For higher differential pressure applications, two additional revisions are recommended as follows:

1. The hardness of the valve housing and secondary sleeve tested were 53.5 and 64 respectively, as measured on the Rockwell "A" scale. The piston ring hardness was measured at 69 on the Rockwell "A" scale. The valve housing exhibited much greater wear than the sleeve, as shown in figures 394 and 398. An increase in the hardness of the valve housing parent material, to exceed that of the piston ring, is recommended to prevent housing material deformation below the chrome coat.
2. The pressure loading effects of the piston rings can be reduced by a piston ring redesign. By increasing the bearing area of the ring on the low pressure side, the unit compressive stress can be reduced, thus improving the wear characteristics.

(C) The pre- and post-test water calibrations, shown in figure 400, indicate little effect from piston ring wear.

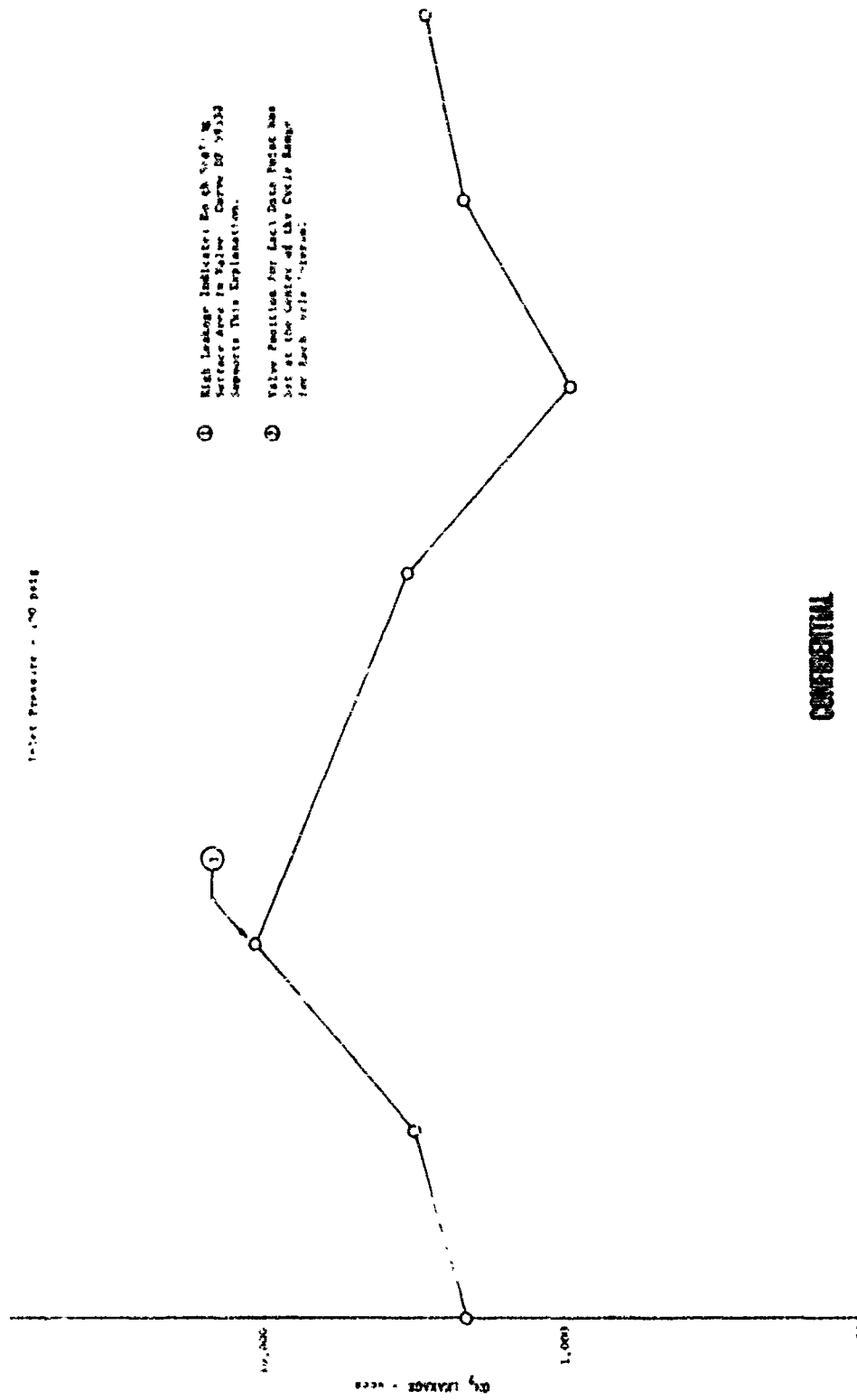
(C) The effect of operating pressure and mechanical cycling on seal drag was determined during an endurance test on the piston seal rig. Maximum seal drag remained essentially constant after 5000 mechanical cycles and indicated an increase of 100 lb force over the ambient pressure force levels. A maximum breakaway force of 200 pounds was defined by combining the results of these tests.

(C) The valve horsepower requirements as a function of required response is shown in figure 401 for a valve stroke of .125 inches.

f. Translating Seal Rig

(U) The flow divider valve test activity is summarized in tables XXXVII, XXXVIII, and XXXIX.

CONFIDENTIAL



CONFIDENTIAL

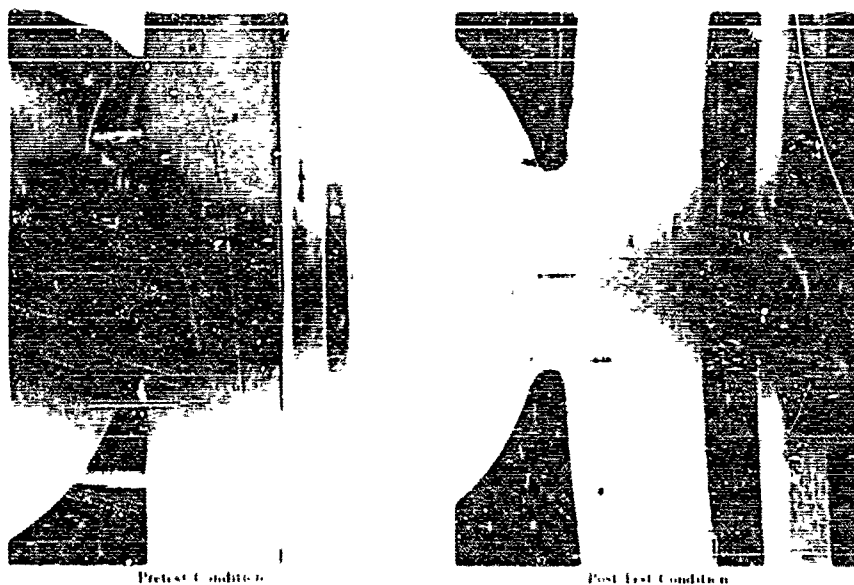


Figure 397. Pretest and Post-Test Condition of Upper Secondary Piston Ring FD 23020

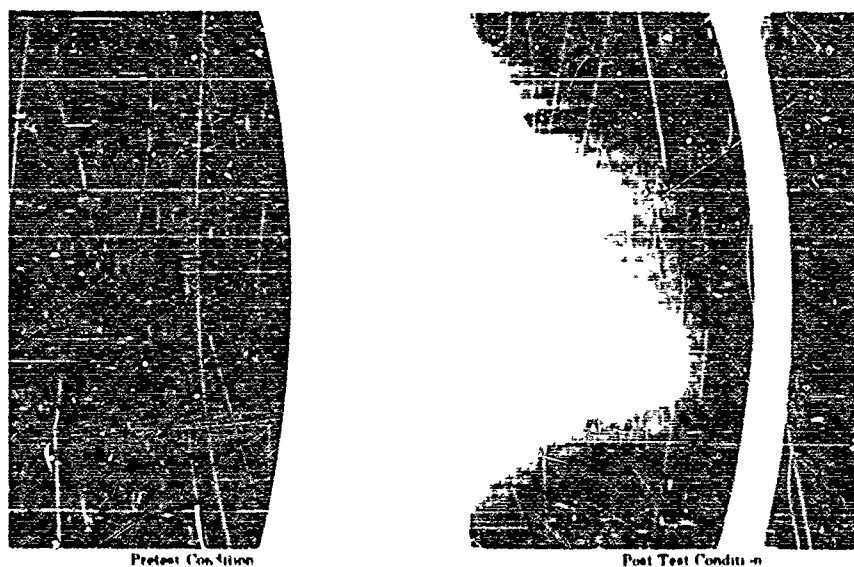


Figure 398. Pretest and Post-Test Condition of Lower Secondary Piston Ring FD 23021

CONFIDENTIAL

(This page is Unclassified)

CONFIDENTIAL

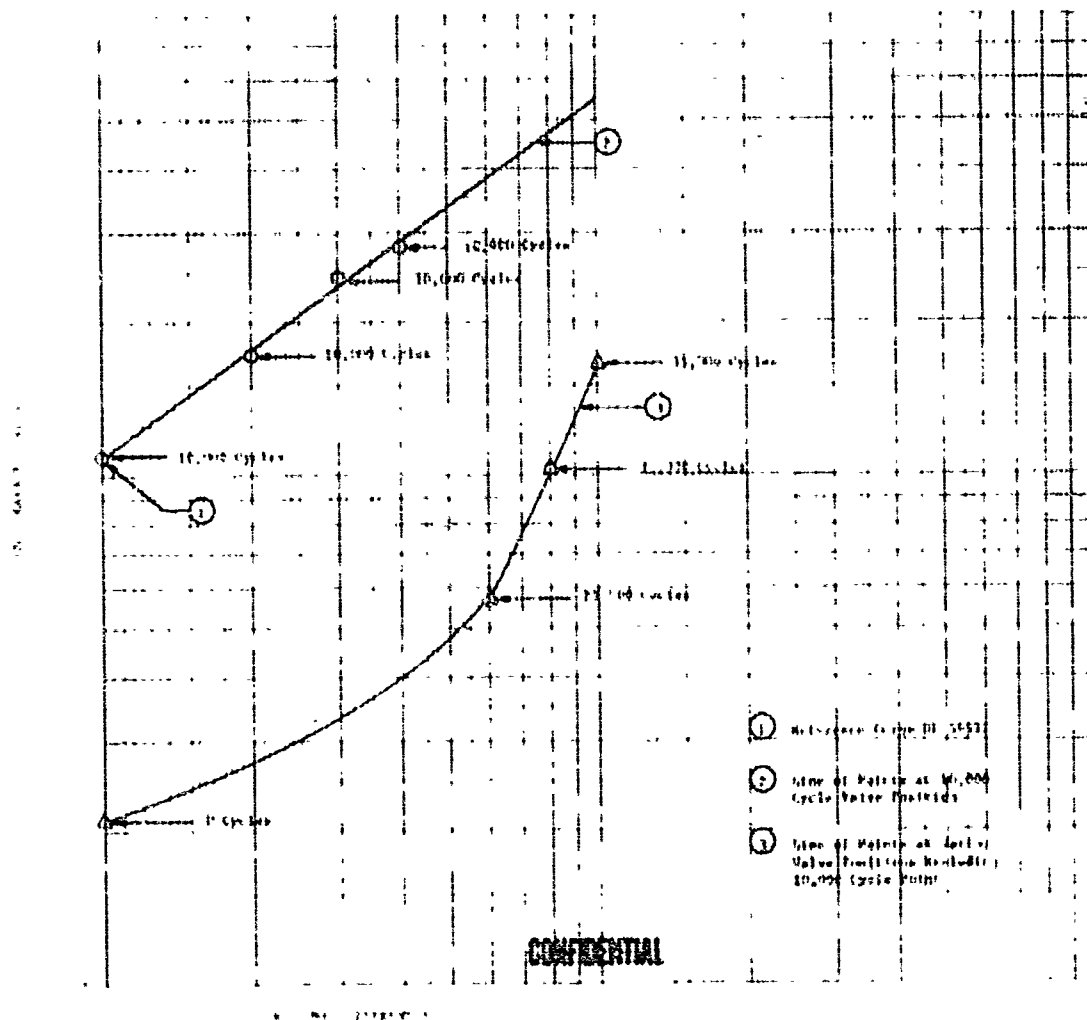
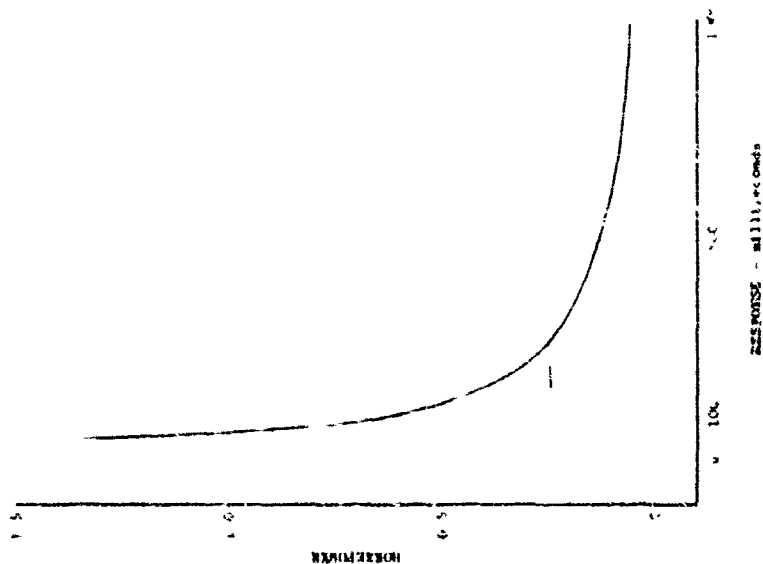


Figure 39c. Piston Seal Ring Leakage vs Differential Pressure

DF 59538

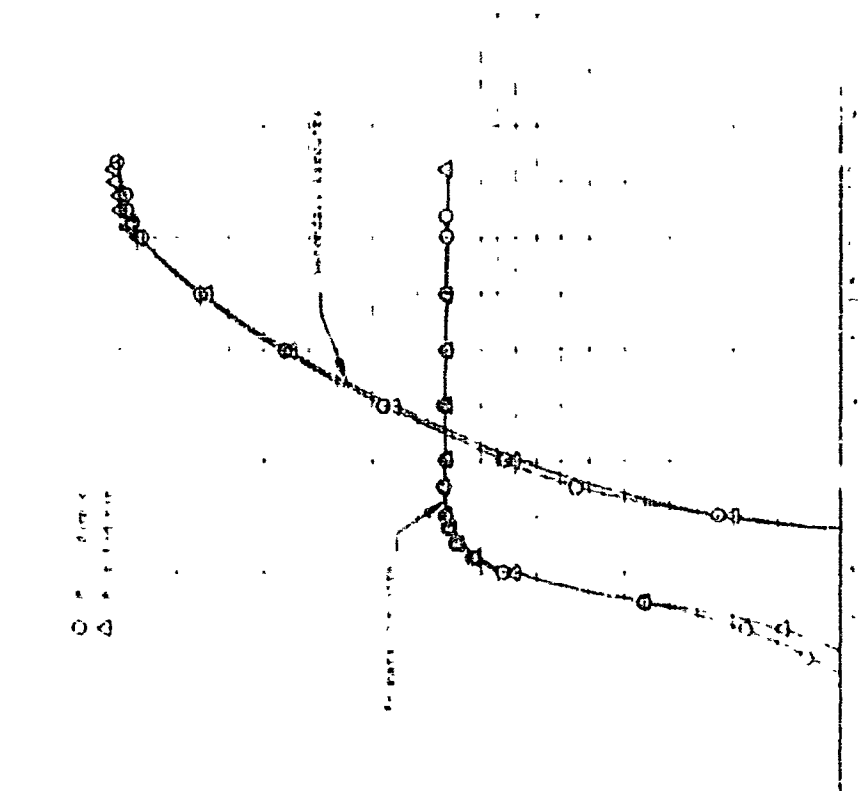
CONFIDENTIAL

CONFIDENTIAL



DF 59796

Figure 401. Flow Divider Valve
Maximum Power Requirements
for Full Stroke of 2.25 in.



DF 59539

Figure 400. Flow Divider Valve
Effective Area vs Stroke
Rig F-3348-6

CONFIDENTIAL

(This page is Unclassified)

CONFIDENTIAL

(Catalog Table XXXVII). Flow Divider Valve 1-33458

| Case No. | Date | Page | Subject | Remarks |
|------------|---------|------|---------|---------|
| 100-100000 | 10-1-40 | 1 | ... | ... |
| 100-100000 | 10-1-40 | 2 | ... | ... |
| 100-100000 | 10-1-40 | 3 | ... | ... |
| 100-100000 | 10-1-40 | 4 | ... | ... |
| 100-100000 | 10-1-40 | 5 | ... | ... |
| 100-100000 | 10-1-40 | 6 | ... | ... |
| 100-100000 | 10-1-40 | 7 | ... | ... |
| 100-100000 | 10-1-40 | 8 | ... | ... |
| 100-100000 | 10-1-40 | 9 | ... | ... |
| 100-100000 | 10-1-40 | 10 | ... | ... |
| 100-100000 | 10-1-40 | 11 | ... | ... |
| 100-100000 | 10-1-40 | 12 | ... | ... |
| 100-100000 | 10-1-40 | 13 | ... | ... |
| 100-100000 | 10-1-40 | 14 | ... | ... |
| 100-100000 | 10-1-40 | 15 | ... | ... |
| 100-100000 | 10-1-40 | 16 | ... | ... |
| 100-100000 | 10-1-40 | 17 | ... | ... |
| 100-100000 | 10-1-40 | 18 | ... | ... |
| 100-100000 | 10-1-40 | 19 | ... | ... |
| 100-100000 | 10-1-40 | 20 | ... | ... |
| 100-100000 | 10-1-40 | 21 | ... | ... |
| 100-100000 | 10-1-40 | 22 | ... | ... |
| 100-100000 | 10-1-40 | 23 | ... | ... |
| 100-100000 | 10-1-40 | 24 | ... | ... |
| 100-100000 | 10-1-40 | 25 | ... | ... |
| 100-100000 | 10-1-40 | 26 | ... | ... |
| 100-100000 | 10-1-40 | 27 | ... | ... |
| 100-100000 | 10-1-40 | 28 | ... | ... |
| 100-100000 | 10-1-40 | 29 | ... | ... |
| 100-100000 | 10-1-40 | 30 | ... | ... |
| 100-100000 | 10-1-40 | 31 | ... | ... |
| 100-100000 | 10-1-40 | 32 | ... | ... |
| 100-100000 | 10-1-40 | 33 | ... | ... |
| 100-100000 | 10-1-40 | 34 | ... | ... |
| 100-100000 | 10-1-40 | 35 | ... | ... |
| 100-100000 | 10-1-40 | 36 | ... | ... |
| 100-100000 | 10-1-40 | 37 | ... | ... |
| 100-100000 | 10-1-40 | 38 | ... | ... |
| 100-100000 | 10-1-40 | 39 | ... | ... |
| 100-100000 | 10-1-40 | 40 | ... | ... |
| 100-100000 | 10-1-40 | 41 | ... | ... |
| 100-100000 | 10-1-40 | 42 | ... | ... |
| 100-100000 | 10-1-40 | 43 | ... | ... |
| 100-100000 | 10-1-40 | 44 | ... | ... |
| 100-100000 | 10-1-40 | 45 | ... | ... |
| 100-100000 | 10-1-40 | 46 | ... | ... |
| 100-100000 | 10-1-40 | 47 | ... | ... |
| 100-100000 | 10-1-40 | 48 | ... | ... |
| 100-100000 | 10-1-40 | 49 | ... | ... |
| 100-100000 | 10-1-40 | 50 | ... | ... |

CONFIDENTIAL

SECRET

(C, Table XXVII. Flow Divider Valve F-33458 (Continued)

| Page No. | Date | Particulars | Debit | Credit | Balance |
|----------|------|----------------|--------|--------|---------|
| 1 | 1950 | By Balance b/d | | 100.00 | 100.00 |
| 2 | 1950 | To Balance c/d | 100.00 | | 100.00 |
| 3 | 1950 | By Balance b/d | | 100.00 | 100.00 |
| 4 | 1950 | To Balance c/d | 100.00 | | 100.00 |
| 5 | 1950 | By Balance b/d | | 100.00 | 100.00 |
| 6 | 1950 | To Balance c/d | 100.00 | | 100.00 |
| 7 | 1950 | By Balance b/d | | 100.00 | 100.00 |
| 8 | 1950 | To Balance c/d | 100.00 | | 100.00 |
| 9 | 1950 | By Balance b/d | | 100.00 | 100.00 |
| 10 | 1950 | To Balance c/d | 100.00 | | 100.00 |
| 11 | 1950 | By Balance b/d | | 100.00 | 100.00 |
| 12 | 1950 | To Balance c/d | 100.00 | | 100.00 |
| 13 | 1950 | By Balance b/d | | 100.00 | 100.00 |
| 14 | 1950 | To Balance c/d | 100.00 | | 100.00 |
| 15 | 1950 | By Balance b/d | | 100.00 | 100.00 |
| 16 | 1950 | To Balance c/d | 100.00 | | 100.00 |
| 17 | 1950 | By Balance b/d | | 100.00 | 100.00 |
| 18 | 1950 | To Balance c/d | 100.00 | | 100.00 |
| 19 | 1950 | By Balance b/d | | 100.00 | 100.00 |
| 20 | 1950 | To Balance c/d | 100.00 | | 100.00 |
| 21 | 1950 | By Balance b/d | | 100.00 | 100.00 |
| 22 | 1950 | To Balance c/d | 100.00 | | 100.00 |
| 23 | 1950 | By Balance b/d | | 100.00 | 100.00 |
| 24 | 1950 | To Balance c/d | 100.00 | | 100.00 |
| 25 | 1950 | By Balance b/d | | 100.00 | 100.00 |
| 26 | 1950 | To Balance c/d | 100.00 | | 100.00 |
| 27 | 1950 | By Balance b/d | | 100.00 | 100.00 |
| 28 | 1950 | To Balance c/d | 100.00 | | 100.00 |
| 29 | 1950 | By Balance b/d | | 100.00 | 100.00 |
| 30 | 1950 | To Balance c/d | 100.00 | | 100.00 |
| 31 | 1950 | By Balance b/d | | 100.00 | 100.00 |
| 32 | 1950 | To Balance c/d | 100.00 | | 100.00 |
| 33 | 1950 | By Balance b/d | | 100.00 | 100.00 |
| 34 | 1950 | To Balance c/d | 100.00 | | 100.00 |
| 35 | 1950 | By Balance b/d | | 100.00 | 100.00 |
| 36 | 1950 | To Balance c/d | 100.00 | | 100.00 |
| 37 | 1950 | By Balance b/d | | 100.00 | 100.00 |
| 38 | 1950 | To Balance c/d | 100.00 | | 100.00 |
| 39 | 1950 | By Balance b/d | | 100.00 | 100.00 |
| 40 | 1950 | To Balance c/d | 100.00 | | 100.00 |
| 41 | 1950 | By Balance b/d | | 100.00 | 100.00 |
| 42 | 1950 | To Balance c/d | 100.00 | | 100.00 |
| 43 | 1950 | By Balance b/d | | 100.00 | 100.00 |
| 44 | 1950 | To Balance c/d | 100.00 | | 100.00 |
| 45 | 1950 | By Balance b/d | | 100.00 | 100.00 |
| 46 | 1950 | To Balance c/d | 100.00 | | 100.00 |
| 47 | 1950 | By Balance b/d | | 100.00 | 100.00 |
| 48 | 1950 | To Balance c/d | 100.00 | | 100.00 |
| 49 | 1950 | By Balance b/d | | 100.00 | 100.00 |
| 50 | 1950 | To Balance c/d | 100.00 | | 100.00 |
| 51 | 1950 | By Balance b/d | | 100.00 | 100.00 |
| 52 | 1950 | To Balance c/d | 100.00 | | 100.00 |
| 53 | 1950 | By Balance b/d | | 100.00 | 100.00 |
| 54 | 1950 | To Balance c/d | 100.00 | | 100.00 |
| 55 | 1950 | By Balance b/d | | 100.00 | 100.00 |
| 56 | 1950 | To Balance c/d | 100.00 | | 100.00 |
| 57 | 1950 | By Balance b/d | | 100.00 | 100.00 |
| 58 | 1950 | To Balance c/d | 100.00 | | 100.00 |
| 59 | 1950 | By Balance b/d | | 100.00 | 100.00 |
| 60 | 1950 | To Balance c/d | 100.00 | | 100.00 |
| 61 | 1950 | By Balance b/d | | 100.00 | 100.00 |
| 62 | 1950 | To Balance c/d | 100.00 | | 100.00 |
| 63 | 1950 | By Balance b/d | | 100.00 | 100.00 |
| 64 | 1950 | To Balance c/d | 100.00 | | 100.00 |

CONFIDENTIAL

CONFIDENTIAL

CONFIDENTIAL

40 Table XXXIV. Flow Divider Valve P-3346

| Test | | Description | | Test Results | |
|------|--|--|--------------|--------------|--|
| No. | | Test Description | | Test Results | |
| 1 | | Valve assembled in test rig A run of three 1/2" dia. 10' long pipes with 1/2" dia. 10' long pipes with 1/2" dia. 10' long | Test Results | Test Results | |
| 2 | | Valve assembled in test rig A run of three 1/2" dia. 10' long pipes with 1/2" dia. 10' long pipes with 1/2" dia. 10' long | Test Results | Test Results | |
| 3 | | Valve assembled in test rig A run of three 1/2" dia. 10' long pipes with 1/2" dia. 10' long pipes with 1/2" dia. 10' long | Test Results | Test Results | |
| 4 | | Valve assembled in test rig A run of three 1/2" dia. 10' long pipes with 1/2" dia. 10' long pipes with 1/2" dia. 10' long | Test Results | Test Results | |
| 5 | | Valve assembled in test rig A run of three 1/2" dia. 10' long pipes with 1/2" dia. 10' long pipes with 1/2" dia. 10' long | Test Results | Test Results | |
| 6 | | Valve assembled in test rig A run of three 1/2" dia. 10' long pipes with 1/2" dia. 10' long pipes with 1/2" dia. 10' long | Test Results | Test Results | |
| 7 | | Valve assembled in test rig A run of three 1/2" dia. 10' long pipes with 1/2" dia. 10' long pipes with 1/2" dia. 10' long | Test Results | Test Results | |
| 8 | | Valve assembled in test rig A run of three 1/2" dia. 10' long pipes with 1/2" dia. 10' long pipes with 1/2" dia. 10' long | Test Results | Test Results | |
| 9 | | Valve assembled in test rig A run of three 1/2" dia. 10' long pipes with 1/2" dia. 10' long pipes with 1/2" dia. 10' long | Test Results | Test Results | |
| 10 | | Valve assembled in test rig A run of three 1/2" dia. 10' long pipes with 1/2" dia. 10' long pipes with 1/2" dia. 10' long | Test Results | Test Results | |

422
CONFIDENTIAL

CONFIDENTIAL

(C) The translating seal rig was constructed to duplicate the flow divider valve shaft and balance seal configuration.

(U) The seal candidates shown in figure 402 were subjected to mechanical and pressure cycles at the maximum operating pressure and LN₂ temperatures. The Omniseal shaft seal dimensions are 0.811-in. OD, 0.681-in. ID, and 0.055-in. axial thickness. The Omniseal face seal dimensions are 1.187-in. OD, 1.357-in. ID, and 0.075-in. axial thickness. The Bal-Seal piston seal dimensions are 0.683-in. OD, 0.563-in. ID, and 0.060-in. axial thickness.

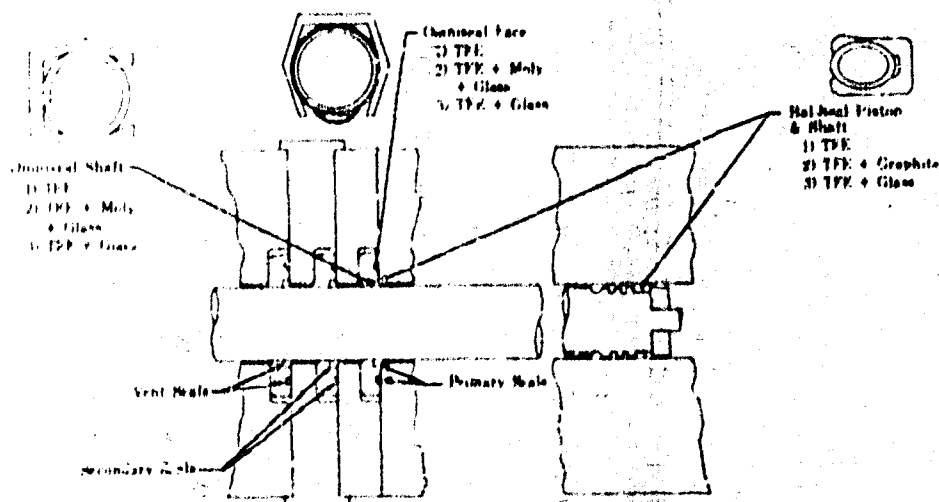


Figure 402. Piston Seal Test Rig and Seal Candidates

FD 18400D

(C) The seal rig was submerged in LN₂ with a 10 psig GN₂ purge in all lines. After the rig was cooled to LN₂ temperature, the purge was dropped, the inlet pressure was increased and maintained between 5,000 and 6,400 psig, and cycling was initiated. The rig was translated a total stroke of 1.375 in. by a pneumatically actuated piston. Leakage measurements were taken at intervals during cycling.

(C) The results of these tests are summarized in table XL. The primary objective of these tests was to define a suitable seal configuration for the flow divider valve with vent leakage less than 10 scfm for 10,000 cycles. Pressure cycles were defined as an increase in inlet pressure from 0 psig to 5,000-6,400 psig and then a decrease to 0 psig.

(C) The selected seal configuration is discussed in the following paragraphs.

Best Available Copy

CONFIDENTIAL

CONFIDENTIAL

(C) Table XI. Translating Seal Rig Test Summary

| Seal Configuration | | Seal Configuration | | Seal Configuration | | Shaft Cycles | Pressure Cycles | Test Notes | Data Plot Figure | Teardown Notes |
|--------------------|----------------|--------------------|----------------|--------------------|----------------|--------------|-----------------|---|------------------|---|
| Primary Seal | Secondary Seal | Primary Seal | Secondary Seal | Primary Seal | Secondary Seal | | | | | |
| Full Seal | Full Seal | Full Seal | Full Seal | Full Seal | Full Seal | 11,000 | 0 | 1. Piston Seal Seal failed between 250 and 100 shaft cycles. At approximately 250 shaft cycles, the primary seal face radial failed. | 403 | 1. Slight pitting and rubbing of the shaft and seal segment were indicated. 2. All shaft lip seals exhibited evidence of failed wear on the ID. 3. The Teflon on the piston seal was split at the corner of the OD and base surface (figure 404). 4. The primary static face seal split along the face (figure 405). |
| Full Seal | Full Seal | Full Seal | Full Seal | Full Seal | Full Seal | 0 | 10 | 1. During initial testing, shaft binding was noted and the test was terminated. | | 1. Wear on the OD was found on the piston seal. The seal was split at the corner of the ID (figure 406). 2. The primary shaft seal exhibited ID wear and slight chipping and was split at the corner (figure 407). 3. The secondary and vent shaft seals exhibited ID wear and chipping. 4. Shaft binding was attributed to shaft lip seal degradation and breakdown. |
| Full Seal | Full Seal | Full Seal | Full Seal | Full Seal | Full Seal | 5150 | 125 | 1. Piston Seal Seal failed between 125 and 175 pressure cycles. | 408 | 1. All shaft lip seals exhibited ID wear. 2. The piston lip seal exhibited ID wear and was split at the corner of the OD and base surface (figure 409). |
| Full Seal | Full Seal | Full Seal | Full Seal | Full Seal | Full Seal | 127 | 0 | 1. Piston Seal Seal failed at 10 shaft cycles. | | 1. The piston lip seal exhibited slight ID wear and was split at the corner of the OD and base surface (figure 410). |
| Full Seal | Full Seal | Full Seal | Full Seal | Full Seal | Full Seal | 127 | 0 | 1. Shaft and face seals were found to be OK. 2. No seal failures. 3. Vent leakage exceeded 10 gpm. | 411 | 1. All seals evidenced slight wear. 2. There was slight wear on the chrome-coated shaft. |
| Full Seal | Full Seal | Full Seal | Full Seal | Full Seal | Full Seal | 10,000 | 0 | 1. No seal failures. 2. Vent leakage exceeded 10 gpm. | 412 | 1. Slight contamination and wear was found on shaft and piston seals. |
| Full Seal | Full Seal | Full Seal | Full Seal | Full Seal | Full Seal | 10,000 | 500 | 1. No seal failures. 2. Vent leakage exceeded 10 gpm. | 413 | 1. All seals in good condition. |
| Full Seal | Full Seal | Full Seal | Full Seal | Full Seal | Full Seal | 10,000 | 500 | 1. No seal failures. 2. Vent leakage exceeded 10 gpm. | 414 | 1. Contamination and wear was found on shaft and piston seals. |
| Full Seal | Full Seal | Full Seal | Full Seal | Full Seal | Full Seal | 10,000 | 500 | 1. Previous tests indicated that the glass-filled Teflon seals had the best resistance to splitting failure. While Teflon seals exhibited superior sealing capabilities. 2. Vent leakage (air) 10 gpm for 10,000 cycles. | 415 | 1. Contamination and wear was found in the shaft and piston seals. |
| Full Seal | Full Seal | Full Seal | Full Seal | Full Seal | Full Seal | 10,000 | 1,700 | 1. The chrome-coated surface on the shaft was subjected to a light electro-polish in an effort to reduce seal wear and improve sealing characteristics. 2. Test should be repeated for continued results. | 416 | 1. The shaft chrome-coated surface was in good condition, except for several small metal protrusions in the shaft seal area (figure 417). The primary shaft seal was destroyed during teardown, however, examination of the seal fragments and the secondary and vent seals showed that small bore and chrome chips were lodged in the seal lip and were the cause of seal failure (figure 418). These chips were generated by the chrome-plated shaft rubbing on the Teflon seal lip due to misalignment of mating assembly. |

Best Available Copy

CONFIDENTIAL

CONFIDENTIAL

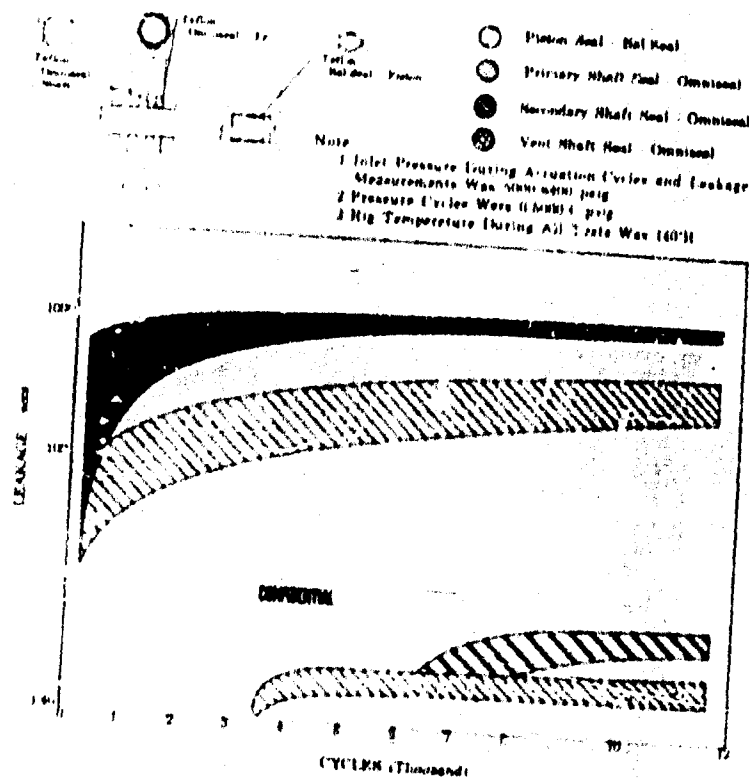


Figure 403. Piston Seal Test Rig Leakage vs Cycles for Rig F-33435-1

FD 20153A

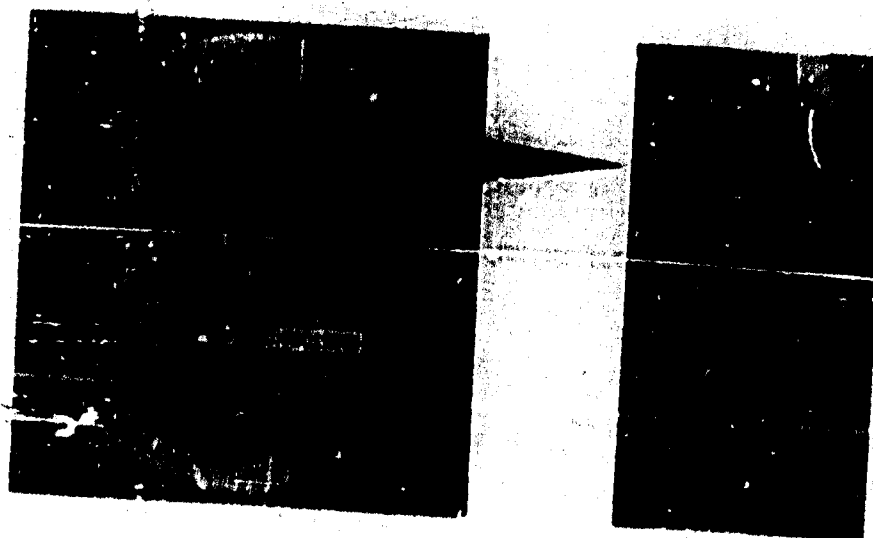


Figure 404. Bal Seal After Test

FD 20069A

CONFIDENTIAL



Figure 405. Omnineal After Test

FD 20066A

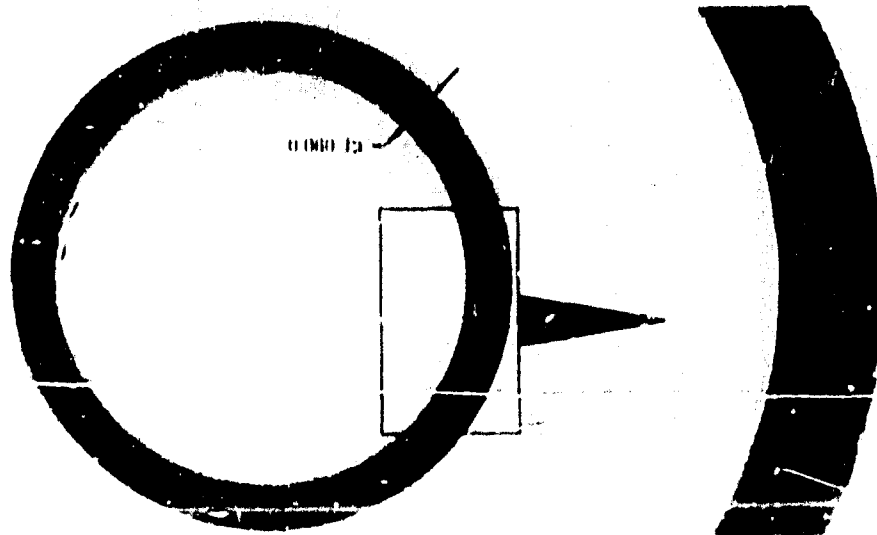


Figure 406. Piston Bal Test After Test

FD 20066A

Best Available Copy

426

CONFIDENTIAL

(This page is Unclassified)

CONFIDENTIAL

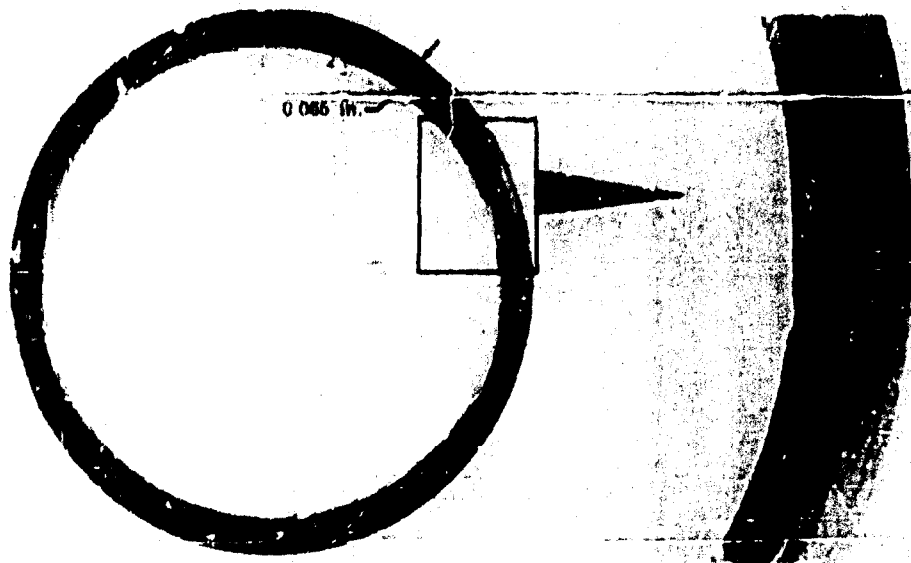


Figure 407. Primary Omniseal After Test

FD 20070A

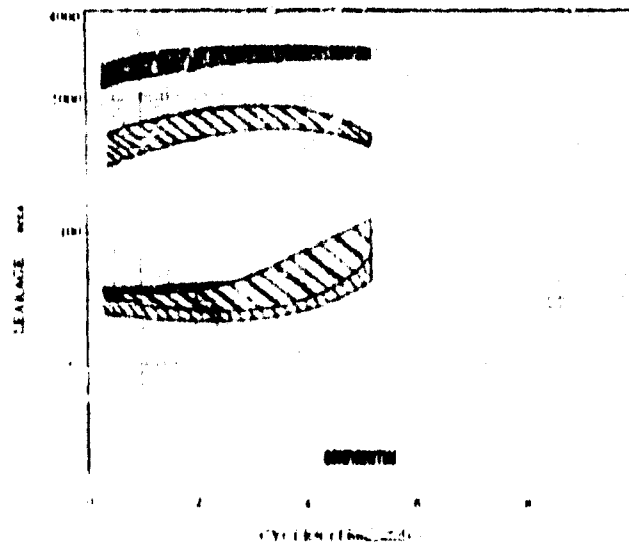
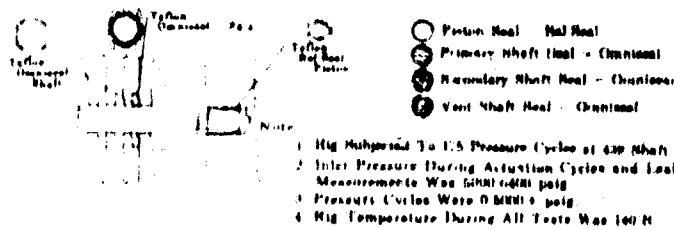


Figure 408. Piston Seal Test Rig Leakage vs Cycle for Rig F-33435-3

FD 20154B

CONFIDENTIAL

Best Available Copy

CONFIDENTIAL

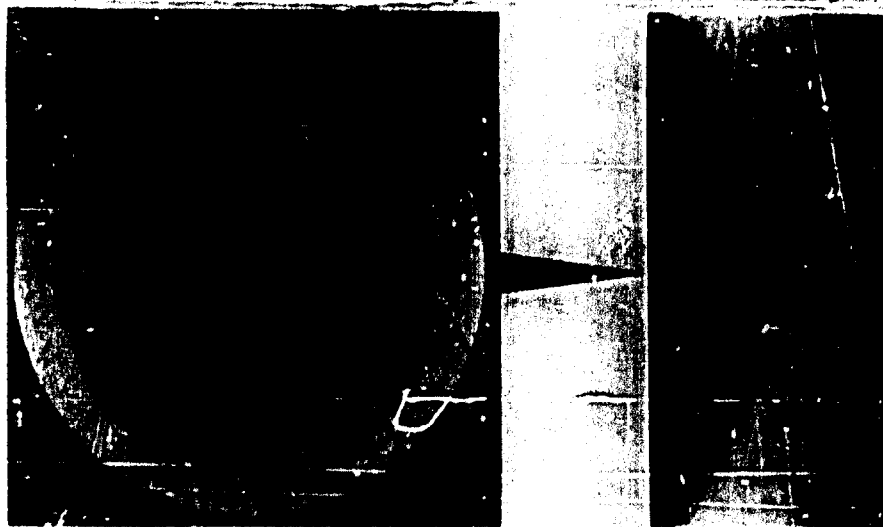


Figure 409. Teflon Piston Bal-Seal After Test FD 20065A

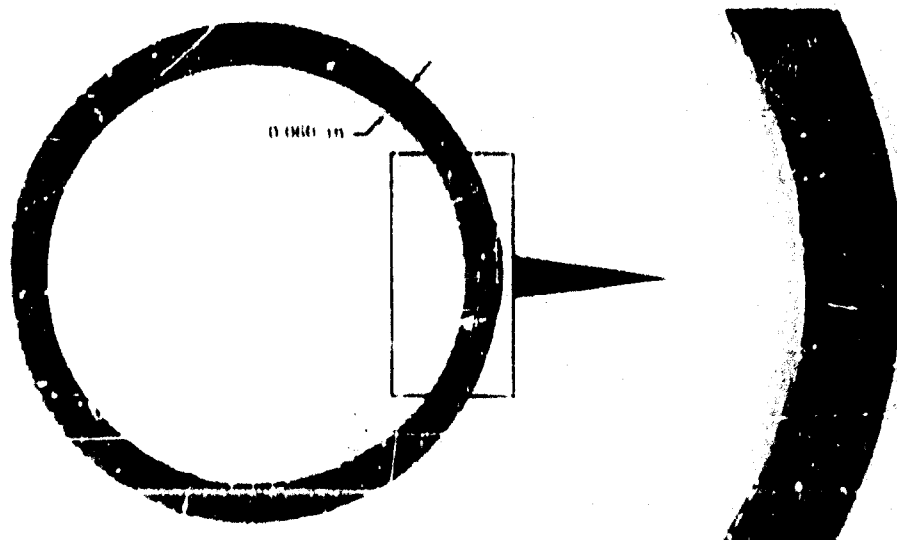


Figure 410. Piston Bal-Seal After Test,
Riv. F 145 G 1

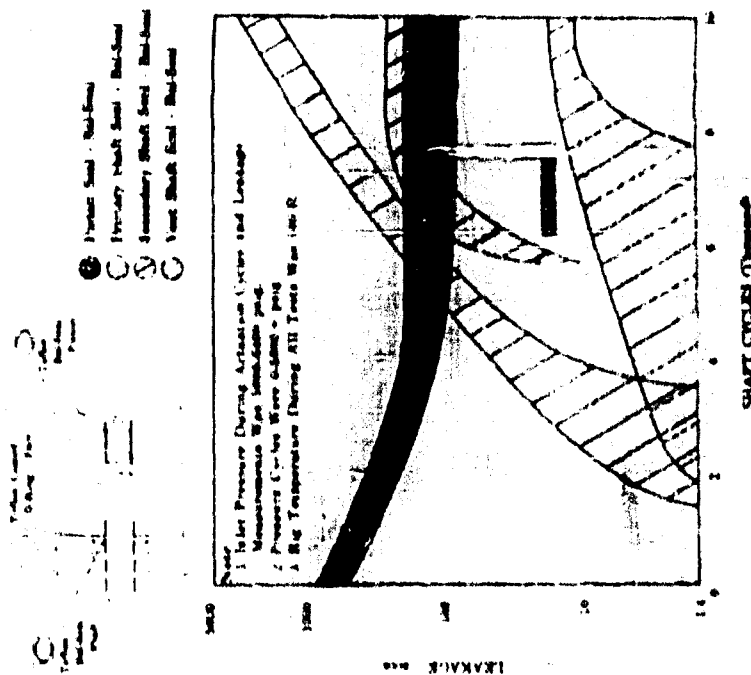
FD 20066A

Best Available Copy

428

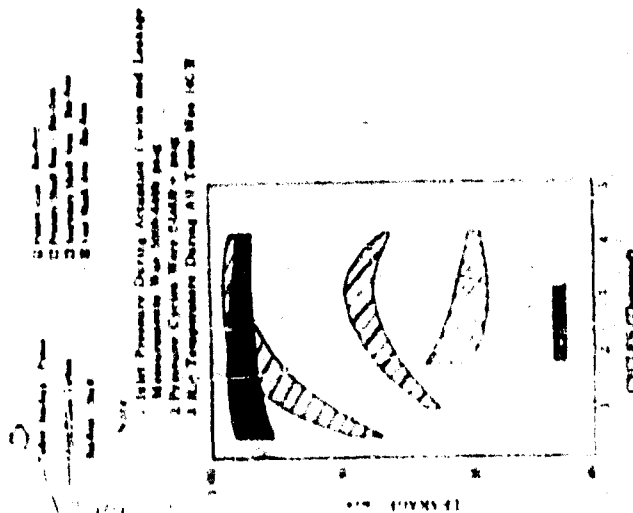
CONFIDENTIAL

CONFIDENTIAL



FD 20177A

Figure 412. Piston Seal Test #19
Leakage vs Cycles for
Rig F-33435-6



FD 20152B

Figure 411. Piston Seal Test Rig
Leakage vs Cycles for
Rig F-33435-5

429
CONFIDENTIAL

Best Available Copy

CONFIDENTIAL

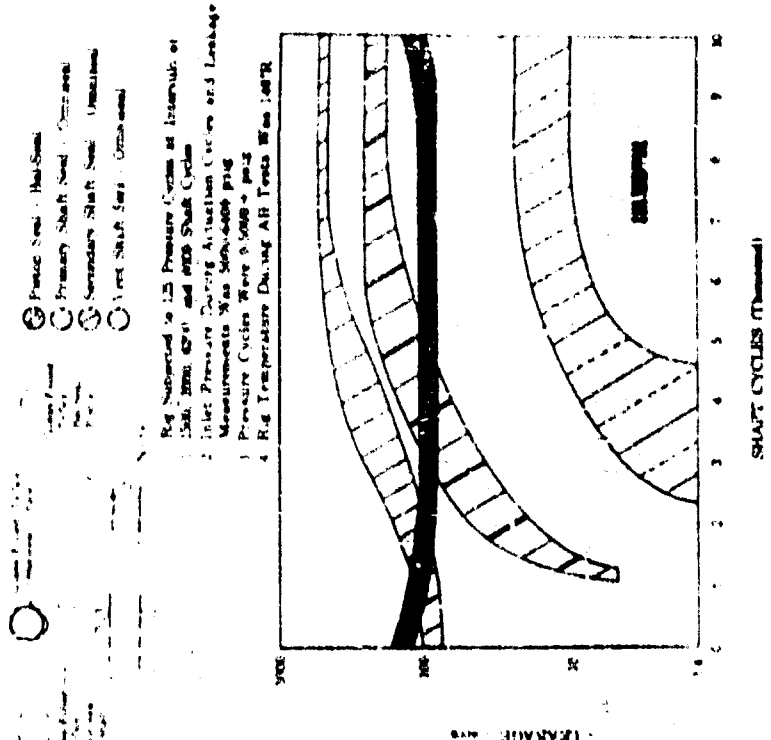


Figure 414. Piston Seal Test Rig Leakage FD 20178A vs Cycles for Rig F-33435-7

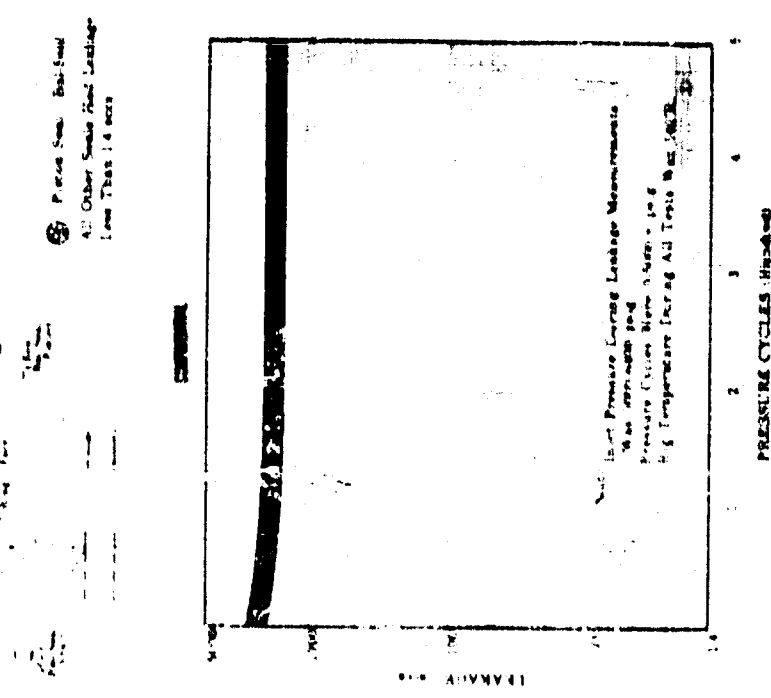


Figure 413. Piston Seal Test Rig Leakage vs Cycles for Rig F-33435-6A FD 20179A

Best Available Copy

CONFIDENTIAL

CONFIDENTIAL

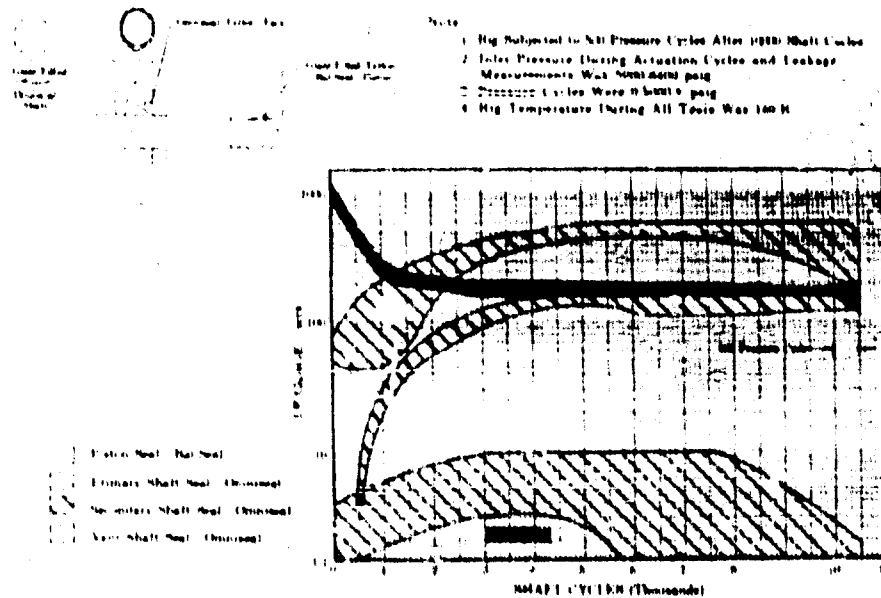


Figure 415. Piston Seal Test Rig Leakage vs Cycles for Rig F-33435-8

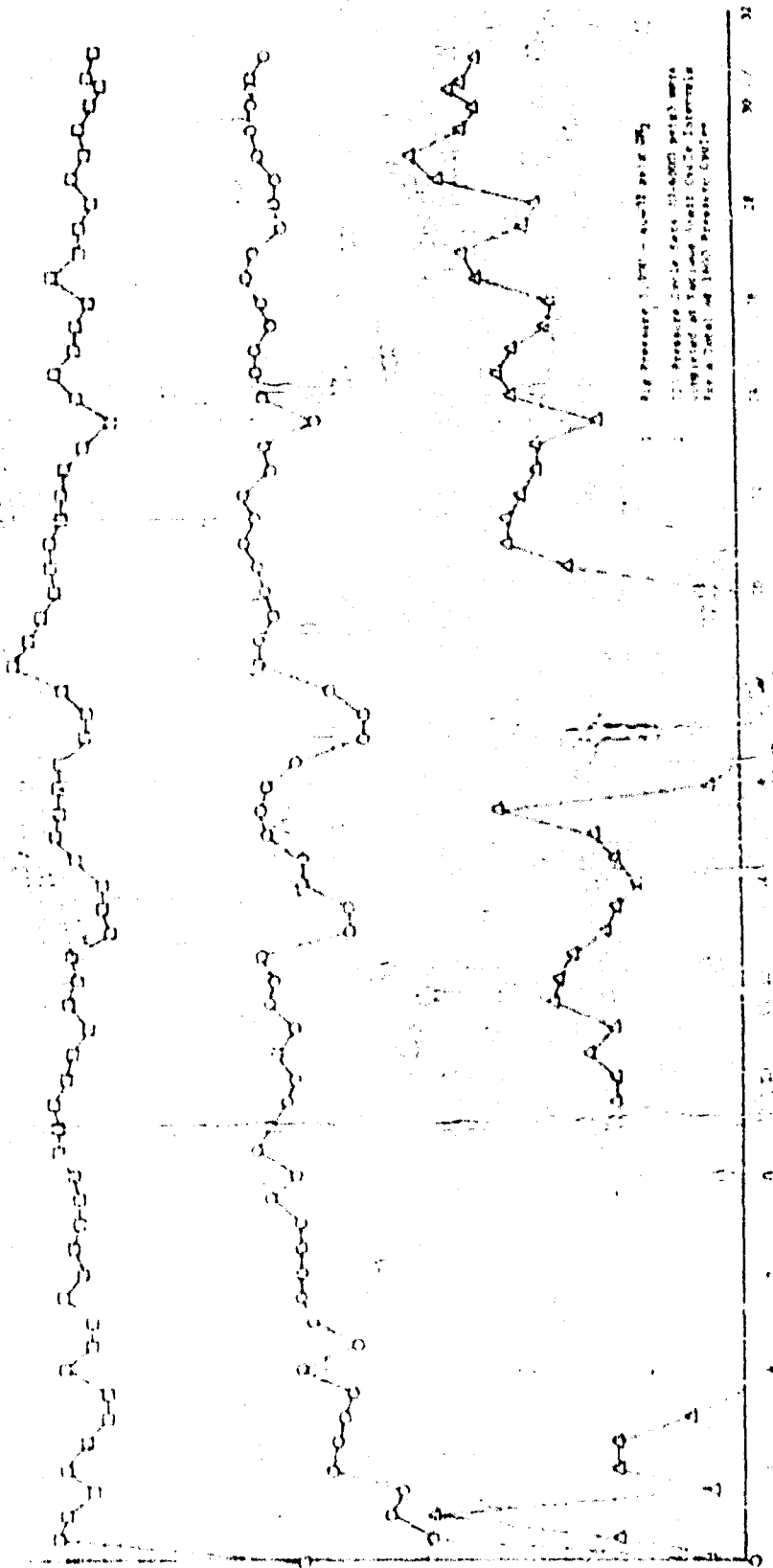
FD 22580A

Best Available Copy

CONFIDENTIAL

CONFIDENTIAL

12.000 - 12.010 Seal
12.010 - 12.020 Seal
12.020 - 12.030 Seal



12.000 - 12.010 Seal
12.010 - 12.020 Seal
12.020 - 12.030 Seal

DF 59793

Figure 416. Piston Seal Rig Leakage, Rig F-33435-9

Best Available Copy

CONFIDENTIAL

(This page is Unclassified)

UNCLASSIFIED

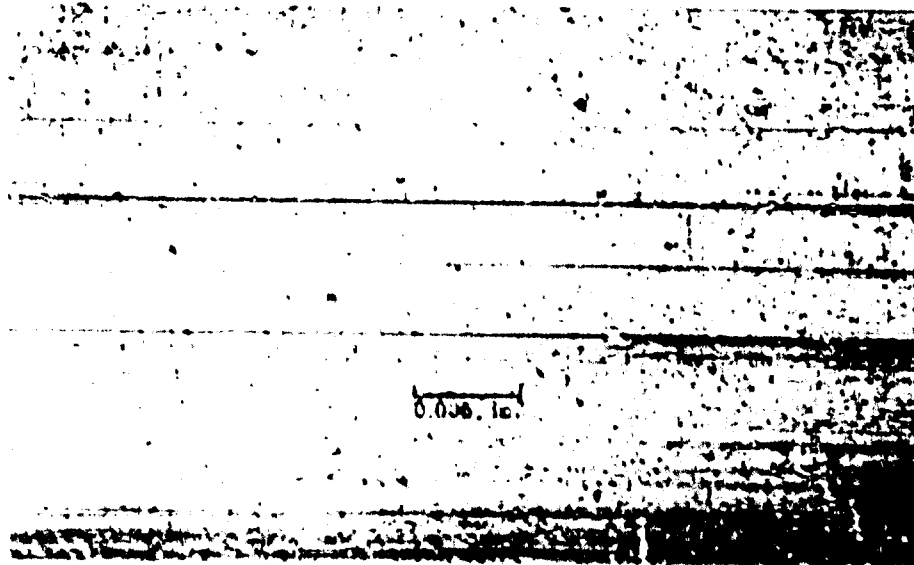
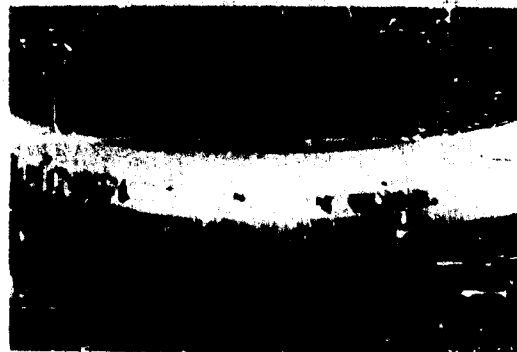
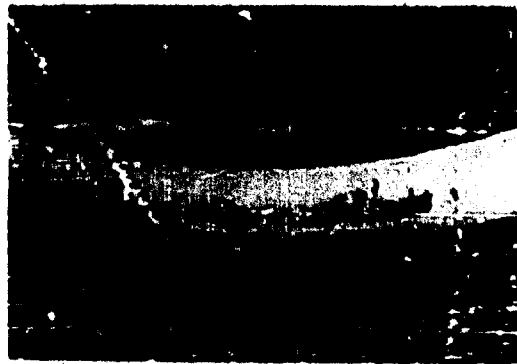


Figure 117. Post-Test Condition of Shell

FD-7318



Best Available Copy

FD-7318

UNCLASSIFIED

UNCLASSIFIED

(1) Shaft Seal

| <u>Location</u> | <u>Configuration</u> | | <u>Material</u> | |
|-----------------|----------------------|----------------|------------------------|------------------------|
| | <u>Static</u> | <u>Dynamic</u> | <u>Static</u> | <u>Dynamic</u> |
| Vent | Omniseal | Omniseal | Teflon | Teflon |
| Secondary | Omniseal | Omniseal | Teflon | Teflon |
| Primary | Omniseal | Omniseal | Glass-filled Teflon | Glass-filled Teflon |

(2) Balance Piston

Bal-Seal

Glass-Filled Teflon

(U) This configuration was selected because the glass-filled teflon seals are better suited for the high differential pressure locations because of the reduced tendency of the filled material to cold flow. The fibrous glass fillers impart greater dimensional stability, reduce the effect of thermal changes, and improve abrasion resistance.

(U) The teflon seals were retained at the lower pressure locations because of their improved sealing characteristics.

(U) Test results indicated that further reduction in seal leakages as a function of time would require an improvement in the shaft surface finish as a means of reducing seal wear.

(U) Electropolishing was evaluated as a means of improving surface finish by removing sharp edges by chemical means. Several chrome-plated samples were electropolished with various solutions and current densities until a suitable process was defined. The translating seal rig shaft was first vapor blasted with number 400 grit aluminum oxide (0.0015-in. maximum diameter particle size) at 150 psig air pressure to provide a uniform matte finish. The distance from the vapor blast nozzle to the shaft surface was 3-in. Then the shaft was electropolished as shown in figure 419. The process is outlined as follows: Solution: (concentrated sulfuric acid - 520 CC, concentrated phosphoric acid - 1700C, citric acid - 90gm, methanol - 120CC, and water to make 1 liter) Current density, 1.0 amp/in² of surface area for three minutes at a temperature of 80 to 90°F.

(U) The results of a test to evaluate the electropolished shaft surface were clouded by the axial scratches incurred on the shaft during the test. The test should be repeated for conclusive results.

(U) Electropolish offers a means of improving the wear characteristics of a mechanically polished surface by removal of sharp edges.

UNCLASSIFIED

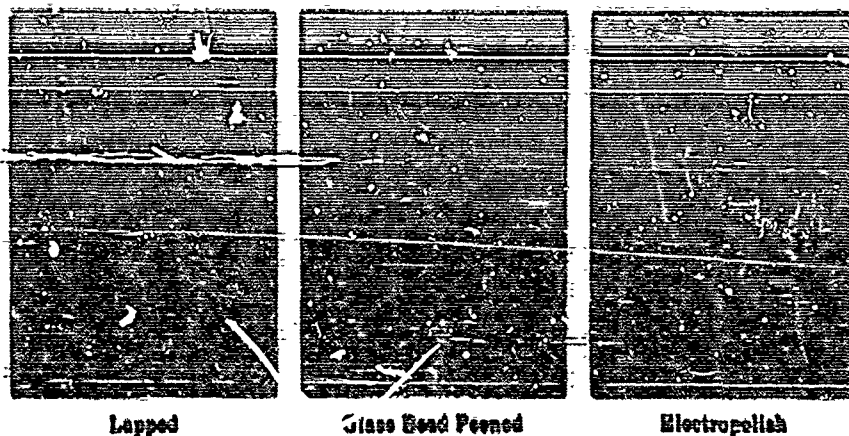


Figure 419. Polishing Techniques

FD 22414

3. Test Facilities and Procedures

a. B-21 and B-22 Test Stands (See figures 420 and 421.)

(U) Control calibrations and cycle tests were obtained through the use of closed loop water blowdown facility on the B-21 stand and the high pressure GN_2 flow bench with cryogenic cooldown capabilities, on the B-22 stand. The water flow loop consisted of a 2100-gallon run tank, which, when filled, was pressurized to the required level from a 5000-psia nitrogen source. The tank was capable of supplying water at 1500-psia to the inlet of the test item at flow rates from 1% to 100% of the equivalent 250K main oxygen flow rate. The water passes through electrohydraulic control valves that set the preprogrammed flow versus pressure ramp to the test item. A 20-channel analog computer was used for this purpose. The water flows through the test section and into a catch tank that recovers the working fluid. The recovered water was then pumped back to the run tank for reuse. Turbine flowmeters were used for flow measurement, and data were recorded on strip charts and on an 18-channel oscillograph. A minimum test duration of 30 seconds was attained with this system when operating at the maximum flow rate.

(U) The high pressure GN_2 flow loop on the B-22 stand consists of a 10,000 psig GN_2 supply, electropneumatic control valves, and turbine flowmeters. A large dowar cooldown tank was available for cryogenic temperature tests. This stand used the same analog computer, strip-charts, and other control and recording facilities as the B-21 stand.

b. Test Procedures

(1) Water Calibration

(U) For water calibration, the flow divider valve was installed in the test block and mounted on the B-21 stand as shown in figure 422.

(U) The valve was instrumented as shown on figure 423 and the data were recorded on strip charts during the test.

UNCLASSIFIED

UNCLASSIFIED

(U) Primary and secondary circuits were calibrated separately; one circuit was blanked off while the other was flowed. A fixed differential pressure was set and maintained through closed loop control on the stand control valves. A valve position was set and the system was allowed to stabilize before parameters were recorded. The procedure was repeated for other valve positions.

(U) From the temperature, flow, and valve pressure drop data recorded, a valve effective areas as a function of valve stroke was calculated.

(2) Cryogenic Checkout and Cycle Test Procedure

(U) Flow divider valve cryogenic tests were conducted on the B-22 stand. The valve was mounted in the test block and installed on the stand LN₂ catch tank (figure 424). The valve was instrumented as shown in figure 425.

(U) Liquid nitrogen was used to cool the valve to cryogenic conditions.

(3) Translating Seal Rig Test Procedure

(C) The piston seal rig cryogenic cycling tests were conducted on the B-22 stand with the test rig shown in figure 426. The rig was immersed in a dewar of LN₂ high pressure ON₂ (3,000 to 6,400 psig) was introduced into the rig and seal vent flows and temperatures were monitored.

(U) A schematic of the rig as installed in the stand is shown on figure 427.

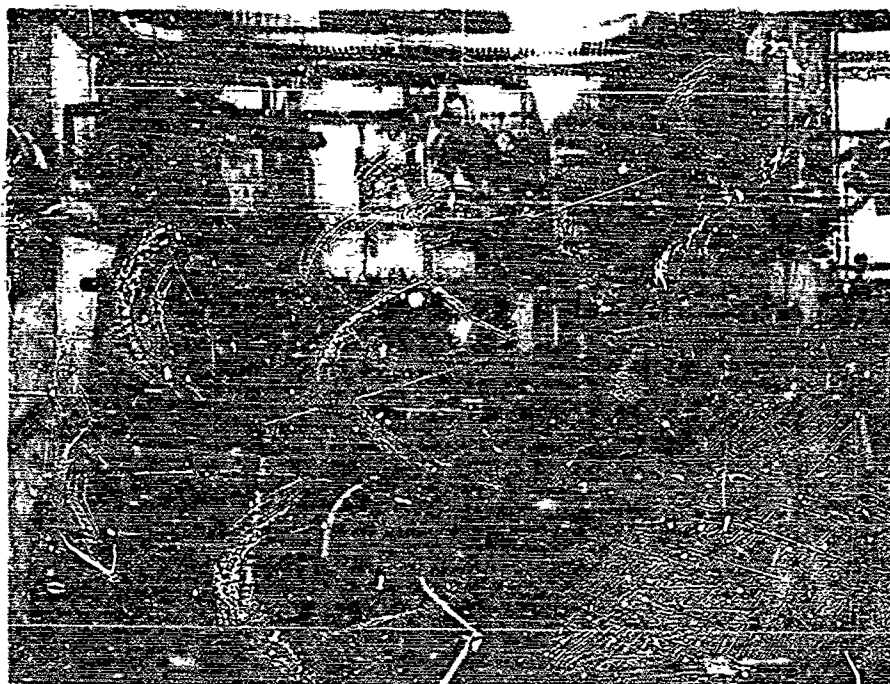


Figure 420. B-21 Control Calibration Facility

FC 13775

UNCLASSIFIED

UNCLASSIFIED

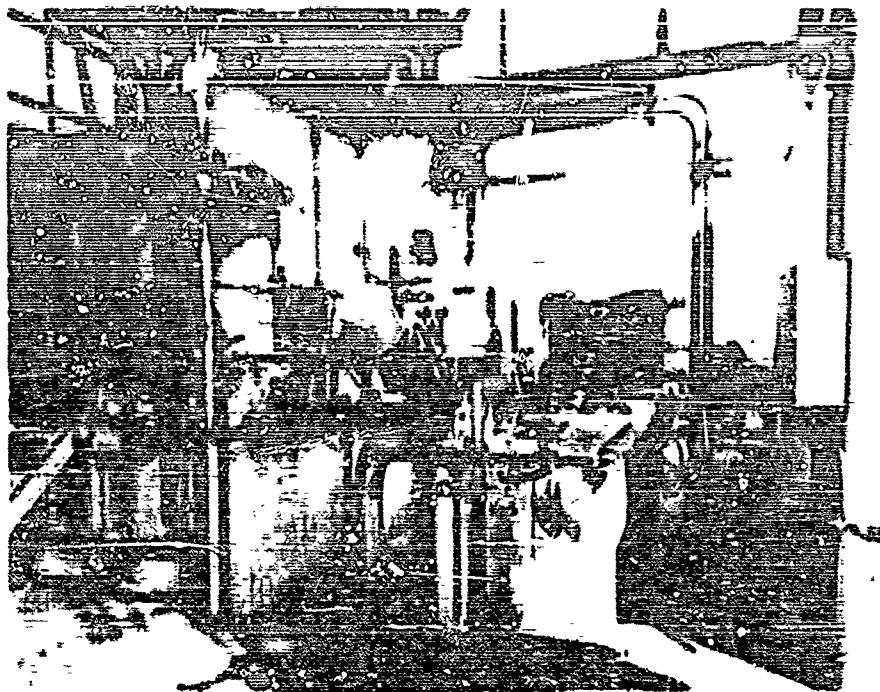


Figure 421. B-22 Cryogenic Static Cycle Stand FC 13799

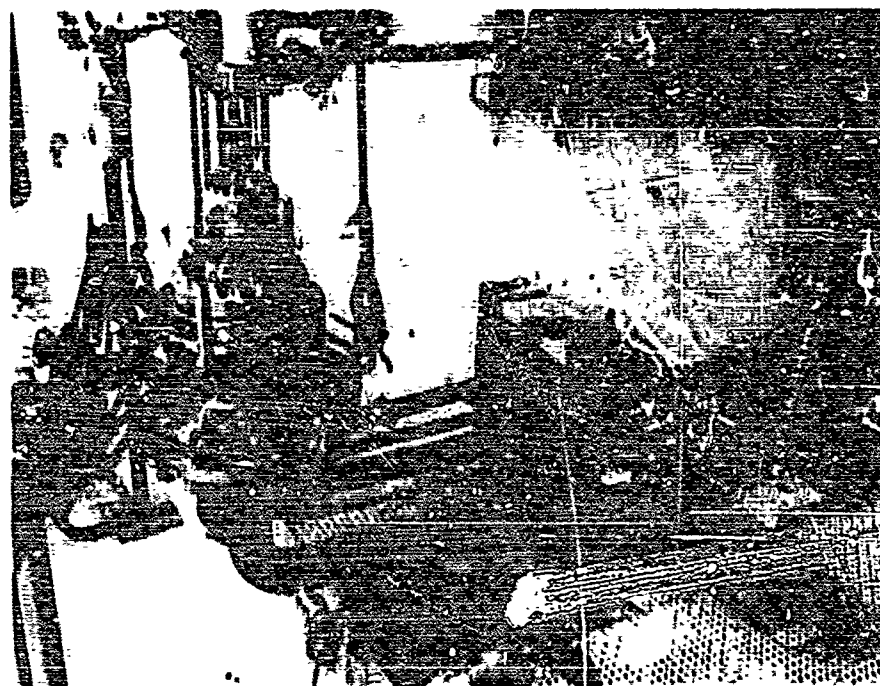
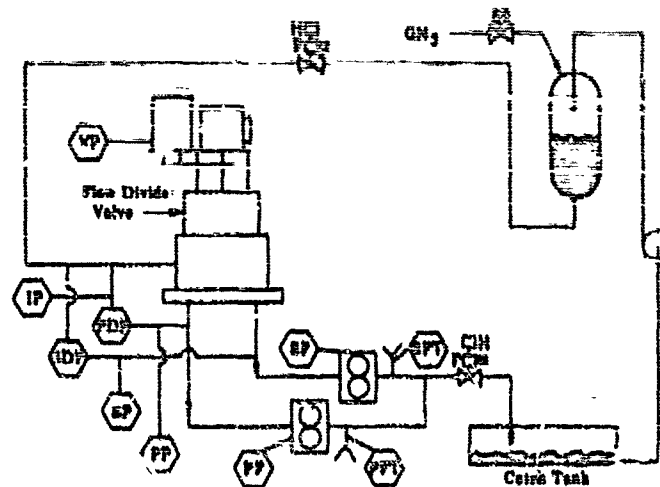


Figure 422. Flow Divider Valve Mounted on b-21 Stand FE 68234

437

UNCLASSIFIED

UNCLASSIFIED



| Header | Description |
|--------|-----------------------------|
| VP | Valve Position |
| IP | Inlet Pressure |
| IDP | Inlet Differential Pressure |
| SP | Secondary Pressure |
| PP | Primary Pressure |
| SPT | Secondary Flow Temperature |
| PPT | Primary Flow Temperature |

Figure 423. Schematic of Flow Divider Valve Mounted on B-21 Stand

FD 23069



Figure 424. Flow Divider Valve Mounted on Test Block for Cryogenic Endurance Test

FE 68532

CONFIDENTIAL

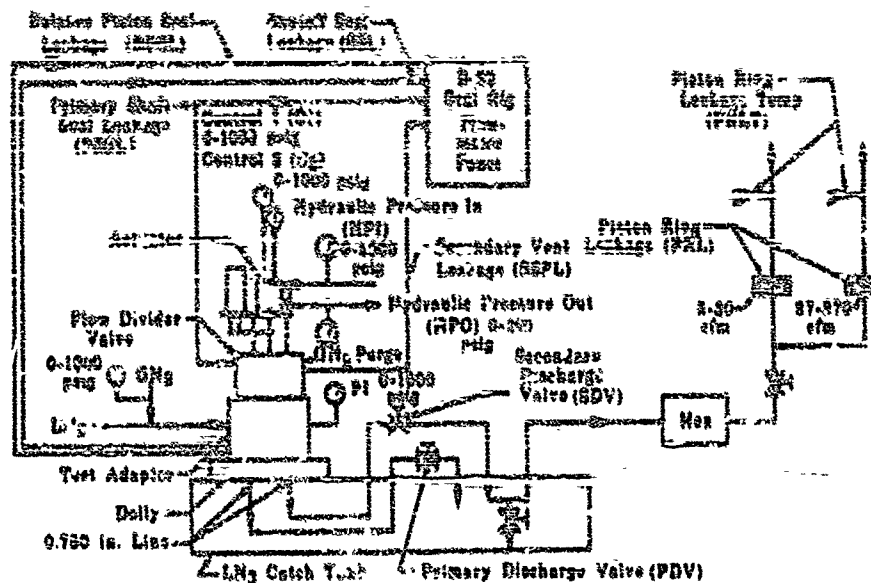


Figure 425. Schematic of 2-way Dividing Valve Test Stand Installation

FD 22151A

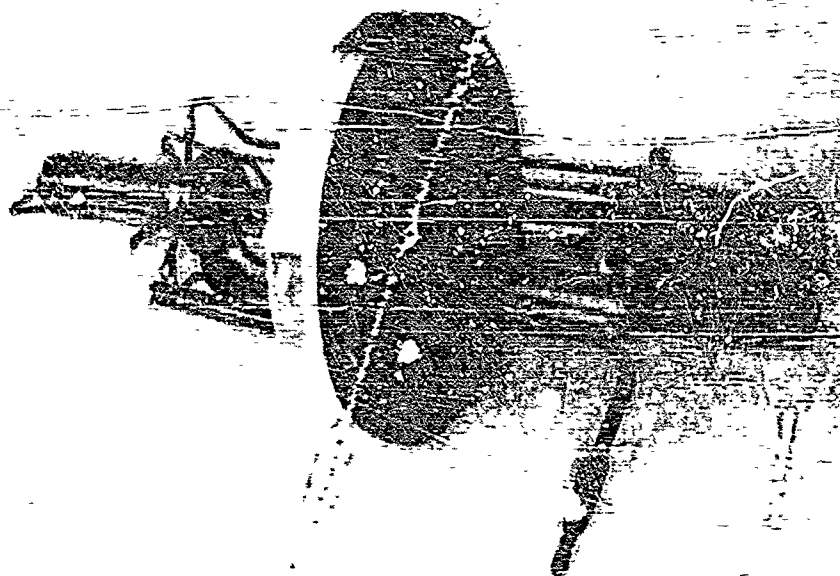


Figure 426. Piston Seal Test Rig

FE 6615c

439
CONFIDENTIAL

(This page is Unclassified)

CONFIDENTIAL

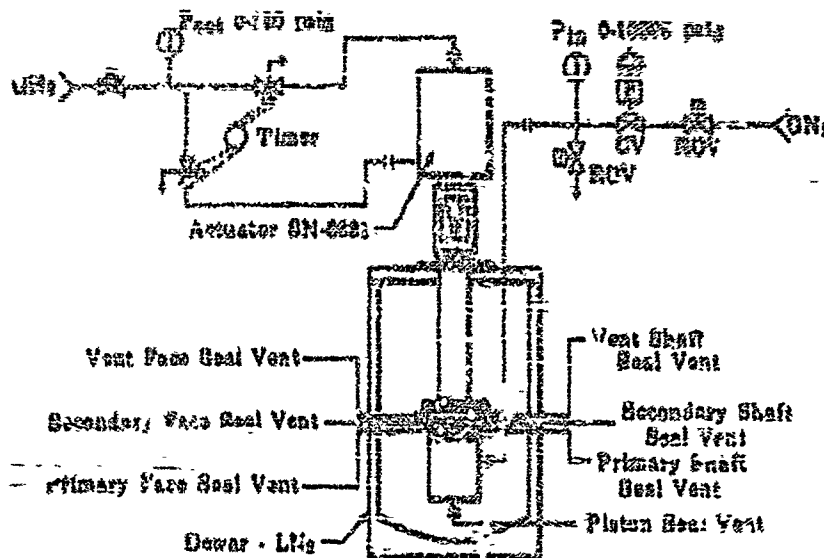


Figure 427. Translating Seal Rig As Installed FD 13070
in H-22 Bench

4. Conclusions

(U) The design selection studies indicated that a translating sleeve valve would best accommodate the system requirement for this valve. Three flow divider valves were fabricated, water flow calibrated, and tested at cryogenic conditions. Some procurement delays were encountered in fabrication of the main valve housing and the secondary sleeve piston rings. The first valve was used for endurance testing and general component development; the second and third valves were used with the staged combustion test rig.

(C) The water flow calibrations showed close agreement with the design predictions and confirmed the design analysis. Cryogenic endurance tests included 41,000- and 35,000-cycle tests to investigate durability characteristics of the component parts. Design improvements indicated by the first endurance test were evaluated during the second endurance test and resulted in acceptable component wear at the original design conditions.

(U) A translating seal rig was designed and nine endurance tests were conducted to evaluate seal configurations. Translating seal rig endurance tests demonstrated acceptable leakage characteristics (less than 10 secs vent seal leakage) for the selected seal package configuration.

(U) Testing with the staged combustion rig demonstrated acceptable component operating characteristics with no failures or excessive overboard or shutoff leakage.

CONFIDENTIAL

~~CONFIDENTIAL~~

B. THRUST CONTROL

1. Hardware Description

a. General

(C) The thrust control was required to regulate the preburner oxidizer flow over transient and steady-state operating ranges to control desired thrust as a function of the required pumping power level. The control system concept uses direct measurement of propellant flow rate. The control valving required was a regulating-type valve that was positioned as a function of the flow error signal between the desired flow, as determined by the control system computer, and the actual flow, as determined by the control system flowmeters. The thrust control regulating valve design requirements were established through engine cycle analyses and are shown in figure 425.

(C) An ideal thrust control configuration would possess the following characteristics: (1) wide turndown ratio, (2) pressure and flow balance, (3) minimum pressure drop, (4) light weight, and (5) capability of being developed to the reliability levels required for a 10-hour TBO application. Because no single valve configuration was an obvious choice, it was required to investigate several configurations analytically to make a reasonable selection.

(1) Sleeve Valve Candidates (figures 429 and 430)

(U) The translating sleeve valve is more widely used as a regulating valve than any other type where low actuation forces are desired, providing no shutoff function is required. This type of valve is inherently force balanced except for the pressure gradient caused by flow, which is discussed in a later paragraph.

(U) In the translating sleeve valve candidate, a sharp-edged type metering port was used to provide the proper flow - pressure drop characteristics. The geometric area of the metering port may be determined as a function of fluid density, valve pressure drop, and flow rate as follows:

$$A_{\text{geometric}} = \frac{\dot{W}}{K\sqrt{\rho(\Delta P)}}$$

where

\dot{W} = Weight flow

ρ = Density

ΔP = Pressure drop

K = Constant (C_d is absorbed)

(U) Because these variables are functions of thrust level and mixture ratio, the required geometric area may be determined and is plotted in figure 431 as a function of thrust level and mixture ratio.

~~CONFIDENTIAL~~

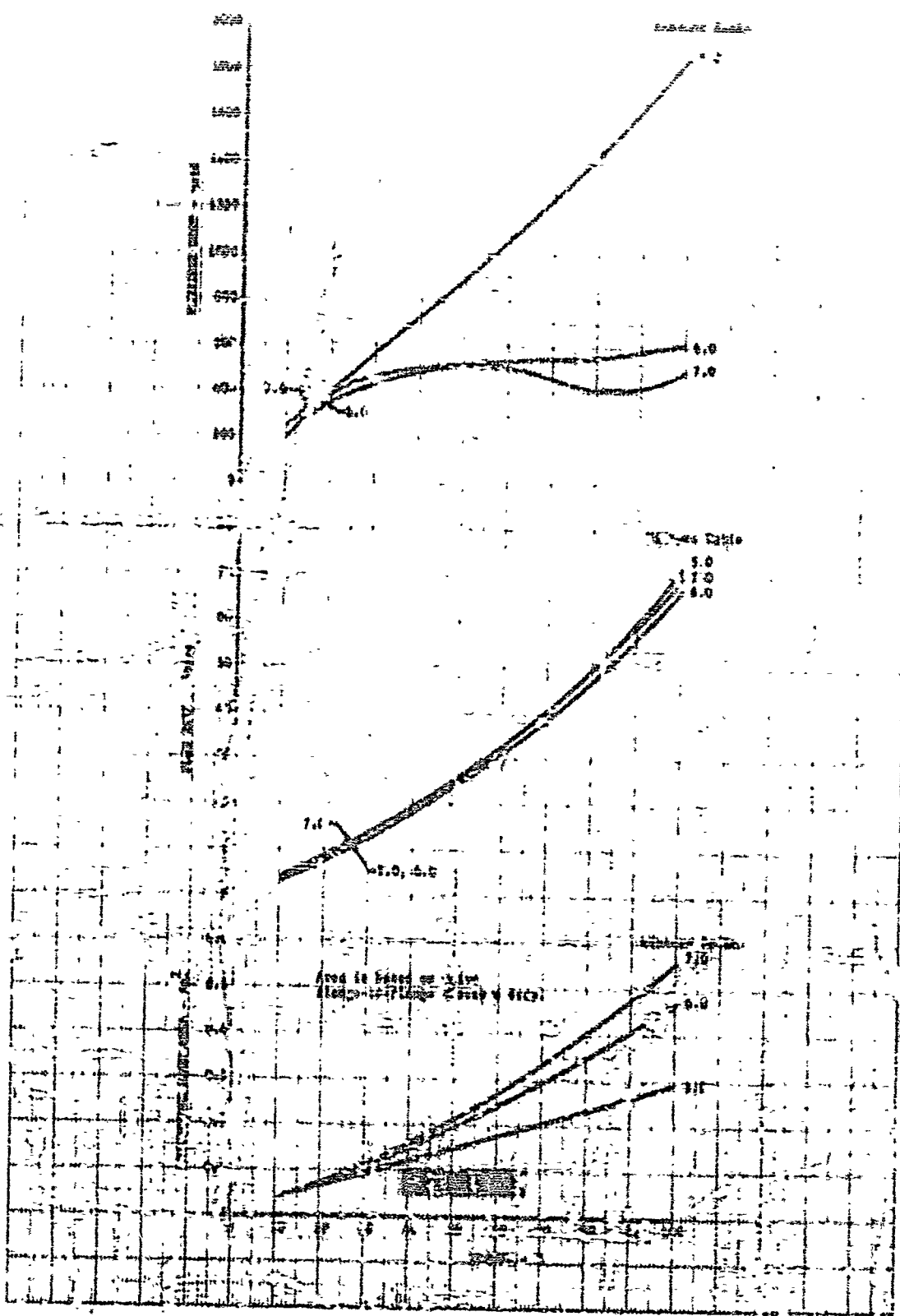


Figure 428. Thrust Control Valve Requirements for Operation DF 92131

CONFIDENTIAL

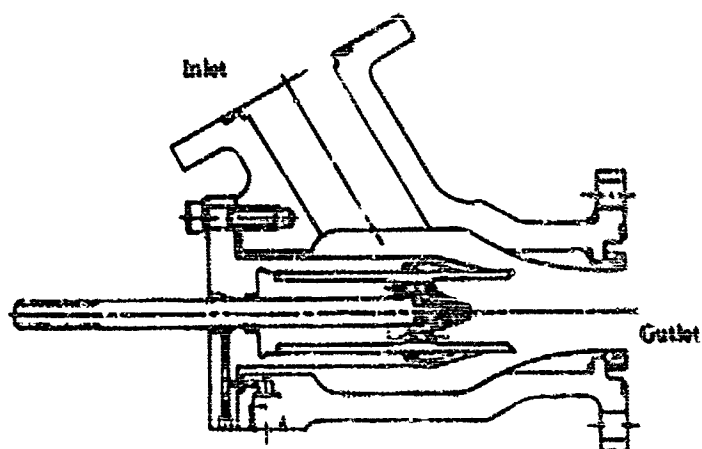


Figure 429. Thrust Control Translating
Sleeve-Inverted Pintle Valve
Candidate

FD 18234

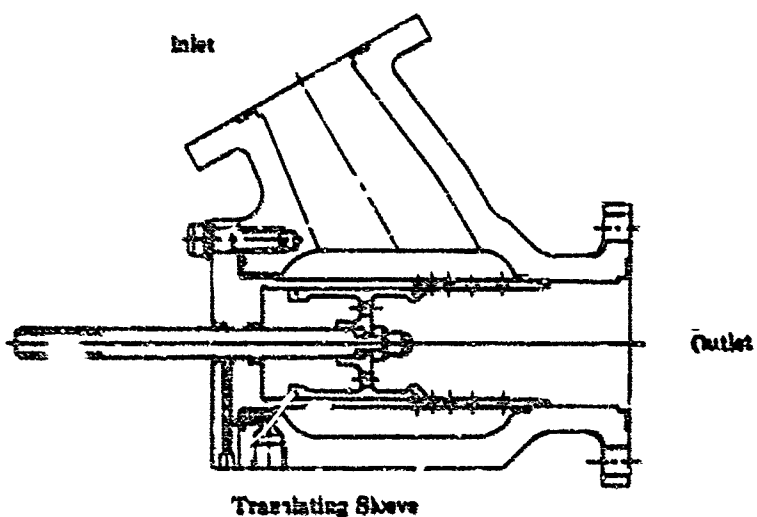


Figure 430. Thrust Control Translating
Sleeve-Port Contoured

FD 18231

443

CONFIDENTIAL

(This page is Unclassified)

CONFIDENTIAL

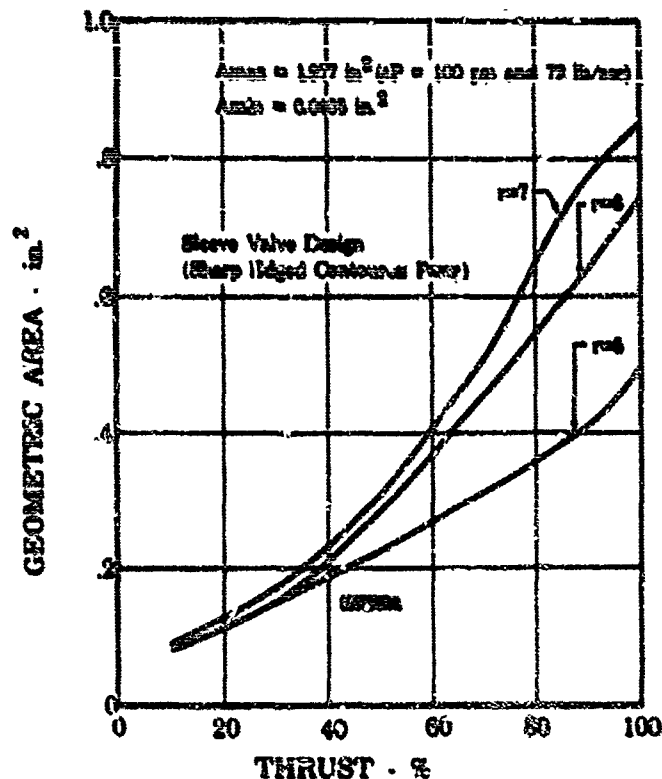


Figure 431. Geometric Flow Area Required vs Percent Thrust (Thrust Control Valve)

FD 18162

(U) A constant percentage error port contour yields an area versus stroke relationship that may be expressed in the form

$$A_p = A_m e^{Cx}$$

where

A_p = Port area

A_m = Maximum port area

x = Valve travel from a reference datum

(U) Differentiating the above equation with respect to valve travel,

$$\frac{dA_p}{dx} = CA_m e^{Cx}$$

(U) Dividing dA_p/dx by A_p ,

$$\frac{dA_p/dx}{A_p} = \frac{CA_m e^{Cx}}{A_m e^{Cx}} = C = \frac{dA_p/A_p}{dx}$$

444

CONFIDENTIAL

CONFIDENTIAL

(U) The value of C , therefore, is the area fractional change with respect to a positional movement of the valve; or, C is the percent area error per positional error. The value of C may be established from the boundary conditions of the original equation.

(U) If $x = 0$, then this is the position where the port area is a maximum and, therefore, when $x = x_{\max}$ the port area must be a minimum and C must be negative.

$$A_{p_{\min}} = A_m e^{Cx_{\max}}$$

Dividing both sides of the equation by A_m :

$$\frac{A_{p_{\min}}}{A_m} = A_{\text{ratio}} = e^{Cx_{\max}}$$

therefore,

$$C = \frac{1}{x_{\max}} \left[\ln(A_{\text{ratio}}) \right]$$

(U) It can be concluded that the accuracy sensitivity of the valve is a function of the total stroke and the valve area turndown ratio. From the value of C , the percent error in valve area may be determined and is plotted in figure 432 as a function of percent of total stroke positional error. A range of valve turndown ratios is used in addition to the design ratio to show the accuracy sensitivity to turndown ratio.

(C) A major mechanical problem with the translating sleeve valve is the inherent bypass leak path through the clearance between the sleeve and the housing. To accurately control the minimum valve flow area for a high turndown ratio valve, it is necessary to minimize this leakage area. The smallest effective flow area that would be called for by the engine is 0.025-in.². For four equally spaced square ports and a 0.002-inch radial clearance, the leakage area could be 0.014-in.², or more than 50% of the flow area. This leakage problem dictates the use of piston ring seals on the translating element, thereby reducing the effective leak path area to slightly more than 2% of the minimum valve area. Incorporation of piston rings increases the actuation forces by approximately 200 pounds.

(U) The rotating sleeve valve has an inherent leak path similar to that in the translating sleeve, except that it is virtually impossible to seal except through use of extremely close running clearances between the sleeve and housing. For this reason, the rotating sleeve was not given serious consideration as a candidate.

CONFIDENTIAL

CONFIDENTIAL

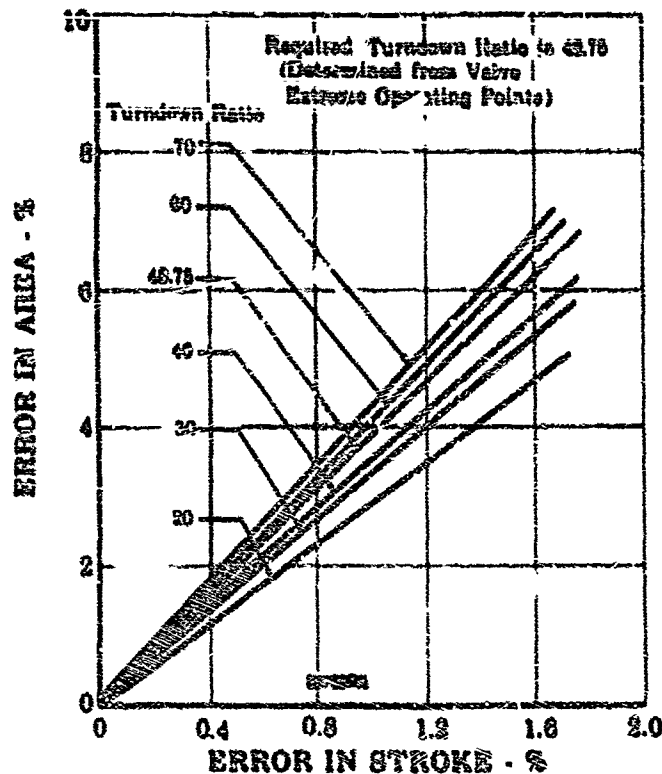


Figure 432. Percent Error in Area vs Percent Error in Stroke (Thrust Control Valve) FD 16165

(U) For a constant percentage metering port, once the maximum-to-minimum port area ratio has been established, the maximum port width is a function of valve stroke. Figure 433 is a plot of the maximum port width for a single port valve as a function of total valve stroke. For multiple port configurations the maximum port width would reduce proportionally to the number of ports.

(U) To size a sleeve valve it would be convenient to define a valve parameter, η . This parameter, η , is defined as the fraction of maximum total valve port width to valve circumference.

$$\eta = \frac{W_{p \max}}{\pi D_v}$$

Where

$W_{p \max}$ = Maximum port width, total

D_v = Valve diameter

CONFIDENTIAL

UNCLASSIFIED

By rearranging the above equation, it may be solved for the valve diameter;

$$D_v = \frac{W_{P_{MAX}}}{\pi \eta}$$

(U) Because the maximum port width is a function of total valve stroke, the required valve diameter may be determined from figure 434 as a function of valve stroke and η .

(U) Figures 435, 436, and 437 are plots of the port contours for valve strokes of 3.0, 2.5 and 2.0 inches, respectively. These contours are constant percentage error metering ports, and the effective area versus stroke curve associated with each of the above valve strokes is shown with its respective port contour.

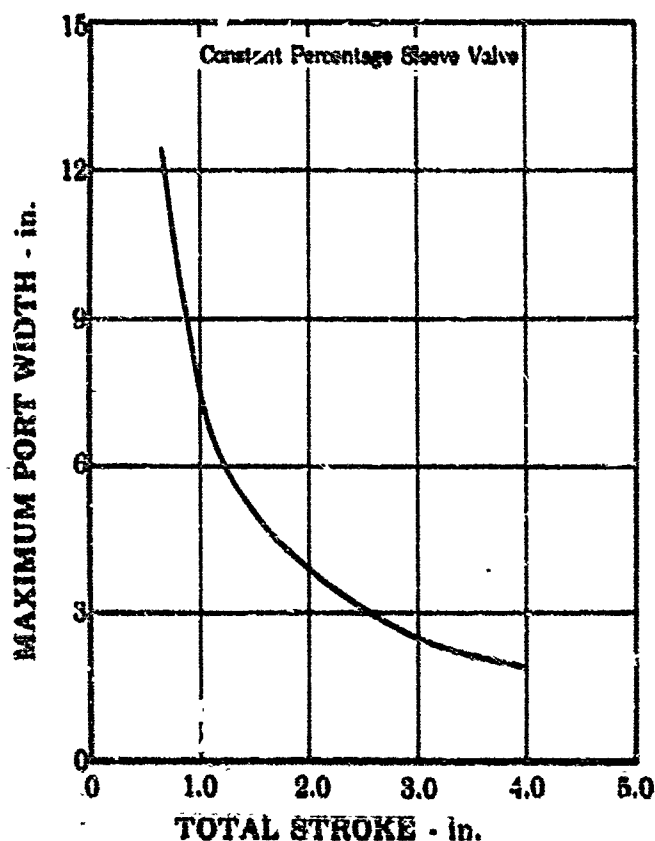


Figure 433. Maximum Port Width Required for a Constant Percentage Sleeve Valve as a Function of Total Stroke (Thrust Control Valve)

FD 18200

UNCLASSIFIED

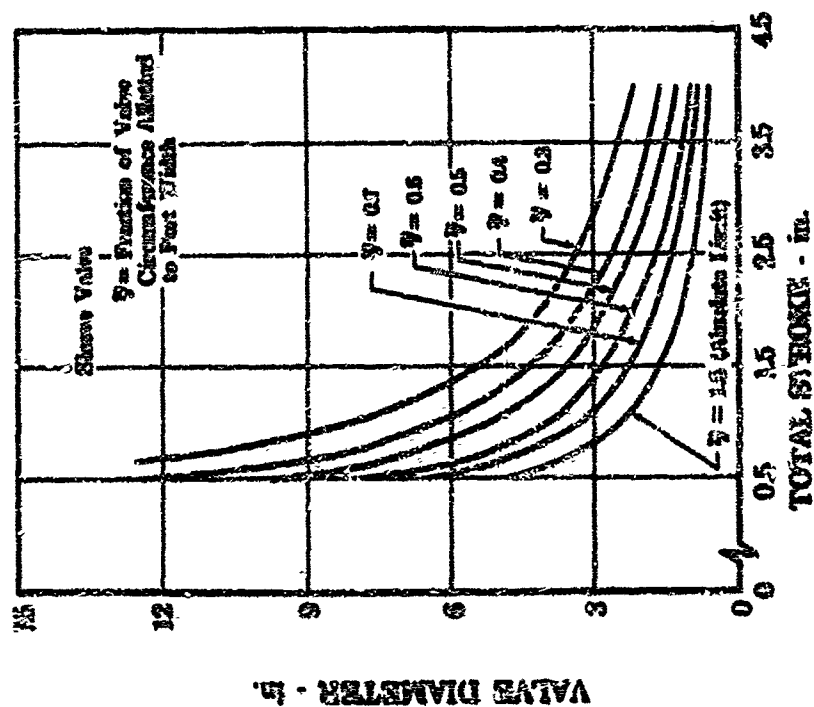


Figure 434. Diameter Required vs Total Stroke (Thrust Control Valve)

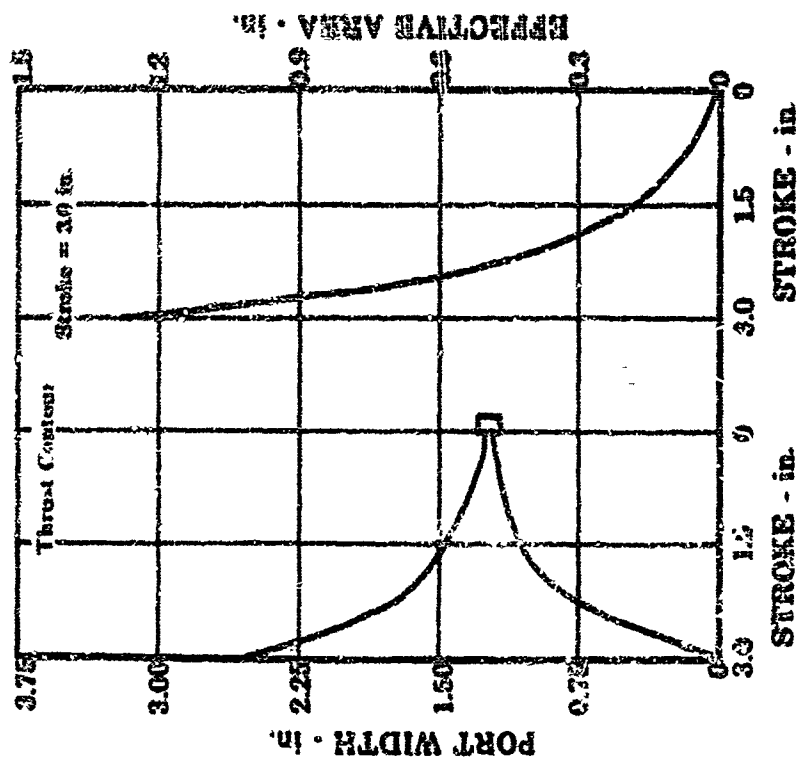


Figure 435. Sleeve Valve Port Contour and Port Effective Area vs Arisel Valve Stroke (3.0-inch Stroke)(Thrust Control Valve)

FD 18213

CONFIDENTIAL

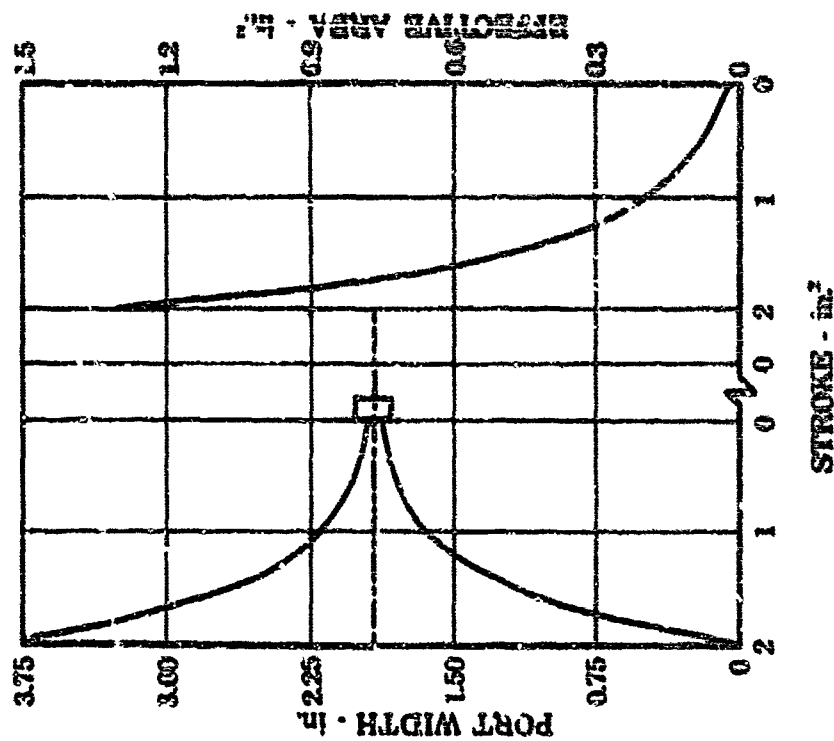


Figure 437. Sleeve Valve Port Contour and Port Effective Area vs Axial Valve Stroke (2.0-inch Stroke) (Thrust Control Valve)

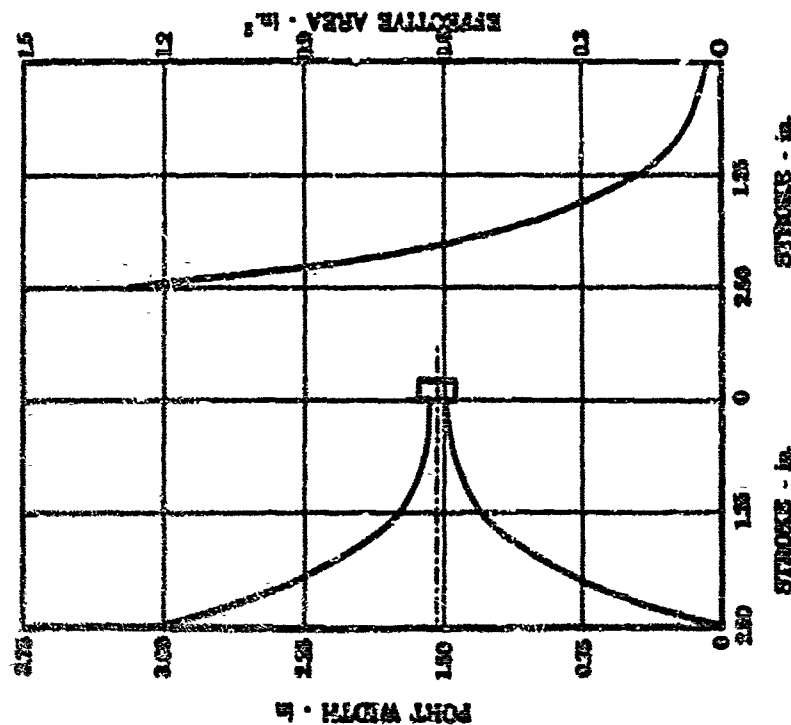


Figure 436. Sleeve Valve Port Contour and Port Effective Area vs Axial Valve Stroke (2.5-inch Stroke) (Thrust Control Valve)

CONFIDENTIAL

(C) The fluid medium generates axial flow forces that are sometimes called Bernoulli Forces as it passes through the contoured port. These forces are developed as the fluid accelerates to the vena contracta and, in so doing, generates a static pressure gradient in the radial direction along the sleeve wall acting along the circumferential port width. This pressure gradient acting along the port face (exposed circumferential width multiplied by the radial sleeve thickness) is opposed by a force at the other end of the sleeve made by a stagnation pressure acting over the same area. The difference in the two forces yields the net axial force exerted by the fluid on the valve. Figure 438 is a plot of this force as a function of thrust level ($r = 5.0$ worst condition) for two types of sleeve valves. The inverted pintle type (figure 429) yields considerably higher loads than the port contoured sleeve valve (figure 430) because the static pressure gradient, which is fluid induced, is exposed to a larger area.

(U) The horsepower required is established in a similar fashion to the butterfly candidate. The demonstrator engine simulation yields an area rate of change requirement, dA/dt . The valve has a relationship between area and stroke, dA/dx . Dividing the area rate of change by the area-stroke relationship yields:

$$\frac{dA/dt}{dA/dx} = \frac{dA}{dx} \left(\frac{dx}{dt} \right) = \frac{dx}{dt} = v$$

where v is the required axial valve velocity. Knowing the axial forces (Bernoulli) and the shaft axial velocity, the horsepower required to overcome the flow forces in accordance with an engine transient is determined from:

$$hp = \frac{(F_w)(v)}{K}$$

where

F_w = Flow forces

v = Axial valve velocity

hp = Horsepower required

K = Constant

Figure 439 shows the horsepower required for two types of sleeve valves.

CONFIDENTIAL

CONFIDENTIAL

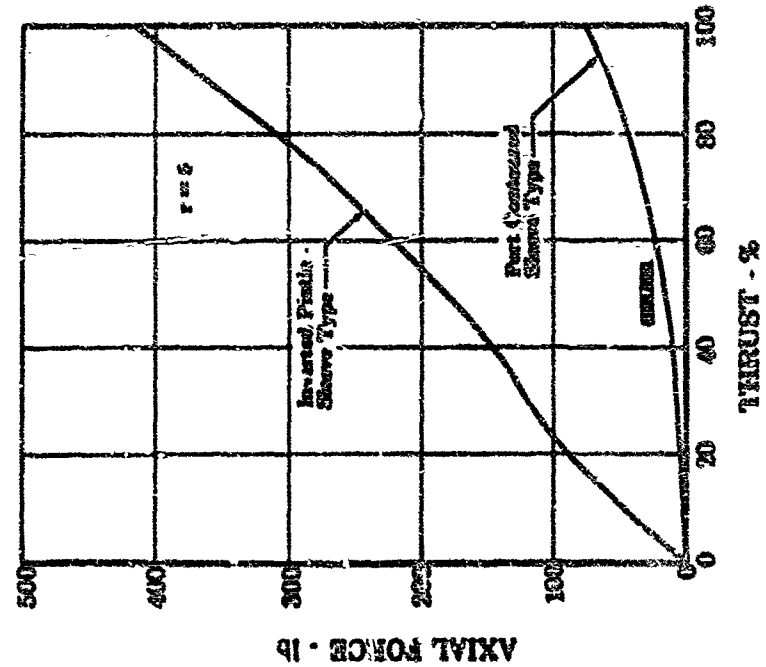


Figure 438. Axial Dynamic Flow Forces vs Percent Thrust at $r = 5$ (Thrust Control Valve)

FD 18263

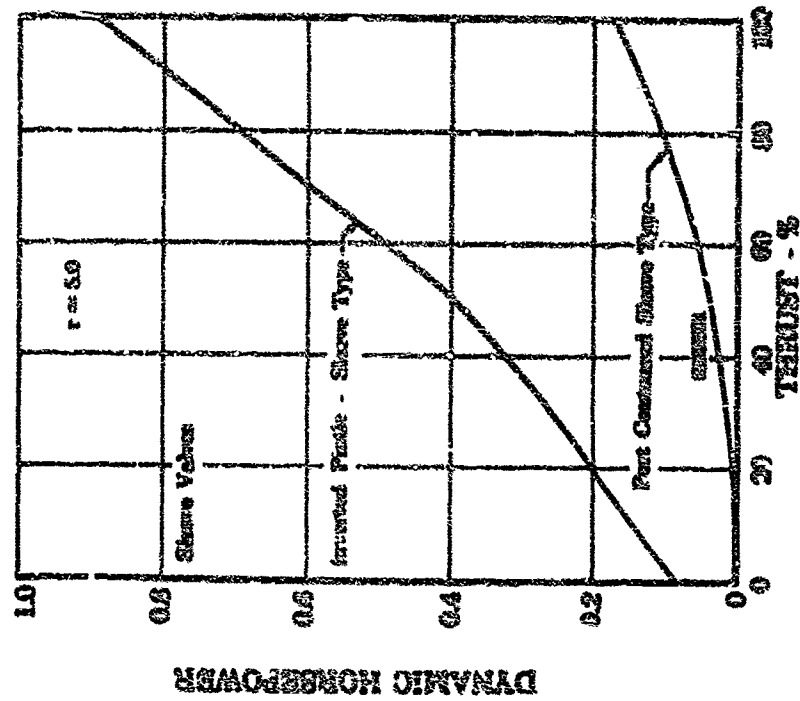


Figure 439. Horsepower Required to Overcome Flow Force vs Percent Thrust at $r = 5$ (Thrust Control Valve)

FD 18212

CONFIDENTIAL

CONFIDENTIAL

(2) Pintle Orifice Valve Candidate (Figure 440)

(U) The pintle of the pintle-orifice valve is merely a translating plug, contoured to yield the desired relationship of flow area to axial position in the orifice. The pintle contours investigated in this study were determined by the constant percent of area error method previously described.

(U) At the low flow conditions of operation, the clearance between the pintle and the housing becomes extremely small, thus requiring close control of concentricities and providing a possible area of contamination sensitivity. In addition, eccentricity in a narrow annulus produces a great effect on coefficient of discharge of the orifice or venturi and would result in uncertainty of valve performance prediction.

(U) In determining the required geometric flow area for a pintle-orifice valve, an analysis similar to that for the sleeve valve is performed. The pressure recovery factor influences the pintle-orifice calculation. Essentially, the pressure recovery factor results in a valve metering pressure drop (total valve inlet pressure minus valve throat static pressure) that exceeds the valve flange-to-flange pressure loss. This results in smaller area requirements for a given flow than in a sleeve valve where port metering contours yield low recovery factors. Figure 441 is a plot of the required geometric flow area as a function of thrust level and mixture ratio. The percent recovery factor is plotted in figure 442. The recovery factor varies according to the variation in throat area and the shape of the pintle contour at the throat. Consequently the recovery factor varies with thrust level and mixture ratio.

(U) Integrating the static pressure profile over the bullet face of the pintle provides the pintle valve opening force. This force is plotted in figure 443 as a function of thrust level and mixture ratio, because the pressure profile on the bullet face varies with the environmental pressures.

(U) If the pressures acting on areas opposing the opening force were integrated, the results would yield an axial valve closing load. This closing load can be altered to obtain "matching characteristics" with the valve opening load by varying the pintle shaft diameter or providing a balance piston. Figure 444 is a plot of the net axial valve force (opening plus closing loads) as a function of thrust level and mixture ratio for a 1.49-inch diameter shaft.

(U) As the system demand for geometric valve area change is made, because of engine throttling and mixture ratio excursion, the valve must be positioned according to thrust level and mixture ratio as shown in figure 445. This position plot is in accordance with the required geometric flow area plot shown in figure 441.

CONFIDENTIAL

(This page is Unclassified)

CONFIDENTIAL

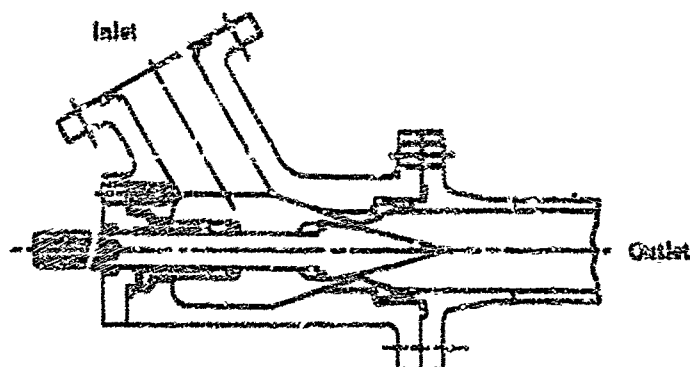


Figure 440. Thrust Control Pintle Orifice Valve Candidate

PD 15263

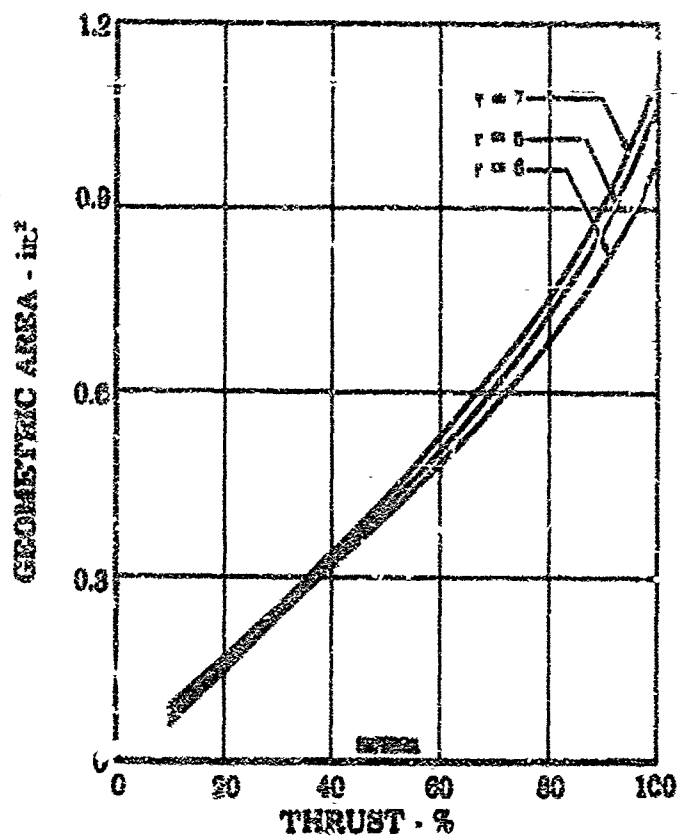


Figure 441. Geometric Flow Area vs Percent Thrust (Thrust Control Valve)

PD 16218

CONFIDENTIAL

CONFIDENTIAL

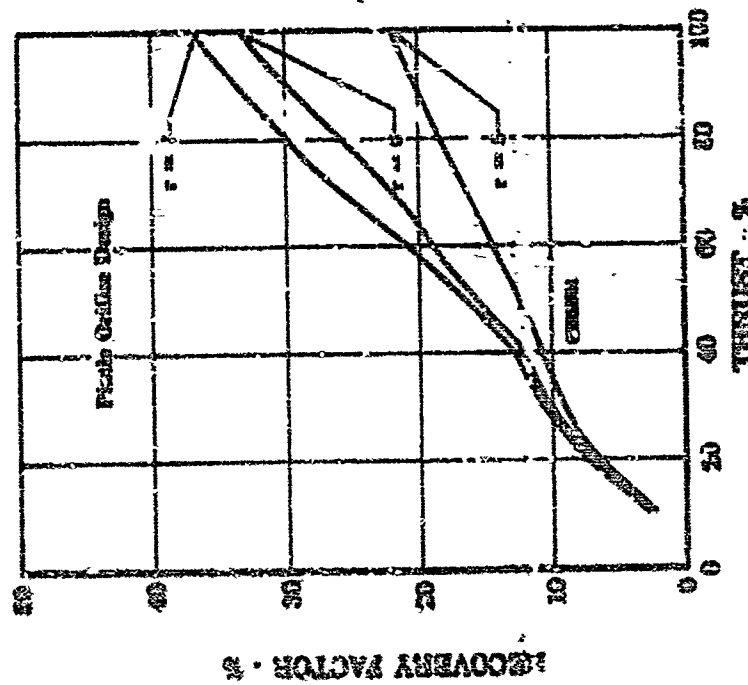
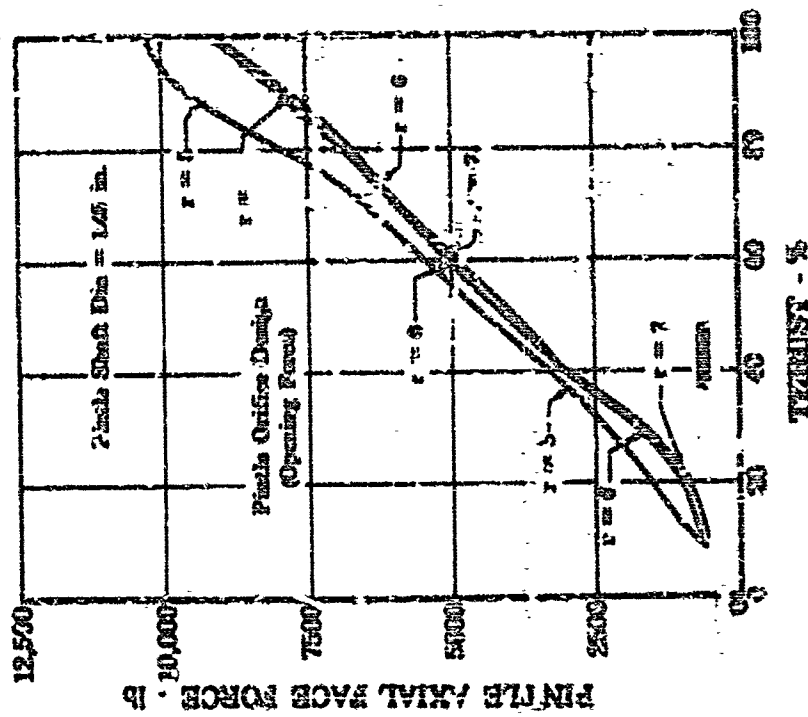


Figure 443. Pintle Axial Force vs. Percent Thrust (Control Valve)

Figure 442. Percent Recovery Factor vs. Percent Thrust (Control Valve)

ED 1316C

ED 23156

CONFIDENTIAL

CONFIDENTIAL

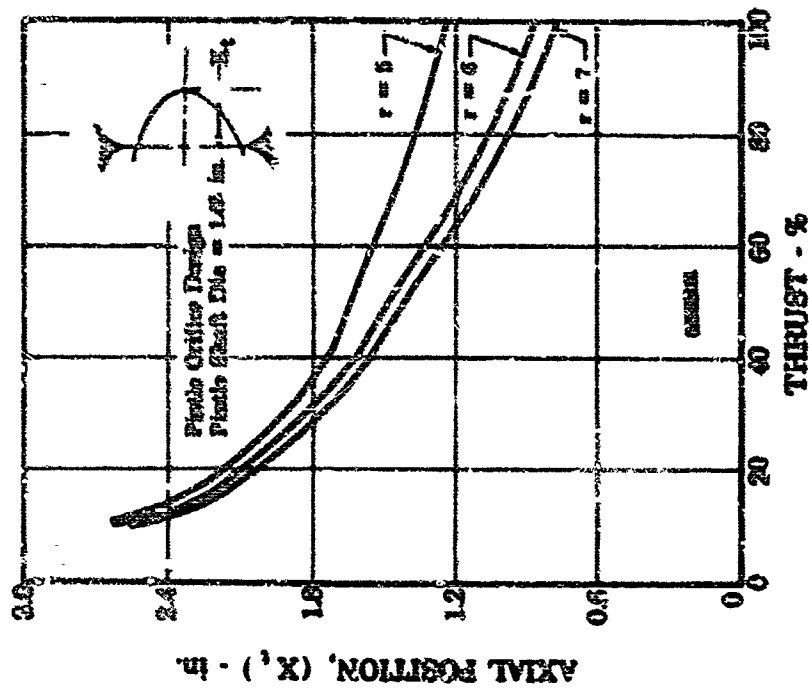


Figure 445. Axial Pintle Position vs Percent Thrust (Thrust Control Valve) FD 18193

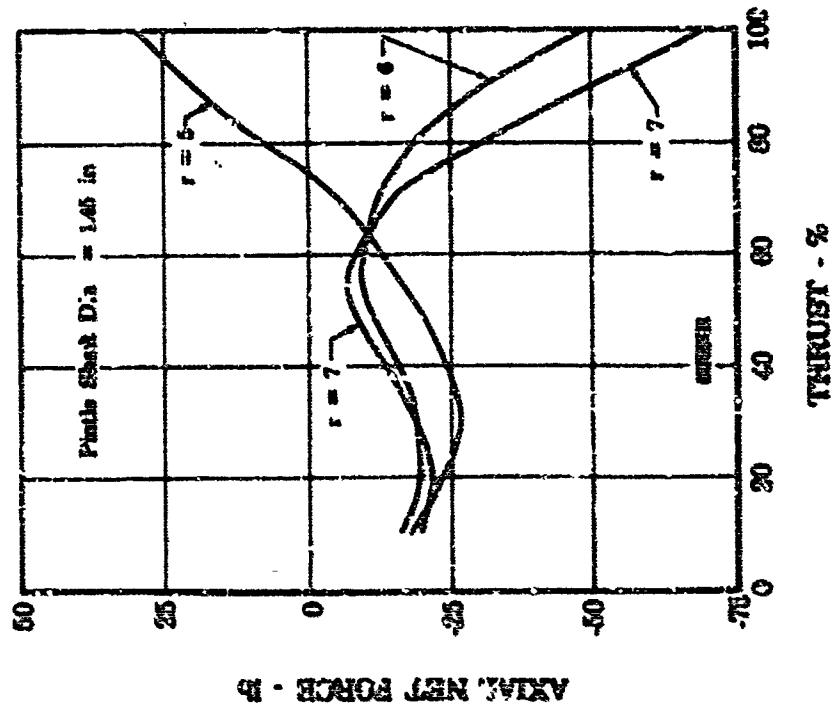


Figure 444. Pintle Net Axial Force vs Percent Thrust (Thrust Control Valve) FD 18157

CONFIDENTIAL

CONFIDENTIAL

(C) The accuracy of the pintle orifice valve candidate is 3.6 percent area error per 1 percent positional error. The power required to follow a simulated engine transient is 0.113 horsepower.

(3) Pintle Venturi Valve Candidate (figure 446)

(a) Cavitating Venturi Scheme

(U) It is necessary that the venturi throat static pressure be maintained at the saturation pressure of the fluid or slightly lower to maintain cavitation.

(U) The throat static pressure may be calculated knowing the venturi inlet and discharge pressure and the pressure recovery.

(U) Defining the following variables;

P_{in} = Venturi inlet pressure, (total)

P_D = Venturi discharge pressure, (total)

R_f = Recovery factor

P_t = Throat pressure (static)

Then the throat head may be written in terms of the recovery factor, throat static pressure, and the venturi discharge pressure as follows:

$$(P_{in} - P_t)(R_f) + P_t = P_D$$

Solving for P_t ,

$$P_t = \frac{P_D - (R_f)(P_{in})}{(1 - R_f)}$$

(C) As long as the throat pressure remains at or below the fluid saturation pressure, the venturi will be in a cavitating regime. Figure 447 is a plot of the throat pressure as a function of thrust level at a mixture ratio of 7. The venturi will not operate in a cavitation mode above 79.0% thrust level.

(b) Noncavitating Venturi Scheme

(C) To operate a venturi successfully in a noncavitating mode, the static pressure in the throat must be maintained above saturation pressure of the fluid. Figure 448 shows that the venturi would cavitate at any thrust level at a mixture ratio of 5.0, and at a thrust level below 35% regardless of mixture ratio, thus eliminating the pintle-venturi from consideration because accurate engine control cannot be maintained with the valve passing through a transitional flow condition.

CONFIDENTIAL

CONFIDENTIAL

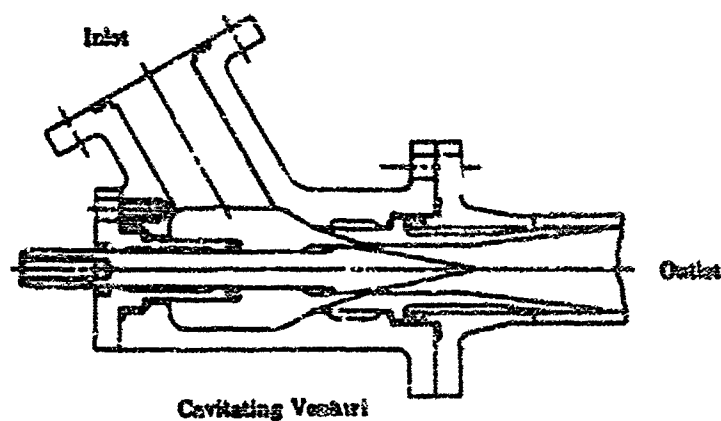


Figure 446. Thrust Control Pintle Venturi Valve Candidate

FD 18267

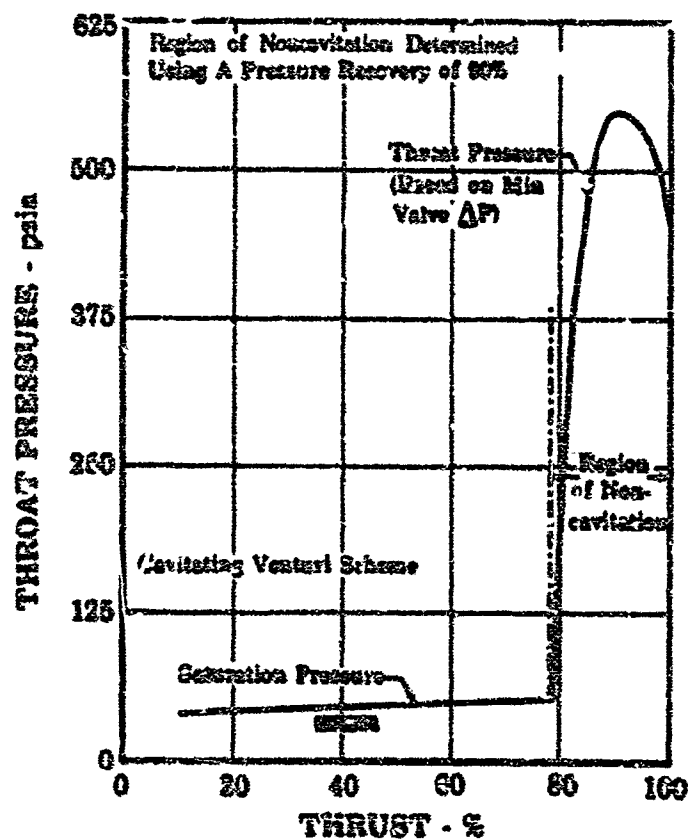


Figure 447. Throat Pressure vs Percent Thrust Defining Region of Noncavitation (Thrust Control Valve)

FD 18152

CONFIDENTIAL

CONFIDENTIAL

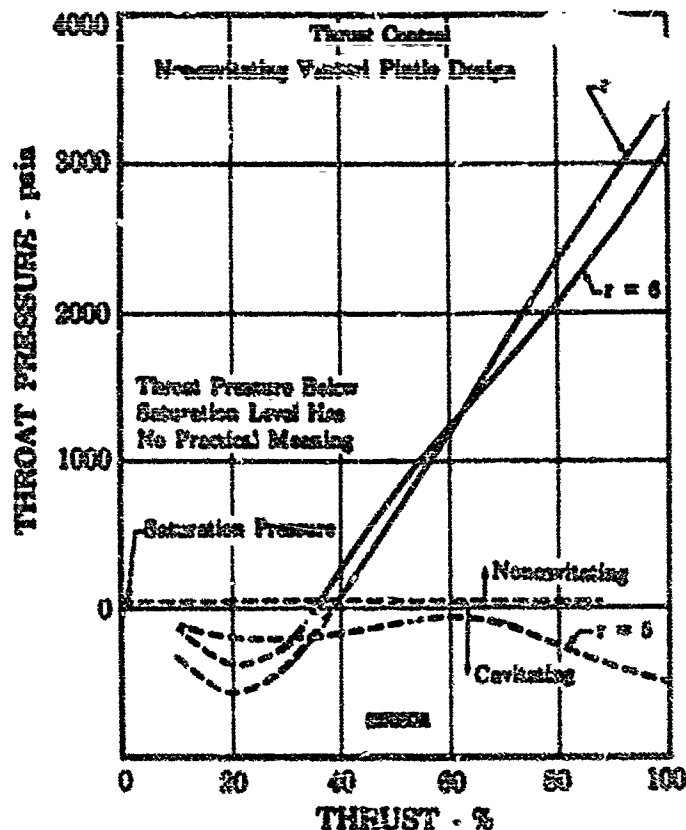


Figure 448. Throat Pressure Required to Meter Scheduled Flow and ΔP Loss Across Venturi vs Percent Thrust

FD 18187

(4) Rotating Plate Valve Candidate (Figure 449)

(U) The rotating plate valve scheme consists of two plates, one stationary and the other rotating, regulating flow by exposing area common to both.

(U) A thrust bearing, which is not shown in the design sketch, supports the load imposed by a valve pressure difference to minimize actuation force requirements. Face seals are incorporated to reduce bypass and port-to-port leakage. The valve shown in figure 449 has circular ports and face seals for manufacturing ease and compact size. If contoured ports were required, as in other schemes, for equal percentage error characteristics, the secondary face seal would be difficult to manufacture and the size of the valve would be necessarily larger to accommodate the long ports.

(5) Butterfly Valve Candidate (figure 450)

(U) The butterfly valve candidate for the thrust control valve uses a straight-through actuation shaft configuration with a removable flapper. The design was evaluated with both journal and roller bearings on either end of the shaft. Use of roller bearings reduced the actuation forces

CONFIDENTIAL

~~CONFIDENTIAL~~

imposed by bearing friction from 21 ft-lb to approximately 0.2 ft-lb. Dynamic seals were incorporated on both ends of the shaft to eliminate thrust loading.

(U) A streamlined flapper of 0.750-inch maximum thickness was selected to minimize base pressure loss.

(C) The thrust control is required to pass the maximum flow rate with a maximum pressure drop of 100 psi. In general, if a flow rate and pressure drop are specified for a butterfly valve, the required valve throat diameter depends on the flapper opening angle. Figure 451 illustrates the required valve flapper position as a function of valve throat diameter for maximum flow rate and 100 psi and 50 psi pressure drop conditions. This comparison reflects the sensitivity of the valve size with respect to pressure loss across the valve at maximum flow conditions. For a given throat diameter, the minimum flapper opening can be determined using the flow rate and pressure drop corresponding to the minimum required thrust level. Therefore, figure 451 illustrates the required throttling range of the butterfly valve in terms of angular opening as a function of valve throat diameter. The valve throat diameter corresponding to a valve flapper opening angle of 50 degrees was selected because it yielded the smallest size valve. This selection gave a throat diameter of 1.5-inches.

(U) With the valve throat diameter selected, a plot of required butterfly angular opening versus percent thrust for various mixture ratios is provided in figure 452. These curves were established by taking the flow rate and pressure drop across the valve from rig data as a function of thrust and mixture ratio and solving for the required head loss factor "K".

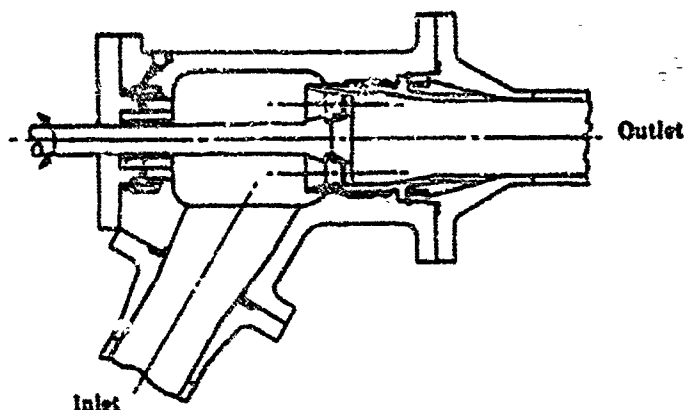


Figure 449. Thrust Control Rotating Plate Valve Candidate

FD 18250

~~CONFIDENTIAL~~

CONFIDENTIAL

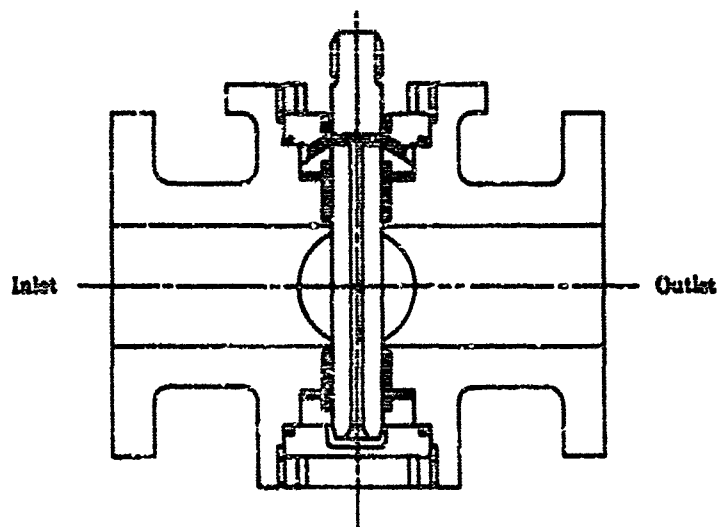


Figure 450. Thrust Control Butterfly Valve Candidate

FD 18232

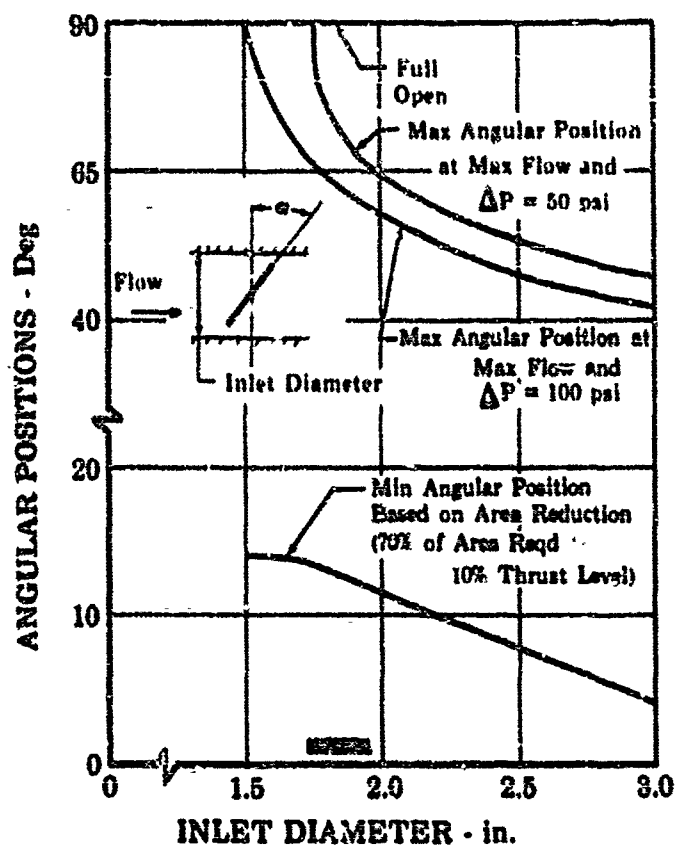


Figure 451. Butterfly Angular Position (Min + Max) vs Butterfly Inlet Dia (Thrust Control Valve)

FD 18244

CONFIDENTIAL

CONFIDENTIAL

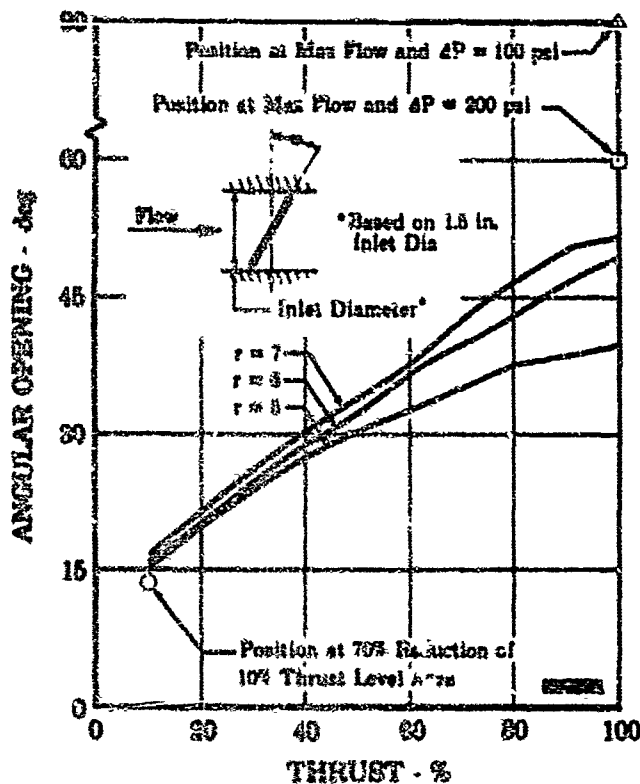


Figure 452. Butterfly Angular Opening vs Percent Thrust (Thrust Control Valve)

FD 18264

(U) For a fixed pressure drop and throat diameter of 1.5 inches, the flow rate through the valve would vary as a unique function of flapper opening. If an orifice was considered instead of a butterfly valve, the effective area of the orifice would regulate the flow versus pressure drop characteristics. Because the butterfly is a variable effective area, it can be related to the area of an equivalent orifice by considering the variable flow/pressure drop characteristics as a function of flapper opening. Figure 453 illustrates butterfly valve effective area versus angular opening.

(C) It was desirable to know the effective area sensitivity with respect to positional error for all the valve candidates. A plot of percent area error per angular positional error can be prepared from figure 453. This was accomplished by taking the slope of the effective area versus angular position curve at a point and dividing by the effective area at that point. Figure 454 is the result of plotting many such points. Operating the valve within the 7% to 100% thrust limits shown in figure 454 allows a reasonable constant error of 5 to 7% per degree of flapper position.

5 Secondary Injection Thrust Vector Control Study (U): Volume I, "Data and Appendix," Lockheed Missiles and Space Company, Huntsville Research and Engineering Center, February 28, 1964 (Confidential).

CONFIDENTIAL

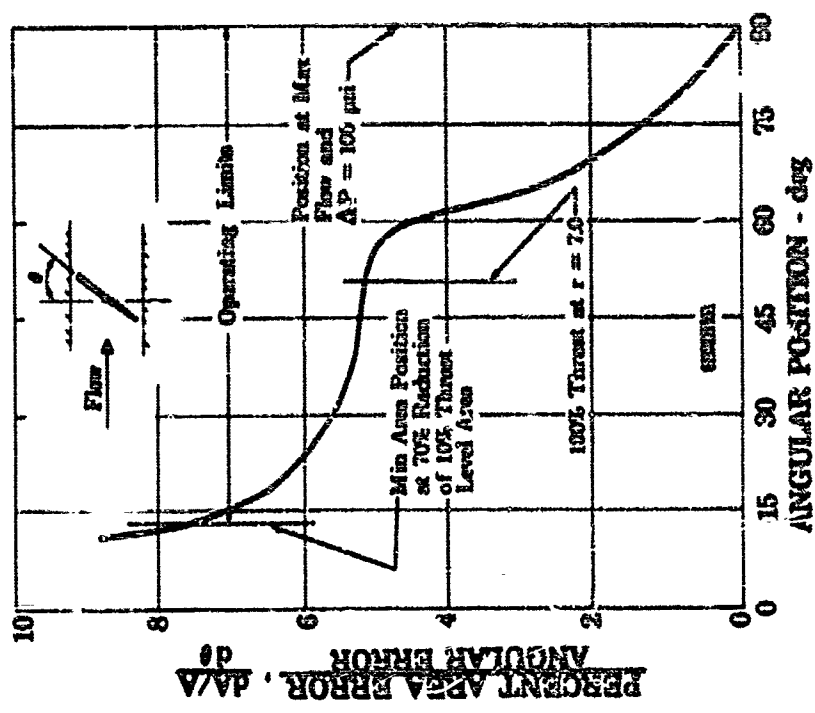


Figure 454. Area Error Per Degree Angular Error vs Butterfly Angular Position (Thrust Control Valve)

FD 18252

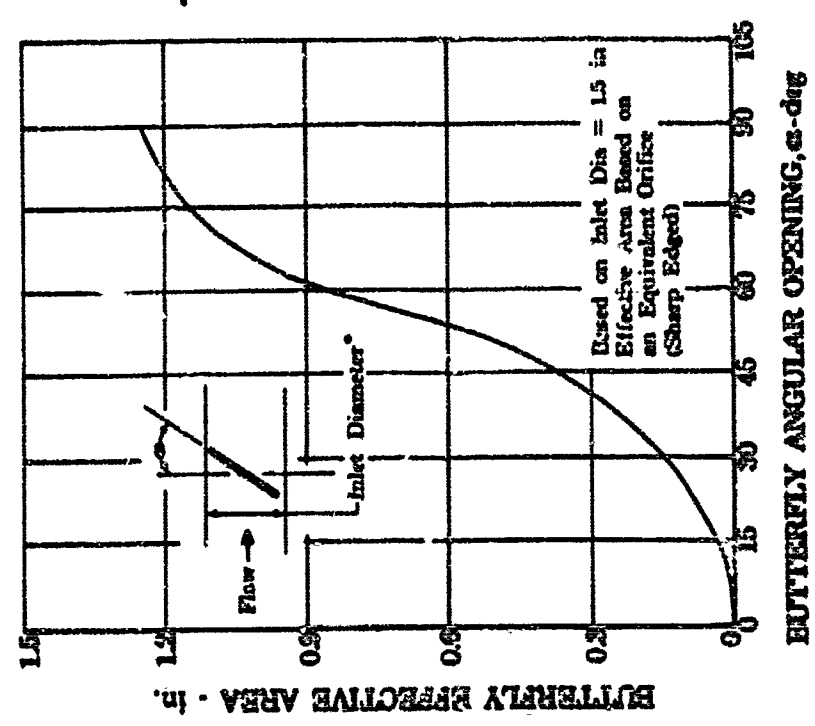


Figure 453. Butterfly Effective Area vs Butterfly Angular Opening (Thrust Control Valve)

FD 18248

~~CONFIDENTIAL~~

(U) To size actuator requirements, it was necessary to determine the dynamic torque characteristics of the butterfly flapper. The dynamic torque is a function of flapper angle, throat diameter, and pressure drop. Flapper angle and pressure drop are functions of thrust level and mixture ratio, and may be determined from figure 432. Therefore the dynamic torque for the 1.5-inch throat diameter valve is shown in figure 433 as a function of thrust level and mixture ratio.

(U) The horsepower required to turn the butterfly shaft depends on the shaft torque and the angular velocity of the shaft. From the transient simulation of the demonstrator engine, a required rate of change of valve area (valve area rate of change to keep up with the engine rate of change of flow and pressure drop) is determined. The required rate of change may be expressed as da/dt and, at a particular engine operating point, there is a relationship between valve effective area and angular opening that may be expressed as $da/d\phi$.

(U) Dividing the area rate of change by the area-angle relationship provides the required valve angular shaft velocity,

$$\frac{da/dt}{da/d\phi} = \frac{da}{dt} \left(\frac{d\phi}{da} \right) = \frac{d}{dt} = \omega$$

where ω is the shaft rotational velocity or frequency. The combination of rig transient shaft frequency and maximum torque required yields a power requirement of 0.306 horsepower. Figure 456 is a plot of required horsepower versus shaft rotational frequency at the maximum shaft torque operating point.

(U) Anticipated problems in the development of the butterfly valve are: the necessity for dynamic seals, which in the high-pressure, low-temperature environment will be subject to wear and leakage; and corner loading of the shaft bearings caused by shaft deflection. Also possible, but unpredictable, is oxidizer cavitation downstream of the flapper resulting in damage to the valve.

(6) Summary and Conclusions

(U) The design selection studies indicated that a butterfly valve would best accommodate the system requirements for this valve.

(U) A butterfly valve with a rotary actuator was selected for development on the basis of advantages in size, weight, and simplicity and the capability to provide the desired schedules with reasonable power requirements. No major procurement problems were encountered during fabrication of two valve assemblies. These units were not assembled or tested after it was decided to use an existing facility valve for this function during the staged combustion rig tests.

c. Design of Selected Configuration

(U) The demonstrator engine thrust control butterfly valve shown in figure 447 was designed to regulate the preburner oxidizer flow to control thrust by controlling turbine power to the main turbopumps. The thrust control valve and mounting block are located on the preburner dome.

463

~~CONFIDENTIAL~~

(This page is Unclassified)

CONFIDENTIAL

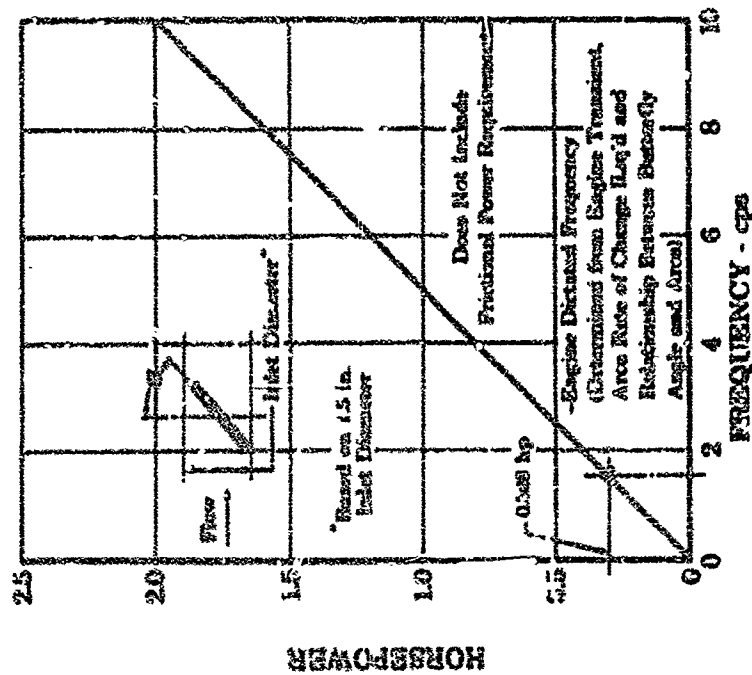


Figure 456. Butterfly Actuator Horsepower vs Frequency of Actuation at Max Torque Point of Operation (Thrust Control Valve)

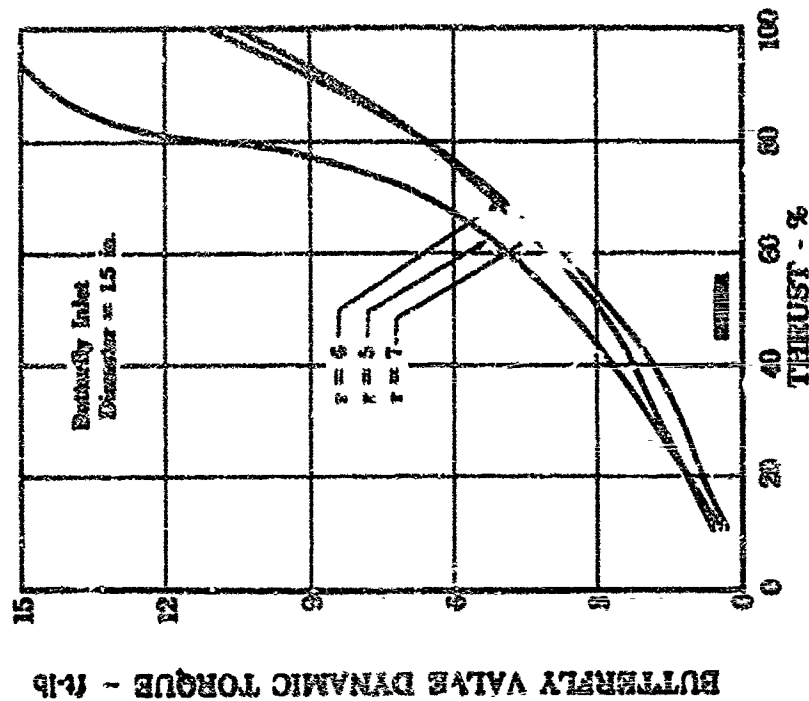


Figure 455. Dynamic Torque vs Percent Thrust (Thrust Control Valve)

464
CONFIDENTIAL

UNCLASSIFIED

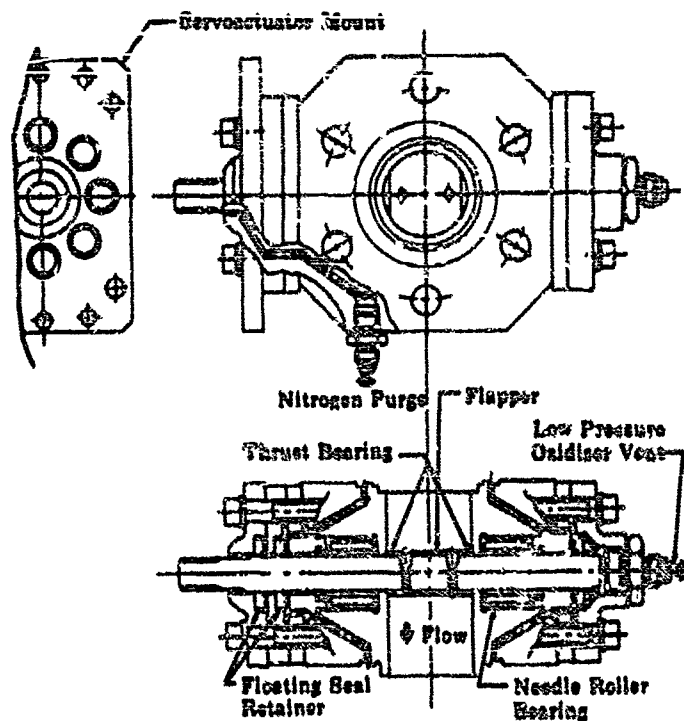


Figure 457. Thrust Control Valve

FD 18910

(U) The butterfly valve straight through shaft configuration was made possible by incorporating the oxidizer shutoff seal into the flow divider valve. The valve construction with the removable flapper has the advantage of simplicity, a high turndown ratio, and can provide the desired performance with reasonable actuation power.

(U) The thrust control valve housing was fabricated from AMS 5646 (stainless steel) and the streamlined flapper and shaft, which are shown in figure 458, were fabricated from Inconel 718. These materials have the strength requirement necessary for these highly loaded parts. The flapper was riveted to the shaft to permit uninterrupted flow past the flapper in the open position, which results in a minimum base pressure loss.

(U) Because the shaft was pressure balanced with low pressures on the ends, thrust loads on the valve shaft are small. Positioned on each side of the flapper was a thrust bearing made of Berylco 25 (AMS 4650) that acts as a snub bearing to prevent the flapper from contacting the valve housing and also to absorb possible shaft loads caused by the servo-actuator installation. Radial shaft loads caused by the pressure difference across the valve flapper and misalignment of the valve servo-actuator are transmitted through needle roller bearings to the housing. The torque required to turn the shaft on the roller bearings is 0.21 ft-lb and is small compared to the seal breakaway and flow torque.

(U) Commercially available Teflon (AMS 2515) dynamic shaft seals are used on each end of the valve shaft. These seals are held by floating seal retainers (figure 459) that allow a small shaft deflection without

UNCLASSIFIED

UNCLASSIFIED

unloading the seals. The for development problem associated with this valve is the wear and leakage associated with these dynamic shaft seals when subjected to a high pressure differential and a low temperature environment.

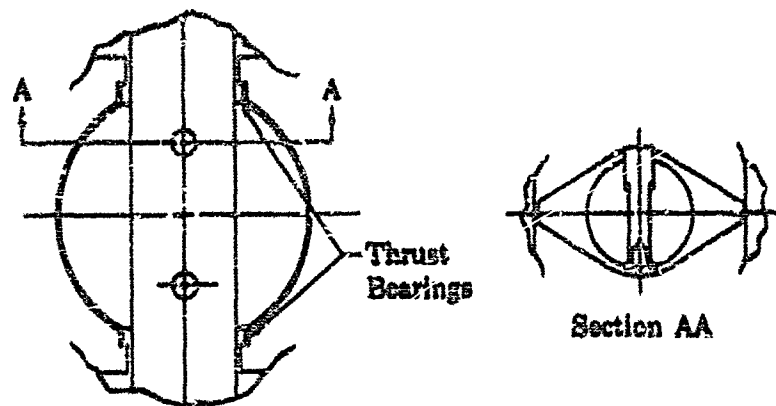


Figure 458. Thrust Control Valve Vane

FD 18892

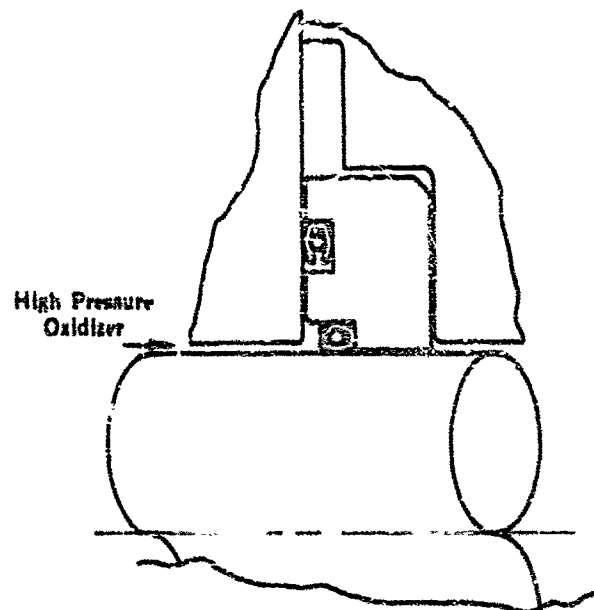


Figure 459. Thrust Control Valve Floating Seal Retainer

FD 19001

(U) Seal leakage past the high-pressure dynamic seal on the servoactuator side of the valve is vented through the passage between the static O-ring seals at the valve interfaces. This leakage is then combined with leakage past the other high-pressure dynamic seal and vented overboard. A nitrogen purge provides leakage past the low-pressure labyrinth seal on the shaft where the servoactuator is mounted to prevent ice from accumulating around the shaft and interfering with the valve operation.

UNCLASSIFIED

CONFIDENTIAL

(U) The shaft seal dimensions are 0.811-in. OD x 0.681-in ID x 0.065-in. axial thickness. The face seal dimensions are 1.187-in. OD x 1.357-in. ID x 0.075-in. axial thickness. Leakage criterion for the seal package is 10 acs GN₂ maximum leakage overboard over the operating range.

(U) The predicted thrust control valve operating characteristics are shown in figures 460 and 461.

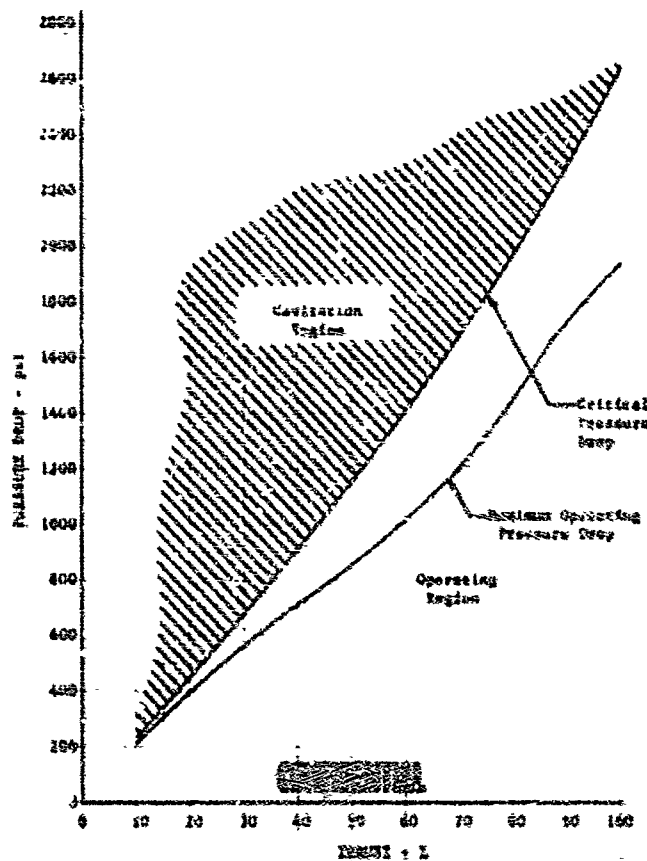


Figure 460. Thrust Control Valve Pressure Drop vs Percent Thrust

DF 52335

CONFIDENTIAL

CONFIDENTIAL

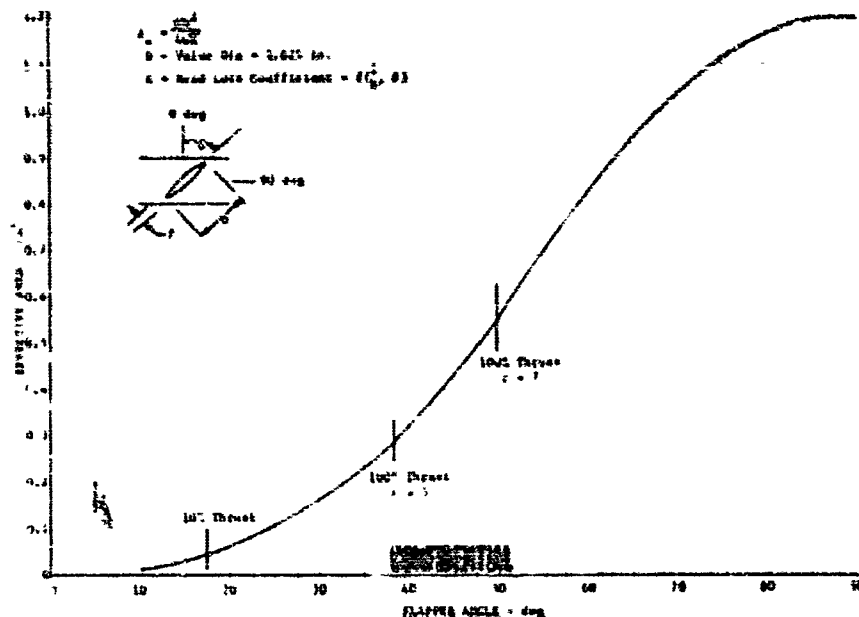


Figure 461. Thrust Control Valve Effective Area vs Flapper Angle

DF 52332

E. CHAMBER COOLANT VALVE AND SEAL RIG

1. Hardware Description

(U) The initial engine cycle concept required a control valve to regulate the main chamber transpiration coolant flow.

(U) The original location of the valve downstream of the fuel pump discharge variable-area venturi was shown by cycle studies to require a valve with maximum flow area at low pressure and flow. Curves of the area and pressure drops required for that valve concept are shown in figures 462 and 463. In addition, a position feedback signal from the inducer turbine bypass valve was required to prevent unacceptable variations in the transpiration coolant flow.

(C) An investigation of other possible supply locations showed that a more reasonable flow area schedule could be provided by a valve that was supplied from upstream of the fuel pump discharge variable-area venturi. Further analysis revealed that sufficient pressure was available to allow incorporation of a venturi valve that would be choked or cavitated in the 10% to 100% thrust range. With the valve cavitated or choked, variations in fuel inducer turbine bypass area and other downstream flow disturbances do not affect the total coolant flow rate. A disadvantage of the fuel pump discharge location was the addition of a shutoff requirement to prevent propellant loss through the transpiration coolant passages when the engine is not operating. A curve of a typical operating point for this valve is shown in figure 464. As indicated, a considerable change in downstream pressure can be tolerated before flow rate is affected. Required valve operating areas, flows, and pressure drops are shown in figure 465.

CONFIDENTIAL

CONFIDENTIAL

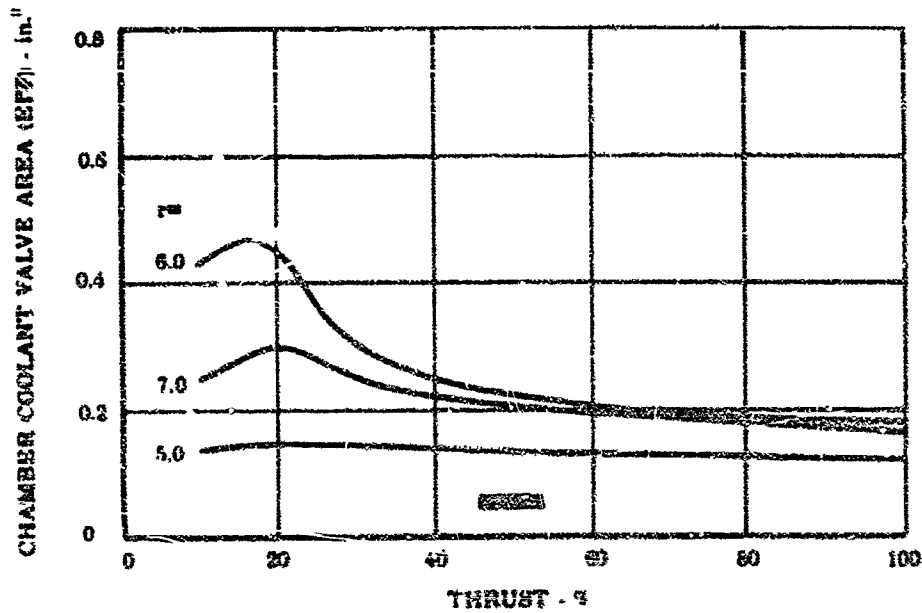


Figure 462. Noncavitating Chamber Coolant Valve Effective Area vs Thrust

FD 16068

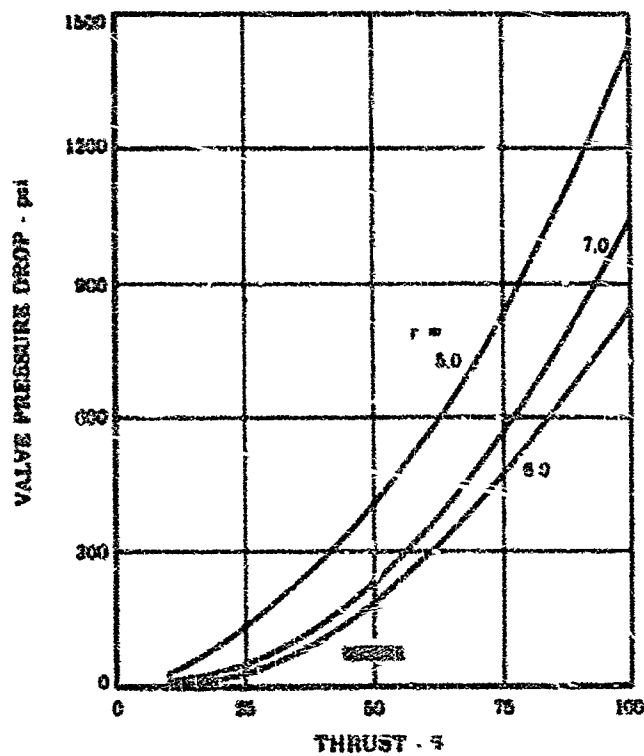


Figure 463. Noncavitating Chamber Coolant Valve (Flange-to-Flange) Pressure Drop vs Thrust

FD 16069

CONFIDENTIAL

CONFIDENTIAL

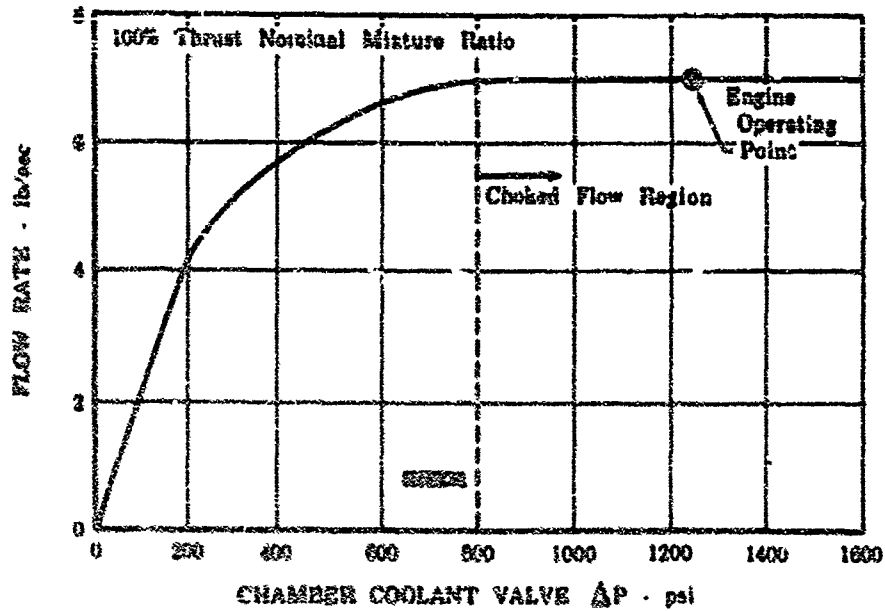


Figure 464. Chamber Coolant Valve Flow vs Total Pressure Drop

FD 16067

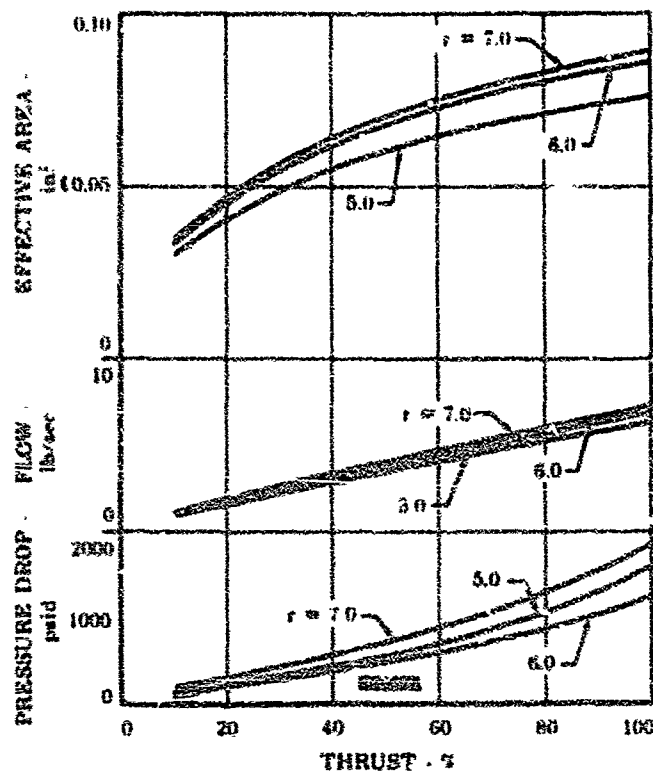


Figure 465. Cavitating Chamber Coolant Valve Operating Requirements

FD 16059

CONFIDENTIAL

CONFIDENTIAL

2. Design of Selected Configuration

(C) The valve design (figure 466) incorporates a plenum chamber, an acceleration section, a throat shutoff seal and a diffuser or pressure recovery section. The inlet to the plenum is at 90 degrees to the throat for ease of manufacturing and packaging. The plenum chamber ensures that the velocity and pressure profiles entering the throat are relatively uniform. In the acceleration section, the static pressure is decreased until sonic velocity is attained at the throat. At this condition, downstream disturbances, such as variations in fuel low-speed inducer turbine bypass area, will not affect the coolant flow. Approximately 90% of the inlet total pressure is recovered in the diffuser section.

(C) The venturi flow area is varied by moving a contoured pintle in and out of the venturi throat. The valve has a required area turndown ratio of approximately 3:1. The pintle design provides a low force unbalance to minimize actuator load requirements and simultaneously ensures that the net force is always in the same direction to prevent actuator load oscillations. Shutoff is accomplished by a seal installed on the pintle that is inserted into the venturi throat as shown in figure 467.

(U) Figure 468 shows a cross-sectional view of the chamber coolant valve flow passage. The inlet and outlet diameters are approximately 1.2-inches. The acceleration section leading to the venturi throat has a wall half angle of 20 degrees. The first diffuser section is the tapered section of the pintle that forms a cone with an 8.1-degree half angle. The second part of the diffuser is a 7-degree cone leading to the valve outlet. The pintle contour is designed for constant percentage area error in the valve flow control range.

(U) Type 6061 aluminum was selected as the housing material because of its good AMS 2468 hardcoating characteristic, availability, and relatively high strength-to-weight ratio. Housing surfaces subjected to rubbing by the pintle and shaft are hardcoated to minimize wear.

(U) The pintle is made in two pieces to facilitate the installation of a shutoff seal. The pintle is made of AMS 5735 (stainless steel), which was selected for its high strength, high elastic modulus, and good machining qualities. The pintle shaft is chrome coated to minimize wear. The tapered portion of the pintle features three streamlined fins 120 degrees apart, which act as stabilizers to prevent pintle flutter. These fins slide on the cylindrical wall of the throat with a 0.002-inch minimum clearance. The pintle stroke required for maximum area turndown is approximately 1.0-inch. An additional 0.5-inch is provided for shutoff, making the total valve stroke 1.5-inches. The actuator end of the pintle features a pressure-assisted Teflon dynamic seal with an internal spring. (See figure 469.)

(U) Flanges have double static seals of the Teflon-coated metal O-ring type with an interseal vent. The housing tie bolts are made of beryllium copper to take advantage of its low modulus of elasticity and high coefficient of expansion to maintain the required joint preload at cryogenic operating temperature.

CONFIDENTIAL

CONFIDENTIAL

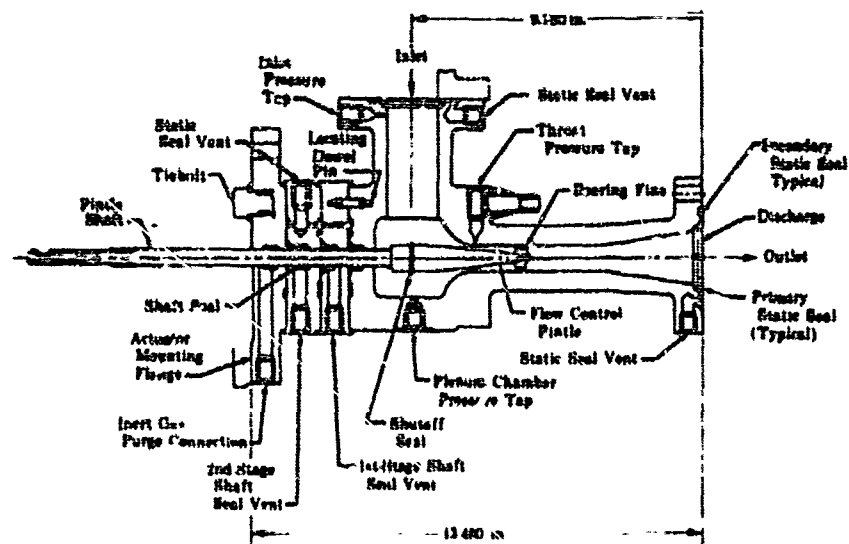


Figure 466. Chamber Coolant Valve

FD 174148

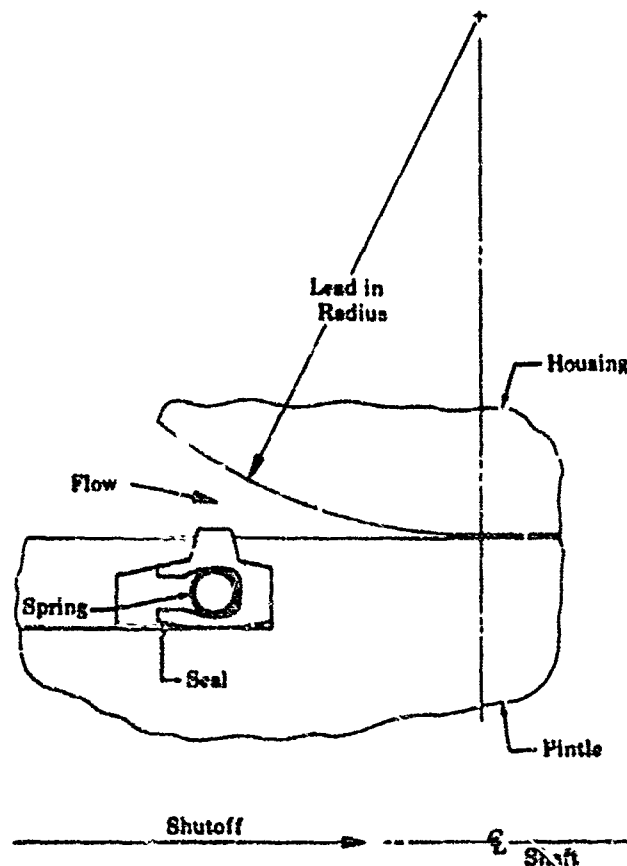


Figure 467. Shutoff Seal

FD 17456

CONFIDENTIAL

(This page is Unclassified)

CONFIDENTIAL

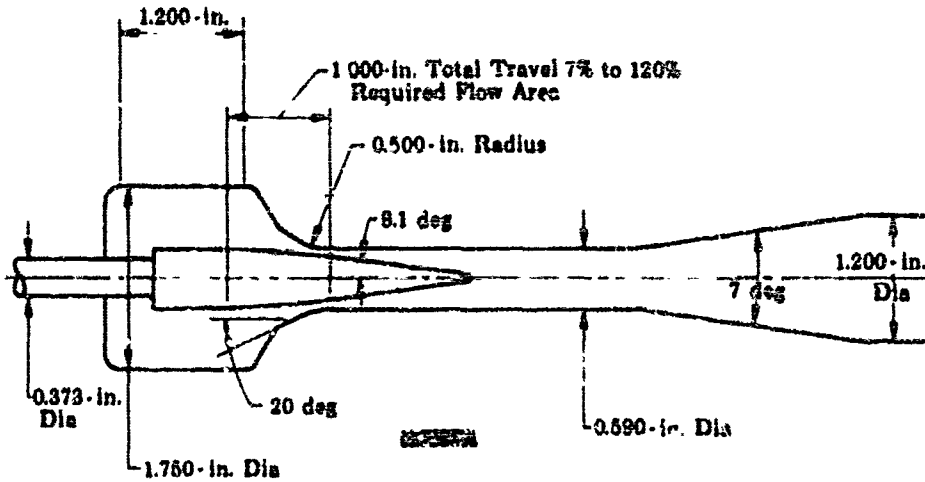


Figure 468. Flow Path Dimensions

FD 17455

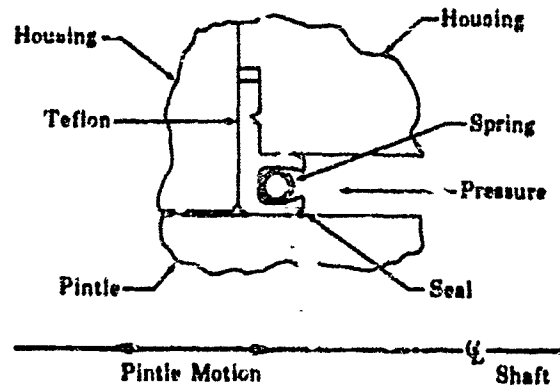


Figure 469. Shaft Seal

FD 17457

(C) The stress margins of the chamber coolant valve parts are shown in table XLI. The stress level in each major valve part is given at the maximum inlet pressure condition (100% thrust, mixture ratio = 7). The limiting pressure on the valve is 8800 psia. Above this pressure the tie bolt preload is exceeded and the joints would tend to separate. The externally applied loads (when applied individually) are limited to those values shown in Table XLII. These values are based on the allowable yield strength of the material.

CONFIDENTIAL

CONFIDENTIAL

(C) The chamber coolant valve was designed to operate in a critical flow regime throughout the entire engine thrust and mixture ratio envelope. The valve operates in the range of engine thrust from 10% to 50% and is choked in the range from 50% to 100% for mixture ratios of 5 to 6. The actual and maximum allowable valve downstream pressures are shown in figure 470; defined in the range from 10% to 30% thrust at a mixture ratio of 5 and from 30% to 100% at a mixture ratio of 6. The pressure recovery assumed for these curves is 90%.

(C) The pintle thrust unbalance reaches a maximum of approximately 390 lb at 100% thrust. The static, or shaft seal breakaway force, and dynamic forces are shown as a function of thrust in figures 471 and 472.

(C) The pintle contour is a constant percentage error design, as shown in figure 473. The required effective flow area of the valve is shown in figure 474 as a function of mixture ratio and thrust. Valve inlet pressure, inlet temperature, and flow rate are shown as a function of engine thrust for mixture ratios of 5, 6, and 7, in figures 475, 476, and 477.

J. Test Program and Test Results

(U) The chamber coolant valve seal test rigs were designed to test chamber coolant valve shaft seal packages. Each rig consisted of seven segments that housed two sets of three shaft seals each, and a 0.375-inch diameter translating shaft driven by a pneumatic actuator (See figure 478.) The primary seals were at the center segment, and fittings for measuring leakage were provided downstream of each seal. Two additional fittings vent leakage that passes the metallic O-ring seals at the segment interface.

(U) The seals were arbitrarily named primary, secondary, and "vent". The primary seal is adjacent to the center segment and was pressurized by full supply pressure. The secondary seal was pressurized by the primary seal leakage vent restriction, and the "vent" seal was pressurized by the corresponding secondary seal leakage. While low primary and secondary seal leakages are desirable, minimum "vent" seal leakage was required for safe staged combustion rig operation.

(U) Table XLI. Chamber Coolant Valve
Parts Stress Margins

| Valve Part | A | B | C |
|--------------------------|--------|--------|---------|
| Shaft | 22,700 | 76,500 | 124,000 |
| Inlet and Exit Flanges | 15,300 | 29,700 | 41,700 |
| Inlet Duct and Exit Cone | 14,500 | 29,700 | 41,700 |
| Plenum Chamber | 12,300 | 29,700 | 41,700 |

A - Actual stress at maximum operating pressure, psi
B - 85% yield at room temperature, psi
C - 85% yield at operating temperature, psi

CONFIDENTIAL

*Support valve at the other numbered station.

| Condition | Load Type | *Station of Applied Load | | Station Load Limit | | C | B = 0.001 | Limiting Station Condition | |
|--|-----------|--------------------------|--------|--------------------|--------|--------|--------------|----------------------------|------------|
| | | 1 | 2 | A | B | | | Station | Condition |
| Pressure 6600 psia Temp 420°R | Tensile | 1 | 9,700 | 1,960 | 7,610 | 79,500 | | 2 | Bending |
| | | 2 | 690 | 9,700 | 82,000 | 8,950 | 3,260 | 622 | Deflection |
| | Shear | 1 | 2,420 | 645 | 2,590 | 2,205 | | 200 | Deflection |
| | | 2 | 1,630 | 3,880 | 7,610 | 4, | | 425 | Deflection |
| | Moment | 1 | 7,040 | 7,040 | 27,450 | 17,800 | | 1,530 | Deflection |
| | | 2 | 7,040 | 7,040 | 27,450 | 17,800 | | 1,530 | Deflection |
| Pressure 0 psia Room Temp | Torque | 1 | 5,600 | 7,040 | 27,250 | 34,800 | | 1 | Shear |
| | | 2 | 7,040 | 5,600 | 25,000 | 17,800 | | 1,530 | Deflection |
| | Tensile | 1 | 62,100 | 12,500 | 6,075 | 59,500 | | | Bending |
| | | 2 | 4,400 | 62,100 | 65,200 | 6,650 | 2,420 | | Bending |
| | Shear | 1 | 24,800 | 4,100 | 2,075 | 1,650 | | | Bending |
| | | 2 | 10,400 | 24,800 | 37,200 | 3,470 | | | Bending |
| Moment | | 1 | 45,000 | 45,000 | 21,750 | 13,300 | | | Bending |
| | | 2 | 45,000 | 45,000 | 21,750 | 13,300 | | | Bending |
| | Torque | 1 | 36,600 | 45,000 | 21,750 | 15,100 | | | Bending |
| | | 2 | 45,000 | 33,900 | 43,500 | 13,300 | | | Bending |

CONFIDENTIAL

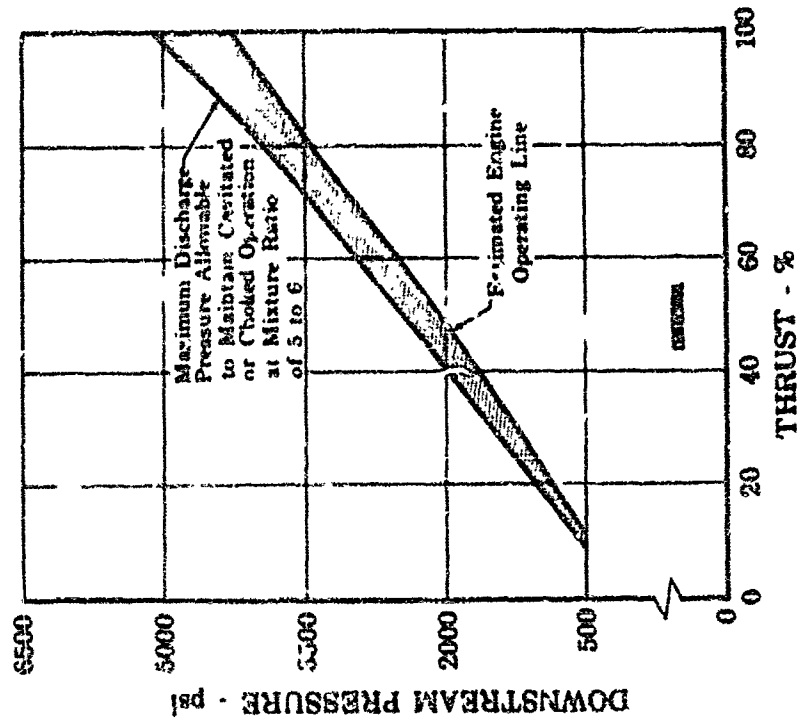
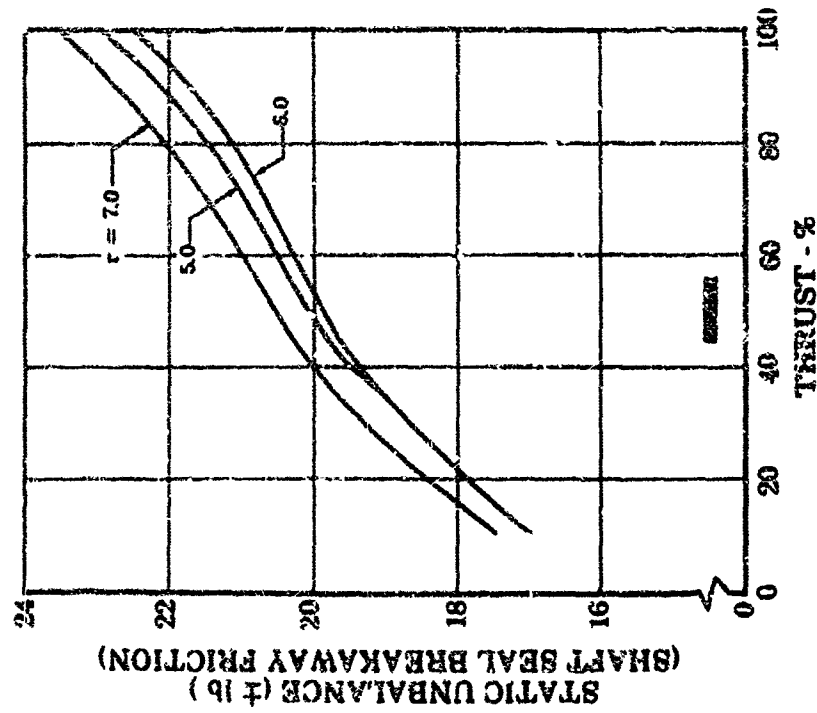


Figure 470. Operating Margin
FD 17458 Figure 471. Pintle Breakaway Force vs Percent Thrust
FD 17489

CONFIDENTIAL

CONFIDENTIAL

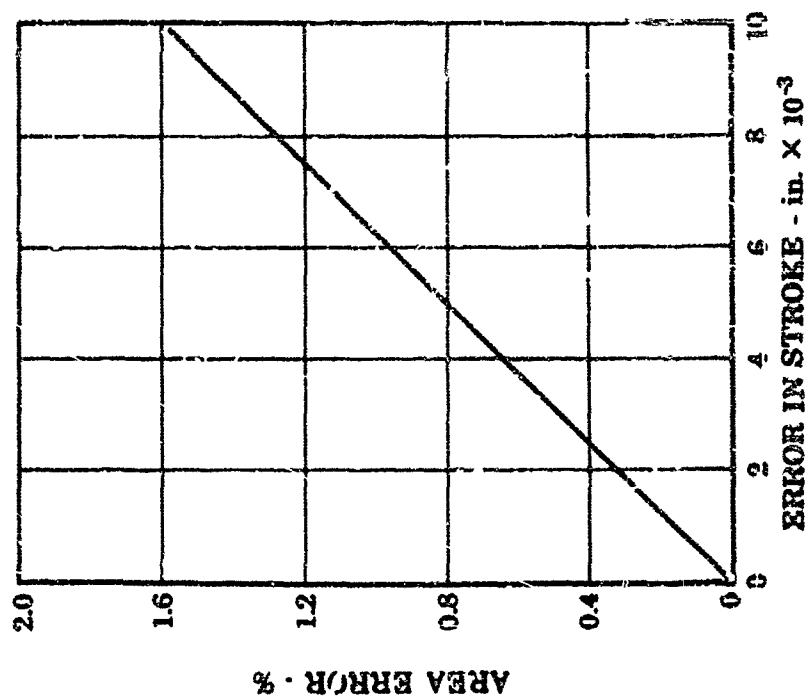
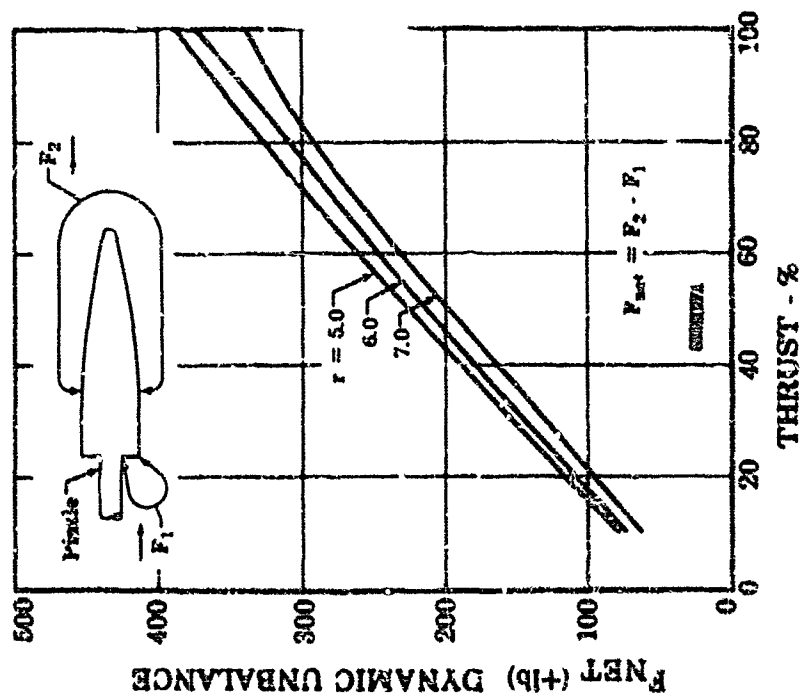


Figure 473. Area Error vs Error in Stroke

FD 17459

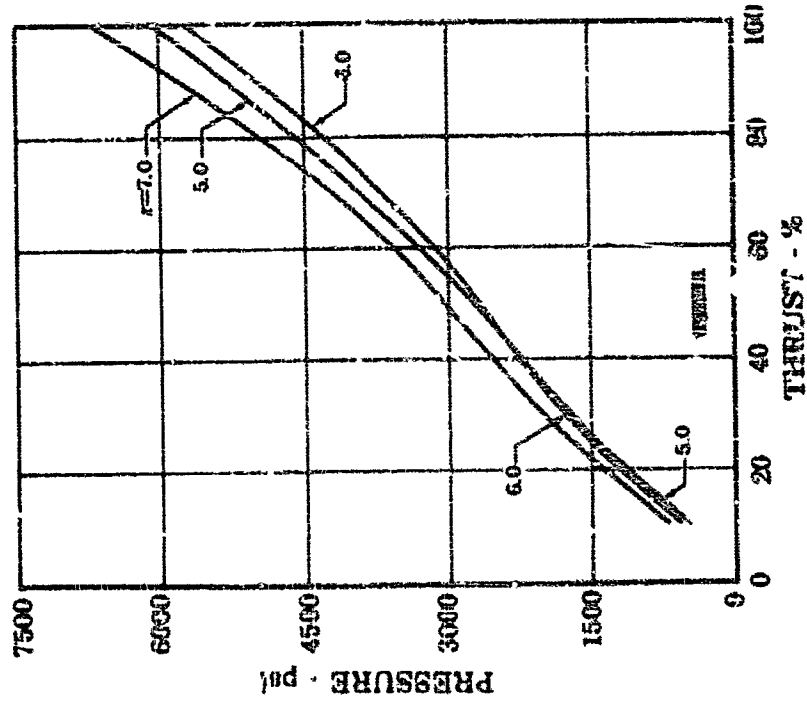
Figure 472. Pintle Dynamic Force vs Percent Thrust

FD 17460



CONFIDENTIAL

CONFIDENTIAL



FD 17462

Figure 475. Inlet Pressure vs Percent Thrust

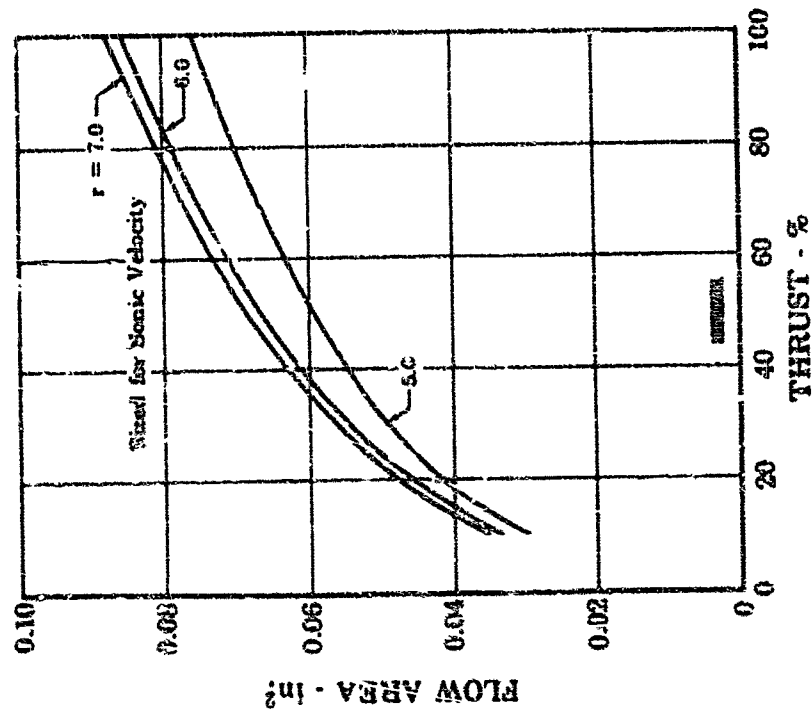
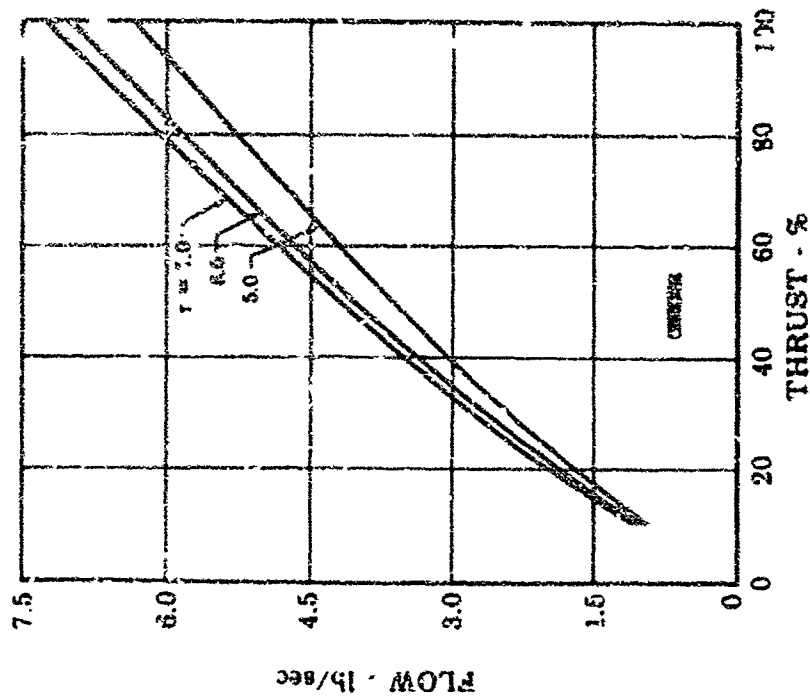


Figure 474. Effective Flow Area vs Percent Thrust

FD 17461

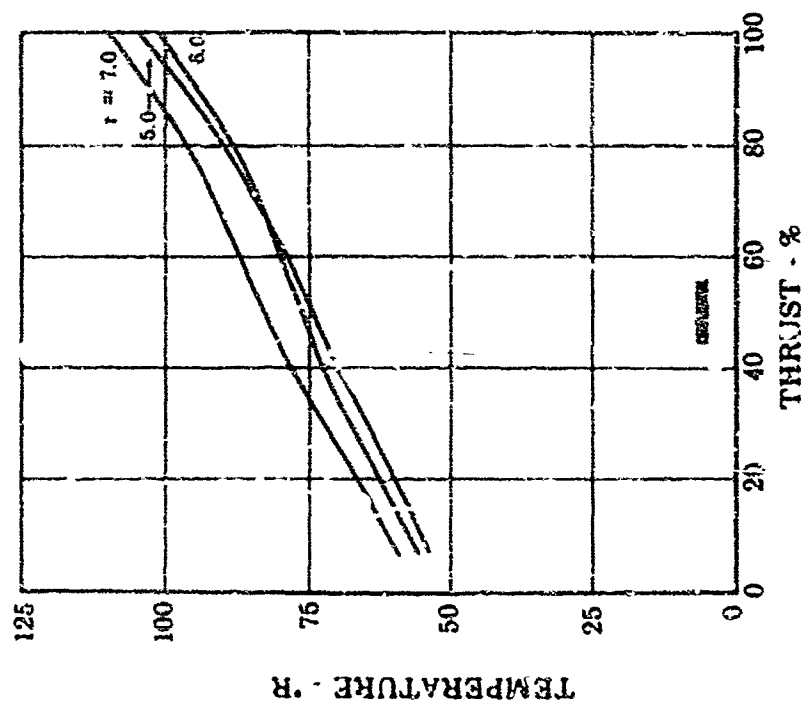
CONFIDENTIAL

CONFIDENTIAL



FD 17487

Figure 477. Flow Rate vs Percent Thrust



FD 17486

Figure 476. Inlet Temperature vs Percent Thrust

CONFIDENTIAL

CONFIDENTIAL

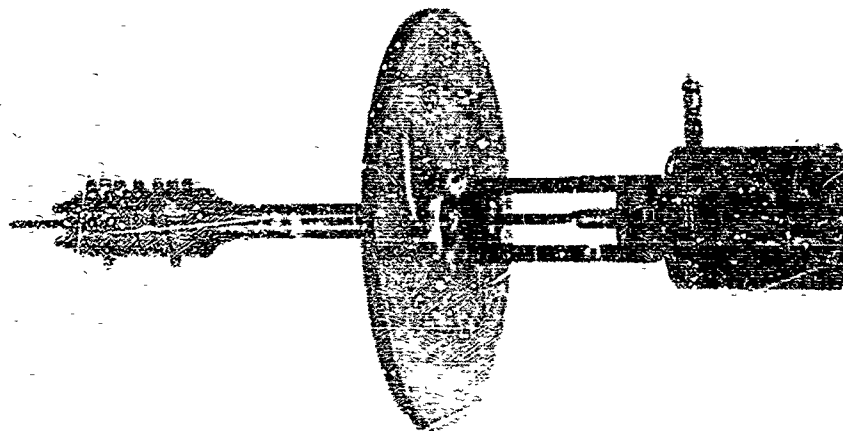


Figure 478. Chamber Coolant Valve Seal Test Rig FE 62470

(B) Three 0.375-inch diameter translating shaft seal test rigs were designed and procured to test six types of seals. The rigs were designed to test two different type seals simultaneously. (1) Antiblowlout omni-seal and Mylar TFE Teflon Lip-Seal, (2) Standard omni-seal and Bal-Seal, (3) Garlock Teflon V-rings and Garlock Chevron packings. Figure 479 is a schematic assembly of the seal test rig illustrating the types of seals tested.

(C) Seal rig materials and dimensional details duplicate chamber coolant valve parts. Figures 480, 491 and 478 show seal test rig parts in exploded detail and assembly.

(D) Two build, test, and inspection cycles were completed on these rigs when the chamber coolant valve was dropped from the program. Further testing of the translating shaft seal test rig was suspended, and the rig parts were stored.

(E) The rigs were mounted on G-6 stand for environmental endurance testing. See figures 482 through 484. Cycle tests were performed at inlet pressures up to 1700 psig GN_2 and 1500 psig GH_4 . Seal leakages were measured at these conditions. Following is a summary of the two tests performed on these rigs.

CONFIDENTIAL

UNCLASSIFIED

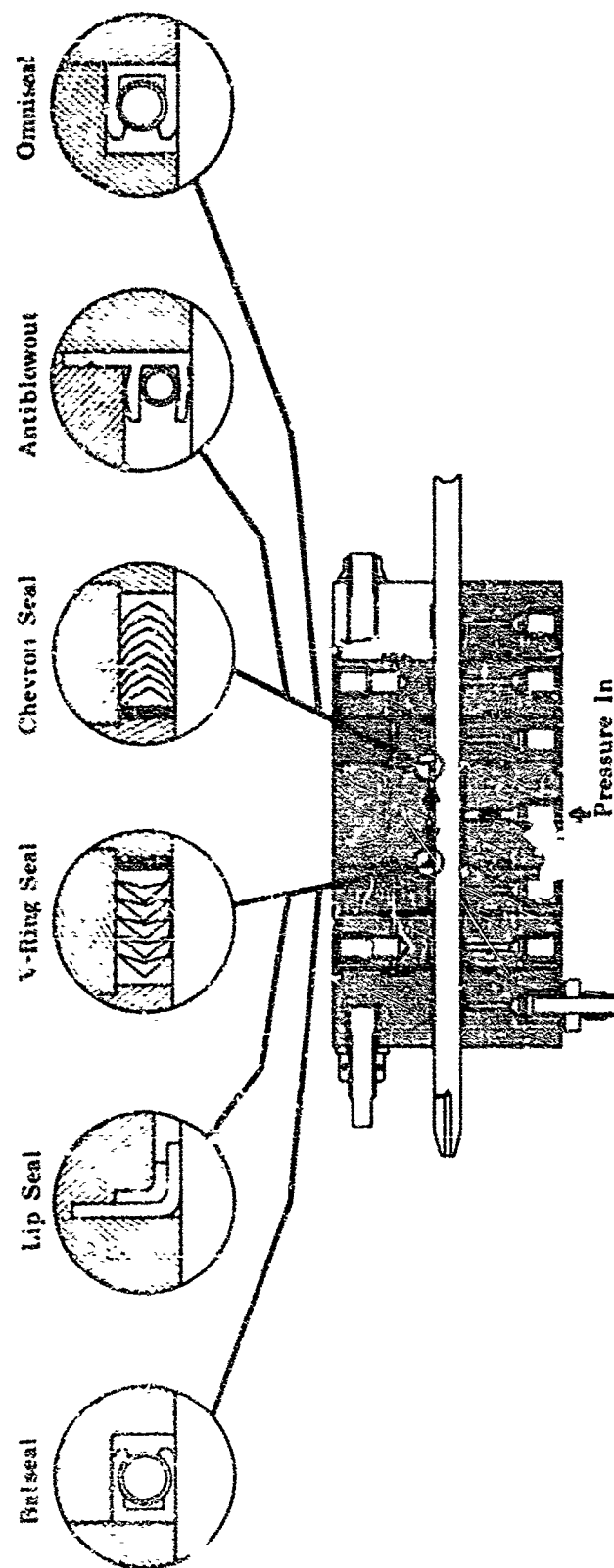


Figure 479. Seal Test Rig Configuration

FD 18107A

UNCLASSIFIED

UNCLASSIFIED

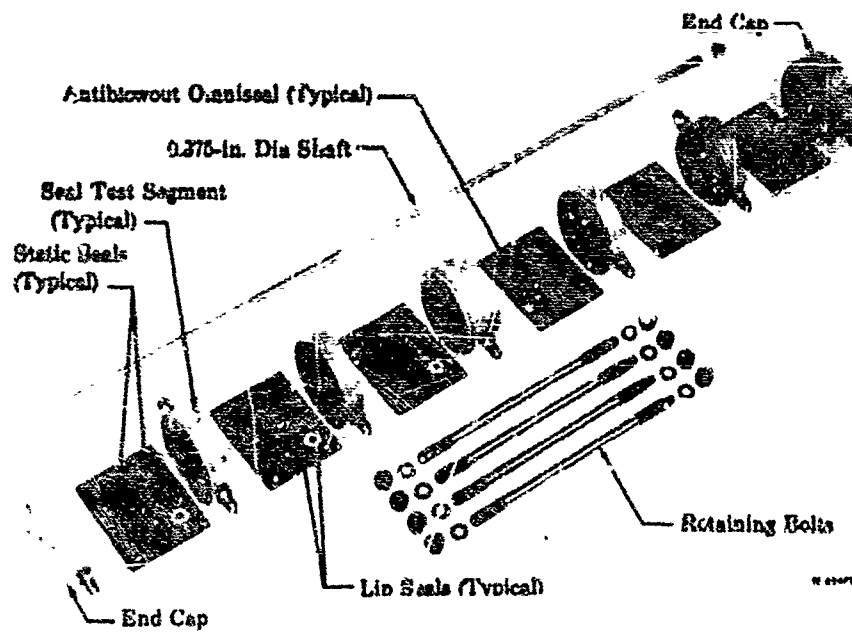


Figure 480. Seal Test Rig Parts

FD 23416

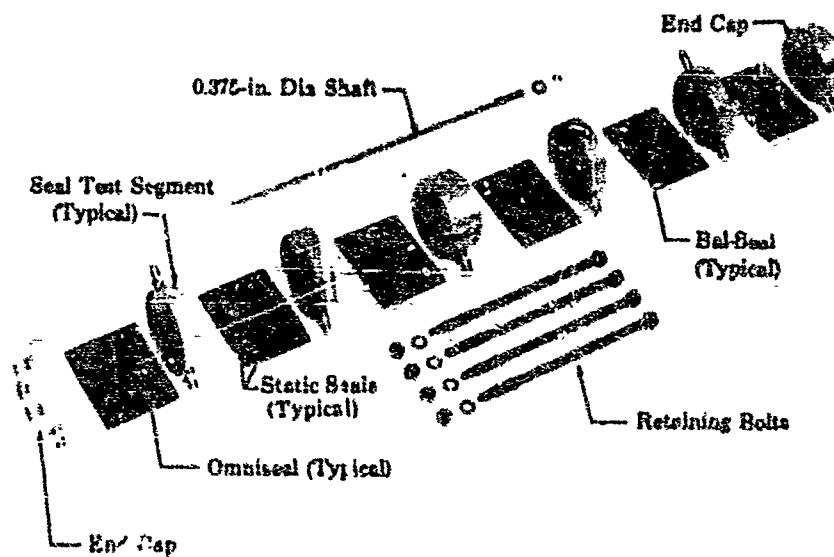


Figure 481. Seal Test Rig Parts

FD 23415

UNCLASSIFIED

CONFIDENTIAL

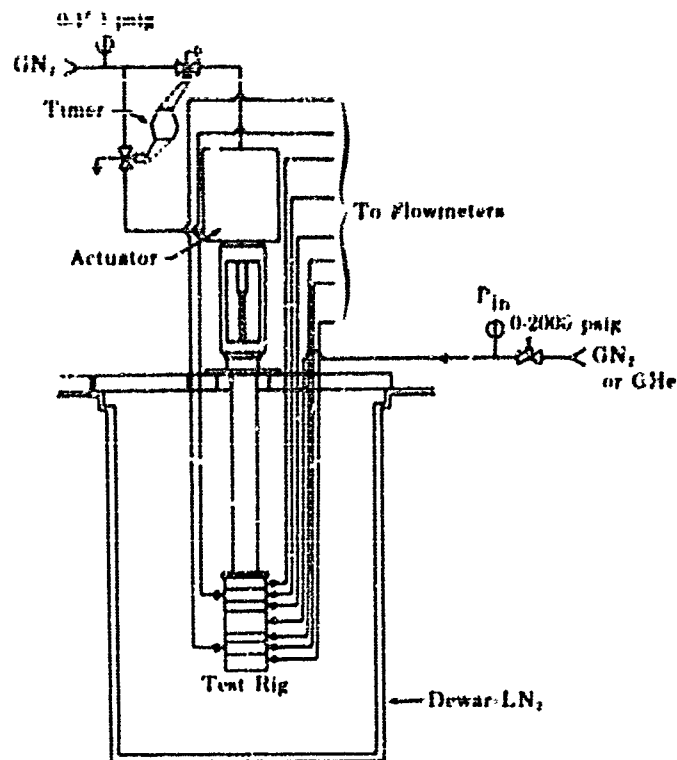


Figure 482. Chamber Coolant Valve Seal
Test Rig Schematic

FD 23081

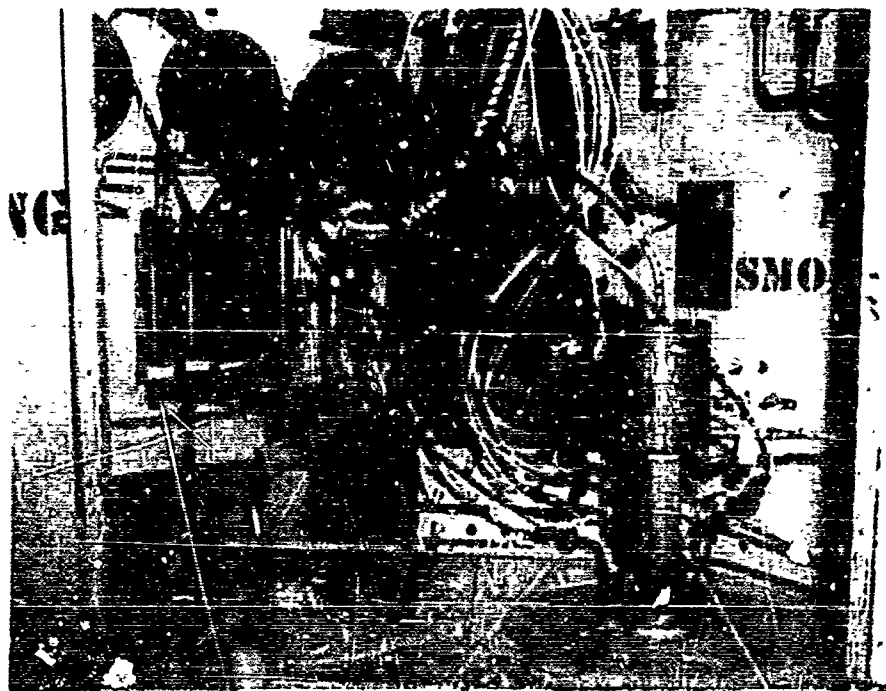


Figure 483. Translating Shaft Seal Rig
Mounted in G-6 Stand

FE 62783

483

CONFIDENTIAL

(This page is Unclassified)

CONFIDENTIAL

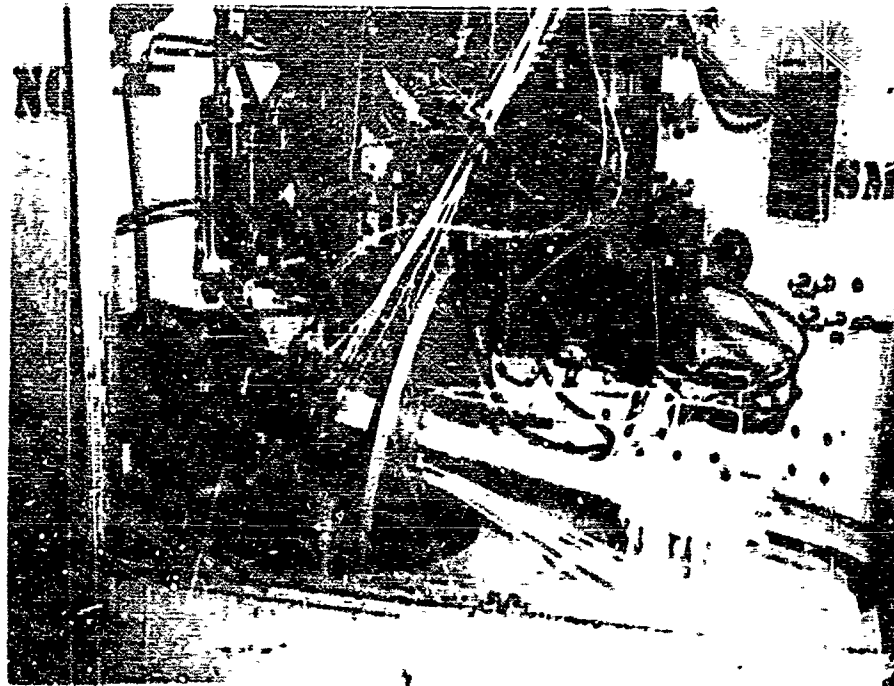


Figure 484. Translating Shaft Seal Rig During Test FE 62784

a. Chamber Coolant Valve Seal Test Rig F-33424 - Build No. 1

(U) This build of the translating shaft seal test rig was to investigate the leakage and endurance of Mylar-TFE Teflon lip seals and antiblowout TFE leflon Omniseals.

(C) The rig was mounted in G-6 Stand and during the test accumulated a total of 604 cycles composed of:

| CH ₄ inlet pressure | Conditions | Cycles |
|--------------------------------|-----------------|------------|
| 0 | Ambient | 2 |
| 0 | Ambient | 24 |
| 0 | LN ₂ | 2 |
| 500 psig | LN ₂ | 101 |
| 1000 psig | LN ₂ | 75 |
| 1500 psig | LN ₂ | <u>400</u> |
| | | 604 |

CONFIDENTIAL

CONFIDENTIAL

(U) The maximum shaft seal leakages during the test were as follows:

| SEAL DESCRIPTION | MAX. GHe LEAKAGE |
|--------------------|------------------|
| Primary Omniseal | 867 acce |
| Secondary Omniseal | 383 acce |
| Primary Lip Seal | 1,833 acce |
| Secondary Lip Seal | 200 acce |

(U) Secondary seal leakages were measured with 100 psig GHe applied to the primary seal vents. The actuator pressure required to move the shaft varied from 3 to 11 psid throughout the test.

(U) After test, disassembly of the rig revealed the following:

1. All lip seals were in good condition - no splitting was detected.
2. All antiblowout seals showed little sign of wear with no splitting on the ID. The vent omniseal was split circumferentially. This was attributed to faulty assembly.
3. Moisture was found in the lip seal segments.

b. Chamber Coolant Valve Seal Test Rig F-33444 - Build No. 1

(U) This build of the translating shaft seal test rig was to investigate the leakage and endurance of TFE Teflon Bal-Seals and TFE Teflon Omniseals.

(U) The test rig incorporated three spring loaded Bal-Seal cup seals on one end, and three similar Omniseals on the other end as shown in figure 481.

(C) The test rig was mounted in the G-6 stand and during the test accumulated a total of 4977 cycles composed of:

| GN ₂ Inlet Pressure | Conditions | Cycles |
|--------------------------------|-----------------|-------------|
| 1500 psig | LN ₂ | 500 |
| 1650 psig | LN ₂ | 3001 |
| 1700 | LN ₂ | <u>1476</u> |
| | | 4977 |

(U) The maximum shaft seal leakages during the test were as follows:

| Seal Description | Max. GN ₂ Leakage |
|--------------------|------------------------------|
| Primary Bal-Seal | 1790 acce |
| Secondary Bal-Seal | 755 acce |
| Primary Omniseal | 1180 acce |
| Secondary | 614 |

CONFIDENTIAL

(U) The above secondary seal leakages were measured with 100 psig GN_2 applied to the primary seal vents. The actuator pressure required to move the rig shaft varied from 4.0 to 6.6 psig throughout the run.

(U) Following test, disassembly of the rig revealed the following:

1. All shaft seals indicated slight ID wear, however no splitting was detected.
2. No moisture was found in the rig.

4. Summary and Conclusions

(U) The main thrust chamber coolant control valve was required to regulate the fuel flow for transpiration cooling. The valve-type selection study resulted in a variable-area venturi valve being selected for design, procurement, and test. The valve was to be located at the fuel pump discharge and to be choked or cavitated throughout the engine operating range. A commercial translating hydraulic servomotor was adapted to the valve and two valve assemblies were placed on order.

(U) A translating shaft seal test rig was designed and parts for testing six types of 0.375-inch diameter shaft seals were procured. The shaft seal rig was intended to evaluate the types of seals applicable to the chamber coolant valve shaft seal package design. Two rig builds were completed and four types of seals were tested as summarized in table XLIII.

(U) Chamber coolant valve procurement and translating shaft seal testing were discontinued when the program scope was changed. All outstanding orders were canceled and parts on hand were stored for possible future use.

(U) The limited amount of data accumulated during the translating shaft seal testing was not sufficient to draw any definite conclusions except that the shaft seal design approach was practical.

F. ELECTRICAL IGNITION SYSTEMS

1. Hardware Description

a. General

(U) Ignition for the preburner chamber and the main chamber was provided by a hydrogen-cooled, continuous-burning, oxygen-hydrogen torch in each chamber. These torch igniters provided a flame to ignite the propellant mixtures in the respective combustion chambers. The ignition system was designed to operate either at sea level or in a vacuum, and was capable of multiple relights. The flame from each torch was spark ignited prior to propellant flow from the injector to prevent excessive propellant accumulation inside the combustion chamber.

CONFIDENTIAL

(C) Table XLIII. Translating Seal Test Rig

| Build No. | Features | Configuration | Seal Description | Cryogenic Test Results | | Remarks |
|-----------|--|---------------------------------|---------------------------------------|------------------------|-------------------------|---|
| | | | | Leakage Range, SCCS | Cycles | |
| 33424-1 | 1. Rig was designed to test two types of seals simultaneously. | Vent Secondary Primary | TFE Teflon Antiblowout Omniseal | 333 867 | 604 Shaft Cycles | 1. During the test inlet pressure was varied from 500 to 1500 psig GHe. |
| | 2. Pacific actuator was used to translate the rig shaft. | Primary Secondary Vent | Mylar - TFE Teflon Lip-Seal | 1833 200 | | |
| 33444-1 | 1. Rig was designed to test two types of seals simultaneously. | Vent Secondary Primary | TFE Teflon Omniseals | 614 1180 | 4977 Shaft Cycles | 1. During test inlet pressure was 1500-1700 psig (N ₂). |
| | 2. Pacific actuator was used to translate the rig shaft. | Primary Secondary Primary | TFE Teflon Bal-Seals | 1790 755 | | |

487

CONFIDENTIAL

CONFIDENTIAL

(U) Each torch igniter had provisions for two separate spark ignition systems to increase the reliability of the ignition system. Each spark plug was energized by a hermetically sealed exciter that converts the 28-vdc input to a minimum of 20 high-voltage (30 kv) sparks per second output at a nominal stored energy level of 0.5-joule per spark. An electrical schematic of the exciter is shown in figure 485.

b. Mechanical Description

(1) Preburner Igniter Assembly

(U) The preburner igniter assembly shown in figure 486 was bolted to the preburner combustion chamber housing. The assembly consists of two spark ignition systems, an igniter chamber liner, and a mounting flange. Figure 487 shows a preburner ignition system.

(U) The Inconel 718 spark plug housings were brazed to the igniter assembly flange as shown in figure 488. The torch igniter is a welded assembly consisting of the throat section, chamber section, and head section. The spark plug housings were brazed into the head section. An expansion joint sleeve was welded to the chamber liner throat section to provide structural support. A labyrinth seal, shown in figure 488, was located in the expansion sleeve to minimize coolant flow leakage between the igniter combustion chamber and the preburner combustion chamber housing.

(U) The oxidizer was injected into the igniter combustion chamber through a single orifice element. The fuel filled the cavity between the chamber liner and igniter assembly flange and was introduced into the chamber through an orifice that was concentric to the oxidizer element. A portion of the fuel flow was used as coolant for the igniter chamber liner and discharges into the preburner combustion chamber between the stability liner and the cooling liner as shown in figure 489.

(U) Three seal vents were provided; one for the O-ring seal between the igniter assembly flange and the preburner combustion chamber housing, and one each for the O-ring seal between the sparkplug housing and each spark plug.

(U) The preburner igniter spark plug, shown in figure 490, consisted of an outer housing of Inconel, ceramic insulator, and a nickel electrode. A mechanical joint at the end of the spark plug joined the plug to the spark exciter high tension lead. The entire spark ignition assembly is weld-and solder-sealed and inert-gas-pressurized to prevent arcing.

(2) Main Burner Igniter

(U) The main burner igniter, shown in figure 491, consists of a combustion chamber, two spark plugs, and a propellant supply probe. Figure 492 shows a main burner electrical ignition system secured to a handling bracket.

CONFIDENTIAL

(This page is Unclassified)

UNCLASSIFIED

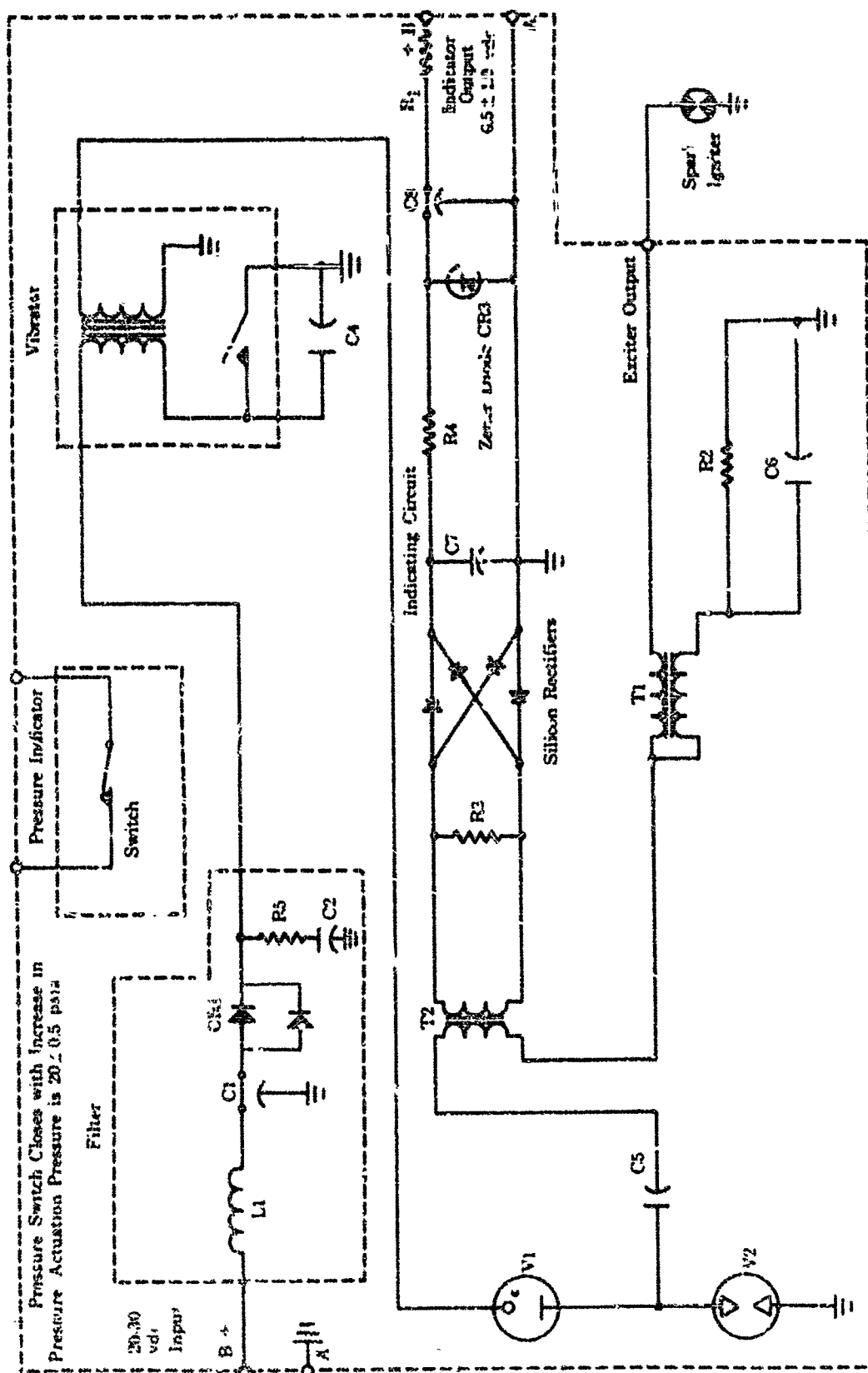


Figure 495. Ignition System Schematic.

FD 3154C

489

UNCLASSIFIED

UNCLASSIFIED

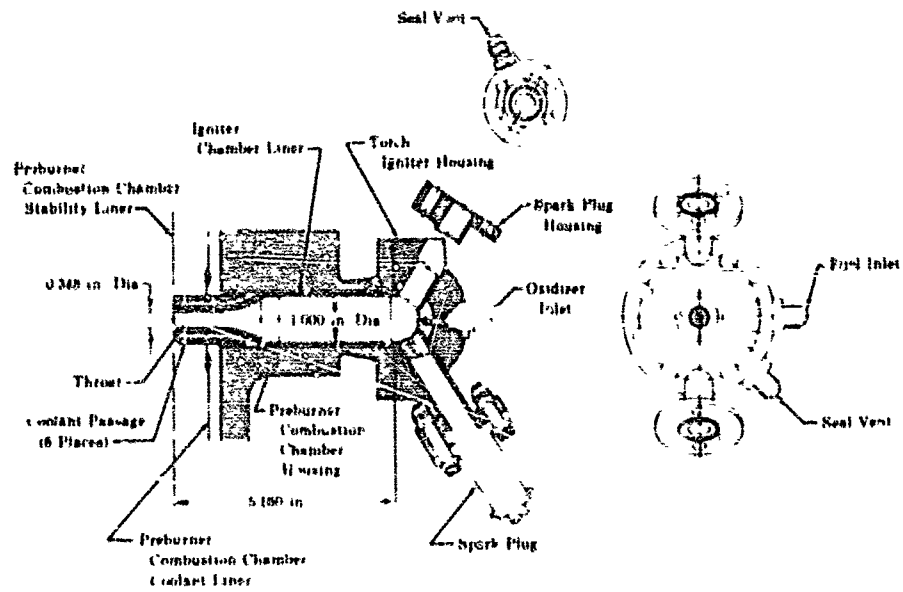


Figure 486. Preburner Igniter Assembly

FD 19590

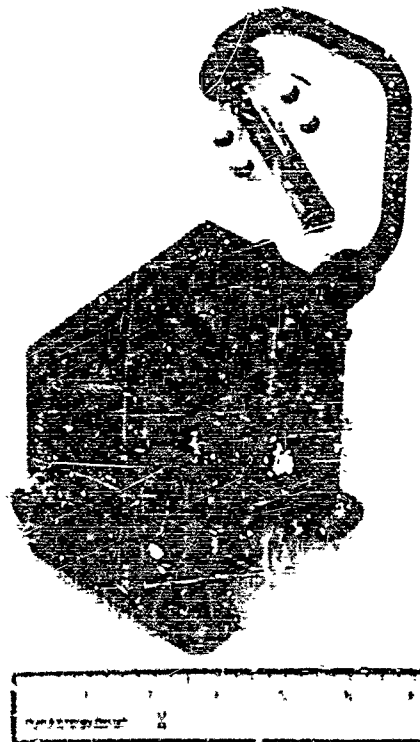


Figure 487. Preburner Igniter Assembly

FE 67911

UNCLASSIFIED

UNCLASSIFIED

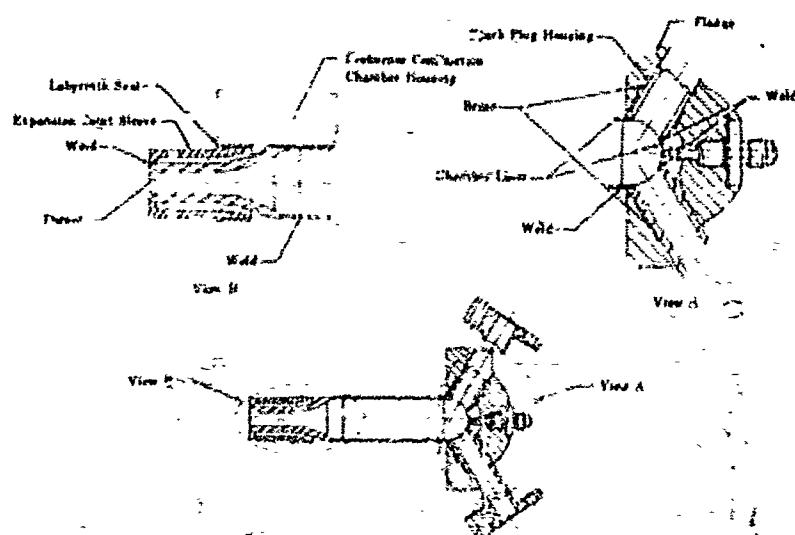


Figure 488. Details of Preburner Igniter Assembly

FIG 19679

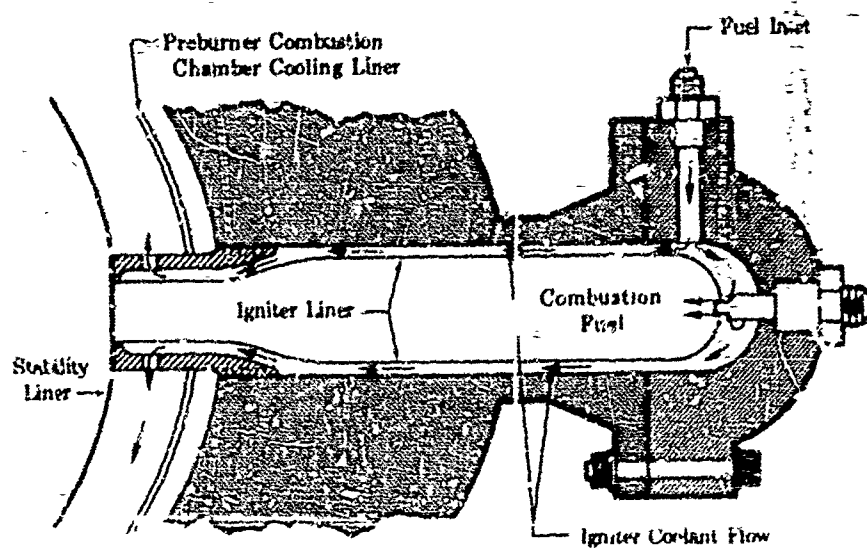


Figure 489. Preburner Igniter Cooling Flow Schematic

FIG 19689

UNCLASSIFIED

UNCLASSIFIED

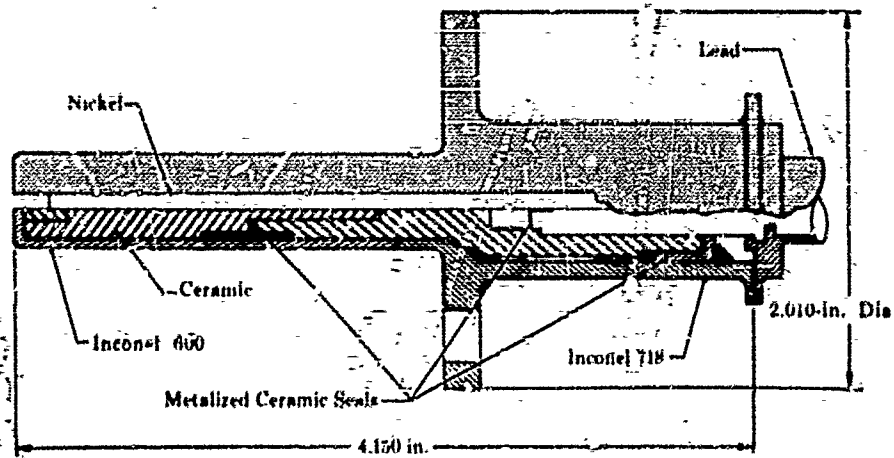


Figure 490. Preburner Igniter Spark Plug FD 19691

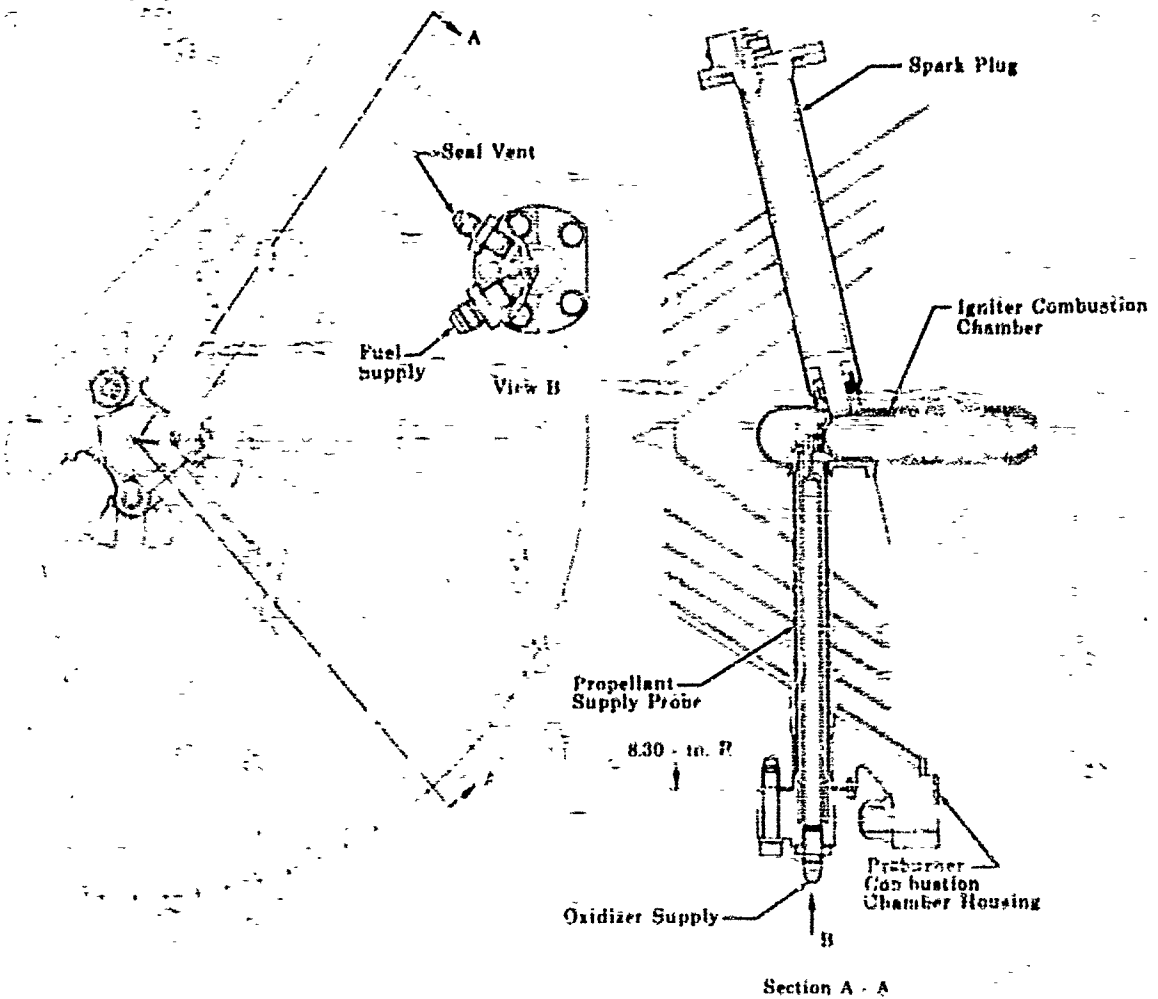


Figure 491. Main Chamber Igniter Assembly

FD 15986

UNCLASSIFIED

UNCLASSIFIED

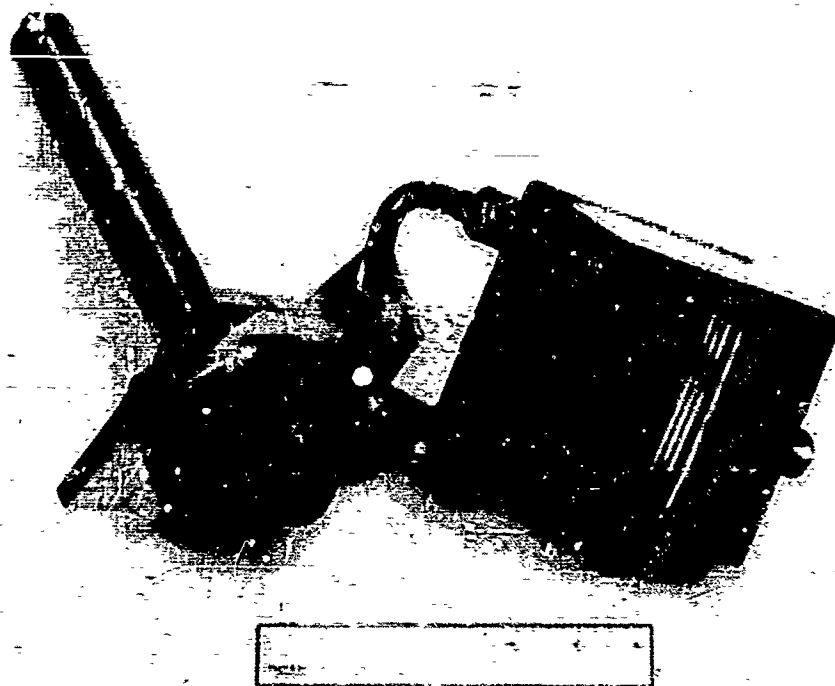


Figure 492. Main Chamber Igniter Assembly

FE 68314

(U) The combustion chamber is located centrally in the main injector and discharges along the engine thrust axis to prevent impingement on the main chamber walls. The combustion chamber is a welded and brazed assembly of Inconel 625 and is bolted to the main injector as shown in figure 493. The igniter combustion chamber housing has four tangs to assure proper alignment of the combustion chamber with the main injector for insertion of the spark plug and propellant supply probe.

(U) The two spark plugs and the propellant supply probe are inserted into the igniter combustion chamber and bolted to the preburner combustion chamber housing.

(U) The main igniter spark plug, shown in figure 494, consists of a housing of Inconel and stainless steel, ceramic and Teflon insulator, and a nickel and copper electrode. Metalized ceramic seals are located at the aft end of the spark plug. Spark plug cooling flow is taken from the preburner combustion chamber cooling liner. Teflon coated metal O-rings, with inter-seal vent, are located between the spark plug flange and the preburner combustion chamber housing. A piston ring seal is provided at the spark plug and igniter chamber joint to prevent excess hydrogen coolant flow into the combustion chamber.

UNCLASSIFIED

UNCLASSIFIED

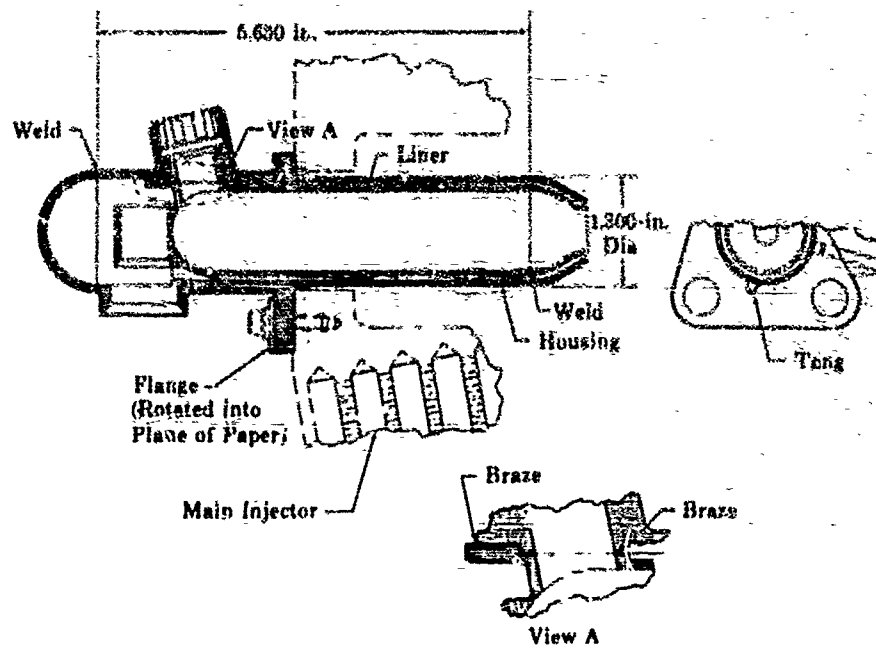


Figure 493. Igniter Combustion Chamber

FD 19680

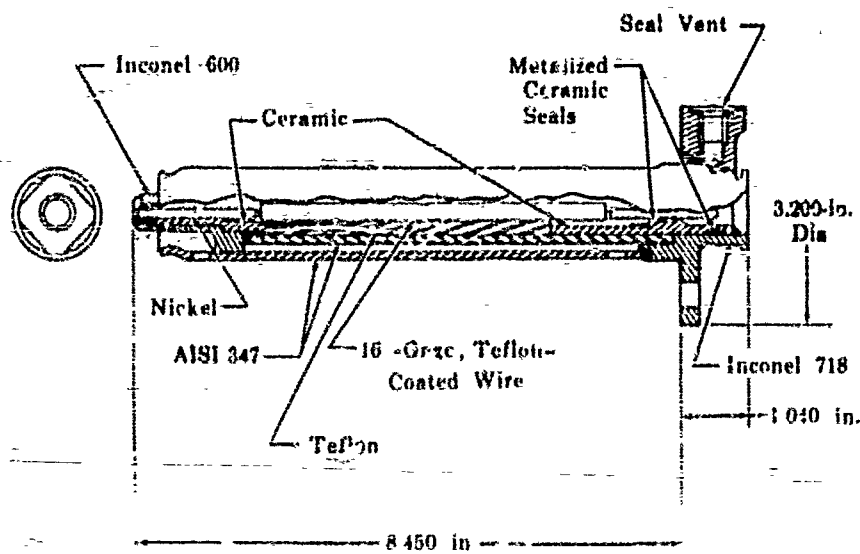


Figure 494. Main Chamber Igniter Spark Plug

FD 19690

UNCLASSIFIED

UNCLASSIFIED

c. Summary and Conclusions

(U) The ground rules established for the 250K engine ignition systems permitted the use of developed RL10 engine high tension spark exciters for ignition power. Spark plugs and igniter chambers were new designs for this program. The preburner and main chamber ignition systems were similar in that both incorporated continuous burning torch type igniters with separate propellant supplies and provisions for dual electrical exciter and spark plug system.

(U) One complete set of electrical ignition systems was procured for both the preburner and main burner, along with four spare plugs for each. No development or life testing was performed on the electrical ignition systems other than the acceptance calibration tests and check firing tests when units were returned from the rig. The electrical exciter and plug systems performed satisfactorily during all rig and staged combustion tests with no problems. Both of the preburner units were used (separately) for full-stage rig firing tests. One of the main burner units was used for all of the main chamber firings.

(U) The electrical ignition systems utilized in this phase of the high pressure engine program did not introduce any development problems. Ignition system performance was satisfactory throughout all firing tests during this program.

495/496

UNCLASSIFIED

SECTION IX
PREBURNER DEMONSTRATION

| | |
|------------------------------------|-----|
| A. Introduction | 497 |
| B. Summary and Conclusions | 500 |
| C. Hardware Description | 504 |
| D. Testing | 529 |
| 1. Facility Checkout | 529 |
| 2. Preburner Torch Igniter Testing | 531 |
| 3. Preburner Testing | 537 |
| E. Facilities and Procedures | 599 |

CONFIDENTIAL

SECTION IX PREBURNER DEMONSTRATION

A. INTRODUCTION

(U) The preburner demonstration program was directed toward the selection, fabrication, and demonstration testing of a preburner injector and combustion system that could be used in the 250K engine. The development schedule of this preburner program required that it be completed prior to incorporation of the preburner injector and combustion chamber into the staged-combustion system for the final performance evaluation. In addition to checking the preburner injector, these early tests developed a satisfactory ignition and start sequence for all preburner and staged-combustion testing and checked out the new high pressure facility. Approximately 80 nonfiring tests and 36 firing tests were conducted in checking the new high pressure facility. These tests established a start sequence and facility control system that provided accurate and repeatable control of the start and acceleration transients. The performance evaluation of the preburner combustion system was conducted in a series of 36 tests prior to the staged-combustion testing. Figure 495 exhibits the milestones of the preburner program.

(C) The preburner injector uses pump-fed propellants that are metered at an approximate mixture ratio of 6.9 and burned in the preburner combustion chamber. The hot gases from the preburner combustion chamber are divided and flowed through the oxidizer and fuel pump turbines prior to being discharged into the main combustion chamber through the main injector. This propellant flow is illustrated in figure 496. Because the preburner gases are used to drive the fuel and oxidizer turbines, this combustion system must be efficient while providing an acceptable temperature profile to permit operating the turbine at the maximum allowable temperature. The selection of the preburner injector was based on the requirements to provide stable and efficient combustion with an acceptable temperature profile over the 20% to 100% operation range. The preburner injector configuration chosen was a dual-orifice oxidizer and variable-area fuel configuration, as shown in figure 497. The combustion chamber selected for use in this test program duplicated the configuration proposed for the 250K engine. The test rig included engine-type cooling and stability liners with added provisions for pulsing the combustion system and measuring the temperature profile, which are shown in figure 498.

(C) The entire preburner test program was devoted to the development of a satisfactory start and ignition sequence and the investigation of the temperature profile at 20%, 50%, and 100% flow conditions. In addition, the combustion system was pulsed at the 20% and 100% levels to demonstrate the dynamic stability of the system.

CONFIDENTIAL

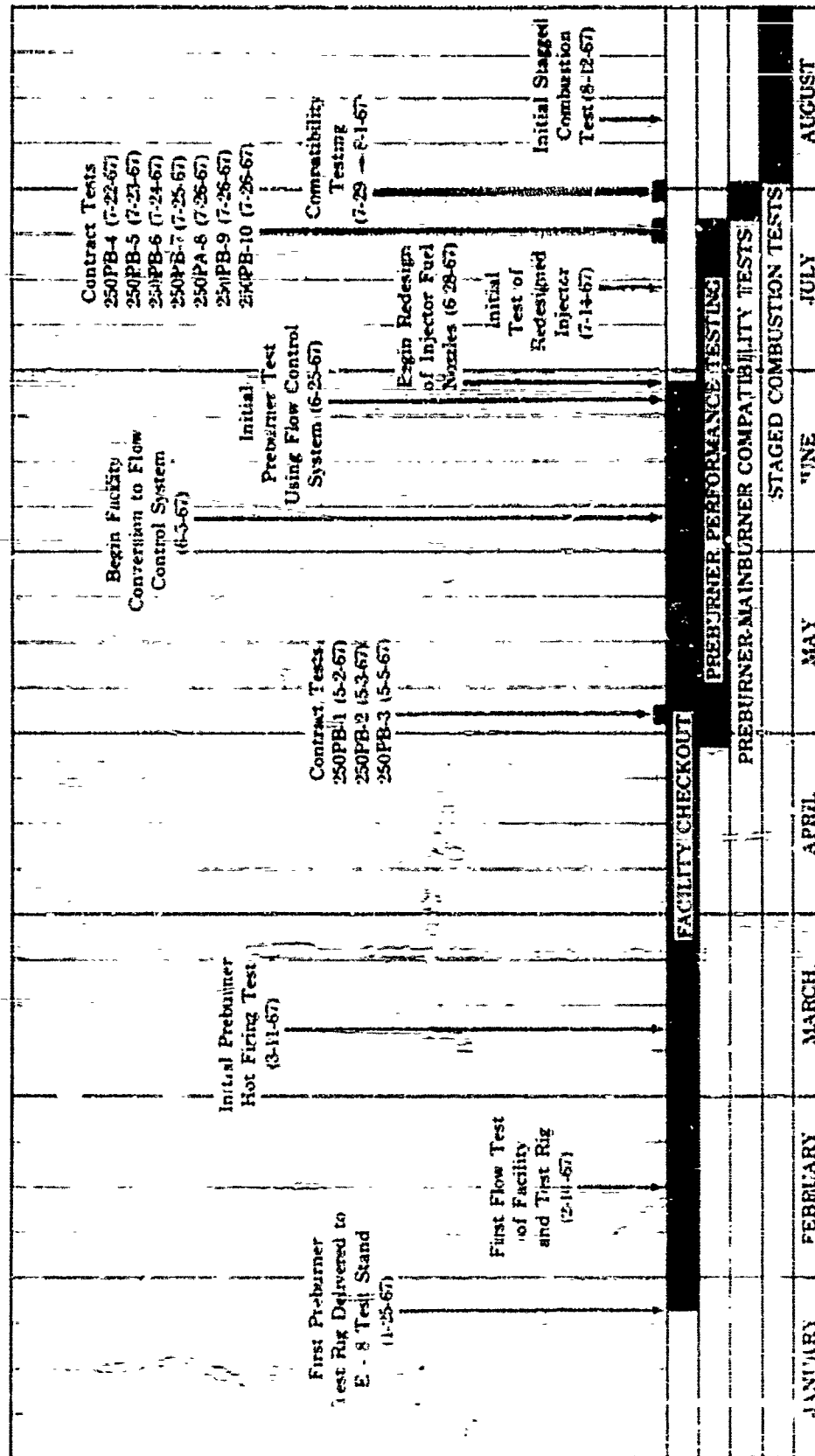


Figure 495. 250K Preburner Test Rig Milestones - 1967

FD 23040

CONFIDENTIAL

(This page is Unclassified)

CONFIDENTIAL

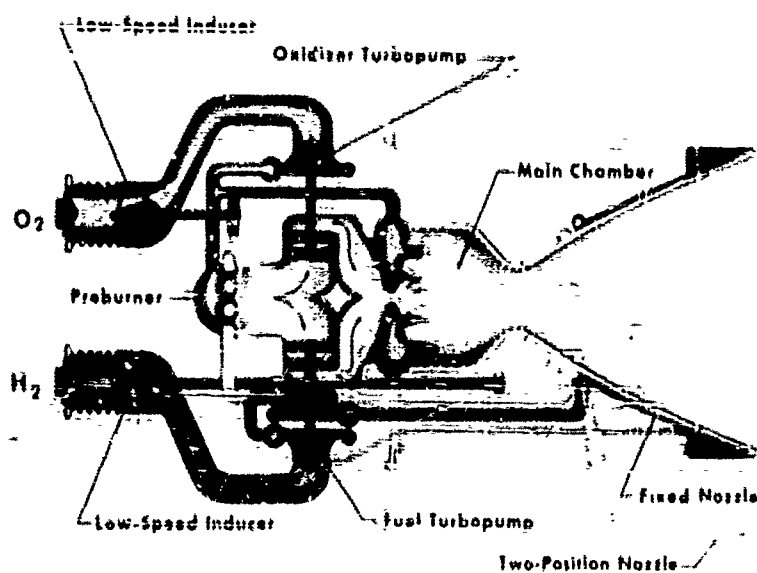
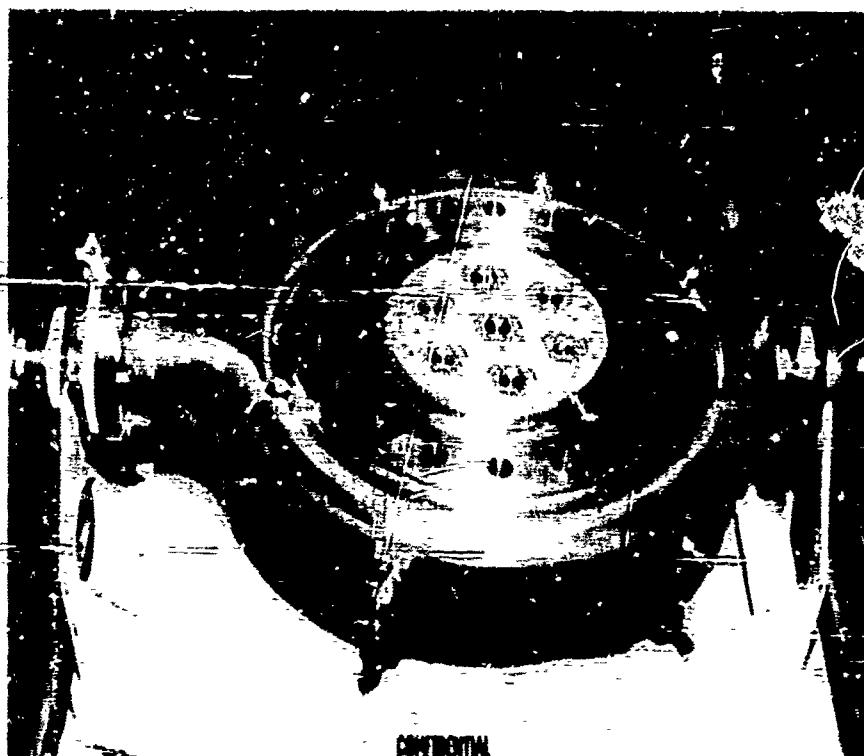


Figure 596. Propellant Flow Schematic

FD 21602



CONFIDENTIAL

Figure 597. Preburner Injector Final Configuration

FF 59801

CONFIDENTIAL

CONFIDENTIAL

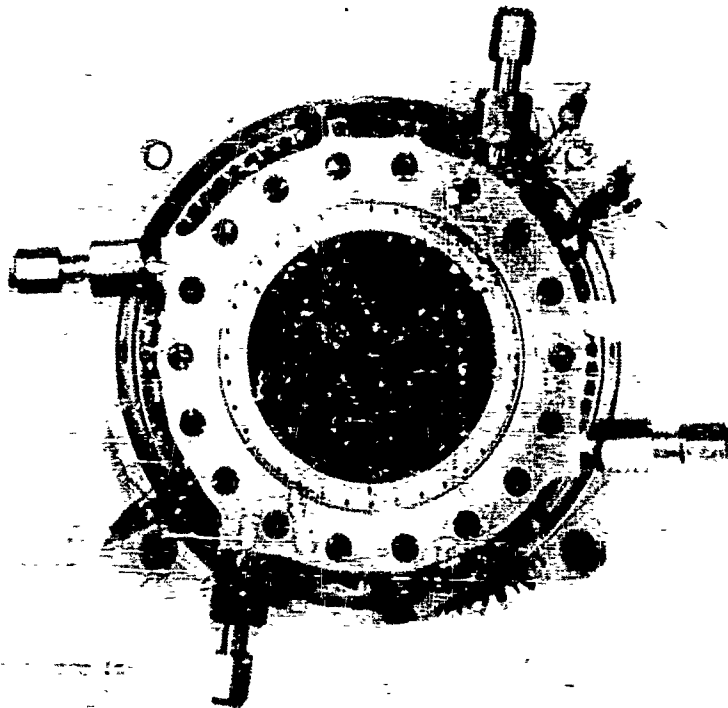


Figure 498. Preburner Instrumentation Installation FL 69220

B. SUMMARY AND CONCLUSIONS

(C) During the test program, the preburner was operated in 22 preburner test rig firings and 12 three-combustion tests. Stable preburner operation was demonstrated from approximately 100 to 1000 g rated flow. Pressure levels were limited to 3600 psia of the required 5000 psia because of an inadequate dome flange.

(C) The most significant achievements of the preburner test program were the resolution of test stand control issues and the development of a preburner injector that provided a stable preburner operation for the three-combustion tests. The injector configuration did not provide a satisfactory temperature profile. Modification of the fuel element produced a temperature profile that approximated the R. at a rated temperature of 2000 K, 11.4% O₂, and 10% water vapor.

500
CONFIDENTIAL

CONFIDENTIAL

staged-combustion testing. Further development is necessary to provide a temperature profile of 150°R or less at an average temperature of 2325°R which is required for the demonstrator engine.

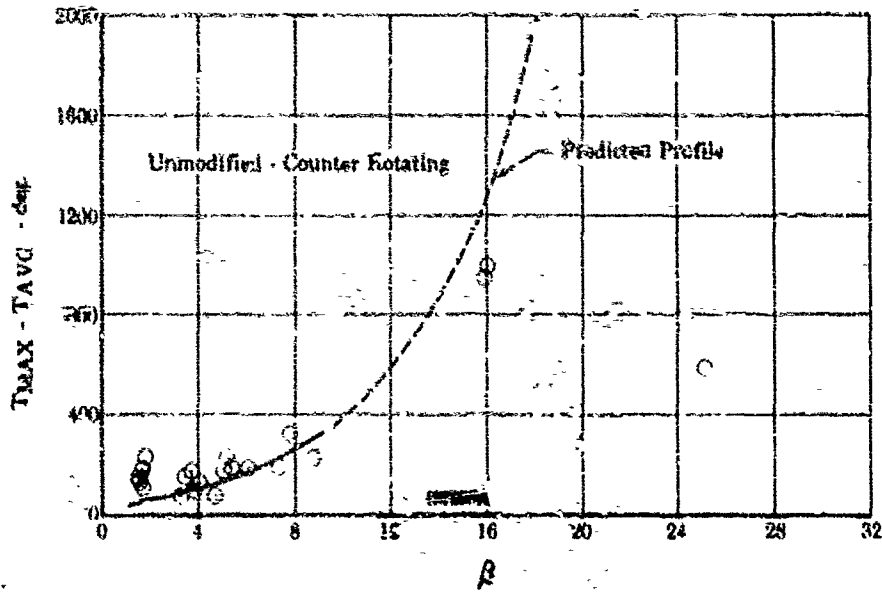


Figure 499. Fuel Element Temperature Profile FD 23450

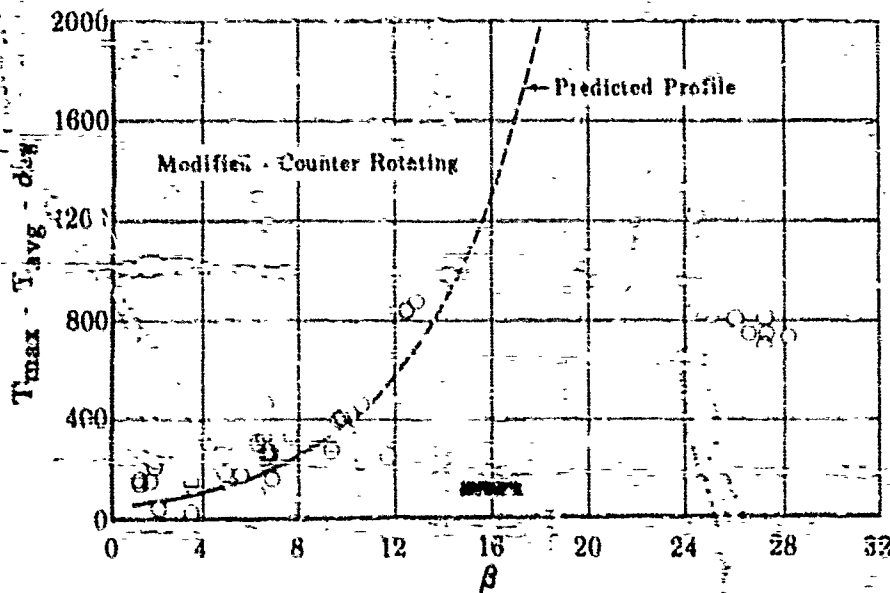


Figure 499. Fuel Element Temperature Profile - FD 23451
Continued

561

CONFIDENTIAL

CONFIDENTIAL

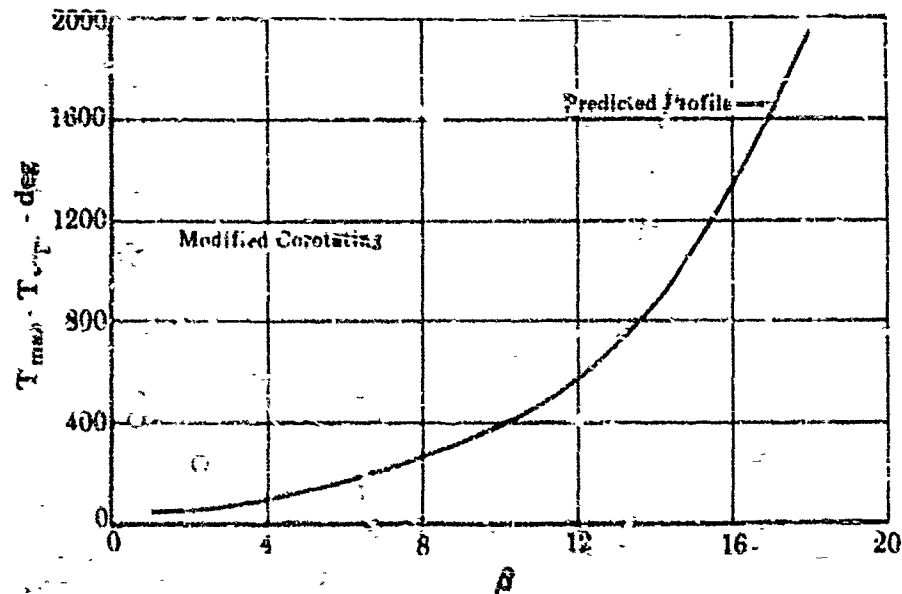


Figure 499. Fuel Element Temperature Profile - FD 23452
Concluded

(C) The pulsing tests conducted on the preburner demonstrated the dynamic stability of the combustion system at the extreme operating conditions. Pulsing the rig at the 20% operating level, with fuel at 118°R supplied to the injector, caused an instantaneous 40% overpressurization that was damped to within 0.5% of nominal operating pressure within 5 milliseconds.

(b) Using the torch igniter with electrical excitation, preburner ignition was demonstrated to be smooth, repeatable, and reliable. The close-coupled injector oxidizer shutoff feature, which was incorporated in the flow divider valve to minimize the injector volume, did eliminate the starting temperature spike associated with the transition from gaseous to liquid oxygen.

(C) Thirty-six successful preburner tests were conducted accumulating 1082 seconds of run time. As shown in the comparison between figures 497 and 500, the final injector configuration shows no deterioration after 21 tests and 421 seconds of hot firing time (run No. 51 to 72). Included in these tests was preburner operation to the 10% level in five separate tests. The component showed no effect of the testing except for slight discoloration on the center element fuel zone plate. The only critical period for the preburner injector was found to be on shutdown. When the final oxidizer purge system was employed, no further injector deterioration was detected.

(U) The preburner combustion chamber deterioration during the 10% tests was restricted to the temperature rakes and the uncooled stability liner. The stability liner showed erosion after testing with the intermediate injector, as shown in figure 501. The temperature profile distortion

CONFIDENTIAL

CONFIDENTIAL

with this injector configuration resulted in a high temperature at the walls in the area between elements, as shown in figure 502. Otherwise, the original cooling liners were used throughout the program, and the combustion chamber housings show no effects of testing.

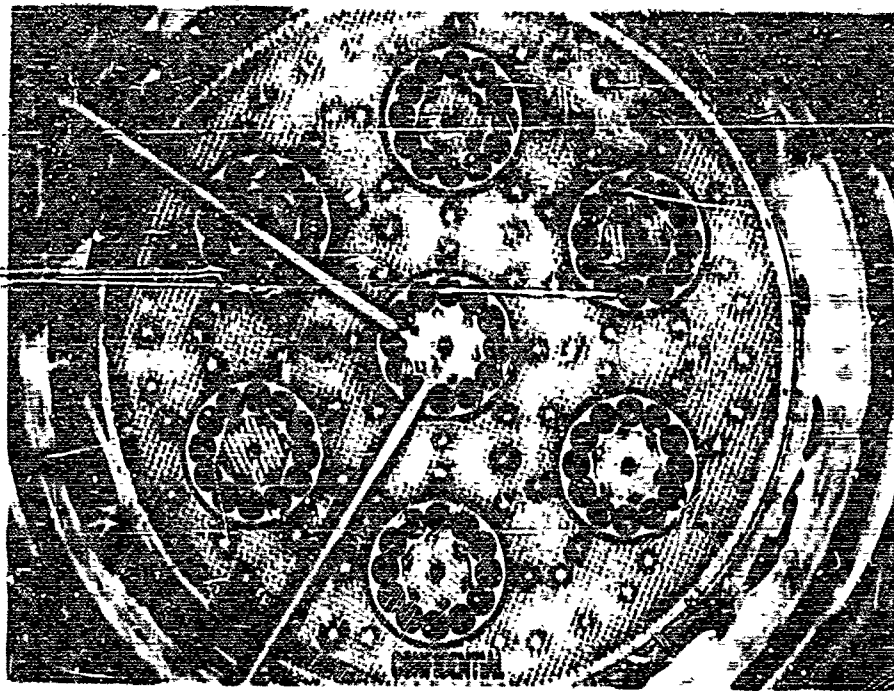


Figure 500. Preburner Injector Configuration
After Testing

FE 71079

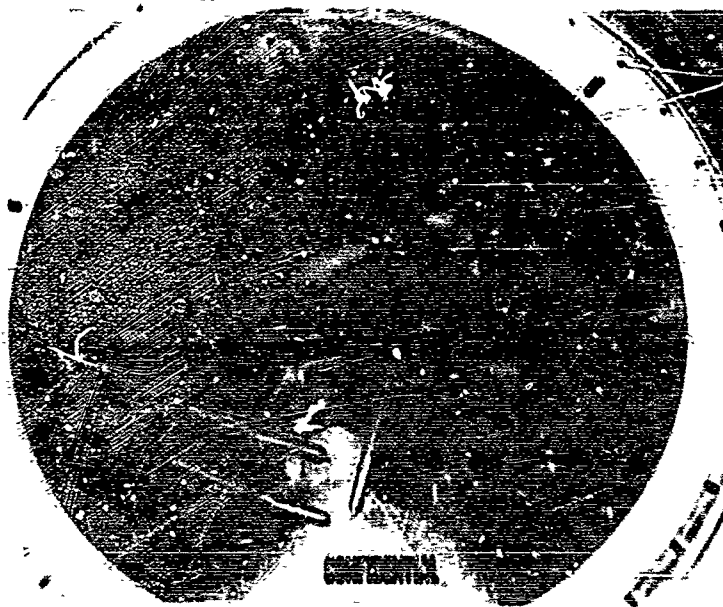


Figure 501. Stability Liner Showing Erosion
After Testing With Intermediate
Injector

FE 70913

503
CONFIDENTIAL

CONFIDENTIAL

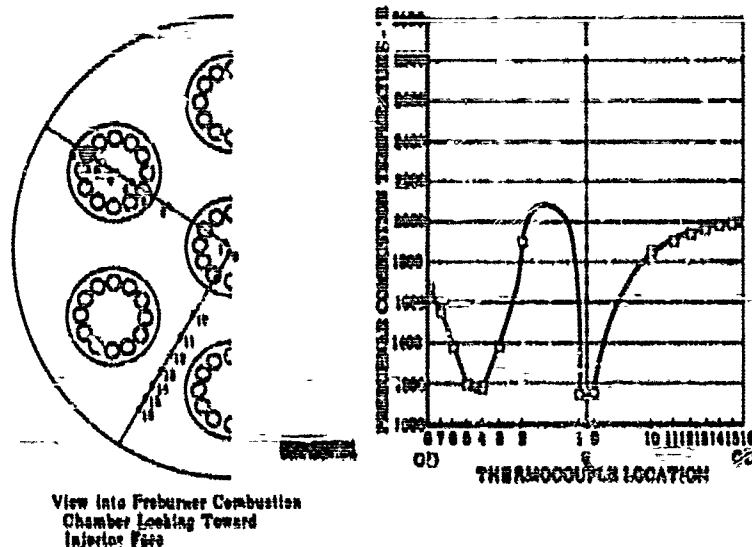


Figure 502. Temperature Profile for Tent No. 51 FD 23042

(U) The preburner torch igniters accumulated more than 250 firing tests, including rig tests, preburner prerun check firings, and preburner tests. This design has demonstrated excellent ignition characteristics because first spark ignition was achieved on all tests, except for limit survey rig tests and preburner tests, when the GN₂ purge contaminated the igniter oxidizer supply because of a faulty facility check valve. No deterioration of the igniter housing or electrical components was detected.

G. HARDWARE DESCRIPTION

(U) The design of the hardware for the preburner program was based on the requirement to provide a preburner injector and combustion system that would be used in a 250K high pressure demonstrator engine. The early portion of the program was directed toward the selection of an injector configuration and combustion system. The selected configuration was then designed, fabricated, and tested.

(C) An analytical study of the dual-orifice oxidizer injector and the variable-area fuel preburner injector was conducted to establish the operating characteristics during ignition, starting, throttling, and steady-state operation. (A detailed discussion of the ignition and start analysis phases of this study is presented in Section IV.) The study showed that a close-coupled oxidizer shutoff, which minimizes the injector volume, reduced the starting time and the phase change that occurred during the filling and start cycle. This close-coupled shutoff feature was easily incorporated in the flow divider valve for the dual-orifice injector. The analytical design study of the preburner starting requirements indicated that the volume of the oxidizer primary and secondary flow passages must be reduced to a minimum to reduce (1) the fill time, and (2) the probability of turbine overheating at start. The volume of the primary passage was held to 3.8 in³. The primary flow to the 7 elements was supplied from the flow divider valve through 15 flow passages, as shown

CONFIDENTIAL

CONFIDENTIAL

in Figure 503. The predicted pressure loss in these passages was 60 psi at the 100% flow condition. The volume of the secondary flow passage was maintained at 36.4 in³. This secondary volume was somewhat larger than desired and resulted in some increases in the fill time, but did not cause an excessive temperature during start. The secondary flow to the seven elements was supplied from the 2" side valve through six passages, as shown in Figure 504. The predicted pressure loss for these passages was 70 psi at 100% flow condition. Pressure taps were incorporated into the injector design to permit measuring the primary and secondary passage pressure separately during test. The dual-orifice injector provides a system with good stability margin at the 20% throttle point as well as the 100% operating point, in addition to providing adequate stability margin at the starting levels.

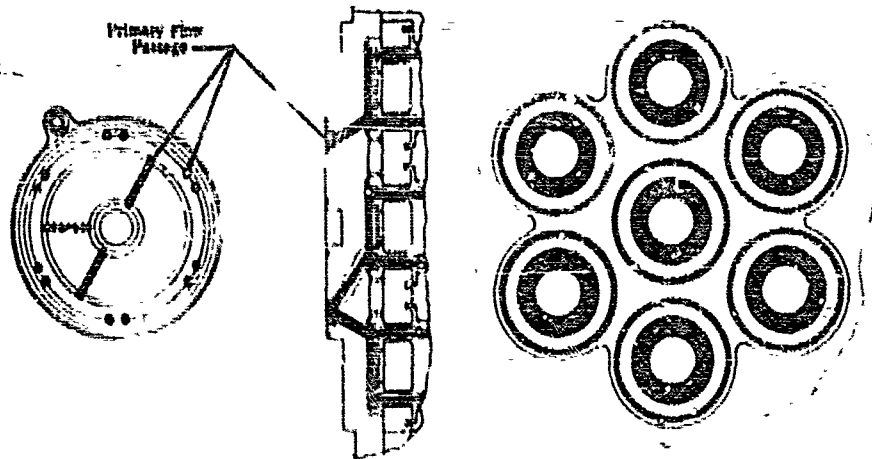


Figure 503. Primary Manifold Configuration

FD 18110A

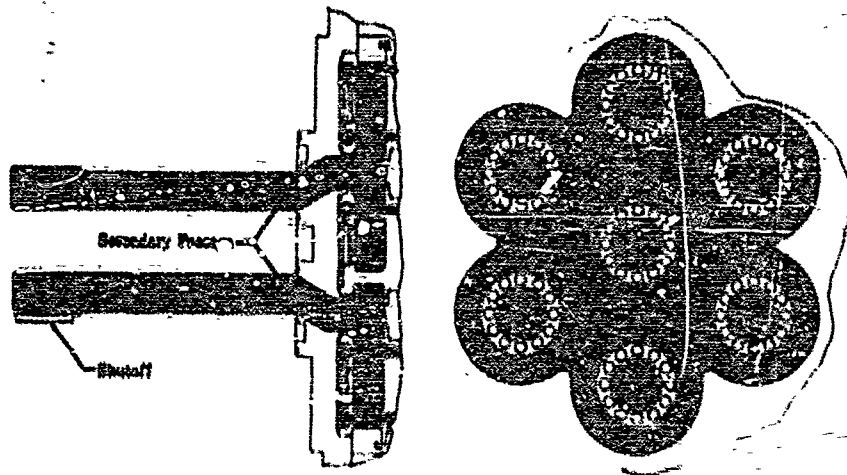


Figure 504. Cross Section of Secondary Manifold

FD 18109

CONFIDENTIAL

THIS PAGE CONTAINS SUBJECT MATTER COVERED BY A SECRET
ORDER WITH A MODIFIED "SECURITY REQUIREMENTS PERMIT"
ISSUED BY U.S. COMMISSIONER OF PATENTS.

CONFIDENTIAL

(C) A study of the effect of primary-to-secondary flow ratio on dual-orifice injector performance was made to optimize the primary-to-secondary area. In this study, these primary-to-secondary area splits were studied to assess the effect on injection velocity stability and the ability to provide a flat temperature profile. The three primary-to-secondary flow splits are shown in figure 505. The results of this study indicated that the larger primary area would provide higher oxidizer injection velocity at low thrust levels, which was desirable for distribution and system stability at all thrust levels. For each of the primary-to-secondary area splits, a primary flow-to-total flow split was calculated, as shown in figure 506. Testing conducted under Contract AF 04(611)-9575 indicated that the best performance was obtained at the low thrust levels with a large percentage of the flow injected through the primary orifice. From this study, the configuration with a primary area of 0.0093 in² and a secondary area of 0.8524 in² was selected for the basic design. This primary-to-secondary area split provided an injection velocity of 20 ft/sec at the 10% thrust level, 90 ft/sec at the 75% thrust level, and 155 ft/sec at the 100% thrust level, as shown in figure 507.

(C) Considering the system stability requirements, these predicted operating conditions provided a satisfactory stability margin at ignition and over the 5 to 1 operating range.

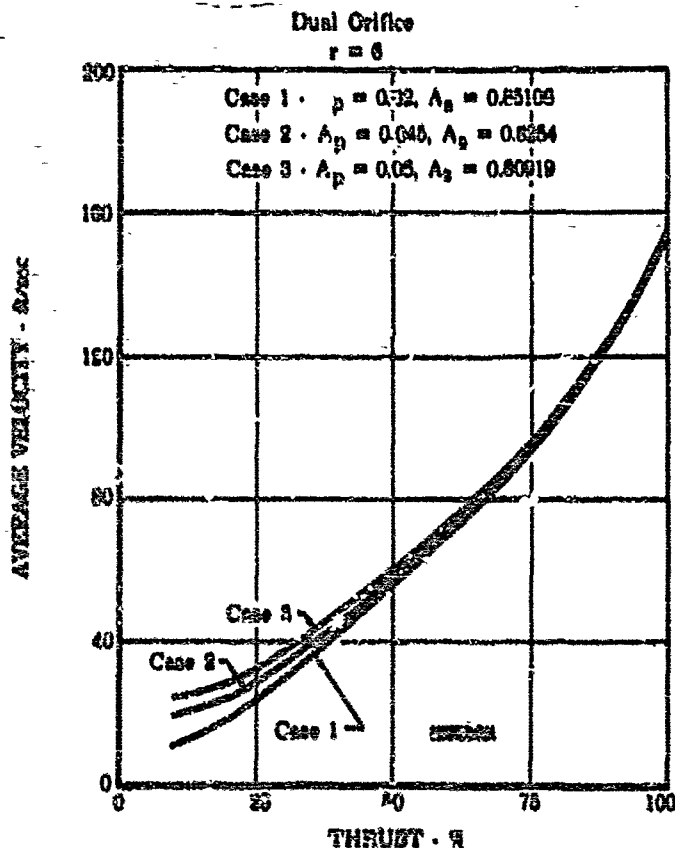


Figure 505. Variation in Velocity With Thrust

FD 16031

CONFIDENTIAL

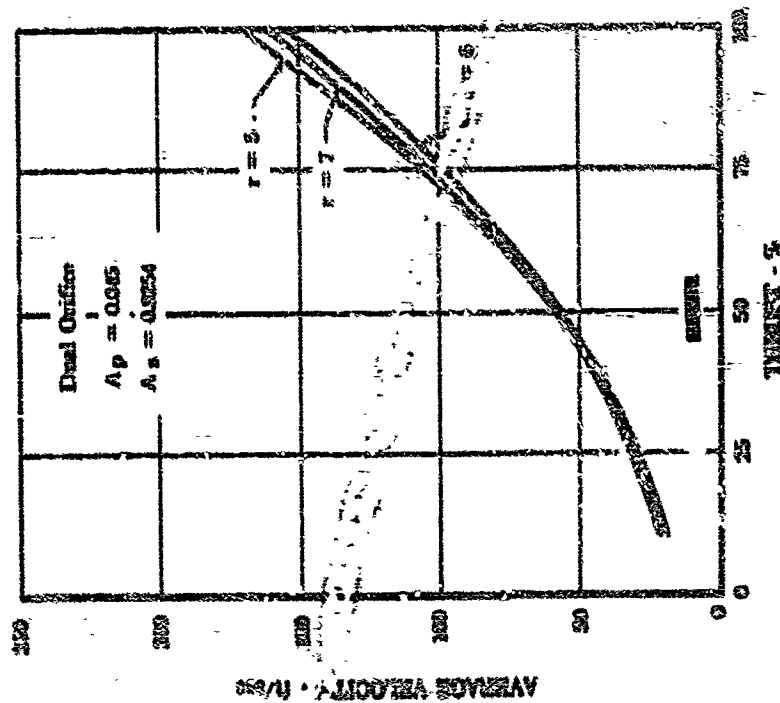


Figure 506. Orifice Primary-to-Total Flow Split vs Percent Thrust

PD 16217

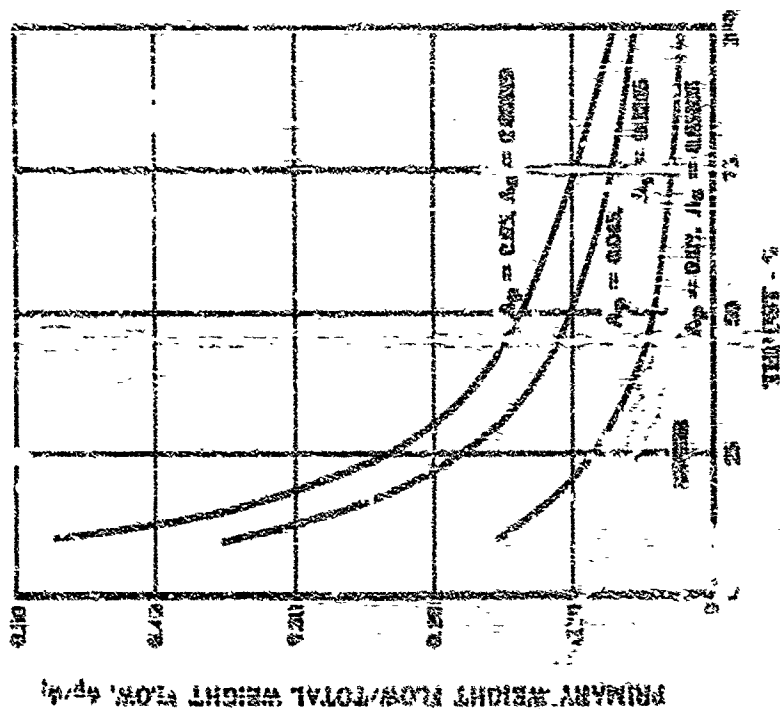


Figure 507. Variation in Velocity With Thrust Dual Orifice

CONFIDENTIAL

(C) Full-scale models of a dual-orifice oxidizer nozzle were fabricated to permit water flow test evaluation of the oxidizer atomization and overall nozzle performance at 10%, 50%, and 100% flow conditions. Flow tests confirmed the validity of the dual-orifice oxidizer nozzle configuration (straight through primary and tangential slot secondary) and demonstrated that the 15-degree secondary flow convergence angle was best for this dual oxidizer nozzle design. Flow tests were also conducted on a water model consisting of six dual-orifice nozzles in line, simulating the maximum cross section of the preburner injector mounted in the vertical plane. The objective of these tests was to evaluate the filling characteristics and hydrostatic head on preburner mixture ratio and temperature profile. These tests indicated that the hydrostatic head was sufficient to cause a 100° F temperature profile distortion at thrust levels less than 15 ft. It was then demonstrated that an increase in preburner injector pressure drop of 300 psid at nominal thrust would diminish the hydrostatic head effects. The injector secondary passages were therefore adjusted to provide a pressure drop of 325 psid at 100% flow and an engine mixture ratio of 7.

(C) A study of the fuel system performance and operating characteristics was conducted. An analysis of the effect of the fuel velocity on the combustion process and the resulting effect on temperature profile indicated that the fuel injection velocity significantly affected the preburner temperature profile, particularly at the high operating temperatures. To aid in the analysis of the data, a regression-type correlation was made using the data obtained during the 10% and 50% high pressure preburner tests. This correlation indicated that the difference between the maximum preburner temperature and the average preburner temperature was a function of momentum ratio, combustion products, velocity, chamber geometry, oxidizer atomization, and injection density, as shown in figure 306. In this analysis, a 50% preburner injector containing 34 elements with swirlers, a 50% preburner injector containing 320 elements without swirlers, and a 10% single-element variable-area injector configuration were correlated. This correlation indicated that a variable-area swirler configuration would provide the best temperature profile at the critical high temperature operating points. The ability to adjust the loss in the fuel system at the various operating points provided more injector pressure drop, which provided greater mixing and an improved profile. The fuel injection velocity for the variable-area configuration was approximately 1500 ft/sec at the nominal operating conditions. The momentum ratio for the variable-area configuration was optimized by rebalancing the engine fuel system pressure losses to provide higher injection velocity at a mixture ratio of 7, as shown in figure 309.

(C) The combination of the dual-orifice oxidizer and variable-area fuel injector configuration was selected for the engine system. The selection of the variable-area fuel injector required that the elements be clustered to provide a gear train that permits variability. The single 10% element that had been satisfactorily tested was used as the basic concept. The element was enlarged and clustered into a seven-element arrangement for the 250% preburner injector, as shown in figures 310 and 311. The injector has 84 dual-orifice oxidizer elements arranged in 7 clusters of 12 elements each, as shown in figure 312. The dual-orifice concept requires that the oxidizer flow for the primary and secondary passages be separated. This

CONFIDENTIAL

CONFIDENTIAL

separation permits the use of only the primary flow at start, where the flow and pressure loss is low, and as thrust level is increased the secondary flow is increased. This flow distribution is accomplished with the flow divider valve. An adapter plate is provided at the rear of the injector to accommodate flow divider valve mounting, as shown in Figure 513. Teflon-coated, self-energizing, O-ring seals have been used between the primary and secondary passages and between the mount ring adapter plate. The primary flow enters the injector through 15 individual ports in the adapter plate and is distributed to the front of each of the seven assemblies. The secondary flow enters the injector through six passages in the adapter plate and is distributed to the secondary plenum of the preburner injector housing, as shown in Figure 514. Pressure measurement taps have been included to permit measuring the primary and secondary passage pressure during test.

(4) The injector housing, which incorporated seven dual-orifice oxidizer assemblies, was fabricated from Inconel 718. This high strength material was selected to reduce the amount of deflection in the plate, which could cause a binding in the variable fuel system. The seven dual-orifice assemblies were fabricated separately and welded into this housing to simplify the manufacturing. Each of the seven assemblies was fitted into the housing with a line-to-line fit and welded at the backface to provide a positive seal to prevent the mixing of fuel and oxidizer within the injector housing as shown in Figure 515. This method of manufacturing permits replacement of individual elements rather than replacing a complete injector in the event of damage or design changes. This technique reduced injector construction costs and provided greater flexibility for testing.

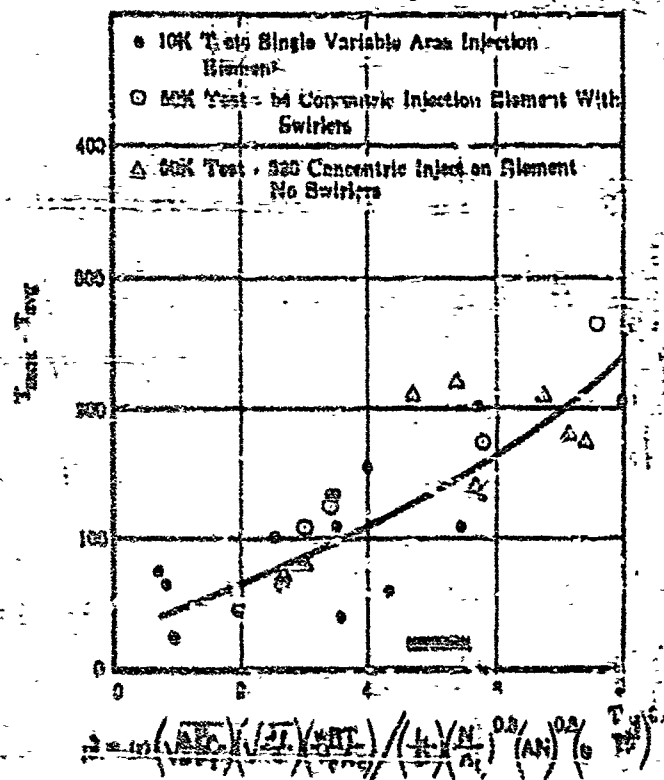


Figure 508. Correlation of Injector and Combustion Chamber Parameters vs Temperature Profile

CONFIDENTIAL

CONFIDENTIAL

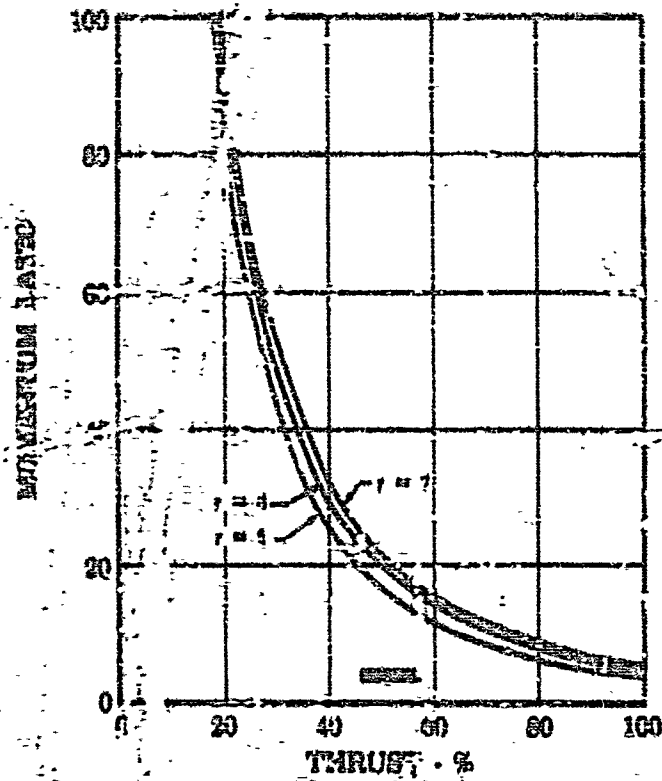


Figure 309, Momentum Ratio vs Percent Thrust

FD 17940

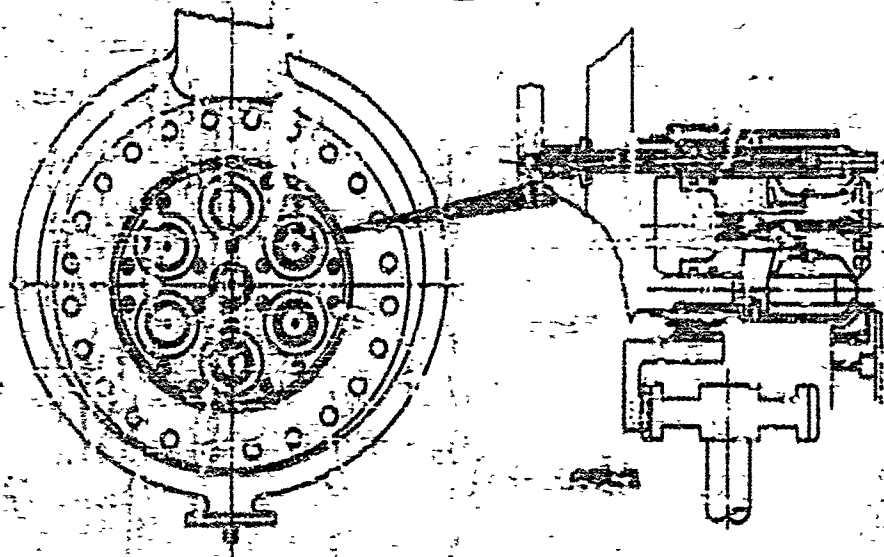


Figure 310, Preburner Injector Configuration

FD 15965

THIS PAGE CONTAINS SUBJECT MATTER COVERED BY A PATENT GRANTED TO THE U.S. GOVERNMENT WITH A RESERVING "SECURITY REQUIREMENTS PERMIT" AS USED BY U.S. COMMISSIONER OF PATENTS.
THIS PAGE CONTAINS SUBJECT MATTER COVERED BY A PATENT GRANTED TO THE U.S. GOVERNMENT WITH A RESERVING "SECURITY REQUIREMENTS PERMIT" AS USED BY U.S. COMMISSIONER OF PATENTS.

CONFIDENTIAL

CONFIDENTIAL

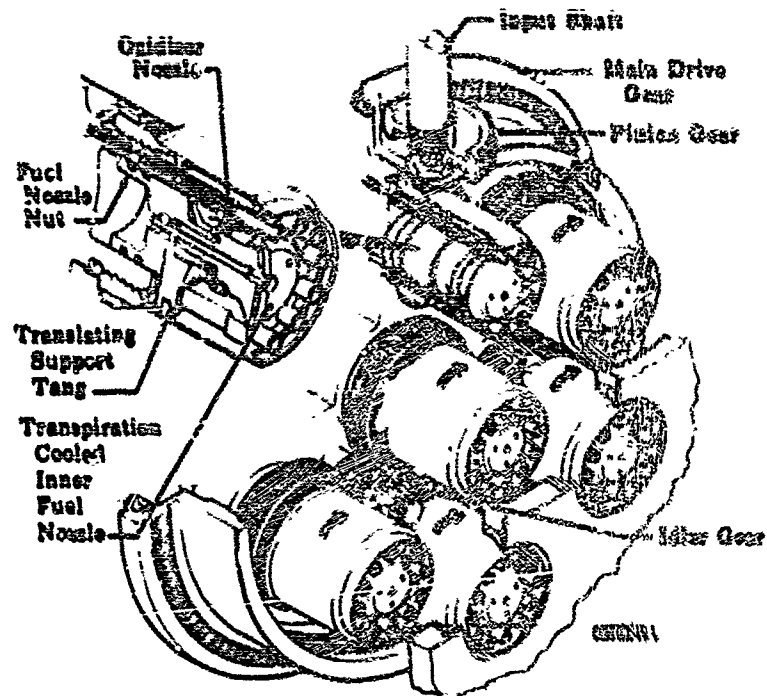


Figure 511. Variable Fuel Element Gear Arrangement

FD 181200

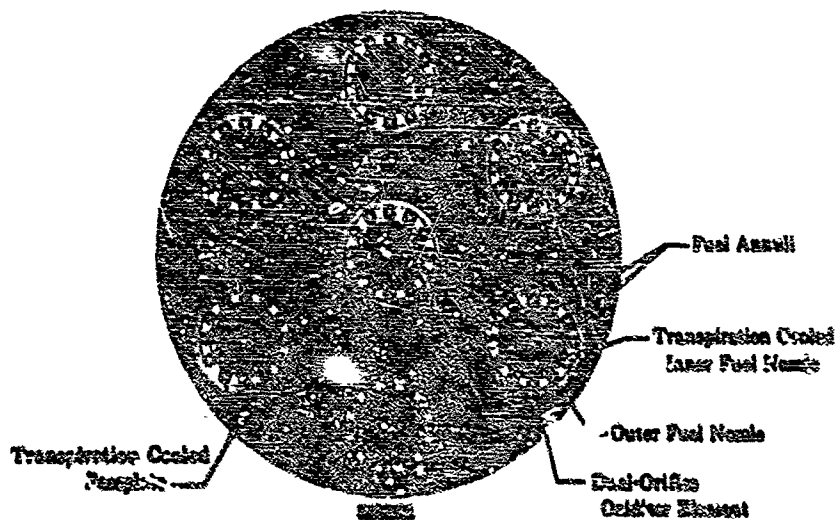


Figure 512. Preburner Injector Face Schematic

FD 19732

311
CONFIDENTIAL

THIS PAGE CONTAINS SUBJECT MATTER COVERED BY A PATENT GRANT ISSUED BY THE U.S. PATENT OFFICE UNDER THE PATENT ACT OF 1952, AS AMENDED, AND IS NOT TO BE RELEASED OR DISCLOSED IN ANY MANNER WITHOUT THE WRITTEN PERMISSION OF THE U.S. GOVERNMENT.

THIS PAGE CONTAINS SUBJECT MATTER COVERED BY A PATENT GRANT ISSUED BY THE U.S. PATENT OFFICE UNDER THE PATENT ACT OF 1952, AS AMENDED, AND IS NOT TO BE RELEASED OR DISCLOSED IN ANY MANNER WITHOUT THE WRITTEN PERMISSION OF THE U.S. GOVERNMENT.

CONFIDENTIAL

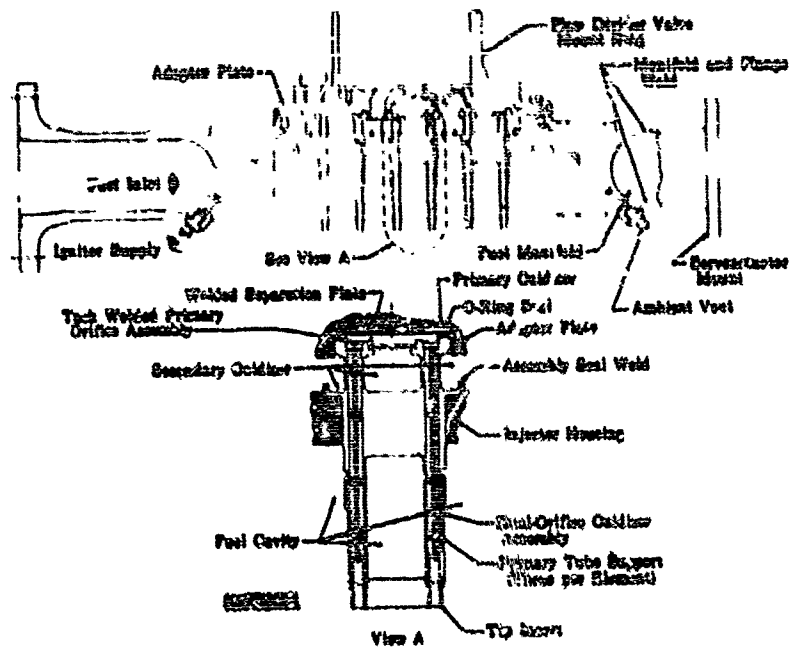


Figure 513. Injector Housing Assembly

FD 19549

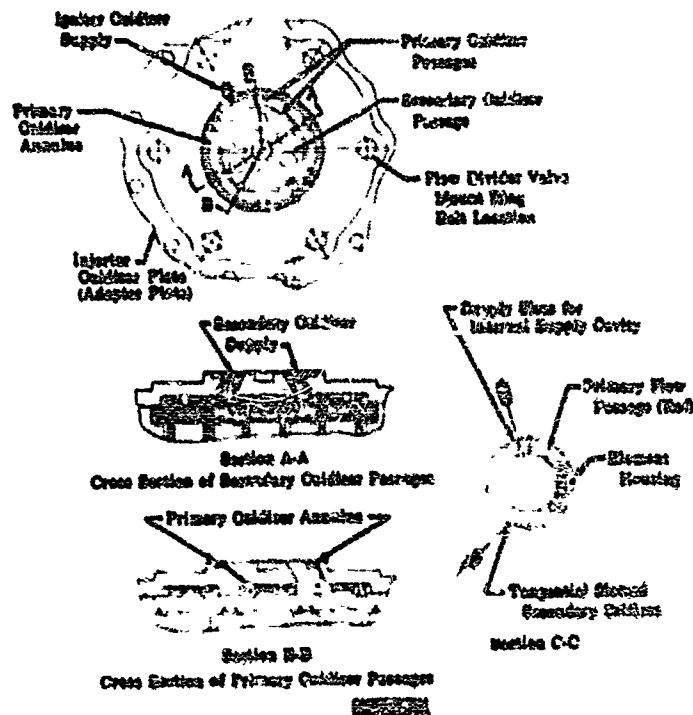


Figure 514. Primary and Secondary Oxidizer Supply Passages

FD 19589

512

CONFIDENTIAL

THIS PAGE CONTAINS SUBJECT MATTER COVERED BY A GOVERNMENT ORDER WITH A MODIFYING "SECURITY REQUIREMENTS DELETED" ISSUED BY U.S. COMMISSIONER OF PATENTS.

CONFIDENTIAL

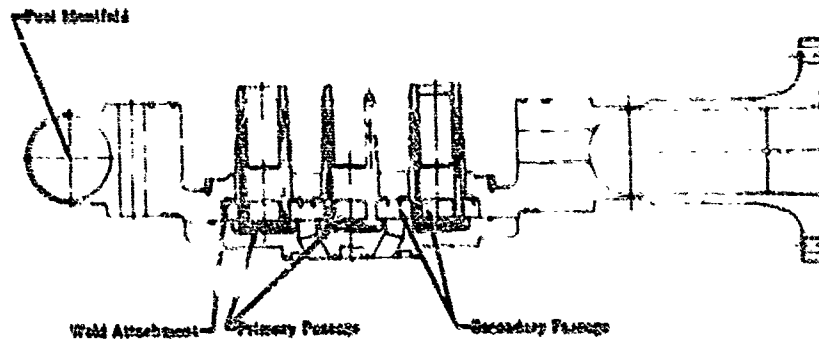


Figure 513. Cross Section of Welded Preburner
Injector Main Housing

FD 18116

(C) The 7 dual-orifice oxidizer assemblies that were fitted into the main housing were designed with 12 dual-orifice elements. The primary tube of the element had a 0.040-inch inside diameter and an L/D of 101. The wall thickness of the primary tube was 0.026 inch. Three collar post supports were provided for locating the primary tube, as shown in figure 513, and to provide accurate positioning of the primary tube in the secondary passage. The inlet collar, which was brazed to the primary tube, was pressed into the dual-element assembly and tack welded at the face to prevent the element from shifting location during operation. The primary tube was fabricated from stainless steel tubing (AMS 5580), which has a coefficient of expansion similar to that of Inconel 718 and good brazing characteristics. The secondary passage had two tangential-entry slots that were 0.035 by 0.283 inch. The oxidizer for the outer tangential slot was supplied from the main secondary flow path. The oxidizer for the inner tangential slot was supplied through transfer slots in the housing that permitted the oxidizer to flow to the inner annulus of the dual-orifice element, as shown in figure 514. This inner annulus supplied the oxidizer for all the inner tangential slots, which provided a tangential velocity to the secondary flow. The tangential velocity caused the secondary flow to discharge into a fine cone of oxidizer as the primary and secondary flows were exhausted into the preburner combustion chamber. The inside diameter of the secondary passage was 0.2375 inch. The axial location of the primary tube discharge was positioned in the converging section of the secondary flow path to obtain a maximum ejector action between the primary and secondary streams. At the low flows, the high velocity primary stream reduced the static pressure at the exit of the secondary stream, thereby increasing the flow through the secondary passage. The tip of the dual-orifice oxidizer assembly was constructed from TD Nickel to obtain the maximum heat conduction and thus avoid local overheating. This TD Nickel tip was brazed to the Inconel 718 dual-orifice assembly body to seal the oxidizer from the fuel and prevent mixing of the propellants in the injector. The dual-orifice elements were fabricated from Inconel 718 to avoid thermal problems with the housing.

(D) The fuel flow was supplied to the injector through one inlet manifold in the housing and was routed around the injector through a 1.420-inch diameter manifold. The fuel was uniformly distributed from this manifold through seventeen 1.060-inch diameter holes into the fuel compartment of the injector. Instrumentation bosses were included in the fuel manifold to measure the fuel manifold pressure. A mount flange was provided

513

CONFIDENTIAL

THIS PAGE CONTAINS SUBJECT MATTER COVERED BY A PATENT GRANT WITH A SPECIFIC "SECURITY REQUIREMENTS" LABEL BY U.S. COMMISSIONER OF PATENTS.

SECRET

On the injector housing, as shown in figure 513, to mount the servo-actuator for the variable-area fuel drive system. Each dual-orifice element housing incorporated a variable inner and outer fuel orifice with fuel sleeves, as shown in figure 515. These fuel annuli were adjustable and formed two concentric cylinders of fuel that were dispersed into the oxidizer to obtain thorough mixing of the two propellants. The outer sleeve of the variable fuel assembly contained 16 slots that permitted fuel to flow to the inside diameter of the element through the 12 slots in the dual-orifice housing to provide uniform distribution. The total area of the fuel annuli was varied through a gear drive system. The outer and inner sleeves of the fuel assembly were made of AMS 4650 (Borlyco 25) to reduce thread and sliding pilot surface galling and to provide a path to conduct heat away from the sleeve tips. The inner translating sleeve of the variable assembly was attached to the outer sleeve by tangs that extended through 3 of the 12 slots in the dual-orifice housing. The tangs rode on an annular land on the outer sleeves and assured uniform axial travel for the inner fuel sleeves. The front surface of the inner fuel nozzle was fabricated from a pyrolytic material (Kigimash) to provide transpiration coolant to reduce the possibility of overheating the surface. The transpiration coolant for this face was metered through two holes in the inner sleeve. The area of the translating sleeve was pressure balanced to minimize the bending load imposed on the three support tangs and to reduce the torque required to translate the element. Fuel leakage between the inside diameter of the element housing and the outside diameter of the inner sleeve nut assembly was minimized by two, stepped, piston ring seals that were pressure-loaded (1.2 to 3.3 pounds) in the closed position, as shown in figure 516. The backface of the inner sleeve was vented to chamber pressure by a hole drilled through the center of the assembly. The vent served to reduce the pressure drop across the seals and also provided a path to vent the small leakage that flowed past the piston seals.

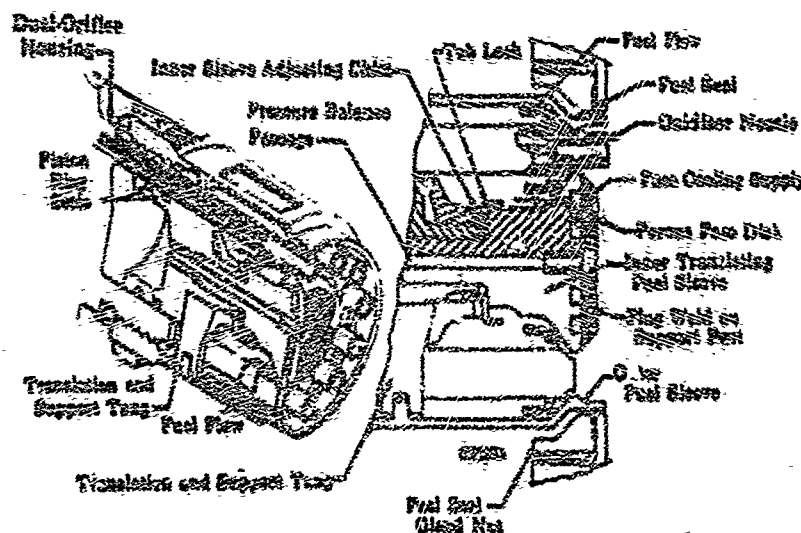


Figure 316. Adjustable Fuel Arrangement

018072

THIS PAGE CONTAINS SUBJECT MATTER COVERED BY A FOREST
ORDER WITH RESPECTING "FOUNTAIN" (FOUNTAIN) OF U.S. FOREST.
SIGNED BY FOREST.

THIS MARK CONTAINS NO COPY RIGHTS CLAIMED BY A PERSON
OTHER THAN A PERSON WHO HAS A PATENT RIGHT IN THE MARK
ISSUED BY U.S. PATENT OFFICE IN 1904.

雙龍

SECRET

CONFIDENTIAL

(C) The gearing system that was used for varying the area of the fuel annuli of the seven elements is illustrated in figure 511. The gearing consisted of (1) a driving pinion with a pitch diameter of 2.0 inches; (2) a main drive ring gear with a driven pitch diameter of 9.8 inches and a driving pitch diameter of 8.5 inches; (3) seven element gears with a pitch diameter of 2.5 inches; and (4) an idler gear with a pitch diameter of 0.89 inch. Each of the element gears was made of Inconel 718, had 90 gear teeth on the outer diameter, and was splined with 89 teeth on the inner diameter to the outer fuel sleeve inner gear. The difference of one tooth between the gear and spline permitted the individual elements to be indexed to the main drive ring gear or the idler gear to minimize the fuel area variation between elements. The main drive ring gear was made of Inconel 718 and the mating pinion gear was made of Berylco 25. The main drive ring gear was mounted on a 10.0-inch diameter ball bearing and was loaded by three needle bearing preload units. This provision accurately located the main drive gear with respect to the element gears and driving pinion. The preload units also served to reduce gear backlash and system friction. The pinion gear was splined to an Inconel 718 shaft, as shown in figure 517. The shaft was radially supported by a Bearnium B-10 sleeve bearing at one end and a series of four Teflon coated "Bal-seals" and Berylco 25 retainers at the other end. The Bal-seal retainers were finish machined during assembly to closely control the concentricity between the retainer and housing. In the machining operation, the press-fitted retainers without seals were line reamed. The retainers were then removed, the seals installed, and the retainers replaced in the fuel housing in the same radial position as before machining. The axial load on the input shaft assembly, which was caused by the fuel manifold pressure, was absorbed through a roller thrust bearing, which was inserted between the pinion gear and the main fuel housing, as shown in figure 517. At the input end of the shaft, the coupling connecting the shaft to the hydraulic servo-actuator was splined on both ends to facilitate assembly. A four-bolt, piloted flange was incorporated in the main fuel housing assembly to support the hydraulic actuator mount.

(C) The torque required to turn the drive shaft was approximately 250 in.-lb, with a response time of 0.5 second from the open position to the closed position. To rotate the fuel element one revolution (the equivalent of 0.0625-inch axial travel), it was necessary to rotate the fuel control shaft 1.44 revolutions. The fuel elements were adjustable over the required operating range from 20% to 100% thrust. The corresponding change in fuel injector pressure drop was from 20 to 640 psi. The main drive ring gear incorporated two fixed position mechanical stops that were located outside the range of the 20% and 100% thrust operating areas. These stops prevented a servos actuator malfunction from running the translating sleeves into the element housing or running the outer sleeves into the faceplate in the opposite direction. The mechanical stop on the main drive ring gear was precisely located with the translating sleeves of the outer elements at the minimum area stop, and the orientation of the indexing element gear was adjusted until the distance between the outer orifice metering surfaces was 0.011 to 0.014 inch. The center element was positioned in the same manner with respect to the idler gear. This positioning assured that the stop was contacted before the element area was completely closed.

CONFIDENTIAL

CONFIDENTIAL

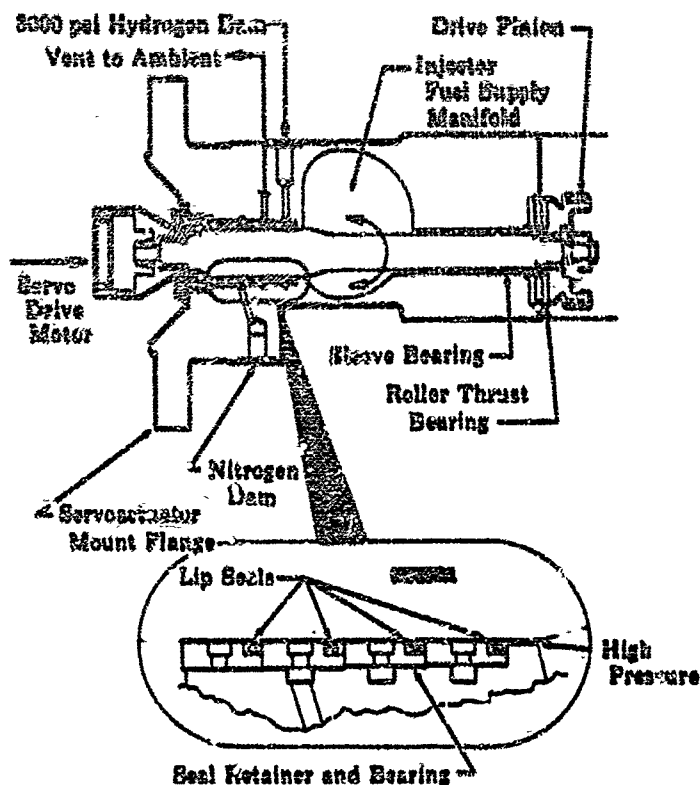


Figure 517. Variable-Area Drive and Seal Package FD 19731

(C) The faceplate assembly, shown in figure 518 consisted of (1) a conical load carrying member to take the fuel injector pressure drop of 700 psi with a minimum deflection, and (2) a porous Rigimesh faceplate to prevent overheating of the injector face. The faceplate was a conical design that incorporated rib-type supports for maximum stiffness. This stiffness was provided to prevent bending of the plate and subsequent binding of the translating fuel nozzles. Metering holes in the fuel plate regulated the fuel flow that was distributed through the porous faceplate. The fuel flow that passed through the porous plate created a heat transfer barrier that prevented recirculating combustion products from burning the face. The injector face cooling flow requirements were established to provide a maximum faceplate temperature of 850°R at 10% thrust and a mixture ratio of 7. The injector faceplate incorporated floating seals at the outside diameter of each of the seven elements to minimize fuel leakage around the outside diameter of the translating outer sleeves. Added coolant slots and distribution annuli were incorporated in each of the floating seal supports to direct supplemental cooling flow to the outside diameter of the outer sleeve. In addition, 36 holes on the outside diameter of the faceplate provided the hydrogen cooling flow that was used in the upper combustion chamber cooling liner. The faceplate assembly is shown in figure 519.

CONFIDENTIAL

CONFIDENTIAL

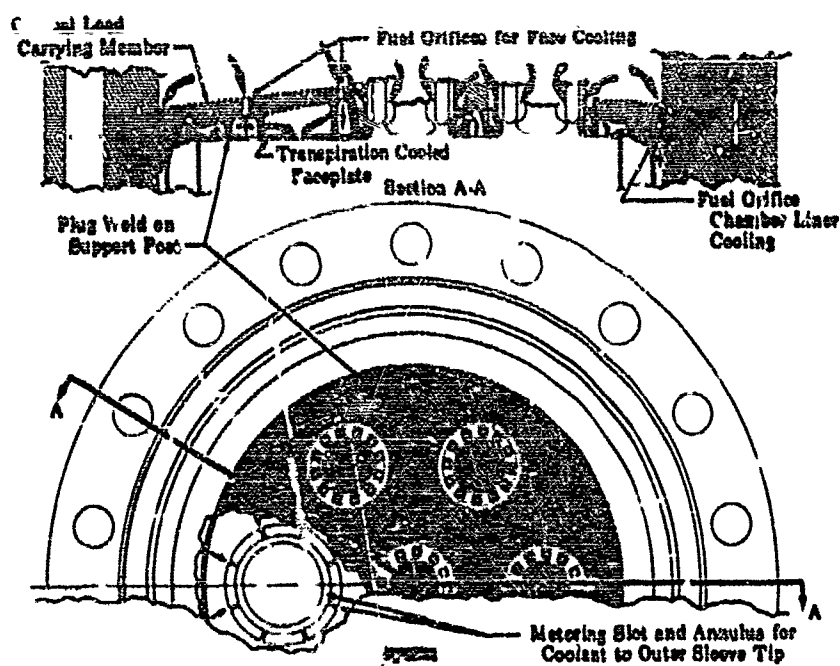


Figure 518. Facoplate Assembly

FD 19730

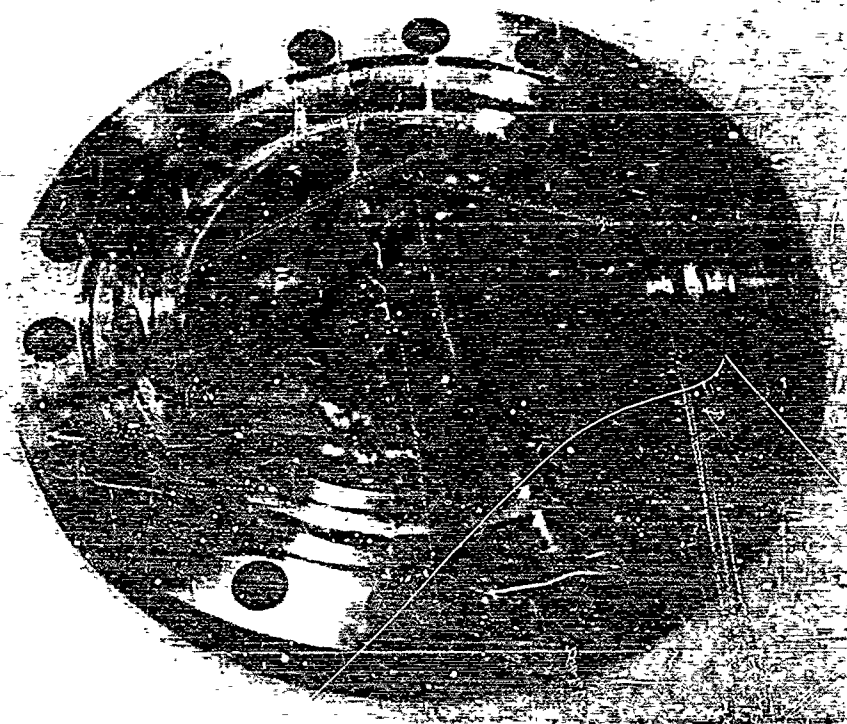


Figure 519. Preburner Injector Transpiration Cooled Faceplate

FE 64598

CONFIDENTIAL

(C) The design of the preburner combustion chamber section was predicated on the requirements for the 250K engine cycle. The combustion chamber length of 11.2 inches and the chamber diameter of 9.7 inches were based on the combustion chamber length and diameter that would be provided in an engine-type combustion system, as shown in figure 520. Therefore, this combustion rig would provide data representative of the engine-type combustion system. To maintain the wall temperatures at 800°R and to obtain the maximum strength of the housing material, a 0.034-inch thick Hastelloy X cooling liner, as shown in figure 521, was provided that used approximately 2% of the injector hydrogen flow as coolant. Tight sleeves were incorporated around the probes that extended into the gas stream to reduce the leakage of the hydrogen coolant. The coolant was metered through the 32 holes in the injector faceplate, passed between the housing and the cooling liner, and discharged into the combustion gas stream at the 11.2-inch station, as shown in figure 521. In addition to the cooling liner, acoustic liners fabricated from 0.050-inch thick Hastelloy X were designed for this combustion system. These liners were designed with 2% and 5% open area to provide damping if instability were encountered. A solid wall liner was provided for use in the stability testing. The preburner stability liners are shown in figure 522.

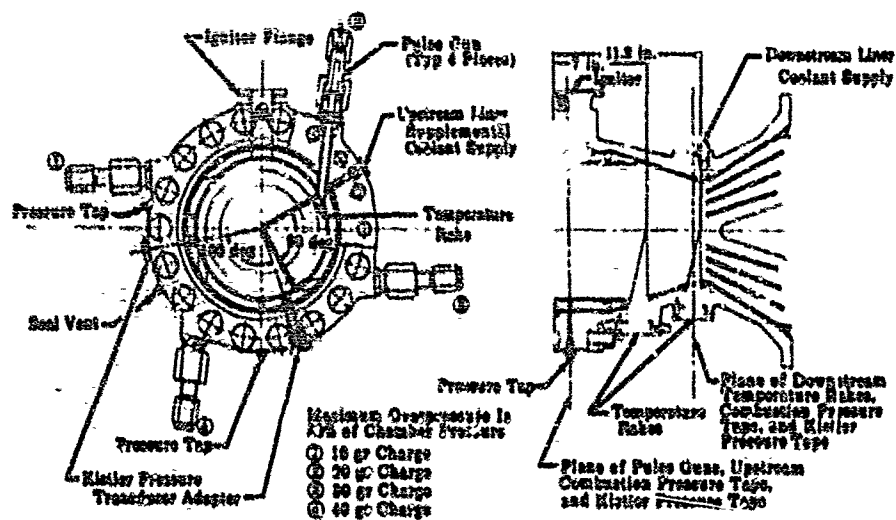
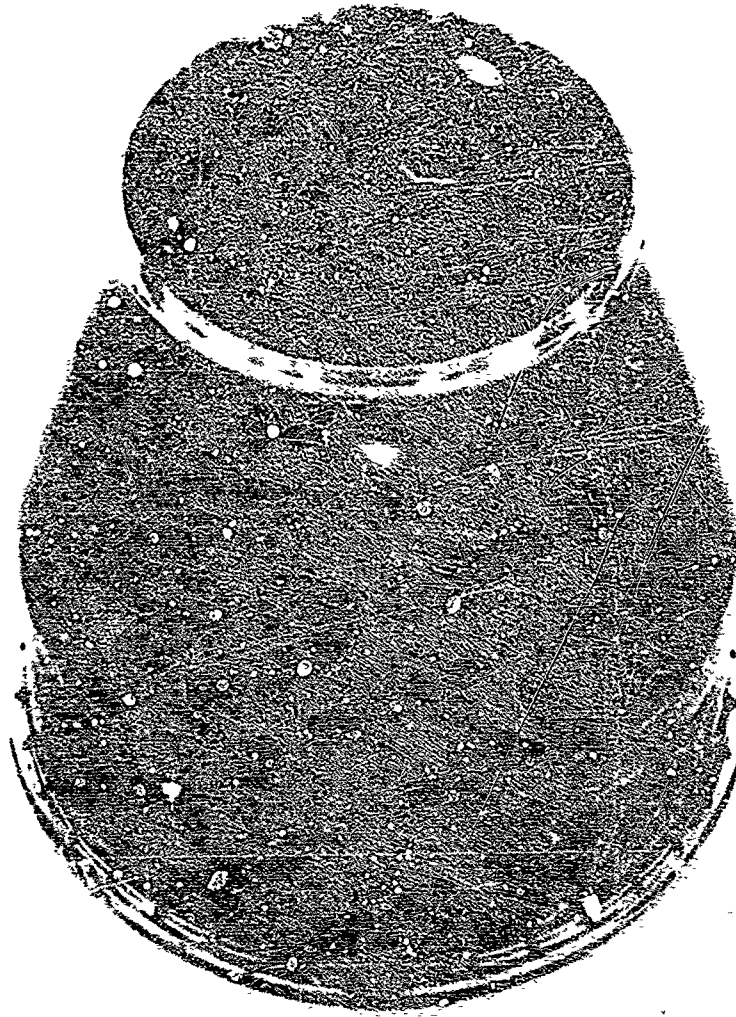


Figure 520. Preburner Combustion Chamber Instrumentation

FD 19650

CONFIDENTIAL

CONFIDENTIAL



INFORMATION REPORT U
FI

Figure 521. Preburner Chamber Cooling Liner
Combustion Section

FE 65612

519

CONFIDENTIAL

(This page is Unclassified)

CONFIDENTIAL

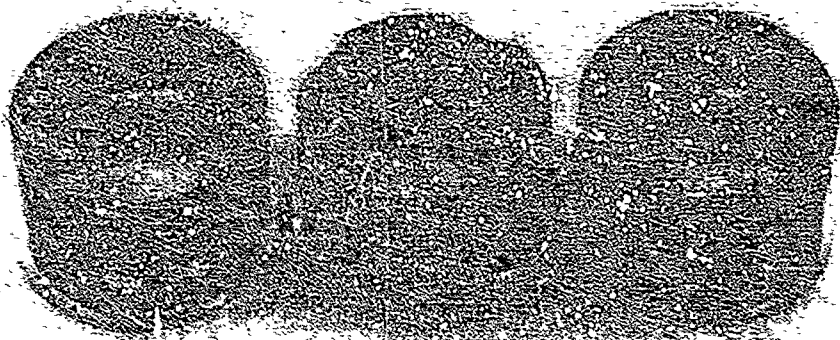


Figure 522. Preburner Chamber Acoustic Liner

PS 65610

(C) The preburner combustion chamber had included provisions for incorporating four tangential pulse guns to permit pulsing the chamber with pulse charges of 20-, 30-, 40-, and 80-grain charges, as shown in figures 523, 524, and 525. Three pulsing ports were designed to initiate the pulsing charge at a location that was 80% of the radius. This was the plane where the maximum energy was released and the system was the most sensitive to a pulsing charge. Two ports were added in the plane of the pulse guns to adapt Kistler transducers for measuring the combustion frequency. In addition, a third Kistler probe port was added at the 11.2-inch station to permit measuring dumping characteristics of the combustion system. This additional Kistler port was in line with one of the upstream ports, as shown in figure 523. In the preburner combustion chamber, four temperature take ports were provided at two planes. One plane was located 7.2 inches downstream from the injector face, and a second plane was located at the 11.2-inch station. Two raker were positioned across the elements, and the other two between elements, as shown in figure 526.

(C) The preburner dome, shown in figure 527, was designed as a plenum chamber for the oxidizer and as a flow divider valve housing, which is shown in figure 528. Prior to rig operation, the oxidizer was circulated through the dome to precondition the system by removing the latent heat. Because the dome was to be exposed to the maximum test stand pressure, the design was predicated on a maximum operating pressure of 7000 psi. To withstand these pressures, an Inconel 718 forging was selected for its high strength properties and to obtain added strength by definition of the grain flow at the attachment point where the minimum cross section was required. A facility thrust structure was mounted on the dome flange, which is shown in figure 529. This was a facility structure that was designed for the test program only. The bolts that were used to attach the dome, injector, main chamber, and thrust structure were fabricated from tensitized Inconel 718. These bolts were stretched to obtain a uniform preload on the attachment flanges and O-ring seals.

CONFIDENTIAL

UNCLASSIFIED

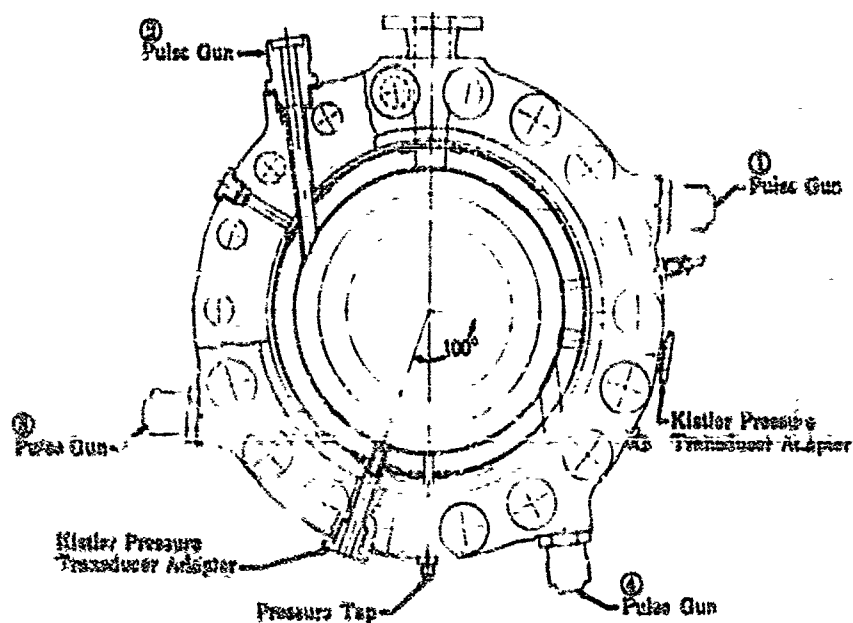


Figure 523. Pulse Gun and Kistler Probe Configuration

FD 18105



Figure 524. Pulse Gun and Kistler Probe Installation

FE 69219

UNCLASSIFIED

UNCLASSIFIED

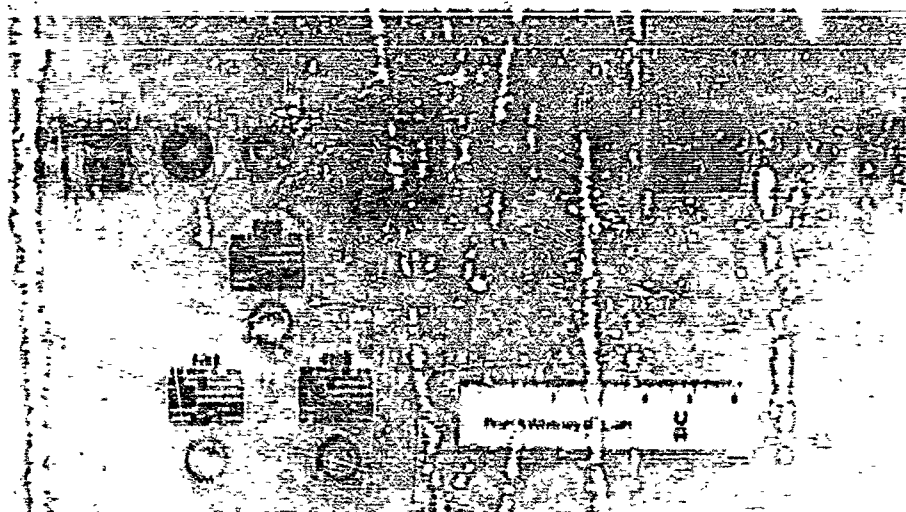


Figure 525. Preburner Pulse Gun Details

FE 65605

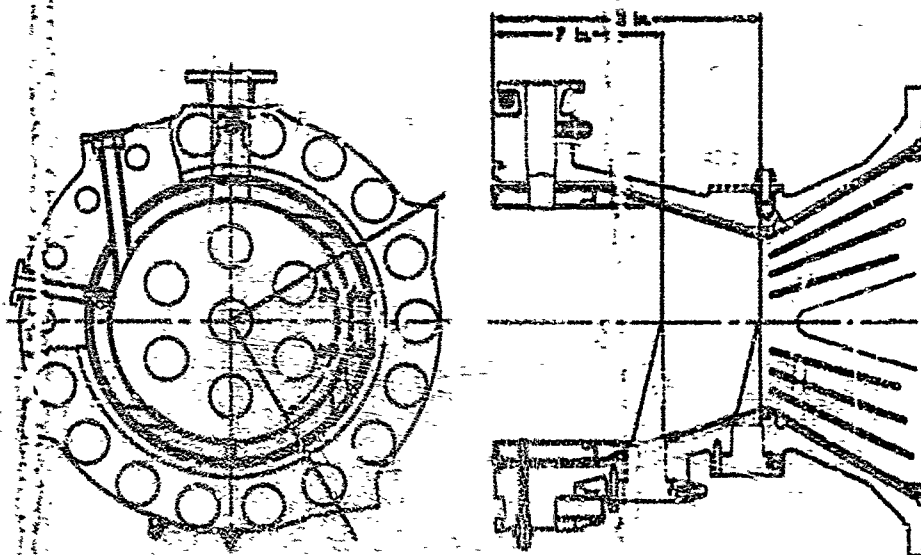


Figure 526. Temperature Probe Installation

GS 2623

UNCLASSIFIED

CONFIDENTIAL



Figure 527. Preburner Flow Divider Valve
Housing

FE 55604

523

CONFIDENTIAL

(This page is Unclassified)

CONFIDENTIAL

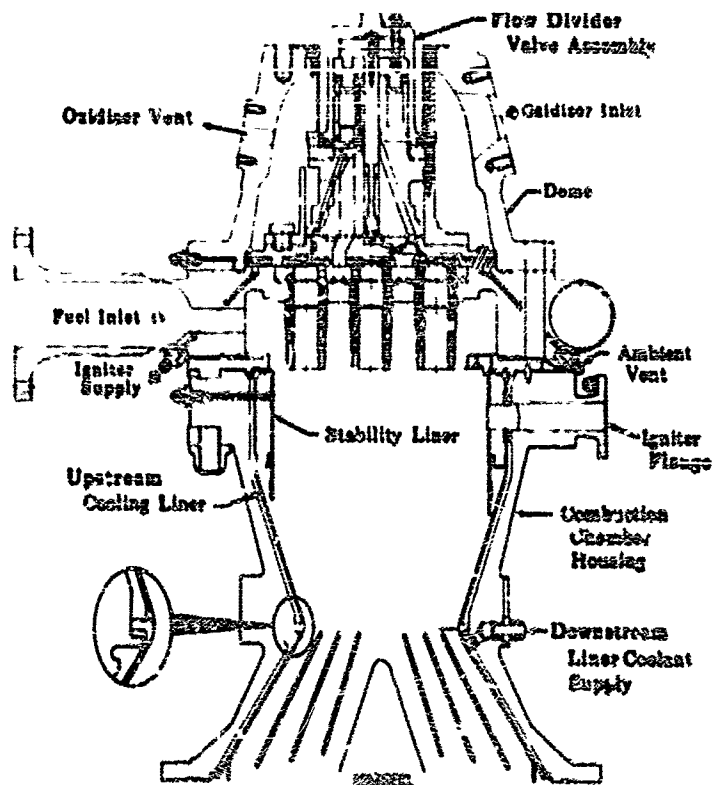


Figure 528. Preburner Combustion Rig Configuration

FD 19258A

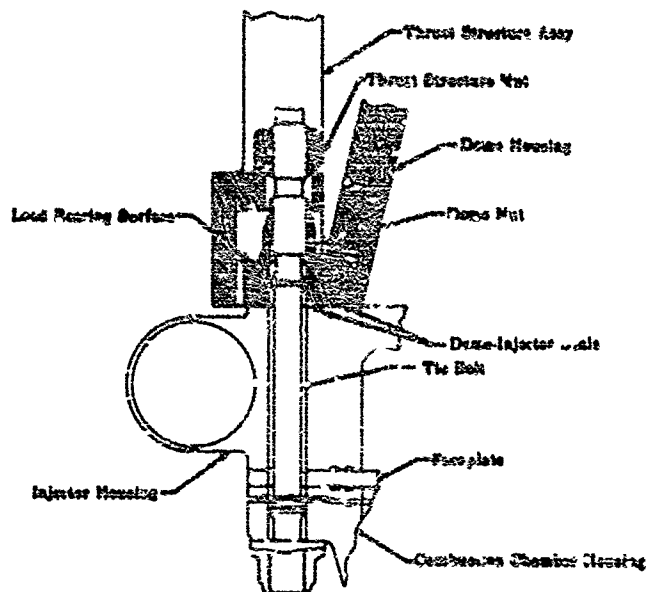


Figure 529. Facility Thrust Structure Attachment for Preburner Combustion Rig

FD 19648A

CONFIDENTIAL

CONFIDENTIAL

(C) For the preburner rig testing, a back pressure plate incorporated a 2.94 inch diameter exit hole that would provide a 5100-psi back pressure at the 100% operating point. This back pressure plate was fabricated from a Waspaloy forging to obtain the desired strength at the operating temperature and is shown in figure 530. A series of 48 stretch-type bolts were used to mount the back pressure plate to the main preburner housing. These same bolts were used to attach the preburner and main injector for the staged-combustion testing.



CONFIDENTIAL

Figure 530. Back Pressure Nozzle Plate

FE 65602

CONFIDENTIAL

CONFIDENTIAL

(U) The preburner torch igniter, shown in figure 531, was a hydrogen-cooled, continuous-burning, oxygen-hydrogen, electrically ignited device. This ignition system was designed to operate at either sea level or in a vacuum, with either gaseous or liquid propellants, and was capable of multiple relights. The flame from the torch was ignited prior to the initiation of preburner propellant flow to prevent excessive propellant accumulation inside the combustion chamber.

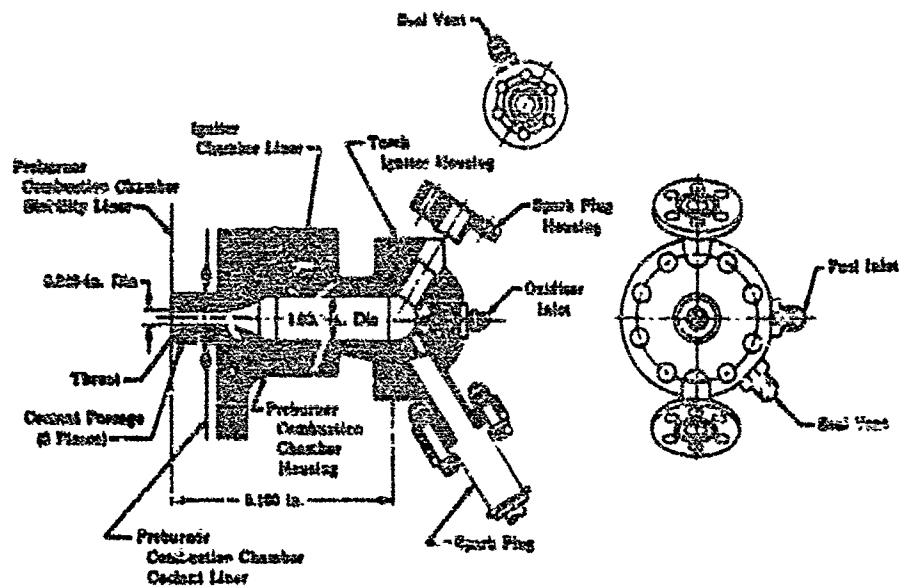


Figure 531. Preburner Igniter Assembly

FD 19590

(U) The torch igniter was a welded assembly consisting of the throat section, chamber section, and head section. The spark plug housings were brazed into the head section. An expansion joint sleeve was welded to the chamber liner throat section to provide structural support. A labyrinth seal, shown in figure 532, was located in the expansion sleeve to minimize the coolant flow leakage between the igniter combustion chamber and the preburner combustion chamber housing.

(U) The oxidizer was injected into the igniter combustion chamber through a single orifice element. The fuel filled the cavity between the chamber liner and igniter assembly flange and was introduced into the chamber through an orifice concentric with the oxidizer nozzle. A portion of the fuel flow was used as coolant for the igniter chamber liner and discharged into the preburner combustion chamber between the stability liner and the cooling liner, as shown in figure 533.

(U) The torch igniter had two separate spark ignition systems to increase the reliability of the electrical system. Each spark plug was energized by a hermetically sealed exciter that converted the 28 vdc input to a minimum of 20 high voltage (30 kv) sparks per second output at a nominal stored energy level of 0.5-joule per spark. An electrical schematic of the exciter is shown in figure 534.

CONFIDENTIAL

(This page is Unclassified)

UNCLASSIFIED

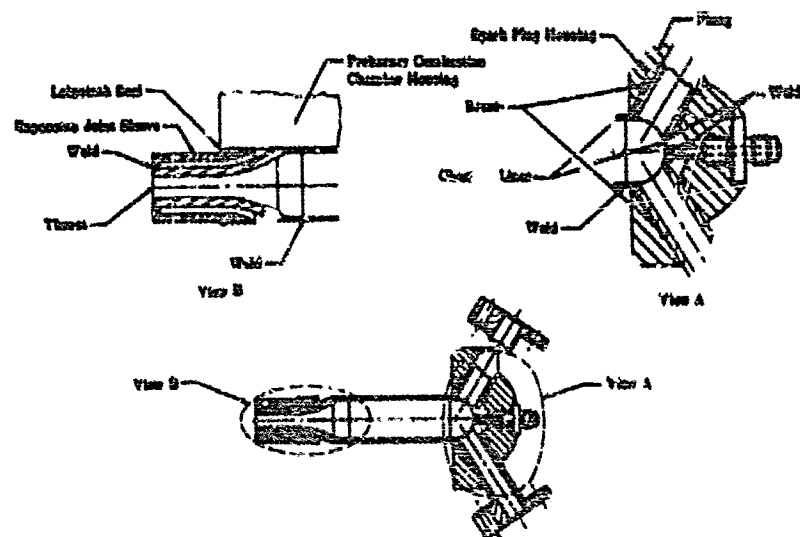


Figure 532. Details of Preburner Igniter Assembly

FD 19679

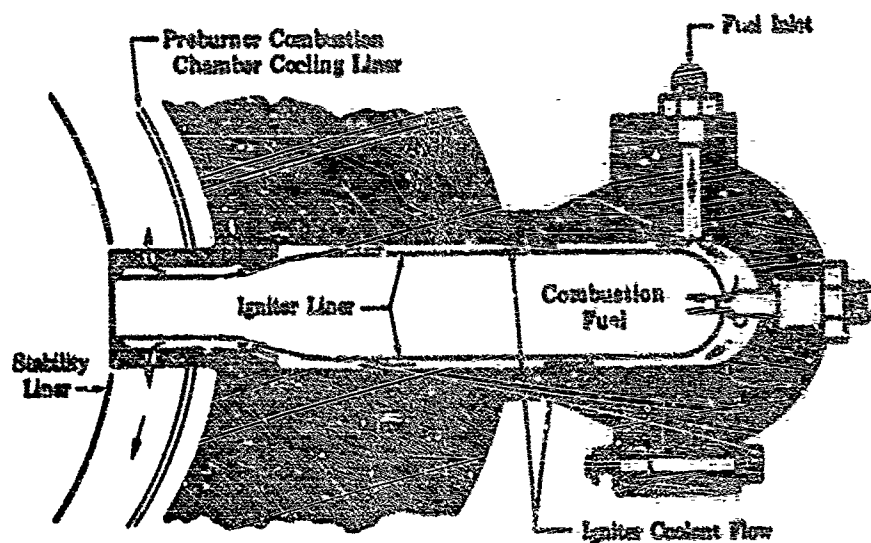
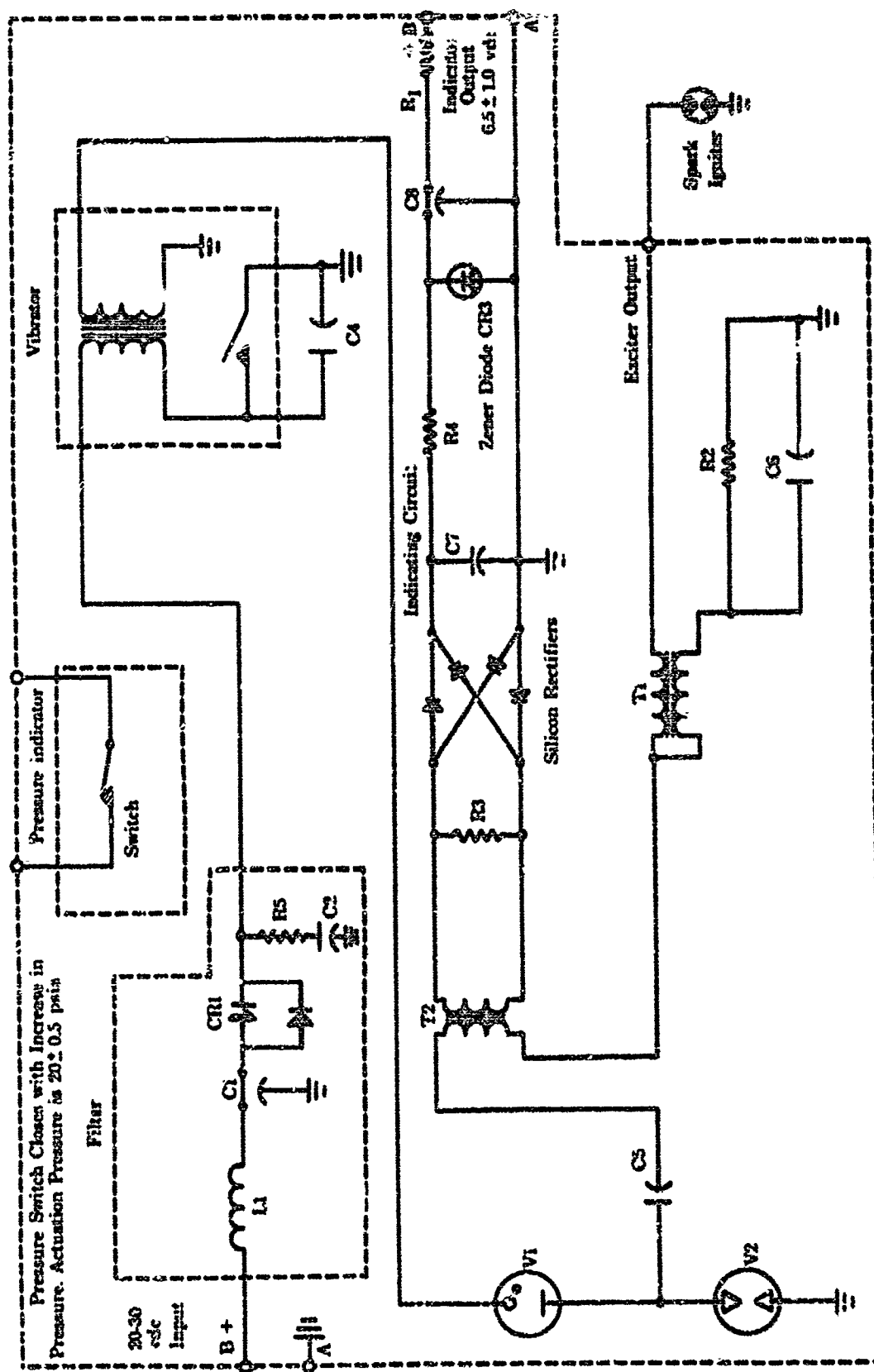


Figure 533. Preburner Igniter Cooling Flow Schematic

FD 19689

UNCLASSIFIED

UNCLASSIFIED



FD 3154C

Figure 534. Ignition System Schematic

UNCLASSIFIED

CONFIDENTIAL

(U) The preburner igniter spark plug, shown in figure 535, consisted of an outer housing of Inconel, a ceramic insulator, and a nickel electrode. A mechanical joint at the end of the spark plug joined the plug to the spark exciter high tension lead. The entire spark ignition assembly was weld- and solder-sealed and inert-gas-pressurized to prevent arcing.

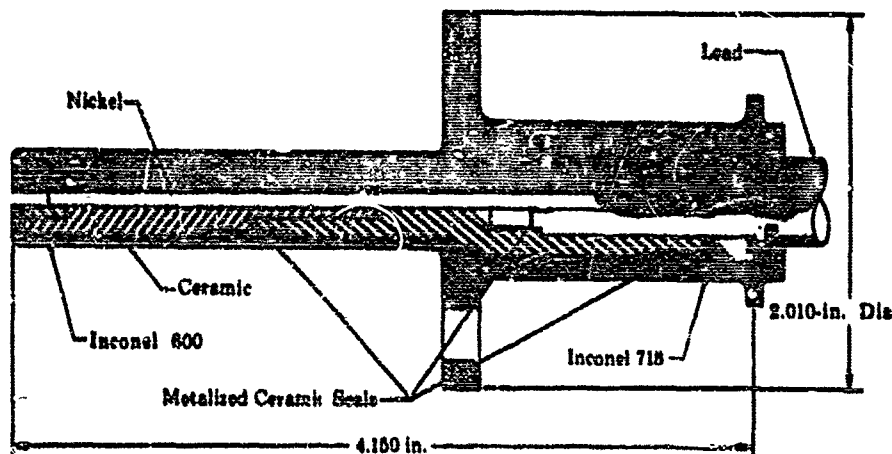


Figure 535. Preburner Igniter Spark Plug

FD 19691

D. TESTING

1. Facility Checkout

(U) The objectives of the initial phase of the preburner test program were (1) the operational check of the new E-8 test facility, and (2) establishment of operating procedures for this new test facility. A series of 53 nonfiring flow tests were conducted to evaluate the facility. Thirty hot firing tests were conducted to establish an acceptable ignition and start sequence that provided propellant flows within the engine cycle requirements. The overall objectives of the tests were:

1. Valve and control functional checks
2. Proof testing of the high pressure systems
3. Run tank pressurization tests
4. Purge and cooldown tests
5. Calibration tests
6. Valve and control sequencing tests
7. Establishment of computer gain settings
8. Establishment of operational procedures and techniques
9. Definition of operational limits and incorporation of automatic protective devices
10. Control of propellant flows to permit test rig operation over a wide range of pressure levels.

CONFIDENTIAL

(This page is Unclassified)

CONFIDENTIAL

(U) The initial preburner test rig was delivered to the E-8 test facility on 25 January 1967. Final facility fabrication and functional checks were completed during installation of the test item. On 14 February 1967, flow tests of the facility and test rig were initiated. The initial flow test objectives were to establish cooldown procedures. Facility checks were conducted to establish these starting flow conditions. At the beginning of the rig tests, the liquid propellant run tanks were pressurized to a relatively low level to maintain a more accurate control of the starting flows. The starting flows were established by diverting the flow overboard through orifices in the hydrogen and liquid oxygen vent lines to set the desired flow rates. After the starting flow orifices were sized, diversion tests were performed to evaluate injector fill rates. As a result of the flow diversion tests, a valve and control sequencing was established that provided smooth, stable, and controlled preburner ignition.

(U) The initial preburner hot firing test was conducted on 11 March 1967. These preliminary tests indicated that the rig ignition characteristics were repeatable. Additional tests were conducted to establish operating levels and timing of automatic ignition sensing devices. These automatic abort systems were incorporated for protection against late ignition, interrupted flows, or other conditions that would permit accumulation of unburned propellants and endanger the facility and test rig.

(C) Further testing was continued with the primary objective of attaining a control system that would regulate propellant flow rates and permit preburner operation up to 100% rated flows. After ignition and stabilization, the preburner was accelerated to approximately 7%. At this level, the propellant flow control system had to be switched from position control to an automatic system that would control preburner propellant flow rates regardless of the run tank operating pressure. Once the automatic propellant control system was actuated, the run tanks could be pressurized to rated pressure and the test rig could then be operated to 100% flows. Initially, the automatic control system sampled preburner combustion pressure and temperature. However, the sensitivity of this control system to varying stand characteristics (propellant temperatures, pressures, control interactions, system volumes, response, etc.) caused wide fluctuation in preburner combustion temperature during the attempted acceleration transient and prevented successful preburner acceleration over 50% of rated flows. These problems, coupled with the inherent response lag in the control systems (sense time, valve action, and change in combustion process), required that a new system of facility control be adopted.

(C) The control system was converted to a system that used the flowmeter signal to position the facility control valves according to a predetermined flow schedule, thereby controlling the mixture ratio and combustion temperature. A series of 27 single and dual cold flows were made to check this system and establish timing and control gains. The flow control schedule that was established in these nonfiring flow tests to maintain a mixture ratio of approximately 0.5 during the acceleration transient is shown in figure 536. Using this flow schedule, a prediction of the

CONFIDENTIAL

CONFIDENTIAL

injector mixture ratio was made from the first series of tests. The small variation from the preset mixture ratio noted during the transient, as shown in figure 536, was caused by the overlap and flow characteristics of the facility valves.

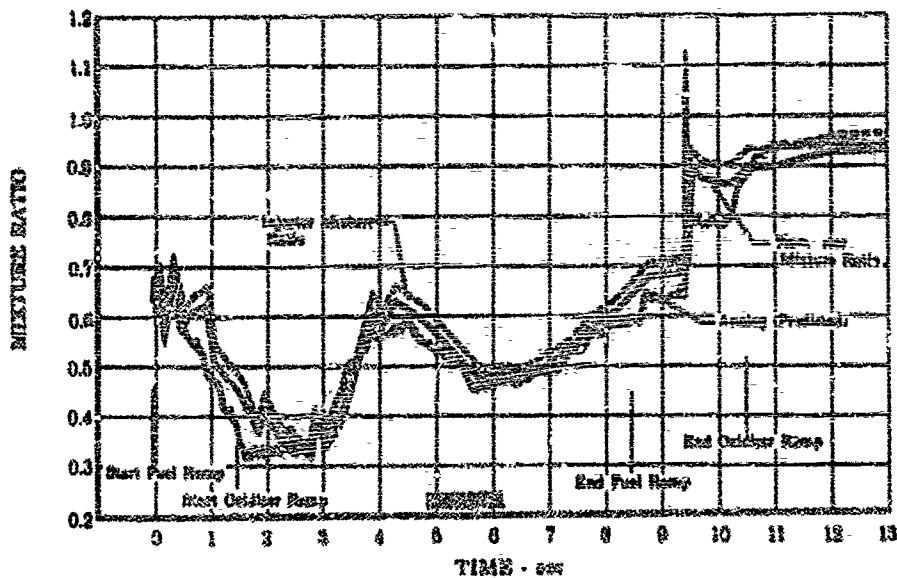


Figure 536. 250K Preburner Mixture Ratio
Profile - Run 46 (Transient from
7% to 80% Rated Flows)

FD 22922

(C) After the 27 nonfiring flow tests were completed with this revised control system, preburner testing was resumed with the primary objective of evaluating the flow control system. Preburner run No. 38 was the initial hot firing using the revised control system. Evaluation of the flow control system was considered complete on run No. 46, when successful preburner rig acceleration to 80% rated flows was accomplished. Flow control was used on all preburner tests after run No. 46 and on all staged-combustion tests.

(C) Once the flow control system was operational, preburner testing was continued. The only facility problem that continued during the test program was nonrepeatability of the starting flows. Both preburner and initial staged-combustion testing demonstrated that the facility could not repeatedly control the low preburner ignition flows and the subsequent transient to 7%. This facility problem was circumvented by igniting the preburner at 7% flows. With the incorporation of the 7% preburner starting flows (staged-combustion run No. 16), predictable testing was achieved.

2. Preburner Torch Igniter Testing

(U) In the early phase of the preburner program, component torch igniter tests were conducted to develop a torch igniter system that would provide consistent, reliable ignition for the preburner test rig. The two preburner torch igniter units were received early in the program. They were

CONFIDENTIAL

CONFIDENTIAL

mounted in the B-8 component test stand and underwent 24 test firings totaling approximately 503 seconds before being incorporated on the preburner test rig. While the igniter unit was designed for dual spark excitation, as shown in figure 537, single spark exciter units were used in all tests. To aid in the acquisition of test data, an instrumentation probe was installed in the second spark plug housing to provide combustion gas temperature and pressure measurement.

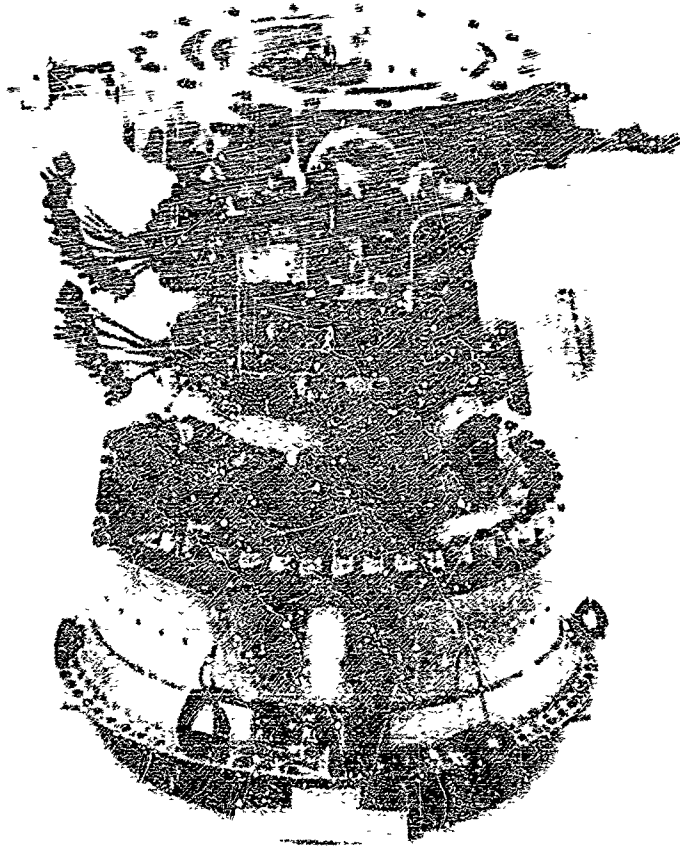


Figure 537. Preburner Igniter Installation
With Dual Electrical Exciter Units

FE 66823

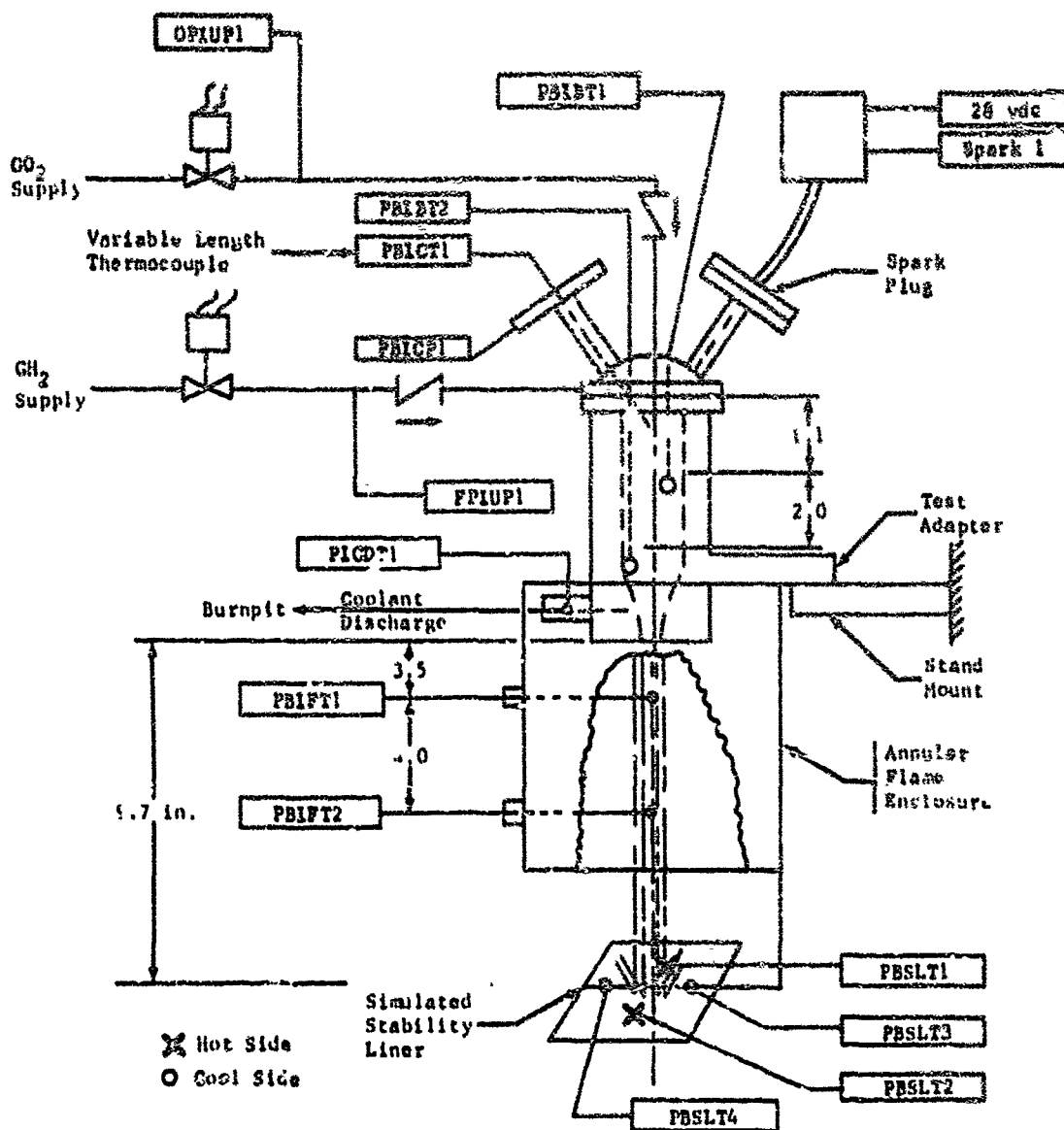
(U) The objectives of the preburner torch igniter rig tests were to establish a reliable ignition procedure, to evaluate the component durability, to establish the ignition limits, and to define the acceptable operating levels. A schematic of the test rig and test facility is presented in figure 538. The test items were mounted in both the horizontal and vertical attitudes during ignition testing. On all but three limit survey tests (test No. 11 to 13), successful first spark ignition was achieved. In all three limit survey tests, at igniter mixture ratios less than 1, the igniter failed to light. Test No. 3 to 8 were devoted to exploring the flame temperature and establishing the optimum immersion depth for the ignition-sensing thermocouple. This device was calibrated to permit torch igniter flame sensing and analysis before opening the preburner propellant valves during preburner testing. Figure 539 describes the various thermocouple immersion depths and resulting temperature indications. Typical preburner torch igniter test data are presented in figure 540.

532

CONFIDENTIAL

(This page is Unclassified)

UNCLASSIFIED



- OPIUP1 Igniter Oxidizer Inlet Pressure
- FPIUP1 Igniter Fuel Inlet Pressure
- PBICT1 Igniter Combustion Temperature (variable length)
- PBIST2 Igniter Barrel Temperature - Cool Side
- PBSLT3 Simulated Stability Liner Temperature - Cold Side
- PBSLT1 Simulated Stability Liner Temperature - Hot Side
- PBIFT1 Igniter Flame Temperature - Upstream
- PBIFT2 Igniter Flame Temperature - Downstream
- PICDT1 Igniter Coolant Discharge Temperature

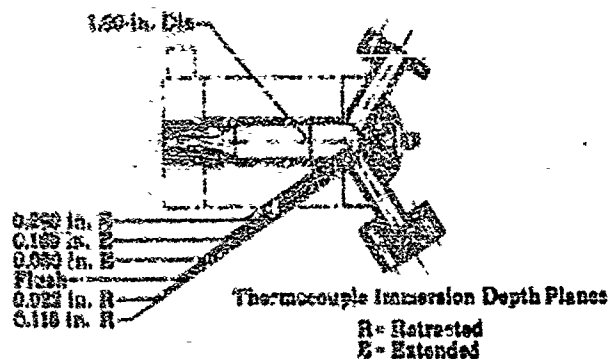
Figure 538. 250K Preburner Igniter Test Stand
Schematic (Rig F-35100B)

FD 21892

533

UNCLASSIFIED

UNCLASSIFIED



| Run No. | Fuel Pressure, psia | GO ₂ Pressure, psia | r | Immersion Depth, in. | Chamber Temperature, R |
|---------|---------------------|--------------------------------|------|----------------------|------------------------|
| 4.01 | 535 | 520 | 1.99 | 0.118R | 1750 |
| 5.01 | 535 | 520 | 2.01 | 0.022E | 1160 |
| 6.01 | 501 | 502 | 1.99 | Flush | 1237 |
| 6.01 | 535 | 520 | 1.99 | 0.050E | 1775 |
| 7.01 | 512 | 527 | 2.13 | 0.180E | 2432 |
| 8.01 | 535 | 520 | 2.01 | 0.250E | 2750 |

Figure 539. Variable Length Thermocouple Location and Temperature Recorded

FD 21893

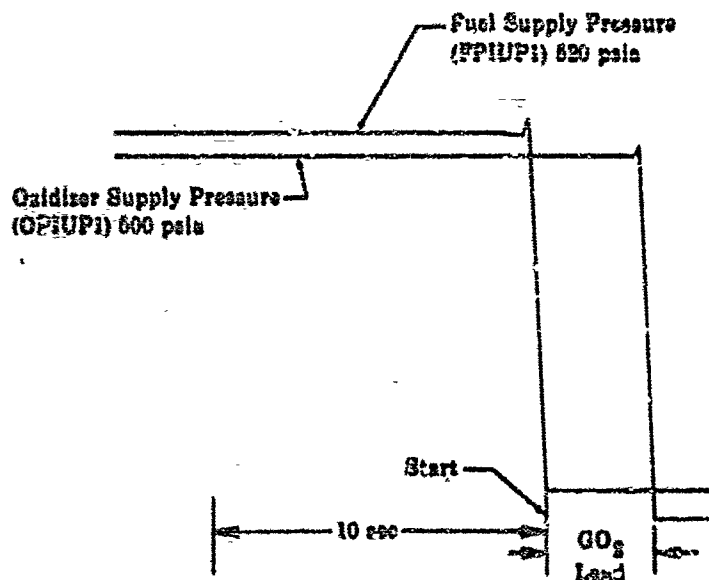


Figure 540. Test Data from Test 2501S4PB

FD 19681

UNCLASSIFIED

UNCLASSIFIED

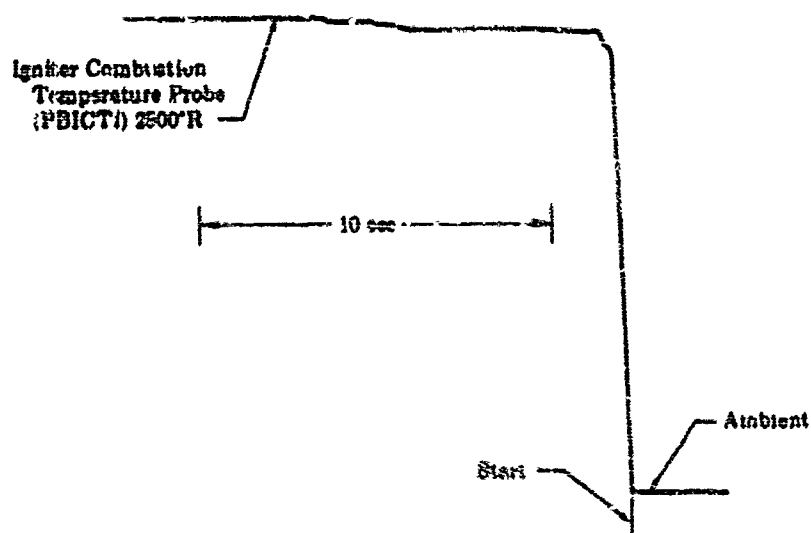


Figure 540. Test Data from Test 250IS4PB -
Continued

FD 19683

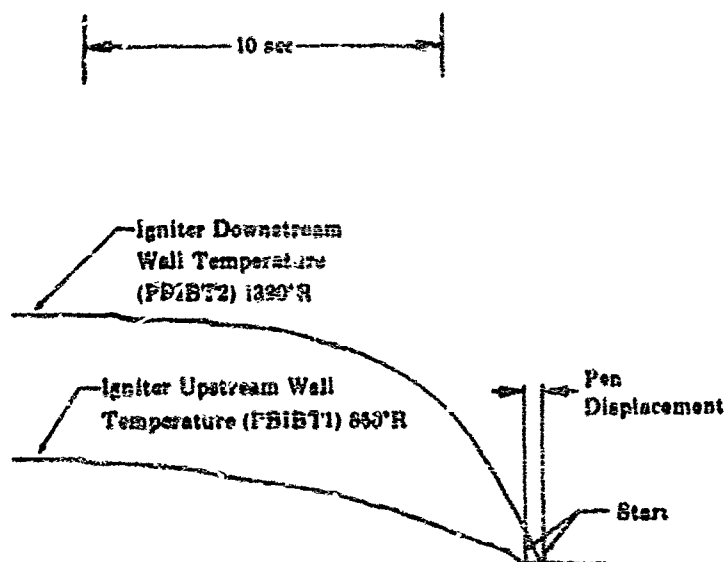


Figure 540. Test Data from Test 250IS4PB -
Continued

FD 19684

UNCLASSIFIED

UNCLASSIFIED

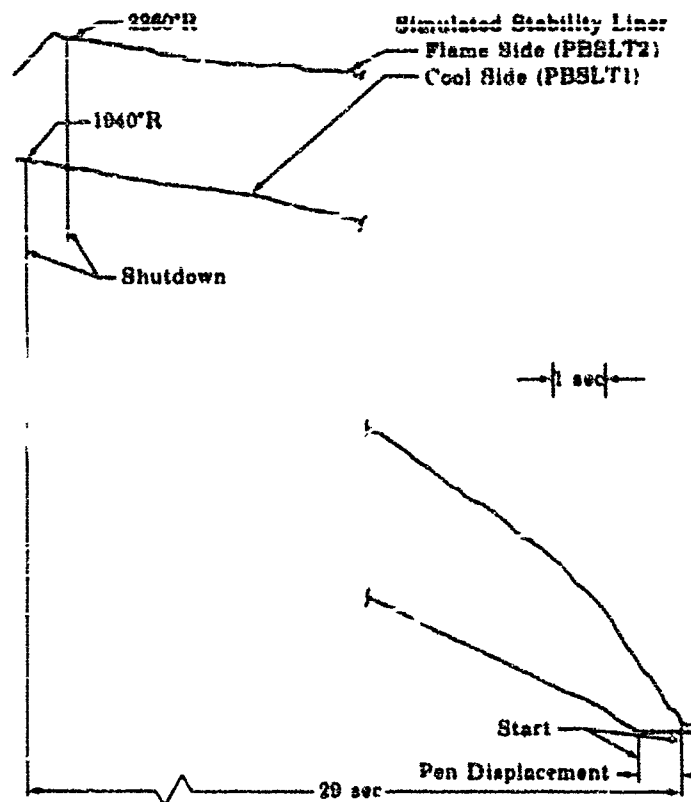


Figure 540. Test Data from Test 250194PB -
Concluded

FD 19682

(U) As a result of the preburner torch igniter tests, an ignition procedure was established for use on the preburner test rigs. It was determined that the following sequence of events would provide reliable preburner ignition:

- 7 seconds Supply gaseous oxygen to the igniter
- 3.5 seconds Supply gaseous hydrogen to the igniter and energize the spark exciter
- 2.5 seconds Turn OFF exciter voltage
- 1 second Sample igniter combustion temperature (abort burner test if temperature not in the acceptable operating region)
- 0 seconds Preburner ignition, open preburner propellant valves.

UNCLASSIFIED

CONFIDENTIAL

(U) Test results further indicated that prolonged and continuous torch operation was feasible. Igniter tests showed that the torch impingement on a simulated stability liner for 29 seconds did not over-temperature the part, and igniter barrel wall temperatures never exceeded 1500°R. During Phase I testing, no igniter problems (ignition characteristics or parts distress) were encountered. A tabulated summary of 250K preburner igniter tests is presented in table XLIV.

3. Preburner Testing

a. General

(C) During testing of the 250K preburner, a total of 104 hot firings tests accumulating 1836 seconds of run time were conducted on two preburner test rigs; 46 were preburner rig performance tests, 6 were for preburner-main burner compatibility evaluation prior to staged-combustion testing, 32 were staged-combustion tests, and 20 were facility checkout tests. Twelve of the preburner performance tests attained all test objectives, 36 tests were classified as partially successful, 20 tests were classified as facility checkout runs, and 8 tests were aborted before useful data were obtained. Table XLV lists the preburner hot firing tests and provides test time accumulated on the two preburner test rigs. During this preburner program, ignition and scarting characteristics, temperature profile, and dynamic stability of the combustion system were investigated. The temperature profile, as well as the overall preburner performance, were evaluated, based on tests conducted at 20% and 100% flows and at an engine mixture ratio of approximately 6.8⁶. The preburner fuel supply temperature during the stability testing was set to approximately 100°R.

(U) Two preburner test rigs were used during this program. The injector incorporated on each test rig was identical except for the swirl direction of the elements of the preburner injector. One injector incorporated a co-rotating secondary swirl and the other incorporated a counter-rotating swirl configuration. On the co-rotating injector, all oxidizer nozzles swirled the secondary flow in one direction. The counter-rotating injector was designed with adjacent oxidizer nozzles swirling the secondary flow in opposite directions. Figure 542 illustrates the two types of oxidizer nozzles. These preburner injector configurations were changed as the test results demonstrated the need for the required modifications.

(U) The preburner test rigs consisted of five primary components: dome, flow divider valve, injector, combustion chamber, and torch igniter. For the preburner test program, a back pressure simulator nozzle was installed on the combustion chamber discharge flange to permit preburner rig testing at pressures simulating either the staged-combustion rig or the engine cycle. Figure 543 shows the 250K preburner test rig assembled for test and figure 544 shows the 250K preburner test rig installed in the hot firing test facility.

⁶ Mixture ratios quoted are engine mixture ratios. For conversion to preburner mixture ratios, see figure 541.

CONFIDENTIAL

CONFIDENTIAL

(C) Table XLIV. 250K Preburner Igniter

| Run No. | Test No. | Gaseous Oxygen Pressure, psia | Fuel Pressure, psia | Mixture Ratio, r | Gaseous Oxygen Lead Time, sec | Sparks Required for Ignition | Combustion Pressure, psia | Igniter Combustion Temperature, °R | Maximum Igniter Chamber Liner Temperature, °K Upstream Downstream | Igniter / Upstream | so Temp D |
|---------|----------|--|---------------------------|------------------------|--|---------------------------------------|---------------------------------|---|--|-----------------------|--------------|
| -- | 250181PB | 580 | 640 | 1.8 | 3.3 | 1 | 0.1 | 2810* | 643* | 710* | -- |
| -- | 250182PB | 580 | 610 | 1.8 | 3.3 | 1 | 0.1 | 2830 | 930 | 1025 | -- |
| -- | 250183PB | 530 | 540 | 2.0 | 3.3 | 1 | 0.1 | 2913 | 797 | 1102 | -- |
| -- | 250184PB | 300 | 520 | 2.6 | 3.3 | 1 | 0.1 | 2900 | 900 | 1390 | -- |
| -- | 250185PB | 520 | 535 | 1.9 | 3.3 | 1 | 0.1 | 1350 | 900 | 1150 | -- |
| -- | 250186PB | 530 | 560 | 2.7 | 3.3 | 1 | 0.1 | 1427 | 918 | 1100 | -- |
| -- | 250187PB | 335 | 560 | 2.0 | 3.3 | 1 | 0.1 | 1438 | 914 | 1161 | -- |
| -- | 250188PB | 520 | 535 | 2.1 | 3.3 | 1 | 0.1 | 1430 | 914 | 1200 | -- |
| -- | 250189PB | 520 | 525 | 2.1 | 3.3 | 1 | 0.1 | 1423 | 923 | 1261 | -- |
| 1.01 | -- | 500 | 550 | 1.8 | 3.3 | 1 | 0.2 | 600* | --- | 820* | 2800* |
| 2.01 | -- | 648 | 648 | 2.1 | 3.3 | 1 | 0.2 | 820 | --- | 1062 | 2985 |
| 3.01 | -- | 582 | 601 | 2.0 | 3.3 | 1 | 0.2 | 1287 | --- | 1050 | 2791 |
| 4.01 | -- | 520 | 535 | 2.6 | 3.3 | 1 | 0.2 | 750 | --- | 1075 | 2750 |
| 5.01 | -- | 520 | 530 | 2.0 | 3.3 | 1 | 0.2 | 1100 | --- | 1100 | 2800 |
| 6.01 | -- | 520 | 535 | 2.0 | 3.3 | 1 | 0.2 | 1775 | --- | 1000 | 3200 |
| 7.01 | -- | 527 | 512 | 2.1 | 3.3 | 1 | 0.1 | 2432 | --- | 1088 | 2855 |
| 8.01 | -- | 520 | 525 | 2.0 | 3.3 | 1 | 0.2 | 2750 | --- | 1075 | 2800 |
| 9.01 | -- | 420 | 535 | 2.0 | 3.3 | 1 | 0.2 | 1248 | --- | 975 | 2750 |
| 10.01 | -- | 370 | 530 | 1.0 | 3.3 | 1 | 0.2 | 900 | --- | 750 | 1200 |
| 11.01 | -- | 260 | 535 | 0.8 | 3.3 | * | 0.2 | -- | --- | -- | -- |
| 12.01 | -- | 240 | 535 | 0.9 | 3.3 | * | 0.2 | -- | --- | -- | -- |
| 13.01 | -- | 240 | 535 | 0.9 | 3.3 | * | 0.2 | -- | --- | -- | -- |
| 14.01 | -- | 871 | 554 | 3.2 | 3.3 | 1 | 0.4 | 935 | --- | 1200 | 3430 |
| 15.01 | -- | 946 | 1018 | 1.9 | 3.3 | 1 | 0.2 | 1030 | --- | 1150 | 2800 |

*Insufficient run duration to permit attaining steady-state conditions.

CONFIDENTIAL

CONFIDENTIAL

250K Preburner Igniter Tests

| Chamber Temperature, °F Downstream | Igniter Flame Temperature, °R | | Maximum Stability Liner Temperature, °R | | Coolant Discharge Temperature °R | Hot Time, sec | Remarks |
|---------------------------------------|-------------------------------|------------|---|-----------|----------------------------------|---------------|--|
| | Upstream | Downstream | Flame Side | Cool Side | | | |
| 713* | -- | -- | 727* | 530* | --- | 1.5 | High chamber temperature abort (automatic) |
| 1025 | -- | -- | 2100 | 1750 | --- | 18.0 | High liner temperature shutdown |
| 1102 | -- | -- | 1080 | 801 | --- | 6.0 | High chamber temperature shutdown |
| 1390 | -- | -- | 2260 | 1940 | --- | 29.0 | Full duration test |
| 1150 | -- | -- | 1500 | 1100 | --- | 30.0 | Full duration test |
| 1100 | -- | -- | 1600 | 1216 | --- | 30.0 | Full duration test |
| 1141 | -- | -- | 1768 | 1477 | --- | 31.0 | Full duration test |
| 1200 | -- | -- | 1641 | 1244 | --- | 31.0 | Full duration test |
| 1261 | -- | -- | 1467 | 1056 | --- | 31.0 | Full duration test |
| 800* | 2800* | 2900* | 1400* | 1100* | 590* | 5.0 | Checkout test |
| 1062 | 2985 | 2634 | 2269 | 2149 | 709 | 30.0 | Full duration rerun of 1 01 |
| 1050 | 2791 | 3165 | 2329 | 2208 | 702 | 30.0 | FBICT1 flush with chamber wall |
| 1075 | 2750 | 3030 | 2300 | 2100 | 700 | 30.0 | FBICT1 retracted 0.118 inch |
| 1100 | 2800 | 3125 | 2300 | 2100 | 700 | 30.0 | FBICT1 retracted 0.022 inch |
| 1000 | 3200 | 3200 | 2000 | 2150 | 700 | 30.0 | FBICT1 extended 0.020 inch |
| 1022 | 2855 | 3166 | 2277 | 2099 | 718 | 30.0 | FBICT1 extended 0.105 inch |
| 1075 | 2800 | 3200 | 2300 | 2300 | 700 | 30.0 | FBICT1 extended 0.240 inch |
| 975 | 2750 | 3130 | 2000 | 2000 | 650 | 60.0 | |
| 750 | 1200 | 1750 | 1550 | 1750 | 620 | 60.0 | |
| -- | -- | -- | -- | -- | --- | 0 | No ignition |
| -- | -- | -- | -- | -- | --- | 0 | No ignition |
| -- | -- | -- | -- | -- | --- | 0 | No ignition |
| 1200 | 3450 | 3550 | 2400 | 2267 | 775 | 30.0 | High mixture ratio run |
| 1150 | 2800 | 3250 | 3456 | 2340 | 736 | 30.0 | High flow run |

CONFIDENTIAL

539/540

2

(C) Table XLV. 250K Preburner Test Summary

| Preburner Rig No. | Preburner Run No. | Date | Test Duration, sec | Maximum Chamber Pressure Sought, Attained, psia psia | Remarks |
|----------------------|----------------------|---------|--------------------------|---|---|
| 33447-1 | 1 | 3/11/67 | 1.53 | 30 | 29 Program: Starting flow test. Smooth ignition with preburner pressure stabilized at 29 psia (1600°R average combustion temperature). |
| | | | | | Fuel Oxidizer |
| | | | | | Starting flow 0.515 lb/sec 0.36 lb/sec |
| | | | | | Inlet pressure 43 psia 42 psia |
| | | | | | Inlet temperature 300°R 171°R |
| 33447-1 | 2 | 3/16/67 | 0.96 | 30 | 42 Program: Starting flow test. Smooth ignition with preburner still in transient condition when low temperature advance circuit advanced the run. Burn wire had burned at 0.7 second. Reset low combustion temperature sample time to make it compatible with ignition characteristics. |
| 33447-1 | 3 | 3/17/67 | 3.15 | 300 | 45 Program: 7% (idle) test to establish control settings. Run advanced because of low oxidizer system response. Reschedule oxidizer control valve timing. |
| 33447-1 | 4 | 3/17/67 | 3.41 | 300 | 40 Program: 7% test. Slow oxidizer system response caused low combustion temperature advance. Make cold flow tests prior to continuing hot firing runs. |
| 33447-1 | 5 | 3/27/67 | 5.82 | 300 | 103 Program: 7% test. Improper control valve sequencing during the transient to 7%. Reset fuel control valve opening relative to oxidizer valve. |

CONFIDENTIAL

(C) Table XLV. 250K Preburner Test Summary (Continued)

| Preburner Rig No. | Preburner Run No. | Date | Test Duration, sec | Maximum Chamber Pressure Sought, Attained, psia psia | Remarks |
|----------------------|----------------------|---------|--------------------------|---|---|
| 33447-1 | 6 | 3/28/67 | 10.28 | 300 322 | Program: 7% test and run tank pressurization. Transient to 7% successful, but instability during run tank pressurization caused the high temperature advance. Steady-state preburner pressure was 322 psia. Instability attributed to low oxidizer control valve gains. |
| 33447-1 | 7 | 3/29/67 | -- | 300 0 | Program: 7% test and run tank pressurization. Torch igniter failed to provide flame intensity required for smooth preburner ignition because of restricted igniter oxidizer supply. Dirt found in the oxidizer flow orifice caused the torch problem. |
| 33447-1 | 8 | 3/30/67 | 11.58 | 300 315 | Program: 7% test and run tank pressurization. Successful ramp to 7% and preburner pressure stabilized at 300 psia. During tank pressurization ramps, the control system became unstable and caused the high temperature advance. Reset the oxidizer control valve gains for the next run. |
| 33447-1 | 9 | 3/31/67 | 5.96 | 300 60 | Program: 7% test and run tank pressurization. Combustion temperature profile distortion caused the low temperature sampling probe to go cold. Bulk combustion temperature was normal. Change sampling thermocouple for the next run. |
| 33447-1 | 10 | 3/31/67 | 2.51 | 300 39 | Program: 7% test and run tank pressurization. High oxidizer starting flow resulted in excessive combustion temperature. Adjust starting flow to previous level and repeat run. |

CONFIDENTIAL

CONFIDENTIAL

(C) Table XLV. 750K Preburner Test Summary (Continued)

| Preburner Rig No. | Preburner Run No. | Date | Test Duration, sec | Maximum Chamber Pressure Sought, Attained, psia psia | Remarks |
|----------------------|----------------------|---------|--------------------------|---|--|
| 33447-1 | 11 | 3/31/67 | 11.59 | 300 330 | Program: 7% test and run tank pressurization. Rig stabilized at 330 psia, but control system instability during tank pressurization ramps caused the high combustion temperature advance. Run procedure revised to ramp propellant tanks individually to prevent interaction between mixture ratio and chamber pressure control systems. |
| 33447-1 | 12 | 4/4/67 | 5.94 | 500 110 | Program: 7% test with individual tank ramps. High combustion temperature advance during transient to 7% thrust. Adjust control gains and repeat run. |
| 33447-1 | 13 | 4/4/67 | 11.59 | 500 435 | Program: 7% test with individual tank ramps. Slow response and instability in the oxidizer control system during oxidizer run tank pressurization caused an injector oxidizer differential pressure advance. Sequencer malfunction during the shutdown transient failed to provide the scheduled sequence of events. Injector purges were not energized and damage to the injector was detected, necessitating rig disassembly and inspection. |
| 33463-2A | 14 | 4/20/67 | 10.28 | 500 237 | Program: 15% test. Shutdown from 7% equivalent thrust just prior to tank ramps because of fuel system instability resulting from excessive gains in the mixer temperature control system. Gains reduced and run repeated. |

CONFIDENTIAL

(C) Table XLV. 250K Preburner Test Summary (Continued)

| Preburner Rig No. | Preburner Run No. | Date | Test Duration, sec | Maximum Chamber Pressure Sought, Attained, psia psia | Remarks |
|----------------------|----------------------|---------|--------------------------|---|---|
| 33463-2A | 15 | 4/22/67 | 27.93 | 500 477 | Program: 15% test. Shutdown from 15% equivalent thrust level because of fuel system instability resulting from saturation of the fuel control valve. Steady-state chamber pressure 477 psia. Prior to run No. 16, the mid-range fuel valve was armed to also control flow and throttle to higher level for checkout. This was the first successful attempt to pressurize the propellant run tanks without affecting the rig operation. |
| 33463-2A | 16 | 4/27/67 | 7.93 | 500 248 | Program: 35% test. Shutdown during transient to 7% equivalent thrust because of excessive combustion temperature profile distortion resulting from insufficient injector fuel area setting. Injector area reset and test repeated. |
| 33463-2A | 17 | 4/28/67 | 38.40 | 1270 1351 | Program: 35% test with engine mixture ratio of 6. Steady-state preburner pressure 1351 psia, combustion temperature approximately 1420°R. Attained all test objectives. Post-run inspection showed rig in good condition. |
| 33463-2A | 18 | 4/29/67 | 31.32 | 650 639 | Program: 20% test with cold flow. Fuel temperature decreased from 300°R to 190°R during 7% operation. During the transient to 20%, the combustion temperature dropped to the advance level (650°R) because of a malfunction of the facility fuel control system; the large fuel control valve opened during the run and caused a severe reduction in mixture ratio. |

CONFIDENTIAL

CONFIDENTIAL

544

(C) Table XLV. 250K Preburner Test Summary (Continued)

| Preburner Rig No. | Preburner Run No. | Date | Test Duration, sec | Maximum Chamber Pressure | | Remarks |
|----------------------|----------------------|--------|--------------------------|-----------------------------|-------------------|--|
| | | | | Sought, psia | Attained, psia | |
| 33463-2A | 19 | 5/2/67 | 62.97 | 650 | 730 | Program: 20% test with mixture ratio excursion and 300°R fuel. Attained all test objective with combustion temperatures of 1625°R, 1800°R, and 1350°R observed during mixture ratio excursion at 730 psia preburner pressure. Post-run rig condition good. |
| 33463-2A | 20 | 5/3/67 | 23.09 | 650 | 259 | Program: 20% test (same as run 19 except with an increased injector fuel area schedule). Run advanced during transition to 20% because of excessive combustion temperature caused by insufficient injector fuel differential pressure. Injector fuel area ramp rescheduled to decrease the rate of opening from 5 to 10 seconds for the next run. |
| 33463-2A | 21 | 5/3/67 | 37.02 | 650 | 684 | Program: 20% test (same as run 20 except with a 10-second rate of opening injector fuel area during transient to 20%). Run advanced during power lever ramp (preburner pressure level of 684 psia) due to deterioration of the temperature profile. Data indicated that the injector fuel area setting at the 20% level should be reduced from 75% to 55%. |

(C) Table XLV. 250K Preburner Test Summary (Continued)

| Preburner Rig No. | Preburner Run No. | Date | Test Duration, sec | Maximum Chamber Pressure Sought, psia | Attained, psia | Remarks |
|----------------------|----------------------|--------|--------------------------|---|-------------------|--|
| 33463-2A | 22 | 5/3/67 | 62.96 | 650 | 735 | Program: 20% test (same as run 21 except with injector fuel area setting of 55%). Fuel inlet temperature adjusted from 300°R to 280°R during power lever ramp. Attained all test objectives with combustion temperatures of 1625°R, 1850°R, and 1325°R observed during mixture ratio excursion at preburner pressure of 735 psia. Post-run rig condition good. |
| 33463-2A | 23 | 5/4/67 | 33.61 | 1950 | 1950 | Program: 50% test with mixture ratio excursion and 250°R fuel. At 50% level (approximately 1950 psia preburner pressure), the facility oxidizer system developed a leak causing oscillations in the preburner pressure. Test manually advanced. |
| 33463-2A | 24 | 5/5/67 | 33.50 | 1950 | 2002 | Program: 50% test (same as run 23). Rig ramped to the 50% level, but injector fuel area hung at 35% (scheduled to open to 75%) on power ramp. After approximately 5 seconds at steady-state at 2002 psia preburner pressure (1500°R combustion temperature), the injector fuel area drive system freed and the fuel area snapped open to the 75% setting. The rapid change in injector fuel differential pressure disrupted the combustion temperature profile and caused the abort shutdown. Post-run checks of the drive system revealed the problem to be in the injector. The rig was pulled from the test stand on 5 May 1967 and inspection revealed the idler gear galling with the pivot post. |

CONFIDENTIAL

346

CONFIDENTIAL

(C) Table XLV. 250K Preburner Test Summary (Continued)

| Preburner Rig No. | Preburner Run No. | Date | Test Duration, sec | Maximum Chamber Pressure Sought, Attained, psia psi | Remarks |
|----------------------|----------------------|---------|--------------------------|--|---|
| 33447-2 | 25 | 5/12/67 | 32.00 | 1950 90' | Program: 50% test (initial test with flow straightener). During the power lever ramp to 50%, run was advanced due to distorted temperature profile. Control temperature parameters went cold during the acceleration transient as the bulk combustion temperature was increasing. The divergent control temperatures caused a mixture ratio increase. The combustion temperature exceeded 3000°R for approximately 3 seconds, causing damage to the chamber liners, flow straightener assembly, and temperature spikes. No injector damage was detected. The rig was pulled from the test stand on 13 May 1967. |
| 33463-3 | 26 | 5/13/67 | 6.42 | 1950 170 | Program: 50% test. Test advanced during transient to 7% because of a malfunction of the control system. The run was normal with minimum transient combustion temperature of 990°R or 340°R above the low temperature advance limit. |
| 33463-3 | 27 | 5/14/67 | 6.38 | 1950 160 | Program: 50% test. Manually aborted during transient to 7% because of low combustion temperature caused by slow oxidizer system response to the control valve opening. Vacillating flow vent valve leaking. |
| 33463-3 | 28 | 5/15/67 | 6.43 | 1950 172 | Program: 50% test. Manually aborted during transient to 7% because of low oxidizer starting flow which caused a significant increase in the system fill time. Flow rate was adjusted to establish the level and test was repeated. |

CONFIDENTIAL

(C) Table XLV. 250K Preburner Test Summary (Cont. next)

| Preburner Rig No. | Preburner Run No. | Date | Test Duration, sec | Sought, psia | Maximum Chamber Pressure Attained, psia | Remarks |
|----------------------|----------------------|--------|--------------------------|-----------------|--|--|
| 33447-3 | 32 | 6/2/67 | 4.6 | 20 | 32 | Starting flow test to evaluate shutdown purges and temperature spike from ignition levels. No rig deterioration. Run successful for full duration. No temperature spike, purges on as scheduled. Temperature spike to 1700°K, steady-state temperature was 1600°K, sequenced shutdown. |
| 33447-3 | 33 | 6/3/67 | 17.2 | 300 | 298 | Program: 7% hot firing test to check temperature spike and establish back flow protection. There was a 2800°K spike at shutdown and consequently high temperature abort. Purges worked well; sequenced shutdown. |
| 33447-3 | 34 | 6/4/67 | 8.6 | 3450 | 225 | Program: 90% hot firing test to establish performance and temperature profile for staged combustion rig operation. Automatic advance on high temperature as CV6 and CV46 went on control prior to tank ramps. High combustion temperature advance when energizing pressure control because of system shift resulting from erratic control transducer (oscillating between 190-225 psia) high temperature advance shutdown. |

89
CONFIDENTIAL

Best Available Copy

(C) Table XLV. 250K Preburner Test Summary (Continued)

| Preburner Rig No. | Preburner Run No. | Date | Test Duration, sec | Maximum Chamber Pressure | | Remarks |
|----------------------|----------------------|---------|--------------------------|-----------------------------|-------------------|--|
| | | | | Sought, psia | Attained, psia | |
| 33447-3 | 39 | 6/26/67 | 10.1 | 3450 | 310 | Program: 80% hot firing test. Same as previous test except reset reference flows for flowmeter control, and incorporate variable liquid fuel density circuit. Run was shutdown because of high combustion temperature caused by erratic LH ₂ flow signal. Post-run checks showed LH ₂ flowmeter vidar was emitting a bad signal, input to vidar from flowmeter was good. |
| | 40 | 6/26/67 | 00.1 | 3450 | 31 | Program: 80% hot firing test. This test was automatically shut down just after start because of false liquid fuel depletion signal. |
| | 41 | 6/27/67 | 25.3 | 3450 | 1800 | Program: 80% hot firing test. This test was shut down during power ramp to 80% because of high combustion temperature. Data review showed good preburner operation. Selected new combustion temperature control parameters. |
| 33447-3 | 42 | 6/27/67 | 15.4 | 3450 | 307 | Program: 80% hot firing test. Test was automatically shut down just before the power ramp because of false fuel depletion signal. |
| | 43 | 6/27/67 | 8.7 | 3450 | 298 | Program: 80% hot firing test. Test was automatically shut down by faulty burnwire sampling circuit. |

(C) Table XLV. 250K Preburner Test Summary (Continued)

| Preburner Rig No. | Preburner Run No. | Date | Test Duration, sec | Maxim Chamber Pres Sought, psia | Attained, psia | Remarks |
|----------------------|----------------------|---------|--------------------------|--|-------------------|---|
| 32447-3 | 44 | 6 28 67 | 1.1 | 3450 | | Program: 80% hot firing test. Test automatically shut down by a malfunction of the burnwire sampling circuit. Data indicated a normal start and the burnwire was burned out in 0.5 second (normal 0.7 sec). |
| 33447-3 | 45 | 6 28 67 | 27.0 | 3450 | 2950 | Program: 80% hot firing test. Test automatically shut down during power ramp because of high combustion temperature. Control data indicated the gains on the LH ₂ were too low when flow was within the 200 gpm error band causing a lag in the fuel flow acceleration. |
| 33447-3 | 46 | 6 28 67 | 31.34 | 3450 | 3450 | Program: 80% hot firing test. Reset the LH ₂ flow error band to 100 gpm and reset the low LH ₂ integral gain (K _i) to 9%. LIFT/lb _m /sec ² . Run was successful 80% hot firing test. Preburner pressure was 3450 psia and all parameters were stable. After 4 seconds of steady-state operation the run was automatically shut down because of a fire on the test stand. It was determined that a small oxidizer leak had developed in the dose-to-injector O-ring seals. Damage to the dome housing necessitated pulling the rig for inspection. |

552
CONFIDENTIAL

CONFIDENTIAL

(C) Table XLV. 250K Preburner Test Summary (Continued)

| Preburner Rig No. | Preburner Run No. | Date | Test Duration, sec | Sought, psia | Maximum Chamber Pressure Attained, psia | Remarks |
|----------------------|----------------------|---------|--------------------------|-----------------|--|---|
| 33447-4 | 47 | 7/14/67 | 17.9 | 1950 | 188 | Program: 50% hot firing test. Run was advanced to shut down after completion of tank ramps because of insufficient oxidizer flow to rig. CV6 closed because of leakage out CV4 vent system. Restroke valve (CV4) to reseal and repeat test. |
| 33447-4 | 48 | 7/14/67 | 14.4 | 1950 | 188 | Program: 50% hot firing test. Run was advanced to shut down during tank ramps because of another leak in CV4. New seal put in valve. It was then determined that oscillations induced in the oxidizer system by the tank pressurizing valve contributed to the faulty flow signal. |
| 33447-4 | 49 | 16/67 | 6.3 | 1950 | --- | Program: 50% hot firing test. Run was advanced to shut down during transient to 7% by low combustion temperature. Low temperature caused by excessive injector fuel area setting. Readjusted fuel control valve ramp timing during transient. |
| 33447-4 | 50 | 7/16/67 | 26.0 | 1950 | 2300 | Program: 50% hot firing test. Run was advanced to shut down just after reaching 50% because of leakage past large oxidizer pump simulator valve (CV5). The extra oxidizer caused rapid increase in combustion temperature and pressure. The valve (CV5) was disarmed for the next test. |

(C) Table XLV. 250K Preburner Test Summary (Continued)

| Preburner Rig No. | Preburner Run No. | Date | Test Duration, sec | Maximum Chamber Pressure Sought, psia | Attained, psia | Remarks |
|----------------------|----------------------|---------|--------------------------|--|-------------------|--|
| 33447-4 | 51 | 7 16 67 | 37.7 | 1450 | 1990 | Program: 50% hot firing test. Program complete. Data analysis showed improved, but insufficient temperature profile. Oxidizer leak out dome O-ring seals neces- sitated pulling the rig. |
| 33447-5 | 52 | 7 22 67 | 5.8 | 1500 | 45 | Program: 50% hot firing test (r = 6). Rig configuration includes injector with concentric fuel annuli and counter-rotating oxidizer flow pattern, 3.4-inch diameter back pressure nozzle. Run was advanced during transient to 7 because of excessive com- bustion temperature caused by excessive delay of fuel pressure buildup. Reschedule CV46 to open 400 milliseconds earlier and repeat test. |
| 33447-5 | 53 | 7 22 67 | 5.2 | 1500 | 23 | Program: 50% hot firing test (r = 6). Run was advanced after 5.2 sec because of excessive starting oxidizer flow. Reprogram starting flow rates and repeat test. |
| 33447-5 | 54 | 7 22 67 | 27.6 | 1500 | 1507 | Program: 50% hot firing test (r = 6). Full duration test with approximately 2-sec steady-state run duration at 50% flows. |

554
CONFIDENTIAL

CONFIDENTIAL

(C) Table XLV. 250K Preburner Test Summary (Continued)

| Preburner Rig No. | Preburner Run No. | Date | Test Duration, sec | Sought. psia | Maximum Chamber Pressure Attained, psia | Remarks |
|----------------------|----------------------|---------|--------------------------|-----------------|--|---|
| 33447-5 | 55 | 7/22/67 | 1.9 | 3450 | 35 | Program: 100% hot firing test (r = 6). Run advanced because of high combustion temperature caused by excessive injector fuel area setting. Reschedule fuel area and repeat test. |
| 33447-5 | 56 | 7/22/67 | 2.5 | 3450 | 24 | Program: 100% hot firing test (r = 6). Run advanced because of low combustion temperature caused by insufficient oxidizer flow. Reschedule oxidizer flow and repeat test. |
| 33447-5 | 57 | 7/23/67 | 26.7 | 3450 | 2181 | Program: 100% hot firing test (r = 6). Run advanced during the acceleration ramp because of inadvertent low setting on injector fuel differential pressure advance circuit. Reschedule the advance level and repeat test. |
| 33447-5 | 58 | 7/23/67 | 31.0 | 3450 | 3400 | Program: 100% hot firing test (r = 6). Program duration test with approximately 2-sec steady-state run duration at rated flows. |
| 33447-5 | 59 | 7/24/67 | 3.6 | 3450 | 28 | Program: 100% hot firing test (r = 6) for 6 sec and pulse test. Run advanced during starting flow level because of high combustion temperature caused by excessive oxidizer flow. Reset flow rates and repeat test. |

(C) Table XLV. 250K Preburner Test Summary (Continued)

| Preburner Rig No. | Preburner Run No. | Date | Test Duration, sec | Maximum Chamber Pressure | | Remarks |
|----------------------|----------------------|---------|--------------------------|-----------------------------|-------------------|---|
| | | | | Sought, psia | Attained, psia | |
| 33447-5 | 60 | 7-24-67 | 31.9 | 3650 | 3484 | Program: 100% hot firing (r = 6) and pulsing test. Test advanced by high oxidizer differential pressure circuit, OPADH; was normal 575 psia and circuit should not have been energized until 600 psia. Profile good with T_{max} -Avg. 276°K. All pulse charges (20, 30, 40, and 80 grains) detonated during the test before sequenced to fire. |
| 33447-5 | 61 | 7-24-67 | 26.6 | 3602 | 3850 | Program: 100% hot firing (r = 5). The test was terminated during the transition to 100% because of fuel flow oscillations and resultant high injector differential pressure. Data analysis indicated the low fuel control gain settings were energized too late in the acceleration ramp. Resequenced the low fuel gains to energize 1.150 sec earlier and reset the low integral gain (K_i) to 2% lb_m/sec^2 to prevent fuel ramp delay. |
| 33447-5 | 62 | 7-25/67 | 35.0 | 3602 | 3600 | Program: 100% hot firing (r = 5). Full duration test with all test objectives accomplished. Energized the four pulse gun circuits for a final evaluation of the control system. |

(C) Table XLV. 250K Preburner Test Summary (Continued)

| Preburner Run No. | Preburner Run No. | Date | Test Duration, sec | Sought, psia | Manifold Chamber Pressure, psia | Attained, psia | Remarks |
|----------------------|----------------------|---------|--------------------------|-----------------|---------------------------------------|-------------------|---|
| 33447-3 | 63 | 7/25/67 | 3.4 | 333 | 28 | | Program: 100% stability test with cold fuel, $r = 6$. Run was advanced during transient to 7% because of high combustion temperature caused by excessive oxidizer starting flow. |
| 33447-5 | 64 | 7/26/67 | 35.1 | 333 | 326 | | Program: 100% stability test with cold fuel, $r = 6$. Successful test with all test objectives accomplished. Charges of 20, 20, 40, and 80 grains were detonated within 220 milliseconds and the combustion system remained stable. The injector fuel inlet temperature was 101°R during the pulsing period. |
| 33447-5 | 65 | 7/26/67 | 28.7 | 300 | 490 | | Program: 20% stability test with cold fuel, $r = 6$. Successful test with none of the four charges exciting the combustion system. Injector fuel inlet temperature was 118°R during the pulsing period. |
| 33447-5 | 66 | 7/26/67 | 35.1 | 3298 | 3765 | | Program: 100% hot firing test, $r = 7$. Accomplished all test objectives. Post-run r/p condition good except for some burning on the temperature rakes. Change back pressure simulator nozzle from 3.40 to 3.28-inch diameter for simulation of stage combustion starting pressures. |

CONFIDENTIAL

CONFIDENTIAL

(C) Table XLV. 450K Preburner Test Summary (Continued)

| Preburner Rig No. | Preburner Run No. | Date | Test Duration, sec | Sought, psi | Maximum Chamber Pressure Attained, psi | Remarks |
|----------------------|----------------------|---------|--------------------------|----------------|---|---|
| 33447-5 | 67 | 7/29/67 | 28.0 | 333 | 1025 | Program: 20% and 100% hot firing tests to evaluate transient combustion temperature profile. The test was advanced during the transient from 20% to 100% rated flows because of a faulty injector oxidizer differential pressure signal. |
| 33447-5A | 68 | 7/30/67 | 27.0 | 333 | 978 | Program: 20% and 100% hot firing test to evaluate transient combustion temperature profile. The test was advanced during the transient from 20% to 100% rated flows because of high preburner combustion temperature caused by oxidizer pump simulator valve malfunction. |
| 33447-5B | 69 | 7/31/67 | 5.4 | 500 | | Program: 20% hot firing test to evaluate 6.1 lb/sec fuel shutdown purge. The run was advanced during start transient by low preburner combustion temperature. |
| 33447-5B | 70 | 8/1/67 | 6.7 | 500 | | Program: 20% hot firing test to evaluate cold GN2 purge of fuel manifold prior to start on fill time of norwood elements. Run advanced by faulty burnwire circuit. |

CONFIDENTIAL

CONFIDENTIAL

(C) Table ZLV. 250X Preburner Test Summary (Continued)

| Preburner Rig No. | Preburner Run No. | Date | Test Duration, sec | Maximum Chamber Pressure | | Remarks |
|----------------------|----------------------|--------|--------------------------|-----------------------------|-------------------|---|
| | | | | Sought, psia | Attained, psia | |
| 33447-5B | 71 | 8/1/67 | 26.4 | 500 | | Program: Repeat of run 70. Run made for full duration. Start transient still exhibited dip in combustion temperature at +5.3 sec after start. |
| 33447-5B | 72 | 8/1/67 | 26.3 | 500 | | Program: 20% hot firing to evaluate start transient. Run full duration. Combustion temperature dipped low at +3 sec after start and again at +5.5 sec after start. Pull preburner rig for incorporation of injector in staged combustion rig. |

CONFIDENTIAL

(C) Table 117. 250K Preburner Test Summary (Continued)

| Rig No. Staged Combustion Preburner | Preburner Run No. | Date | Test Duration, sec | Maximum Chamber Pressure Sought. psia | Attained, psia | Remarks |
|--|----------------------|---------|--------------------------|---|-------------------|--|
| 35108-1 33463-5 | 73 | 8/14/67 | 2.2 | 3050 | 20 | Program: Acceleration to 100% thrust with data points at 20% and 100% to check out engine startup and shutdown sequence and to evaluate combustion performance and cooling requirements. Test aborted by erroneous main chamber CH ₂ coolant ΔP signal. |
| 35108-1 33463-5 | 74 | 8/16/67 | 1.3 | 1050 | 20 | Program: Acceleration to 3% thrust with a data point at 20% to check out engine startup and shutdown sequence and to evaluate combustion performance and cooling requirements. Test aborted by high preburner temperature during initial propellant fill period. |
| 35108-1 33463-5 | 75 | 8/16/67 | 3.1 | 1050 | 20 | Program: Same as run No. 74. Test aborted by low preburner temperature during initial propellant fill period. |
| 35108-1 33463-5 | 76 | 8/17/67 | 5.3 | 1050 | 30 | Program: Same as run No. 74. Test aborted by low preburner temperature during initial propellant fill period. |
| 35108-1 33463-5 | 77 | 8/18/67 | 5.3 | 1050 | 30 | Program: Same as run No. 74. Test aborted by low preburner temperature during initial propellant fill period. |
| 35108-1 33463-5 | 78 | 8/18/67 | 5.3 | 1050 | 30 | Program: Same as run No. 74. Test aborted by low preburner temperature during initial propellant fill period. |

CONFIDENTIAL

CONFIDENTIAL

(C) Table XLV. 250K Preburner Test Summary (Continued)

| Rig No. Stage Combustion Preburner | Preburner Run No. | Date | Test Duration, sec | Maximum Chamber Pressure, psia | Sought, psia | Attained, psia | Remarks |
|---|----------------------|---------|--------------------------|--------------------------------------|-----------------|-------------------|--|
| 35108-1 33463-5 | 79 | 8/18/57 | 27.5 | 1050 | | | Program: Same as run No. 74. Acceleration was satisfactory. Post-test inspection of the rig was good. |
| 35108-1 33463-5 | 80 | 8/19/57 | 5.4 | 1600 | | | Program: Acceleration to 50% thrust with data points at 20 and 50%. Test aborted by high preburner temperature during acceleration to 7% thrust. The main injector, cooled chamber, and primary nozzle case were damaged when high pressure CH ₂ coolant was introduced during post-test purge. |
| 35108-1A 33463-5 | 81 | 8/27/57 | 0.9 | 2400 | | | Program: Acceleration to 75% with data points at 20 and 50% to check out engine startup and shutdown sequence and to evaluate combustion performance and cooling requirements. Test aborted by high preburner temperature during initial pre-pellant fill period. |
| 35108-1A 33463-5 | 82 | 8/27/57 | 5.9 | 2400 | | | Program: Same as run No. 81. Test aborted by high preburner temperature during ramp from starting flows to the 7% thrust level. |
| 35108-1A 33463-5 | 83 | 8/28/57 | 9.5 | 2400 | | | Program: Same as run No. 81. Test aborted by low preburner temperature. Preburner flamed out during ramp to 7% thrust. |

CONFIDENTIAL

CONFIDENTIAL

() Table IV. 25% Preburner Test Summary (Continued)

| Rig No. Staged Combustion Preburner | Preburner Run No. | Date | Test Duration | Maximum Temperature psi | Remarks |
|--|----------------------|---------|------------------|-------------------------------|--|
| 35108-1A 33463-5 | 81 | 8/28/67 | 1.2 | 2400 | Program: Same as run No. 81. Test aborted by high preburner temperature during initial propellant fill period. |
| 35108-1A 33463-5 | 85 | 8/29/67 | 10.5 | 2400 | Program: Same as run No. 81. Test aborted by low preburner temperature. Preburner flamed out during initial propellant fill period. |
| 35108-1A 33463-5 | 86 | 8/29/67 | 0.8 | 2400 | Program: Same as run No. 81. Test aborted by high preburner temperature during initial propellant fill period. |
| 35108-1A 33463-5 | 87 | 8/30/67 | 7.3 | 2400 | Program: Same as run No. 81, except preburner ignition flows increased from 2 to 7%. Test advanced during run tank pressurization ramps because of high preburner temperature. The advance was attributed to inadvertent failure to arm oxidizer control valves to flow control. |
| 35108-1A 33463-5 | 89 | 8/30/67 | 29.4 | 2400 | Program: Same as run No. 87. Test was completed per program. No coolant supplied to primary or secondary nozzles and maximum skin temperature was 1200°F on the primary nozzle. No post-test parts distress noted. |

CONFIDENTIAL

CONFIDENTIAL

(C) Table XIV. 250K Preburner Test Summary (Continued)

| Rig No. Staged Combustion Preburner | Preburner Run No. | Date | Test Duration, sec | Maximum Chamber Pressure | | Remarks |
|--|----------------------|---------|--------------------------|-----------------------------|-------------------|---|
| | | | | Sought, psia | Attained, psia | |
| 35108-1A 33463-3 | 84 | 8/30/67 | 32.6 | 3150 | 3020 | Program: Acceleration to 100% with data points at 20 and 50% initial test using translating secondary nozzle. Water coolant to primary and secondary nozzles through test except during sampling probe data points. Test was completed per program. No parts distress detected. |
| 35108-1B 33463-5 | 90 | 9/1/67 | 35.6 | 3150 | 3090 | Program: Same as run No. 89. Test was completed per program. No parts distress noted. |
| 35108-1C 33463-5 | 91 | 9/8/67 | 35.9 | 3150 | 3095 | Program: Same as run No. 89, except main chamber cooling flow reduced 11%. Test was completed per program. No parts distress noted. |
| 35108-1B 33463-5 | 92 | 9/9/67 | 35.9 | 3150 | 3060 | Program: Same as run No. 89, except preburned mixture ratio adjusted to operate at nominal 0.7 at 100%. Test was completed per program. |
| 35108-1C 33463-5 | 93 | 9/12/67 | 35.9 | 3150 | 3120 | Program: Same as run No. 92. Test completed per program. No parts distress detected. |
| 35108-1C 33463-5 | 94 | 9/15/67 | 36.4 | 3150 | 3130 | Program: Same as run No. 92. Results same. |

CONFIDENTIAL

CONFIDENTIAL

(C) Table XLV. 250K Preburner Test Summary (Continued)

| Rig No. Staged Combustion Preburner | Preburner Run No. | Date | Test Duration, sec | Maximum Chamber Pressure Sought, psia | Attained, psia | Remarks |
|--|----------------------|---------|--------------------------|--|-------------------|--|
| 35108-1C 33463-5 | 95 | 9/15 67 | 36.4 | 3150 | 2953 | Program: Same as run No. 92. Results same. |
| 35108-1C 33463-5 | 96 | 9/18 67 | 1.4 | 3150 | 25 | Program: Same as run No. 92. Test advanced by main chamber hydrogen coolant ΔP . The advance was attributed to erroneous ΔP limit. |
| 35108-1C 33463-5 | 97 | 9/18 67 | 26.5 | 3150 | 2400 | Program: Same as run No. 92. Test advanced by high preburner combustion temperature. |
| 35108-1C 33463-5 | 98 | 9/19 67 | 36.4 | 3150 | 2880 | Program: Same as run No. 92 except mixture ratio adjusted to operate at a nominal 0.65 at 100%. Test completed per program. No parts distress detected. |
| 35111-1 33463-6 | 99 | 9/28 67 | 3.8 | 650 | 40 | Program: Acceleration to 20% with main chamber combustion stability investigation at steady state. Test advanced by low main igniter combustion temperature. Advance attributed to incorrect instrumentation hookup. |
| 35111-1 33463-5 | 100 | 9/28 67 | 19.5 | 650 | 594 | Program: Same as run No. 99. Test completed per program. |

CONFIDENTIAL

CONFIDENTIAL

(C) Table XLV. 250K Preburner Test Summary (Continued)

| Rig No. Staged Combustion Preburner | Preburner Run No. | Date | Test Duration, sec | Maximum Chamber Pressure Sought, psia | Attained, psia | Remarks |
|--|----------------------|---------|--------------------------|--|-------------------|---|
| 35111-1 33463-6 | 101 | 9/29/57 | 28.7 | 3150 | 3030 | Program: Acceleration to 20 and 100% with main chamber combustion stability investigation at 100%. Test advanced by low main chamber coolant ΔP . Advance occurred before combustion stability investigation. |
| 35111-1 33463-6 | 102 | 9/29/57 | 24.9 | 3150 | 1880 | Program: Same as run No. 101. Test advanced by high main chamber coolant ΔP . |
| 35111-1 33463-6 | 103 | 9/30/57 | 31.4 | 3150 | 3180 | Program: Same as run No. 101. Test completed per program. No parts distress noted. |
| 35111-1 33463-6 | 104 | 9/30/57 | 30.6 | 2700 | 2770 | Program: Same as run No. 101. Test completed per program. |

CONFIDENTIAL

CONFIDENTIAL

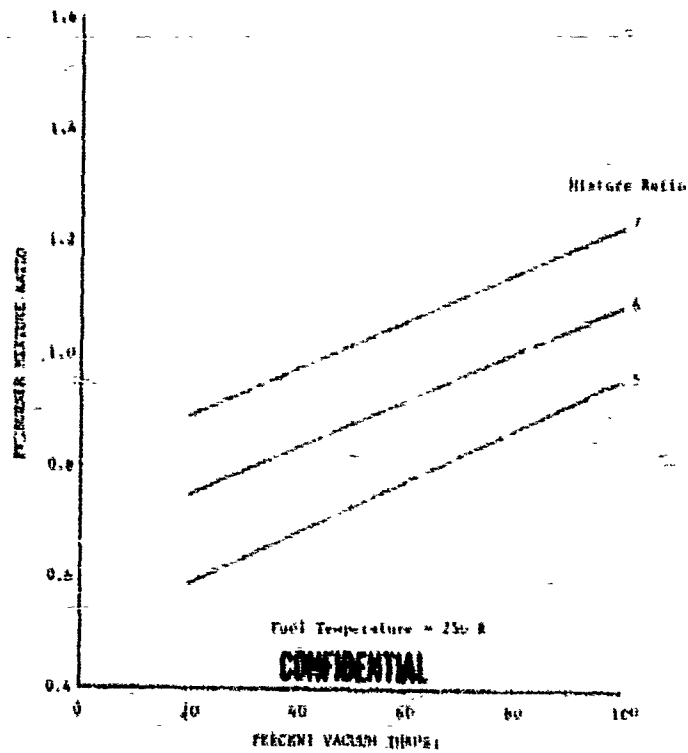


Figure 561, Preburner Mixture Ratio
vs Percent Vacuum Thrust
ADP Demonstration Engine

DF 59530

CONFIDENTIAL

CONFIDENTIAL

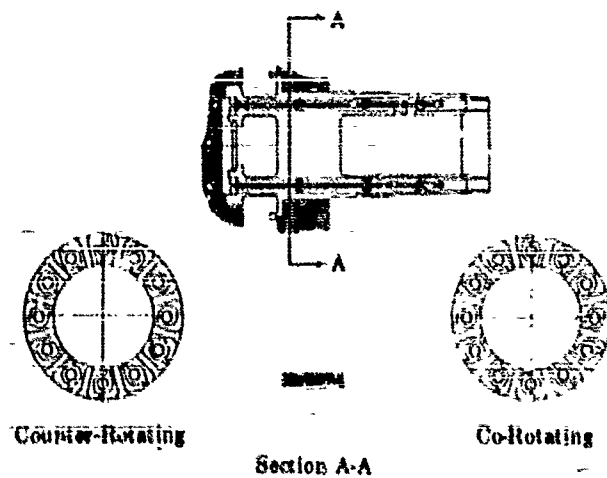


Figure 542. Alternative Secondary Slot Configuration

FD 20083

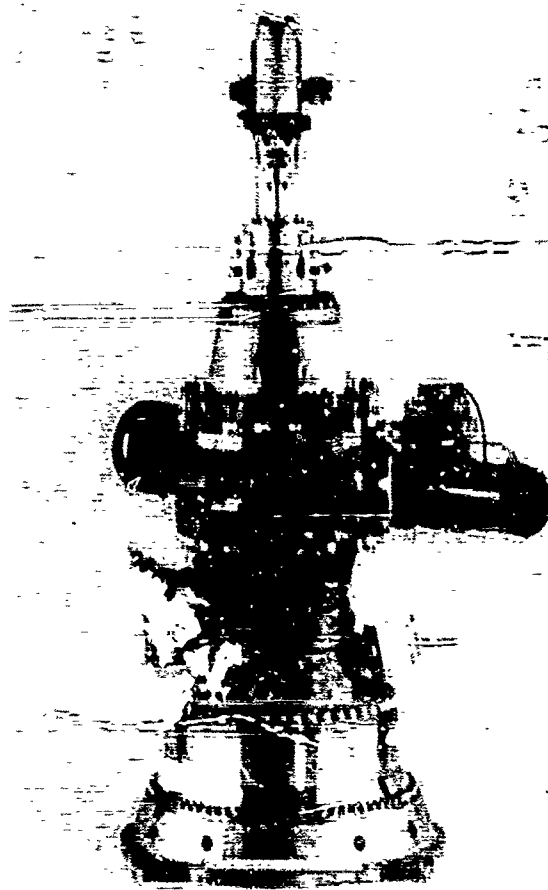


Figure 543. 250K Preburner Test Rig Assembled for Test

FE 66403

567

CONFIDENTIAL

THIS PAGE CONTAINS SUBJECT MATTER COVERED BY A SECURITY ORDER WITH A MODIFYING SECURITY REQUIREMENTS PERMIT ISSUED BY U.S. COMMISSIONER OF PATENTS

CONFIDENTIAL

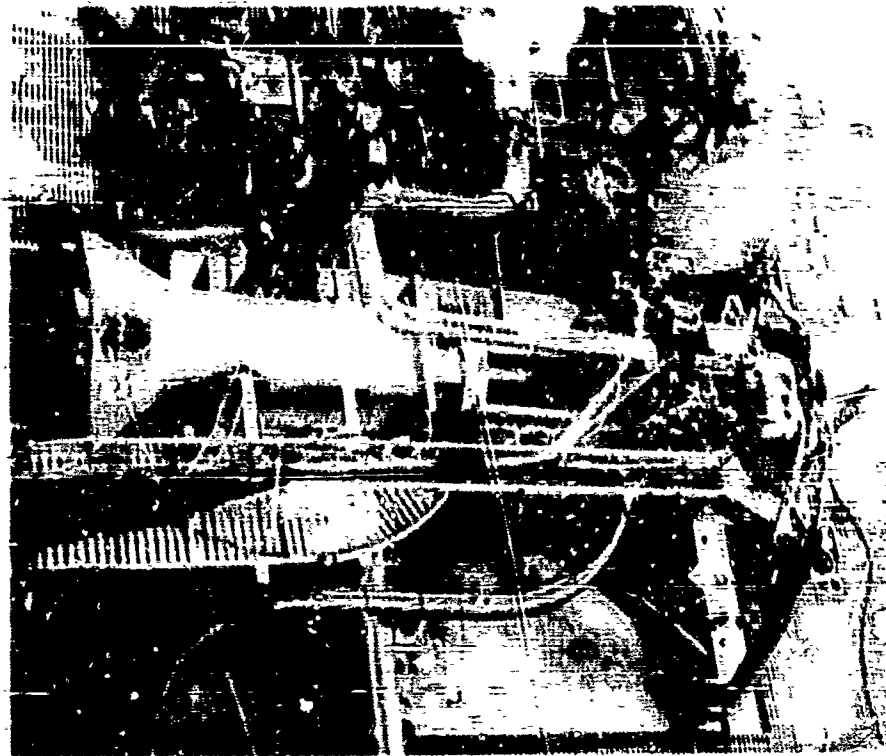


Figure 546, 250K Preburner Test Rig
Installed in Test Facility

FC 14324

(C) The early portion of the test program was directed to the investigation of the ignition and start transient requirements. The early tests were of short duration to assure that the torch igniter, which had been checked out in separate component tests, could consistently ignite the preburner. These tests are shown in Figure 545. After the test rig ignition sequence was established, the transition from starting flows to the 7% operating level was investigated, and the start operating procedures were established to permit operation to the 7% level and above. Figure 546 describes a typical acceleration transient from 1% to 7% preburner operation.

(V) During early preburner testing, several injector elements were damaged because of a backflowing condition that occurred at shutdown. The injector flow reversal (fuel-rich combustion products backflowed into the oxidizer system) caused burn damage to the injector elements, as shown in Figure 547. The delays resulting from the injector damage were minimized because of the preburner injector design, which permits easy removal and replacement of the individual elements, as described in Figure 548. The repaired injectors were ready for further testing, generally within three days. Figures 549 and 550 show the repaired injector configuration. In addition to repairing the injectors, a salvage technique was developed for the damaged nozzle that removed the damaged entry slot section, as shown in Figure 551, and replaced it with a new end section, shown in Figure 552.

CONFIDENTIAL

CONFIDENTIAL

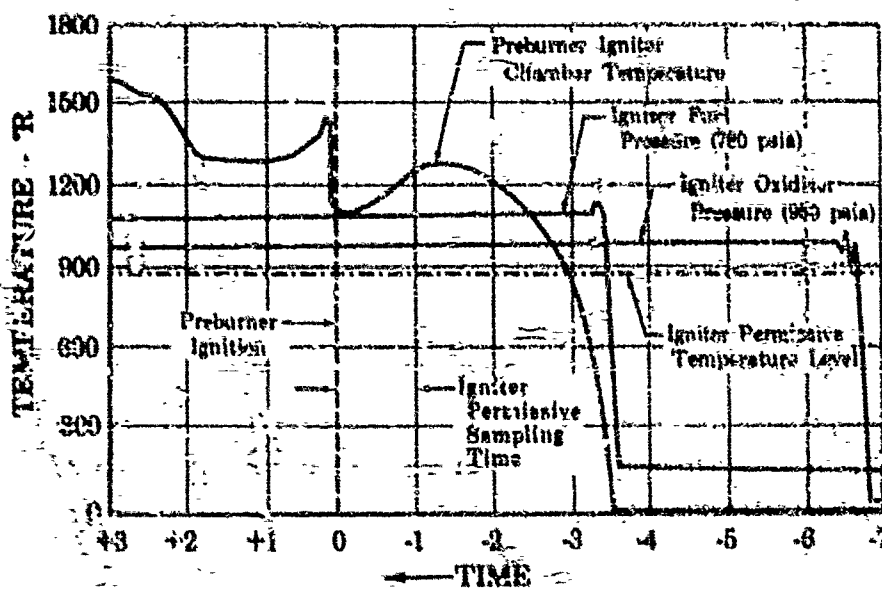


Figure 545. 550K Torch Igniter Start Transient FD 21398
on Preburner Test Rig (Run 22)

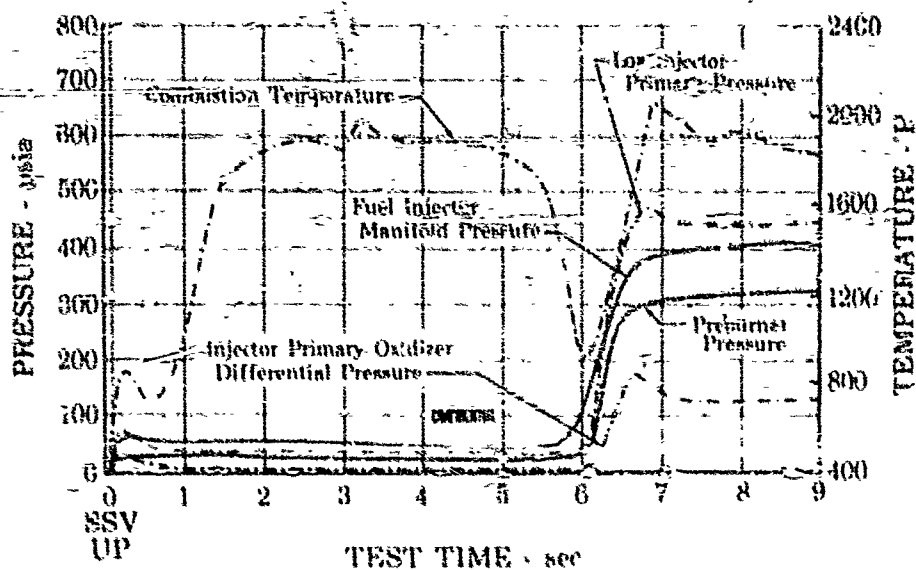


Figure 546. 250K Preburner Test Rig
(Run 6)

FD 21406

CONFIDENTIAL

CONFIDENTIAL



Figure 547. 250K Preburner Injector - View
Showing Built Damage to Dual-
Griff Oxidizer Nozzles in
Plane of Transfer and Entry
Slots

FB 88544

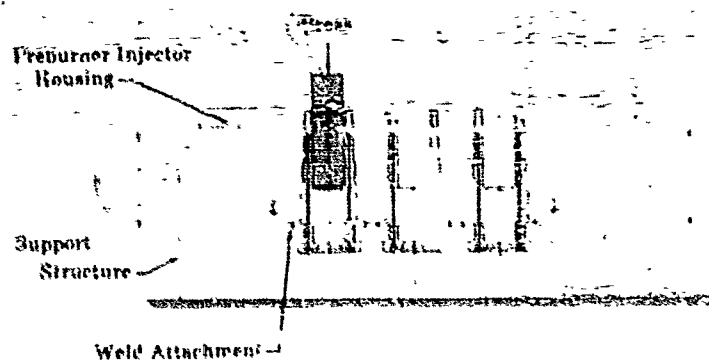


Figure 548. Schematic of 250K Preburner
Injector Showing Method of
Removal of Damaged Dual-
Griff Oxidizer Nozzle

FD 18116A

CONFIDENTIAL

CONFIDENTIAL

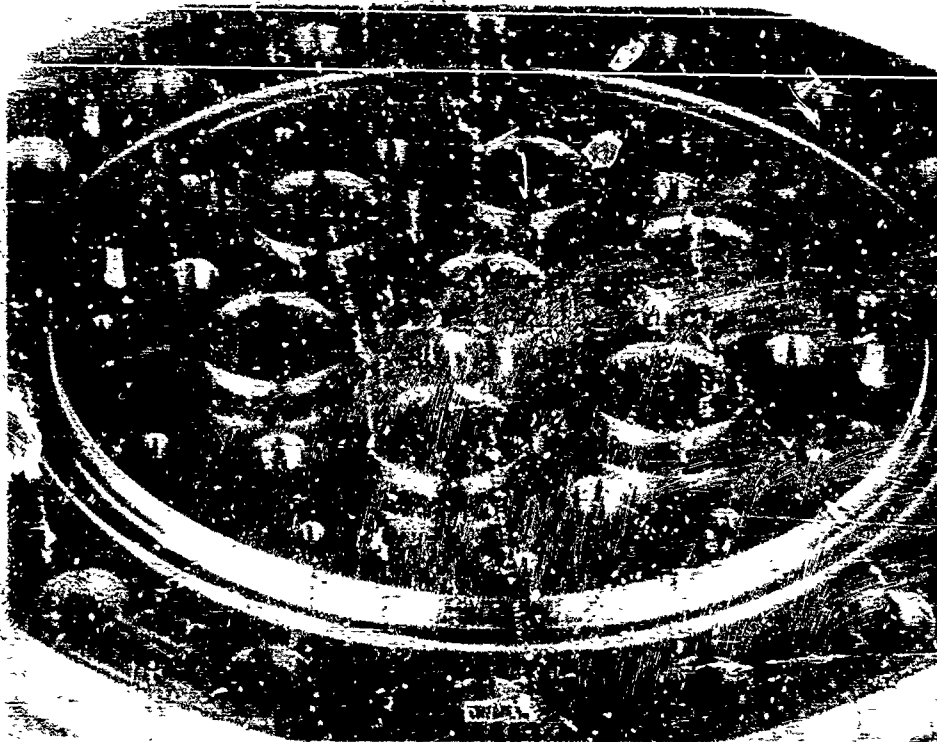


Figure 549. 250K Preburner Injector - View Showing FE 68895
the Injector from Test Rtg F-33447-1
After Replacement of Five Damaged Dual-
Orifice Oxidizer Nozzles, View 1.

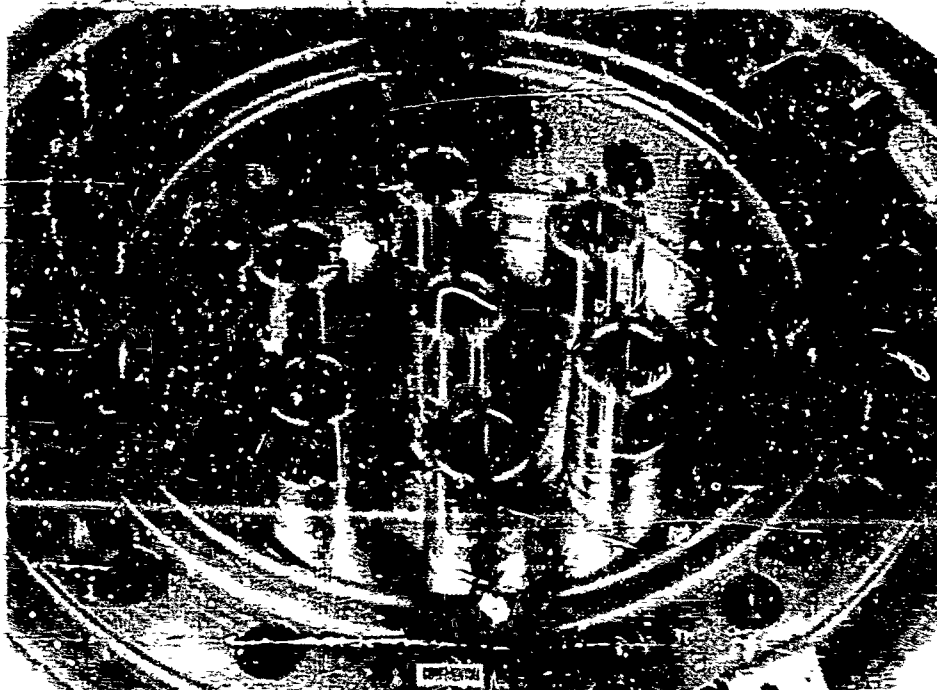


Figure 550. 250K Preburner Injector - View Showing FL 68896
the Injector from Test Rtg F-33447-1
After Replacement of Five Damaged Dual-
Orifice Oxidizer Nozzles, View 2.

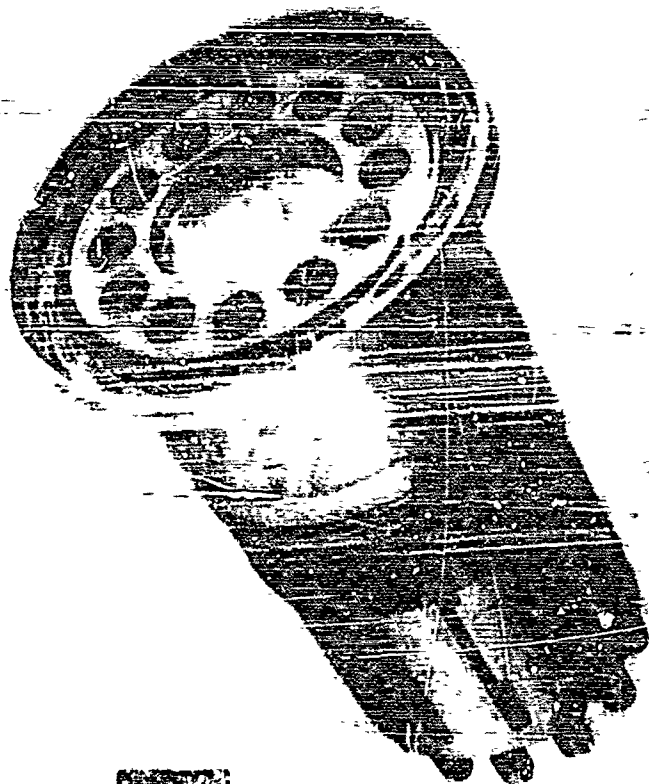
571

CONFIDENTIAL

THIS PAGE CONTAINS SUBJECT MATTER COVERED BY A TECHNICAL
ORDER WITH PROHIBITORY EFFECTS. IT IS TO BE KEPT IN U.S. GOVERNMENT
POSSESSION OR CONTROL.

THIS PAGE CONTAINS SUBJECT MATTER COVERED BY A TECHNICAL
ORDER WITH PROHIBITORY EFFECTS. IT IS TO BE KEPT IN U.S. GOVERNMENT
POSSESSION OR CONTROL.

CONFIDENTIAL



CONFIDENTIAL

Figure 531. 250K Preburner Injector Dual-Orifice Oxidizer Nozzle View Showing a Nozzle Unit With Damaged Slot Section Removed FR 68732

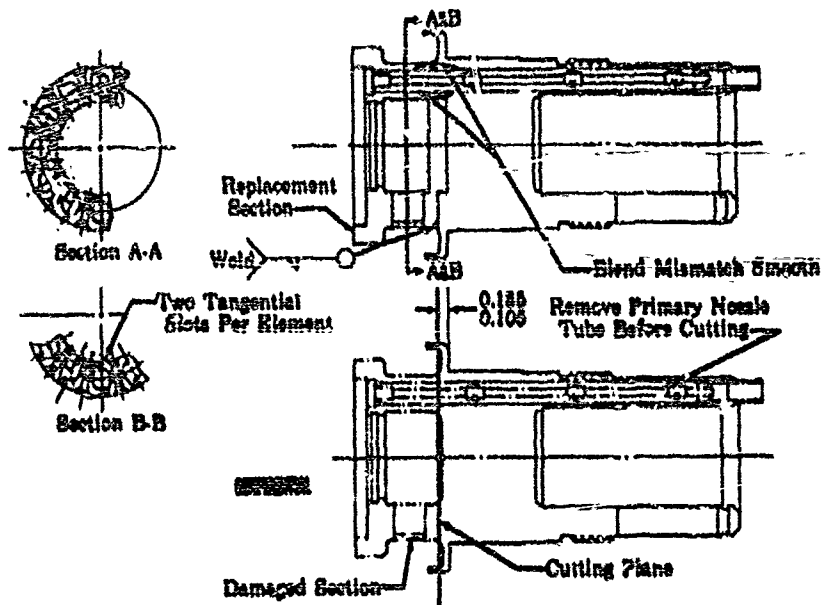


Figure 532. Schematic of 250K Preburner Injector Dual-Orifice Nozzle Assembly Showing the Replacement of Damaged Entry Slot Section FD 21408

CONFIDENTIAL

(G) To prevent a recurrence of the backflow conditions and to obtain a reduced shutdown temperature spike, an analysis of the injector purge requirements was completed. This analysis indicated that the problem could be corrected by adding an additional purge port that would remove the oxidizer from the flow divider valve and injector passages after shutdown. This additional purge port, shown in figure 553, would provide a 50% increase in the gaseous nitrogen purge flow. As an added precaution, the purge passages to the primary and secondary cavities were increased to provide increased flow, and orifices were installed to better control the purge flow rate. It was determined that primary and secondary purge rates of 0.02 lb/sec and 0.20 lb/sec, respectively, were required to purge the primary and secondary cavities and maintain an injector cavity pressure that would prevent injector backflow. Prior to run No. 32, the modified preburner purge systems that are shown in figure 554, were incorporated. The results of subsequent tests indicated that the modified preburner injector purge systems satisfactorily protected the preburner injector and reduced the shutdown temperatures.

(U) During the Phase I test program, three preburner injector configurations were tested. The original variable fuel area configuration consisted of an inner and outer fuel annuli surrounding the 12 oxidizer nozzle elements, as shown in figure 516. The initial preburner tests (run No. 1 to 46) indicated that this injection configuration provided an unacceptable temperature profile at the higher operating pressures, which are shown in figure 555.

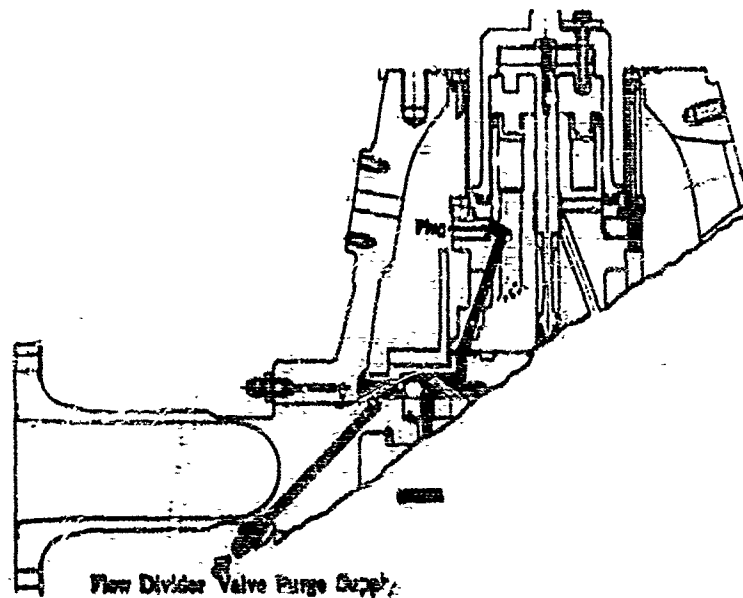


Figure 553. Revised 350K Preburner Injector
Oxidizer Purge Schematic

FD 19733B

CONFIDENTIAL

CONFIDENTIAL

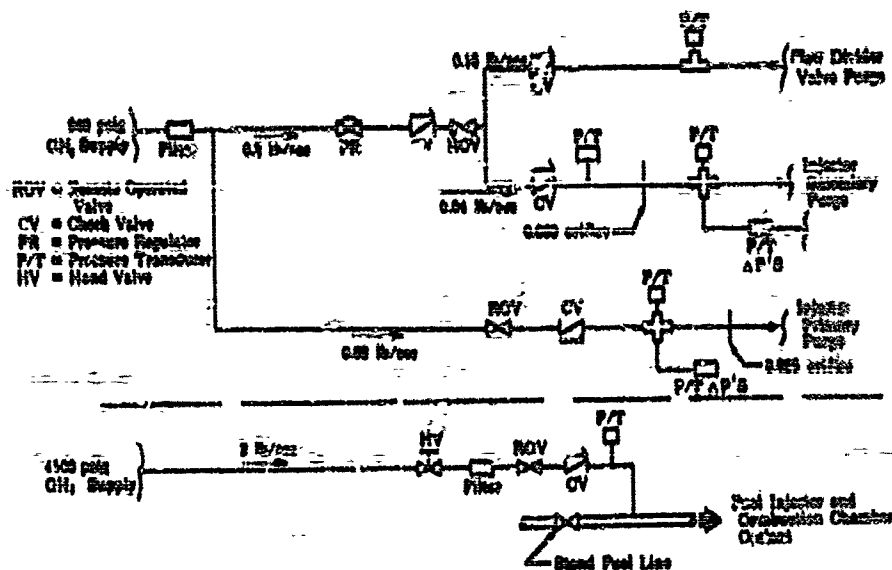


Figure 554. Modified Purge Systems for 250K Preburner Testing (Effective Run 32)

FD 21596

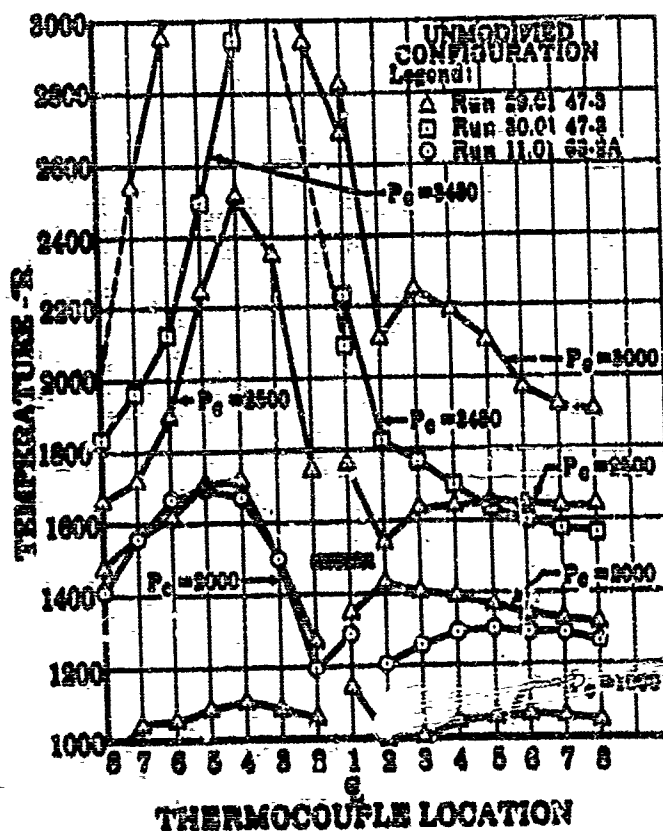


Figure 555. Temperature Profile for Run 46

FD 22456

CONFIDENTIAL

CONFIDENTIAL

(G) The factors that could cause this distorted temperature profile were investigated by flowing a preburner injector on the water flow stand. The flows were collected from each of the seven oxidizer elements when the injector was flowing at the 80% water flow rates. These tests disclosed the maximum variation between the seven elements to be 2.4%. Additional water flow tests were conducted to determine the variation between the 12 dual-orifice tubes in an element. These tests showed the maximum variation between the 12 primary tubes to be 4%. In analyzing these water flow test results, the variation between the oxidizer elements was determined not to be the cause of the temperature profile distortion. A single dual-orifice element was then flow tested to evaluate the flow split between the inner and outer fuel annuli. These tests substantiated that the fuel flow ratio between the inner and outer annuli was 0.593, as the design requires.

(G) Because these flow calibration tests indicated that the fuel and oxidizer flow variations were not the cause of the distorted temperature profile, an analysis of the injector design was made. These flow data, coupled with data from earlier flow tests that had been conducted on a single dual-orifice element, indicated that the problem was caused by expansion of the fuel prior to impingement with the oxidizer cones. The premature fuel expansion decreased the fuel velocity and reduced atomization and mixing between the two propellants. The alternative preburner injector configuration, which was designed to correct this problem and which is shown in figure 556, consisted of concentric fuel annuli around each of the oxidizer nozzles. In addition, the fuel metering surface was moved forward to obtain more direct impingement of the high velocity hydrogen into the oxidizer cone. Figure 557 shows the contrast between the two injector fuel arrangements. This alternative fuel metering configuration was incorporated on the preburner injector with co-rotating oxidizer nozzles.

(G) In addition to modifying the preburner injector to improve the temperature profile, these early tests indicated that the operating pressure in the test rig would have to be reduced to avoid overcracking of the attachment bolts and deflection of the dome flange which had caused static seal overboard leakage. To permit testing the combustion system at the 100% flow condition, the area of the back pressure plate was increased. This increased area permits operation at approximately 3500 psia (simulating the staged-combustion preburner pressure) and 100% propellant flow rates. All subsequent preburner tests were conducted at the reduced pressure level to avoid the dome flange deflection and overboard leakage.

CONFIDENTIAL

CONFIDENTIAL

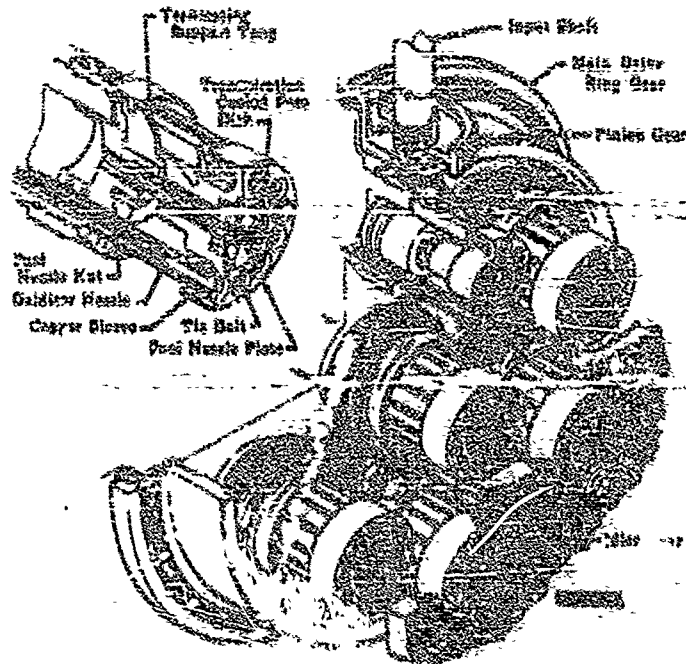


Figure 556. Preburner Injector Fuel Drive System

FD 18120X

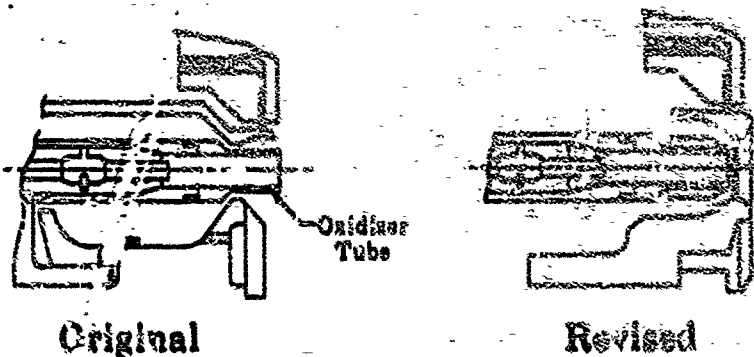


Figure 547. Preburner Injector Modification

PT 22505A

(C) Testing of the alternative preburner injector configuration began on 14 July 1967. The alternative injector contained the co-rotating oxidizer nozzle spray pattern in conjunction with the new concentric fuel nozzle arrangement. After five tests (run No. 47 to 51), it was determined that the preburner temperature profile was still unsatisfactory for staged-combustion testing. A review of the test data indicated that this alternative injector configuration provided a significant shift in the preburner temperature profile, but the overall

THIS PAGE CONTAINS SUBJECT MATTER COVERED BY A SECRETARY ORDER WITH MODIFICATION FROM A-1 ISSUED BY U.S. COMMISSIONER OF PATENTS.

THIS PAGE CONTAINS SUBJECT MATTER COVERED BY A SECRETARY ORDER WITH A MODIFICATION FROM A-1 ISSUED BY U.S. COMMISSIONER OF PATENTS.

576

CONFIDENTIAL

CONFIDENTIAL

variation in temperature was only slightly reduced. As shown in figure 502, the temperature profile was cold over the elements and hot between elements. Because the propellant atomization and mixing were improved with this alternative design, a review of the design indicated that a redistribution of the oxidizer was required. A comparison of the spray pattern obtained from the co-rotating and counter-rotating elements is shown in figure 558. The co-rotating oxidizer swirl pattern provides a homogeneous distribution of liquid particles as compared with the counter-rotating arrangement. Further review of the comparison photos of the co- and counter-rotating configurations indicated that the relatively cold areas over the center of the nozzle could be eliminated by substituting the counter-rotating type oxidizer nozzles.



Figure 558. Preburner Dual-Orifice Oxidizer
Element Water Flow Test at
300 psia

FD 2008C

(C) The alternative fuel metering configuration was incorporated into the backup preburner injector with a counter-rotating oxidizer swirl pattern, and the test program was continued. This alternative injector configuration, used on preburner run No. 52 to 104, showed a significant improvement in the combustion temperature profile. Figures 559 and 560 show a temperature profile comparison of three preburner configurations evaluated during Phase I testing.

(C) Because the alternative preburner injector demonstrated an acceptable temperature profile, it was possible to conduct testing at 100% rated flow and an overall mixture ratio of 3, 6, and 7. Figure 561 shows the preburner being tested at the 100% level. In addition, the pulsing tests at 20% and 100% were conducted with a cold fuel inlet temperature. These tests demonstrated the dynamic stability of the preburner combustion system.

CONFIDENTIAL

0 Point Rad

8 Point Rad

16 Point Rad

View into Preburner Combustion Chamber Looking toward 1, loc of F39

TEMPERATURE (°C)

1000

800

600

400

200

0

0 4 8 12 16

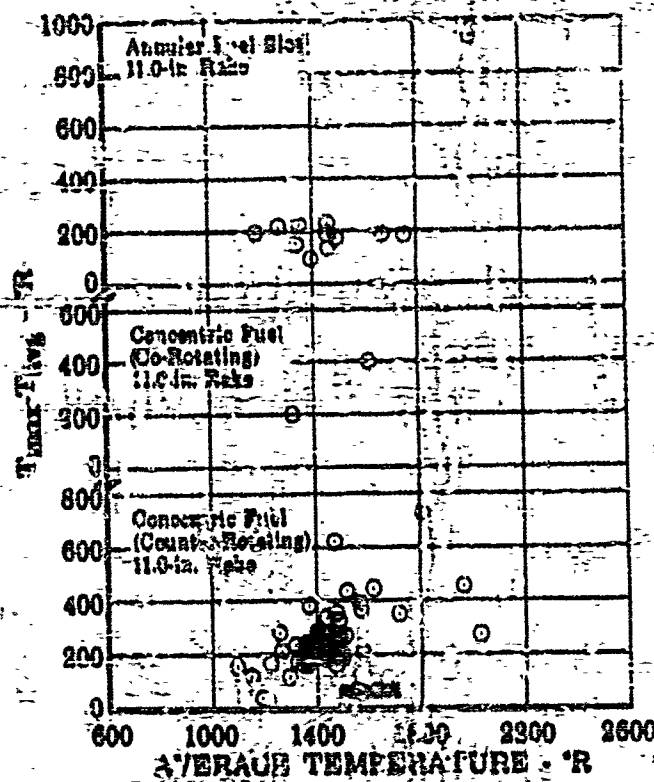
0D THERMOCOUPLE LOCATION 0D

Wall 1: 1000

Flame: $\Delta T = 255^\circ K$

Inlet: 1000

FD 25641



ET-23471

476

CONFIDENTIAL

CONFIDENTIAL

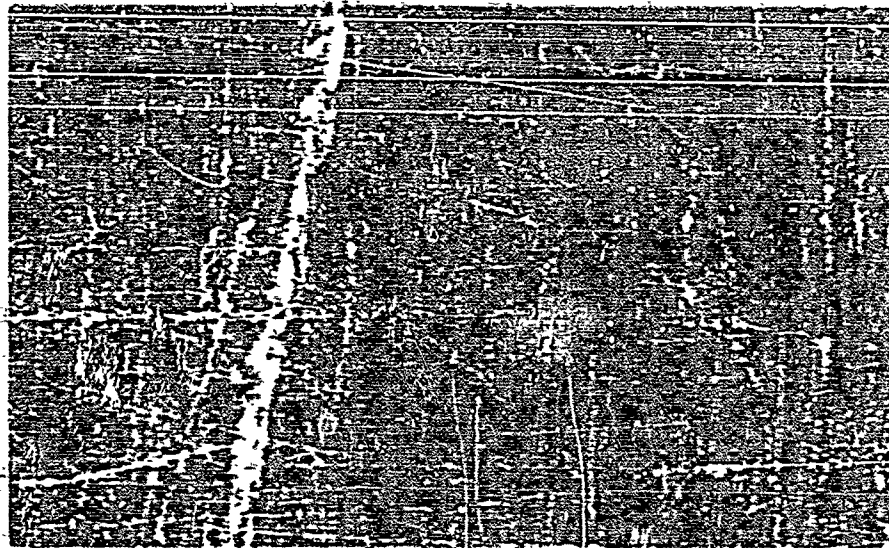


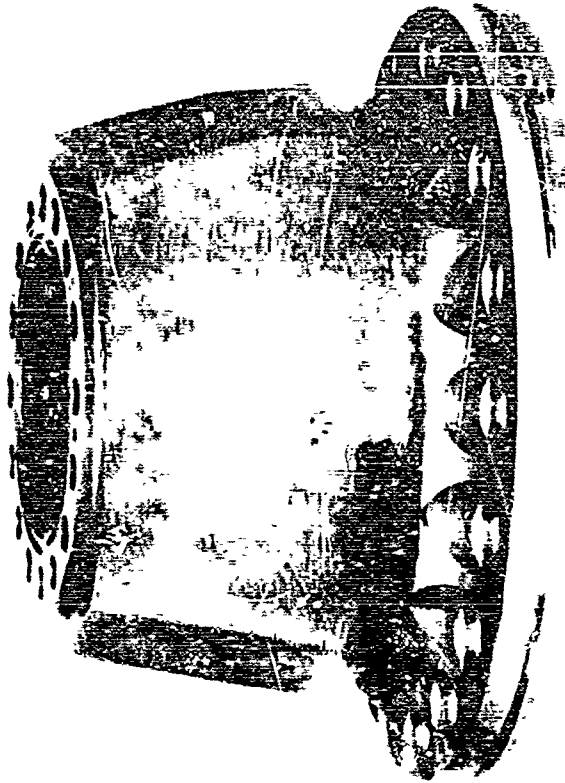
Figure 551. Preburner Test at 100% Level

WZ 71/05

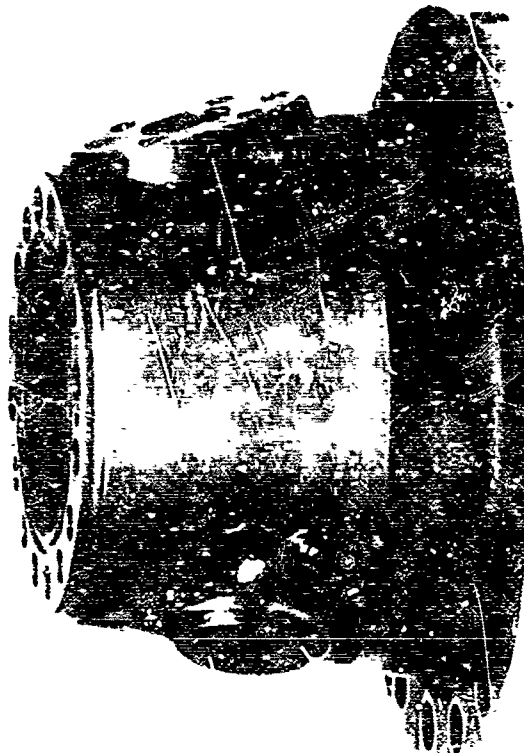
(C) The static seal leakage problem in the dome to injector housing flanges, previously discussed, was determined to have been caused by flange deflection from unloading of the stretch bolts because of the combined effects of operating temperature and pressure, see figure 529. This problem was initially encountered on preburner run No. 46. After approximately 2 hours of stabilized operation at a preburner pressure of 3450 psia the dome seal began leaking and a fire developed in the injector seal groove. After disassembly of the preburner both the remaining seal material and the injector internal surface were tested for contamination; the results were negative. Numerous pin seals were examined, inspected for contamination, and tested for liquid oxygen compatibility. Again the results of analysis were negative. Because the fire in the dome to injector seal groove was unexplained, revised C-ring seal cleaning procedures were devised and more stringent injector cleaning, handling, and assembly procedures were instituted. The leakage problem was evaluated on a preburner dome seal test rig using liquid nitrogen as the pressurizing medium. It was determined that the leak could be corrected with a stiffened dome flange and by tensioning the existing stretch bolts to 100,000 lb. Preburner testing would have been delayed approximately 6 weeks if the revised dome had been incorporated. Instead, the back pressure nozzle was revised to permit 100% preburner operation at reduced pressures. The revised operating level was selected to simulate the 100% preburner pressures on the staged combustion rig. The 18 stretch bolts underwent the tensioning operation, and the assembly preload was increased from 62,500 to 90,500 lb. The subsequent preburner test rig fabrication of the revised dome housing was completed after staged combustion testing had begun. A comparison of the original and revised preburner dome housings is shown in figure 552. On all preburner tests after run No. 51, the revised stretch bolt loading was used and the operating pressures were limited to 3600 psia (72% of the required 5000 psia). No further leakage problems were encountered either in the dome flange or at any other preburner static seal flange during the final preburner testing and staged combustion testing.

CONFIDENTIAL

CONFIDENTIAL



(Revised Design)



(Original Design)

12 270119

FD 23472

Figure 562. 250K Preburner Dome Housings - View Showing Comparison of Revised Dome Housing to Original Design

580

CONFIDENTIAL

(This page is Unclassified)

CONFIDENTIAL

B. Preburner Test Results

(C) Nineteen successful 250K preburner tests are discussed in the following listing. The first ten tests conducted in this program used the original preburner injector configuration (annular fuel sleeve arrangement). The remaining tests were conducted with the alternative preburner injector configuration (concentric fuel nozzles around each oxidizer nozzle). The stability tests were included as part of the last nine tests.

| Test No. | Rig No. | Run No. | Date | Operating Level |
|----------|---------|---------|---------------|-----------------|
| | 33447-1 | 1 | 11 March 1967 | Ignition |

Program: Conduct an ignition test to demonstrate satisfactory ignition and shutdown. Ignition was instantaneous and ran for 1.6 seconds. No rig deterioration observed after shutdown. Starting flows were as follows:

0.33 lb/sec oxidizer and 0.47 lb/sec fuel.

| Test No. | Rig No. | Run No. | Date | Operating Level |
|----------|---------|---------|---------------|-----------------|
| | 33447-1 | 6 | 28 March 1967 | 7% Thrust |

Program: The objective of this test was to demonstrate successful rig operation at high propellant tank pressures and to operate at 7% rated thrust. Run was terminated during propellant tank pressurization because of high combustion temperature caused by improper response of facility oxidizer valve; however, operation at 7% rated thrust was successful.

| Test No. | Rig No. | Run No. | Date | Operating Level |
|----------|---------|---------|---------------|-----------------|
| | 33447-1 | 8 | 30 March 1967 | 7% Thrust |

Program: Conduct a test to demonstrate successful operation during propellant tank pressurization and at 7% rated thrust. Rig operation was successful at ignition and at 7% rated thrust levels, but was unstable during tank pressurizations because of improper response of facility propellant valves.

CONFIDENTIAL

CONFIDENTIAL

| Test No. | Rig No. | Run No. | Date | Operating Level |
|-------------|------------|------------|---------------|--------------------|
| | 33447-1 | 11 | 31 March 1967 | 7% Thrust |

Program: Conduct a test to demonstrate successful operation during propellant tank pressurization and at 7% rated thrust. Rig operation was successful at ignition and at 7% rated thrust levels, but was unstable during tank pressurizations because of improper response of facility propellant valves.

| Test No. | Rig No. | Run No. | Date | Operating Level |
|-------------|------------|------------|---------------|--------------------|
| | 33463-2A | 17 | 28 April 1967 | 35% Thrust |

Program: Conduct a test to evaluate propellant transient control characteristics and successful operation at 35% of rated thrust. The test was completely successful for full duration.

| Test No. | Rig No. | Run No. | Date | Operating Level |
|-------------|------------|------------|------------|--------------------|
| 250PB1 | 33463-2A | 19 | 2 May 1967 | 20% Thrust |

Program: Conduct a test at the 20% thrust level to establish the performance and temperature profile over the full mixture ratio range. The facility control system was programmed so that at the 20% level the mixture ratio was varied to establish the combustion temperature at approximately 1625°, 1800°, and 1930°R to correspond to preburner operation at engine mixture ratios of 6, 7, and 5. Figure 563 shows the transient to 20% thrust and figure 564 shows the temperature (mixture ratio) excursion. In addition, during the simulated acceleration transient from 7% to 20%, the open injector fuel area was adjusted from 16.5% to 35% to obtain a close simulation of the fuel system pressure drop. The measured temperature profile (maximum to average) varied from 153° to 193°R during the mixture ratio excursion. The test duration was 63.0 seconds.

| Test No. | Rig No. | Run No. | Date | Operating Level |
|-------------|------------|------------|------------|--------------------|
| 250PB2 | 33463-2A | 22 | 3 May 1967 | 20% Thrust |

Program: This test was similar to test 250PB-1 except for the increased injector fuel area setting and different mixture ratio settings. The facility control system was varied to provide combustion temperatures of 1625°, 1850°, and 1925°R during the test. Data from the 20% operation are shown in Figure 555. During this test run, the injector fuel area

CONFIDENTIAL

CONFIDENTIAL

was adjusted to be 55% open at the 20% level. While the average combustion temperatures attained during this test were lower than those of test No. 250FD-1, the temperature profile was slightly larger, which is associated with the larger injector fuel area setting (reduced fuel momentum). The test duration was 63.0 sec.

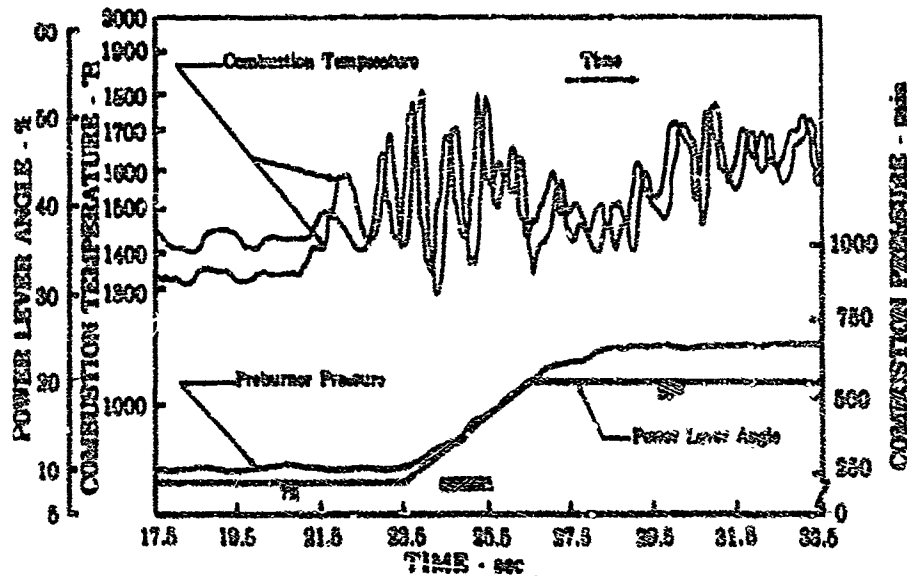


Figure 563. Data from Run 19 (Rig F-33463-2A)
Describing Power Level Ramp to
20% Thrust

FD 21404

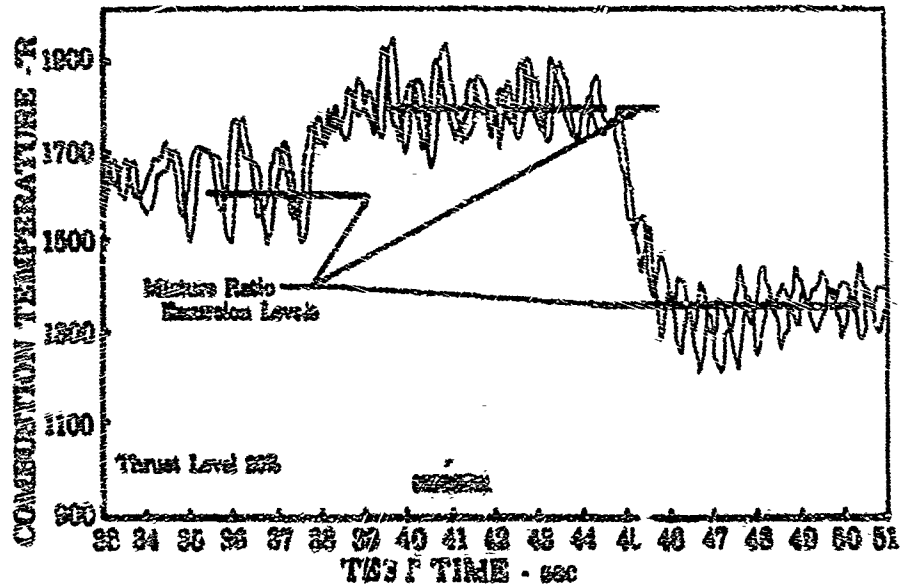


Figure 564. 250K Preburner Test Rig (Run 19)

FD 21402

CONFIDENTIAL

CONFIDENTIAL

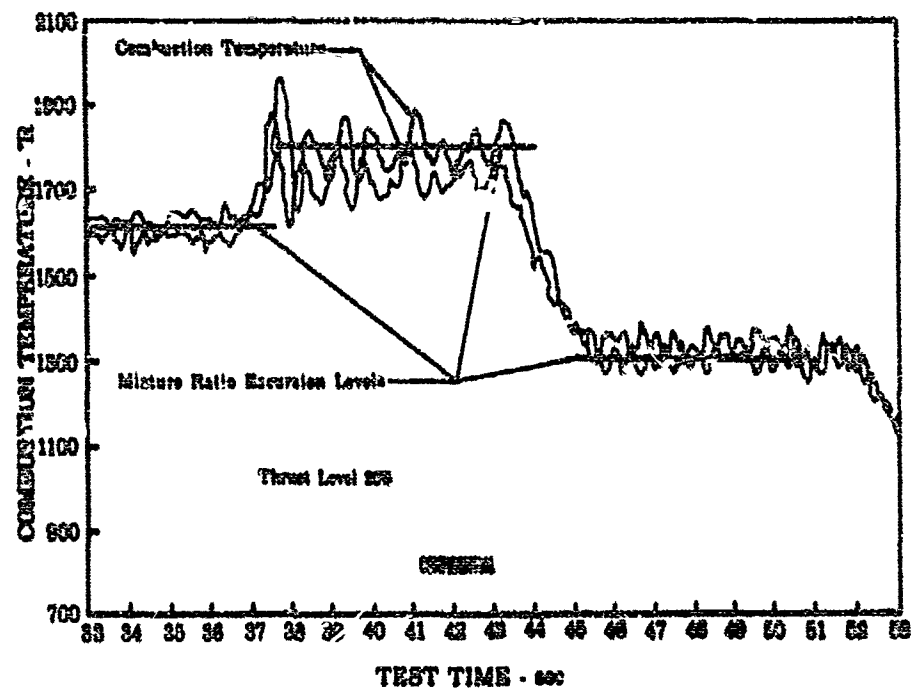


Figure 565. 250K Preburner Test Rig (Run 22)

FD 21403

| Test No. | Rig No. | Run No. | Date | Operating Level |
|----------|----------|---------|------------|-----------------|
| 250PB3 | 33463-2A | 24 | 5 May 1967 | 50% Thrust |

Program: The objective of this test was to operate the preburner at 50% thrust and establish the combustion performance and temperature profile over the full range of mixture ratio. The simulated acceleration transient from 7% to 50% is shown in figure 566. During this transient, the injector fuel area was programmed to open from 30% to 75%, but the area opened only to 35% during the programmed period. The preburner stabilized at a preburner combustion chamber pressure of 2002 psia and a combustion temperature of 1465°R. After approximately 5 seconds of stable operation, the fuel area snapped open to the 75% setting. The rapid change in injector fuel differential pressure disrupted the combustion temperature profile and the test was automatically terminated. The test duration was 33.5 seconds.

During the period prior to test No. 250PB4, 29 preburner tests were conducted. In this series of tests, the preburner temperature profile was determined to have been excessive, and an alternative preburner injector design was provided. During this series of tests, the control of the facility propellant was changed from a temperature-pressure sense to a flowmeter volumetric sense.

CONFIDENTIAL

CONFIDENTIAL

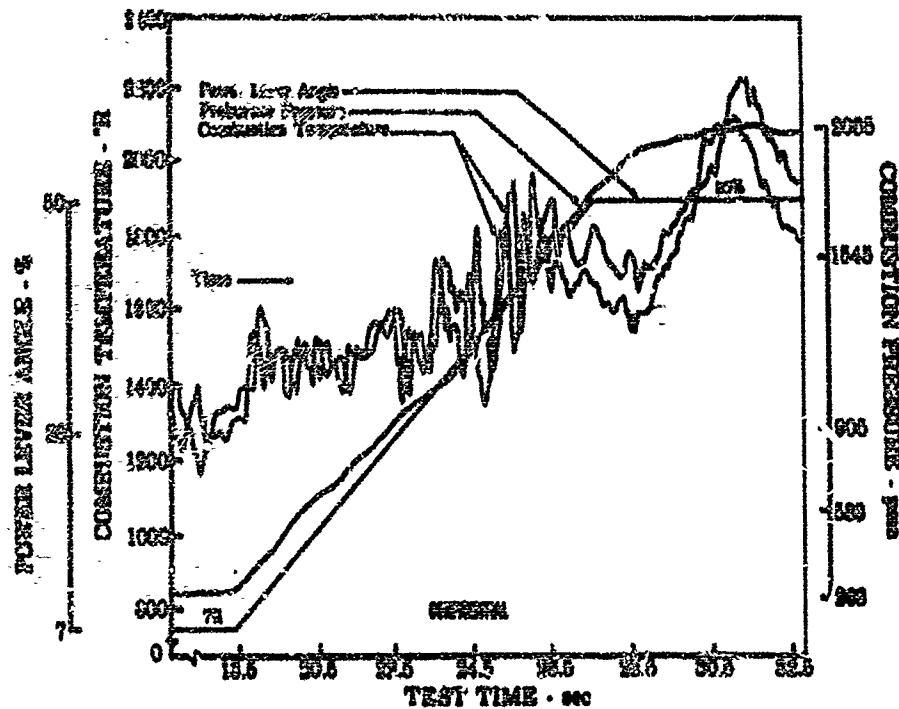


Figure 566. Data from Run 24 (Rig F-33463-2A) FD 21397
Describing Power Level Ramp to
50% Thrust

| Test No. | Rig No. | Run No. | Date | Operating Level |
|----------|---------|---------|--------------|-----------------|
| | 33447-3 | 46 | 28 June 1967 | 80% Thrust |

Program: Conduct a test to evaluate rig operation at 80% rated thrust. The 80% level was obtained. Preburner pressure was 3450 psia and all parameters were stable. After 4 seconds of steady-state operation, the run was automatically shut down because of a fire. It was determined that a small oxidizer leak had developed in the dome-to-injector O-ring seals.

| Test No. | Rig No. | Run No. | Date | Operating Level |
|----------|---------|---------|--------------|-----------------|
| | 33447-4 | 51 | 16 July 1967 | 50% Thrust |

Program: Conduct a test at 50% rated thrust level to evaluate temperature profile characteristics. The 50% level was obtained but the temperature profile was excessive.

CONFIDENTIAL

CONFIDENTIAL

| Test No. | Rig No. | Run No. | Date | Operating Level |
|----------|---------|---------|--------------|-----------------|
| 250PB4 | 33447-5 | 54 | 22 July 1967 | 50% Thrust |

Program: The objective of this test was to evaluate the preburner temperature profile and combustion performance at 50% rated flow with the alternative preburner injector configuration. In this test, the simulated acceleration transient from 7% to 50% flow condition was achieved using flow control. The preburner fuel injector area was not varied in the test but held fixed at 3.5 in². The temperature profile was approximately 450°R. This large variation was caused by the short duration of the test and the fixed fuel area set at the large opening. This was the initial contract test with the enlarged back pressure nozzle. The test duration was 27.6 seconds.

| Test No. | Rig No. | Run No. | Date | Operating Level |
|----------|---------|---------|--------------|-----------------|
| 250PB5 | 33447-5 | 58 | 23 July 1967 | 100% Thrust |

Program: This was the initial test with the preburner operating at 100% rated flow. The preburner stabilized at 3400 psia. Because the run duration at the 100% flow was limited, these tests were conducted at one preburner combustion gas temperature, 1960°R. During this test, a satisfactory acceleration transient to 100% flow was achieved using the facility control system. The measured temperature profile was 460°R, but the momentum ratio was higher than desired (6.2). The test duration was 31.0 seconds.

| Test No. | Rig No. | Run No. | Date | Operating Level |
|----------|---------|---------|--------------|-----------------|
| 250PB6 | 33447-5 | 60 | 24 July 1967 | 100% Thrust |

Program: The objective of this test was to investigate the combustion performance and establish the temperature profile at the 100% flow condition and to check the pulsing circuitry. The operating conditions for this test were similar to those for test No. 250PB5, except that the propellant momentum ratio was decreased from 6.2 to 6.0 and the temperature profile was reduced to 278°R in spite of the 70°R increase in the average operating temperature. During this test, the pulsing circuits fired prematurely because of a facility problem that was corrected for subsequent tests. The preburner pressure during this test was 3484 psia. The test duration was 31.9 seconds.

CONFIDENTIAL

CONFIDENTIAL

| Test No. | Rig No. | Run No. | Date | Operating Level |
|----------|---------|---------|--------------|-----------------|
| 250PB7 | 33447-5 | 62 | 25 July 1967 | 100% Thrust |

Program: The objective of this test was to establish pre-burner performance and temperature profile at the 100% flow condition with the preburner combustion system operating at an overall engine mixture ratio of 5. Satisfactory rig operation was attained with a stable operating pressure of 3600 psia and an average combustion gas temperature of 1787°R. The temperature profile was 350°R, which was attributed to the momentum ratio increase to 6.2. During this test, a satisfactory check of the four pulse triggering systems was conducted. The test duration was 35.0 seconds.

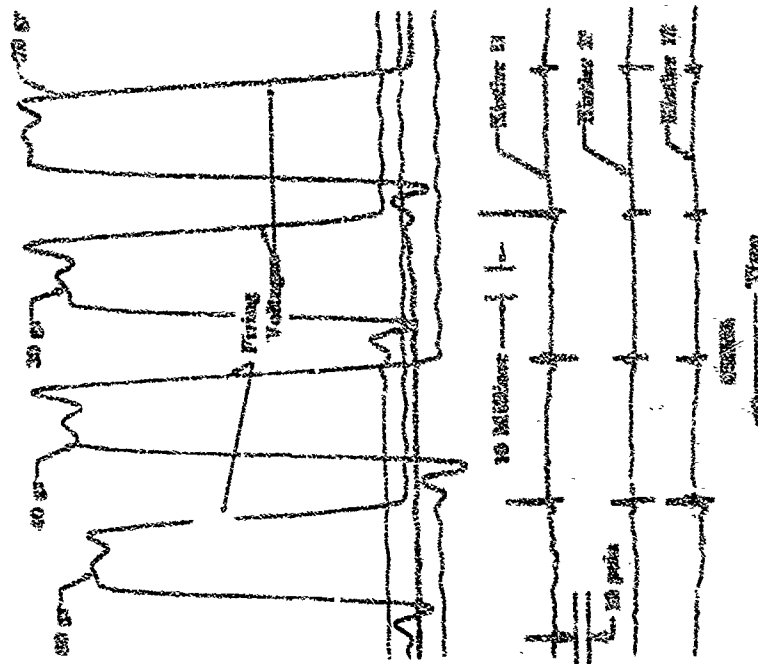
| Test No. | Rig No. | Run No. | Date | Operating Level |
|----------|---------|---------|--------------|-----------------|
| 250PB8 | 33447-5 | 64 | 26 July 1967 | 100% Thrust |

Program: The objective of this test was to evaluate the dynamic stability of the preburner combustion system at the 100% flow condition with a fuel injector inlet temperature of 102°R. During this test, the preburner combustion system stabilized at a combustion pressure of 3200 psia at the desired inlet temperatures, and the four pulse charges of 20, 30, 40, and 80 grains were detonated at 60-millisecond intervals. The stability data, which were measured on three Kistler transducers, are presented in figure 567. The maximum overpressurization detected was 3% (96 psia) and the maximum damping time was 30 milliseconds (recovery to within 0.5% of nominal combustion pressure). The test duration was 35.1 seconds.

| Test No. | Rig No. | Run No. | Date | Operating Level |
|----------|---------|---------|--------------|-----------------|
| 250PB9 | 33447-5 | 65 | 26 July 1967 | 20% Thrust |

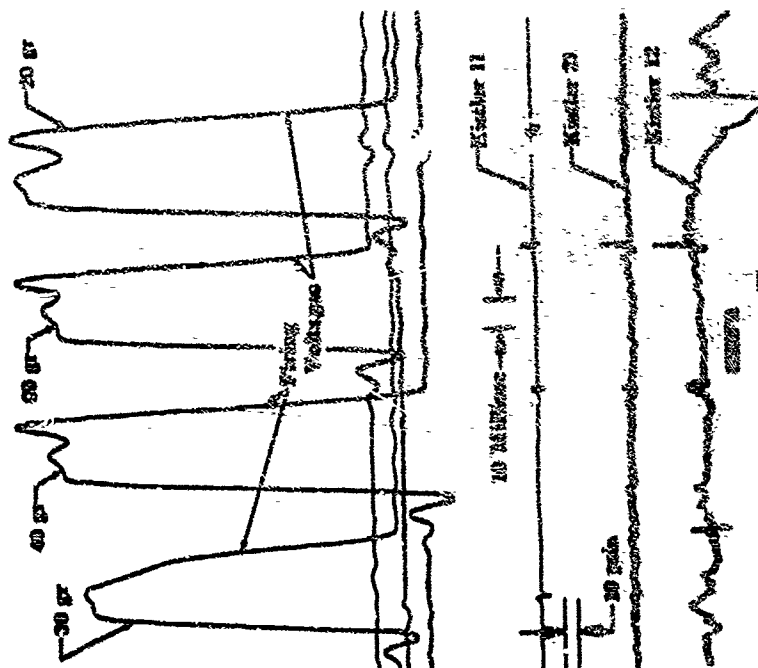
Program: This test was a 20% pulse test to evaluate the dynamic stability of the preburner combustion system at 20% rated thrust with an injector fuel inlet temperature of 118°R. During this test, the preburner stabilized at a combustion pressure of 475 psia, and the four pulse charges of 20, 30, 40, and 80 grains were detonated at 60-millisecond intervals. The overpressure pulses, which were recorded during this test on three Kistler transducers, are presented in figure 568. The maximum overpressurization recorded at 20% thrust was 96 psia. The duration of this overpressure condition was 5 milliseconds. This damping characteristic was well within the specification requirements for this system. The test duration was 28.7 seconds.

CONFIDENTIAL



FD 22925A

Figure 568. 250K Preburner Dynamic Stability Data - Run 57 (20% Flow)



FD 22925A

Figure 567. 250K Preburner Dynamic Stability Data - Run 54 (100% Flow)

CONFIDENTIAL

CONFIDENTIAL

| Test No. | Rig No. | Run No. | Date | Operating Level |
|----------|---------|---------|--------------|-----------------|
| 2307810 | 33447-5 | 56 | 26 July 1967 | 100% Thrust |

Program: Investigate the performance and temperature profile at 100% flow and an overall engine mixture ratio of 7. On this test, the preburner was operated at 3290 psia preburner pressure and 2224°R average combustion temperature. The temperature measurements indicated that the profile was distorted approximately 674°R. These data are not conclusive because several thermocouples were lost during the transient. However, one other factor that could contribute to the distorted profile was the low momentum ratio (4.0). All operating parameters, with the exception of 5 combustion temperature sampling points, were within the pre-established operating limits. All parts were in excellent condition, except for some burning on the temperature rakes. The test duration was 33.2 seconds.

| Test No. | Rig No. | Run No. | Date | Operating Level |
|----------|----------|---------|---------------|-----------------|
| | 33447-5B | 71 | 1 August 1967 | 20% Thrust |

Program: Conduct a test at 20% rated thrust level to evaluate effect of cold ON₂ purge of fuel manifold prior to start on oxidizer element filling time. Start transient exhibited dip in combustion temperature during ramp to 7% thrust level, but 20% level was obtained for full test duration.

| Test No. | Rig No. | Run No. | Date | Operating Level |
|----------|----------|---------|---------------|-----------------|
| | 33447-5B | 72 | 1 August 1967 | 20% Thrust |

Program: Conduct a test at 20% rated thrust level to further evaluate start transient. Test was for full duration but dips in combustion temperature were experienced just after ignition and during the ramp to 7% rated thrust.

(U) A summary of preburner test data is presented in tables XLVI through XLIX. Tables XLVI and XLVII provide measured and calculated preburner test rig data, and tables XLVIII and XLIX list the preburner data from the staged combustion tests.

389/590

CONFIDENTIAL

CONFIDENTIAL

(C) Table XLVI. Summary of Measured Parameters

| Test No. | Date | Exp. No. / Serial No. | Ambient Pressure, psia | LM ₂ Flow Rate, gpm (1) | CH ₄ Flow Rate, sfc (1) | Oxidizer Flow Rate, gpm (2) | LM ₂ Flowmeter Temperature, °K | CH ₄ Flowmeter Temperature, °K | Oxidizer Flowmeter Temperature, °K | Oxidizer Injector Inlet Temperature, °K | Fuel Injector Inlet Temperature, °K | Liquid Oxidant Inlet Temperature, °K | LM ₂ Press, ps |
|----------|-------------|-----------------------|------------------------|------------------------------------|------------------------------------|-----------------------------|---|---|------------------------------------|---|-------------------------------------|--------------------------------------|---------------------------|
| | 11 May 1967 | P-33447-1 | 14.73 | -- | -- | -- | 31.4 | 344 | 163.9 | 163 | 302 | 302 | 15 |
| | 20 May 1967 | P-33447-1 | 14.73 | 264 | 93 | 26 | 49.4 | 331 | 163.8 | 161 | 302 | 302 | 22 |
| | 30 May 1967 | P-33447-1 | 14.73 | 267 | 95 | 24 | 49.8 | 332 | 163.6 | 151 | 307 | 302 | 21 |
| | 31 May 1967 | P-33447-1 | 14.73 | 227 | 117 | 24 | 51.8 | 332 | 164.5 | 161 | 305 | 302 | 24 |
| | 25 Apr 1967 | P-33447-2A | 14.73 | 1143 | 414 | 93 | 54.9 | 332 | 163.0 | 191 | 307 | 302 | 34 |
| 250731 | 2 May 1967 | P-33447-2A | 14.73 | 393 | 234 | 33.1 | 37.2 | 330 | 172.1 | 182 | 302 | 302 | 34 |
| | | | 14.73 | 333 | 237 | 37.1 | 37.1 | 334 | 175.9 | 186 | 300 | 300 | 31 |
| | | | 14.73 | 310 | 234 | 36.0 | 37.0 | 332 | 177.2 | 190 | 302 | 302 | 33 |
| | | | 14.73 | 612 | 290 | 31.7 | 36.6 | 330 | 177.1 | 191 | 301 | 301 | 33 |
| 250732 | 2 May 1967 | P-33447-2A | 14.73 | 473 | 237 | 49.8 | 35.4 | 337 | 176.9 | 183 | 303 | 303 | 46 |
| | | | 14.73 | 633 | 248 | 53.2 | 35.5 | 338 | 177.1 | 187 | 303 | 303 | 47 |
| | | | 14.73 | 600 | 241 | 52.4 | 35.5 | 332 | 177.4 | 190 | 303 | 303 | 47 |
| | | | 14.73 | 583 | 221 | 50.1 | 35.5 | 330 | 178.9 | 191 | 302 | 302 | 47 |
| 250733 | 2 May 1967 | P-33447-2A | 14.80 | 3403 | 318 | 137 | 56.8 | 333 | 203.4 | 254 | 196 | 196 | 51 |
| | 28 Jun 1967 | P-33447-3 | 14.70 | 3327 | 323 | 302 | 66.2 | 334 | 179.3 | 183 | 219 | 219 | 51 |
| | 16 Jul 1967 | P-33447-4 | 14.74 | 1920 | 393 | 173 | 33.0 | 333 | 173.2 | 185 | 227 | 227 | 54 |
| 250735 | 22 Jul 1967 | P-33447-5 | 14.76 | 1917 | 282 | 168 | 36.8 | 341 | 177.7 | 186 | 238 | 238 | 56 |
| 250736 | 23 Jul 1967 | P-33447-5 | 14.74 | 3317 | 637 | 411 | 36.7 | 332 | 173.8 | 184 | 240 | 240 | 54 |
| 250737 | 24 Jul 1967 | P-33447-5 | 14.74 | 5632 | 693 | 418 | 37.2 | 333 | 174.6 | 190 | 238 | 238 | 54 |
| 250738 | 25 Jul 1967 | P-33447-5 | 14.76 | 4922 | 713 | 431 (3) | 36.7 | 337 | 176.7 | 186 | 190 | 190 | 54 |
| 250739 | 26 Jul 1967 | P-33447-5 | 14.78 | 5427 | 110 | 408 (3) | 36.8 | 339 | 174.3 | 184 | 182 | 182 | 53 |
| 250740 | 26 Jul 1967 | P-33447-5 | 14.73 | 970 | 73 | 34 (3) | 37.9 | 340 | 180.8 | 197 | 110 | 110 | 54 |
| 250741 | 26 Jul 1967 | P-33447-5 | 14.75 | 3354 | 715 | 429 (3) | 36.0 | 339 | 176.9 | 191 | 214 | 214 | 50 |
| | 2 Aug 1967 | P-33447-5B | 14.74 | 648 | 213 | 42 | 37.5 | 338 | 176.9 | 188 | 248 | 248 | 53 |
| | 1 Aug 1967 | P-33447-5B | 14.74 | 643 | 212 | 42 | 38.1 | 333 | 175.1 | 189 | 234 | 234 | 48 |

(1) Flowmeter flow

(2) Pressure flowmeter

(3) Oxidizer controlled through CH₄ (no ignition adjustment was made)

(4) Primary supply

(5) Secondary supply

(6) Measured between primary supply and combustion pressure

(7) Measured between secondary supply and combustion pressure

CONFIDENTIAL

CONFIDENTIAL

Measured Parameters of Preburner Tests

| Prel Injector Inlet Temperature, °R | Liner Coolant Inlet Temperature, °R | High Pressure puls | High Pressure puls | Out-lier Flowmeter Pressure, puls | Out-lier Injector Inlet Pressure, puls | Out-lier Injector Inlet Pressure, puls | Prel Injector Inlet Pressure, puls | Liner Coolant Inlet Pressure, puls | Chamber Pressure (Injector Stator), puls | Prel Injector Inlet puls | Out-lier Primary Inlet puls | Out-lier Secondary Inlet puls |
|---|---|--------------------------|--------------------------|--|--|--|--|--|--|-----------------------------------|--------------------------------------|--|
| 393 | 320 | 1334 | 1323 | 1452 | 38 | 33 | 47 | 63 | 32 | 10 | 5 | 0 |
| 393 | 302 | 1315 | 1301 | 1387 | 447 | 321 | 407 | 407 | 323 | 34 | 122 | 0 |
| 397 | 307 | 1187 | 1171 | 1341 | 433 | 315 | 385 | 390 | 315 | 82 | 141 | 0 |
| 393 | 293 | 1093 | 1079 | 1307 | 423 | 310 | 354 | 434 | 333 | 106 | 127 | 0 |
| 397 | 297 | 1476 | 1463 | 1444 | 1421 | 1372 | 1401 | 1401 | 1230 | 255 | 64 | 25 |
| 349 | 285 | 1443 | 1430 | 1470 | 765 | 732 | 853 | 853 | 735 | 146 | 46 | 19 |
| 330 | 300 | 1455 | 1440 | 1470 | 781 | 752 | 830 | 870 | 740 | 128 | 40 | 12 |
| 302 | 302 | 1390 | 1370 | 1412 | 732 | 704 | 840 | 840 | 740 | 112 | 43 | 21 |
| 301 | 301 | 1375 | 1360 | 1413 | 779 | 755 | 893 | 893 | 740 | 165 | 41 | 8 |
| 373 | 375 | 1480 | 1470 | 1440 | 754 | 721 | 783 | 773 | 710 | 94 | 40 | 10 |
| 383 | 383 | 1713 | 1703 | 1440 | 773 | 742 | 800 | 800 | 723 | 90 | 39 | 8 |
| 383 | 383 | 1710 | 1703 | 1440 | 778 | 744 | 850 | 790 | 730 | 75 | 41 | 0 |
| 373 | 373 | 1710 | 1700 | 1433 | 771 | 740 | 813 | 813 | 723 | 103 | 35 | 6 |
| 306 | 306 | 1110 | 1100 | 1430 | 2143 | 2049 | 2350 | 2350 | 2000 | 235 | 120 | 34 |
| 310 | 310 | 1337 | 1324 | 1410 | 3767 | 3678 | 3786 | 3756 | 3429 | 277 | 239 | 183 |
| 327 | 327 | 1407 | 1393 | 1344 | 3142 | 3090 | 3702 | 3608 | 3073 | 231 | 170 | 160 |
| 328 | 328 | 1423 | 1408 | 1304 | 1702 | 1631 | 1733 | 1733 | 1615 | 227 | 176 | 114 |
| 349 | 340 | 1416 | 1398 | 1389 | 3842 | 3849 | 3803 | 3803 | 3293 | 441 | 430 | 438 |
| 328 | 328 | 1433 | 1415 | 1374 | 3917 | 3916 | 3877 | 3877 | 3457 | 448 | 447 | 458 |
| 190 | 190 | 1406 | 1389 | 1323 | 4096 | 4086 | 4073 | 4073 | 3407 | 472 | 469 | 458 |
| 162 | 162 | 1321 | 1302 | 1321 | 3603 | 3600 | 3571 | 3531 | 3213 | 326 | 282 | 271 |
| 110 | 110 | 1410 | 1394 | 1344 | 323 | 303 | 347 | 557 | 474 | 73 | 31 | 15 |
| 314 | 314 | 1007 | 1003 | 1321 | 3718 | 3713 | 3408 | 3405 | 3287 | 321 | 414 | 413 |
| 360 | 360 | 1387 | 1374 | 1376 | 390 | 383 | 440 | 440 | 300 | 137 | 89 | 41 |
| 334 | 334 | 1355 | 1340 | 1380 | 370 | 358 | 413 | 417 | 285 | 138 | 83 | 24 |

CONFIDENTIAL

2

CONFIDENTIAL

(C) Table XLVII. Summary of Calculated Perform

| Test No. | Test Date | Rig No. - Build No. | Total Fuel Flow Rate, lb _m /sec | Oxidizer Flow Rate, lb _m /sec | Total Liner Flow Rate, lb _m /sec | Overall Mixture Ratio | Injector Mixture Ratio ⁽¹⁾ | Ideal ⁽²⁾ Temperature, °R | Average ⁽³⁾ Combustion Temperature, °R | ΔT ⁽⁴⁾ Profile °R |
|----------|-------------|---------------------|--|--|---|-----------------------|---------------------------------------|--------------------------------------|---|------------------------------|
| | 11 Mar 1967 | 7-3347-1 | -- | -- | -- | -- | -- | -- | 1529 | 260 |
| | 28 Mar 1967 | F-33447-1 | 5.4 | 4.1 | 0.28 | 0.77 | 0.81 | 1724 | 1653 | 296 |
| | 30 Mar 1967 | F-33447-1 | 5.1 | 3.8 | 0.28 | 0.74 | 0.78 | 1679 | 1680 | 283 |
| | 31 Mar 1967 | 7-33447-1 | 6.1 | 3.9 | 0.31 | 0.63 | 0.66 | 1467 | 1443 | 257 |
| | 28 Apr 1967 | F-33463-2A | 26.0 | 16.1 | 1.00 | 0.62 | 0.64 | 1421 | 1313 | 303 |
| 250PB1 | 2 May 1967 | F-33463-2A | 13.4 | 8.7 | 0.57 | 0.63 | 0.65 | 1490 | 1490 | 181 |
| | | | 12.7 | 9.3 | 0.53 | 0.74 | 0.77 | 1635 | 1665 | 193 |
| | | | 12.2 | 9.6 | 0.91 | 0.79 | 0.77 | 1745 | 1750 | 183 |
| | | | 14.8 | 8.4 | 0.61 | 0.57 | 0.59 | 1395 | 1235 | 153 |
| 250PB2 | 3 May 1967 | F-33463-2A | 14.2 | 8.1 | 0.48 | 0.57 | 0.59 | 1320 | 1265 | 221 |
| | | | 11.9 | 8.7 | 0.47 | 0.63 | 0.55 | 1425 | 1350 | 226 |
| | | | 13.2 | 9.0 | 0.44 | 0.68 | 0.71 | 1330 | 1435 | 231 |
| | | | 19.1 | 8.2 | 0.50 | 0.54 | 0.56 | 1270 | 1175 | 196 |
| 250PB3 | 5 May 1967 | F-33463-2A | 37.0 | 25.3 | 1.46 | 0.67 | 0.70 | 1410 | 1465 | 192 |
| | | | 34.3 | 30.7 | 1.80 | 0.93 | 0.96 | 1883 | 2011 | 229 |
| | | | 34.1 | 28.3 | 1.26 | 0.65 | 0.56 | 1727 | 1604 | 408 |
| 250PB4 | 22 Jul 1967 | F-33447-3 | 34.6 | 27.0 | 1.12 | 0.73 | 0.81 | 1648 | 1618 | 430 |
| 250PB5 | 23 Jul 1967 | F-33447-3 | 65.6 | 66.8 | 2.01 | 1.02 | 1.05 | 2058 | 1962 | 460 |
| 250PB6 | 24 Jul 1967 | F-33447-3 | 67.2 | 68.2 | 2.03 | 1.01 | 1.05 | 2030 | 2028 | 278 |
| 250PB7 | 25 Jul 1967 | F-33447-3 | 78.7 | 70.0 | 2.35 | 0.89 | 0.92 | 1788 | 1717 | 350 |
| 250PB8 | 26 Jul 1967 | F-33447-3 | 68.1 | 66.5 | 2.34 | 0.93 | 1.01 | 1853 | 1809 | 734 |
| 250PB9 | 26 Jul 1967 | F-33447-3 | 12.4 | 9.7 | 0.54 | 0.71 | 0.74 | 1416 | 1470 | 626 |
| 250PB10 | 26 Jul 1967 | F-33447-3 | 36.6 | 70.0 | 1.75 | 1.24 | 1.20 | 2384 | (9) | (9) |
| | 1 Aug 1967 | F-33447-5B | 13.4 | 6.4 | 0.40 | 0.68 | 0.50 | 1145 | 1092 | 146 |
| | 1 Aug 1967 | F-33447-5B | 12.8 | 6.5 | 0.39 | 0.91 | 0.53 | 1176 | 1146 | 121 |

- (1) Injector fuel flow rate = total fuel flow rate - total liner coolant flow rate
 (2) Based on injector mixture ratio
 (3) Based on area-weighted thermocouple data 11.2 inches downstream of injector
 (4) ΔT = maximum temperature - average temperature
 (5) Stagnation pressure equals static pressure within data roundoff
 (6) Corrected for C_d = 0.954 (geometric throat area = 6.78 in²)
 (7) $\bar{T}_{0.5} = (\text{average temperature/ideal temperature})^{0.5} \times 100\%$
 (8) Using C_D = 0.956 (throat area = 7.0792 in²)
 (9) Calculations could not be made because 5 T/C were overscaled
 (10) Corrected for C_d = 0.954 (geometric throat area = 3.94 in²)
 (11) Not calculated. Throat A_C not available for this configuration.

CONFIDENTIAL

CONFIDENTIAL

Calculated Performance for Preburner Tests

| Average (3) Combustion Temperature, °R | ΔT (4) Profile °R | Chamber (5) Stagnation Pressure | η_{01} (6) (corr) | η_{02} (7) | Fuel Injection Velocity, ft/sec | Outliner Injection Velocity, ft/sec | Fuel/Outliner Momentum Ratio | Remarks |
|---|---------------------------------|---------------------------------------|---------------------------|-----------------|--|--|------------------------------------|--|
| 1329 | 260 | 32 | -- | -- | -- | -- | -- | Ignition Check, Flow Meters Out of Range |
| 1688 | 296 | 323 | 88.4 (10) | 99.0 | 1788 | 129.9 | 13.5 | |
| 1680 | 285 | 315 | 92.4 (10) | 100.0 | 1797 | 121.3 | 16.3 | |
| 1445 | 337 | 335 | 90.6 (10) | 99.3 | 1847 | 127.8 | 18.8 | |
| 1513 | 302 | 1351 | 100.0 (5) | 103.2 | 1462 | 33.0 | 39.1 | |
| 1490 | 181 | 725 | 100.7 (6) | 100.0 | 1455 | 34.4 | 35.5 | |
| 1665 | 193 | 740 | 100.4 (6) | 100.3 | 1410 | 35.5 | 46.8 | |
| 1750 | 185 | 740 | 100.0 (6) | 100.1 | 1365 | 36.3 | 41.5 | |
| 1545 | 153 | 740 | 100.5 (6) | 99.5 | 1345 | 32.6 | 70.0 | |
| 1265 | 211 | 725 | 100.9 (6) | 97.5 | 1235 | 32.5 | 39.2 | 5 T/C Out |
| 1350 | 216 | 725 | 100.1 (6) | 97.5 | 1210 | 33.1 | 52.2 | 5 T/C Out |
| 1455 | 231 | 730 | 99.8 (6) | 97.5 | 1150 | 31.4 | 43.8 | 5 T/C Out |
| 1175 | 199 | 725 | 100.0 (6) | 99.2 | 1270 | 31.7 | 66.6 | 5 T/C Out |
| 1465 | 192 | 2000 | 100.7 (6) | 101.9 | 1090 | 61.0 | 17.5 | 5 T/C Out |
| 2011 | 929 | 1491 | 98.6 (6) | 103.4 | 1045 | 149.3 | 6.7 | |
| 1606 | 408 | 1975 | 94.6 (6) | 96.4 | 1124 | 90.6 | 13.2 | |
| 1618 | 450 | 1518 | 99.9 (6) | 99.1 | 1235 | 87.2 | 17.0 | 1 T/C Out |
| 1962 | 460 | 3390 | 98.1 (6) | 97.6 | 1329 | 197.5 | 6.2 | 1 T/C Out |
| 2028 | 278 | 3464 | 98.2 (6) | 99.5 | 1328 | 203.5 | 6.0 | 3 T/C Out |
| 1717 | 350 | 3514 | 97.1 (6) | 98.0 | 1241 | 209.7 | 6.2 | 3 T/C Out |
| 1809 | 734 | 3217 | 95.8 (6) | 98.2 | 907 | 196.9 | 4.4 | 3 T/C Out |
| 1470 | 624 | 475 | 97.0 (6) | 101.9 | 751 | 37.2 | 26.2 | 3 T/C Out |
| (9) | (9) | 3293 | 97.1 (6) | (9) | 1117 | 207.6 | 4.0 | 5 T/C Overscaled |
| 1692 | 256 | 300 | (11) | 97.7 | 1624 | 55.4 | 61.5 | |
| 1140 | 121 | 286 | (11) | 90.7 | 1654 | 51.5 | 59.5 | |

CONFIDENTIAL

593/594

CONFIDENTIAL

(C) Table XLVIII. Summary of Measured Parameters for Preburner D

| Test No. | Date | Rig P., Staged Combustion/Preburner | Ambient Pressure, psia | LN ₂ Flow Rate, gpm | O ₂ Flow Rate, slm | Outflow Flow Rate, gpm | 1st Flowmeter Temperature, °F | O ₂ Flowmeter Temperature, °F | Outflow Flowmeter Temperature, °F | Outflow Injector Inlet Temperature, °F | Post Injector Inlet Temperature, °F |
|----------|--------------|-------------------------------------|------------------------|--------------------------------|-------------------------------|---------------------------------|-------------------------------|--|-----------------------------------|--|-------------------------------------|
| 2506C1C | 18 Aug 1967 | F-35108-1/P-33463-5 | 14.76 | 656 | 211 | 59.0 | 58.6 | 547 | 160 | 195 | 279 |
| 2506C2C | 23 Aug 1967 | F-35108-1/P-33463-5 | 14.74 | 641 1710 | 211 551 | 59.4 142 | 58.5 57.6 | 540 535 | 176 177 | 191 192 | 297 278 |
| 2506C3C | 31 Aug 1967 | F-35108-1/P-33463-5 | 14.74 | 630 1703 3470 | 211 551 1067 | 48.5 141.8 747.0 | 58.3 57.3 57.1 | 549 540 524 | 178 178 178 | 175 192 189 | 308 280 254 |
| 2506C4C | 1 Sept 1967 | F-35108-1/P-33463-5 | 14.74 | 652 1727 3504 | 212 547 1034 | 50.5 141.3 243.5 | 58.7 57.2 56.9 | 546 536 523 | 180 178 176 | 195 194 184 | 298 276 263 |
| 2506C5C | 8 Sept 1967 | F-35108-1/P-33463-5 | 14.74 | 666 1725 3596 | 210 543 1075 | 49.5 140.5 240.0 | 57.9 57.2 57.4 | 540 531 520 | 180 179 180 | 195 194 189 | 290 277 254 |
| 2506C6C | 9 Sept 1967 | F-35108-1/P-33463-5 | 14.74 | 664 1730 3165 | 210 546 551 | 49.5 139.0 239.0 | 57.8 57.2 56.9 | 534 531 519 | 179 177 178 | 190 191 187 | 282 270 249 |
| 2506C7C | 16 Sept 1967 | F-35108-1/P-33463-5 | 14.69 | 658 1719 4109 | 209 540 966 | 49.6 138.4 318.6 | 57.7 57.2 57.3 | 542 534 520 | 179 178 180 | 192 193 182 | 293 281 278 |
| 2506C8C | 15 Sept 1967 | F-35108-1/P-33463-5 | 14.69 | 642 1735 3250 | 173 682 1020 | 47.4 177.4 220.6 | 57.7 57.0 57.0 | 540 528 516 | 177 178 179 | 192 190 190 | 276 274 254 |
| 2506C9C | 15 Sept 1967 | F-35108-1/P-33463-5 | 14.69 | 531 7178 2138 3119 | 172 680 987 956 | 45.0 178.0 267.8 265.6 | 58.2 57.4 57.0 57.7 | 538 528 521 522 | 176 177 178 178 | 192 197 194 192 | 283 276 260 283 |
| 2506C10C | 18 Sept 1967 | F-35108-1/P-33463-5 | 14.69 | 807 | 257 | 65.2 | 58.3 | 539 | 177 | 197 | 292 |
| 2506C11C | 18 Sept 1967 | F-35108-1/P-33463-5 | 14.69 | 799 3496 5211 | 255 617 912 | 54.7 214.9 237.9 | 57.6 57.5 60.1 | 537 524 516 | 176 178 179 | 197 197 193 | 289 216 204 |
| 2506C12C | 28 Sept 1967 | F-35111-1/P-33463-6 | 14.64 | 685 | 257 | 64.3 | 57.9 | 535 | 177 | 197 | 288 |
| 2506C13C | 29 Sept 1967 | F-35111-1/P-33463-6 | 14.70 | 687 2989 | 212 903 | 49.2 226.6 | 57.8 56.7 | 529 511 | 176 177 | 190 187 | 275 278 |
| 2506C14C | 29 Sept 1967 | F-35111-1/P-33463-6 | 14.70 | 640 2722 | 210 867 | 50.0 213.6 | 57.1 55.5 | 530 512 | 176 177 | 190 188 | 276 265 |

CONFIDENTIAL

CONFIDENTIAL

Parameters for Preburner During Staged-Combustion Tests

| Test No. | Outdoor Injector Inlet Temperature, °F | Fuel Injector Inlet Temperature, °F | Liner Coolant Inlet Temperature, °F | 1/2 Flowmeter Pressure, psia | 1 Flowmeter Pressure, psia | Outdoor Flowmeter Pressure, psia | Outdoor Injector Inlet Pressure, psia | Fuel Injector Inlet Pressure, psia | Liner Coolant Inlet Pressure, psia | Chamber Pressure (Injector Stall), psia | Fuel Injector ΔP, psia | Outdoor Primary ΔP, psia | Outdoor Secondary ΔP, psia |
|-------------|--|---|---|---------------------------------------|-------------------------------------|---|---|--|--|---|---------------------------------|-----------------------------------|-------------------------------------|
| 173 | 279 | 279 | 279 | 5507 | 5552 | 6357 | 667 | 815 | 815 | 588.7 | 202 | 61 | 34 |
| 181 | 297 | 297 | 297 | 5656 | 6311 | 6399 | 686 | 703 | 703 | 603.7 | 105 | 56 | 31 |
| 182 | 278 | 278 | 278 | 5624 | 5936 | 6358 | 1788 | 1851 | 1851 | 1593.9 | 267 | 194 | 114 |
| 187 | 296 | 296 | 296 | 5468 | 6223 | 6300 | 656 | 710 | 710 | 605.1 | 99 | 52 | 29 |
| 192 | 280 | 280 | 280 | 5467 | 5961 | 6313 | 1758 | 1859 | 1859 | 1598.1 | 261 | 143 | 110 |
| 189 | 274 | 274 | 274 | 5-17 | 5102 | 6126 | 2324 | 2324 | 2324 | 1018.1 | 910 | 284 | 283 |
| 145 | 293 | 293 | 293 | 5416 | 6215 | 6283 | 687 | 736 | 736 | 617.2 | 128 | 57 | 32 |
| 184 | 276 | 276 | 276 | 5433 | 5836 | 6282 | 1780 | 1904 | 1904 | 1597.6 | 213 | 158 | 127 |
| 186 | 245 | 245 | 245 | 5372 | 4975 | 6038 | 2394 | 2465 | 2465 | 2091.7 | 564 | 267 | 270 |
| 195 | 290 | 290 | 290 | 5401 | 6611 | 6256 | 713 | 765 | 765 | 643.3 | 128 | 59 | 35 |
| 184 | 277 | 277 | 277 | 5445 | 6197 | 6197 | 1783 | 1921 | 1921 | 1597.9 | 330 | 167 | 129 |
| 189 | 269 | 269 | 269 | 5438 | 5233 | 5999 | 2401 | 2707 | 2707 | 2093.3 | 623 | 286 | 288 |
| 190 | 283 | 283 | 283 | 5390 | 6063 | 6298 | 689 | 734 | 734 | 616.1 | 118 | 59 | 30 |
| 191 | 270 | 270 | 270 | 5415 | 5704 | 6374 | 1781 | 1886 | 1886 | 1585.0 | 297 | 167 | 118 |
| 187 | 249 | 249 | 249 | 5282 | 4911 | 6005 | 2415 | 2551 | 2551 | 2061.9 | 686 | 260 | 204 |
| 191 | 287 | 287 | 287 | 5381 | 6732 | 6376 | 709 | 761 | 761 | 632.7 | 129 | 58 | 32 |
| 192 | 281 | 281 | 281 | 5364 | 6391 | 6219 | 1788 | 1931 | 1931 | 1593.6 | 333 | 168 | 174 |
| 188 | 228 | 228 | 228 | 5376 | 5423 | 6068 | 1720 | 2891 | 2891 | 2260.7 | 626 | 289 | 292 |
| 187 | 296 | 296 | 296 | 5386 | 4802 | 6309 | 624 | 671 | 671 | 576.3 | 97 | 51 | 24 |
| 186 | 274 | 274 | 274 | 5390 | 5480 | 6215 | 2117 | 2556 | 2556 | 2177.5 | 379 | 209 | 163 |
| 191 | 254 | 254 | 254 | 5381 | 5226 | 6038 | 2480 | 2682 | 2682 | 2129.6 | 595 | 305 | 206 |
| 187 | 292 | 292 | 292 | 5372 | 6604 | 6307 | 635 | 293 | 293 | 560.3 | 96 | 49 | 26 |
| 187 | 276 | 276 | 276 | 5381 | 5984 | 6231 | 2422 | 2595 | 2595 | 2181.0 | 372 | 202 | 161 |
| 184 | 280 | 280 | 280 | 5348 | 5416 | 6150 | 2422 | 2674 | 2674 | 2086.1 | 542 | 283 | 289 |
| 192 | 282 | 282 | 282 | 5373 | 5511 | 6152 | 2703 | 2567 | 2567 | 2953.2 | 543 | 285 | 288 |
| 197 | 292 | 292 | 292 | 5393 | 6574 | 6315 | 764 | 821 | 821 | 688.3 | 152 | 75 | 42 |
| 187 | 290 | 290 | 290 | 5324 | 6523 | 6308 | 741 | 769 | 769 | 656.6 | 134 | 71 | 43 |
| 187 | 216 | 216 | 216 | 5346 | 5498 | 6216 | 2598 | 2598 | 2598 | 2316.8 | 284 | 345 | 222 |
| 197 | 204 | 204 | 204 | 5275 | 5232 | 6224 | 2384 | 2517 | 2517 | 2884.0 | 632 | 435 | 431 |
| 192 | 288 | 288 | 288 | 5467 | 6640 | 6249 | 714 | 767 | 767 | 594 | 116 | 58 | 26 |
| 190 | 275 | 275 | 275 | 5432 | 5843 | 6277 | 714 | 740 | 740 | 577 | 107 | 55 | 22 |
| 187 | 218 | 218 | 218 | 5176 | 4890 | 6128 | 2560 | 2579 | 2579 | 2116 | 462 | 172 | 177 |
| 193 | 276 | 276 | 276 | 5364 | 5478 | 6281 | 696 | 710 | 710 | 577 | 89 | 52 | 20 |
| 188 | 245 | 245 | 245 | 4837 | 4584 | 6100 | 2992 | 3102 | 3102 | 2666 | 934 | 178 | 142 |

CONFIDENTIAL

2

CONFIDENTIAL

(C) Table XLIX. Summary of Calculated Performance for Prebur

| Test No. | Date | Rig No. Staged Combustion/Preburner | Total Fuel Flow Rate, lb _m /sec | Oxidizer Flow Rate, lb _m /sec | Total Liner Flow Rate, lb _m /sec | Overall Mixture Ratio | Injector Mixture Ratio ⁽¹⁾ |
|----------|--------------|--|---|---|--|-----------------------|---------------------------------------|
| 2508C1C | 18 Aug 1967 | F-35108-1/F-33463-5 | 13.3 | 6.4 | 0.68 | 0.48 | 0.50 |
| 2508C2C | 30 Aug 1967 | F-35108-1/F-33463-5 | 13.8 | 8.3 | 0.47 | 0.60 | 0.62 |
| | | | 35.9 | 23.3 | 1.21 | 0.65 | 0.67 |
| 2508C3C | 31 Aug 1967 | F-35108-1/F-33463-5 | 13.6 | 8.0 | 0.46 | 0.59 | 0.61 |
| | | | 35.4 | 23.2 | 1.21 | 0.65 | 0.68 |
| | | | 68.1 | 40.8 | 2.25 | 0.60 | 0.62 |
| 2508C4C | 1 Sept 1967 | F-35108-1/F-33463-5 | 13.7 | 8.3 | 0.50 | 0.60 | 0.62 |
| | | | 35.6 | 23.2 | 1.29 | 0.65 | 0.67 |
| | | | 68.1 | 39.8 | 2.40 | 0.58 | 0.60 |
| 2508C5C | 8 Sept 1967 | F-35108-1/F-33463-5 | 14.2 | 8.1 | 0.23 | 0.57 | 0.58 |
| | | | 36.3 | 23.0 | 0.58 | 0.63 | 0.64 |
| | | | 70.9 | 39.2 | 1.10 | 0.55 | 0.56 |
| 2508C6C | 9 Sept 1967 | F-35108-1/F-33463-5 | 13.8 | 8.2 | 0.23 | 0.59 | 0.60 |
| | | | 35.5 | 23.0 | 0.57 | 0.64 | 0.66 |
| | | | 62.1 | 45.7 | 0.95 | 0.73 | 0.74 |
| 2508C7C | 14 Sept 1967 | F-35108-1/F-33463-5 | 14.2 | 8.1 | 0.25 | 0.57 | 0.58 |
| | | | 36.4 | 22.9 | 0.60 | 0.63 | 0.64 |
| | | | 74.3 | 52.4 | 1.17 | 0.70 | 0.71 |
| 2508C8C | 15 Sept 1967 | F-35108-1/F-33463-5 | 11.7 | 7.0 | 0.19 | 0.60 | 0.61 |
| | | | 44.8 | 29.1 | 0.71 | 0.65 | 0.66 |
| | | | 65.3 | 44.2 | 1.01 | 0.67 | 0.68 |
| 2508C9C | 15 Sept 1967 | F-35108-1/F-33463-5 | 11.5 | 7.4 | 0.21 | 0.64 | 0.66 |
| | | | 44.6 | 29.2 | 0.75 | 0.65 | 0.66 |
| | | | 63.6 | 43.9 | 1.05 | 0.69 | 0.70 |
| | | | 63.6 | 43.5 | 1.08 | 0.68 | 0.69 |
| 2508C10C | 18 Sept 1967 | F-35108-1/F-33463-5 | 17.3 | 10.7 | 0.23 | 0.62 | 0.63 |
| 2508C11C | 18 Sept 1967 | F-35108-1/F-33463-5 | 17.1 | 9.0 | 0.23 | 0.52 | 0.53 |
| | | | 59.2 | 35.2 | 0.82 | 0.59 | 0.60 |
| | | | 85.5 | 53.7 | 1.20 | 0.63 | 0.63 |
| 2508P1C | 28 Sept 1967 | F-35111-1/F-33463-6 | 14.0 | 8.1 | 0.23 | 0.55 | 0.56 |
| 2508P2C | 29 Sept 1967 | F-35111-1/F-33463-6 | 14.0 | 8.0 | 0.22 | 0.57 | 0.58 |
| | | | 69.7 | 35.7 | 0.93 | 0.53 | 0.53 |
| 2508P3C | 29 Sept 1967 | F-35111-1/F-33463-6 | 13.2 | 8.2 | 0.19 | 0.63 | 0.63 |
| | | | 52.5 | 35.0 | 0.74 | 0.67 | 0.68 |

(1) Injector fuel flow rate = total fuel flow rate - total liner coolant flow rate

(2) Based on injector mixture ratio

(3) Based on area weighted thermocouple data 11.2 inches downstream of injector

(4) ΔT = maximum temperature - average temperature(5) $\eta_o = (\text{average temperature/ideal temperature})^{0.5} \times 100\%$

CONFIDENTIAL

CONFIDENTIAL

Performance for Preburner During Staged-Combustion Tests

| Test No. | Injector Mixture Ratio | Ideal (2) Temperature, °R | Average (3) Combustion Temperature, °R | ΔT (4) Profile, °R | Chamber Static Pressure | η_c (5) | Fuel Injection Velocity, ft/sec | Oxidiser Injection Velocity, ft/sec | Fuel Oxidiser Momentum Ratio |
|-------------|------------------------------|---------------------------------|---|----------------------------------|-------------------------------|--------------|--|--|---------------------------------------|
| 8 | 0.50 | 1166 | 1188 | 37 | 589 | 100.9 | 1979 | 42.9 | 87.2 |
| 10 | 0.62 | 1397 | 1406 | 281 | 604 | 100.3 | 1546 | 38.1 | 63.0 |
| 13 | 0.67 | 1439 | 1484 | 327 | 1596 | 100.8 | 1520 | 78.3 | 28.0 |
| 19 | 0.61 | 1379 | 1442 | 339 | 606 | 102.3 | 1519 | 36.7 | 66.1 |
| 25 | 0.68 | 1474 | 1472 | 359 | 1600 | 100.0 | 1504 | 77.5 | 27.7 |
| 30 | 0.62 | 1341 | 1314 | 235 | 3021 | 99.0 | 1550 | 125.9 | 19.3 |
| 30 | 0.62 | 1396 | 1433 | 264 | 618 | 101.3 | 1666 | 38.5 | 67.0 |
| 35 | 0.67 | 1460 | 1500 | 196 | 1599 | 101.4 | 1628 | 78.6 | 29.7 |
| 38 | 0.60 | 1306 | 1382 | 226 | 3095 | 102.9 | 1587 | 122.8 | 20.7 |
| 37 | 0.58 | 1308 | 1354 | 164 | 644 | 101.7 | 1630 | 39.0 | 69.9 |
| 43 | 0.64 | 1405 | 1428 | 198 | 1600 | 100.8 | 1670 | 78.9 | 31.9 |
| 45 | 0.56 | 1233 | 1261 | 216 | 3088 | 101.1 | 1677 | 121.8 | 23.7 |
| 48 | 0.60 | 1337 | 1359 | 235 | 615 | 100.8 | 1574 | 38.9 | 65.3 |
| 54 | 0.66 | 1424 | 1459 | 275 | 1587 | 101.2 | 1572 | 78.6 | 29.4 |
| 53 | 0.74 | 1557 | 1571 | 367 | 3065 | 100.4 | 1492 | 138.9 | 13.9 |
| 57 | 0.58 | 1320 | 1326 | 174 | 633 | 100.2 | 1644 | 38.6 | 70.6 |
| 53 | 0.64 | 1404 | 1448 | 265 | 1595 | 101.6 | 1687 | 78.6 | 32.3 |
| 60 | 0.71 | 1472 | 1563 | 399 | 3264 | 103.0 | 1587 | 137.8 | 13.7 |
| 60 | 0.61 | 1367 | 1432 | 264 | 575 | 102.3 | 1515 | 36.4 | 65.0 |
| 65 | 0.66 | 1433 | 1447 | 241 | 2180 | 100.5 | 1570 | 96.0 | 24.0 |
| 67 | 0.68 | 1461 | 1483 | 274 | 3133 | 100.9 | 1494 | 136.1 | 16.5 |
| 64 | 0.66 | 1453 | 1471 | 161 | 587 | 100.6 | 1493 | 35.8 | 61.3 |
| 65 | 0.65 | 1448 | 1485 | 202 | 2183 | 101.3 | 1549 | 95.5 | 23.4 |
| 69 | 0.70 | 1495 | 1510 | 275 | 3089 | 100.5 | 1592 | 135.6 | 15.2 |
| 68 | 0.59 | 1486 | 1466 | 217 | 2956 | 99.3 | 1650 | 133.6 | 17.2 |
| 72 | 0.63 | 1399 | 1513 | 438 | 339 | 104.0 | 1602 | 45.4 | 34.5 |
| 72 | 0.53 | 1231 | 1254 | 282 | 655 | 101.0 | 1638 | 43.0 | 69.3 |
| 79 | 0.60 | 1268 | 1370 | 380 | 2319 | 103.9 | 1380 | 113.0 | 19.7 |
| 83 | 0.63 | 1315 | 1356 | 232 | 2887 | 101.6 | 1579 | 167.0 | 14.4 |
| 85 | 0.56 | 1280 | 1345 | 168 | 642 | 102.5 | 1534 | 38.6 | 68.3 |
| 87 | 0.58 | 1261 | 1407 | 285 | 643 | 105.6 | 1427 | 37.9 | 63.3 |
| 83 | 0.53 | 1121 | 1220 | 166 | 3160 | 104.3 | 1365 | 112.5 | 22.1 |
| 83 | 0.63 | 1383 | 1574 | 210 | 630 | 106.7 | 1361 | 56.7 | 56.7 |
| 87 | 0.68 | 1421 | 1491 | 249 | 2781 | 102.4 | 1286 | 107.4 | 17.2 |

CONFIDENTIAL

597/598

CONFIDENTIAL

E. FACILITIES AND PROCEDURES

(C) The testing of the 250K preburner rig was conducted in the E-8 test facility, shown in figure 569, which was provided by the United Aircraft Corporation. This high pressure facility permits preburner or staged-combustion testing to pressures of 5000 psi at thrust levels up to 250,000 lb. This facility is described in more detail in Section IX of this report. The configuration used for control of the preburner is shown in figure 570.

(C) For the preburner program, a series of 80 nonfiring flow tests and approximately 30 hot firing tests were conducted to establish an accurate and repeatable control system. The early control concept, which utilized combustion gas temperature and chamber pressure to control the valve position during the acceleration transient, was abandoned because of the system response and system interaction, which prevented smooth and repeatable transient and steady-state operation. The alternative control concept, which utilized the flowmeter output as a closed-loop control signal for the position of the propellant valves during the start transient, proved to be a satisfactory and repeatable control system during the start transient. In this configuration, the operating level of the preburner is determined by the power lever angle, which schedules the oxidizer and fuel control valves to maintain and schedule the desired values of preburner liquid oxygen and hydrogen flows into the combustion process. The measured values of these flows are inputted to the control system and then compared with the desired levels, which are functions of the power lever angle.

(C) The preburner starting sequence is accomplished by diverting the required fuel and oxidizer flows from a preset overboard condition to the injector and allowing them to stabilize. The preburner combustion pressure is less than 1% at this point. The fuel and oxidizer valves are then ramped to provide approximately 7% flow and, after stabilization, switched to closed-loop flow control. The run tanks are then pressurized to the operating levels, and the preburner flows are ramped to the desired equivalent thrust level and combustion temperature, as shown in figure 571.

(C) During the starting sequence and ramp to 7%, the fuel mixer temperature control section modulates the gaseous hydrogen valves to regulate the GH_2 flow into the mixing section and provides the desired injector fuel temperature to simulate engine conditions. At 7%, the gaseous hydrogen valves are switched to flow control and ramped with the liquid hydrogen valves in the proper proportions to simulate engine conditions. The total fuel flow is then determined by measuring the gaseous and liquid flow rates. Three parallel valves in the liquid hydrogen system provide a flow range from starting to maximum flow.

CONFIDENTIAL

CONFIDENTIAL

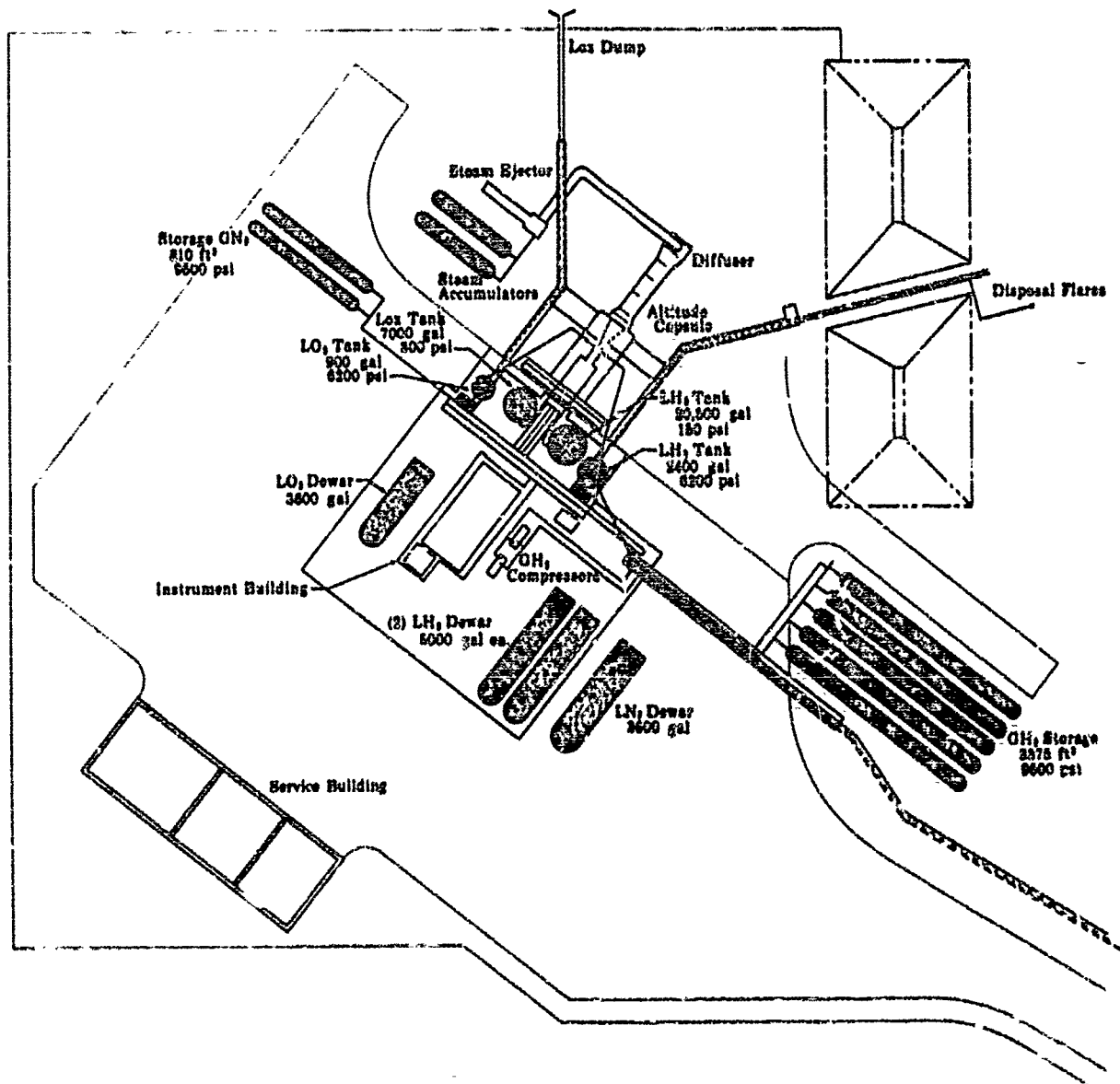


Figure 569. E-8 High Pressure Test Facility

FD 21139

600

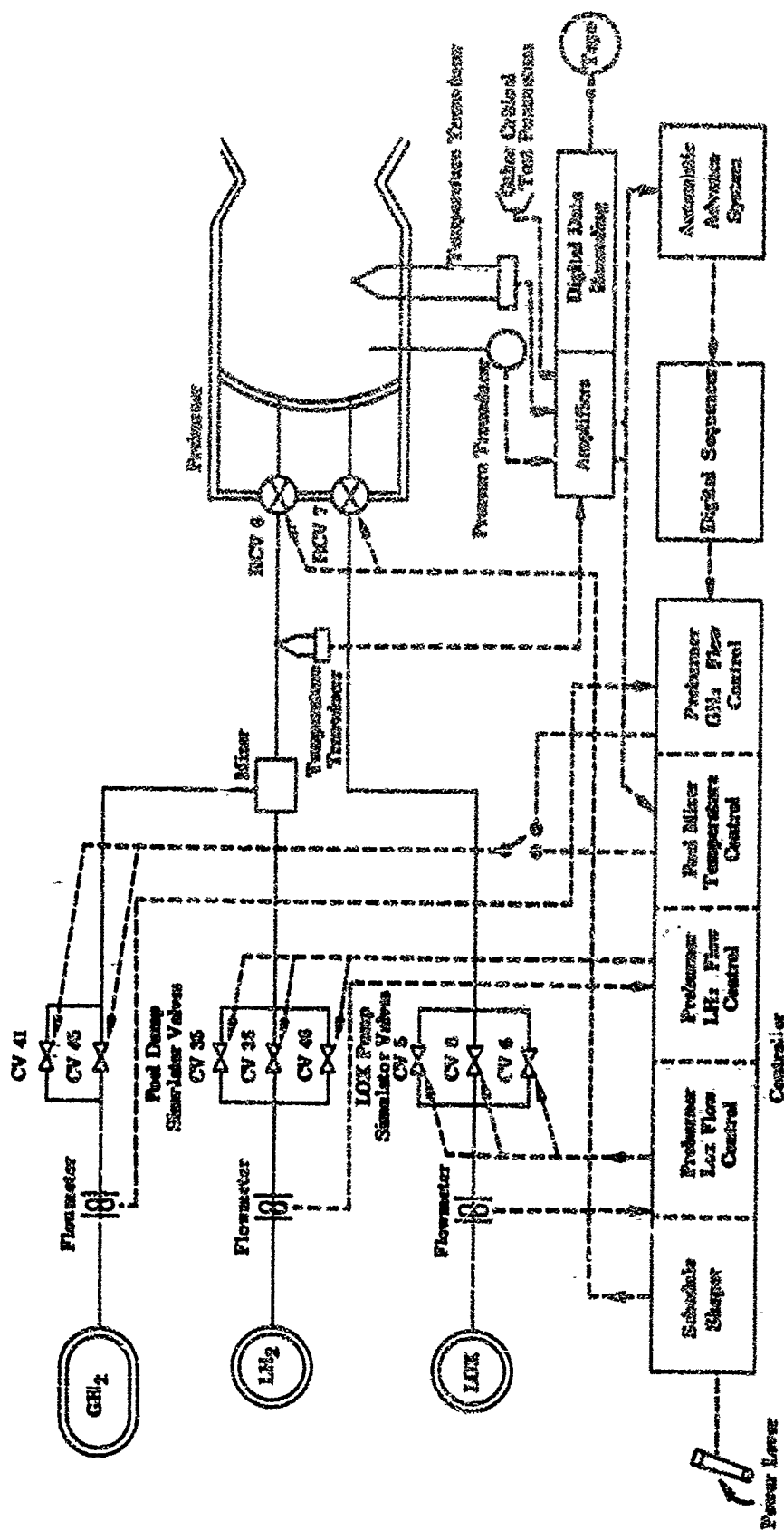
CONFIDENTIAL

(This page is Unclassified)

601

CONFIDENTIAL

(This page is Unclassified)



1551

CONFIDENTIAL

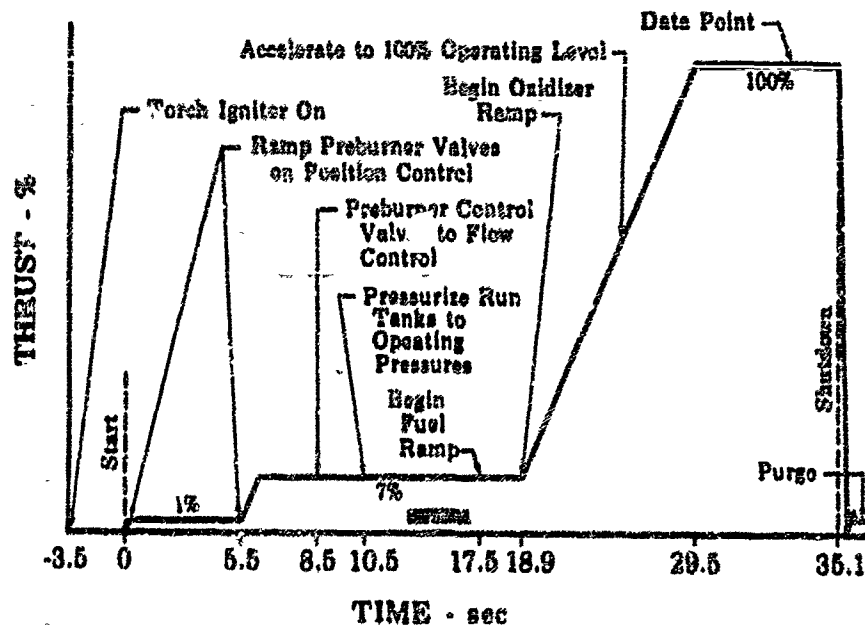


Figure 571. 250K Preburner Test Sequence

FD 23010

(U) The oxidizer flow is likewise closed-loop controlled through the computer with the necessary timing to maintain the required mixture ratio during the transient.

(U) Test conditions, other than those scheduled by power lever, are programmed in and out of the control by the digital sequencer to set starting flows, provide automatic changes of flow level, and provide automatic excursions in test conditions to acquire performance data.

CONFIDENTIAL

SECTION X
250K STAGED-COMBUSTION

| | |
|--|-----|
| A. Introduction | 603 |
| B. Summary and Conclusions | 603 |
| 1. Summary | 603 |
| 2. Conclusions | 603 |
| C. 250K Staged-Combustion Hardware Description | 604 |
| D. Test Program and Test Results | 617 |
| 1. Introduction | 617 |
| 2. Staged-Combustion Performance | 621 |
| 3. Preburner Tests | 621 |
| 4. Main Chamber Coolant Optimization and Performance Tests | 621 |
| 5. Two-Position Nozzle | 637 |
| 6. Main Chamber Combustion Stability Tests | 637 |
| E. Test Facilities and Procedures | 645 |
| 1. Test Facilities | 645 |
| 2. 250K Test Procedures | 648 |

CONFIDENTIAL

**SECTION X
250K STAGED COMBUSTION**

A. INTRODUCTION

(U) The objectives of the 250K staged-combustion program were to:

1. Demonstrate satisfactory ignition
2. Determine performance over the mixture ratio and throttling range
3. Evaluate hardware durability
4. Evaluate combustion stability
5. Demonstrate the operating characteristics of the translating nozzle
6. Demonstrate the functional ability and durability of the regenerative primary nozzle.

B. SUMMARY AND CONCLUSIONS

1. Summary

(U) To accomplish the program objectives, tests were conducted using a 250,000-lb thrust staged-combustion thrust chamber. Main chamber hardware fabricated under a company-sponsored program for the tests included two main injectors, two main igniters, six sets of uncooled graphite chamber liners, two cooled copper wafer liners, and two chamber shells. Nozzle hardware fabricated included one sheetmetal primary nozzle, one regeneratively cooled primary nozzle, and two sheetmetal translating secondary nozzle skirts. Preburner hardware from the 250,000-lb thrust level preburner program was used.

(U) A third chamber shell was fabricated to provide pulsing ports and locations for high frequency response pressure transducers.

(U) A total of 10 successful staged-combustion coolant optimization and performance tests was conducted. Six tests were made to optimize chamber coolant flow rate and four tests were made with optimum coolant flow. Eight of the tests were made using the translating secondary nozzle, and four tests were made using the regeneratively cooled primary nozzle skirt.

(C) To demonstrate combustion stability, three pulsing tests were conducted firing 40- and 80-grain charges into the main chamber at the 20 and 100% thrust levels.

2. Conclusions

(C) The following conclusions were made:

1. Main chamber transpiration cooling flows of less than 1% of total propellant flow were demonstrated.

CONFIDENTIAL

CONFIDENTIAL

2. Vacuum impulse performance exceeding 96% of theoretical was demonstrated at the engine mixture ratios from 5.0 to 6.3. Additional development will be required to attain 96% efficiency at an engine mixture ratio of 7.0.
3. Immediate recovery of the main chamber pressure following 40 and 80 grain pulsing charges at injector mixture ratios of 5.9, 6.7, and 8.5 showed that the combustion process was extremely stable.
4. Dimensional stability of the chamber throat and the condition of the main injector and chamber hardware after 377 seconds of hot time and 42 seconds at full thrust, indicated the durability of the main burner hardware. However, some minor delamination was noted in the combustion chamber.
5. The two-position nozzle demonstrated the desired sea level flow stabilization, but nozzle performance at low chamber-to-ambient pressure ratios was less than expected.
6. The functioning and durability of the regeneratively cooled primary nozzle was demonstrated.

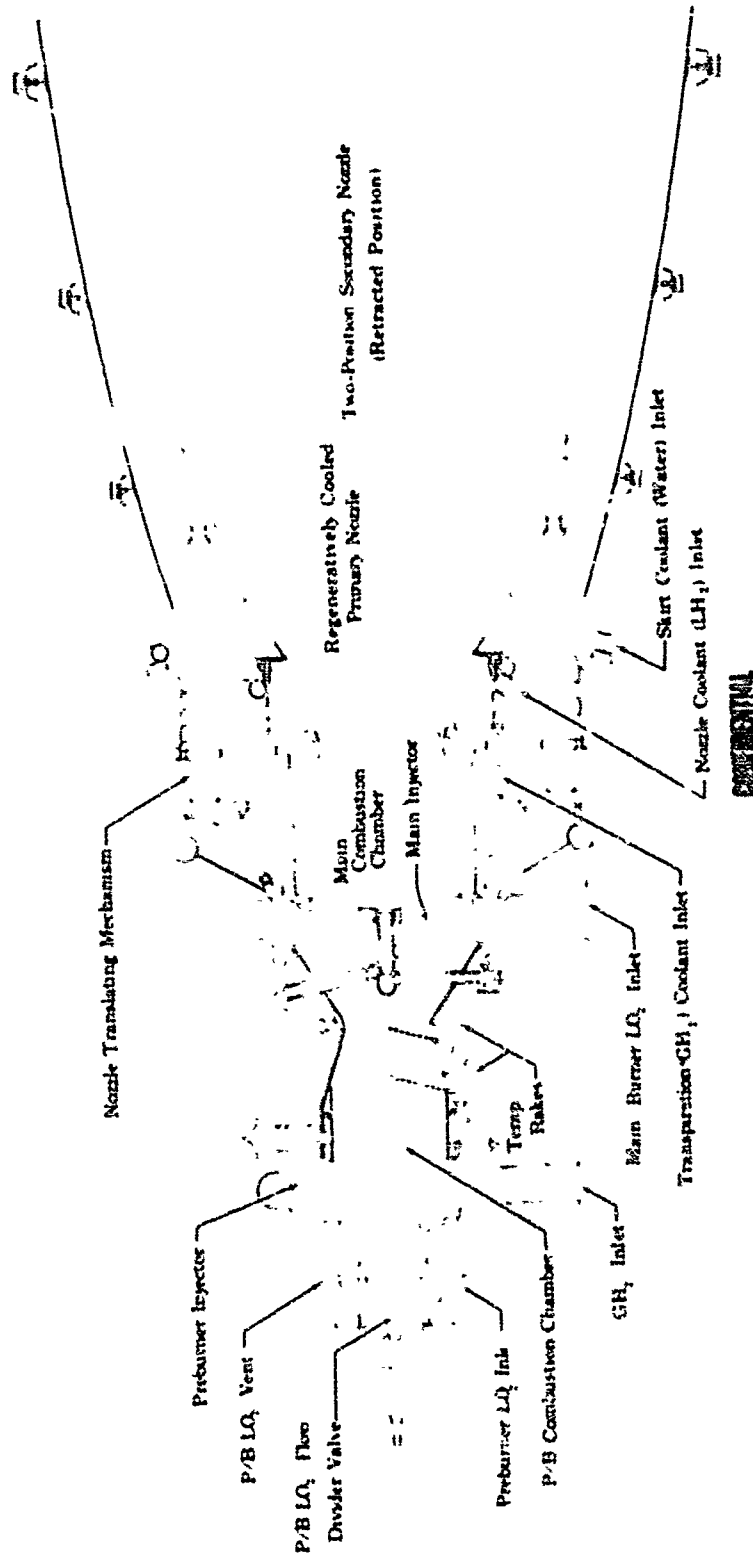
C. 250K STAGED-COMBUSTION HARDWARE DESCRIPTION

(U) The 250K ground test staged combustion thrust chamber configuration is shown in figure 572.

(C) The main burner, illustrated in figure 573, is located between the preburner and nozzle. The main burner consists of the main injector, chamber shell, transpiration-cooled chamber liner, transpiration-cooled nozzle liner, and a torch igniter unit. The preburner combustion products are the main burner fuel supply, supplemented only with the hydrogen required for transpiration cooling the thrust chamber. Eighty five percent of the engine oxidizer is supplied to the main injector as a liquid and is injected into the fuel-rich preburner combustion gases for combustion in the main chamber. These combustion products are then accelerated through the nozzle to produce thrust.

(C) The function of the main injector, shown in figure 574, is to inject, atomize, and mix the liquid oxidizer with the hot combustion products from the preburner in a manner that achieves maximum combustion efficiency in the main chamber. The injector, figure 575, is a radial spraybar design. The oxidizer injection elements are brazed into the radial spraybars and project through slots in the porous Rigmesh injector faceplate as shown in figure 576. These slots in the injector face are sized to direct and distribute approximately 92% of the fuel-rich preburner gases on the injected liquid oxidizer. The remainder of the preburner gases flow through the porous faceplate to form a barrier between the faceplate and the main burner combustion products.

CONFIDENTIAL



CONFIDENTIAL

FD 21190A

Figure 572. Staged-Combustion Rig Configuration

CONFIDENTIAL

CONFIDENTIAL

FD 20691A

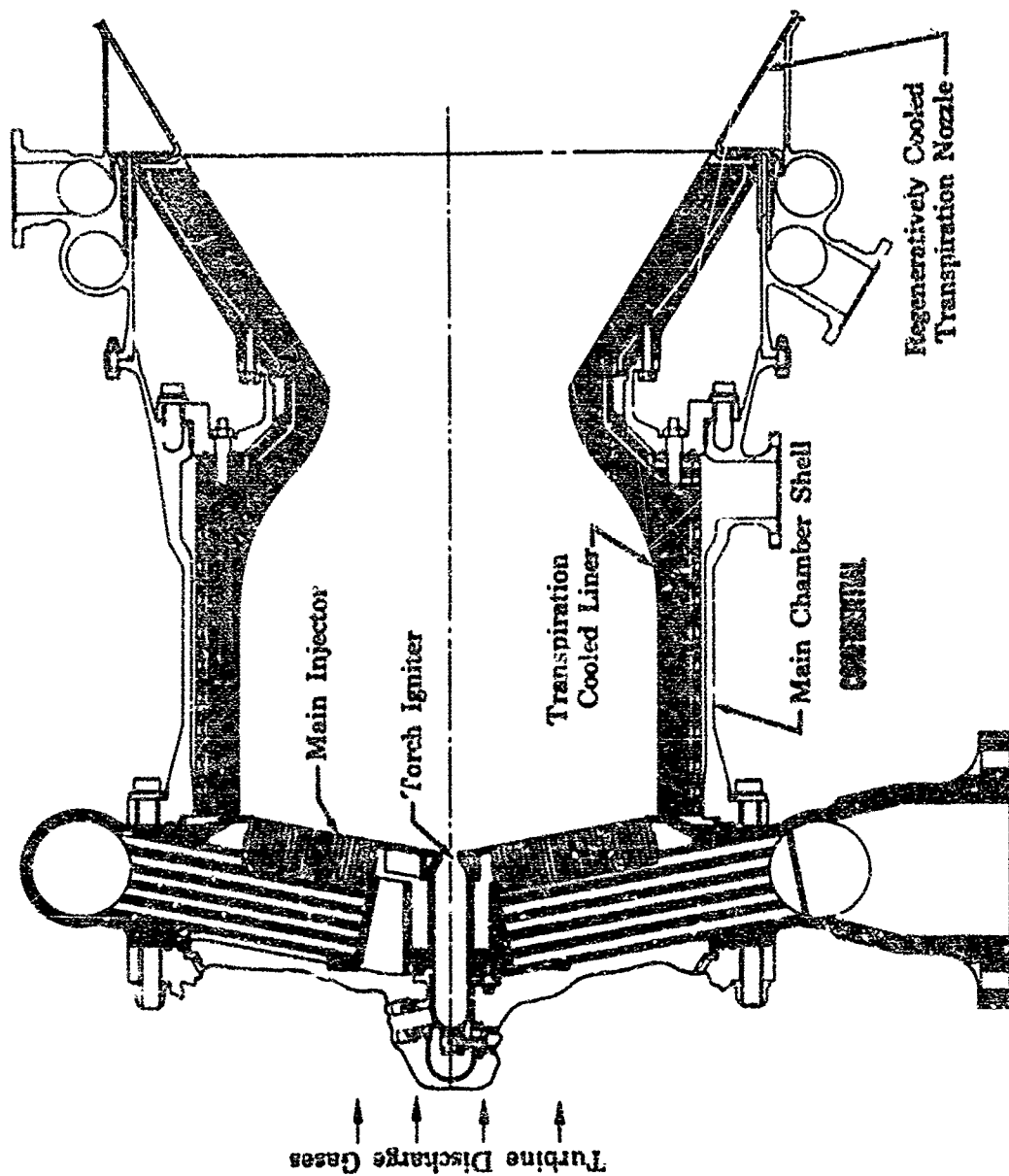


Figure 573. Main Burner

THIS PAGE CONTAINS SUBJECT MATTER COVERED BY A SECRET
ORDER WITH A MODIFYING "SECURITY REQUIREMENTS PERMIT"
ISSUED BY U.S. COMMISSIONER OF PATENTS

606
CONFIDENTIAL

CONFIDENTIAL

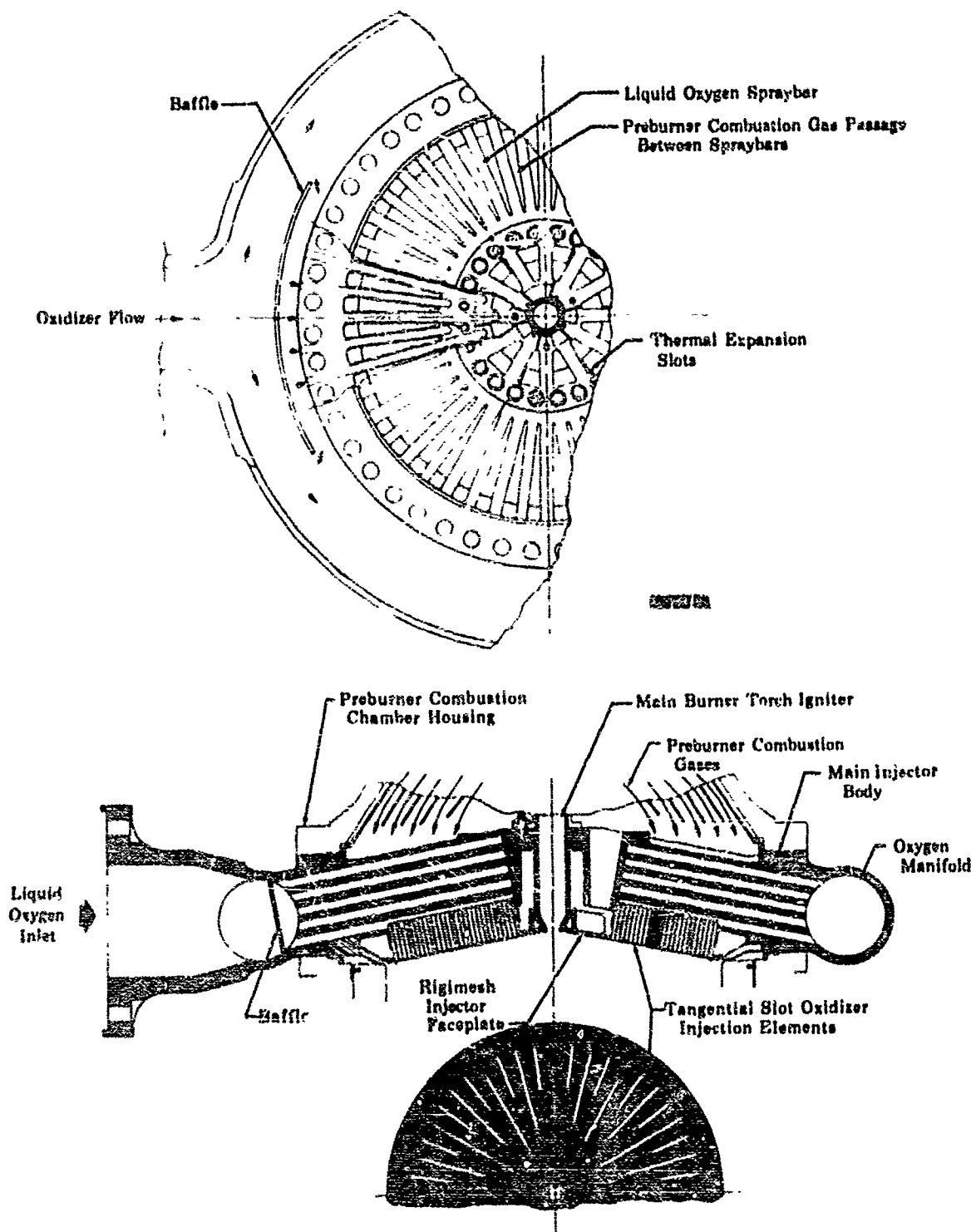
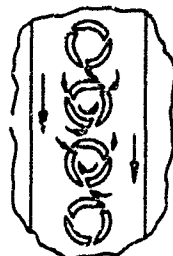
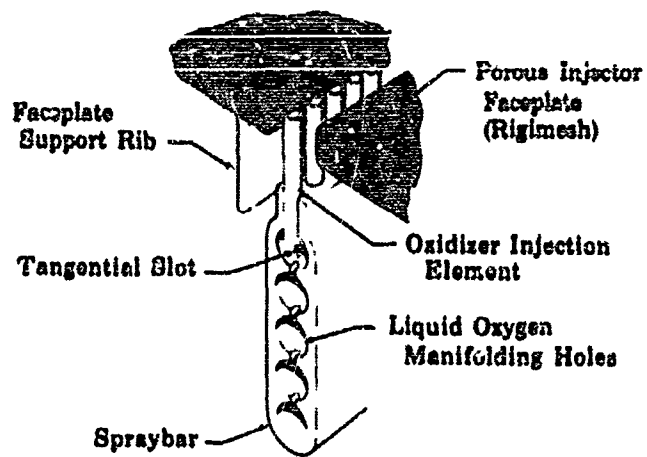


Figure 574. Main Injector Configuration

FD 20693

CONFIDENTIAL

CONFIDENTIAL



Section A-A

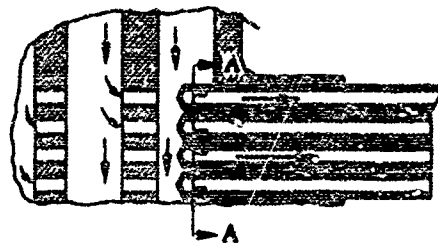


Figure 575. Main Injector Spraybar
Cross-Section

FD 20688



Figure 576. Main Injector Assembly

FE 70340

CONFIDENTIAL

CONFIDENTIAL

(U) The main torch igniter is located in the center of the main injector. The igniter, similar to the preburner torch igniter, is a hydrogen-cooled, continuous-burning, oxygen-hydrogen torch with dual spark ignition systems. The igniter torch is directed axially into the main chamber.

(C) The main combustion chamber, shown in figure 577, includes the main chamber shell, the transpiration-cooled chamber and nozzle liners, and the liner support. The main chamber shell constitutes the pressure vessel for the main burner and is the main structural member of the engine for support of the primary and secondary exhaust nozzles. The transpiration-cooled liners are constructed of thin copper wafers that have spiral grooves etched in both faces. These wafers are brazed bonded to form a controlled porosity unit. Gaseous hydrogen passes through the grooves to convectively cool the liner and then flows into the main chamber to form a relatively cool gaseous barrier along the inner surface of the liner.

(U) The analytical heat transfer model (discussed in Section VI) was used in conjunction with wafer structural requirements to determine acceptable limits in the spiral groove dimensions. A dimensioned cross section of a typical wafer is shown in figure 578, and groove dimensional distribution characteristics are shown in figures 579 through 581. Every wafer was inspected visually and dimensionally. Groove widths were limited to maintain an acceptable braze bonding area.

(C) Figure 582 shows the predicted effect of bulk zone flow area on cooling requirements at different chamber locations. The bulk zone area was kept large enough to ensure a predicted coolant mass flux at a minimum supply pressure of 3400 psia.

(C) The nozzle, shown in figures 583 and 584, consists of the primary nozzle, translating secondary nozzle and drive mechanism. The nozzle has a design area ratio of 89 truncated at an area ratio of 60. The primary portion of the nozzle mates to the rear section of the transpiration cooled liner at an area ratio of 4.75 and extends to an area ratio of 20. The primary nozzle is regeneratively cooled. A sheet-metal skirt extends from an area ratio of 20 to an area ratio of 60. The secondary nozzle is supported on a translating mechanism that allows the secondary to move 15 inches, from the retracted (open) to the extended (closed) position.

CONFIDENTIAL

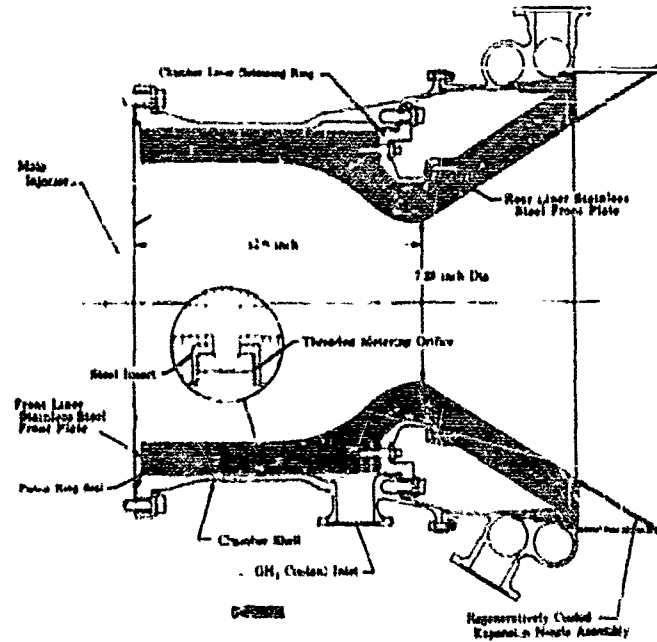


Figure 577. Main Chamber Configuration

FD 16084C

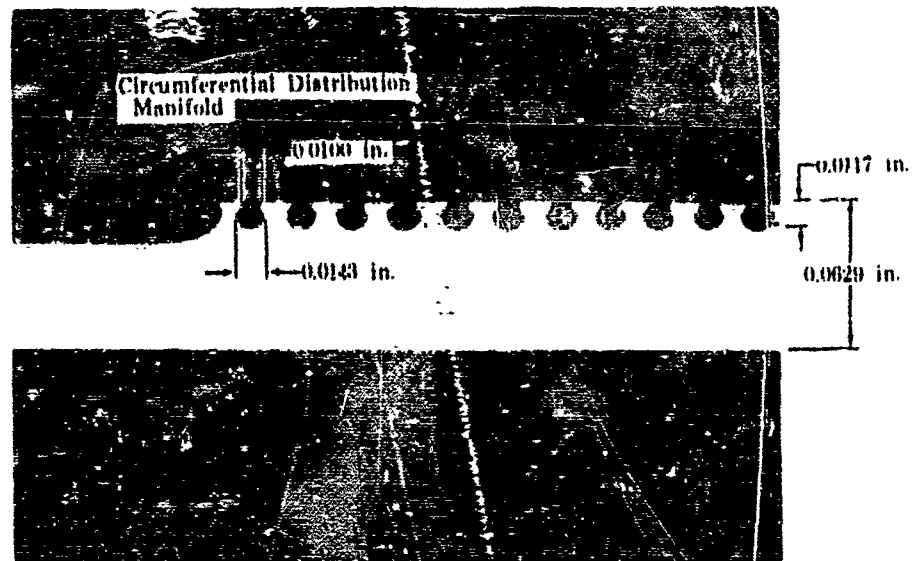
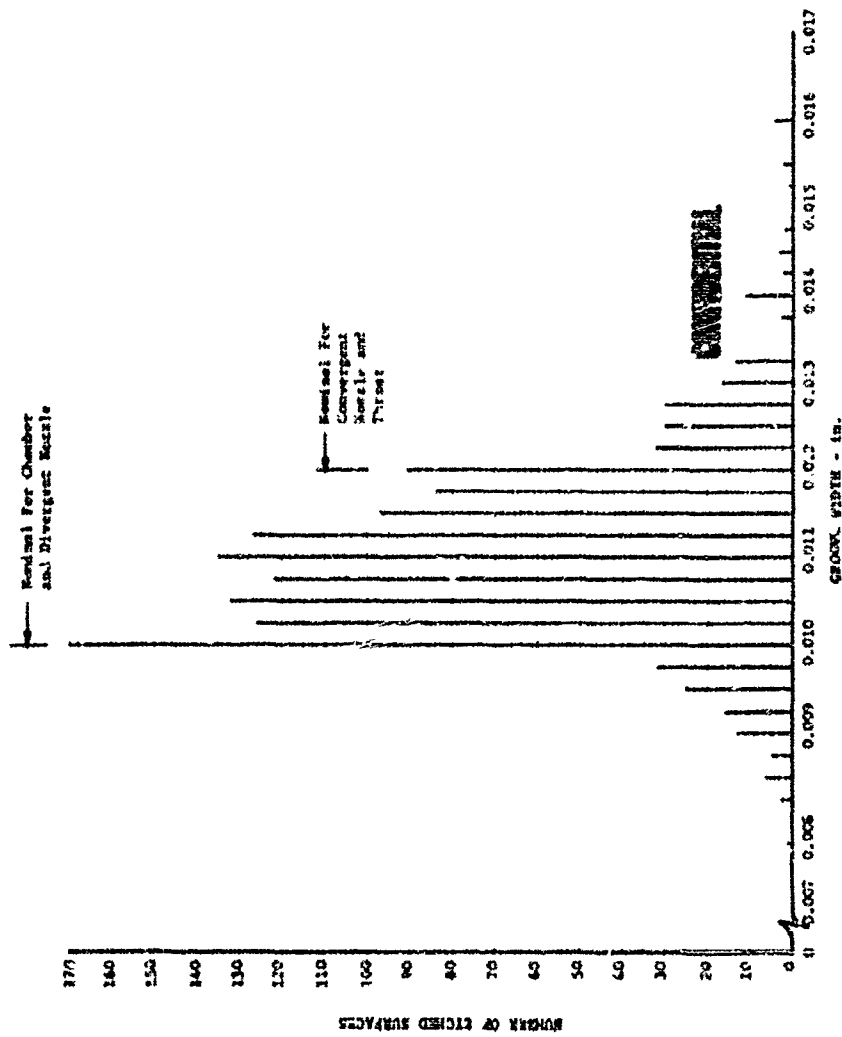


Figure 578. Cross Section of Typical Photoengraved Wafer

FD 23009

CONFIDENTIAL



DF 59392

Figure 579. Photoengraved Spiral Groove Average Widths for 250K Chamber Plates

CONFIDENTIAL

CONFIDENTIAL

DF 59393

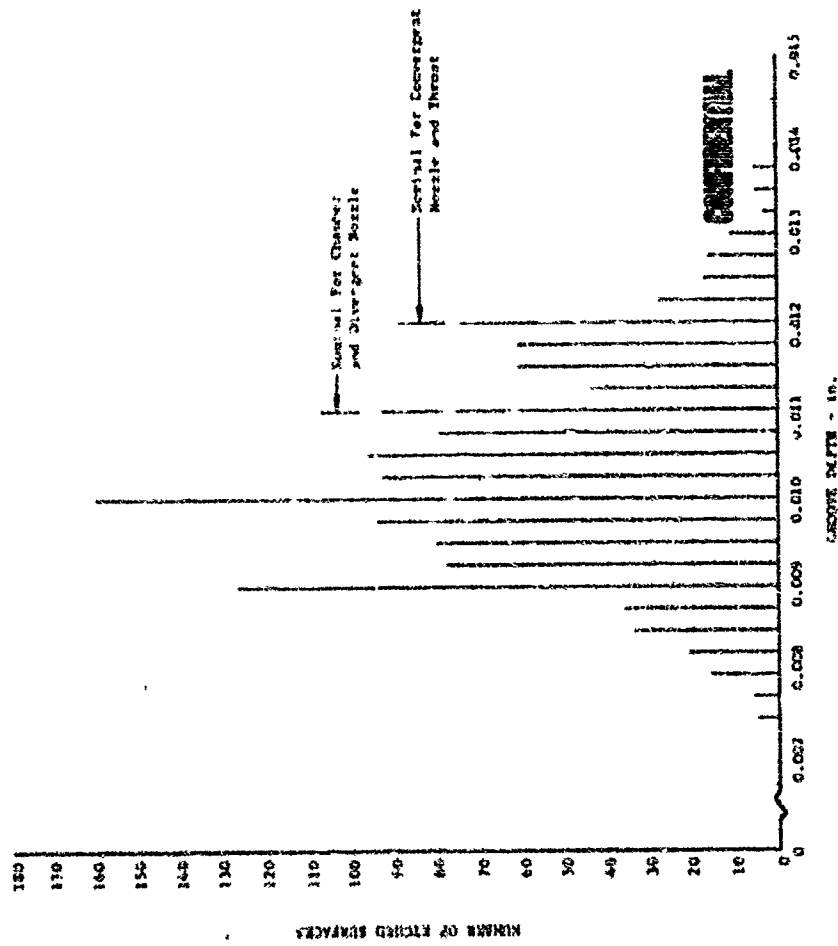
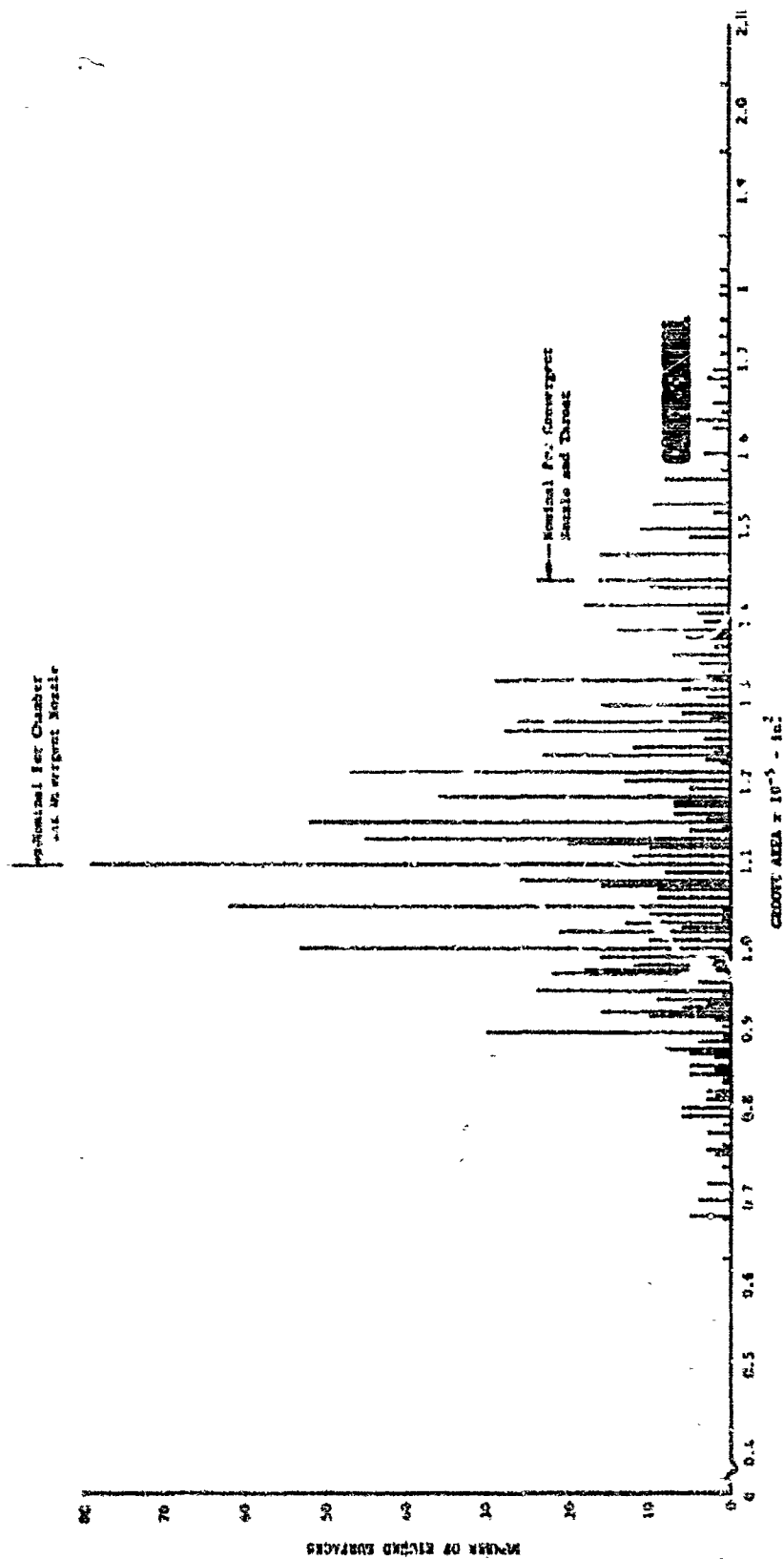


Figure 580. Photoengraved Spiral Groove Average Depths for 250K Chamber Plates

612
CONFIDENTIAL

CONFIDENTIAL



613

CONFIDENTIAL

DF 59394

Figure 581. Photoengraved Spiral Groove Average Areas for 250K Chamber Plates

CONFIDENTIAL

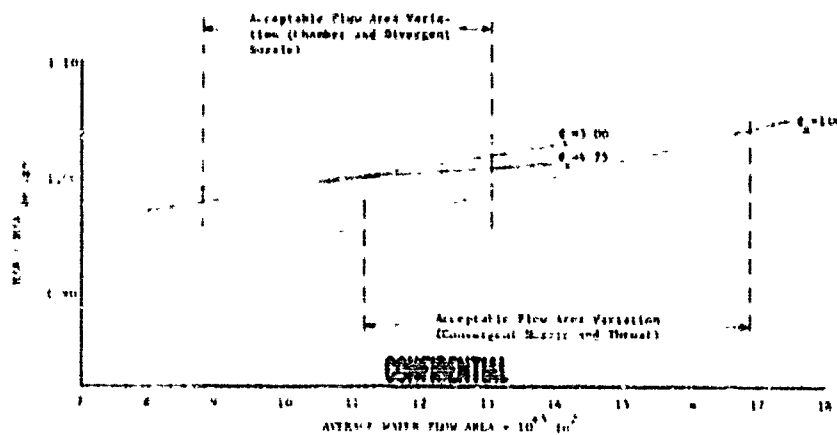


Figure 582. Relative Coolant Flux
vs Average Wafer Flow Area

DF 59505

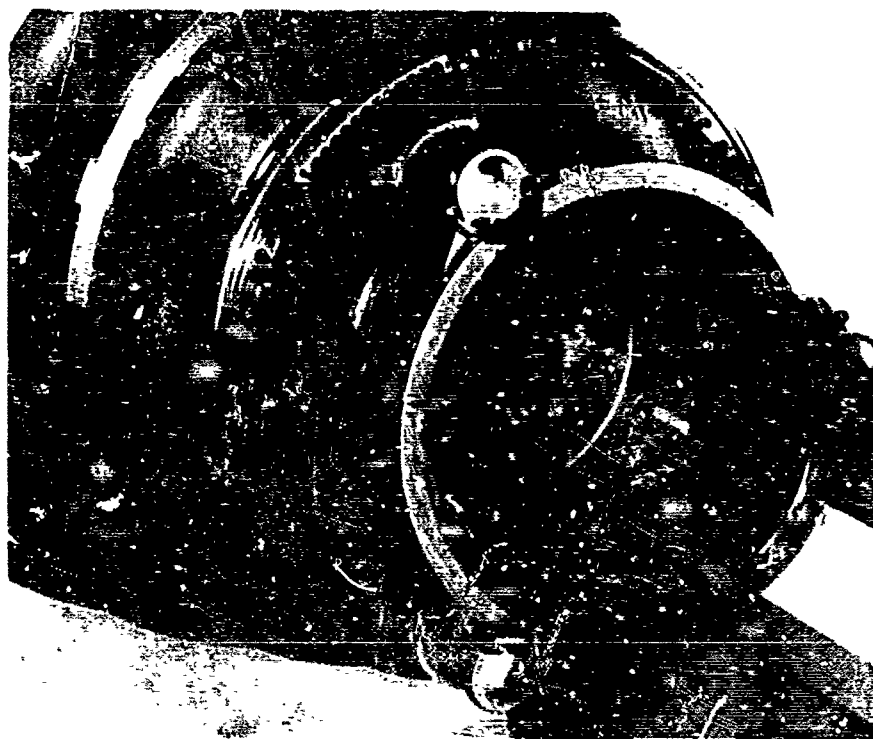


Figure 583. 250K Translating Nozzle
Showing Drive Mechanism

FE 70054

CONFIDENTIAL

CONFIDENTIAL

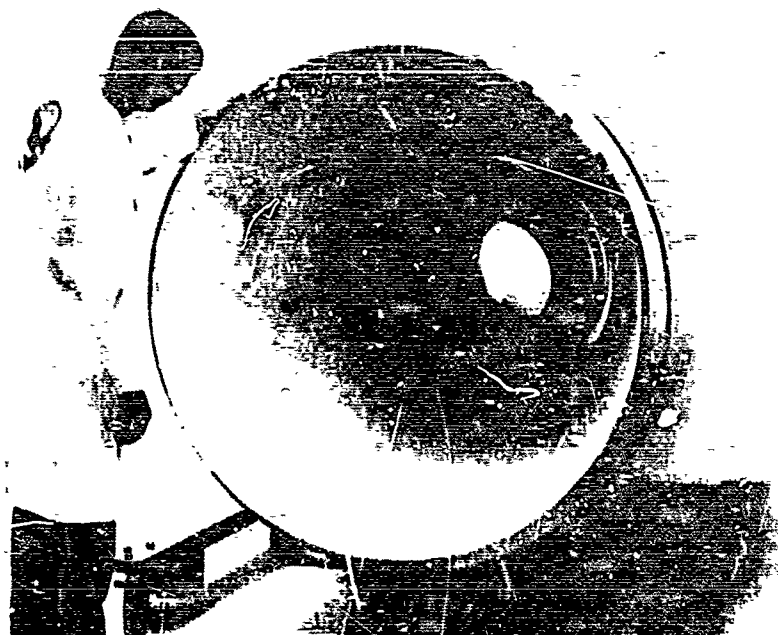


Figure 584. 250K Translating Nozzle Showing
Primary and Sheetmetal Secondary

FE 7035~

(U) Combustion stability chamber pulsing hardware was designed and constructed. Pressure pulses were generated by firing 40 and 80 grain explosive charges in pulse gun chambers with a burst diaphragm rated at 20,000 psi. Pressure fluctuations were measured by piezoelectric dynamic pressure transducers mounted in proximity to the chamber inner wall.

(C) The following main chamber pulsing hardware was procured under the contract: an 8-in. main chamber shell, a 2-in. spacer, a 3-in. housing for the pulse guns and pressure transducers, a combustion chamber liner, and longer tie bolts to attach the new chamber shell, spacer, and housing to the preburner and main injector. The pulse guns from the preburner program were used.

(U) The main chamber liner used a combination of film and transpiration cooling. The convergent nozzle section was salvaged from the transpiration-cooled liner that was damaged after the eighth-staged combustion test, and brazed to a steel cylinder. The steel cylinder formed a housing for two film-cooled combustion chamber liner sections. The liner section adjacent to the transpiration section was made from an uncooled graphite chamber liner. The forward section was made of solid copper brazed to a steel ring at the upstream end which formed a film coolant inlet annulus. The graphite section was located axially inside the steel cylinder with dowel pins and the copper section was retained with countersunk flathead screws. This formed a chamber liner assembly that was inserted inside the chamber shell. The pulse gun barrels and two of the transducer housings enter the chamber through the solid

CONFIDENTIAL

CONFIDENTIAL

copper liner section. Rubber O-rings were used to prevent coolant flow through passages other than the film coolant annulus and the transpiration-cooled section.

(U) Figures 585 and 586 show pulse gun and pressure transducer installation configurations. Figure 587 shows the chamber shell and chamber liner configuration.

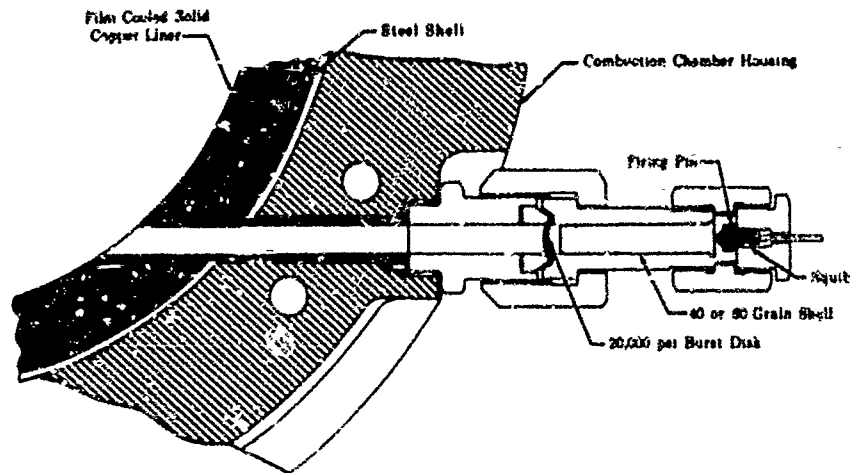


Figure 585. Main Chamber Pulse Gun Installation FD 23015

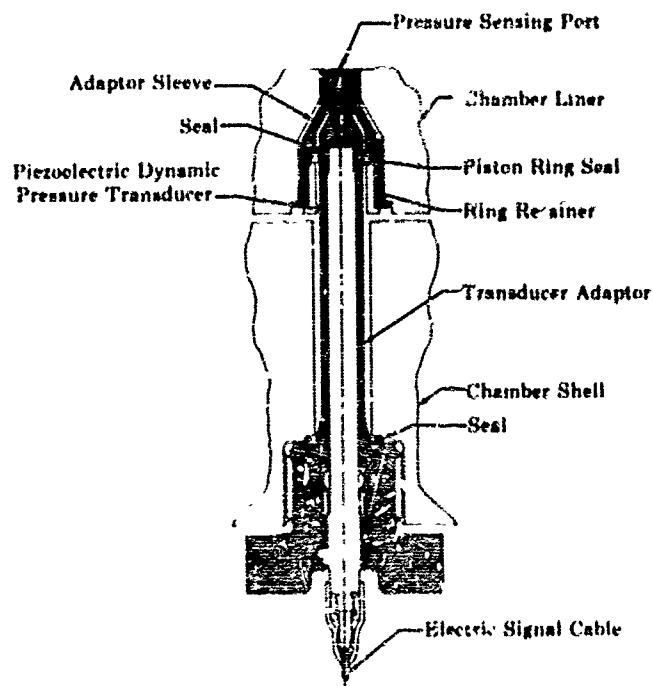


Figure 586. Main Chamber Pressure Transducer Installation

FD 23014

616

CONFIDENTIAL

(This page is Unclassified)

CONFIDENTIAL

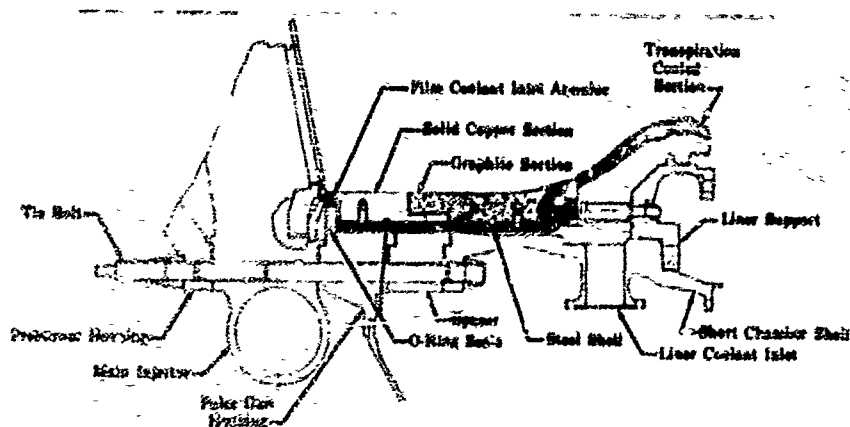


Figure 587. 250K Main Chamber Pulse Testing Configuration

FD 23013

D. TEST PROGRAM AND TEST RESULTS

1. Introduction

(C) Testing of the 250K thrust level stage-1-combustion lightweight design hardware was conducted on the 6600 psi E-8 pressure-fed facility to demonstrate the following:

1. Satisfactory ignition
2. Staged-combustion performance between 20 to 100% thrust and 5.0 to 7.0 engine mixture ratio ranges.
3. Hardware durability.
4. Combustion stability.

(C) To accomplish these objectives, the test program was divided into three phases:

1. Preburner tests
2. Main chamber coolant optimization and performance tests
3. Main chamber combustion stability tests.

(U) The staged-combustion ground test rig, shown mounted in the test stand in figure 588, consists of the preburner and main burner assemblies and the two-position nozzle.

(U) A description of the test facility and test procedures is presented in paragraph E of this Section.

CONFIDENTIAL

CONFIDENTIAL

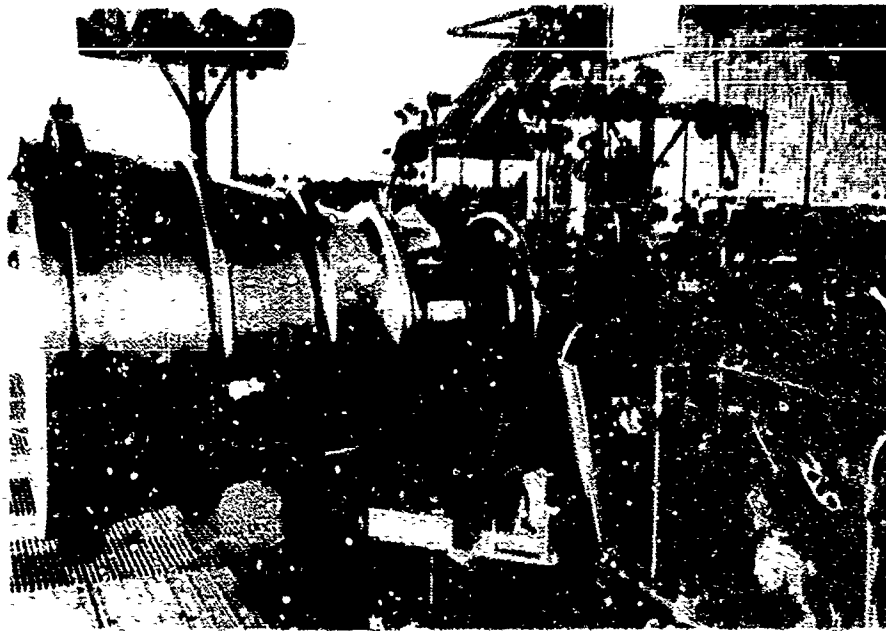


Figure 5A8. Staged-Combustion Rig
Installed in Test Stand

FE 71244

(C) The six additional preburner tests (runs No. 67 to 72 inclusive) were necessary after completion of the preburner performance test series to demonstrate satisfactory preburner chamber temperature profile control required for staged-combustion testing during the startup and shutdown transients.

(C) A total of 10 completely successful stage combustion coolant optimization and performance tests was conducted. The main chamber was reorificed twice to produce a nearly optimized coolant distribution with an approximately uniform surface temperature of 1900°R in the combustion chamber and divergent nozzle, and 1700°R in the convergent nozzle including the throat. The analytical heat transfer model and the temperature sensitive platings were employed to determine coolant reductions. Percent coolant to total flow rate ratios (\dot{w}_c/\dot{w}_p) of less than 1.0% were demonstrated over the engine mixture ratio range.

(C) Chamber and nozzle performance with the cooled primary nozzle was demonstrated over the engine mixture ratio range of 3.9 to 7.1 and over the throttling range of 20 to 100% thrust during the final 5 performance tests. Vacuum specific impulse efficiency, $\eta_{I_{vac}}$, of 97.3, 96.6, and 94.0% based on theoretical one-dimensional isentropic equilibrium values was achieved at overall mixture ratios (r) of 5.0, 6.0, and 7.0, respectively, with the nozzles extended ($\epsilon = 50$), and transpiration cooling flow rates (\dot{w}_c/\dot{w}_p) of approximately 1.0%. Nozzle efficiency (η_{np}) decreased 3.2% between overall mixture ratios of 5 and 7 at 100% thrust. Analytical studies have indicated that this is the result of increasing combustion gas mixture ratio profile variation and/or increasing nozzle friction at higher mixture ratios.

CONFIDENTIAL

CONFIDENTIAL

(C) Reducing transpiration cooling flow (\dot{w}_c/\dot{w}_p) from 1.5% to 1.0% during the cooling optimization tests increased specific impulse approximately 1.5% at 100% thrust, $\tau = 6$.

(C) Preburner combustion temperature level did not appear to significantly influence main chamber performance for the range of 1300°R to 1600°R.

(C) The two-position nozzle demonstrated stabilized sea level nozzle flow. The retracted ($\epsilon = 20$) thrust was 1.0% greater than the nozzle extended thrust at sea level.

(C) A secondary airflow is induced by the primary nozzle flow, which results in reduced static wall pressures along the inside of the secondary nozzle. The effect is a drag force of up to 1% of the sea level thrust.

(C) Estimates of the vacuum specific impulse for nozzle retracted operation shown in figure 589 show performance to be 4.0% lower than the nozzle extended performance. This lower performance is the result of lower nozzle C_d (3%) and secondary nozzle drag (1%). These estimates with the nozzle retracted are probably conservative since they are based on sea level test data, which include the secondary nozzle drag. This drag force would not be present under vacuum conditions.

(C) The primary nozzle flow impinged on the secondary nozzle at chamber pressures greater than approximately 2600 psia at sea level conditions with this nozzle configuration. Secondary nozzle temperatures indicate the possibility of overheating if the engine is operated for a long duration under attachment conditions without cooling the secondary skirt.

(C) Main chamber combustion stability was demonstrated at various thrust levels and mixture ratios. The main chamber was pulsed with 40 grain and 80 grain explosive charges at 20% thrust and 100% thrust.

(C) Main chamber durability was demonstrated by the good condition of the hardware after a total hot firing time of 377 seconds, including 42 seconds at 100% thrust. Dimensional stability of the 250K main chamber throat in contrast to the 50K, shown in figure 590, indicates the effectiveness of the circumferential and axial thermal reliefs in minimizing thermal strain, a requirement for long cyclic fatigue life. The dimensional changes reflect a cyclic strain on the order of a 0.3% strain or less with predicted life of more than 10,000 cycles according to the study by S.S. Manson and C. Halford (Reference NASA TMX-52270), and shown in figure 591. The two-directional thermal strain reliefs are shown schematically in figure 592. The radially directed slots shown on a detail wafer in figure 593a provide thermal strain relief in the circumferential (hoop) direction. Relief in the axial direction was obtained by photoengraving a 0.001-inch annulus at the ID in the ungrooved face as shown in figure 593b. Overpressurization of the main chamber during startup and shutdown transients caused inward bowing of the cylindrical section and was responsible for some wafer plate separation. Overpressurization would not occur in an actual engine since it is a pump-fed and not a pressure-fed system. In addition, some separation occurred in the divergent nozzle because of excessive thermal strain (no thermal reliefs were provided).

CONFIDENTIAL

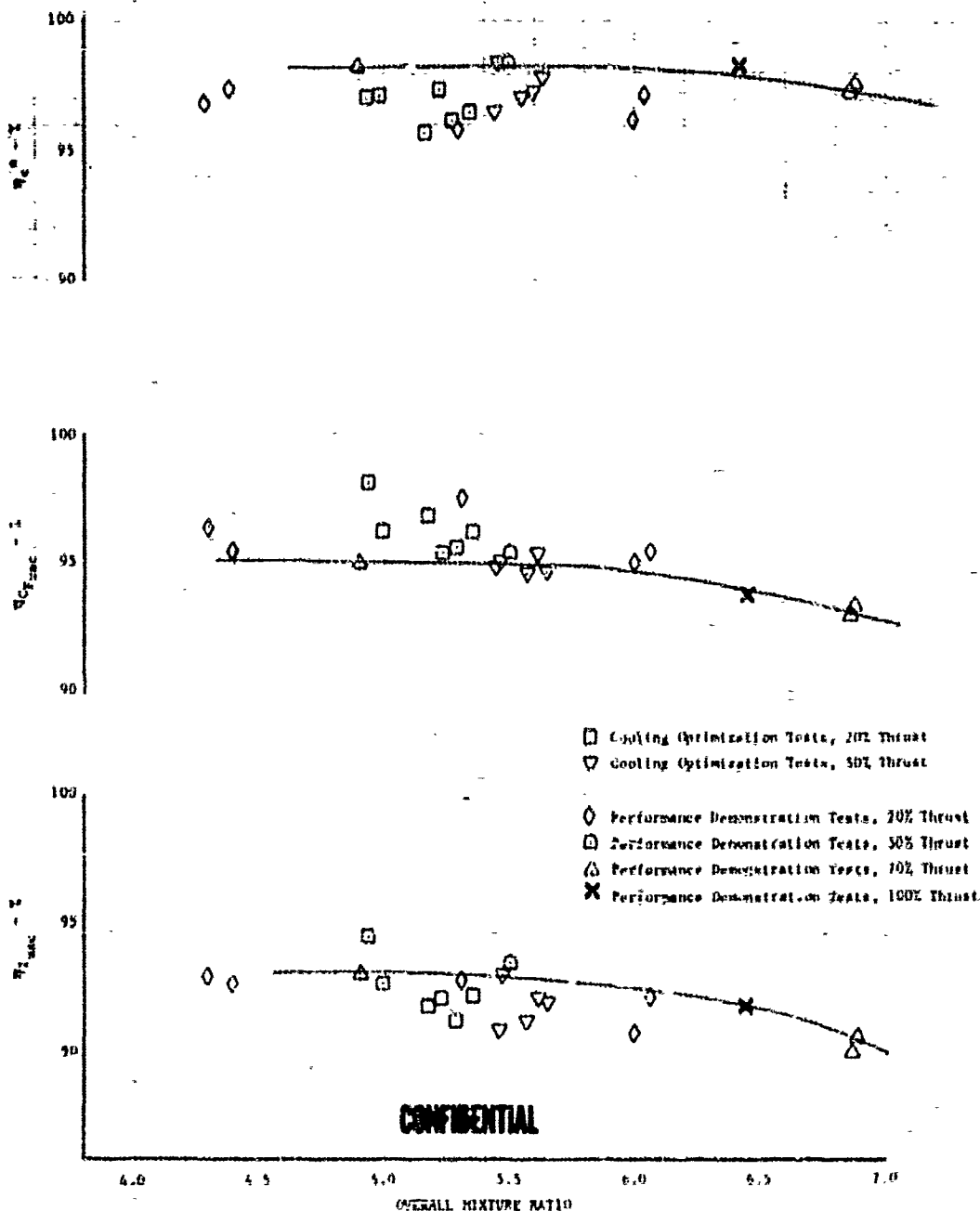


Figure 5F Throttled Vacuum Performance, Area Ratio = 20

DF 60404

620

CONFIDENTIAL

CONFIDENTIAL

(U) The regeneratively cooled primary nozzle demonstrated functional ability and durability.

2. Staged-Combustion Performance

(C) Summaries of measured and calculated performance data for all staged combustion tests are presented in tables I and LI. Performance obtained over the throttling range at sea level and vacuum conditions with the nozzle extended and retracted is compared to theoretical one-dimensional isentropic equilibrium values and is shown as a function of engine mixture ratio in figures 589 and 594 through 596. These data were calculated in a manner similar to the 50K staged combustion tests as described in Appendix IV. Vacuum performance with the nozzle retracted as shown in figure 589 includes secondary nozzle drag. This drag force would not be present under vacuum conditions. Efficiencies at the higher engine mixture ratios may be improved with more uniform preburner temperature profile and a significant exhaust bulk temperature increase. Increasing preburner exhaust bulk temperature would provide higher main burner injector momentum ratios.

(C) Steady-state data were taken at the 20 and 100% thrust levels for all performance tests except tests No. 250SC1C and 250SC2C, which were programmed to shutdown at 33-1/3% and 75% thrust, respectively, and test No. 250SC10C, which was advanced to shutdown during the acceleration to 50% thrust. Fifty percent thrust data were obtained during test No. 250SC2C through 250SC7C and 70% thrust data for test No. 250SC8C, 250SC9C, and 250SC11C. The combustion stability tests were ramped directly from 20 to 100% thrust. The two-position nozzle was extended only at the 100% thrust level and retracted at shutdown to ventilate and minimize the side-loading effects during chamber deceleration.

(U) An exhaust gas sampling probe was used to evaluate the mixture ratio profile at the exit plane of the secondary nozzle and is discussed in Appendix V.

3. Preburner Tests

(C) Six additional preburner tests (run No. 67 to 72) were conducted prior to initiating the staged-combustion tests to improve the starting and shutdown test sequence and to minimize the temperature spike during the shutdown. Incorporating a supplemental fuel flow eliminated the shutdown temperature spike. The back pressure nozzle area was resized for runs No. 71 and 72 to simulate staged-combustion back pressure during the startup to 20% thrust flows. The tests verified that the starting and shutdown were acceptable for staged combustion operation.

4. Main Chamber Coolant Optimization and Performance Tests

(C) A total of 27 cooled tests, 10 of which were completely successful, was conducted (1) to establish starting and operational sequences, (2) to optimize coolant distribution, and (3) to demonstrate performance over the required mixture ratio and throttling ranges. Five tests at

CONFIDENTIAL

100% thrust were required to optimize cooling. Injector mixture ratio was maintained at a nominal 6.5 at the 20, 50, and 100% thrust levels except for test No. 2508C6C, which was a 7:1 mixture ratio test. The condition of the main injector and main chamber during testing is shown in figures 597 and 598, respectively.

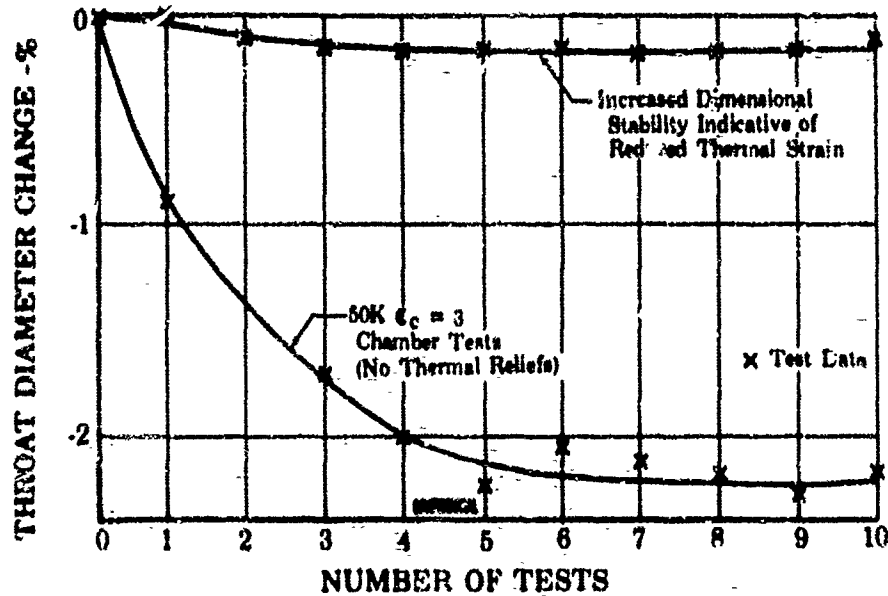


Figure 590. Demonstration of Cooled Thrust Chamber Thermal Strain Relief

FD 21929A

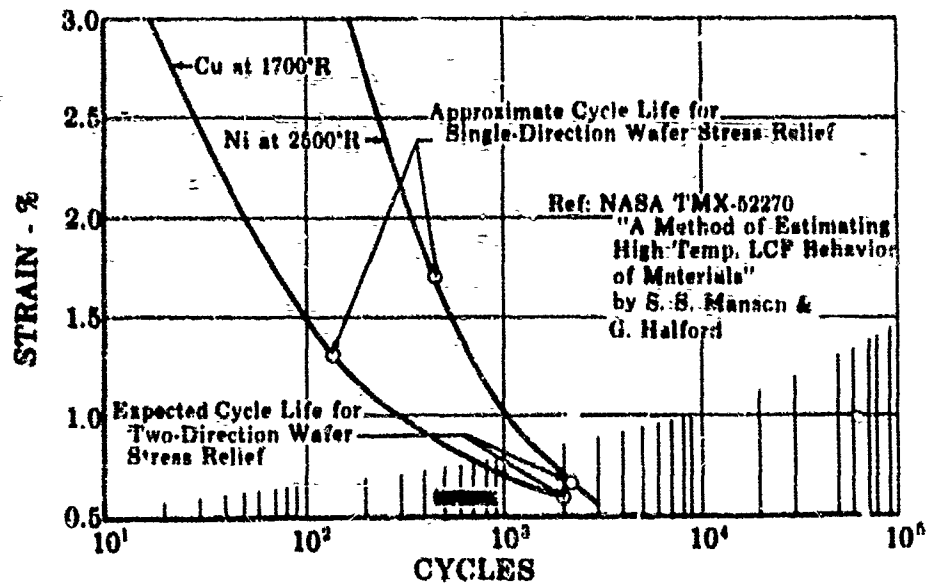


Figure 591. Effect of Strain on Wafer Low Cycle Fatigue Life

FD 21055

CONFIDENTIAL

CONFIDENTIAL

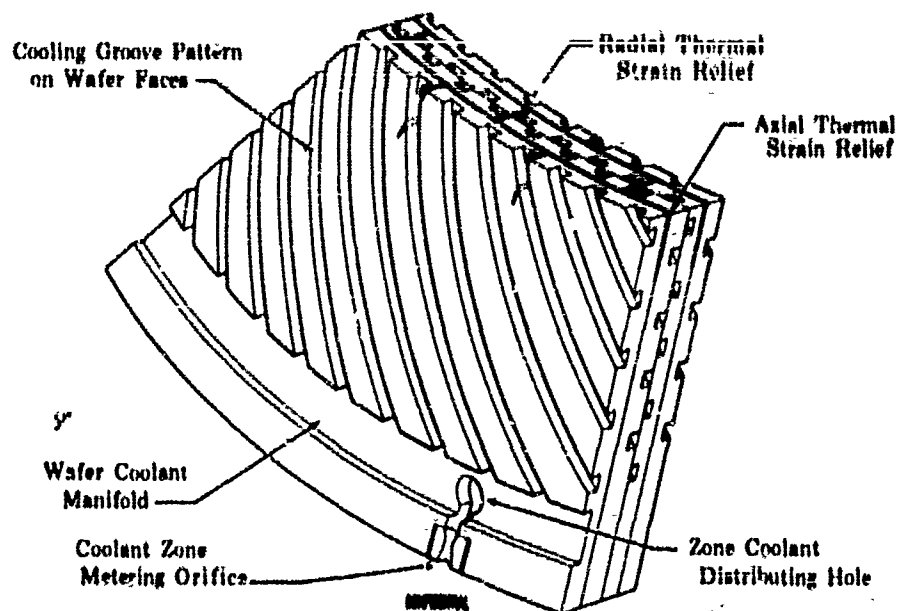


Figure 592. Two-Directional Thermal Strain Reliefs

FD 21319A



(a) Circumferential



(b) Axial

Figure 593. Grooved Wafer Thermal Relief

FD 23432

CONFIDENTIAL

CONFIDENTIAL

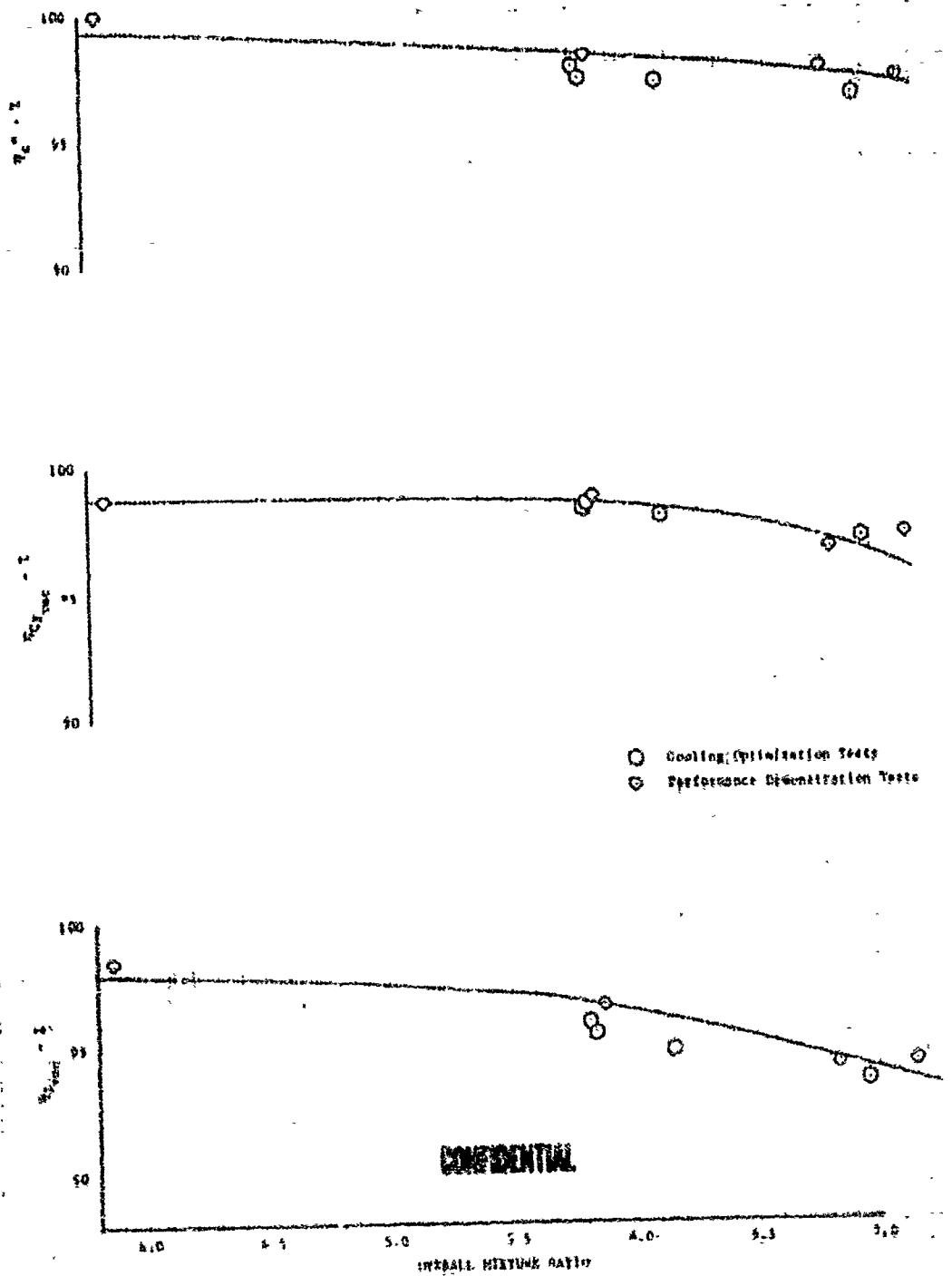


Figure 59a. Vacuum Performance at 100% Thrust-Area Ratio ≈ 60

DP 66433

CONFIDENTIAL

CONFIDENTIAL

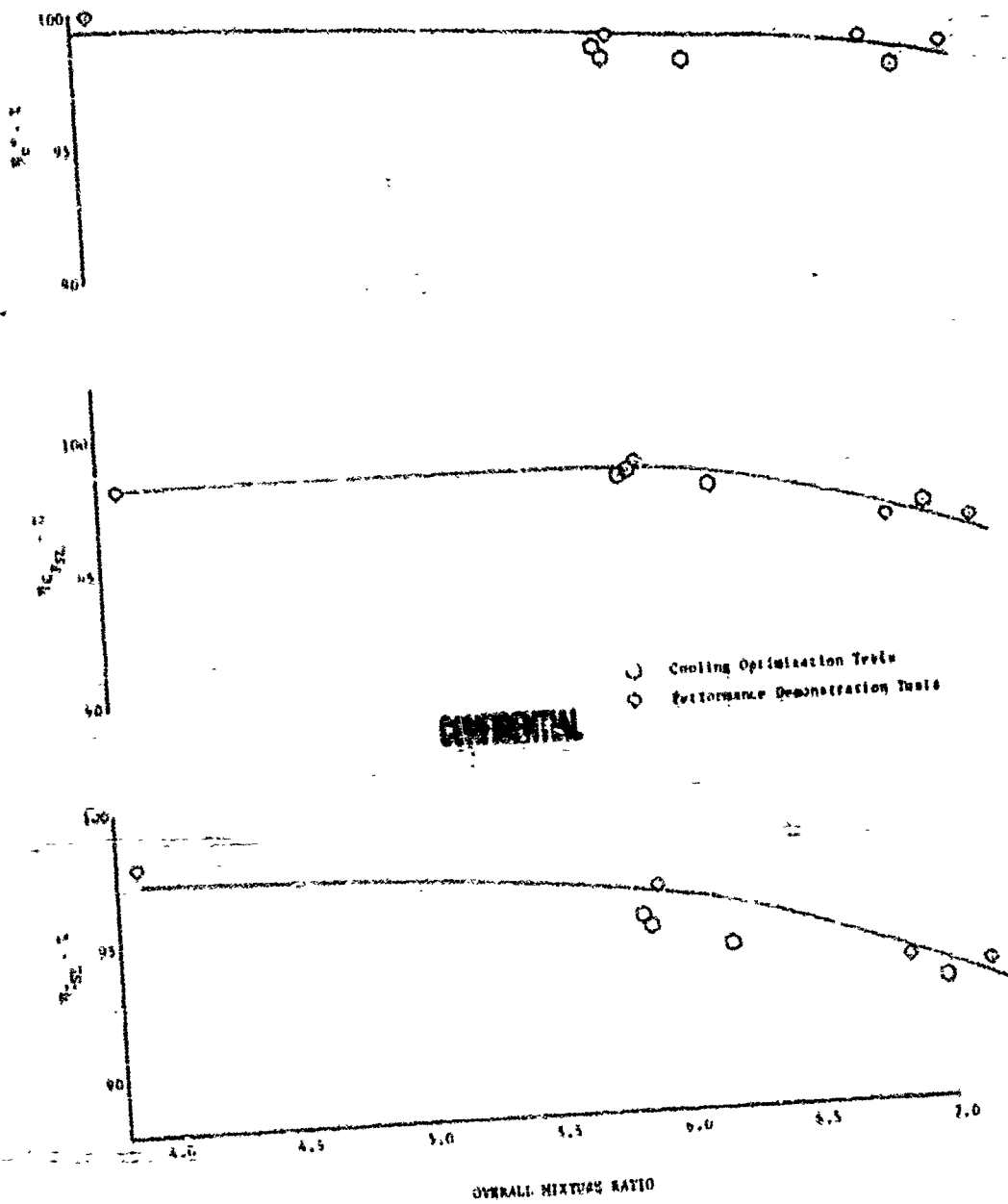


Figure 595. Sea Level Performance at 100% Thrust,
Area Ratio = 60

DF 60403

625

CONFIDENTIAL

CONFIDENTIAL

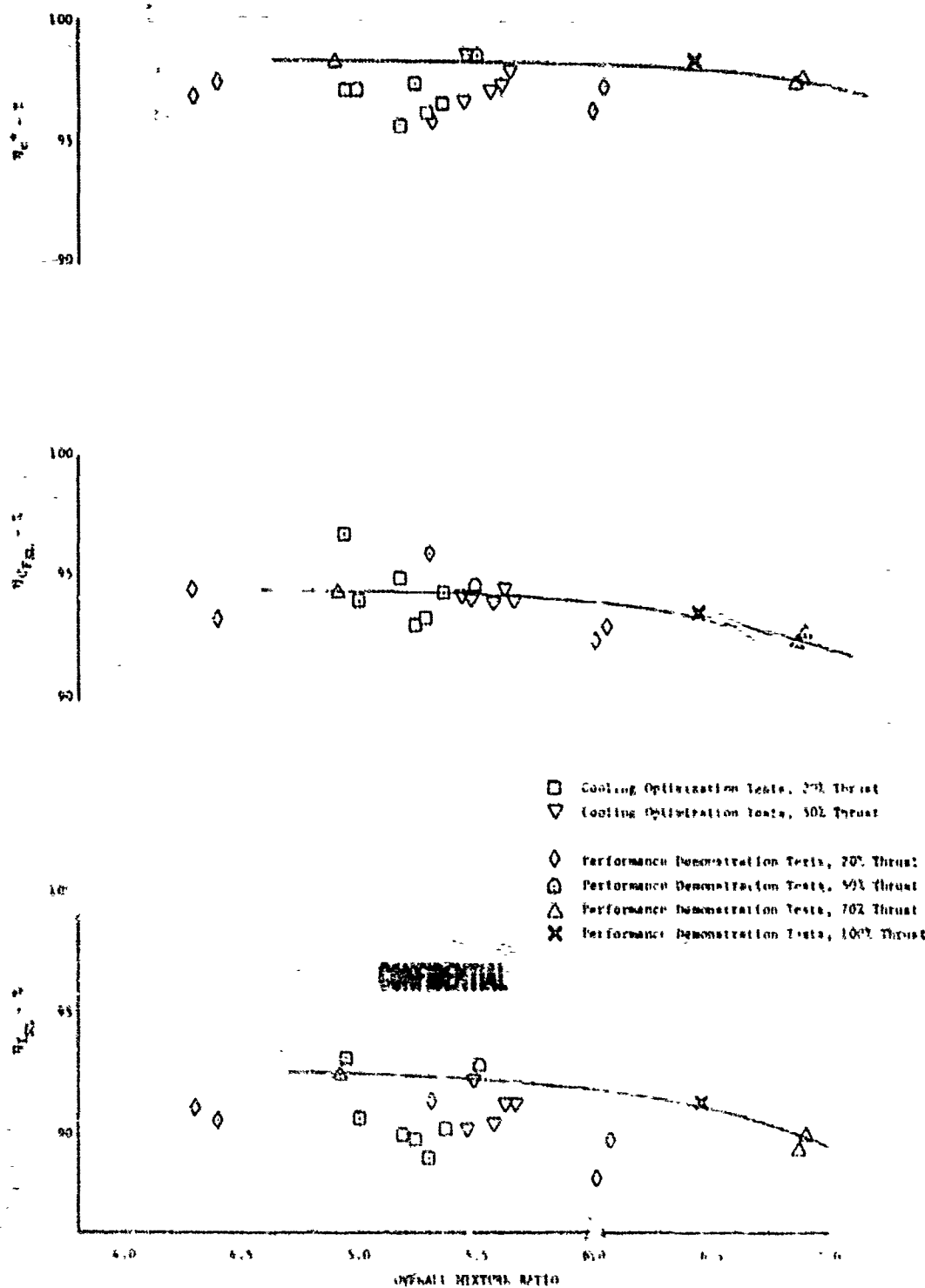


Figure 596. Throttled Sea Level Performance, Area Ratio = 20

DF 60406

CONFIDENTIAL

CONCLUSION

(C) Table L. Summary of Measured Data for 250K Staged

[illegible]

*Values not available. All data unless from previous and subsequent years.

(C) Table LI. Summary of Preliminary Calculated
250L Staged-Combustion Test Series

[illegible]

1 Data for 250% Staged-Combustion Test Series

[illegible][illegible]

Best Available Copy

CONFIDENTIAL

62716211

2

CONFIDENTIAL

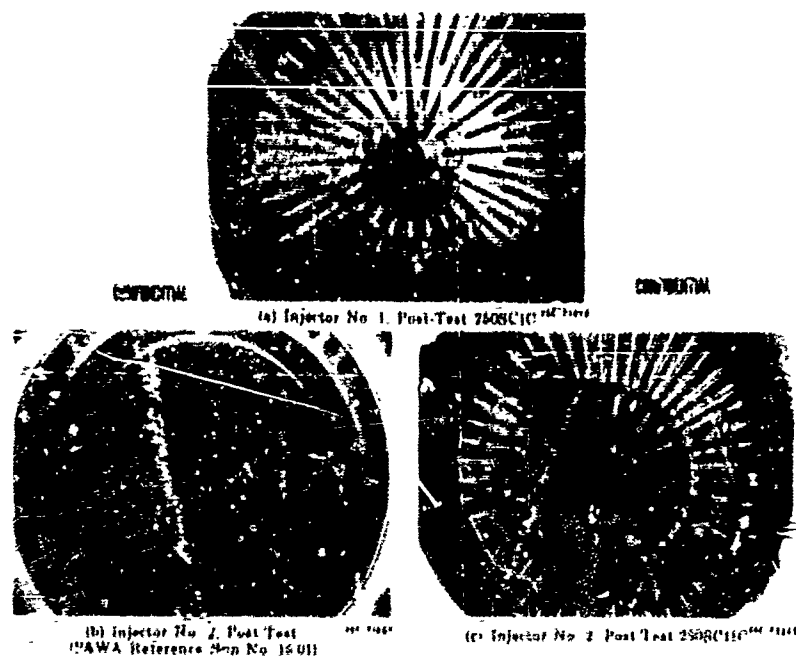


Figure 597. Main Injector History,
Cooling Optimization and
Performance Test Series

FD 23-53

(C) The first six runs were advanced to shut down during ignition flows (17) or during the transient to 7%; five being advanced because of preburner combustion temperatures outside acceptable limits. The seventh test (250SC1C) was a full duration staged-combustion test with steady-state operation at 20% and acceleration to 33% thrust. The post-test inspection showed all the parts were in excellent condition. The next test was scheduled to accelerate to 50% thrust with data points at the 20 and 50% levels, but was advanced to shut down because of high preburner combustion temperatures during the transient to 7% flow. During the post-test facility purge, the main chamber high pressure gaseous hydrogen coolant was inadvertently supplied to the rig, causing overpressurization and collapse of the transpiration-cooled main chamber liner, as shown in figure 598. The main burner and nozzle assemblies were removed from the test stand and the main injector and chamber were replaced with the backup set of hardware. The primary nozzle attachment case was replaced with a new section. The preburner remained mounted in the test facility. The main burner and nozzles were returned to the test stand and the next six runs were advanced to shut down because of preburner combustion temperatures being out of limits.

CONFIDENTIAL

CONFIDENTIAL



(a) Main Chamber No. 1, Post-Test 2508C1C
(12:00 Position)



(b) Main Chamber No 1, Damaged After Shutdown
(P&WA Reference Run No. 8.01)



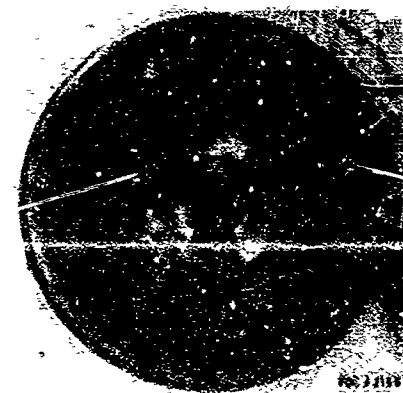
(c) Main Chamber No. 2, Post-Test 2508C3C
(12:00 Position)



(d) Typical Wafer Separations, Main Chamber
No. 2, Post-Test 2508C4C (3:00 Position)



(e) Main Chamber No. 2 Post-Test 2508C7C
(12:00 Position)



(f) Divergent Nozzle Section,
Post-Test 2508C7C

CONFIDENTIAL

Figure 598. Main Chamber History, Cooling,
Optimization and Performance
Test Series

FD 23449

630

THIS PAGE CONTAINS DISCRET MATTER COVERED BY A SECURITY
ORDER WITH A MODERATE SECURITY REQUIREMENTS FRAME
SERIAL NO. 42 COMMISSIONER OF PATENTS

CONFIDENTIAL

CONFIDENTIAL

(C) The problem of repeatable facility control at very low starting flow rates (approximately 1%) delayed staged-combustion rig testing. While this problem was encountered in preburner testing, it was more pronounced in staged-combustion tests because of the lower temperature abort limits required to protect the main burner injector (2400°R). The feasibility of starting at tank head pressures and 1% flows had been demonstrated during the preburner tests and in staged-combustion test No. 250SC10. The preburner starting flows were increased to 7%. The 7% liquid oxygen conditions in the preburner and gaseous oxygen conditions in the main burner were established and then the fuel was rapidly ramped to 7% flow. The preburner transient from oxygen-rich to fuel-rich is so rapid that there was no significant temperature spike. Run No. 15 was the first 7% ignition test; smooth, stable ignition was achieved, as shown in figure 599. All subsequent tests used the new starting flows with complete success. The starting flow control problems encountered during preburner testing and on the initial staged-combustion tests were associated with the high-pressure-fed facility, where it was difficult to provide adequate turndown for accurate starting flow control, and system heat leaks in the facility plumbing at the low starting flows aggravated the problem. On an engine system, low pressures would supply the starting flows, and starting flow control valves would be sized to operate in an acceptable control band. Figure 600 shows a typical test sequence as used on subsequent runs.

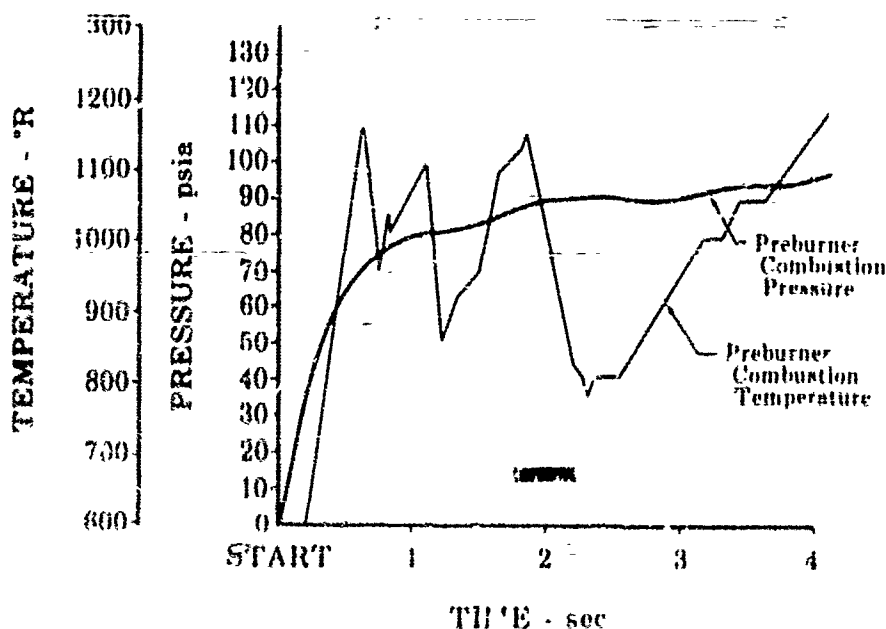


Figure 599. Test No. 15 Preburner Temperature and Pressure

FD 22843

CONFIDENTIAL

CONFIDENTIAL

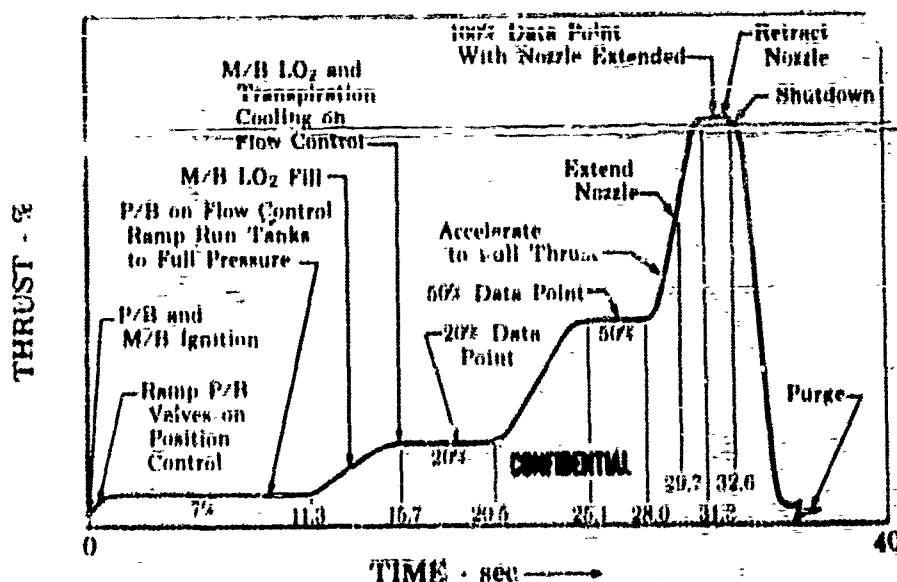


Figure 600. 250K Staged-Combustion Test Sequence - Test No. 250SC3C

FD 22901

(C) The first 7% starting flow test was prematurely advanced to shut down because of an error in failing to arm the preburner oxidizer control system to flowmeter control. During the oxidizer run tank pressurization cycle, the preburner oxidizer flow increased, causing the excessive preburner temperature. The main injector was blued because of the excessive preburner temperature, but was not otherwise damaged, and completed the test series in good condition. The next test, No. 250SC2C, was a full-duration staged-combustion test programmed to stabilize at 20 and 50% thrust and shut down after acceleration to 75% thrust to verify the compatibility of the main burner and preburner flow acceleration ramps. Nominal engine mixture was 3:1 at the 20 and 50% thrust levels. Data analysis and post-test inspection of the test rig verified the validity of the flow control and showed the rig to be operating as anticipated.

(C) Test No. 250SC3C was the first 100% thrust staged-combustion test, and all test objectives were achieved with steady-state operation at 20, 50, and 100% thrust with a nominal engine mixture ratio of 6.0. The secondary translating nozzle was extended at the 100% thrust setting and was retracted and vented at shutdown. The rig operating at 100% thrust is shown in figure 601. The cooling water to the primary and secondary nozzles was off during the data periods at 20, 50, and 100% thrust. The hardware was in good condition.

(C) The cooled chamber front assembly was removed from the shop after Test No. 250SC4C. The supply passages to the rear assembly were reoriented to reduce flow by 30% in the divergent nozzle. The chamber outside diameter in the cylindrical section was bowed inward slightly. This was caused by overpressurization during startup and shutdown.

CONFIDENTIAL

CONFIDENTIAL

(liner ΔP was as high as 1050 psi) when the bypass valve around the main control valve was opened and main chamber pressure was low. Inspection of the bypass line revealed that the flow-restricting orifice had failed, apparently when the first cooled liner was overpressured. A new orifice was installed after being pressure checked above 10,000 psi. The overpressure because of the failed orifice was responsible for inside diameter plate separation in the cylindrical portion of the liner. This was noticed after the first test with the liner.



Figure 601. 250K Staged-Combustion Rig
Operating at 100% Thrust

FE 72190

(C) The chamber was reorificed after test No. 250SC6C and the water-cooled primary nozzle was replaced with the LiH_2 regeneratively cooled nozzle. The temperature sensitive platings indicated that the cylindrical chamber (zones 1 through 7) was operating near 1900°K surface temperature, but that the convergent and divergent nozzle sections could be reduced significantly. As a result, zones 8 through 18 (convergent nozzle and immediately downstream of the throat) were reduced by 25% and the rest of the divergent nozzle (zones 19 through 24) by 33-1/3%. The reductions were to increase surface wall temperatures by 200°K in the convergent nozzle and by 300°K in the divergent nozzle, based on predictions by the analytical heat transfer model. Figure 602 shows how the flow reduction was estimated for the throat (zone 16).

(C) Tests No. 250SC7C, 250SC8C, 250SC9C, and 250SC11C demonstrated nearly optimized coolant distribution at the 100% thrust level over the engine mixture ratio range, as shown in Figure 603. The limited number of tests did not permit coolant optimization over the throttling range, although performance data were obtained at 20, 50, and 70% thrust for different mixture ratios. The 100% thrust level chamber pressure and mixture ratio were lower than programmed for test No. 250SC11C because of restricted flow through a collapsed main injector liquid oxygen inlet filter.

CONFIDENTIAL

CONFIDENTIAL

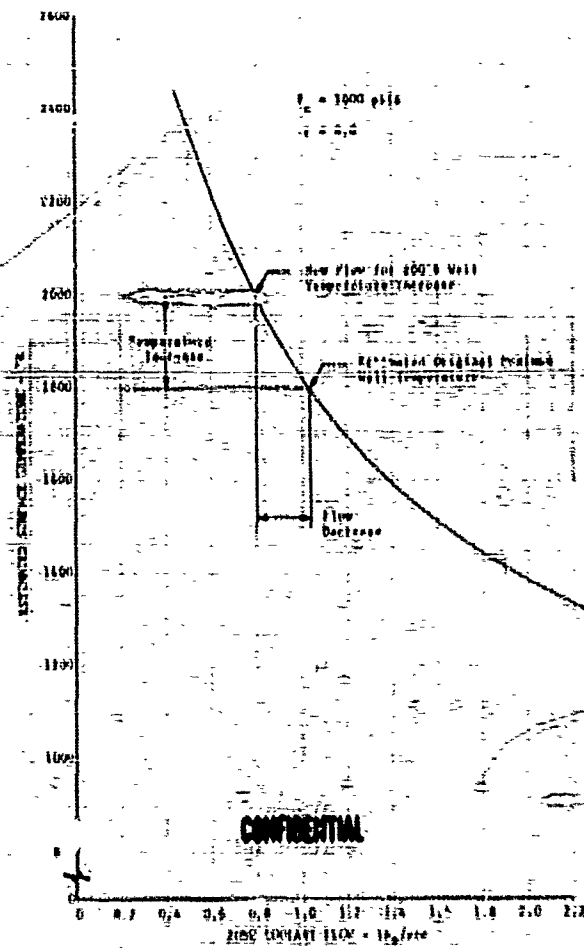


Figure 602. Zone 16 Estimated Surface Temperature vs Zone Coolant Flow

DF 59506

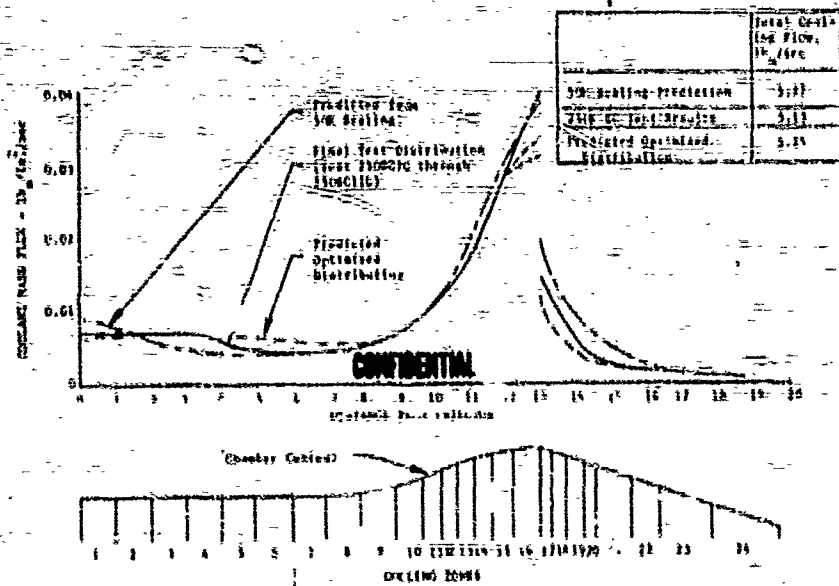


Figure 603. Coolant Mass Flow

DF 59522

CONFIDENTIAL

CONFIDENTIAL

(C) The temperature sensitive platings indicated in the downstream portion of the rear assembly as well as the combustion chamber and in the convergent nozzle during test No. 2508C7C. After this test, only minor increases in the amount of indication occurred during the remainder of the performance tests while cooling flow remained constant. The post-test condition of the main chamber hardware was good; estimated maximum surface temperatures are shown in figure 604. Liner structural strength remained adequate because of the very steep wall temperature gradients, as shown in figure 605. A prediction of the chamber coolant if the distribution were exactly optimized is included in figure 603. All the hardware was generally in good condition except for the preburner injector, which had 5 burned dual-orifice elements (figure 606). Data analysis indicated burning had occurred prior to test No. 2508C2C when the rig was advanced to shut down several times at very low chamber pressures (less than 60 psi). The secondary cavity nitrogen purge flow rate was insufficient to increase cavity pressure faster than the GH_2 purge increased preburner chamber pressure, which caused backflow.

(C) Main chamber durability was indicated by the condition of the hardware. Total hot firing times of 516 and 377 seconds, with 46.4 and 41.8 seconds at 100% thrust, were achieved on the main injector and cooled chamber build, respectively. In contrast to the 50K cooled chamber, the 250K throat diameter experienced only 0.17% diametric shrinkage compared to 2.20% for the 50K. This indicates that the thermal reliefs were effective in minimizing thermal strain, which is a requirement for long cycle fatigue life.

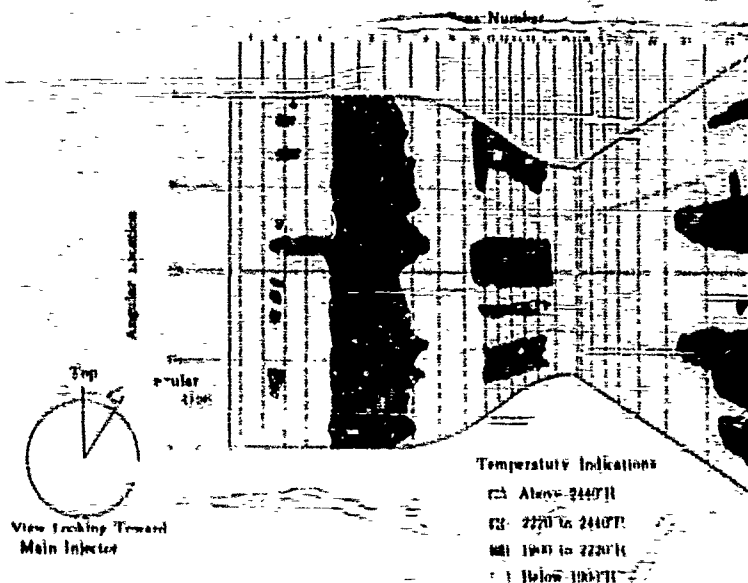


Figure 604. Main Chamber Surface Temperature Pattern (Tests 2508C7C Through 2508C11C)

FD 23039

CONFIDENTIAL

CONFIDENTIAL

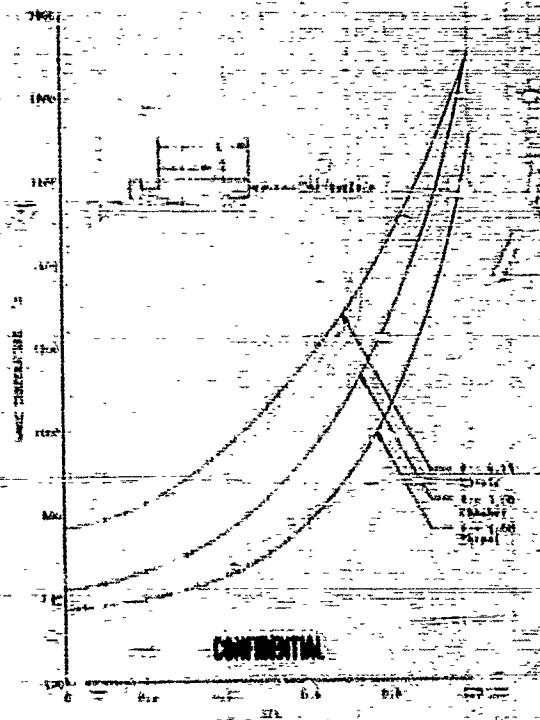


Figure 605. Main Chamber Wall Temperature Profiles

DF 59509

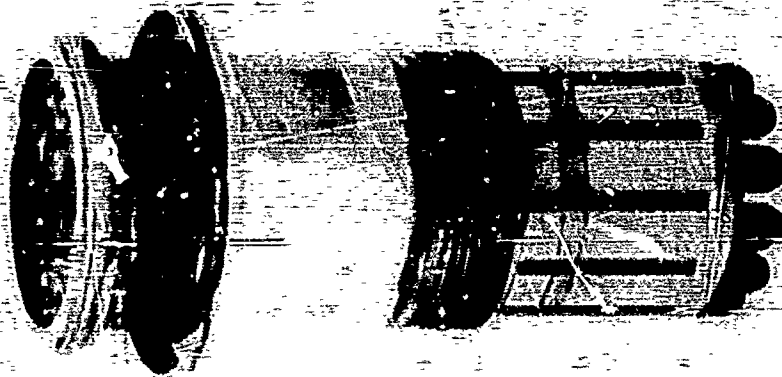


Figure 606. Post-Test Condition of Preburner Injector

FE72493

CONFIDENTIAL

CONFIDENTIAL

5. Two-Position Nozzle

(C) The tests with the lightweight, full-scale, two-position nozzle hardware indicated that the two-position concept was feasible.

(C) The tests showed that retracting the secondary nozzle toward the throat produced stable separation during sea level operation and provided significant gains in performance at low chamber-to-ambient pressure ratios. Translation of the nozzle to the closed position was smooth and provided satisfactory performance at high pressure ratios.

(U) Eleven 250K staged-combustion tests were performed with the two-position nozzle mounted. The nozzle was successfully translated to the closed position and open position at high pressure ratios. In eight of these tests, Figure 607 illustrates the relationship of nozzle translation, pressure ratio, and secondary airflow during a typical test. Reattachment of the primary gas stream to the secondary nozzle skirt did not occur until a significantly high pressure ratio was attained. Figure 608 shows the wall static pressures and temperatures of the secondary nozzle during the start transient of a typical test. Figure 609 shows the favorable agreement between actual and theoretical C_D data with the secondary nozzle in both the open position and closed position. Figure 610 shows the favorable agreement between theoretical wall static pressures and those actually measured on a typical test with the nozzle extended.

(C) The two-pass stainless steel (AISI 347) regeneratively cooled primary nozzle ($\epsilon_x = 20$) was tested during tests No. 250SC7C through 250SC12C. The nozzle demonstrated functional ability and durability. Nozzle coolant was not optimized, with flows remaining approximately 40% above design. However, valuable test data were obtained.

6. Main Chamber Combustion Stability Tests

(U) Tests were conducted to verify combustion stability of the full-scale 250K staged-combustion thrust chamber. Hardware used in these tests included: (1) the backup preburner injector modified to incorporate counter-rotating secondary passages, (2) the designed main injector, (3) the main chamber hardware fabricated and modified for these tests, as described in paragraph C of this Section, and (4) the sheetmetal primary nozzle and the secondary nozzle that was installed and positioned open (retracted) for tests No. 250CP2C and 250CP3C.

(C) Combustion stability of the full-scale main chamber hardware was verified. Both 40- and 80-grain charges were fired during three tests, with a maximum overpressure of 191 psi and a maximum damping time of 8 milliseconds. Investigation of combustion stability over the mixture ratio and thrust ranges was accomplished by testing at nominal values of 20% thrust, $r_{inj} = 5.9$, $r_o = 5.1$; 100% thrust, $r_{inj} = 6.7$, $r_o = 5.4$; and 100% thrust, $r_{inj} = 8.5$, $r_o = 6.5$. A summary of chamber conditions is shown in table LII. (Pressure transducer responses depend on location relative to the pulse gun as well as charge size.) Figure 611 shows the location of the pressure transducers and the pulse guns.

CONFIDENTIAL

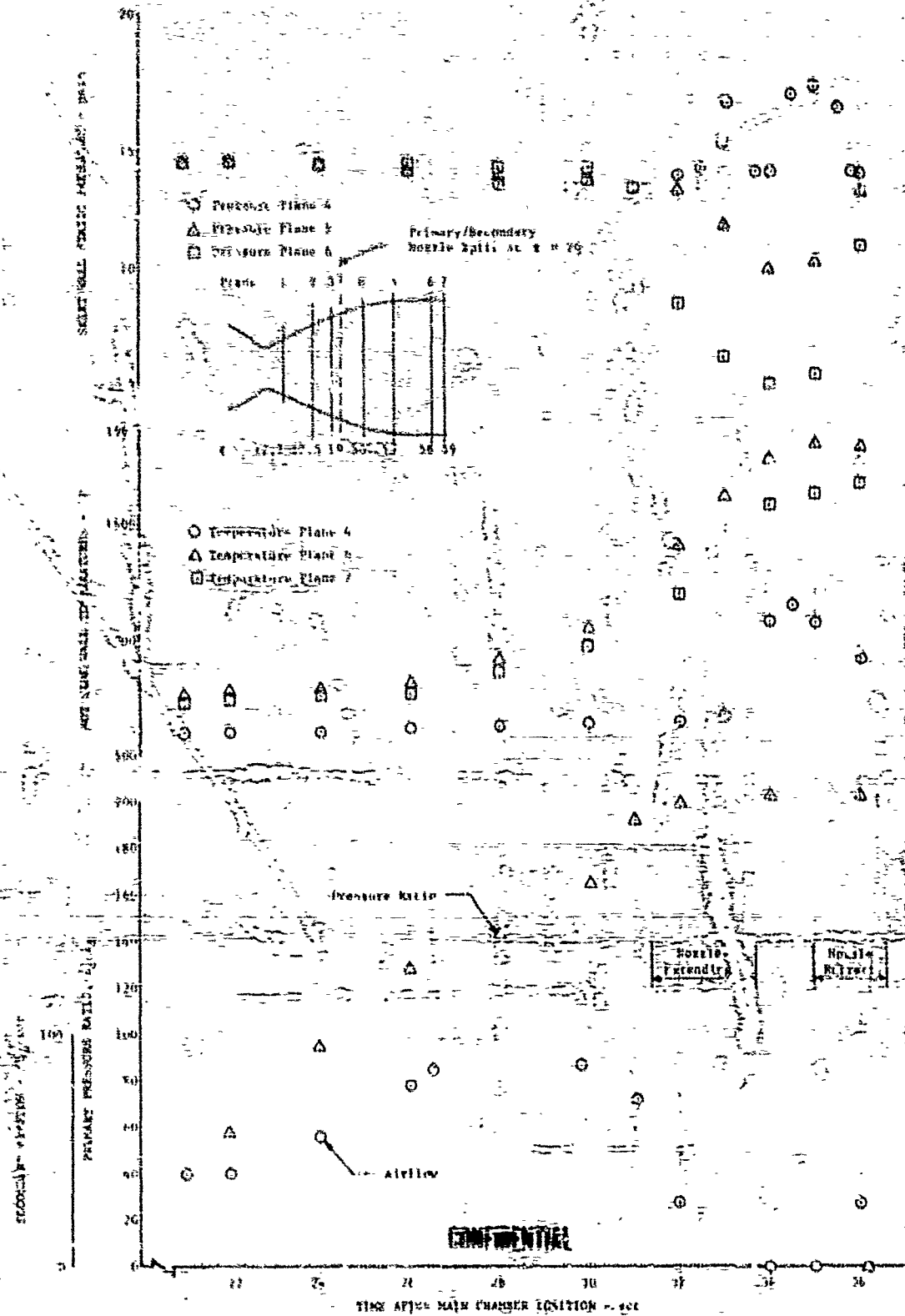


Figure 607. Typical 250K Translating Nozzle Test Data - Test No. 250SC9C

DF 59512

CONFIDENTIAL

CONFIDENTIAL

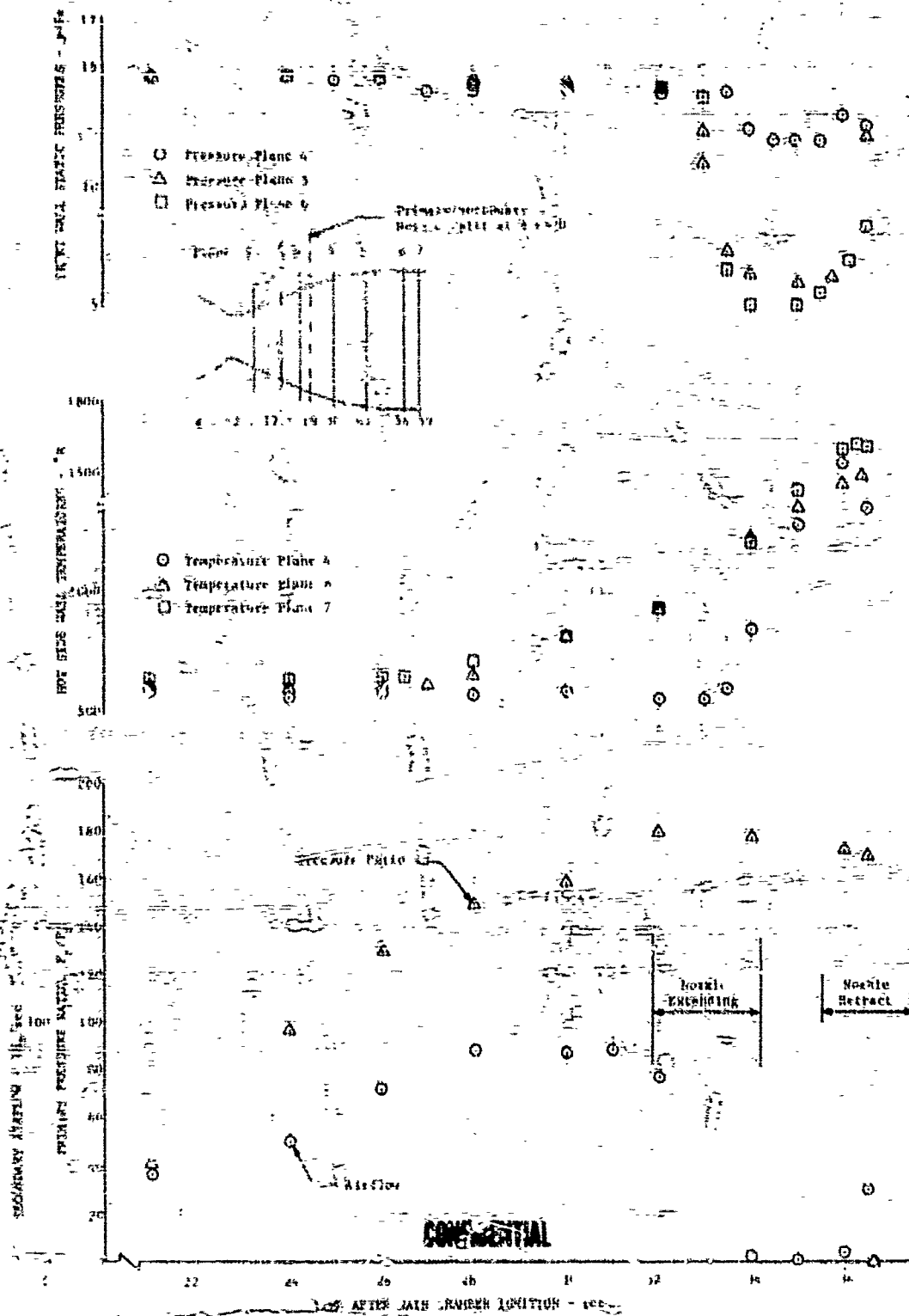


Figure 508. Typical 250K Translating Nozzle Test Data -
Test No. 250SG110

DF 59511

CONFIDENTIAL

CONFIDENTIAL

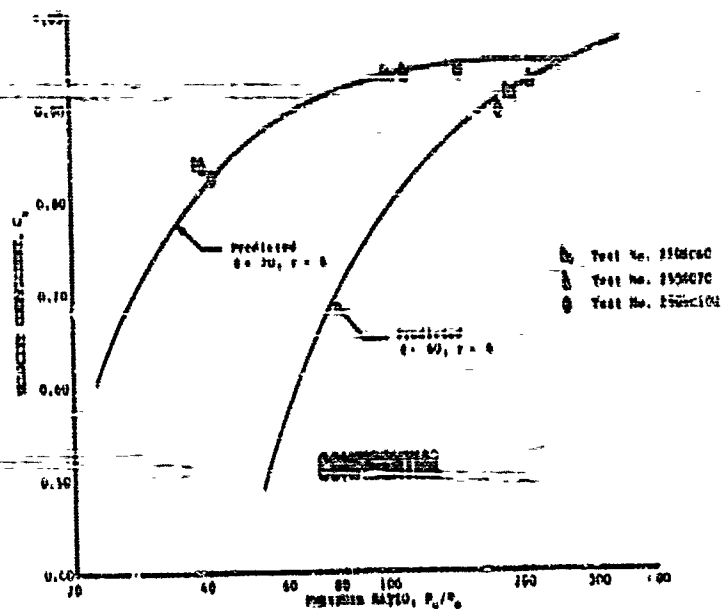


Figure 609. 250K Two-Position Nozzle Tests

DF 59521

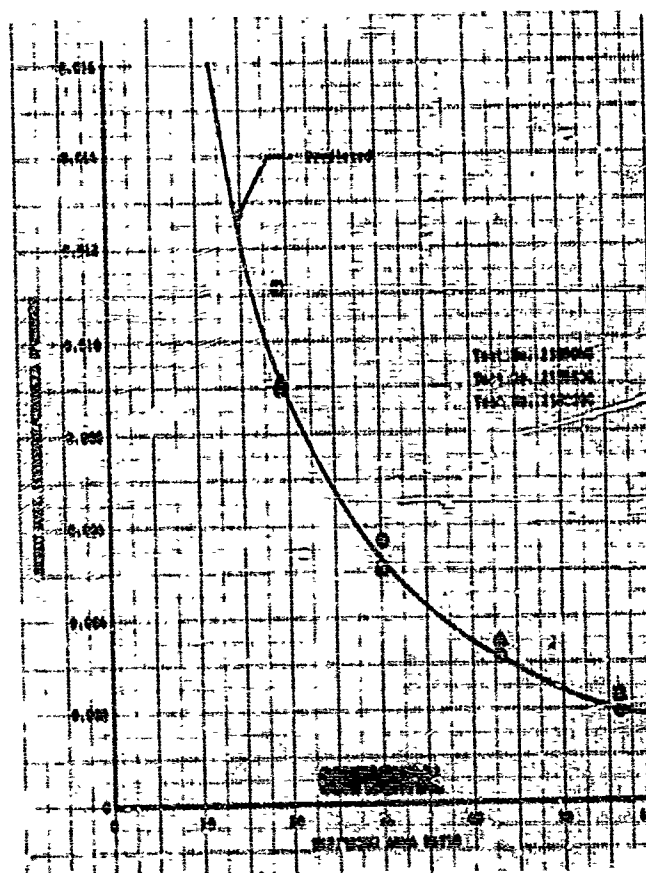


Figure 610. Wall Static Pressures of 250K Translating Nozzle Tests

DF 59510

640

CONFIDENTIAL

CONFIDENTIAL

(7) Table LII. Pulse Test Data Tabulation

| TEST NO. | DATE | TEST DESCRIPTION, sec | P ₀ , psia | P ₁₀ (measured), psia | P ₁₀ (measured) | Location | Maximum Overpressure, psi | | Damping Time, milliseconds | |
|----------|---------|-----------------------|-----------------------|----------------------------------|----------------------------|----------|---------------------------|----------|----------------------------|----------|
| | | | | | | | 40 grain | 80 grain | 40 grain | 80 grain |
| 250CPIC | 9-28-67 | 19.48 | 602 | 5.87 | 1.11 | 2187-12 | 70 | 31 | Immediate | 3 |
| | | | | | | 2187-15 | 70 | 90 | 3 | 6 |
| | | | | | | 2187-16 | 70 | 159 | 3 | 6 |
| | | | | | | 2187-17 | 90 | 83 | 3 | 7 |
| 250CPIC | 9-30-67 | 11.19 | 3028 | 6.70 | 1.43 | 2187-12 | 30 | 38 | Immediate | 3 |
| | | | | | | 2187-15 | 70 | 100 | 3 | 6 |
| | | | | | | 2187-16 | 130 | 191 | 3 | 7 |
| | | | | | | 2187-17 | 83 | 173 | 4 | 7 |
| 250CPIC | 9-30-67 | 30.62 | 2666 | 6.66 | 0.48 | 2187-12 | Not Detected | 49 | Not Detected | 4 |
| | | | | | | 2187-15 | Not Detected | 62 | Not Detected | 3 |
| | | | | | | 2187-16 | Not Detected | 127 | Not Detected | 3 |
| | | | | | | 2187-17 | Not Detected | 143 | Not Detected | 8 |

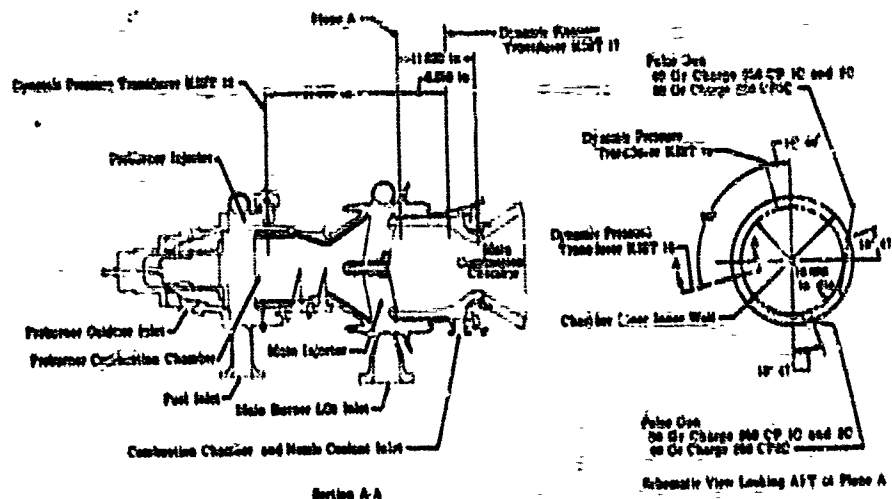


Figure 611. 250K Staged-Combustion Rig Configuration

FD 23003

(C) Of a total of six tests conducted, three were completely successful. The second test, 250CPIC, was conducted at a steady-state chamber pressure of 602 psia. A maximum overpressure of 130 psi was recorded and damping was accomplished within 7 milliseconds. Figure 612 shows the pressure data recorded during this test. The fifth test, 250CP20, was conducted at a steady-state chamber pressure of 3028 psia. As shown in figure 613, the maximum overpressure induced was 191 psi, and all oscillations were damped within 7 milliseconds. Test No. 250CP30 demonstrated a maximum damping time of 8 milliseconds and a maximum overpressure of 143 psi when the 80-grain charge was fired at a chamber pressure of 2666 psia. The firing of the 40-grain charge was undetected as shown in figure 614.

(U) Figure 615 shows the pressure recording of the dynamic transducer from main chamber fill through shutdown for test No. 250CP10. It can be seen that the rapid main injector liquid oxygen fill creates a more severe disturbance than the pulse charges. Even so, this pressure upset is damped in 1.5 cycles and 30 milliseconds and is typical of all tests conducted.

CONFIDENTIAL

CONFIDENTIAL

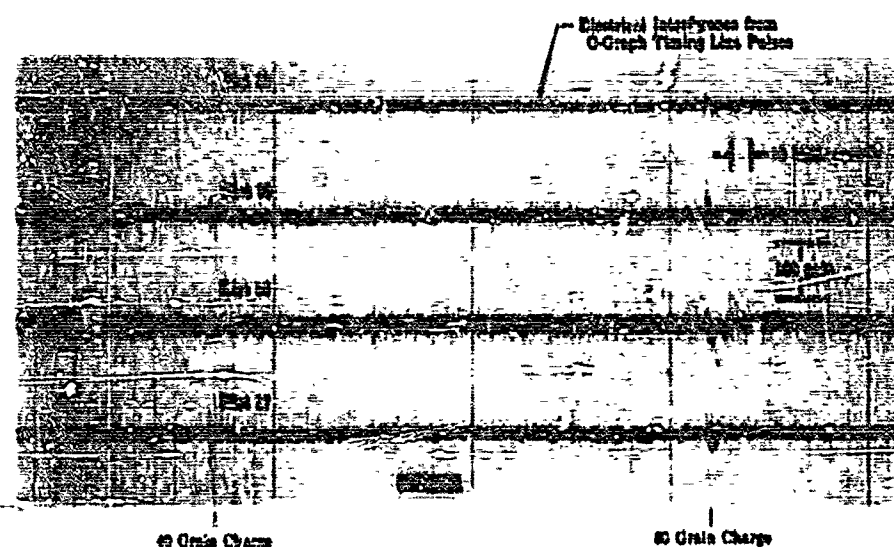


Figure 612. Test 250CP1C Dynamic Pressure
Data (20% Thrust, $r_{inj} = 5.9$,
 $r_0 = 5.1$)

PD 23016

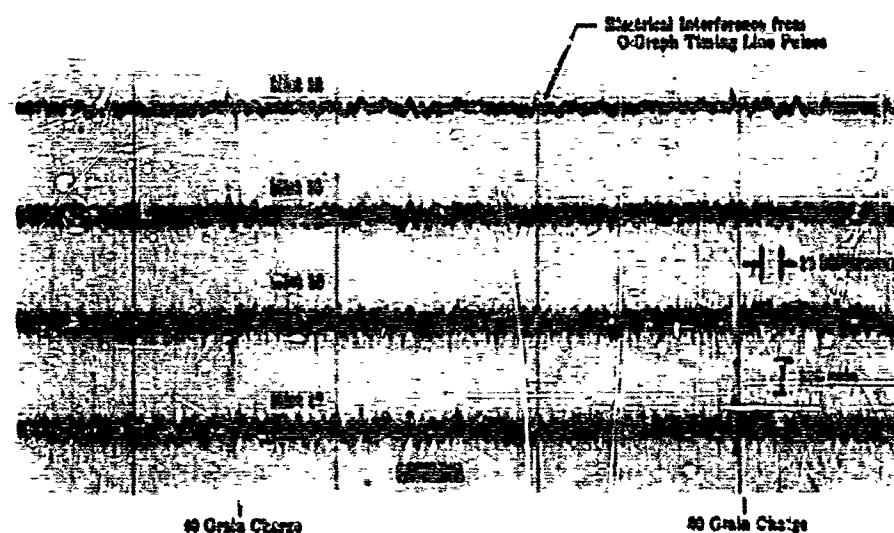


Figure 613. Test 250CP2C Dynamic Pressure
Data (100% Thrust, $r_{inj} = 5.43$,
 $r_0 = 5.43$)

PD 23007

CONFIDENTIAL

CONFIDENTIAL

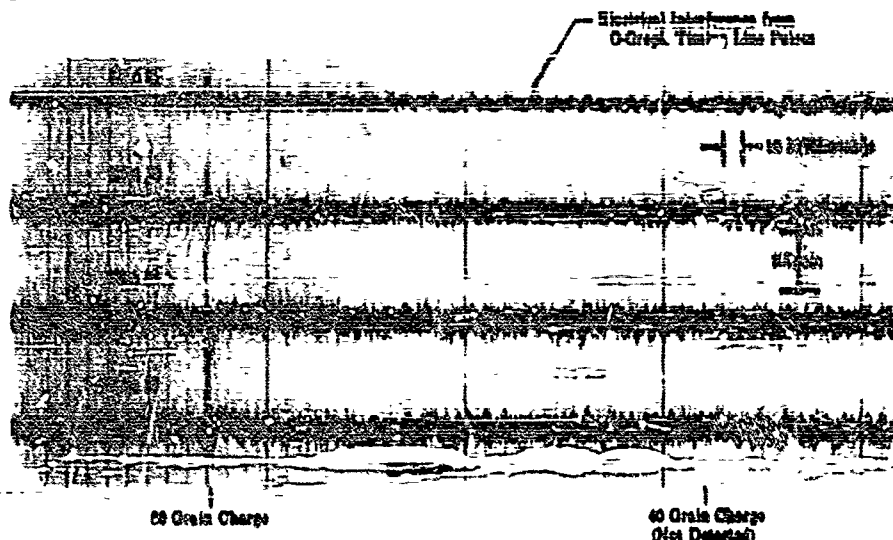


Figure 614. Test 250GP30 Dynamic Pressure Data (100% Thrust, $r_{inj} = 8.46$, $r_o = 6.46$) FD 23008

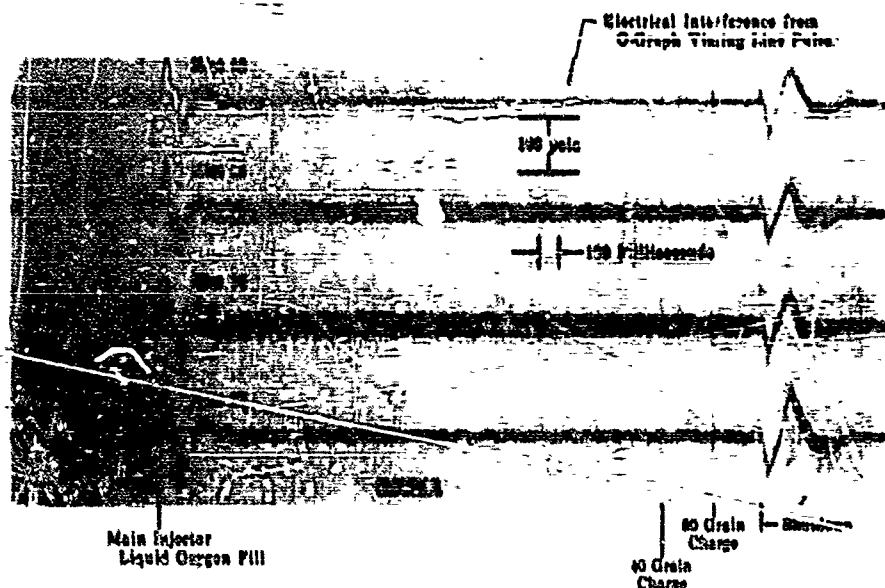


Figure 615. Test 250GP10 Dynamic Pressure Data (20% Thrust, $r_{inj} = 5.87$, $r_o = 5.11$) FD 23022

(U) The third test was advanced to shut down at 100% thrust, but prior to pulsing, by a low GH_2 coolant ΔP resulting from high leakages past axial O-ring seals between the film coolant ring and chamber shell and between the steel shell and copper section, as shown previously in figure 587. The leakage significantly reduced the flow through the film coolant inlet annulus by exposing alternative flow paths, and erosion of the solid copper liner section resulted. The coolant supply flow rate was increased by 30% for succeeding tests. Additional erosion of the copper section occurred, but the hardware was adequate for continued testing. Figure 616 shows the chamber prior to testing, and figure 617 shows the condition at the conclusion of the tests.

CONFIDENTIAL

CONFIDENTIAL

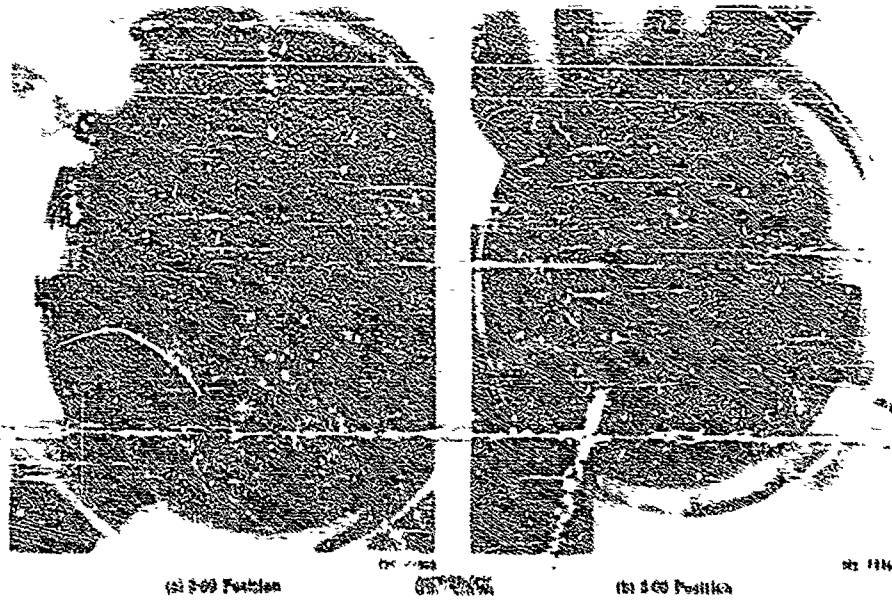


Figure 616. Pretest Condition of Main Chamber

FD 23453

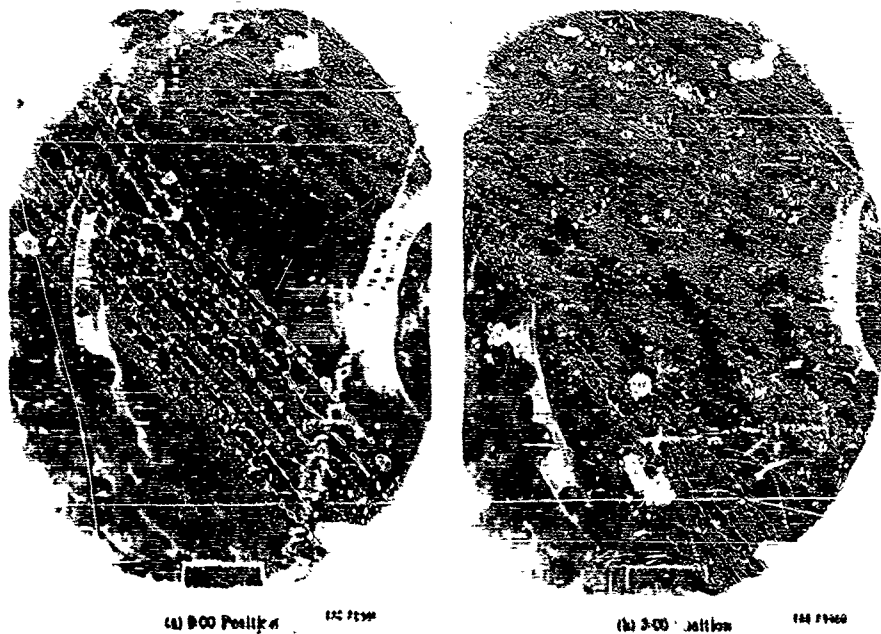


Figure 617. Post-Test Condition of Main Chamber (250CP3C)

FD 23454

THIS PAGE CONTAINS SUBJECT MATTER COVERED BY A SECRET ORDER WITH A MODIFIED "SECURITY REQUIREMENTS" PERMIT ISSUED BY U.S. COMMISSIONER OF PATENTS.

144
CONFIDENTIAL

CONFIDENTIAL

E. TEST FACILITIES AND PROCEDURES

1. Test Facilities

(U) The E-0 test stand, as shown in figure 618, was provided by United Aircraft Corporation to support the Phase I full-scale preburner and staged-combustion test programs. The addition of this large capacity pressurized facility to the existing FRDC facilities has allowed testing of 250K thrust preburners at pressures greater than 5000 psi. The facility consisted of a 2400-gallon, 6600-psi hydrogen tank, and a 500-gallon, 6600-psi oxygen tank. These liquid run tanks were pressurized with gaseous hydrogen and gaseous nitrogen, supplied from seven 9000-psi cylinders with a total storage volume of 4185 cubic ft. The facility included twin 10,000-psi hydrogen gas compressors and 10,000-psi nitrogen vaporizer pumps for charging the tank pressurization bottles. The liquid and gas ~~supply system~~ ^{supply system} along the 250K thrust preburner at design operating pressure for 7 seconds and staged combustion tests for 15 seconds. The thrust measurement system was sized for 350K thrust and allowed accurate thrust measurement with a precision error of less than $\pm 1\%$ over a 10 to 1 thrust range. A liquid-gas mixer was provided to supply hydrogen to the rig at any temperature between -253°C of liquid hydrogen and room temperature to simulate engine operating conditions. In addition, separate hydrogen systems were available for chamber and nozzle coolants. Control of propellants to the test rig was accomplished using 25 electrohydraulic commercial control valves in the gas and liquid systems. These control valves, many of which were in parallel, allowed for a pressure-flow control range of 450 to 1.

(U) The facility control system was based around an analog computer, allowing for closed loop control of the electrohydraulic servovalves, plus associated mathematical computation and nonlinear function generation. The computer system consisted of the following components:

- 200 Coefficient Potentiometers
- 160 Philbrick DC Operational Amplifiers
- 20 BAI Multipliers
- 26 Variable Diode Function Generators
- 26 Voltage Comparators
- 1 NLS Digital Voltmeter
- 1 NLS Digital Printer
- 1 NLS Digital Frequency Counter
- 24 Astrodata Differential Amplifiers
- 1 Vidar Voltage-to-Frequency Converter
- 1 Wavitek Function Generator
- 5 Vidar Frequency-to-Voltage Converters
- 1 HP Dual Trace Oscilloscops

CONFIDENTIAL

CONFIDENTIAL

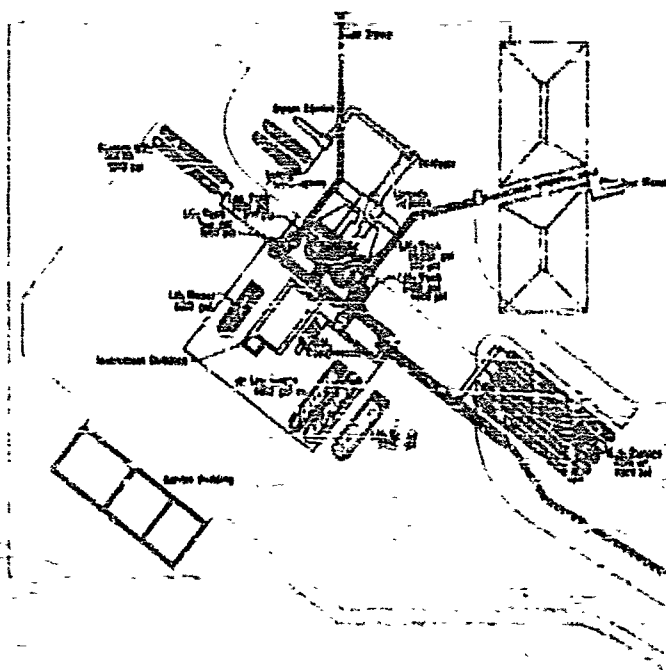


Figure 318. E-8 High Pressure Test Facility

FD 21139

(U) Test program events were controlled by an electronic digital sequencer. This unit converted a constant frequency pulse train into time-controlled switch operations according to a predetermined program sequence. These switches could be operated in series, parallel, cascade, and time-delayed sequence. Event timing could be scheduled in 1 millisecond intervals on any one of 60-relay channels between the time limits of $\pm 999,999$ sec. In conjunction with the analog computer, the sequencer provided for pre- and post-firing valve operation, initiation and shutdown of test, and timing of controlled parametric changes during the test. The sequencer was programmed to interrogate, in conjunction with voltage comparators, certain parameters at specific time intervals, and thus provided a go/no-go indication for test to proceed, advance to a preprogrammed controlled shutdown, or abort. This engine parameter interrogation system has proved invaluable in the protection of rig hardware from damage because of program error, controller error, or valve malfunction.

(U) Control system input as well as data recording were handled through a 200-channel digital data system with a sampling rate of 6666 samples per second. The transmission and signal conditioning system had the capacity to handle the following:

| | |
|---------------------------------------|-------------|
| Pressures (individual power supplied) | 72 channels |
| Thrust | 12 channels |
| Resistance temperature bulbs | 24 channels |
| rpm and flow | 12 channels |

CONFIDENTIAL

(This page is Unclassified)

CONFIDENTIAL

| | |
|--------------------|-------------|
| Flow multiplier | 15 channels |
| Thermocouples, C-A | 68 channels |
| Thermocouples, C-C | 48 channels |
| Vibrations | 18 channels |
| Dynamic pressures | 6 channels |

(U) The data are presented using:

| | |
|-----------------------------------|--------------|
| Strip charts | 28 channels |
| Oscilloscope | 36 channels |
| Analog tape | 24 channels |
| Digital recording | 200 channels |
| Oscilloscope (control parameters) | 18 channels |

(U) In addition, there were two high-speed camera locations and closed-circuit TV for test monitoring.

(U) Figure 619 shows the flow schematic for staged-combustion testing as used in Phase I.

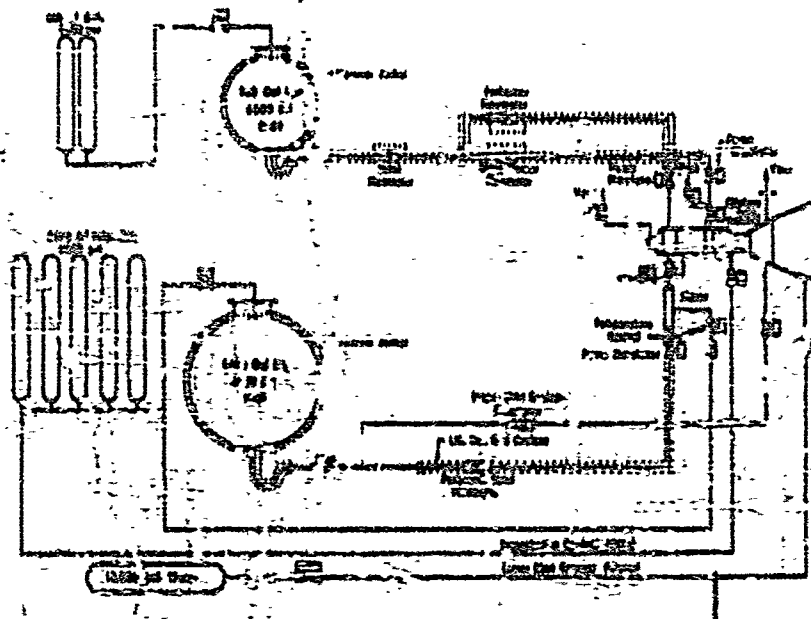


Figure 619. 1-3 Test Stand Flow Schematic UGB 2647A

CONFIDENTIAL

2. 250K Test Procedures

(U) The high-pressure 250K thrust level staged-combustion tests were conducted in the pressure-fed E-8 test stand in the Rocket Test Area. The staged-combustion control block diagram is shown in figure 620. A 60-channel digital sequence was used for test sequencing, and a 160-amplifier analog computer was used to provide propellant run valve ramping. A diagram of the test sequence was provided previously in figure 500.

(U) Pilot ignition gaseous oxygen and hydrogen was provided to the main burner and preburner torch igniters simultaneously from sources at approximately 900 psia for gaseous oxygen and 100 psia for gaseous hydrogen. Flows were controlled by small choked orifices in each of the supply lines. Ignition was initiated in the torches by a spark plug. Satisfactory ignition was sensed by thermocouple probes inserted into both of the torch igniter combustion chambers. If satisfactory ignition was not sensed during a prescribed time interval of the test sequence, the test was automatically advanced to shut down.

(C) If satisfactory ignition was verified for the prescribed period, preburner oxidizer was allowed to enter the injector by opening the rig flow divider valve. Fuel flow was introduced to the rig by opening a remotely operated stand valve. The preburner pump simulator valves were position-ramped to a 7% flow level. Gaseous oxygen for pilot ignition was supplied to the main injector through choked orifices that regulated the flow rate. The flow was introduced downstream of the mixture ratio valve, which was still closed at this point.

(U) The gaseous hydrogen transpiration coolant for the main burner combustion chamber was supplied directly from high pressure storage. Flow was controlled by an electrohydraulic valve in the coolant supply line, which was controlled by the differential pressure across the coolant liner.

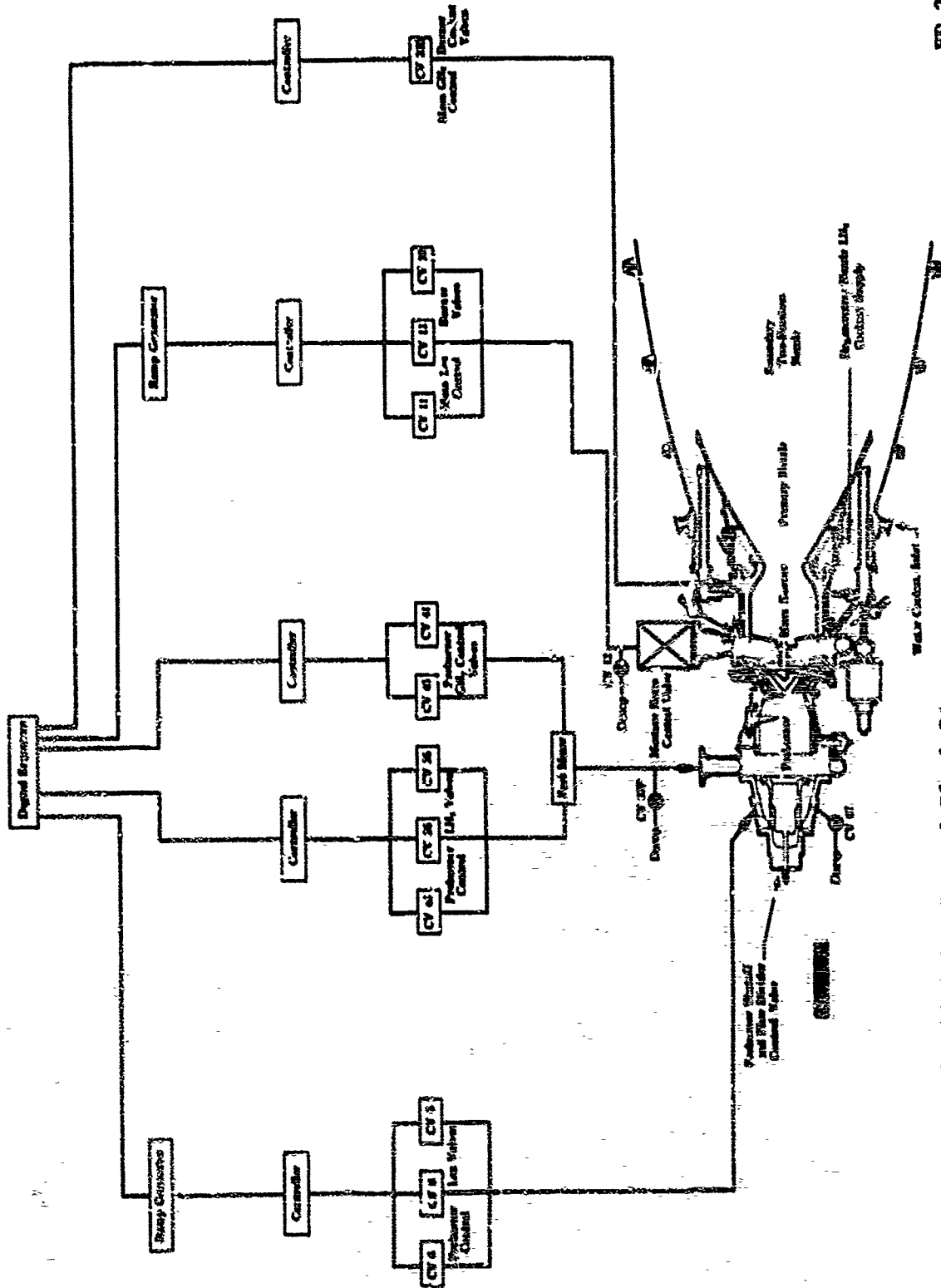
(C) While 7% preburner flows were being established, the chamber coolant bypass valve was opened on position control and provided coolant for this initial ramp. The main chamber coolant valve was later switched to ΔP control and ramped along with main propellant flow rate.

(C) After stabilization at 7% preburner flow rates, preburner fuel and oxidizer pump simulator valves were switched to flow control, and the flow control was used to ramp preburner valves to a 20% flow level. When the preburner 20% flow level was reached, main burner liquid oxidizer flow was allowed to enter by opening the mixture ratio valve while stepping the main chamber pump simulator valve to a position required to deliver the 20% flow rate. After stabilization at the 20% flow rates, control of the main chamber pump simulator valve was switched to flowmeter closed loop control. Using the computer, flow was ramped in conjunction with the preburner. The shape of the flow ramps maintained the desired propellant mixture ratios in the preburner and main burner. Mixture ratio excursions were accomplished by ramping the individual liquid oxygen and/or fuel flow rates to the required set points for the desired mixture ratio.

CONFIDENTIAL

CONFIDENTIAL

FD 211:17A



CONFIDENTIAL

CONFIDENTIAL

(U) After stabilization at the 100% thrust level, the translating nozzle was extended for high area ratio expansion data points.

(U) Shutdown from any chamber pressure level was achieved by closing all liquid pump simulator valves at the maximum slew rates. Gaseous hydrogen was supplied to the preburner injector during shutdown to maintain a fuel-rich condition.

(U) Critical parameters in the test item were monitored both manually and by the automatic advance system. The automatic system would advance a test to an immediate shutdown if a critical parameter exceeded preset limits. This was done by causing the digital sequence to step to the programmed shutdown time, bypassing the remaining portion of the test program. When activated manually, the system operated in the same manner.

630

CONFIDENTIAL

(This page is Unclassified)

SUPPLEMENTARY

INFORMATION

DIVISION OF UNITED AIRCRAFT CORPORATION

OCT - 7 1968

In reply please refer to:
MFB:RPSmb:Corl. Adm.

AD-385-911

Mrs. Mary Racovich, FTMKR-3
Directorate of Materiel
Procurement Division
Edwards Air Force Base, California 93523

- Reference: (a) ^{N/R} PWA FP 67-11, 250K High Performance Reusable Oxygen/Hydrogen Rocket Engine, dated 21 August 1967.
- (b) ^{N/R} PWA FR-1810, Components Design Handbook, Advanced Development Program for a High Performance Oxygen/Hydrogen Rocket Engine, dated 30 June 1966.
- (c) ^{N/R} PWA FR-1911, Quarterly Report No. 1, Advanced Cryogenic Rocket Engine Program Staged - Combustion Concept, dated June 1966.
- (d) ^{N/R} PWA FR-1928, Quarterly Report No. 1, 250K Thrust Chamber Technology Program, dated 30 June 1966.
- (e) ^{N/R} PWA FR-2372, Final Report - Advanced Engine Design Study, Bell, (AEB), dated July 31, 1967.
- (f) ^{N/R} PWA FR-2597, Advanced Cryogenic Rocket Engine Program Staged - Combustion Concept - Final Report, dated December 1967.

Vol. 2 - Dec 67 910 (f)
Vol. 2 - Dec 67 911 (f)
Vol. 2 - Dec 67 912 (f)

Dear Mrs. Racovich:

The U. S. Patent Office has issued a Secrecy Order with a modifying "Security Requirements Permit" against United Aircraft Corporation's U. S. Patent Application No. 725,954, entitled "Dual Slot Swirler Injector Element." This Secrecy Order relates to a single throttleable injection element that provides a wide range of throttleability. You are advised that the referenced documents contain information relating to this concept.

Mrs. Mary Racovich

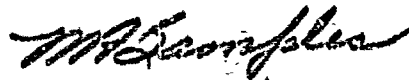
- 2 -

A "Security Requirements Permit" limits disclosure of the subject matter involved to the security requirements of the Government contract which imposes the highest level of security classification thereon. The highest level of security classification on the subject matter of this application is "Confidential". Disclosure of the invention or any material information with respect thereto is prohibited except by written consent of the Commissioner of Patents or as authorized by the permit. By statute, violation of a Secrecy Order is punishable by a fine not to exceed \$10,000 and/or imprisonment for not more than two years.

If this invention has been disclosed to others, the recipients of this letter are requested to notify them of the issuance of the Secrecy Order and "Security Requirements Permit" and of the penalties for violation.

Very truly yours,

UNITED AIRCRAFT CORPORATION
Pratt & Whitney Aircraft Division



M. F. Samples
Senior Contract Administrator
Florida Research and Development Center

cc: see attached.